

**THE HYDROGEOLOGY OF THE TABRIZ  
AREA, IRAN**

By

**Asghar Asghari Moghaddam Heris**

A Thesis

Submitted for the Degree

of

Doctor of Philosophy

**Department of Geological Sciences**

**University College London**

**1991**

ProQuest Number: 10610881

All rights reserved

INFORMATION TO ALL USERS

The quality of this reproduction is dependent upon the quality of the copy submitted.

In the unlikely event that the author did not send a complete manuscript and there are missing pages, these will be noted. Also, if material had to be removed, a note will indicate the deletion.



ProQuest 10610881

Published by ProQuest LLC (2017). Copyright of the Dissertation is held by the Author.

All rights reserved.

This work is protected against unauthorized copying under Title 17, United States Code  
Microform Edition © ProQuest LLC.

ProQuest LLC.  
789 East Eisenhower Parkway  
P.O. Box 1346  
Ann Arbor, MI 48106 – 1346

TO MY MOTHER, MY CHILDREN  
AND  
TO THE MEMORY OF MY FATHER

## ABSTRACT

The present project area lies in East Azarbijan in the north-west part of Iran, and comprises the Tabriz Plain (about 3000 km<sup>2</sup>) and part of the surrounding mountain area (about 4500 km<sup>2</sup>). Climatically, the Tabriz area has hot and dry summers and cold winters with average precipitation ranging from 200mm in the lowland to 500mm in the higher mountain area.

Three main aquifers supply drinking, domestic, industrial and most part of the agricultural water to Tabriz City and its surrounding urban and rural areas. They are (1) the unconfined Sahand Plio-Pleistocene volcanic and volcano-sedimentary Alluvial Tuff aquifer which lies to the south and south-west of Tabriz, (2) the unconfined alluvial fans that lie in the northern and southern parts of the Plain, and (3) the multi-layered aquifer system which lies in the central part of the Plain. The average thickness of these aquifers are about 200m, 50m and 60m respectively. Long-term declines of ground water level are indicated in some parts of the alluvial fans and reverse flow of ground water, in the heavily pumping area in the south-west of the Plain, has produced saline water intrusion into the fresh water aquifer.

Constant-rate and step-drawdown pumping test data available from different parts of the area, have been analysed by analytical as well as numerical methods to determine the aquifer properties and well characteristics. The resultant values of transmissivity for the Plain and alluvial tuff aquifers range from 500 m<sup>2</sup>/d to 3500 m<sup>2</sup>/d, and 240 m<sup>2</sup>/d to 1000 m<sup>2</sup>/d, respectively. Due to the lack of observation well data, direct values of storage coefficient could not be determined for the Plain aquifer. However, the values deduced from the numerical method for the confined aquifer of this area ranges between  $2.2 \times 10^{-3}$  and  $2.0 \times 10^{-5}$ . Values for the alluvial tuff aquifer range from  $2.7 \times 10^{-1}$  to  $1.1 \times 10^{-1}$ . The step-drawdown test data have been analysed by a number of methods. The well loss factor (C) and aquifer loss factor (B) range from  $1.0 \times 10^{-7}$  to  $1.1 \times 10^{-8}$  d<sup>2</sup>m<sup>-5</sup> and  $4.66 \times 10^{-3}$  to  $4.14 \times 10^{-4}$  dm<sup>-2</sup>, respectively.

With respect to geological conditions and ground water quality, the area was divided into three hydrochemical zones i.e., alluvial tuff, northern part of the Plain, and southern and central parts of the Plain. The values of TDS in the ground water of these zones range from 150 to 500 mg/l, 200 to 1200 mg/l, and 1000 to 5000 mg/l, respectively. Bicarbonate type water dominates the alluvial tuff aquifer and higher elevation parts of the northern parts of the Plain. The southern and central parts of the Plain represents a chloride type ground water in some places especially around the River Aji Chay and the area between Tabriz and Soufian. The alluvial tuff water is rich in Ca and Na whereas, the northern part of the Plain is rich in Ca and Mg which reflect the differences in water bearing-layers in the area.

The total amount of annual recharge to ground water is estimated to be about  $782 \times 10^6$  m<sup>3</sup> and discharge about  $763 \times 10^6$  m<sup>3</sup>. Therefore, the present rate of withdrawal indicates that ground water in the area is in an old age state of development and requires careful assessment, protection and management. Hence, a numerical regional ground water model was used to try to understand the hydrogeological behaviour of aquifers and water resource management goals in the area.



## Acknowledgments

The author extends his sincere thanks to his supervisor Professor G. P. Jones for his constructive discussions, guidance, encouragement and support throughout the period of this work.

The author also wishes to acknowledge the University of Tabriz, Ministry of Culture and Higher Education for their financial grants, and the Azarbijan Regional Water Authority (ARWA) for supplying the existing relevant data. I would like to thank Mr. M. Shahmahammadi, A. Alinezhad and A. Ahmadi for their kindness help during the collecting data and field visit.

Special thanks are due to Mrs. Susan White for her whole-hearted co-operation, particularly her skilful computing help, which has played a vital role during the computer analysis of much of the data.

Also many thanks are due to Mrs. Jane Dottridge for her useful discussions and guidance in modelling and for reading the whole of the manuscript.

All academic and departmental staff who extended their support deserve special thanks, particularly, Janet Baker and Colin Stuart for their help during the preparation of some of the drawings.

I am grateful to all my family and friends who helped me one way or another during my studies. I apologise for not naming everyone here, but you know who you are.

Finally, I would like to thank my wife Mrs. Aghdas Shokohi for her patience and encouragement throughout the study time.

# C O N T E N T S

Abstract	page
Acknowledgements	i
Contents	ii
List of figures	iii
List of tables	vi
List of appendices	xii
	xv

## CHAPTER 1 INTRODUCTION

1.1 Purpose and Scope	2
1.2 Size and Location of the Study Area	2
1.3 Soil Types and Characteristics	4
1.4 Vegetation and Land Use	5
1.5 Previous Work	5
1.6 Types and Sources of Data	7

## CHAPTER 2 HYDROLOGY

2.1 Introduction.	9
2.2 Main Geomorphological Units	9
2.2.1 Tabriz Plain.	10
2.2.2 Northern Mountains.	10
2.2.3 The Sahand Mountain	11
2.3 Drainage Basins	11
2.4 Climate	13
2.4.1 Introduction.	13
2.4.2 Precipitation	14
2.4.3 Temperature, Wind and Relative Humidity	21
2.4.4 Evaporation and Transpiration	21
2.5 River Discharge	28
2.5.1 Introduction.	28
2.5.2 Sources and Components of River Discharge	31
2.5.3 Hydrograph Analysis	31
2.5.4 Factors Affecting Baseflow.	34
2.5.5 Flow Duration Curve Analysis.	39

## CHAPTER 3 GEOLOGY

3.1 Geological Setting.	43
3.2 Litho-Stratigraphy.	44
3.3 Geological Structure.	47

## CHAPTER 4 HYDROGEOLOGY

4.1 Introduction.	51
-------------------	----

4.2 Aquifer Systems . . . . .	51
4.2.1 Types of Aquifer. . . . .	51
4.2.2 Boundaries and Thicknesses of Aquifers. . . . .	53
4.3 Ground Water Level Fluctuations . . . . .	59
4.3.1 Long Term Fluctuations. . . . .	60
4.3.2 Seasonal Fluctuations . . . . .	60
4.4 Ground Water Contour and Flow Maps. . . . .	65
4.4.1 Introduction. . . . .	65
4.4.2 Flow in Relation to Minimum Ground Water Contours . . . . .	66
4.4.3 Flow in Relation to Maximum Ground Water Contours . . . . .	68
4.4.4 Annual Ground Water Fluctuation Map . . . . .	68
4.4.4.1 Estimation of Replenishment. . . . .	71

## CHAPTER 5 AQUIFER TESTS

5.1 General . . . . .	75
5.2 Applied Methods . . . . .	77
5.2.1 Analytical Solution . . . . .	77
5.2.1.1 Drawdown Solution . . . . .	77
5.2.1.2 Recovery Solution . . . . .	78
5.2.2 Numerical Solution . . . . .	79
5.3 Analytical Analysis of Data . . . . .	82
5.4 Numerical Analysis of Data . . . . .	121

## CHAPTER 6 STEP-DRAWDOWN TEST

6.1 General . . . . .	143
6.2 Planning a Step-Drawdown Test . . . . .	144
6.3 Step-Drawdown Test Analysis Methods . . . . .	145
6.3.1 Jacob arithmetic method . . . . .	145
6.3.2 Bruin and Hudson method . . . . .	145
6.3.3 Eden and Hazel method . . . . .	146
6.3.4 Rorabaugh graphical method . . . . .	148
6.4 Use of Step-Drawdown Test Analysis . . . . .	149
6.4.1 Determination of well characteristics . . . . .	149
6.4.2 Estimating aquifer properties . . . . .	149
6.5 Data Analysis of Project Area . . . . .	150

## CHAPTER 7 HYDROCHEMISTRY

7.1 Introduction . . . . .	189
7.2 Sample collection and analysis . . . . .	189
7.3 Evaluation and accuracy check of data . . . . .	192
7.4 Representation and interpretation of data . . . . .	193
7.4.1 Numerical classification . . . . .	193
7.4.2 Graphical representation and interpretation . . . . .	198
7.5 TDS and their relation to electrical conductivity . . . . .	210
7.6 Ground water contamination in the Tabriz area . . . . .	212

7.7 Factors and processes controlling ground water compositions . . . . .	217
7.7.1 Major constituents . . . . .	217
7.8 Ground Water Quality Evaluation . . . . .	225
7.8.1 Suitability of Ground Water for Drinking Purposes . . . . .	225
7.8.2 Suitability of Ground Water for Agricultures . . . . .	226

**CHAPTER 8 GROUND WATER RESOURCES**

8.1 Introduction. . . . .	232
8.2 Estimation of Resources . . . . .	232
8.2.1 Introduction. . . . .	232
8.2.2 Ground Water Recharge . . . . .	233
8.2.2.1 Infiltration from Precipitation. . . . .	233
8.2.2.2 Irrigation and Municipal Return Flow . . . . .	236
8.2.2.3 Infiltration from Losing Streams . . . . .	237
8.2.3 Ground Water Discharge. . . . .	239
8.2.3.1 Artificial Withdrawal by Wells and Qanats. . . . .	239
8.2.3.2 Natural Spring Discharge . . . . .	240
8.2.3.3 Actual Evaporation and Transpiration . . . . .	240
8.2.4 Ground Water Budget . . . . .	242
8.3 Ground Water Management . . . . .	244

**CHAPTER 9 GROUND WATER MODELLING**

9.1 Introduction. . . . .	248
9.2 Conceptual Model. . . . .	249
9.3 Numerical Model . . . . .	250
9.3.1 Model Code. . . . .	253
9.3.2 Model Inputs. . . . .	256
9.4 Model Results . . . . .	267
9.4.1 Sensitivity Analysis . . . . .	267

**CHAPTER 10 CONCLUSIONS AND RECOMMENDATIONS**

10.1 Conclusions. . . . .	273
10.2 Recommendations. . . . .	275

<b>REFERENCES.</b> . . . . .	<b>278</b>
------------------------------	------------

<b>APPENDICES</b> . . . . .	<b>284</b>
-----------------------------	------------

## LIST OF FIGURES

1.1 Location map of the study area. . . . .	3
2.1 Physiographic sub-division of the study area. . . . .	12
2.2 Mean annual precipitation for the Tabriz area (1980-87). . . . .	15
2.3 Mean annual precipitation for the Tabriz area (1986-87). . . . .	16
2.4 Monthly variation of precipitation: (a) for Daryan station, (b) for Saidabad station. . . . .	18
2.5 Monthly variation of precipitation: (a) for Sahlan station, (b) for Vanyar station. . . . .	19
2.6 Mean seasonal percentage of precipitation for different stations (1980-87). . . . .	20
2.7 Calculated potential evapotranspiration for the Tabriz Airport station (1982) . . . . .	25
2.8 Calculated potential evapotranspiration for the Tabriz Airport station (1984) . . . . .	26
2.9 Hydrograph showing baseflow and surface runoff components (manual analysis) . . . . .	32
2.10 Hydrograph showing baseflow and surface runoff components (computer analysis). . . . .	33
2.11 Comparison of flow duration curves for the same period. . . . .	40
2.12 Comparison of flow duration curves for different periods. . . . .	41
3.1 Geological map of the study area. . . . .	45
4.1 The aquifer systems in the study area . . . . .	52
4.2 Geological cross sections from the Tabriz Plain (after ELC-Electroconsult, 1969). . . . .	54
4.3 Geological cross sections from the Tabriz Plain (after ELC-Electroconsult, 1969). . . . .	55
4.4 Geological cross section from the Tabriz Power Station Exploratory wells (after IRAB Engineering Co., 1978). . . . .	56

4.5 Isopach map of the alluvial tuff and fans (after Abkav Co., 1978). . . . .	57
4.6 Isopach map of the alluvial tuff and fans. . . . .	58
4.7 Location of the ground water levels monitoring wells. . . . .	61
4.8 Ground water level fluctuations in selected monitoring wells. . . . .	62
4.9 Ground water level fluctuations in selected monitoring wells. . . . .	63
4.10 Ground water level fluctuations in selected monitoring wells. . . . .	64
4.11 Ground water contour and flow map for dry period (Oct. 1987). . . . .	67
4.12 Ground water contour and flow map for wet period (May 1987). . . . .	69
4.13 Annual maximum fluctuation contour map of ground water (1987). . .	70
5.1 Well field location map. . . . .	76
5.2 Saidabad well field and location of pumping wells. . . . .	83
5.3 Cross sections showing Saidabad well construction. . . . .	85
5.4 PW SW1, Straight line method: Time-Drawdown plot. . . . .	86
5.5 OW SPW1, Straight line method: Time-Drawdown plot. . . . .	87
5.6 PW SW1, Straight line method: Calculated Recovery plot. . . . .	88
5.7 OW SPW1, Straight line method: Calculated Recovery plot. . . . .	89
5.8 Geological section through Saidabad exploratory wells. . . . .	91
5.9 PW SW3, Straight line method: Time-Drawdown plot. . . . .	92
5.10 PW SW3, Straight line method: Calculated Recovery plot. . . . .	93
5.11 OW SPW3, Time-Drawdown plots: (a) Straight line method, (b) Type curve method. . . . .	94
5.12 OW SPW3, Straight line method: Calculated Recovery plot. . . . .	95
5.13 PW SW7, Straight line method: Time-Drawdown plot. . . . .	97
5.14 OW SPW7, Straight line method: Time-Drawdown plot. . . . .	98
5.15 PW SW7, Straight line method: Calculated Recovery plot. . . . .	99

5.16 OW SPW7, Straight line method: Calculated Recovery plot. . . . .	100
5.17 Geological and technical cross sections of the Tabriz Plain wells (a) Tabriz Power Station well field, (b) Jamshidabad well 1, and (c) Jamshidabad well 2. . . . .	101
5.18 PW JW1, Straight line method: Time-Drawdown plot. . . . .	103
5.19 PW JW1, Straight line method: Calculated Recovery plot. . . . .	104
5.20 PW JW2, Straight line method: Time-Drawdown plot. . . . .	105
5.21 PW JW2, Straight line method: Calculated Recovery plot. . . . .	106
5.22 Tabriz Power Station well field and location of pumping wells. . . . .	107
5.23 PW TPSW1, Time-Drawdown plots: (a) Straight line method, (b) Type curve method. . . . .	110
5.24 PW TPSW1, Calculated Recovery plots: (a) Straight line method, (b) Type curve method. . . . .	111
5.25 PW TPSW3, Straight line method: Time-Drawdown plot. . . . .	112
5.26 PW TPSW3, Straight line method: Calculated Recovery plot. . . . .	113
5.27 PW TAW, Straight line method: Time-Drawdown plot. . . . .	114
5.28 PW TAW, Straight line method: Calculated Recovery plot. . . . .	115
5.29 PW SOW, Straight line method: Time-Drawdown plot. . . . .	117
5.30 PW SOW, Straight line method: Calculated Recovery plot. . . . .	118
5.31 OW SPW3, Model analysis: (a) Without recovery, (b) With recovery. . . . .	119
5.32 PW SW3, Model analysis: (a) Without recovery, (b) With recovery. . . . .	120
5.33 PW SW1, Model analysis: (a) Without recovery, (b) With recovery. . . . .	124
5.34 OW SPW1, Model analysis: (a) Without recovery, (b) With recovery. . . . .	125
5.35 PW SW7, Model analysis: (a) Without recovery, (b) With recovery. . . . .	126
5.36 OW SPW7, Model analysis: (a) Without recovery, (b) With recovery. . . . .	127
5.37 PW JW1, Model analysis: (a) Without recovery, (b) With recovery. . . . .	128

5.38 PW JW2, Model analysis: (a) Without recovery, (b) With recovery. .	129
5.39 PW TPSW1, Model analysis: (a) Without recovery, (b) With recovery.	130
5.40 PW TPSW3, Model analysis: (a) Without recovery, (b) With recovery.	131
5.41 PW TAW, Model analysis: (a) Without recovery, (b) With recovery. .	133
5.42 PW SOW, Model analysis: (a) Without recovery, (b) With recovery. .	134
6.1 PW SW1, Step-Drawdown test: Bruin & Hudson method, (a) data handling, (b) data plot. . . . .	153
6.2 PW SW1, Step-Drawdown test: Eden & Hazel method, (a) data handling (b) data plot. . . . .	154
6.3 PW SW1, Step-Drawdown test: Rorabaugh method. . . . .	155
6.4 Step-Drawdown test: Theoretical drawdown-yield curve, (a) PW SW1, (b) PW SW8. . . . .	156
6.5 PW JW2, Step-Drawdown test: Bruin & Hudson method, (a) data handling, (b) data plot. . . . .	158
6.6 PW JW2, Step-Drawdown test: Eden & Hazel method, (a) data handling, (b) data plot. . . . .	159
6.7 PW JW2, Step-Drawdown test: Rorabaugh method, (a) data handling, (b) data plot. . . . .	160
6.8 Step-Drawdown test: Theoretical drawdown-yield curve, (a) PW JW1, (b) PW JW2. . . . .	161
6.9 PW TPSW6, Step-Drawdown test: Bruin & Hudson method, (a) data handling, (b) data plot. . . . .	163
6.10 PW TPSW6, Step-Drawdown test: Eden & Hazel method, (a) data handling, (b) data plot. . . . .	164
6.11 PW TPSW6, Step-Drawdown test: Rorabaugh method. . . . .	165
6.12 Step-Drawdown test: Theoretical drawdown-yield curve, (a) PW TPSW4, (b) PW TPSW6. . . . .	166
6.13 PW TAW, Step-Drawdown test: Bruin & Hudson method, (a) data handling, (b) data plot. . . . .	168



6.14 PW TAW, Step-Drawdown test: Eden & Hazel method, (a) data handling, (b) data plot. . . . .	169
6.15 PW TAW, Step-Drawdown test: Rorabaugh method. . . . .	170
6.16 Step-Drawdown test: Theoretical drawdown-yield curve, (a) PW TAW, (b) PW SOW. . . . .	171
6.17 PW SOW, Step-Drawdown test: Bruin & Hudson method, (a) data handling, (b) data plot. . . . .	173
6.18 PW SOW, Step-Drawdown test: Eden & Hazel method, (a) data handling, (b) data plot. . . . .	174
6.19 PW SOW, Step-Drawdown test: Rorabaugh method. . . . .	175
6.20 Technical cross sections of the Park, Tabriz wells. . . . .	177
6.21 PW PTW1, Step-Drawdown test: Bruin & Hudson method, (a) data handling, (b) data plot. . . . .	178
6.22 PW PTW1, Step-Drawdown test: Eden & Hazel method, (a) data handling, (b) data plot. . . . .	179
6.23 PW PTW1, Step-Drawdown test: Rorabaugh method. . . . .	180
6.24 PW PTW2, Step-Drawdown test: Bruin & Hudson method, (a) data handling, (b) data plot. . . . .	181
6.25 PW PTW2, Step-Drawdown test: Eden & Hazel method, (a) data handling, (b) data plot. . . . .	182
6.26 PW SW1, Model analysis: (a) without well loss, (b) with well loss. .	184
7.1 Map showing location of hydrochemical samples. . . . .	191
7.2 Relationship between (a) ground water levels (1987) and (b) TDS (1987) in the Tabriz area. . . . .	199
7.3 Pattern diagrams for the major ions of ground water of the Tabriz area.	200
7.4 Water analysis diagram showing hydrochemical facies, in percent of total equivalent per million (after Back, 1966). . . . .	202
7.5 Alluvial Tuff aquifer; ground water chemical analysis by Piper diagrams . . . . .	203

7.6 The Tabriz Plain aquifers; ground water chemical analysis by Piper diagrams. . . . .	204
7.7 Expanded Durov diagrams, demonstrating major ions in ground water of alluvial tuff aquifer (Oct. 1987). . . . .	207
7.8 Expanded Durov diagrams, demonstrating major ions in ground water of the northern part of the Plain (Oct. 1987). . . . .	208
7.9 Expanded Durov diagrams, demonstrating major ions in ground water of the southern and central parts of the Plain (Oct. 1987). . . . .	209
7.10 The relation between TDS and EC in ground water of the Tabriz Plain area. . . . .	213
7.11 The monthly variations of TDS (a) in water of the River Gomanab Chay and (b) in the River Aji Chay (1986-87). . . . .	215
7.12 The variations of TDS of River Aji Chay by discharge rate (1986-87). . . . .	216
7.13 Hydrochemical sections along the ground water principal flow directions (a) along the A-A, and (b) along the B-B. . . . .	222
7.14 Hydrochemical sections along the ground water principal flow directions (a) along the C-C, and (b) along the D-D. . . . .	223
7.15 Hydrochemical sections along the ground water principal flow directions (a) along the E-E, and (b) along the F-F. . . . .	224
7.16 Classification of ground waters of the Tabriz area for irrigation purposes. . . . .	229
8.1 The hydrological components of the adjacent areas and the behaviour of the ground water in these areas. . . . .	243
9.1 Map showing the aquifer types, model boundaries, and pumping centres. . . . .	251
9.2 Flow chart of program structure. . . . .	255
9.3 Pre-processor chart for Modflow. . . . .	257
9.4 (a) Ground water levels for wet season (1987) and (b) initial head in model from measured data and topographical extrapolation. . . . .	259
9.5 Map showing the resultant final heads (a) for no-flow boundary conditions and (b) for constant head boundary conditions. . . . .	269

## LIST OF TABLES

	Page
2.1 Pan evaporation data from different meteorological stations . . . . .	27
2.2 Calculated soil moisture deficit and actual evaporation for the Liguvan sub-catchment . . . . .	29
2.3 Calculated soil moisture deficit and actual evaporation for the Tazekand sub-catchment . . . . .	30
2.4 River discharge analysis results . . . . .	35
3.1 Stratigraphic sequence in the project area . . . . .	49
4.1 Annual volumetric change of water levels in the Tabriz Plain . . . . .	73
5.1 Total and completed depths and screen lengths of Saidabad wells . . . . .	84
5.2 Time-drawdown and recovery data analytical analysis results from the Saidabad well-field . . . . .	138
5.3 Time-drawdown and recovery data analytical analysis results from the Tabriz Plain well-fields . . . . .	139
5.4 Time-drawdown data numerical analysis results from the Saidabad well-field. . . . .	140
5.5 Time-recovery data numerical analysis results from the Tabriz Plain well-fields. . . . .	141
6.1 Resultant well loss factors calculated by Jacob arithmetic method. . . . .	185
6.2 Calculated values of transmissivity and well characteristics (a) Bruin & Hudson, and Eden and Hazel methods, and (b) Rorabaugh method. . . . .	186
6.3 Comparison of well loss values deduced from numerical method and the other methods. . . . .	187
7.1 Tabular graph of alluvial tuff aquifer ground water type frequency. . . . .	195
7.2 Tabular graph of the northern part of the Tabriz Plain ground water type frequency. . . . .	196
7.3 Tabular graph of the south and central parts of the Tabriz Plain ground water type frequency. . . . .	197

7.4 Classification of the ground water of the study area with respect to the dissolved solids concentration. . . . .	211
7.5 concentrations of nitrate, BOD, and COD in some parts of the study area. . . . .	214
7.6 TDS changes in the ground water of the Tabriz City over three year period. . . . .	217
7.7 Hardness classification of the study area. . . . .	221
7.8 Comparison of the alluvial tuff ground water with EEC guide levels . . .	226
7.9 Standard water for different livestock (after McKee & Wolf, 1963). . . . .	227
7.10 Relative tolerances of crops to salt concentrations (after Richards, in Todd, 1980). . . . .	230
8.1 Artificial withdrawal of ground water from the study area. . . . .	239
8.2 Percentage and volumetric evaporation amounts from the different parts of the area. . . . .	241
8.3 Ground water budget for the study area. . . . .	244
9.1 The model boundary conditions of the modeled area. . . . .	252
9.2 List of the various packages used in Modflow. . . . .	254
9.3 Initial head data distribution. . . . .	260
9.4 Aquifer thicknesses distribution. . . . .	261
9.5 (a) River input data and (b) pumping centre locations and abstraction rates. . . . .	262
9.6 The estimated areal recharges for no-flow boundary conditions. . . . .	263
9.7 The estimated areal recharges for constant-head boundary conditions . .	264
9.8 Final transmissivity distribution for no-flow boundary conditions . . . . .	265
9.9 Final transmissivity distribution for constant-head boundary conditions. . . . .	266
9.10 Final head under no-flow boundary conditions at end of time step 1 in stress period 1. . . . .	270

9.11 Final head under constant-head boundary conditions at end of time step 1 in stress period 1. . . . .	271
9.12 Volumetric budget for entire model (a) under no-flow boundary conditions (b) under constant-head boundary conditions. . . . .	272

## LIST OF APPENDICES

	Page
Appendix 1 Constant Test and Calculated Recovery Data. . . . .	284
Appendix 2 Step-Drawdown Test Data. . . . .	294
Appendix 3 Basic Program Used in Numerical Analysis for Pumping Test Data. . . . .	301
Appendix 4 Ground Water Level Fluctuations from some Selected Monitoring Wells. . . . .	308
Appendix 5 Plots of Constant Rate Test Analyses. . . . .	316
Appendix 6 Plots of Step-Drawdown Test analysis. . . . .	335
Appendix 7 Results of Chemical Analyses for Ground- Water in the Area (Oct. 1987) . . . . .	358

## **CHAPTER 1**

### **INTRODUCTION**

**1.1 Purpose and Scope**

**1.2 Size and Location of the Study Area**

**1.3 Soil Types and Characteristics**

**1.4 Vegetation and Land Use**

**1.5 Previous Work**

**1.6 Types and Sources of Data**

# CHAPTER 1

## INTRODUCTION

### 1.1 Purpose and Scope

The Tabriz area is a densely populated area of Iran, with 100 percent of its drinking, domestic and industrial water and 80 percent of agricultural water supplied from ground water resources. The rapid increase in the population, with added immigration of people from villages and small towns to Tabriz City, which has occurred during the past 15 years has led to large scale ground water developments around this city. As a result, large amounts of water are locally withdrawn from underground storage. The rate and amount of abstraction creates problems with drawdown distribution.

Another problem is the occurrence of saline surface and ground waters in the Tabriz Plain which poses a serious threat to the quality of some existing ground water resources. Hence, the occurrence of such problems have encouraged the author to attempt a detailed hydrogeological study using the latest available conventional and numerical techniques for understanding ground water behaviour in the area.

The purpose of this study is to consider the present ground water resource potential, its hydrochemical conditions and its relation with surface water, as well as to describe the acceptable principles of assessment, protection and management of this vital resource.

The entire work is based on the collection of pre-existing hydrological and hydrogeological data together with a field visit for supplementary measurement of ground water levels, river discharge gauging, and ground water sampling for hydrochemical analysis.

### 1.2 Size and Location of the Study area

The present study area is located in East Azarbijan in the north-west part of Iran (see Fig. 1.1) and mainly includes the Tabriz Plain and part of the surrounding mountain area. Its total area amounts to about 7500 km<sup>2</sup>, of which 3000 km<sup>2</sup> is located in the Tabriz Plain and 4500 km<sup>2</sup> (above 1500m amsl) in the mountain area. It lies between latitudes 37°43' and 38°18' N, and longitudes 45°26' and 46°37' E.



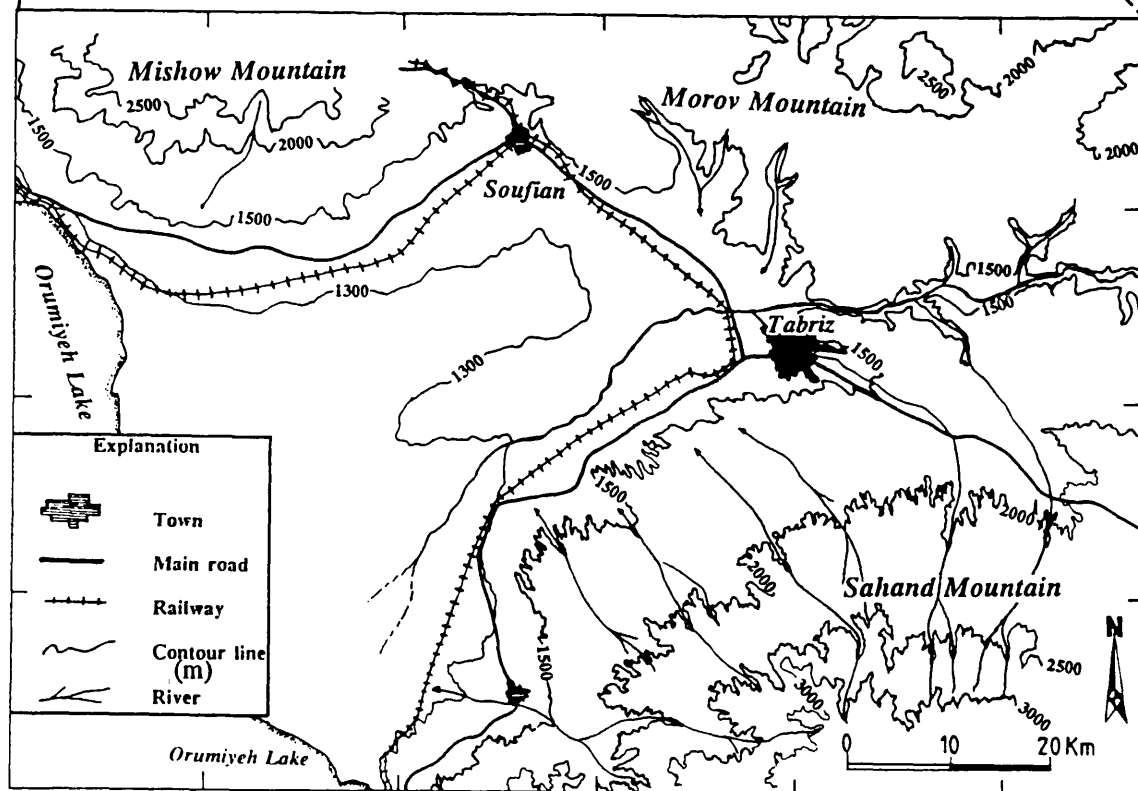
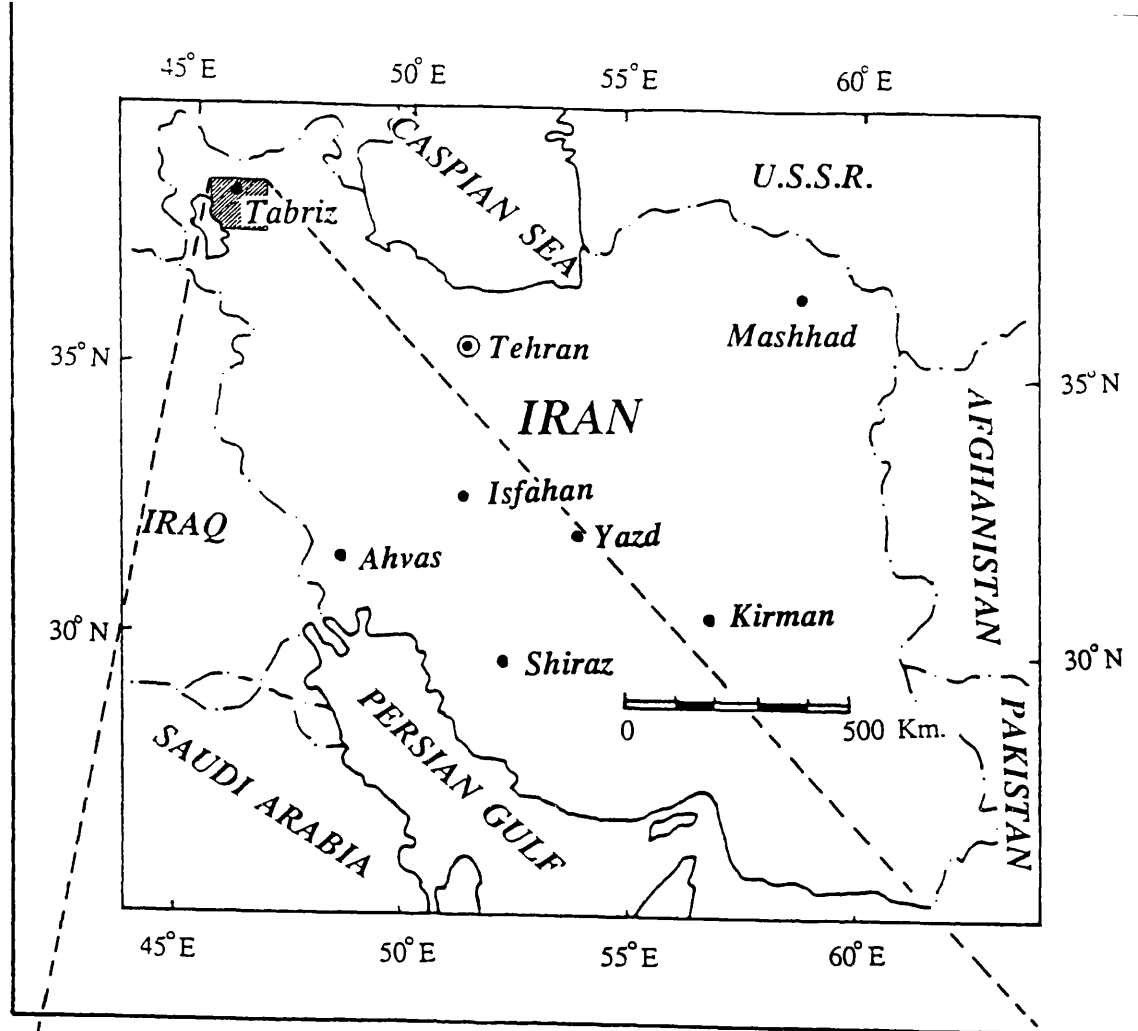


Fig. 1.1 Location map of the study area.

The area is bordered to the west by Orumiyeh Lake, to the north and north-east by the Mishow and Morov mountains, and to the south and south-east by the Sahand mountain (see Fig 1.1).

### **1.3 Soil Types and Characteristics**

The soils and their characteristics form an important contribution to the hydrological cycle with significant effects of both positive and negative nature on the important contributions to ground water replenishment.

A detailed soils map of Iran at a scale of 1:2,500,000 was prepared jointly by the Iranian Ministry of Agriculture and the FAO in 1964. Nineteen soil associations were identified and used as the basis of mapping. For convenience, these mapping units were classified under four physiographic units, e.g., soils of the Caspian piedmont, soils of the plateau, soils of plains and valleys, and soils of the dissected slopes and mountains. Based on the indications of the previously-mentioned map, the soils of the study area were included in the latter three physiographic units.

#### **1.3.1 Soils of the Plain and Valleys**

The soils of the plain and valleys in the study area are formed of material which has been deposited by water and wind. These type of soils can be divided into (a) fine-textured alluvial soils and (b) coarse-textured alluvial and colluvial soils. In the central and western part of the Plain, where drainage is poor, fine-textured alluvial soils including salt-marsh and saline alluvial soils have been deposited. Also, in the central part of the Plain in a few places, sand dunes have been built up by the action of the wind. The sand dunes are classed as part of the coarse-textured alluvial soils.

Coarse-textured alluvial and colluvial soils are also associated with alluvial fans along the foothill regions in the northern and southern parts of the Plain. These types of soils are still in the process of being formed by material carried by flood-water from the mountain area through relatively narrow valleys.

#### **1.3.2 Soils of the Plateaux**

The soils of the plateaux have been formed under modified continental

climatic conditions with marked aridity, at heights of around 1000m or more amsl (Beaumont et al., 1976). Some parts of the project area are covered with this type of soil in the northern and southern lower mountain areas.

The dominant units of these soils are brown and grey coloured soils and lithosols. They form brown to light-brown and calcareous soils horizons in the northern, and grey and light colour in the southern part of the Plain. The lithosols and grey and brown soils have very weakly developed greyish-brown, granular surface A1 horizons, with an organic matter content of about 1 percent.

### **1.3.3 Soils of Dissected Slopes and Mountain**

The soils of the dissected slopes and mountains are stony, shallow over bedrock, without definite profile development, and contain a high proportion of unweathered rock fragments. The dominant units of these soils occupying the higher mountains of the northern and southern parts of the area are more or less the same as above-mentioned plateau type of soils (brown and grey soils and lithosols) but are very shallow over bedrock. These soils indicate areas generally unsuited for crop growth.

### **1.4 Vegetation and Land Use**

Agriculture is the main activity of the people living in the small towns and villages. Most of these activities are concentrated in the Tabriz Plain where the best lands are found; about 30 percent of the Plain area is presently under cultivation. Generally, in the mountainous area only very small parts, in narrow river valleys near the villages, are able to be cultivated.

Irrigation is practised wherever it is possible, since the rainfall is insufficient to obtain rewarding crops. Water for irrigation is obtained through river diversion, qanats and shallow and deep wells. Typical crops grown in the area are cereals (mainly wheat and barley), forage, fruit trees, onions, tomatoes, and vegetables.

### **1.5 Previous Studies**

A fair amount of hydrogeological, geophysical and ground water development studies have been done in the Tabriz area during the past thirty years. As early as

1956, Sir Alexander Gibb and Partners investigated the water supply problems of the city of Tabriz. The study was a broad scheme of development designed to serve as a framework for individual developments, and planned to supply 50 million m<sup>3</sup>/year of water to the 490,000 people expected by 1993 (in fact the population of Tabriz already is more than 1.5 million).

In 1958, a French company (OFER-ETCO) studied the development prospects of the Aji Chay river, with emphasis on the feasibility of irrigation and power generation. The project considered the hydrology, water quality, and soil and irrigation problems of the area. Unfortunately the results and reports of all above-mentioned studies are not available.

Two geophysical surveys have been done in the southern part of the study area on the alluvial tuff formation. Firstly, a geo-electrical survey was carried out in 1964 by the Geophysical Institute of Israel. This study investigated the thickness and quality of the water bearing layer over 1500 km<sup>2</sup> in this area. The second was a geo-electrical and seismic refraction survey run in 1976 by an Iranian company called Abkav Consulting Engineers. One aim of this study also was to assess the thickness and characteristics of the alluvial tuff formation, as well as the type of bedrock in an area larger than the first study.

A French company called CITRA-SOGREAH-CGG-HYDRA studied the ground water resources of the Tabriz Plain in 1965. This feasibility study considered local ground water potential and conditions for developing this water for irrigation and domestic supply. Another work with the same objective was carried out in the Tabriz Plain by ELC-Electroconsult of Milano, Italy, in 1969. This work also considered the ground water potential and development conditions for different sub-basins in the Plain.

Some other local ground water development and water supply studies have been carried out in the study area. The first was done by the AGRO-Water Consulting Engineers (1977) on the assessment and development of ground water resources in the Saidabad area and its vicinity for water supply purposes to the city of Tabriz. The second was run by IRAB-Engineering Company for water supply to the Tabriz Power Station and Tabriz Airport in 1977, and Tabriz Park in 1978.

Finally, some published and unpublished studies have been undertaken by the

Azərbaycan Regional Water Authority (ARWA) during the past twenty years. Data from most of the above-mentioned reports were extracted to make this present detailed and systematic hydrogeological research work more meaningful.

### **1.6 Types and Sources of Data**

The basic data used in this study can be divided into the following categories; hydrogeological and geological reports, pumping test data, ground water level monitoring data, hydrochemical data, and hydrological data (river discharges and climatic data).

There are 1328 deep and 882 shallow wells, 982 qanats and 147 springs in the study area. The historical hydrochemical data are recorded from some of these wells and qanats by the ARWA and the basic location map was provided by this organization. The ground water level monitoring well data were recorded at 120 other non-pumping wells by the ARWA, their locations being shown in Figure 4.7.

Most of above-mentioned data were obtained from the records of ARWA and/or from the Ministry of Water and Power in Tehran. Some of geological reports and maps were collected from the Tabriz branch of the Geological Survey of Iran. Additional data were also collected from the following organizations: the Tabriz Agricultural Development Office, the related Departments of the University of Tabriz, the Climatological Office of Tabriz Airport, Tabriz Governor's Engineering Office, Tabriz Central Plan and Budget Authority, and the Tabriz City Parks Development Office.

## **CHAPTER 2**

### **HYDROLOGY**

#### **2.1 Introduction**

#### **2.2 Main Geomorphological Units**

##### **2.2.1 Tabriz Plain**

##### **2.2.2 Northern Mountains**

##### **2.2.3 The Sahand Mountain**

#### **2.3 Drainage Basins**

#### **2.4 Climate**

##### **2.4.1 Introduction**

##### **2.4.2 Precipitation**

##### **2.4.3 Temperature, Wind and Relative Humidity**

##### **2.4.4 Evaporation and Transpiration**

#### **2.5 River Discharge**

##### **2.5.1 Introduction**

##### **2.5.2 Sources and Components of River Discharge**

##### **2.5.3 Hydrograph Analysis**

##### **2.5.4 Factors Affecting Baseflow**

##### **2.5.5 Flow Duration Curve Analysis**

## CHAPTER 2

### HYDROLOGY

#### 2.1 Introduction

This chapter brings together four aspects; two physically related and two climatically related. From the geomorphologic point of view, the Tabriz area will be considered through two main geomorphic aspects such as morphological units and drainage patterns in the basin, which can give some understanding of the landforms and water courses in the region.

From a climatic point of view, the essential features of meteorological significance are physically related, while the river discharge is both a direct and indirect consequence of topography, catchment and climate.

#### 2.2 Main Geomorphologic Units

The study area is bordered to the north-west and north by the Mishow (<3000m amsl) and Morov (<2000m amsl) mountain ranges, respectively. The Mishow mountain range is mainly composed of metamorphic rocks on the high ground (above 1800m), while alluvial fans cover the lower slope and flat areas (below 1800m), which are known as the Mishow fans or northern part of the Tabriz Plain.

The Morov mountain range mainly includes Cretaceous and Miocene sediments with small alluvial fans, which lie between Soufian and Tabriz City and possibly, from a morphologic point of view, can be considered part of the Tabriz Central Plain.

To the south and south-east, the boundary is formed by the Plio-Pleistocene volcanic Sahand mountain (<3700m), which is mainly formed from andesitic lavas at high elevations and from pyroclastic material reworked by water at lower elevations (below 2100m), known as the Alluvial Tuff Formation. Towards the north, the slope of the Alluvial Tuff surface decreases and becomes flat where it meets the Tabriz Plain.

The western margin is bordered by the Orumiyeh Lake (1274m amsl) with its adjacent salt marshes and swamps.

Thus, the three major geomorphic units can be considered as (1) Tabriz Plain which includes (a) the northern and southern terraces and alluvial fans and (b) the salty, marshy central part, (2) the northern (Mishow-Dagh, Morov-Dagh), and (3) southern (Kuhe-Sahand) mountainous areas.

### **2.2.1 Tabriz Plain**

The Tabriz Plain, which lies between the 1274m (the elevation of Orumiyeh Lake above mean sea level) and 1500m contour lines, is a complex constructed plain that includes a largely unoccupied salty, marshy central plain and a settled horseshoe-shaped belt of terraces and alluvial fans.

The Central Plain below 1300m amsl is formed from semi-pervious loam and clay with a very gentle slope toward Orumiyeh Lake, showing slopes in the range of 0.1 %. The terraces lie mainly between 1300m and 1400m elevation along the River Aji-Chay. At the surface, they include several units composed of fine sandy loam and coarser material, up to 30m above the river level. The slope of this material is also shallow and mainly toward the river.

Alluvial fans are generally located between 1300m and 1500m elevation. In the northern part of the Plain, they form an uninterrupted strip over 600 km<sup>2</sup> in area and made up of coalescing fans extending from Tassoij to Soufian. In the southern part, the fans cover a smaller area (200 km<sup>2</sup>) comprising a chain of independent fans such as Khosrowshahr and Sardrud fans and the isolated Azarshahr fan. They include highly pervious, coarse material at the top, with the percentage of finer material increasing gradually toward the central Plain. The slope is highly variable and changes from 5 % at the apex of the fans to 2 % toward the toe.

### **2.2.2 Northern Mountains**

The northern mountains form a continuous three unit range; the Mishow-Dagh (Mishow mountain, <3155m), the Morov-Dagh (<2187m) and the southern Qara-Dagh foothills (<2842m). The Mishow-Dagh is a steep-walled, rugged body of limestones, schists and igneous rocks flanked by soft rock foothills, where severe erosion phenomena have cut narrow valleys into the above-mentioned fans.

The Morov-Dagh and southern Qara-Dagh mountain foothills made up of



limestones, schists, marls and sandstones, dominate the Plain from Soufian to the east of Tabriz. Aggradation erosion in this part is less important than in the Mishow-Dagh, but degradation has produced significant features such as the Vanyar gorges.

### **2.2.3 The Sahand Mountain**

The Sahand volcanic mountain is located to the south and south-east of the Tabriz Plain. It is a huge cone made up of andesitic lava flows above 2400m elevation which are surrounded by an enormous body of pervious tuff, deeply eroded by streams.

The Alluvial Tuff Formations of the Sahand have relatively high elevation (roughly from 1500m to 2400m elevation) with very variable slope, which in general decreases towards the Plain. At elevations between 1500m and 2000m the general slope ranges from 4 to 6 percent. The Alluvial Tuff formation is mainly comprised of red and green andesitic tuff mixed with quantities of blocks, boulders, gravel and sand of volcanic and alluvial origin. The size of these materials reduces towards the Plain.

## **2.3 Drainage Basins**

The stream network of the Tabriz area may be grouped into three major systems: (1) the general Plain with the River Aji Chay, (2) the northern sub-basins on the right bank of the Aji Chay and (3) the southern sub-basins on the left bank (see Fig. 2.1). The natural destination of the surface water system is the Orumiyeh Lake, but only a small amount of the total volume of water involved actually reaches the Lake. The greater part is absorbed by evaporation and evapotranspiration mainly in natural pasture, swamps and cultivated areas.

**River Aji Chay:** the Aji Chay river enters the Plain at its eastern boundary, through the Vanyar gorge and after some 100km its channel reaches the Orumiyeh Lake. In this part of its course, two hydrometric stations operate to measure the flows of the river placed at Vanyar and at Akhole some 40km downstream of Vanyar.

**The northern sub-basins:** the northern stream system includes seven river sub-basins (see Fig. 2.1), namely, starting from the Orumiyeh Lake, Daryan, Shabestar, Sis, Soufian, Sinekh, Gomanab and Bababaghi. The latter two rivers join the Aji

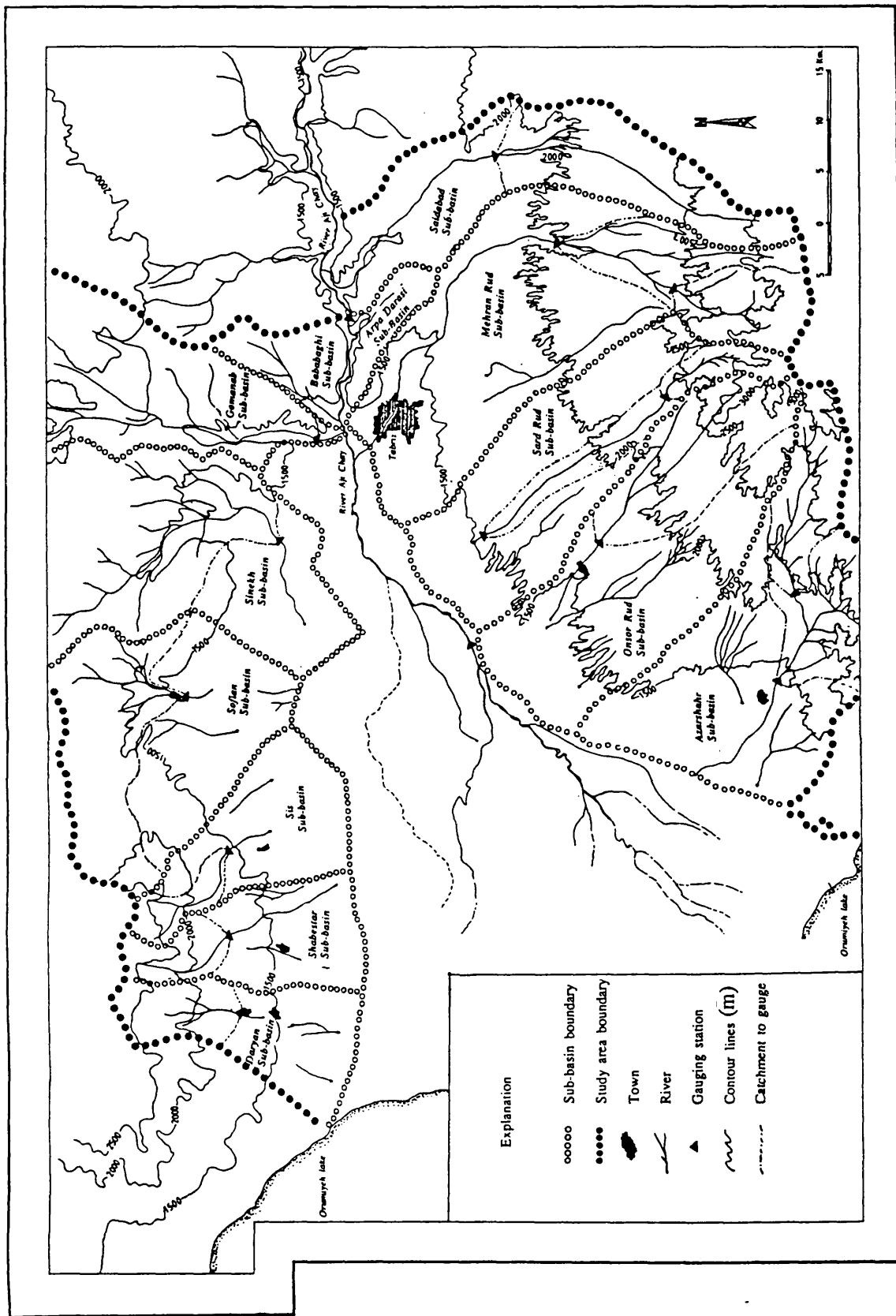


Fig. 2.1 Physiographic sub-division of the study area.

Chay at its right bank, whereas the others become lost in the lower part of their basins and only reach the Central Plain when major floods occur in the rainy season. Hydrometric stations providing flow measurements are located on the main streams of the northern system as follows: on the Gomanab Chay at Anakhaton station, on the Sinekh Chay at Pole-Sinekh and on the Daryan Chay at Daryan(see Fig.2.1).

**The southern sub-basins:** the southern stream system comprises five main river basins on the left bank of the River Aji Chay, namely from west to east they are: Azarshahr Chay, Onsorrud, Sardrud, Mehranrud, and Saidabad Chay. The latter two rivers usually join the Aji Chay river most wet seasons, but the others become dry in their lower parts due to percolation and evaporation losses, as well as diversion of the water for irrigation. There are some gauging stations which operate on the following main streams and tributaries, namely the Ghermezi-Gol station on the River Gombar Chay (itself a tributary of Azarshahr river), Azarshahr station on the Azarshahr Chay, Zinjanab and Sardrud stations both on the Sardrud Chay , Liquvan and Hervi stations on Liquvan Chay, and Saidabad station on the Saidabad Chay.

## **2.4 Climate**

### **2.4.1 Introduction**

The prevailing climate of the Tabriz area has semi-arid characteristics. During the wet season, the area is under the influence of middle-latitude westerlies, and most of the rain that occurs over the region during this period is caused by depressions moving over the area, after forming in the Mediterranean Sea on a branch of the polar jet stream in the upper troposphere (Ganji 1968).

These atmospheric depressions are basically of two different types: 1) the first type is connected with shallow waves moving rapidly in the upper troposphere on a westerly air stream, bringing the main precipitation to the area; 2) the second type of depression is related to the development of cold troughs in the upper atmosphere which tend to create stationary or slow moving depressions in the lower troposphere. These lows, which absorb much moisture from the Persian Gulf and humid lowlands of Iraq, give rise to heavy precipitation over the mountainous area.

According to Ganji (1968), the heating effect from the ground in spring

creates convectional precipitation, especially over the mountains. This is considered to be the main reason why the mountainous areas receive their maximum precipitation during the spring.

The seasons in the study area are considered according to the Iranian calendar: i.e. the year begins on the first day of spring (20 March), and each season covers three calendar months. The 'water year' has been fixed from the 20th September to 19th September of the following year and is used in all hydrological discussions.

In general, the main precipitation of the area occurs during the three seasons of autumn, winter and spring, during which from the third month of the autumn to end of the winter it falls as snow rather than the rain. Usually, in mountainous areas this period may be longer than the above-mentioned four months.

There are fourteen meteorological stations in the study area; in seven of which the main climatological parameters such as precipitation, evaporation, and wind speed, are recorded. However, in the other seven only precipitation data are recorded.

## **2.4.2 Precipitation**

The nature of precipitation in the Tabriz area includes rain, snow and sometimes hail. In general, snow falls in the winter, though in high elevation mountainous areas it comprises five months of the year, from November/December to March/April. Only the two most important aspects of the precipitation such as its variation in space and in time are considered in this study.

### **2.4.2.1 Spatial variations**

The data used to illustrate the spatial variations of precipitation are the mean annual precipitation values for an eight-year period (1980-87) from the ten stations shown on Figure 2.2. The mean values were computed for those stations in the area which had no break in record during that period. In addition, mean values for a two-year period (1986-87), which includes data from four additional stations, are considered and the variation is shown in Figure 2.3. The resultant mean annual isohyetal maps demonstrate that the amounts of rainfall generally increase from the lowland toward the higher altitude mountainous areas.

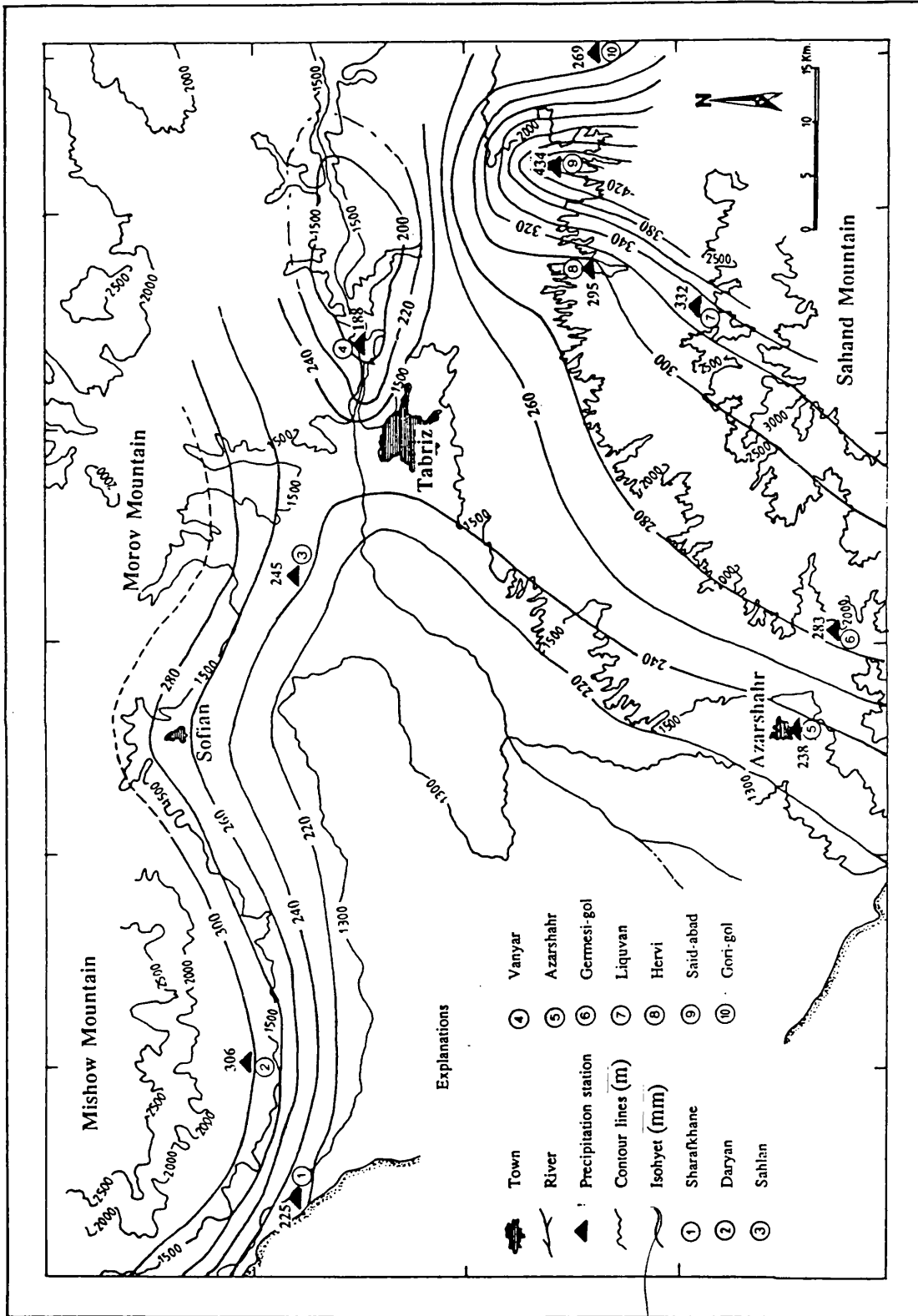


Fig. 2.2 Mean annual precipitation for the Tabriz area (1980-87).

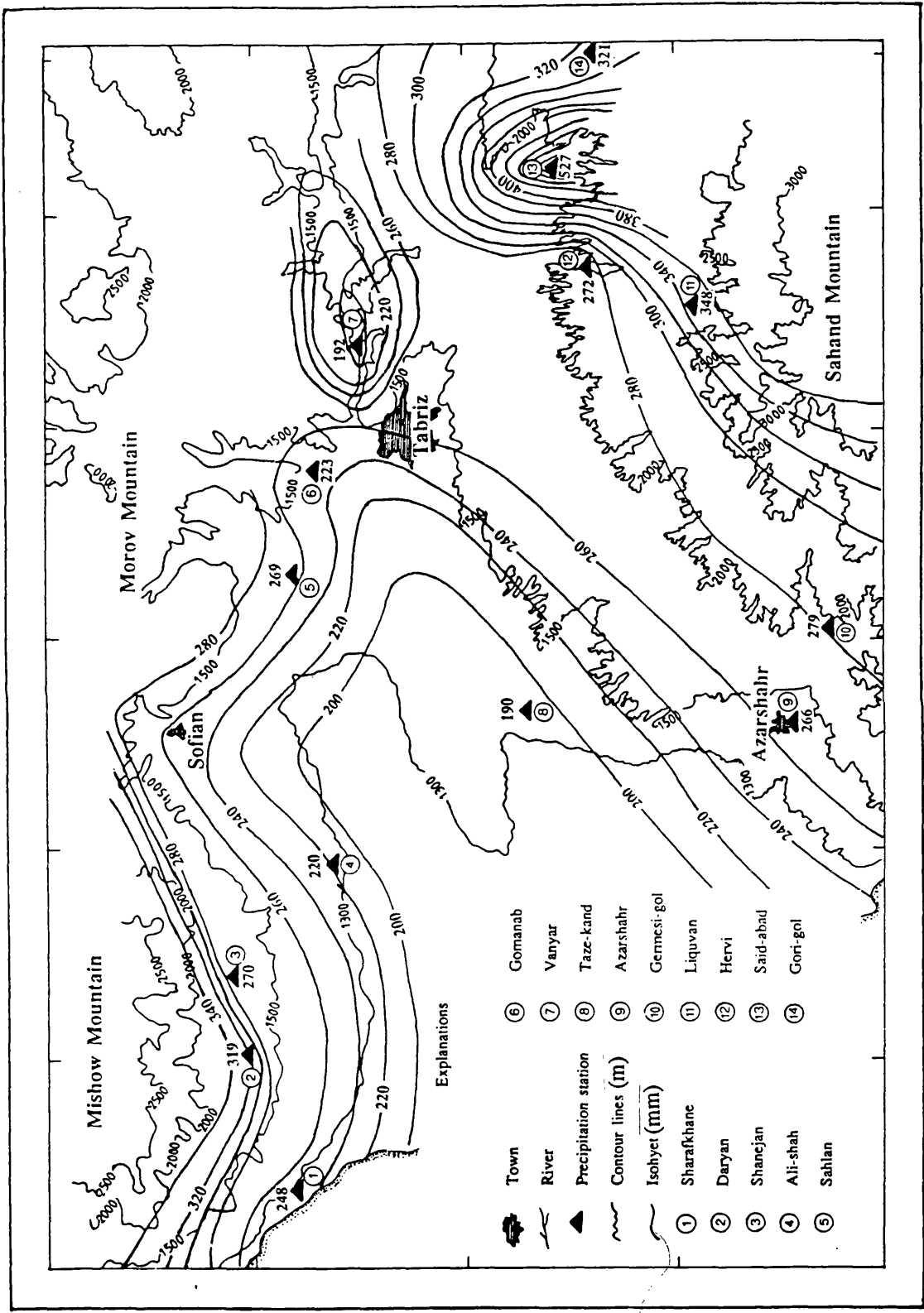


Fig. 2.3 Mean annual precipitation for the Tabriz area (1986-87).

However, the amount of the mean annual precipitation for both the above-mentioned periods show an abnormality for the Vanyar (4) as well as the Saidabad (9) stations, with respect to their elevation. The mean annual precipitation at Vanyar station shows an extremely low value (the lowest in the area), whereas its ground elevation is greater than many other stations. Also the Saidabad station shows the highest mean annual precipitation value for the area, despite its elevation being less than those of the Hervi, Liquvan and Gorigol stations.

The low mean annual precipitation value in Vanyar station is believed to be due to extreme exposure of the station as well as low slope of the land. According to Spreen (1947), considerations other than the elevation of a station include three topographical factors such as (a) maximum slope of the land surface, (b) exposure of the station to the inflow of air masses and (c) orientation of this exposure all of which are important factors when considering the uneven regional distributions of precipitation. However, mechanical failures within the instrument as well as observer and siting errors are virtually unavoidable. It is strongly believed that the above mentioned topographical factors especially the exposure and possibly some human error were influential at Saidabad station.

The effect of the Orumiyeh lake on the distribution of precipitation throughout the area is not very obvious.

#### **2.4.2.2 Variations with Time**

Long term (ten years), seasonal and monthly variations of precipitation for the study area are considered in this sub-section. In Figures 2.4 and 2.5, histograms of the monthly and yearly variations of precipitation for four selected stations are demonstrated. As the figures show, in general the maximum precipitation in the area occurs during the months of May and November with the lowest usually during the summer season, especially from mid-July to mid-October.

There is no obvious trend to the long-term variations of precipitation in the area, though it is possible that the chosen period is not enough long to allow such trends to be identified.

Figure 2.6 demonstrates the percentage mean of seasonal precipitation variation for eight stations during an eight year period (1980-87). As the figure

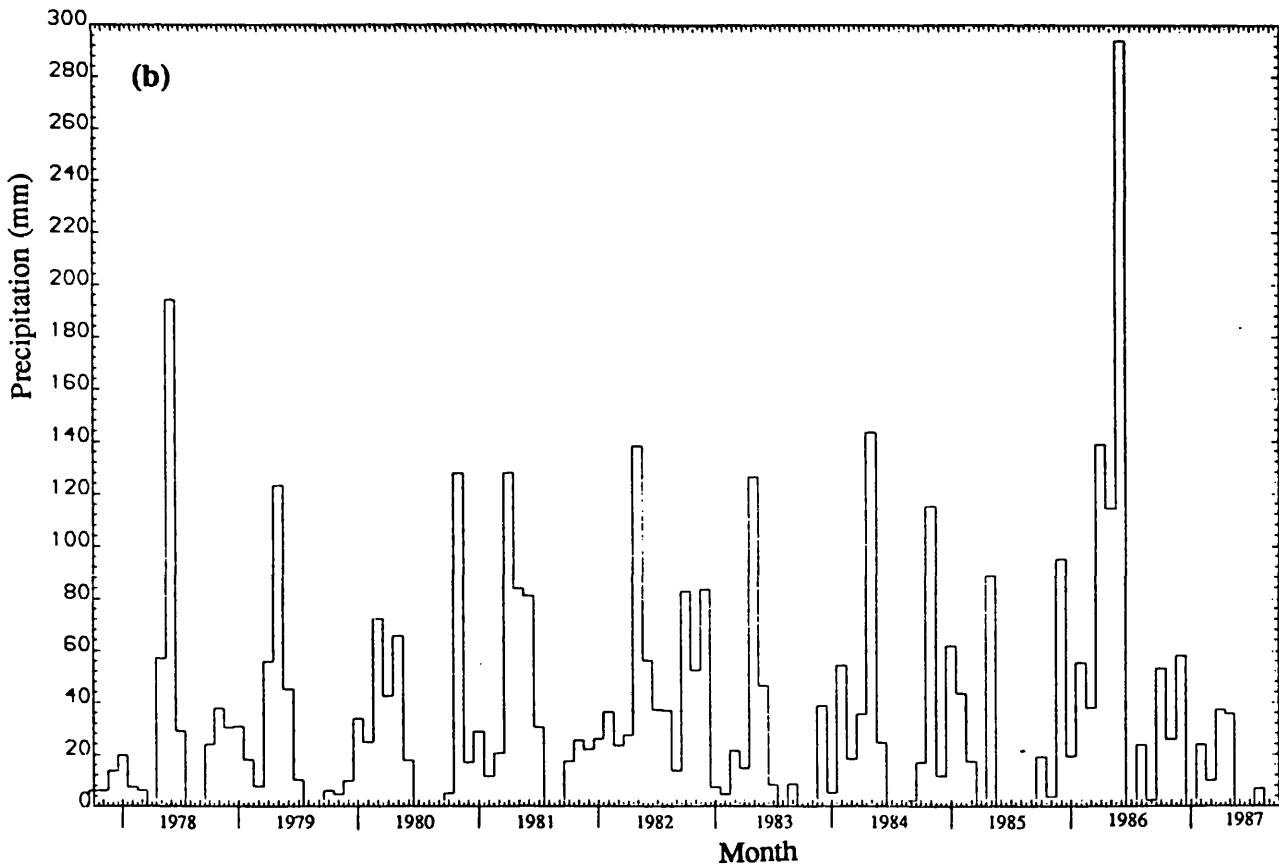
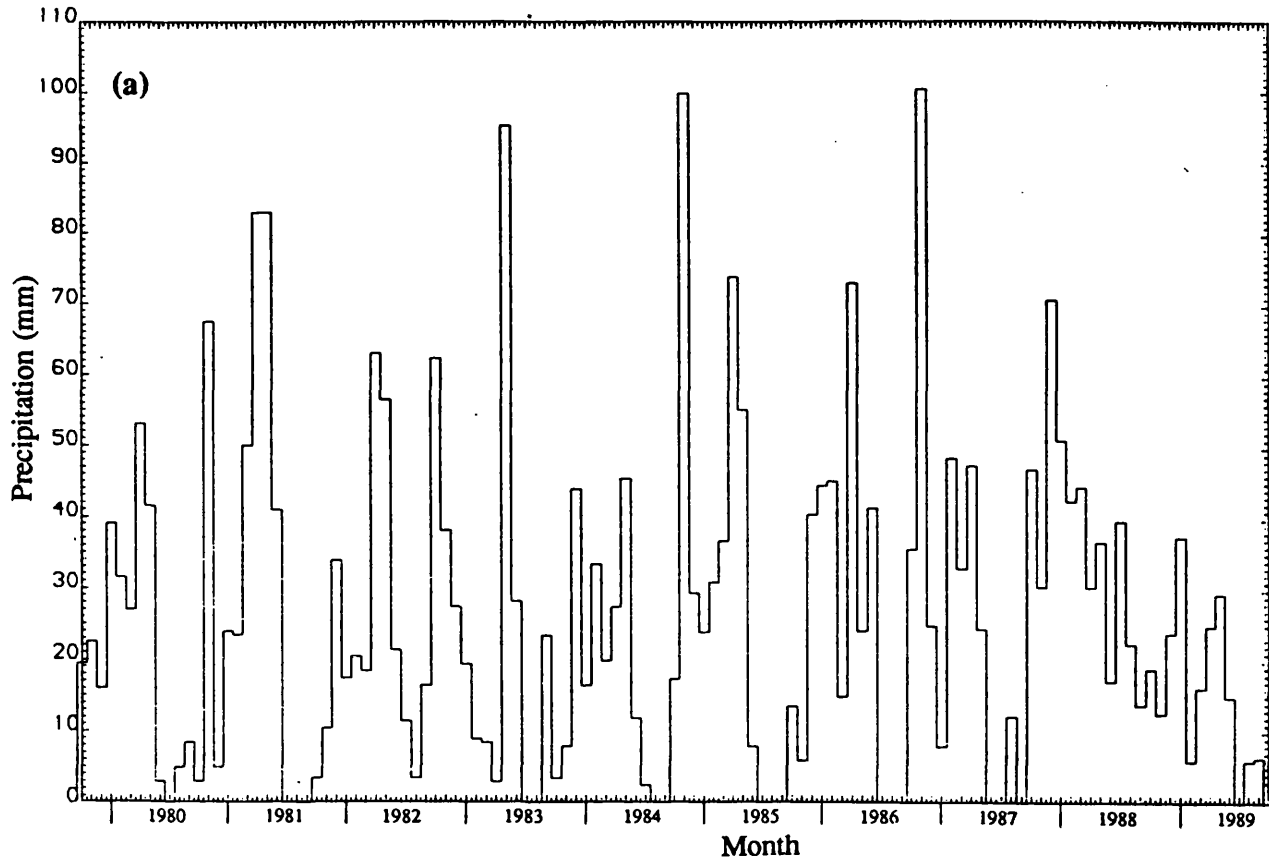


Fig. 2.4 Monthly variation of precipitation: (a) for Daryan station, (b) for Saidabad station.



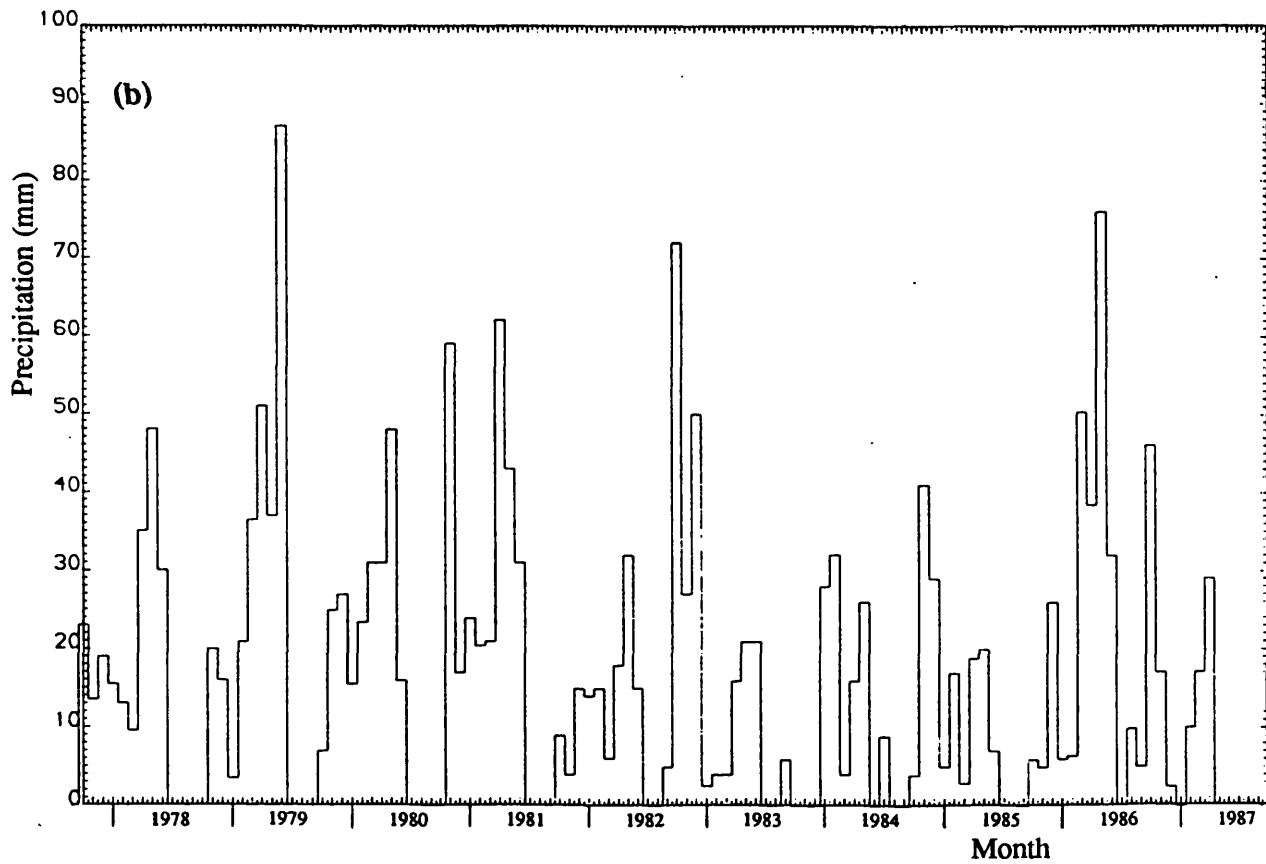
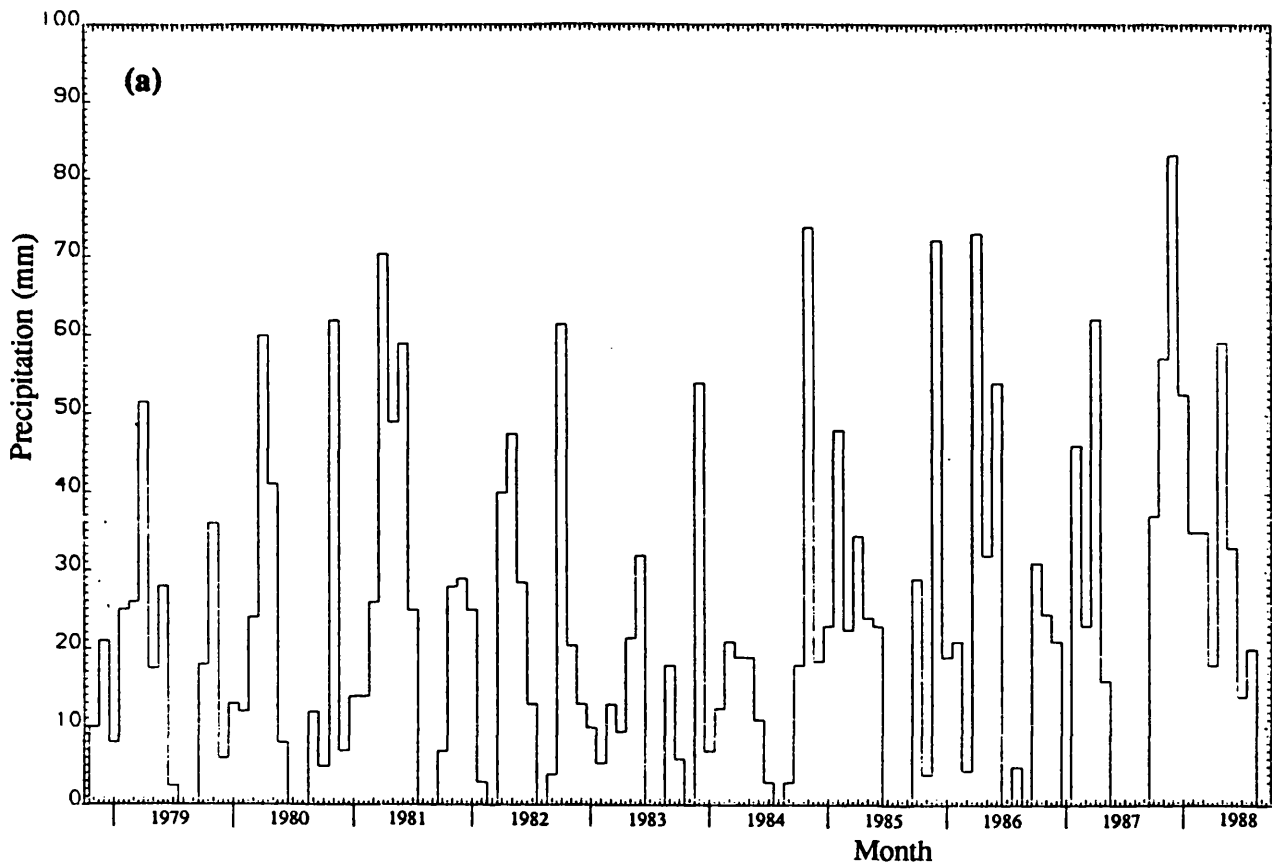


Fig. 2.5 Monthly variation of precipitation: (a) for Sahlan station, (b) for Vanyar station.

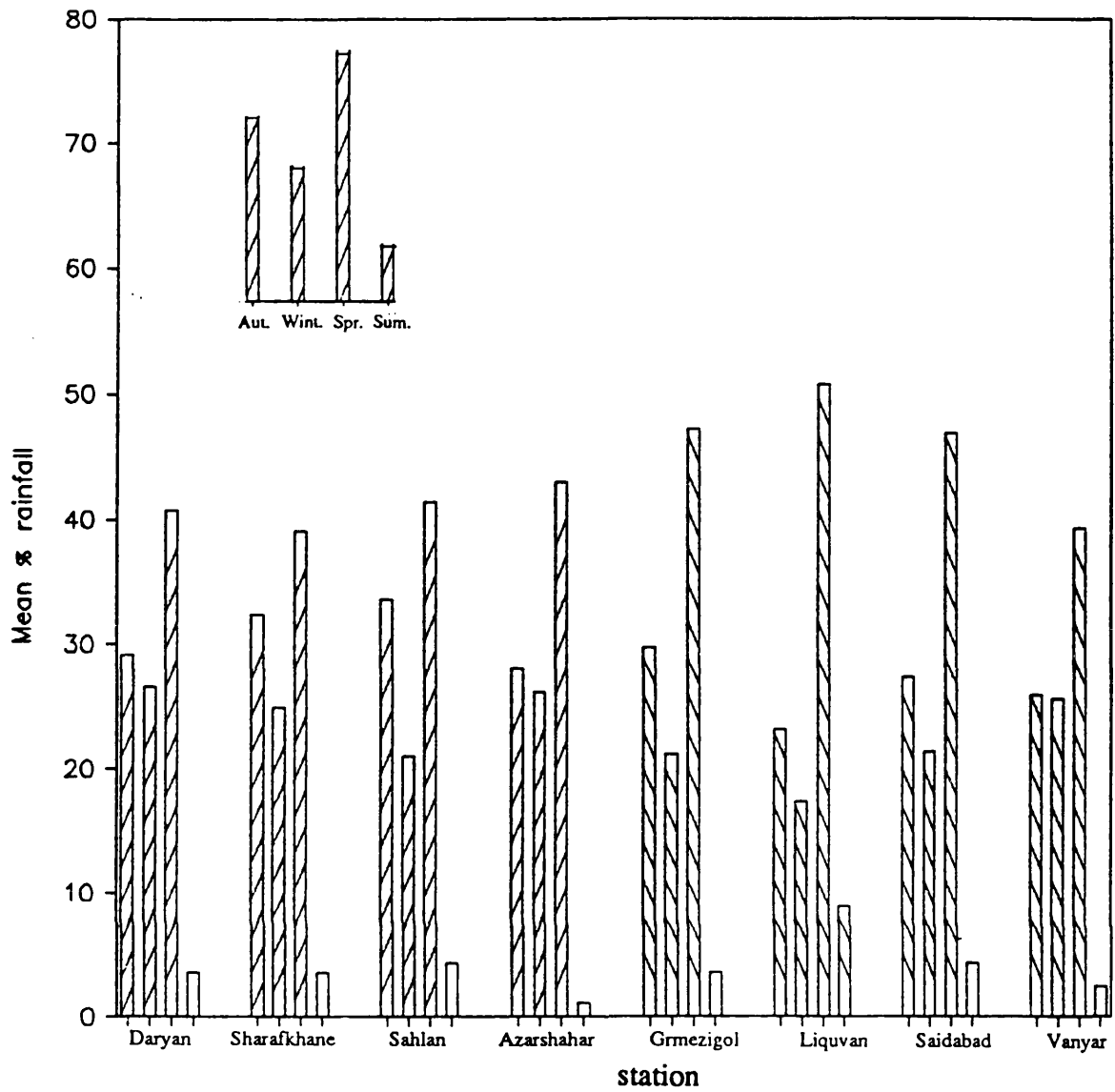


Fig. 2.6 Mean seasonal percentage of precipitation for different stations (1980-87).

shows, about 30 % of the precipitation occurs during the autumn season, 23 % during winter, 45 % during the spring and only 2 % during the summer.

#### **2.4.2 Temperature, Wind and Relative Humidity**

**Temperature:** the altitude is the most important controlling factor in the distribution of temperature in the study area. Mean daily temperatures in Tabriz (1360m amsl) vary from -2°C in January up to 28°C in July with a yearly average of 12°C. At Liguvan (2100m amsl), in the southern mountainous region, the annual average temperature is reduced to 6.5°C, with the mean monthly temperature varying between -5°C in January and 17°C in July. The mean annual temperature at Sharafkhane near the Orumiyeh Lake is the same as in Tabriz but thermal variation throughout the year is lower, varying between 0.50°C in January up to 24°C in July.

**Wind:** The dominant winds over the area blow from the north-east and the south-west, though, winds from the east and the west are also common. The wind speed rarely exceeds 25 m/sec; however, over the mountainous regions they are extremely variable and greatly influenced by topography.

Masses of relatively warm and moist air from the Mediterranean frequently break through the area, not only raising the temperature conditions but also bringing precipitation to the region.

**Relative humidity:** In general, mean monthly relative humidity at the Tabriz station is relatively high during the November-February period, ranging from 75 to 80%, and lower during July and August, when it is about 35 to 45%. A similar case can be assumed for the other parts of the study area, with some higher values for the zones near the Orumiyeh Lake and lower values for the driest period in the mountains.

#### **2.4.4 Evaporation and Transpiration**

Evapotranspiration is one of the most important elements in water resource studies. Its consideration is essential for estimating water requirements for irrigation, and is useful for estimating municipal and industrial water needs, rainfall disposition, ground water recharge and safe yields, and stream flow depletion in river basins (Jensen, 1974). A knowledge of evapotranspiration is necessary in planning and operating water resource development and management.

There are eight meteorological stations in the study area and the available data from these stations can be divided into two types: (i) data from the Tabriz airport meteorological station are reliable and include mean monthly temperature, precipitation, wind speed and direction, mean vapour pressure, and bright sunshine duration; (ii) data from the other seven stations are less reliable and include mean monthly pan evaporations, precipitation, temperature, wind speed and in some case relative humidity.

### **Calculation or Estimation of Potential Evapotranspiration (Pet)**

Of the several parameters in the hydrological cycle, that of evaporation is one of the most difficult to quantify. Furthermore, the actual water loss from vegetated land surface by transpiration adds further complexities to the evaluation of the processes.

In general, the selected methods for estimation or calculation of Pet from the many methods (see Jensen 1974), depend on the availability and accuracy of the recorded metrological data. With respect to these factors only the above-mentioned data from the Tabriz airport station are used for calculating the Pet following two main methods and pan evaporation method for the other stations as described below.

#### **(a) Penman combination methods**

In a classical study of natural evaporation Penman (1948) developed a formula for calculating open water evaporation based on fundamental physical principles, with some empirical concepts incorporated, to enable standard meteorological observations to be used. The physical principles combine the mass transfer (aerodynamic) and the energy budget methods to calculate the evaporation from the open water.

According to Shaw (1988) resulting from later experience, the formula for the open water was modified by MAFF (1967) to allow for the conditions under which evaporation plus transpiration takes place from a vegetated surface.

Then the basic equation for Pet becomes:

$$\text{Pet} = \frac{(\Delta/\gamma)H_T + E_{at}}{(\Delta/\gamma) + 1}$$

where  $\Delta$  is the slope of the saturated vapour pressure versus temperature curve and  $\gamma$  is the psychometric constant. The  $H_T$  is calculated from incoming ( $R_I$ ) and outgoing ( $R_o$ ) radiations determined from sunshine records, temperature and humidity, using:

$$H_T = (1-r)R_I - R_o$$

where  $r$  is the albedo and equals 0.25 for a short grassed surface,  $R_I$  is a function of  $R_s$ , the solar radiation (fixed by latitude and season) modulated by a function of the ratio,  $n/N$ , of measured to maximum possible sunshine duration as:

$$R_I(1-r) = 0.75 R_s \cdot f_s(n/N)$$

where the  $f_s(n/N) = (0.16 + 0.62 n/N)$  for latitudes south of  $54.5^\circ$  N,  $n$  is the sunshine hours and  $N$  is latitude of the station.

The empirical equation for the outgoing radiation takes the form:

$$R_o = \sigma T_a^4 (0.47 - 0.075 \sqrt{e_a}) (0.17 + 0.83 n/N)$$

where  $\sigma T_a^4$  is the black body radiation at average daily temperature ( $T_a$ ) which is modified by functions of the humidity of the air ( $e_a$ ) and the cloudiness ( $n/N$ ).

The term  $E_{at}$  is derived from the aerodynamic equation with empirical function as:

$$E_{at} = 0.35(1 + u_2/100)(e_s - e_a)$$

where,  $u_2$  is the wind speed at 2 m above the surface, and  $(e_s - e_a)$  is the saturation deficit.

### (b) Thornthwaite method

Thornthwaite (1948) carried out much experimental work in east central U.S.A and extensively studied the correlation between temperature and potential evapotranspiration. He derived a formula for calculating potential evaporation on a monthly basis:

$$Pet \text{ (mm)} = 16 N (10T_a/I)^a$$

where  $T_a$  is the mean monthly temperature in  $^\circ\text{C}$ ,  $N$  is the monthly adjustment factor related to hours of daylight, and  $I$  is the heat index for the year, given by:

$$I = \sum_i = \sum(T_a/5)^{1.5} \quad \text{from } a=1,2,\dots,12$$

and

$$a = 6.7 \times 10^{-7} I^3 - 7.7 \times 10^{-5} I^2 + 10^{-2} I + 0.49$$

Given the monthly mean temperatures from the measurements at a

climatological station, an estimate of the potential evaporation for each month of the year can be calculated.

### **(c) Pan evaporation method**

As mentioned above, the direct measurements of evaporation by the Class A U.S.A standard pan were carried out in the area at most of the stations. So the data from these stations can be used to estimate the potential evapotranspiration in the area.

The relatively small capacity and shallow depths of pans, in comparison with lakes and rivers, and their situation at or near the land surface allows proportionately greater amounts of advected heat from the atmosphere to be absorbed by the water in the pan through the sides and bottom, in comparison with natural open water (Wilson, 1983). Also, storage of heat within the pan can be appreciable and may cause almost equal evaporation during night and day, whereas most crops transpire only during the daytime (Doorenbos, 1977). Therefore, pan evaporation is usually too high and a pan coefficient has to be applied. Doorenbos (1977) derived values for such coefficients by taking into account the climatic conditions and the pan environment.

## **Results and discussion**

The resultant values of  $P_{et}$ , for the Tabriz airport station in years 1982 and 1984, which has been calculated by the Penman and Thornthwaite methods, are presented in Figures 2.7 and 2.8. As the plots show, the agreement between two methods is not very good. The total annual  $P_{et}$  calculated using the Penman method for years 1982 and 1984 are 1283mm and 1145mm respectively, whereas, the corresponding results using the Thornthwaite method are 728mm and 755mm.

The results deduced from the Penman method seem much more reliable than those from the Thornthwaite, because they show very close agreement with the values estimated from the pan evaporation method at nearby stations as well as with the previously reported values (Perrin and Wallen, 1963).

According to Jensen (1974), the assumptions of Thornthwaite formula include (a) the albedo of the evaporating surface must be a standard, (b) the rate of

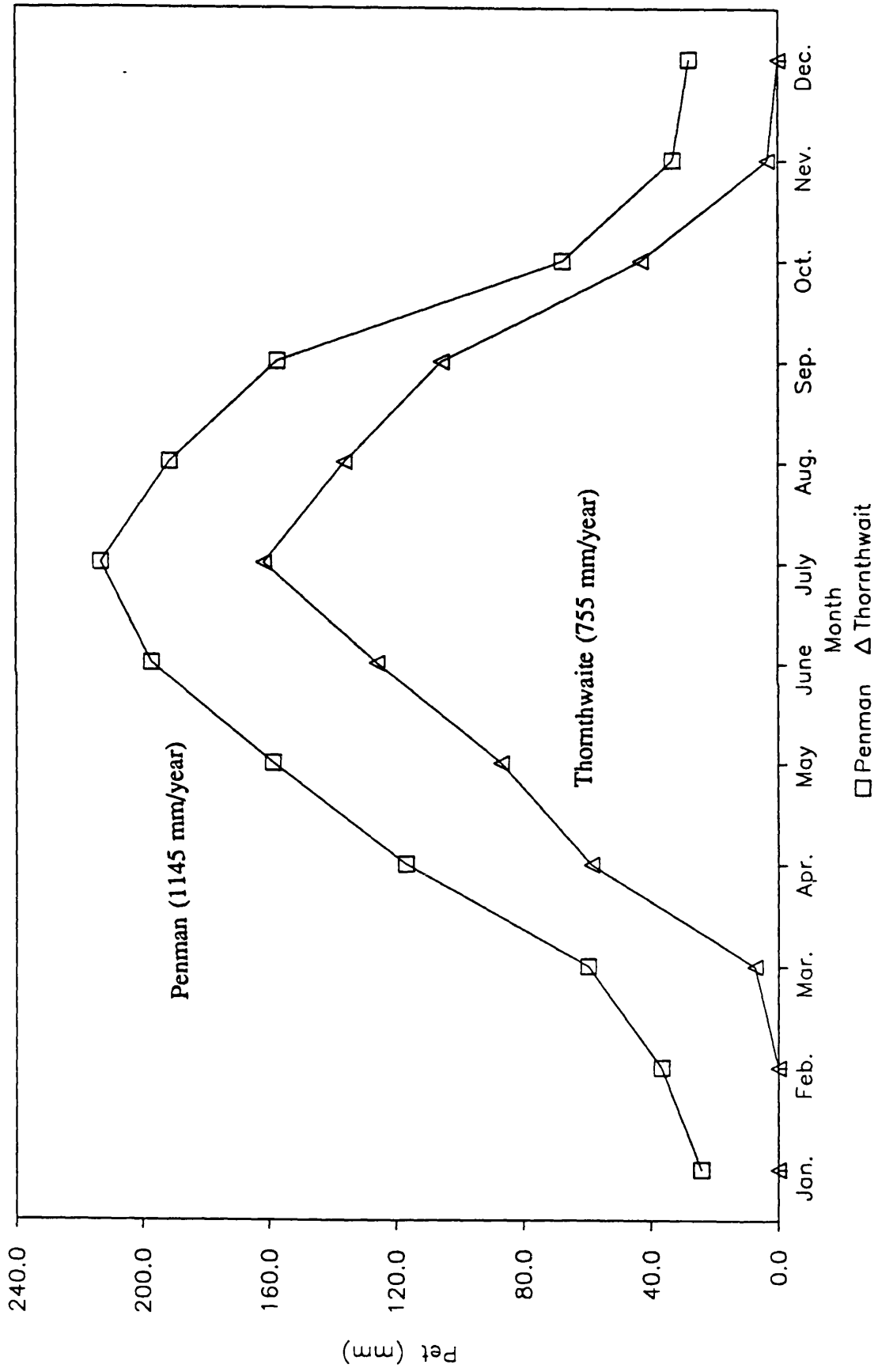


Fig. 2.7 Calculated potential evapotranspiration for the Tabriz Airport station (1982).

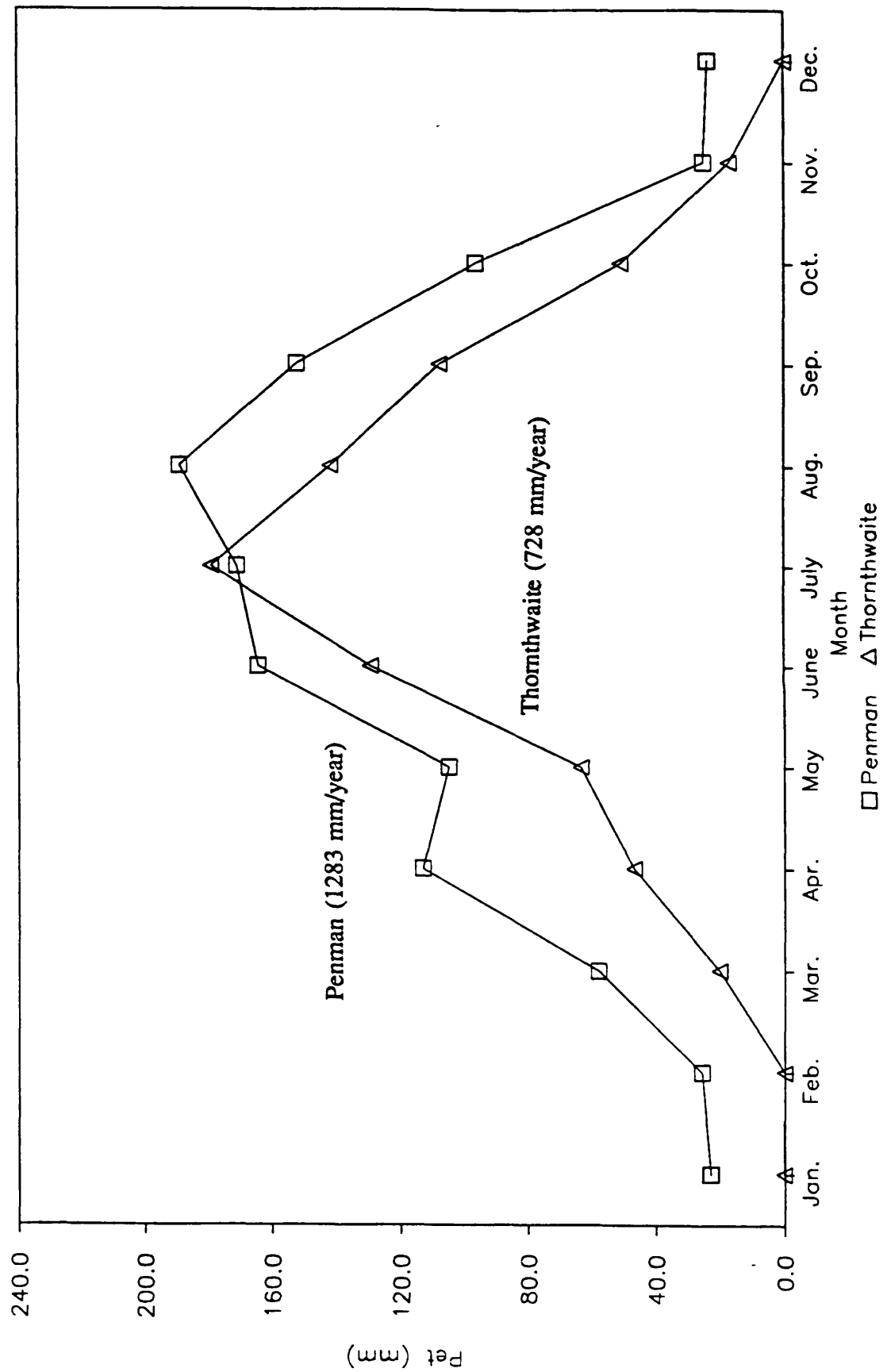


Fig. 2.8 Calculated potential evapotranspiration for the Tabriz Airport station (1984).



evapotranspiration must not be influenced by advection of moist or dry air and (c) the ratio of energy utilized in evaporation to that of heating the air must remain essentially constant and do not exist in arid and semi-arid areas. Thus, the formula should not be expected to provide reliable results for the study area.

The pan evaporation data from the seven other meteorological stations (for the location see Fig 2.3) are used to show the regional variations in Pet during the water year 1985-86 (see Table 2.1). As the table shows, the amounts of Pet generally decrease from the Tabriz Plain towards the mountainous areas as well as towards the Lake sides. The highest value (1300mm) occurred to the north-west of Tabriz City at Sahlan station, while the lowest value (628mm) was determined in the high mountain area at the Gorigol station. Also, it should be mentioned that the pan evaporation estimation of Pet for the stations close to the Tabriz airport station are in closer agreement with the Penman method Pet value rather than that of the Thornthwaite method.

**Table 2.1**

<b><u>Name of Station</u></b>	<b><u>Pan Evaporation (mm)</u></b>	<b><u>Pan Coefficient</u></b>	<b><u>Pet (mm)</u></b>
Sharafkhane	1057.7	0.75	793
Shanejan	913.7	"	685
Sahlan	1734.5	"	1301
Alishah	1528.6	"	1147
Tazekand	1660.6	"	1246
Liquvan	1282.7	"	962
Gorigol	837.4	"	628

**Actual evapotranspiration**

The potential evapotranspiration estimated by either the Penman or pan evaporation method is the amount of water evaporated from a short green crop completely covering the ground and well supplied with water. However, water loss from a catchment area does not always proceed at the potential rate, since this is

dependent on a continuous water supply. When the vegetation is unable to abstract water from the soil then the actual evaporation becomes less than potential. Thus, the relationship between actual and potential evaporation depends on the soil moisture content.

If there is no rain to replenish the water supply, the soil moisture gradually becomes depleted by the transpiration demands of the vegetation and direct evaporation to produce a soil moisture deficit (SMD). As SMD increases, actual evaporation becomes increasingly less than potential. The values of SMD and actual evaporation vary with soil and vegetation types.

Penman (1950) introduced the concept of root constant, that defines the amount of soil moisture which can be extracted from the soil without difficulty by the given vegetation and soil type. Grindley (1970) used this model to calculate the actual evaporation and SMD over Britain.

The model was applied to the Tabriz area (see Tables 2.2 and 2.3), but because of the high SMD carried over from the previous year, the great climatological difference between the two areas ( Britain is a humid area and the study area is an arid or semi-arid region) and very low differences between the calculated annual actual evaporation and precipitation rate introduced some doubts regarding the results. Therefore, the model is not considered to be applicable to the study area(Agnew, 1991, pers. comm.).

## **2.5 River Discharge**

### **2.5.1 Introduction**

As explained in Section 2.3, there are 13 rivers in the project area and 8 of them are gauged by the hydrometric stations. Also, on three of these rivers hydrometric stations are operated at two different places upstream and downstream which increase the number to eleven stations (see Fig. 2.1). The daily gauge readings can be converted directly to river discharge. A typical set of the daily discharge data is presented graphically as the hydrograph in Figure 2.9 . An analysis of river hydrographs and the investigation of the corresponding river regime permits the identification of the ground water (baseflow) component.

Table 2.2 Calculation of soil moisture deficit and actual evaporation (mm) for Liquevan station (1986).

Total Pan Evaporation=1291.8mm

Month	Precip.	Pet(KpxPep)	Pre.-Pet	Poten. SMD	Bare Soil		RC 75		RC 140		Catchment	
					SMD	Et	SMD	Et	SMD	Et	SMD	Et
Jan.	7.5	0	7.5	0	0	0	0	0	0	0	0	0
Feb.	26.5	0	26.5	0	0	0	0	0	0	0	0	0
Mar.	7	0	7	0	0	0	0	0	0	0	0	0
Apr.	32	0	32	0	0	0	0	0	0	0	0	0
May	89.5	134.7	-46.23	46.2	40.2	135.7	46.2	135.7	46.2	135.7	41.1	135.7
Jun.	158.5	161.1	-2.64	48.9	41	159.5	48.9	161.1	48.9	161.1	42.185	159.74
Jul.	0	197.3	-197.3	246.2	50	9	121	72.1	176	127.1	63.4	21.215
Agu.	44	151.6	-107.6	353.8	50	44	125	48	187	55	64.35	44.95
Sep.	4.3	141.3	-137	490.8	50	4.3	125	4.3	190	7.3	64.5	4.45
Oct.	60.5	107.5	-47	537.8	50	60.5	125	60.5	193	63.5	64.65	60.65
Nov.	24.5	56.6	-32.1	569.9	50	24.5	125	24.5	195	26.5	64.75	24.6
Des.	11	0	11	558.9	39	0	125	0	194	0	55.35	0
Total	465.3	950.1				437.5		506.2		576.2		451.305

Catchment SMD= 0.85 SMD(Bare soil)+ 0.1 SMD(RC 75)+ 0.05 SMD(RC 140)

Catchment Et= 0.85 Et(Bare soil)+ 0.1 Et(RC 75)+ 0.05 Et(RC 140)

SMD= Soil Moisture Deficit Et= Actual evaporation RC=Root Constant

Table 2.3 Calculation of soil moisture deficit and actual evaporation (mm) for Tazekand station (1986).

Total Pan Evaporation = 1638.8

Month	Precip.	Pet(KpxPep)	Pre.-Pet	Poten. SMD	Bare Soil		RC 75		RC 140		Catchment	
					SMD	Et	SMD	Et	SMD	Et	SMD	Et
Jan.	2	0	2	0	0	0	0	0	0	0	0	0
Feb.	27	0	27	0	0	0	0	0	0	0	0	0
Mar.	3	0	3	0	0	0	0	0	0	0	0	0
Apr.	36	41.2	-5	5	41.2	5	41.2	5	41.2	5	41.2	5
May	5.5	126.9	-121.4	126.4	50	109	109.5	126.4	126.9	62.4	62.5	62.5
Jun.	36	154.9	-118.9	245.3	50	120	47	176	91	66.8	40.4	40.4
Jul.	0	277.6	-277.6	522.9	50	125	5	190	14	68.25	1.45	1.45
Agu.	8	300	-292	814.9	50	125	8	195	13	68.5	8.3	8.3
Sep.	0	221.6	-221.6	1036.5	50	125	0	200	5	68.75	0.25	0.25
Oct.	16	108.9	-92.9	1129.3	50	125	16	205	21	69	16.25	16.25
Nov.	26	69.7	-43.7	1173	50	125	26	208	29	69.15	26.15	26.15
Des.	38	0	38	1135	12	125	0	207	0	38.7	0	0
Total	197.5	1300.8					177.2	252.7	341.1		196.5	196.5

Catchment SMD= 0.8 SMD(Bare soil)+ 0.15 SMD(RC 75)+ 0.05 SMD(RC 140)

Catchment Et= 0.8 Et(Bare soil)+ 0.15 Et(RC 75)+ 0.05 Et(RC 140)

SMD=Soil Moisture Deficit Et= Actual evaporation RC= Root Constant

### **2.5.2 Sources and Components of River Discharge**

Ward (1975) schematically indicated that total runoff from a typically heterogenous catchment area may be conveniently divided into four component parts: channel precipitation, overland flow, interflow and ground water flow. The sum of channel precipitation, surface runoff and more rapid interflow can be referred to as quickflow which represents the major runoff contribution during storm periods. The sum of ground water runoff and delayed interflow is defined as baseflow.

In addition to the rainfall, due to the high altitudes of some parts of the study area a certain proportion of streamflow may be derived from the melting of snow, which occurs gradually over a period of several months in spring and early summer. Bengtsson (1982) and Stephenson and Freeze (1974) studied the effect of variation of the snowmelt intensity on streamflow and concluded that the ratio between the two different kinds of flow (baseflow and quickflow) strongly depends on basin and snowpack characteristics. However, the contribution of baseflow resulting from snowmelt to streamflow may be considerable.

### **2.5.3 Hydrograph Analysis**

Most of the assumptions made in hydrograph analysis involve simplifying generalizations of an arbitrary nature. Ward (1975) illustrated several types of methods to separate the baseflow from the surface runoff.

Daily flow data from the rivers of the study area were analysed by an arbitrary manual method that took account of individual storm recessions and projected a rise of ground water contribution to coincide with the spring peak(s). An example of this approach is illustrated in Figure 2.9. Also, the data have been analysed using a computer program written by the Institute of the Hydrology (IH) in 1978. The computer program runs with field data and calculates the total volume of flow, baseflow and the ratio of baseflow to total flow which is described as the " base flow index". Also from the manual analysis these values can be obtained by determining the volume of water below the separated hydrograph. Additionally, the value of the baseflow in mm over its catchment can be calculated.

Figures 2.9 and 2.10 illustrate the hydrograph from the River Liguvan at the Liguvan hydrometric station for 1987-88 that was analysed by both the above-

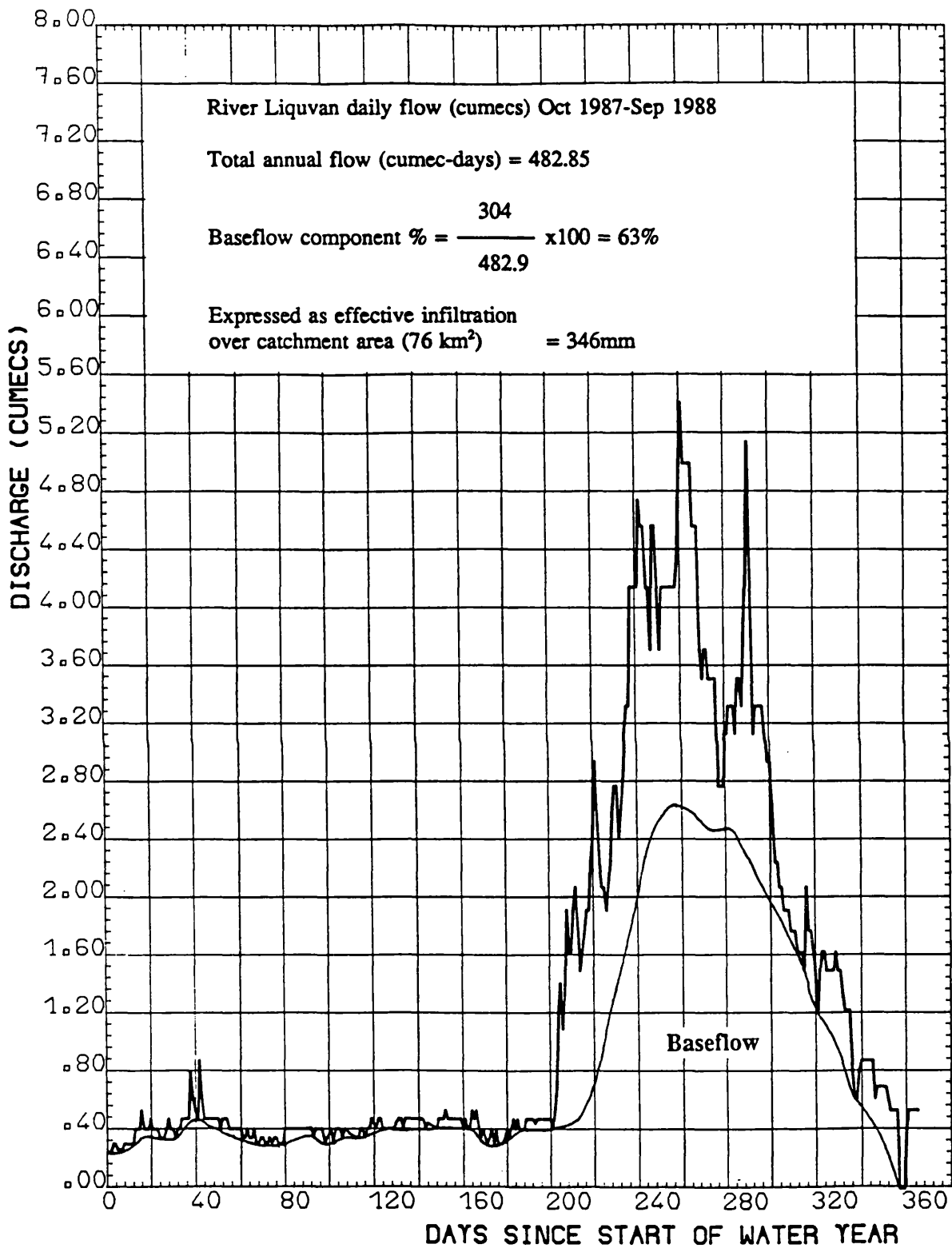


Fig. 2.9 Hydrograph showing baseflow and surface runoff components (manual analysis).

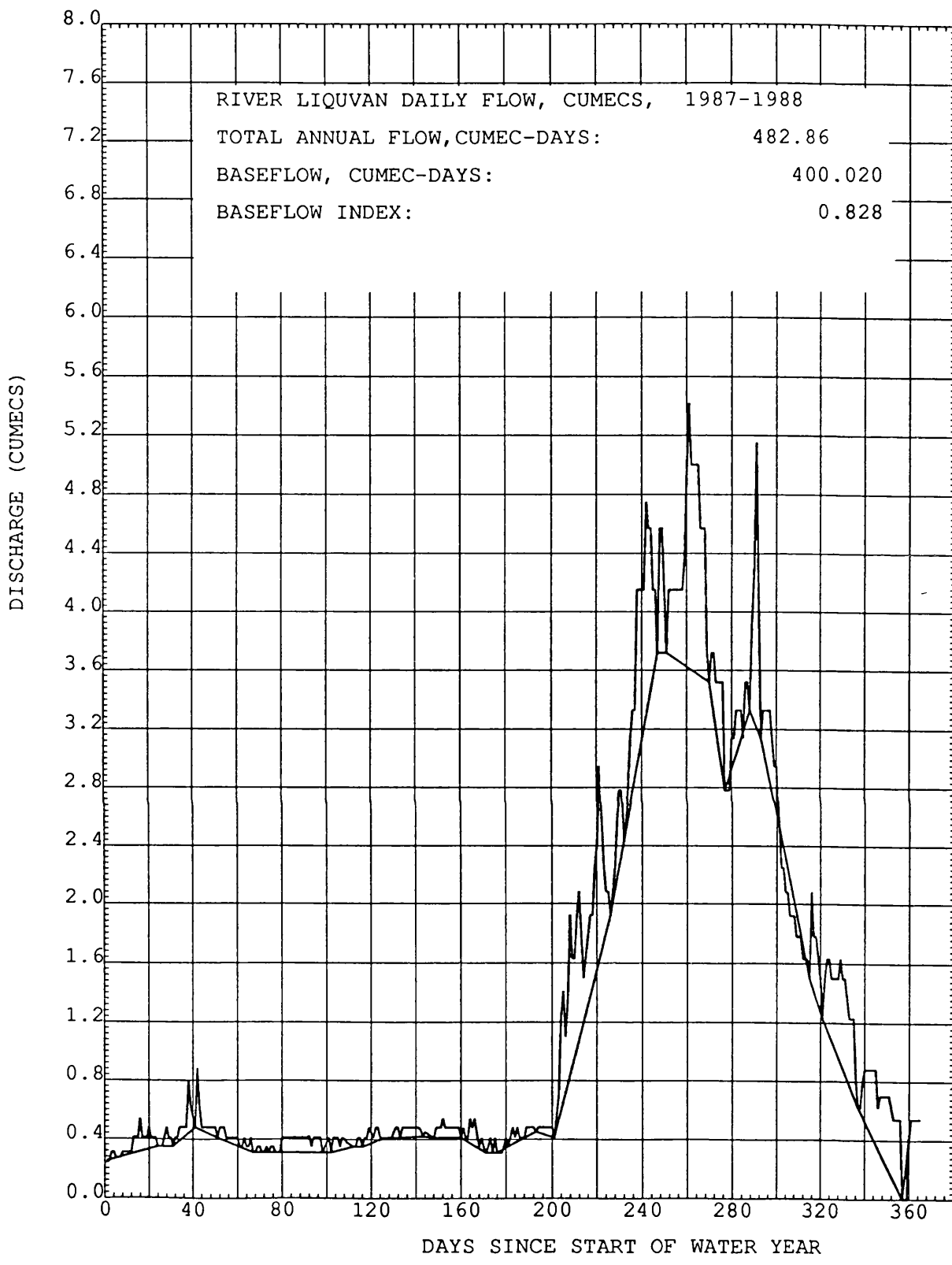


Fig. 2.10 Hydrograph showing the baseflow and surface runoff component (computer analysis).

mentioned methods. Data from the other stations were also analysed for different years by these methods and the results are summarized in Table 2.4.

As the table shows, the baseflow values resulting from the IH method are greater than the manual method and in some cases surprisingly they are equal to or greater than the total flow, which indicates the method is not applicable for the study area. However, the IH method can give some check on the manual analysis result.

#### **2.5.4 Factors Affecting Baseflow**

The ratio of baseflow to the total stream flow from the area is affected by three main groups of factors: (a) climatic factors, (b) catchment factors and (c) human factors. The climatic factors such as evapotranspiration, type of precipitation, rainfall intensity, duration and distribution, as comparatively stable environmental factors, play an important role in the generation of baseflow. The snow blanket in high altitude areas acts as storage, which gradually delivers the meltwater through highly permeable eroded rocks to the streamflow (see Table 2.4).

Most important catchment factors are the topographical, geological and vegetational features of the area. The partitioning of precipitation between overland flow, interflow and ground water flow depends on land slope, soil types and structure and permeability of geological formations. As Table 2.4 shows, the ground water component at stations very close to the high mountainous area (like Liquvan, Zinjanab, Gombar and Daryan stations) is about 25 percent of total precipitation.

This high percentage of infiltration to ground water or baseflow contribution to streamflow is due to gradual snowmelt, the high permeability of the geological formations, and low influence of human factors in the upper stream catchments. However, in downstream stations of these rivers the baseflow components show a lower percentage of ground water contributions, due to agricultural and municipal water uses of ground water as well as diverted river water in the upper parts. Also, with the reduction of the slope of the land surface, the rivers become losing rather than gaining streams. Therefore, the volume of baseflow is reduced in these stations. In Tabriz Plain, for example, where the slope is very low the total river flow reduces by more than 20 percent (see Table 2.4).



Table 2.4 River discharge analysis results (flow in cumec-days and catchment area in km<sup>2</sup>).

No	River & Station	Date	Catch. Area	Total Flow	Synthetic	Method	Manual	Method	G.W Comp. in (mm)
					baseflow	(BFI)	Baseflow	%	
1	Daryan	1983	57.5	152.9	40.7	0.27	34	22	51
2	-	1984	-	121.4	119.3	0.98	80	66	120
3	(Daryan)	1985	-	161.1	120.8	0.75	74	46	111
4	-	1986	-	127	110.9	0.87	86	68	129
5	-	1987	-	140.1	138.2	0.99	88	63	132
6	-	1988	-	281.8	128.9	0.46	150	53	225
	Average	-		164.1	109.8	0.72	85.3	53	128
1	Gomanab	1976	396.3	411.5	412.5	1	200	48	44
2		1977	-	332.3	364.5	1.1	208	63	45
3	(Anakhato)	1978	-	178.1	148.2	0.83	116	65	25
4		1980	-	272.5	200.8	0.74	152	56	33
	Average			298.6	281.5	0.92	169.0	58.0	36.8
1	Sinekh	1975	497.5	98.9	76.3	0.77	56	57	10
2		1976	-	429.5	146.6	0.34	140	33	24
3	(Pole-Sinekh)	1977	-	471.5	225.3	0.48	175	37	30
4		1978	-	286.2	121.1	0.42	130	45	23
5		1979	-	263.2	165	0.63	156	59	27
6		1981	-	251.2	106.9	0.43	103	41	18
7		1983	-	620.7	256.9	0.41	192	30	33
8		1985	-	476.8	220.6	0.46	208	43	36
9		1986	-	230.9	129.3	0.56	116	50	20
	Average	-	-	347.7	160.9	0.50	141.8	43.9	24.6

Table 2.4 (continued)

No	River & Station	Date	Catch. Area	Total Flow	Synthetic	Method	Manual	Method	G.W Comp. in (mm)
					baseflow	(BFI)	Baseflow	%	
1	Azar-shahr	1980	290	160.3	118	0.74	76	47	23
2		1981	-	336.9	139.7	0.42	138	41	41
3		1982	-	369	153.7	0.42	152	41	45
4		1983	-	384.7	174.4	0.45	136	35	41
5		1985	-	355.5	201.3	0.57	120	31	36
6		1986	-	362.4	176.8	0.49	160	44	48
7		1987	-	264.1	170.2	0.65	116	30	35
	Average			319.0	162.0	0.53	128.3	38.4	38.4
1	Gombar (Germezi-Gol)	1969	109.4	1941.2	1579.6	0.81	640	33	506
2		1976	-	300.4	195.2	0.66	160	53	126
3		1984	-	248.5	162.1	0.65	152	61	120
4		1985	-	395.2	258.3	0.65	184	47	145
5		1986	-	335.5	189.4	0.57	150	45	119
6		1987	-	347.8	237.8	0.68	176	51	139
	Average			594.8	437.1	0.67	243.7	48.3	192.5
1	Sard-Rud (Zinjanab)	1981	38.8	126.4	59.3	0.47	56	44	125
2		1982	-	124.5	80.1	0.64	64	51	143
3		1983	-	146.9	70.5	0.48	60	41	134
4		1985	-	134.2	68.7	0.51	60	45	134
5		1986	-	88.5	67.3	0.76	60	68	134
6		1987	-	92.4	67.7	0.52	44	48	98
7		1988	-	153.9	83.8	0.55	62	40	138
	Average			123.8	71.1	0.56	58.0	48.1	129.4

Table 2.4 (continued)

No	River & Station	Date	Catch. Area	Total Flow	Synthetic	Method	Manual	Method	G.W Comp. in (mm)
					baseflow	(BFI)	Baseflow	%	
1	Liquvan	1979	76	261.4	198.6	0.76	173	66	197
2		1980	-	259.9	200.7	0.77	147	57	167
3	(Liquvan)	1981	-	271.1	191.9	0.71	124	46	141
4		1982	-	241.3	161.5	0.67	112	46	127
5		1983	-	285.4	218.2	0.76	130	46	148
6		1984	-	175.4	120.8	0.69	84	48	96
7		1985	-	321	223.6	0.7	192	48	218
8		1986	-	312.3	231.8	0.74	164	53	186
9		1987	-	334.1	213.2	0.64	152	46	173
10		1988	-	482.9	400	0.83	305	63	346
	Average			294.5	216.0	0.73	158.3	51.9	179.9
1	Liquvan	1980	186.3	193.2	101.6	0.53	78	40	36
2		1981	-	260.7	164.2	0.63	108	41	50
3	(Hervi)	1982	-	242.4	137.4	0.57	81	33	38
4		1983	-	303.8	161.1	0.53	87	29	40
5		1984	-	153.4	61.6	0.4	45	29	21
6		1985	-	302.5	156.3	0.52	69	23	32
7		1986	-	262.6	134.6	0.51	114	61	53
	Average			245.5	131.0	0.53	83.1	36.6	38.6
1	Said-Abad	1978	191.3	125.7	102.2	0.82	85	68	38
2		1979	-	107.9	106.9	0.99	92	85	42
3	(Said-Abad)	1980	-	137.8	93	0.68	92	67	42
4		1981	-	122.8	87.6	0.71	88	72	40
5		1982	-	111.9	65.8	0.59	64	57	29

Table 2.4 (continued)

No	River & Station	Date	Catch. Area	Total Flow	Synthetic	Method	Manual	Method	G.W Comp. in (mm)
					baseflow	(BFI)	Baseflow	%	
6		1983	-	160.1	120.9	0.76	92	58	42
7		1985	-	116.7	94.3	0.81	86	74	39
8		1986	-	113.2	75.1	0.66	76	67	34
9		1987	-	83.5	56.3	0.67	44	53	20
10		1988	-	114.2	88.6	0.78	86	75	39
	Average			119.4	92.8	0.07	80.5	67.6	36.5
1	Aji-Chay	1977	7432.4	3873.3	2154.3	0.55	1840	48	21
2		1980	-	3805.4	2806	0.74	1384	36	16
3	(Vanyar)	1981	-	5713.3	3559.5	0.62	2240	39	26
4		1982	-	4965.1	3609.7	0.73	2224	45	26
5		1983	-	6566.8	4750.5	0.72	2400	37	28
6		1984	-	3103.2	1892.5	0.61	1440	46	17
7		1985	-	7822.2	5645.7	0.72	1920	25	22
8		1986	-	5001.8	3017.7	0.6	2000	40	23
9		1987	-	3765.1	2849.1	0.76	1560	41	18
10		1988	-	8611.7	6420.7	0.75	2440	28	28
	Average			5322.8	3670.6	0.68	1944.8	38.5	22.5
1	Aji-Chay	1984	9752.4	2245	1203	0.54	960	48	9
2		1985	-	6415.8	2750.5	0.43	1840	29	17
3	(Akhole)	1986	-	4974.6	2296.6	0.46	1600	32	14
	Average			4545.1	2083.4	0.48	1466.7	36.3	13.3

### **2.5.5 Flow Duration Curves**

The procedure for constructing a flow duration curve was outlined by Searcy (1959) and defined as a cumulative frequency curve that shows the percent of time that specified discharges were equalled or exceeded in a given period. The flow duration curve provides a convenient means for studying the flow characteristics of streams and for comparing one basin with another.

The flow duration data for some rivers (see Fig. 2.11) were prepared by computer program, according to the classified discharges, and the percentage of the total time was computed for each class. Figure 2.11 shows four year period duration curves of daily flow for rivers Liquvan, Sinekh and Saidabad. The latter two rivers show a steep slope which indicated the highly variable nature of the streams, with a large volume of flow from direct runoff, whereas the Liquvan river curve with a generally shallow slope, reveals the presence of surface or ground water storage which tends to equalize the flow.

Also, Figure 2.12 shows the flow duration curves for four rivers for different periods of time. The Liquvan and Daryan rivers indicate a high contribution from ground water and gradual snowmelt water, whereas the Sardrud and Sinekh rivers indicate a lower contribution from storage.

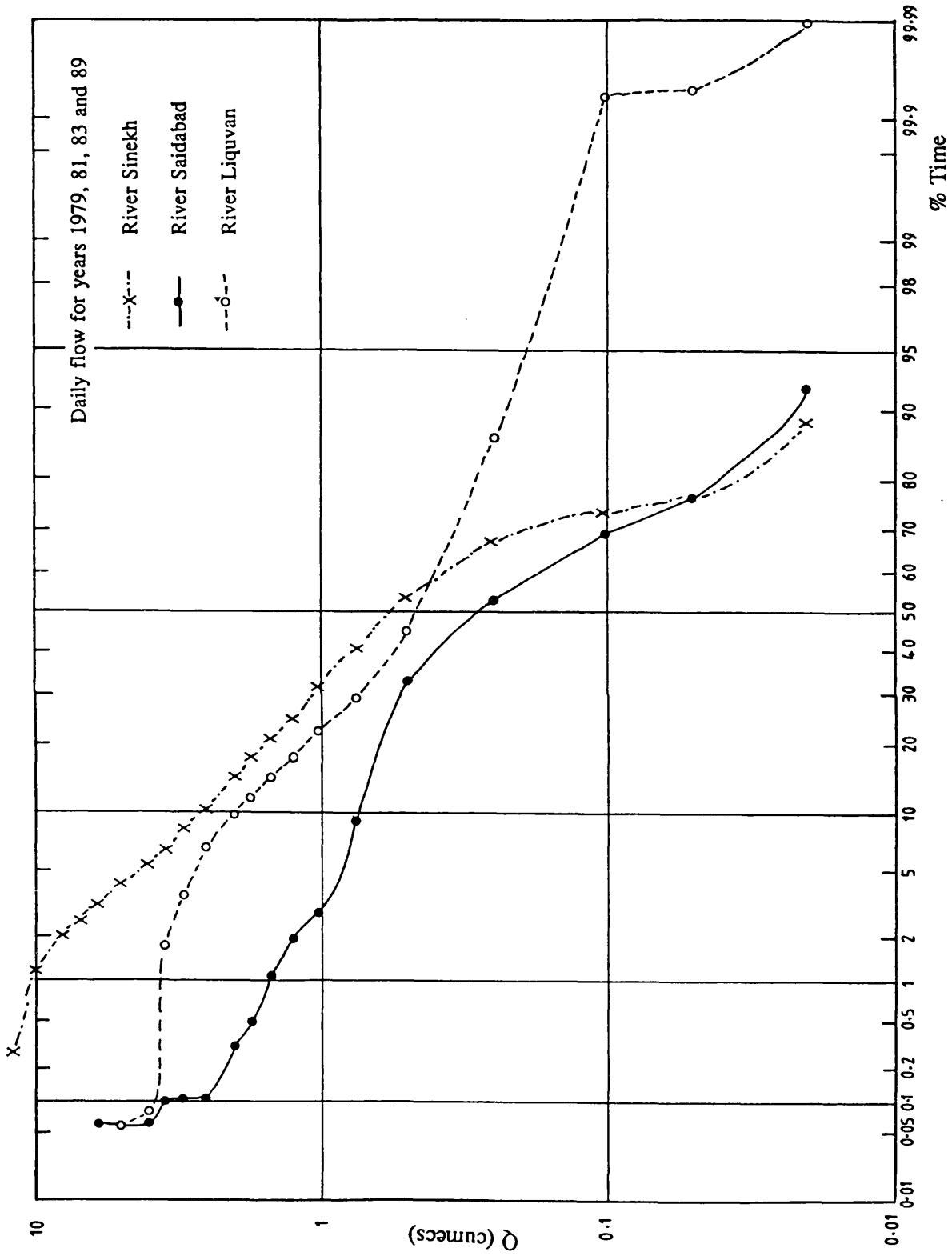


Fig. 2.11 Comparison of flow duration curves for the same period.

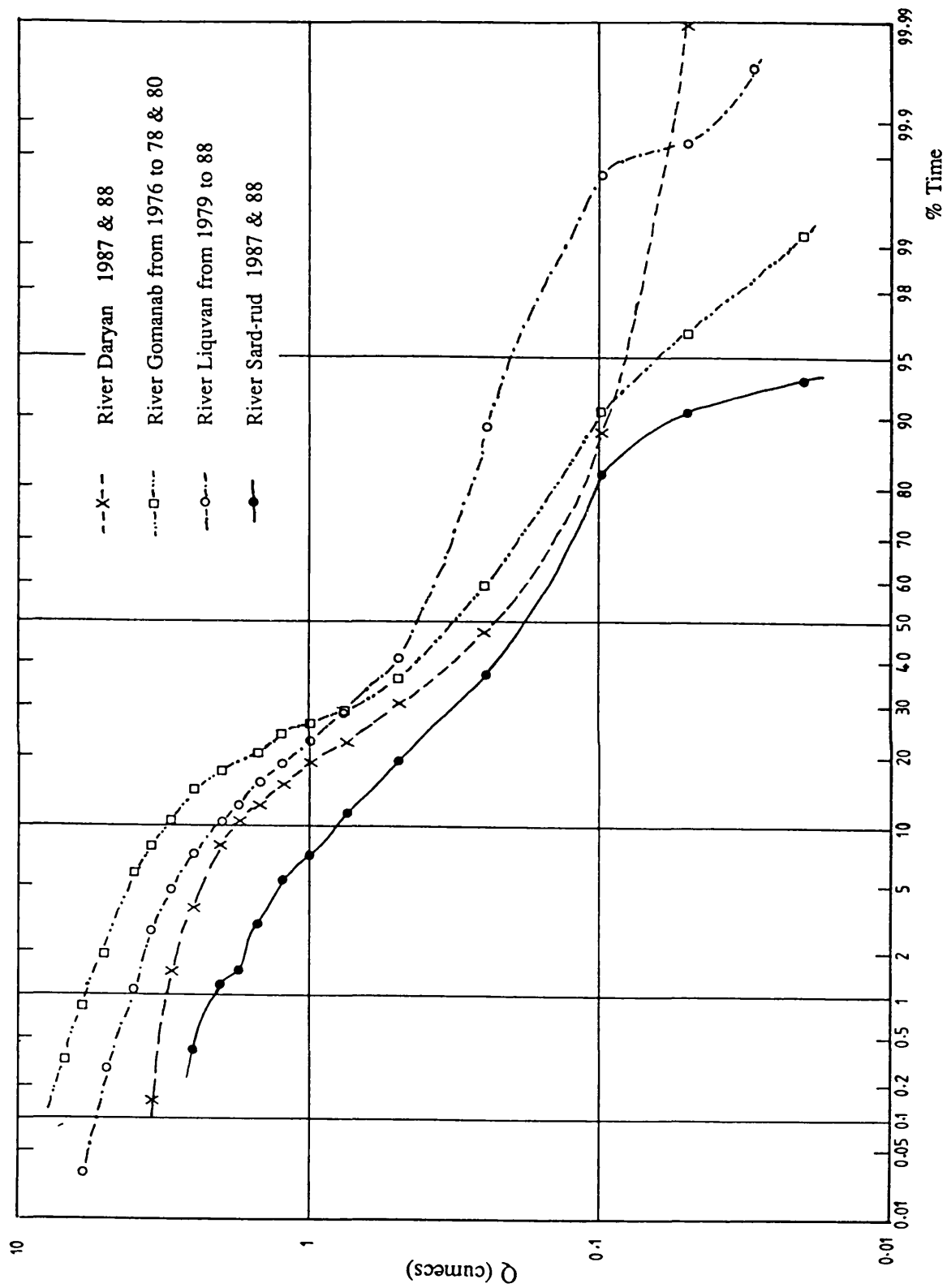


Fig. 2.12 Comparison of flow duration curves for different periods.

## **CHAPTER 3**

### **GEOLOGY**

**3.1 Geological Setting**

**3.2 Litho-stratigraphy**

**3.3 Geological Structure**



## CHAPTER 3

### GEOLOGY

#### 3.1 Geological Setting

The area of investigation lies in East Azarbijan province which is structurally part of Central Iran unit. It is wedged between the Zagros and Alborz mountain-systems. The project area includes representatives of Devonian to Quaternary age with various movements affecting it, most strongly those of Alpine origin.

The oldest geological formations such as the Devonian and Jurassic metamorphic rocks and sediments mainly occupy the northern part in the Mishow and Morov mountains. However, basic and acid intrusive bodies and Tertiary sedimentary rocks also occur in these mountain ranges.

The major Miocene transgression is marked by a thick unconformable conglomerate overlain by an evaporitic facies series. Subsequently, Alpine orogenesis raised the area while forming the Tabriz basin in correspondence with the downthrown block of North Tabriz Fault line and other displacement lines. Thus, the north-eastern part of the Tabriz area which so called south-western Qara Dag is dominated by a thick Miocene sequence of red sandstone, conglomerates and marls including gypsum and salt rocks.

Pliocene time involved a marine regression and a change to continental conditions, mainly lacustrine, coupled with the deposition of clay and clastics. Then the Plio-Pleistocene was marked by significant volcanic activity, with lava flows and pyroclastic masses associated with the continental conditions of that epoch.

Hence, the southern and south-western part of the Tabriz area is occupied by the extinct Sahand volcano which is built up from a volcanic series of rocks. This massif is surrounded by volcanic sediments called "alluvial tuff ", which were deposited around the andesitic and trachytic core. The Sahand alluvial tuff conformably overlies Pliocene marls, sandstones and fishbed layers.

The south-western part of Tabriz or the western side of Sahand mountain also includes Jurassic and Cretaceous limestones with Pliocene travertine; the latter is believed to be connected to the thermal mineral springs issuing from the Cretaceous limestones as well as from the alluvial tuff. According to Issar (1969) the thermo-

mineral springs are associated with late volcanic activity in this region. It is believed that karstic conditions are active in these limestones at present with a solution factor enhanced by the abundance of CO<sub>2</sub> of volcanic origin.

The Pleistocene and late Quaternary followed an alternation of alluviation and degradation phases according to base level changes. Thus, the Tabriz basin was gradually filled with poorly sorted clastic and fine grained material. Base level lowering and/or land uplift due to minor movements were coupled with the cutting of the terraces and with the continued filling of the basin.

Therefore, recent base level changes were associated with an ultimate erosion and aggradation phase including the construction of the recent Aji Chay terraces, the building up of alluvial fans, and the overall alluviation that is still underway.

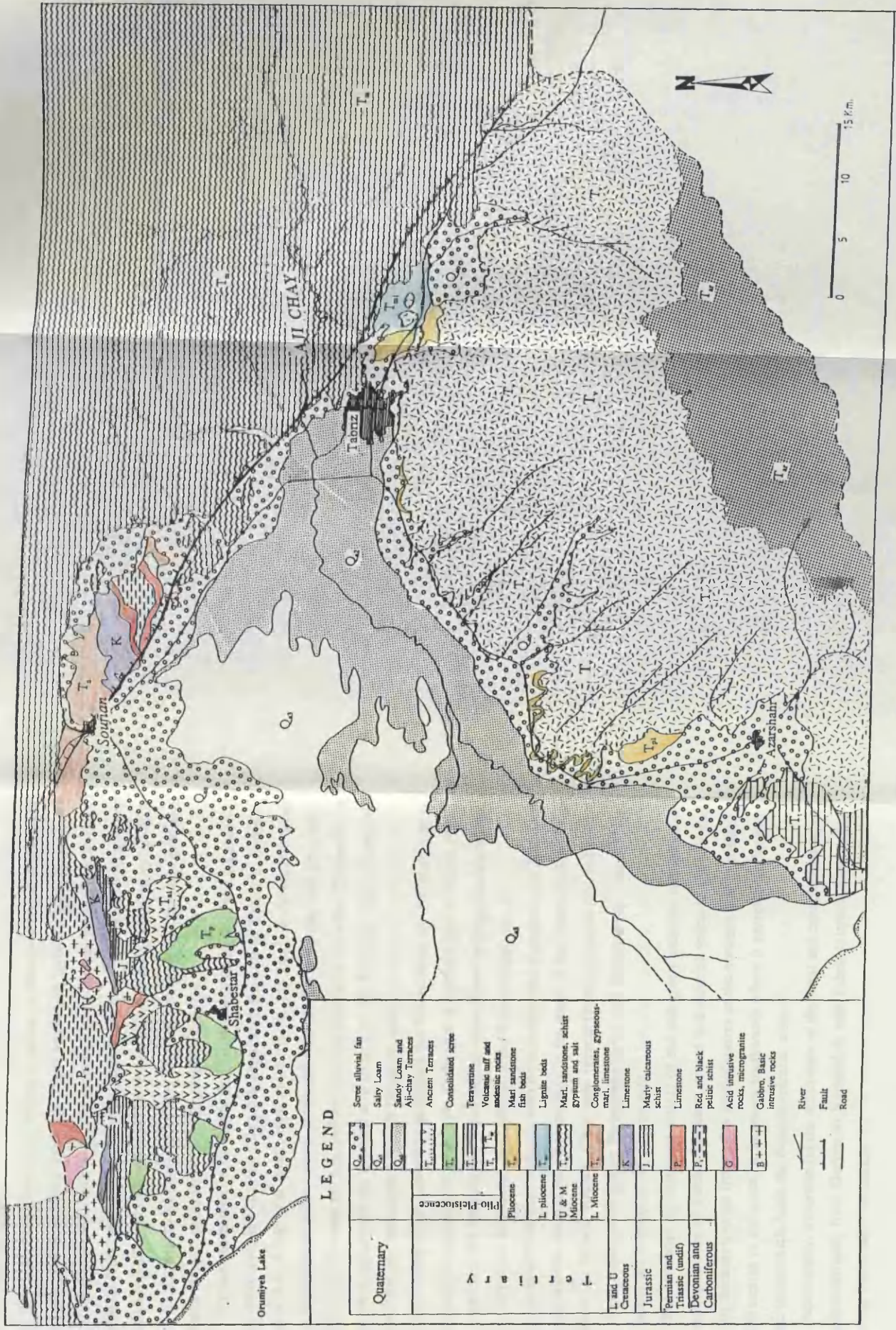
### **3.2 Litho-Stratigraphy**

Palaeozoic sequence outcrops are better developed in the Mishow than the Morov mountains. These formations surround and underlie the Quaternary deposits (see Fig 3.1). The Devonian-Carboniferous sediments and metamorphic rocks occupying the above-mentioned mountains have a thickness between 500 to 1000 metres (ELC-Electroconsult, 1969). They consist of pelitic schists, some limestone and quartzite all disturbed by igneous intrusions.

The Permo-Triassic black bituminous limestone with an average thickness of 75 m is formed only in the Mishow and Morov mountains.

In addition to those of the Mishow and Morov area, Jurassic and Cretaceous limestone formations are widely exposed in the western part of Sahand as well as the southern rim of the Tabriz Plain. The thickness of the Jurassic limestone unit (Lar, Dalichay and Shomshak formations) averages some 100 metres, with the Cretaceous limestone being thicker but largely undetermined. The Jurassic formation consists of marly calcareous schists and sandstone whereas the Cretaceous limestone is made up well bedded grey and black limestone.

According to the Iranian National Oil Company (1978), the Eocene-Oligocene andesite and trachyte volcanic rocks are exposed in the higher elevations of the Sahand volcanic mountain. Additionally, the ELC-Electroconsult Water Company (1969) reported the possibility of the calcareous series underlying the Miocene series



**LEGEND**

Geological Unit	Description	
Quaternary	Q <sub>4</sub> (Dotted pattern)	Some alluvial fan
	Q <sub>3</sub> (Horizontal lines)	Salty Loam
	Q <sub>2</sub> (Vertical lines)	Sandy Loam and Aji-chay Terraces
Tertiary	T <sub>1</sub> (Diagonal lines)	Ancient Terraces
	T <sub>2</sub> (Stippled)	Consolidated silt
	T <sub>3</sub> (Horizontal lines)	Terravene
	T <sub>4</sub> (Vertical lines)	Volcanic tuff and andesite rocks
	T <sub>5</sub> (Stippled)	Mari sandstone fish beds
	T <sub>6</sub> (Diagonal lines)	Lignite beds
	T <sub>7</sub> (Stippled)	Mari, sandstone, schist
	T <sub>8</sub> (Vertical lines)	Syrgan and salt
	T <sub>9</sub> (Stippled)	Conglomerates, gypsum-salt, limestone
	T <sub>10</sub> (Stippled)	Limestone
L and U	L (Stippled)	Mari calcareous schist
	U (Stippled)	Limestone
Jurassic	J <sub>1</sub> (Stippled)	Red and black pelitic schist
	J <sub>2</sub> (Stippled)	Red and black pelitic schist
Permian and Triassic (undif)	P <sub>1</sub> (Stippled)	Acid intrusive rocks, microgranite
	P <sub>2</sub> (Stippled)	Acid intrusive rocks, microgranite
Devonian and Carboniferous	D <sub>1</sub> (Stippled)	Gabbro, Basic intrusive rocks
	D <sub>2</sub> (Stippled)	Gabbro, Basic intrusive rocks

Fig. 3.1 Geological map of the study area.

in the Mishow mountain.

The Upper Red Formation (Miocene series) is widely exposed in the north-eastern part of Tabriz Plain, made up of red marls with gypsum and conglomerate with a total thickness of about 150 metres. The sequence passes upwards into alternations of red sandstone, marls with conglomerate and salt, overlain by gypsum, clay, lignite and marly limestone. The thickness of this sequence is up to 1000 metres. In consequence, the water quality of rivers crossing this series is generally saline and abundantly charged with suspended solids.

Pliocene beds overlie the Upper Red Formation with normal and undisturbed contact (Nowtash, 1984), where they are exposed to the east of Tabriz in Bareng, Gorjan and in Anakhaton (north-west of Tabriz) in the Bareng Formation. They consist of lacustrine yellow marl, sandstone with sand and lignite, and grey, blue, greenish clay. Towards the top, yellow marl and clay with so-called "Fishbeds" as well as sand and gravel are exposed in a cutting on the Basminj- Tabriz Road. All of these Pliocene formations are over 60 metres thick.

According to Oil Company geologists the fish-remains are the same age as the Mamagan Formation (located in the study area in southern part of Tabriz Plain) which extends to the foothills of the Sahand mountain. Some hydrogeologists believe that this formation constitutes the bedrock of the Tabriz Plain.

The Plio-Pleistocene volcanic tuffs have an extended exposure over 2000 km<sup>2</sup>, and conformably overlie the Pliocene beds to the south of the Tabriz Plain around the core of the Sahand volcano. They were formed from pyroclastic material blown out of the Sahand vents during Pleistocene times and subsequently reworked by water, hence the description of alluvial tuff.

The formation is composed mainly of red and green andesitic tuff admixed with large quantities of blocks, boulders, gravel and sand of volcanic and alluvial origin. Its thickness varies from a few tens of metres at the northern end to possibly over 500 metres in the south. It increases southwards where it passes laterally into andesitic lavas which flank the Sahand volcanic area.

Additionally, travertine (in the south-west of the area) and consolidated scree and ancient terraces, from Daryan to Nematollah and Tabriz Airport, form minor parts of the Pleistocene formation.



The Quaternary fluvial deposits have their major outcrop in the Tabriz Plain which forms more than one third of the project area. The alluvium, fans and recent Aji Chay terraces consist of numerous beds of gravel and sand, separated by and grading into silt and clay. They are coarse and very poorly sorted in the fans and the highest parts of the Plain and become progressively finer and more clayey towards the central part and particularly near the Orumiyeh Lake, which is flanked by a salty loam and huge clay plug.

According to the well drilling logs and geophysics, the thickness of the alternating gravel, sand and clay layers ranges from a few metres to 120 metres. The maximum thickness and gravel-sand percentage occur in fans on an axis from Tabriz toward Qezel Dizeh and Qeshlag (southern and northern parts of the Plain). Lesser thicknesses were revealed in the eastern part of the Plain, being coupled with a gentle Miocene bedrock updoming. Additionally, recent deposits and sand dunes are distributed in a few parts of the Tabriz Plain centre.

A summary of the stratigraphic sequence of the project area is shown in Table number 3.1 with the younger strata uppermost.

From the ground water view point, the most important geological formations of the investigation area are the Upper Red Formation (Miocene series), volcanic tuffs (Plio- Pleistocene) and Quaternary deposits. Thus, the pre-Miocene sedimentary and metamorphic rocks have much less effect on ground water availability and quality in the area.

### **1.3. Geological Structure**

The North Tabriz Fault is the most important tectonic structure in the immediate vicinity of Tabriz City (see Fig. 3.1). It continues along the foot of the northern mountains near Tabriz for about 100 km from Mishow mountain in the west to Bostanabad in the east. The fault trace is approximately N 115° E and its dip is vertical.

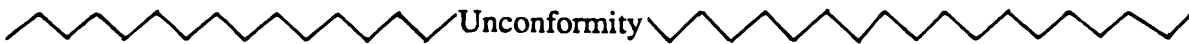
Over its central part, between Soufian and to north of Tabriz City, the North Tabriz Fault forms a well marked boundary between the Miocene Upper Red Formation rocks and Quaternary alluvial deposits of the Tabriz piedmont zone, upthrusting the Miocene rocks against the alluvial deposits.

In the west, the North Tabriz Fault separates Morov mountain from the alluvial deposits. In the east and near to Tabriz it cuts the Miocene marls and continues to Bostanabad in the south-east. According to Berberian (1976), to the east of Soufian (in Cheleh-Khaneh village) the Fault is well marked with a downthrow of the southern block of about 80 metres. The North Tabriz Fault near the surface has a vertical fault plane and the southern block is downthrown by an average 40 metres. It is believed that this fault is a post-Pleistocene age. However, according to Eftekhar-nezhad (1975; in Berberian, 1976) the North Tabriz Fault is an old geological fault which has been reactivated during different periods. He believes that this was a very important tectonic phenomenon of the early Devonian.

Another geological structure existing in the area is the strong folding of the Mishow mountain rocks with their east-west strike and similar direction of faulting. However, the Morov mountain is folded in a southeast-northwest direction.

According to the Electroconsult Water Company (1969), the Pliocene beds which underlie the Sahand mountain tuffs dip south-wards. The bedrock of the Tabriz basin (Pliocene and locally Miocene) is gently disturbed in the eastern part of the plain by Miocene updoming.

**Table 3.1 Stratigraphic sequence in the project area (after ELC-Electroconsult, 1969).**

Age	Lithology	Thickness(m)
Quaternary	-Recent deposits, sand dunes, fans, recent terraces	
	-Brown loam and clay	10-25
	gravel and sand, silt clayey material	15-60
	gravel and sand	5-50
		up to 200
Plio-Pleistocene	-Ancient terraces, consolidated scree, travertine -Reworked volcanic tuffs	up to 550
Pliocene	-Yellow marl and clay(fish beds) with sand and gravel	
	-Lacustrine yellow marl and sandstones with sand and lignite, gary-blue, greenish clay	
		over 60
Miocene	-Gypsum, clay, lignite, marly limestone	
	-Breccia, sandstone, red sandstone and marl sandstone, cong. Salt domes	1000
	-Red, ochre marls with gypsum,cong.	150
 Unconformity		
Eocene-Oligocene	-andesitic, trachytic lava flow; limestone and sandstone	
Cretaceous	-Well bedded gray-black limestone	
Jurassic	-Marly, calcareous schists; sandstone and limestone	100
Permo-Triassic	-Black, bituminous limestone	75
Devonian and Carboniferous	-Red pelitic schists and quartzite	
	-Calcareous schists and black limestone	
	-Thick, black pelitic schists (intrusions of microgranite, gabbro and diorite)	
		500-1000

## **CHAPTER 4**

### **HYDROGEOLOGY**

#### **4.1 Introduction**

#### **4.2 Aquifer Systems**

##### **4.2.1 Types of Aquifer**

##### **4.2.2 Boundaries and Thicknesses of Aquifers**

#### **4.3 Ground Water Level Fluctuations**

##### **4.3.1 Long Term Fluctuations**

##### **4.3.2 Seasonal Fluctuations**

#### **4.4 Ground Water Contour and Flow Maps**

##### **4.4.1 Introduction**

##### **4.4.2 Flow in Relation to Minimum Ground Water Contours**

##### **4.4.3 Flow in Relation to Maximum Ground Water Contours**

##### **4.4.4 Annual Ground Water Fluctuation Map**

###### **4.4.4.1 Estimation of Replenishment**



## CHAPTER 4

### HYDROGEOLOGY

#### 4.1 Introduction

The geological conditions of the study area were explained in the previous chapter, so only the aquifer systems, thicknesses and boundaries will be considered in this chapter. Within the approximately 7500 km<sup>2</sup> study area, only 42 percent contains good water-bearing layers. The pre-Quaternary rocks except the Plio-Pleistocene tuff, generally have the nature of an aquiclude or are very poor aquifers. However, the superficial weathered strata can store and transmit some ground water. Palaeozoic and Mesozoic limestones provide poor aquifer conditions due to their fissured and jointed nature. The Eocene-Oligocene and mainly Miocene gypsum-rich sandy and clayey red marls penetrated by salt domes are definitely aquicludes and are the major sources of salt for the rivers flowing through them.

The Quaternary, semi-pervious, salty loam and clay in the western part of the central plain (roughly below 1300m elevation) is characterized by high water table conditions, with a surface drainage pattern insufficient for the complete removal of water that falls onto it. Therefore, all the above mentioned formations have the status of an aquiclude and there is no point in making a more detailed hydrogeological investigation about this area. Figure 4.1 shows the locations and the types of aquifers in the study area.

#### 4.2 Aquifer Systems

##### 4.2.1 Types of Aquifer

The Alluvial Tuff aquifer, the most important aquifer in the area, has been known for many years as a good aquifer, through qanats, geophysics and an uneven distribution of drilled wells. It has been extensively developed for public water supply and investigated hydrogeologically, particularly in connection with ground water development.

The Plio-Pleistocene tuff is composed mainly of red and green andesitic tuff admixed with large quantities of blocks, boulders, gravel and sand of volcanic and

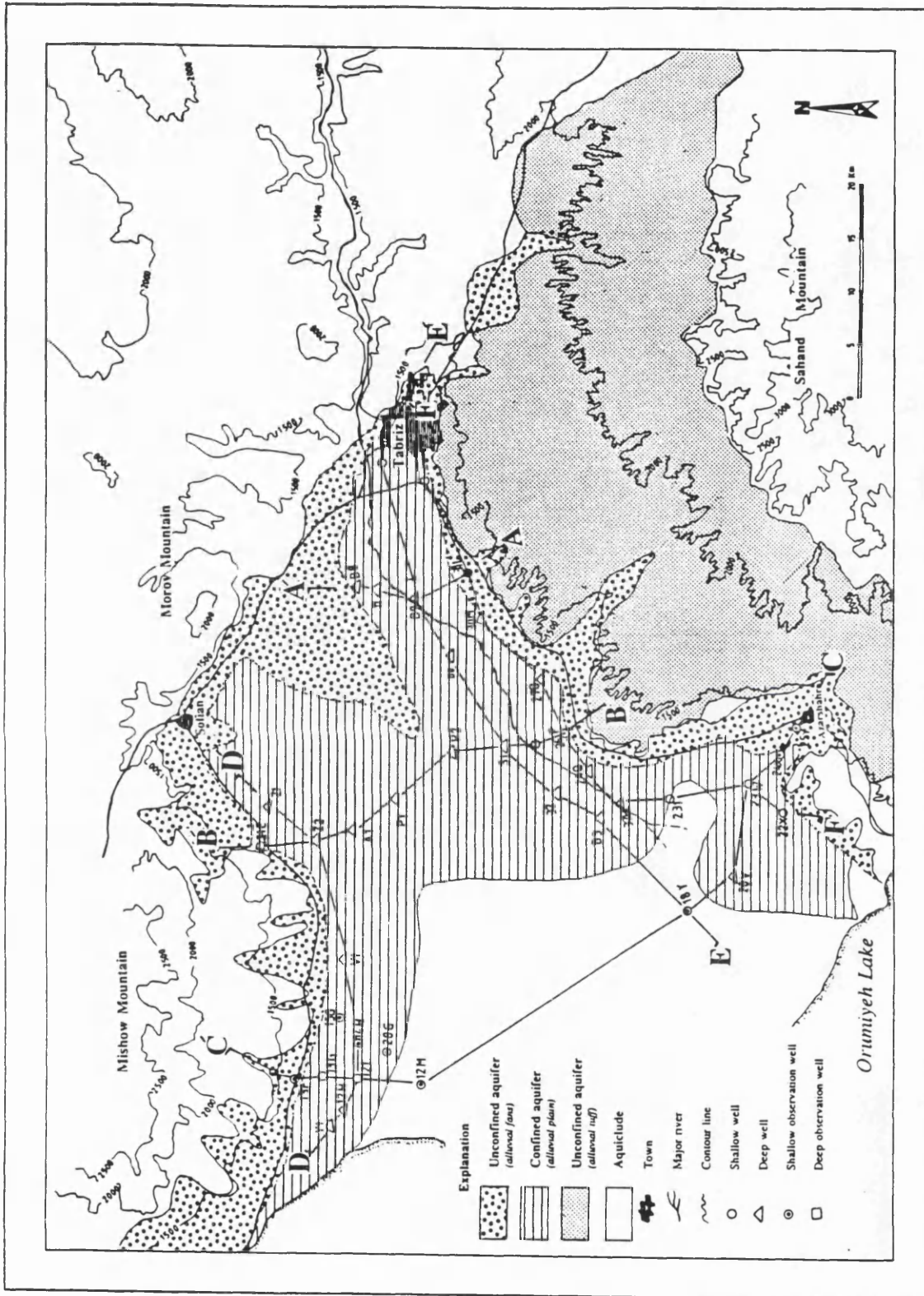


Fig. 4.1 The aquifer systems in the study area.

alluvial origin. In some places, these formations are separated by a local impermeable conglomerate or agglomerate horizon (Geop. Inst. Israel, 1964; Moinvaziri et al., 1975). In general, however, the alluvial tuff aquifer is unconfined, with water level depth changes according to topographical and subsurface geological conditions. For example, the water level is over 100 metres below ground level in the southernmost parts of the area and gradually gets closer to the ground surface towards the Plain.

In the Tabriz Plain itself, there are two types of aquifers; (1) an unconfined aquifer which includes the southern, northern and central alluvial fans and pervious terrace materials, and (2) the multi-layer aquifer system which mainly lies in the central plain as well as in the Aji Chay and Mehran Chay (the river that cross Tabriz City) river terraces and buried channel formations. Figures 4.2 and 4.3 show some geological cross sections from south to north and west to east which were deduced from the correlation of the drilling wells results (after ELC-Electroconsult, 1970). In these cross sections, the great distances between the wells reduces the reliability of the results. However, a geological cross section through exploratory and observation wells in Figure 4.4 (after IRAB, 1976) indicates good correlation between the electrical resistivity logs and gives an unequivocal result for the aquifer systems in the Tabriz Plain. The well-known, fresh water aquifers consist of alternating layers of sand and gravel lying between about 58 and 120 m depth. Water in the upper sands and gravels are brackish as indicated from shallow wells in the area.

#### **4.2.2 Boundaries and Thicknesses of Aquifers**

In addition to some drilled wells, geo-electrical and seismic refraction surveys have been established to determine the thickness, limitations and water-bearing qualities of the alluvial sand and gravel in the Plain and of the alluvial tuff in the mountain areas (Geop. Inst. Israel, 1964; Abkav Consulting Engineers, 1976).

The resultant isopach maps of these investigations (Figs. 4.5 and 4.6), in combination with data from the drilled wells, have provided detailed information from the aquifers and also allowed a comparative consideration of the reliability of these field works. According to the geophysical investigations and drilled wells in the Saidabad area, the thickness of the alluvial tuff increases from the north to the south where it passes laterally into andesitic lavas (see Fig. 5.8). The highest estimated

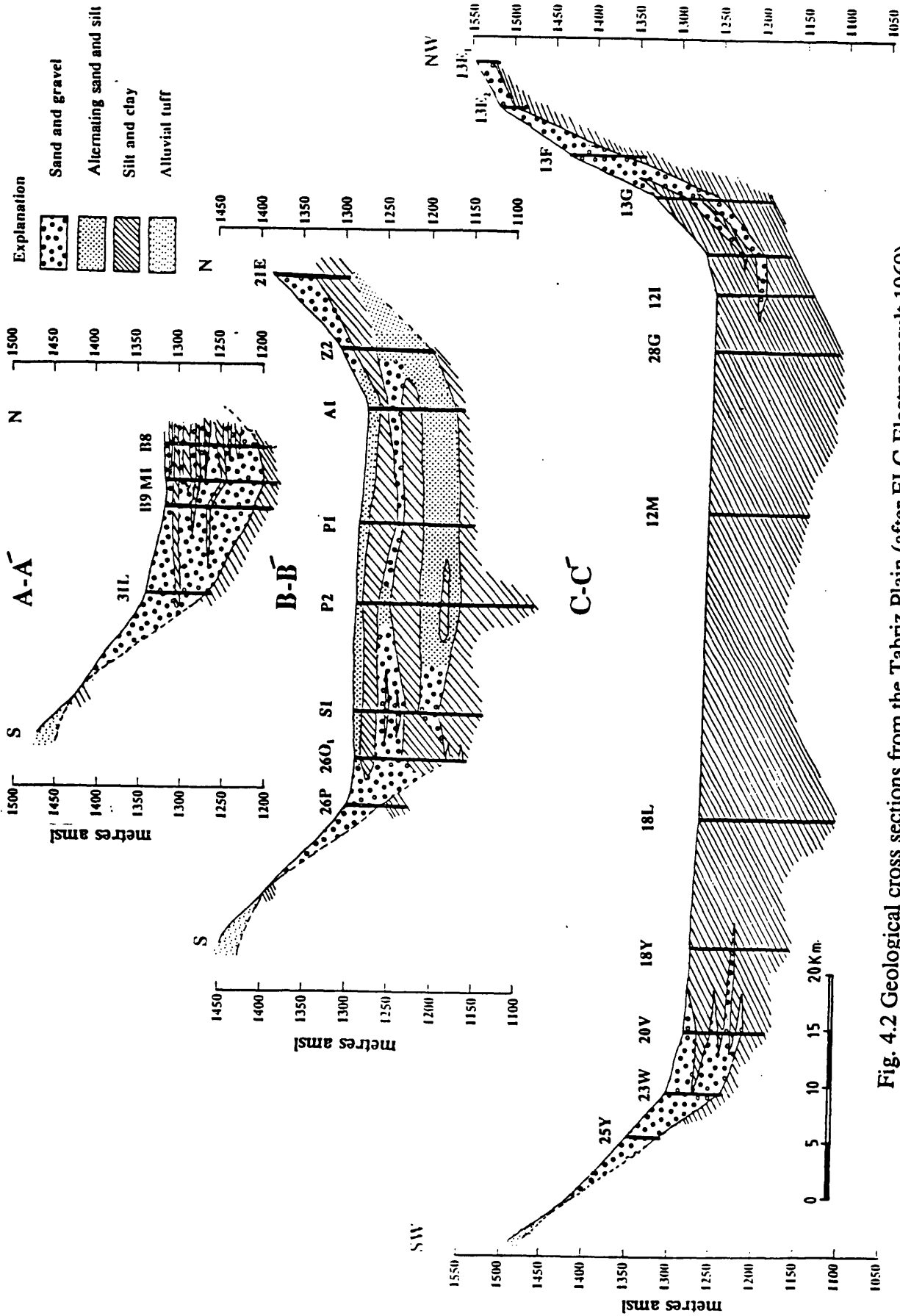


Fig. 4.2 Geological cross sections from the Tabriz Plain (after ELC-Electroconsult, 1969).

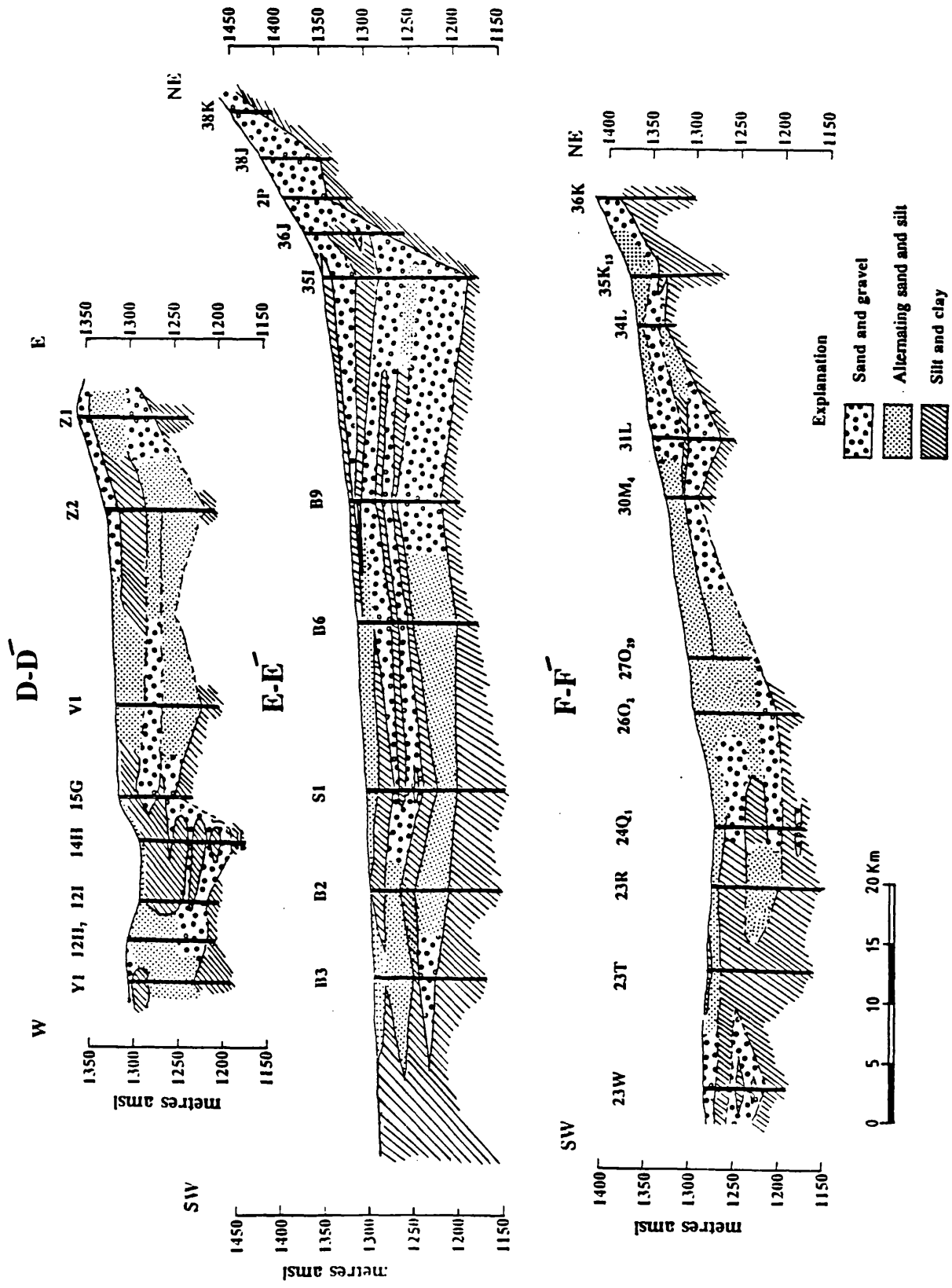


Fig. 4.3 Geological cross sections from the Tabriz Plain (after ELC-Electroconsult, 1969).





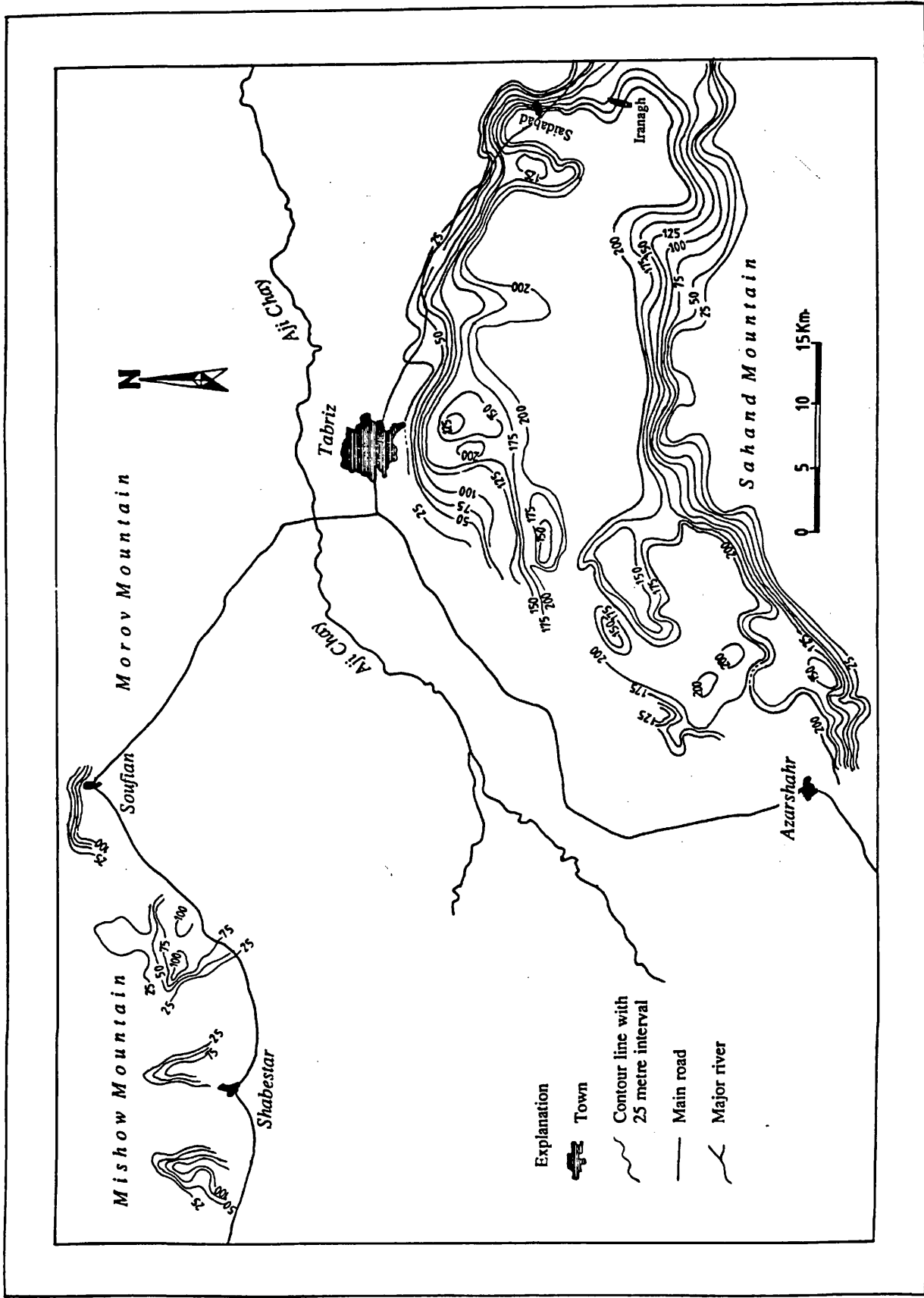


Fig. 4.5 Isopach map of the alluvial tuff and fans (after Abkav Co., 1978).

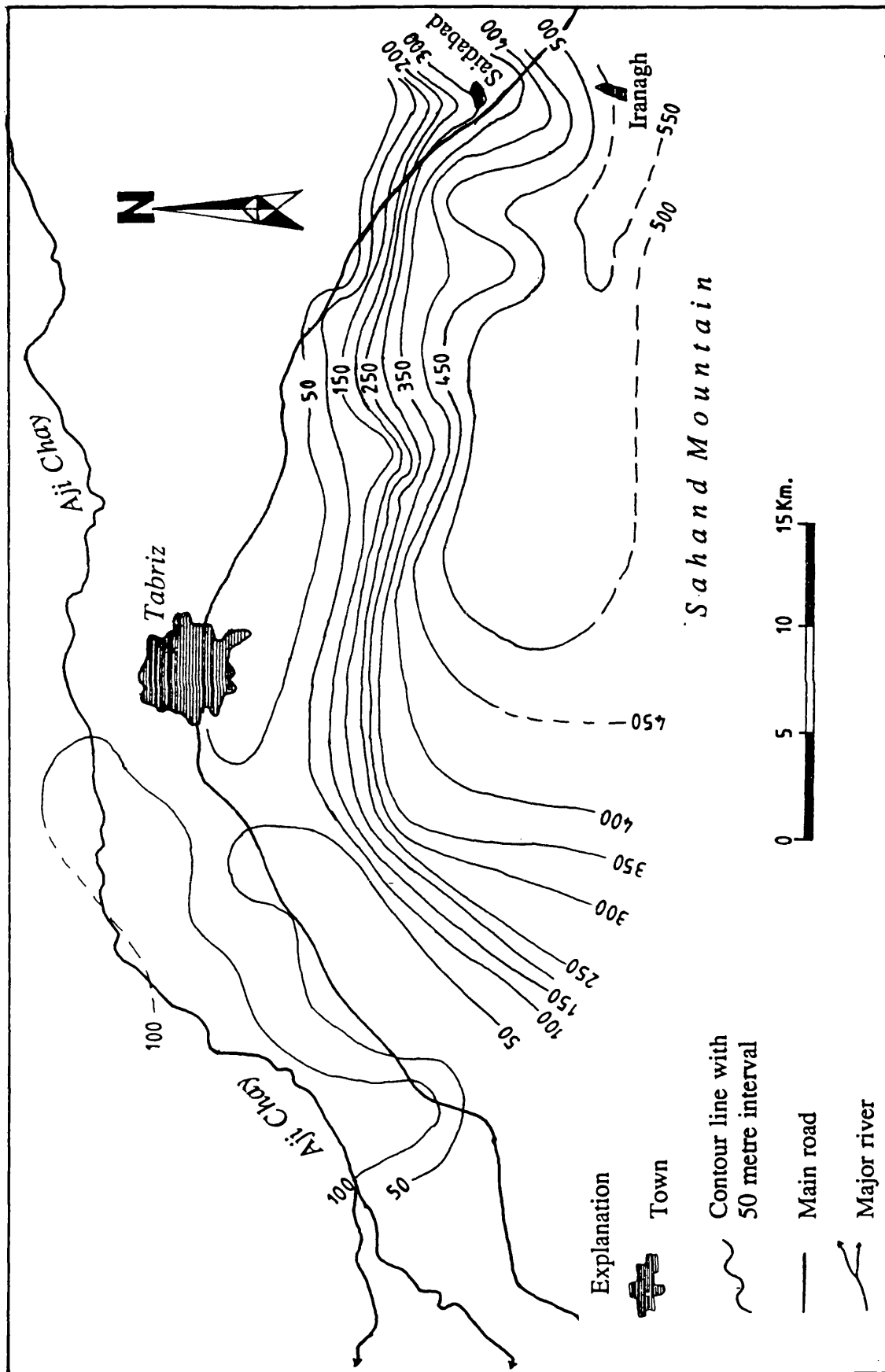


Fig. 4.6 Isopach map of the alluvial tuff and fans (after Geoph. Inst. Israel, 1964).



thickness of the alluvial tuff lies in this area, with an average thickness of 350 metres (average of two above mentioned geophysical investigations and exact values resultant from drilled wells).

In some areas, the boundary between alluvial tuff and southern alluvial fans is a geomorphological boundary between the Plain and mountain. While in other areas, they are separated by Pliocene marls and fish-beds which lie below the tuff (see Fig. 4.1). The southern fans and alluvial tuff are bordered to the north and north-east by upper and middle Miocene and Pliocene marl, sandstone, schist, gypsum and fish-beds; to the south by the andesitic lavas of the Sahand mountain; to the west and north-west by the Jurassic marly calcareous schist and Plio-Pleistocene travertine and Quaternary sand and salty loams respectively. There is no complete ground water continuity between the southern and northern alluvial fans of the Tabriz Plain since they are separated by the salty and sandy loams of the Central Plain.

The thickness (maximum 100m) of the unconfined Tabriz Plain aquifer decreases towards the mountain as well as towards the central part of the Plain areas, with average thickness of about 50m.

### **4.3 Ground Water Level Fluctuations**

Ground water level fluctuations can result from a wide variety of hydrological phenomena, some natural, such as ground water recharge, evaporation, bank-storage effects, earthquakes, and meteorological phenomena, and some man-induced, such as ground water pumping, deep well injection, artificial recharge and agricultural irrigation and drainage. In many cases, there may be more than one mechanism operating simultaneously and if measurements are to be correctly interpreted, it is important that the various phenomena be understood.

The time variations in ground water level can be considered as (a) long term, (b) seasonal, and (c) short term durations. In overdeveloped basins, where extraction exceeds recharge, a downward trend in ground water levels may continue for many years. The seasonal fluctuations usually result from influences of rainfall, bank-storage, and irrigation pumping, all of which follow well-defined seasonal cycles. The short-term fluctuations can occur due to air entrapment during ground water recharge, external loading of confined aquifers and earthquakes. However, there are no

measurements of short-term fluctuations in ground water levels in the study area. Therefore, only the long-term and seasonal fluctuations will be considered.

#### **4.3.1 Long-Term Fluctuations**

Monthly fluctuations of ground water level have been measured in the confined and unconfined aquifers of the Tabriz Plain for a long time. But, unfortunately, there are no water level measurements in the alluvial tuff aquifer which supplies the major proportion of drinking and domestic water for Tabriz City and some of its adjacent towns. The measurement of water level fluctuations in such an aquifer should be essential in order to detect long-term declines in water levels due to aquifer exploitation.

Figure 4.7 shows the locations of the ground water level monitoring wells situated in the Plain. Data obtained from 40 of these wells (especially those are located in fresh water areas) are plotted on arithmetic scale as well hydrographs (see Figs. 4.8 to 4.10 and Appendix 4). The decline of ground water levels is indicated in wells 28I-4S, 26I-1D, 34L-1S, 32M-3D, 30R-1S and 24I-1S (see Fig. 4.8) which are located in the alluvial fans of the northern and southern parts of the Tabriz Plain. The maximum decline of water levels occurs in wells 26I-1D and 28I-4S with about 6 to 8 metres over the 4 to 5 year period. It appears that the decline of water levels is mainly due to the intensive withdrawal of ground water in the area for agricultural purposes.

An unusual response is seen in Figure 4.9 which illustrates the rise of ground water level in well 37K-1D located in western part of Tabriz City. Such long-term rise of ground water levels in this area is believed to be due to the intensive use and recharge of domestic water into the aquifer.

From above discussions, it can be concluded that the long-term fluctuations of ground water level in the area depend on man-induced operating mechanisms and the availability of recharge water.

#### **4.2.2 Seasonal Fluctuations**

Seasonal fluctuations of ground water levels operate in most of the monitoring wells. However, their intensity and periods are generally different. The maximum

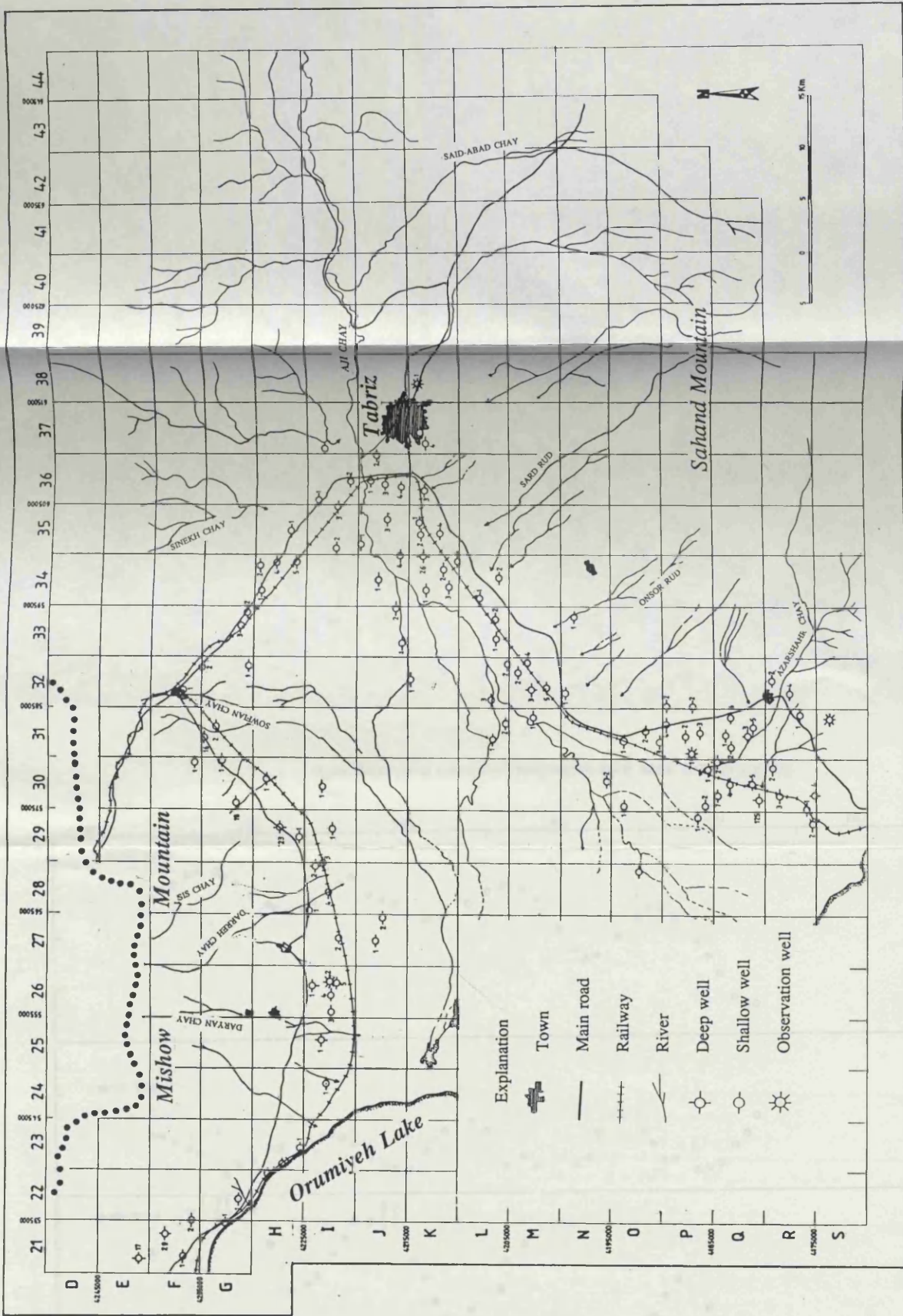


Fig. 4.7 Location of the ground water levels monitoring wells.

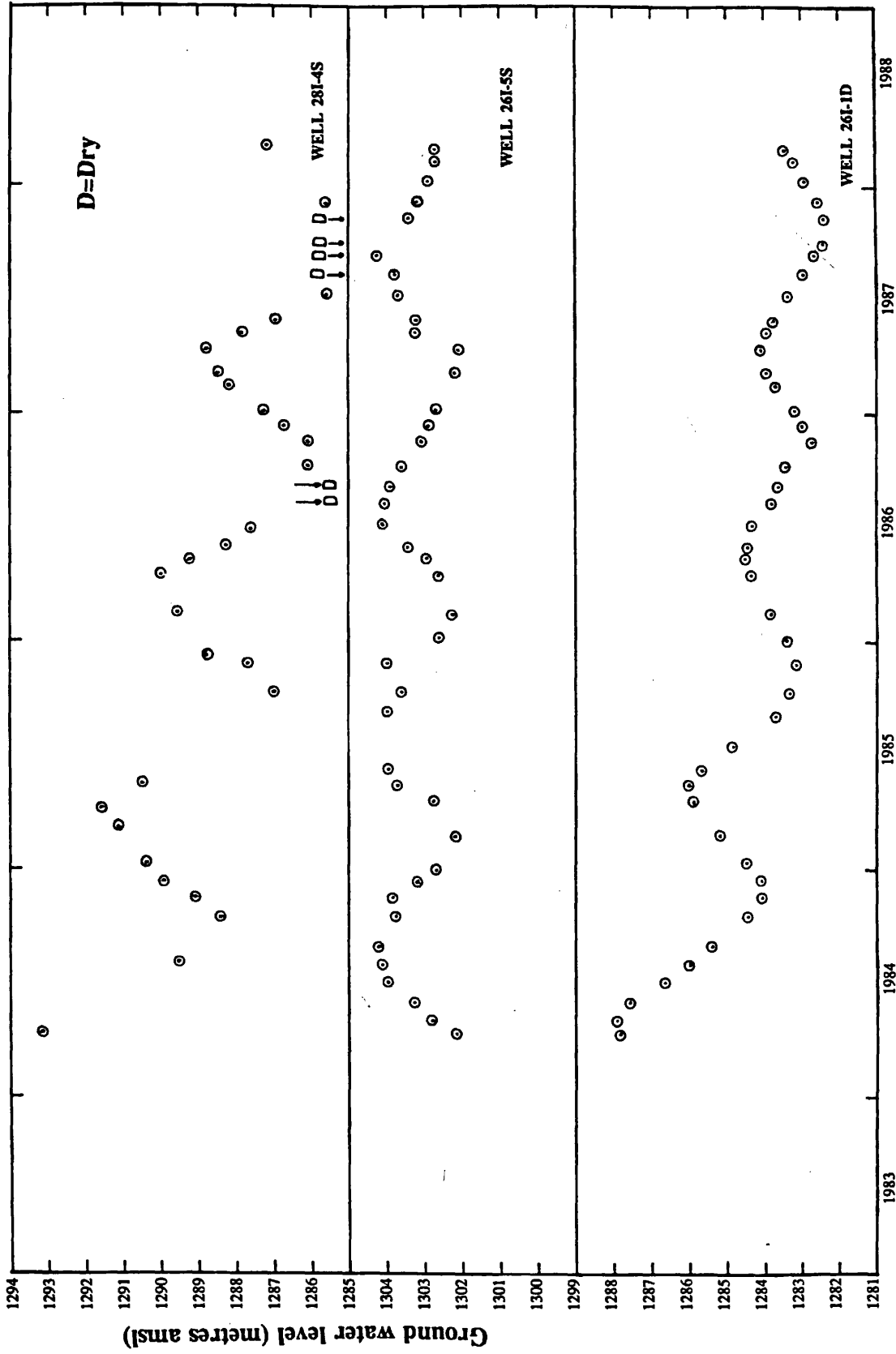


Fig. 4.8 Ground water level fluctuations in selected monitoring wells.

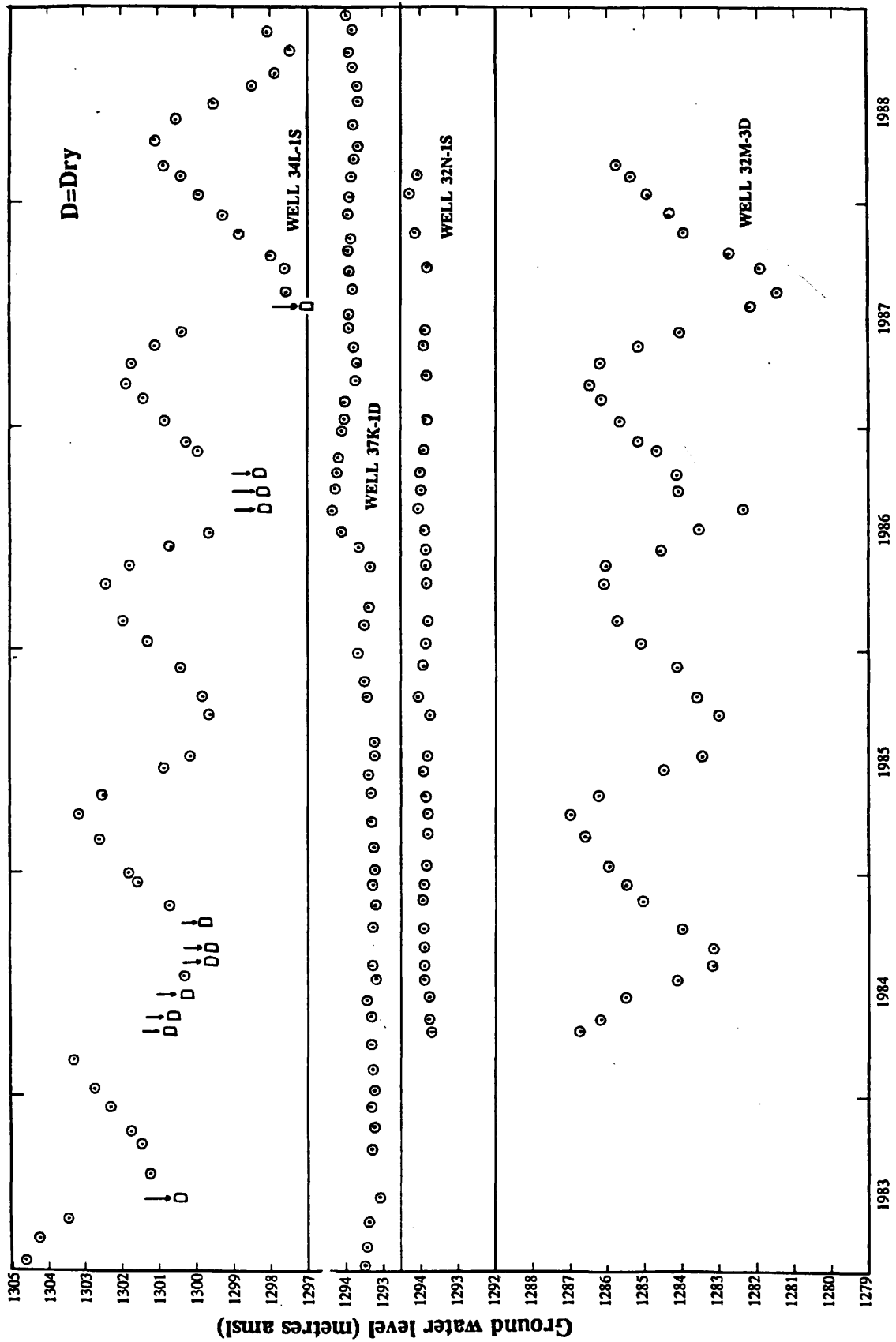


Fig. 4.9 Ground water level fluctuations in selected monitoring wells.

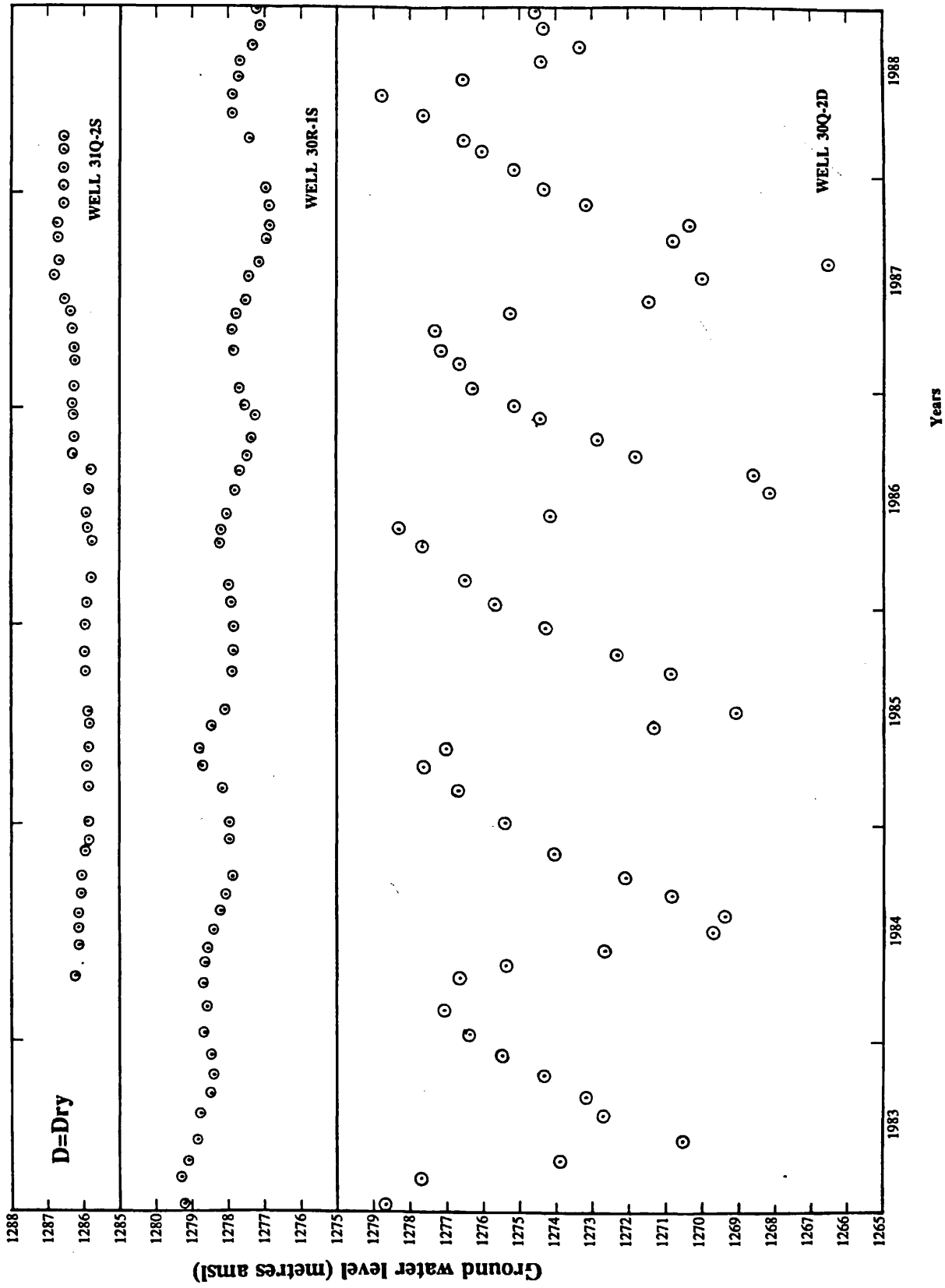


Fig. 4.10 Ground water level fluctuations in selected monitoring wells.

seasonal fluctuations occur in the most western part of the area at well 30Q-2D, located in the end of the River Azarshahr. The average fluctuation of ground water here is about 10 metres over a period of 6 years (see Fig. 4.10). It appears, that these fluctuations result from at least two simultaneous mechanisms such as river water recharge effects and high pumping abstraction of ground water both of which follow a well-defined seasonal cycle. The main reason for the effect of river water recharge is the coincidence of the ground water level rising with stream flow variations.

In general, it may be concluded that the well-defined water level fluctuations are in related with rainfall, losing (i.e influent) rivers, and large abstraction of ground water from the aquifer. In areas with poor quality ground water, the amplitude of these fluctuation is small due to the lower abstraction of ground water. The differences in period of fluctuations depends on the distance of recharge area from the well locations as well as the hydraulic conductivity of the aquifer.

#### **4.4 Ground Water Contour and Flow Maps**

##### **4.4.1 Introduction**

There are 120 deep and shallow wells on the Tabriz Plain in which ground water levels have been monitored monthly. All measurements of depth to the water table are made from a bench mark (fixed at ground level at the edge of well) in metric units. Thus, the measured water levels can be conveniently converted to elevation above mean sea level (amsl).

Data obtained from most of above-mentioned wells have been used to construct the minimum and maximum potentiometric maps for the period 1987. The contour lines are drawn using a 5-metre interval. A maximum fluctuation contour map has been prepared with data determined by subtracting the elevation of minimum water table from the maximum water table in all the wells during the year 1987. The major flow direction map was constructed from the maximum and minimum water level elevations.

Contour maps of static water level are useful for (a) measurement of the hydraulic gradient which can be a measure of the ground water potential, (b) location of new wells, using assumptions that convex contours indicate region of ground water

recharge, while concave contours are associated with ground water discharge, as well as a wider contour spacing representing a decreasing hydraulic gradient, which in turn suggests a more permeable condition, and (c) construction of a flow net map which enables the indication of the major flow directions.

The main principles for the sketching of the flow lines can be summarized as (1) the direction of flow is always from higher elevation (potential) to lower elevation (potential); (2) flow lines and contour lines must intersect at right angles throughout the region; and (3) flow lines must be parallel to impermeable boundaries.

#### **4.4.2 Flow in Relation to Minimum Ground Water Contours**

Figure 4.11 shows the minimum ground water level contour map for the driest season of year 1987 (Oct.1987). During this period, the water levels declined to their minimum elevation due to the dry, hot summer and autumn and also due to the maximum withdrawal of ground water from storage for agricultural purposes.

A very distinctive decline in water levels occurred at the southern margin of the Tabriz Plain in the Sardrud, Khosrowshahr, and Azarshahr sub-basins. The reason for this is the highly fertile croplands and fruit trees in this region. The closed contour lines and reverse flow directions show the locations of these heavily pumped areas.

It is apparent from the geomorphology (see Chapter 2) that the slope of the land surface decreases toward the central plain. Ground water hydraulic gradients are usually subdued replicas of the land surface, and the close spacing between the contour lines in the steep part of the Plain is the consequence of the topographical feature. However, in the south-west part of the Plain (in the Azarshahr sub-basin) the reverse flow of ground water due to artificial discharges is quite clear and contamination of fresh water by saline water intrusion has been reported.

Contour maps of ground water level, together with flow lines, provide useful information about the responses of ground water and also its possible relationship with river flow. The contour lines in the northern sub-basins and along the River Aji Chay show a concave shape along the channel with their flow line directions, which mean that the rivers behave as losing streams. However, most of them in their extreme upstream sections (which are not shown in this map) have the characteristics



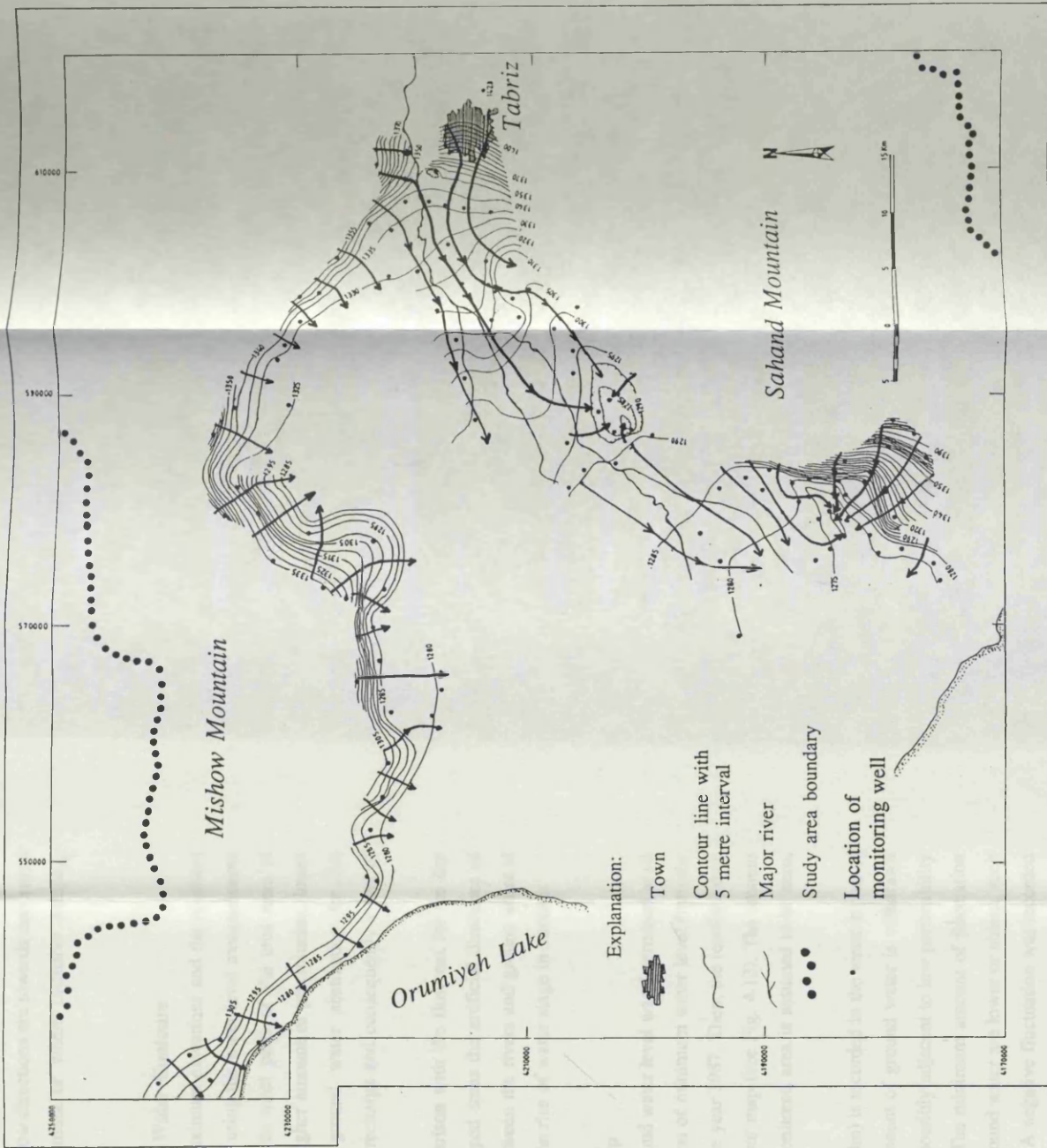


Fig. 4.11 Ground water contour and flow map for dry period (Oct. 1987).

of gaining rivers. In general, the ground water flow directions are towards the central plain except where they meet impermeable strata or where intensive pumping reverses the flow direction.

#### **4.4.3 Flow in Relation to Maximum Ground Water Contours**

The ground water level contours for maximum elevations and the resultant flow nets map (see Fig. 4.12) were prepared by using the water level measurements for May 1987 when the ground water levels in most parts of the area were at maximum elevations. During this period, the higher amount of precipitation, lower rate of evapotranspiration, and absence of ground water abstraction for the agricultural purposes led to a high amount of recharge and consequently a rise of ground water level throughout the area.

The general direction of flow in comparison with the flow net for the dry period is more natural, though in heavily pumped areas the artificial directions of flow are still in operation. The relationship between the rivers and ground water is also more clear than in the dry period due to the rise of water stage in streams.

#### **4.4.4 Annual Ground Water Fluctuation Map**

The maximum annual fluctuation in ground water level was determined at all the monitoring wells by subtracting the elevation of minimum water level from the elevation of the maximum water level during the year 1987. Then, the resultant data were used to draw the annual fluctuation contour map (see Fig. 4.13). The amount of fluctuation at the outer boundaries of the monitored area is assumed to be zero, though in some areas this is not the case.

The maximum amount of fluctuation (13m) is recorded in the western part of the Azarshahr sub-basin, where the greatest amount of ground water is withdrawn during the dry period and where the aquifer is possibly adjacent to low permeability media as well as a local limestone aquiclude. The minimum amount of fluctuation mainly occurred where the abstractions from ground water are lower or absent, such as the north-east and central parts of the Plain. A negative fluctuation was recorded in the western part of Tabriz City (-0.3m) which implies a rise in water level during the dry period. A possible explanation for the rising water level could be that more

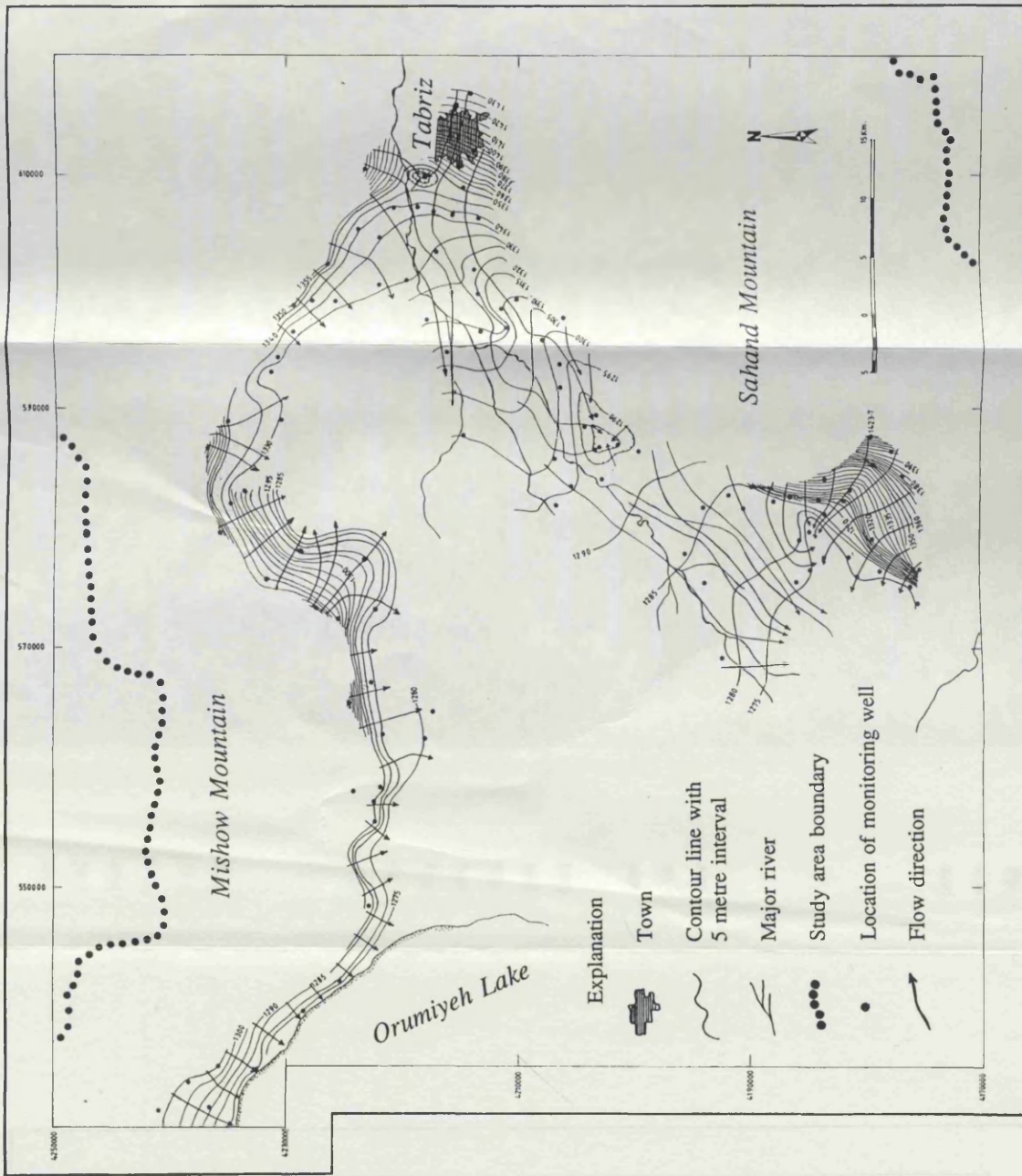


Fig. 4.12 Ground water contour and flow map for wet period (May 1987).



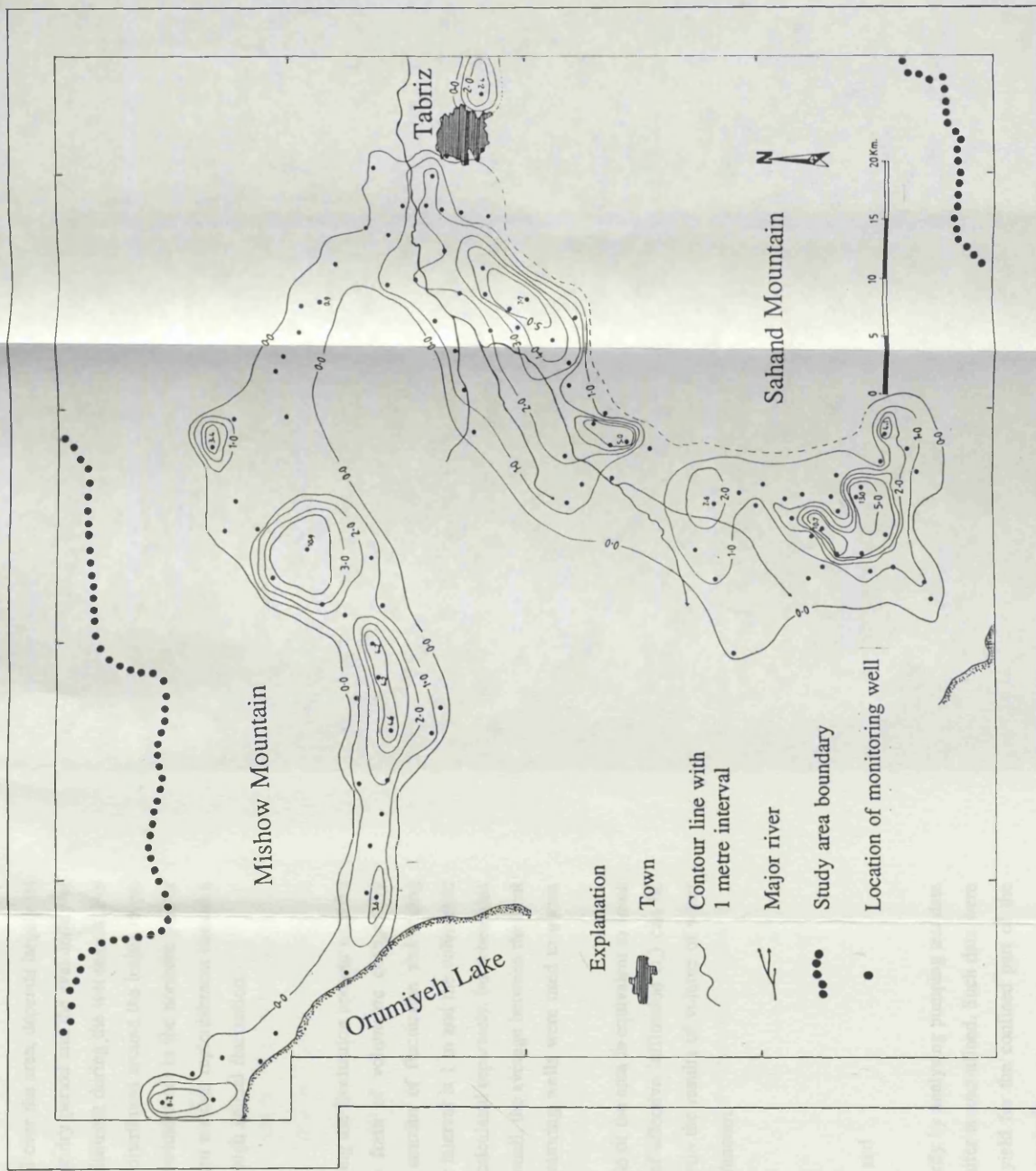


Fig. 4.13 Annual maximum fluctuations contour map of ground water (1987).

water recharges via losses from the municipal, industrial and irrigation water into the aquifer.

The high amount of annual fluctuation, all over the area, depends largely on the amount of ground water withdrawal during the dry period and the availability of enough surface water resources to provide replenishment during the wet season. For this reason, the high annual fluctuation areas are distributed around the losing rivers in the region. The high amount of ground water withdrawal in the northern part of the Plain around wells 28I-4S and 26I-1D without enough replenishment caused a long term decline of ground water rather than a high annual fluctuation.

#### 4.4.4.1 Estimation of Replenishment

The annual replenishment is estimated using the fluctuation contour map for year 1987 (Fig. 4.13). It is calculated in the form of volumetric changes by multiplying the area involved by the average amount of fluctuation and taking account of the available void space. The contour interval is 1 m and the volumetric changes between two consecutive contours were calculated separately, but where this interval is not met or the contour spacing is too small, the average between the final contour and direct calculated values for the monitoring wells were used to obtain better results which are displayed in Table 4.1.

The total volumetric changes for the whole of the area is equivalent to some  $2.1 \times 10^9$  m<sup>3</sup>/year . Therefore, the total amount of effective infiltration ( $I_e$ ) can be calculated from the following expressions to obtain the results of volume of water (m<sup>3</sup>/annum) as well as in terms of height in mm/annum.

$$I_e = W_y \times S_y$$

$$I_e = [(W_y \times S_y)/A]$$

where  $W_y$  = total volumetric change

$A$  = area over which recharge occurred, and

$S_y$  = specific yield.

The specific yield can be determined directly by analysing pumping test data obtained from an observation well, when the aquifer is unconfined. Such data were not available from the study area. The specific yield for the confined part of the aquifer cannot be determined from pumping test analysis.

The specific yield can also be estimated by laboratory measurements and the porosity analysed where the volume of linked porosity is taken as equivalent to specific yield. However, neither the laboratory and nor the pumping test method has been applied to the estimation of specific yield in the area. Under these circumstances one can use values of specific yields for certain rocks and sediment types presented in the literature.

Specific yield values ranging from 5 to 29 percent were estimated for the Tabriz Plain by the ELC-Electroconsult company (1970). However, it might be expected that the actual average value should be greater because this value is supposed to be for the whole area of the Plain, whereas the high fluctuations due to abstraction only occurred where the grain size is relatively greater than at other places.

As explained earlier, most of the ground water level monitoring wells are located in alluvial fans of the Plain and lithologically they penetrate a mixture of coarse sand and gravels. The value of specific yield represented for such material is 15 to 25 percent (Walton, 1970; Johnson Division, 1987). Therefore, an average value of 20 percent has been selected in order to calculate the amount of water replenishment into the aquifer by the expression:

$$I_e = [(W_y \times S_y)/a] = [(2052816000 \times 0.20)/1284960000 = 320\text{mm} = 4.1 \times 10^8 \text{ m}^3 .$$

This amount of replenishment is an estimated value and the water which infiltrated into storage from irrigation activities, ground water flow from out side the considered area, as well as some rainfall during the withdrawal period were not taken into account. Thus, it seems the estimated value is less than the actual replenishment during the year.

Table 4.1 Annual volumetric changes (m ) of ground water of the Tabriz Plain (1987).

No.	Contour interval (m)	Area between contours (m <sup>2</sup> )	Average fluctuation (m)	Volumetric changes (m <sup>3</sup> )
1	0 to 0.8	309760000	0.40	124000000
2	0 to 1	316960000	0.50	158480000
3	1 to 2	339360000	1.50	509040000
4	2 to 3	125280000	2.50	313200000
5	3 to 4	48320000	3.50	169120000
6	4 to 5	38560000	4.50	173520000
7	3 to 8.2	6720000	5.60	37632000
8	2 to 3.6	4000000	2.80	11200000
9	4 to 4.3	9120000	4.15	37848000
10	3 to 10.9	42400000	6.95	294680000
11	3 to 3.4	2240000	3.20	7168000
12	2 to 2.4	5440000	2.20	11968000
13	5 to 7.7	12800000	6.35	81280000
14	2 to 2.6	13120000	2.30	30176000
15	5 to 10.7	3840000	7.85	30144000
16	5 to 13	7040000	9.00	63360000
Total		1284960000		2052816000

## **CHAPTER 5**

### **AQUIFER TESTS**

#### **5.1 General**

#### **5.2 Applied Methods**

##### **5.2.1. Analytical Solution**

###### **5.2.1.1 Drawdown Solution**

###### **5.2.1.1 Recovery Solution**

##### **5.2.2. Numerical Solution**

#### **5.3 Analytical Analysis of Data**

#### **5.4 Numerical Analysis of Data**



## CHAPTER 5

### AQUIFER TESTS

#### 5.1. General

One of the most important aspects of ground water resources investigation is the determination of aquifer properties by analysing data obtained from pumping tests of wells. These characteristics of an aquifer are important for determining future declines in ground water levels associated with pumping and natural flow of water through the aquifer.

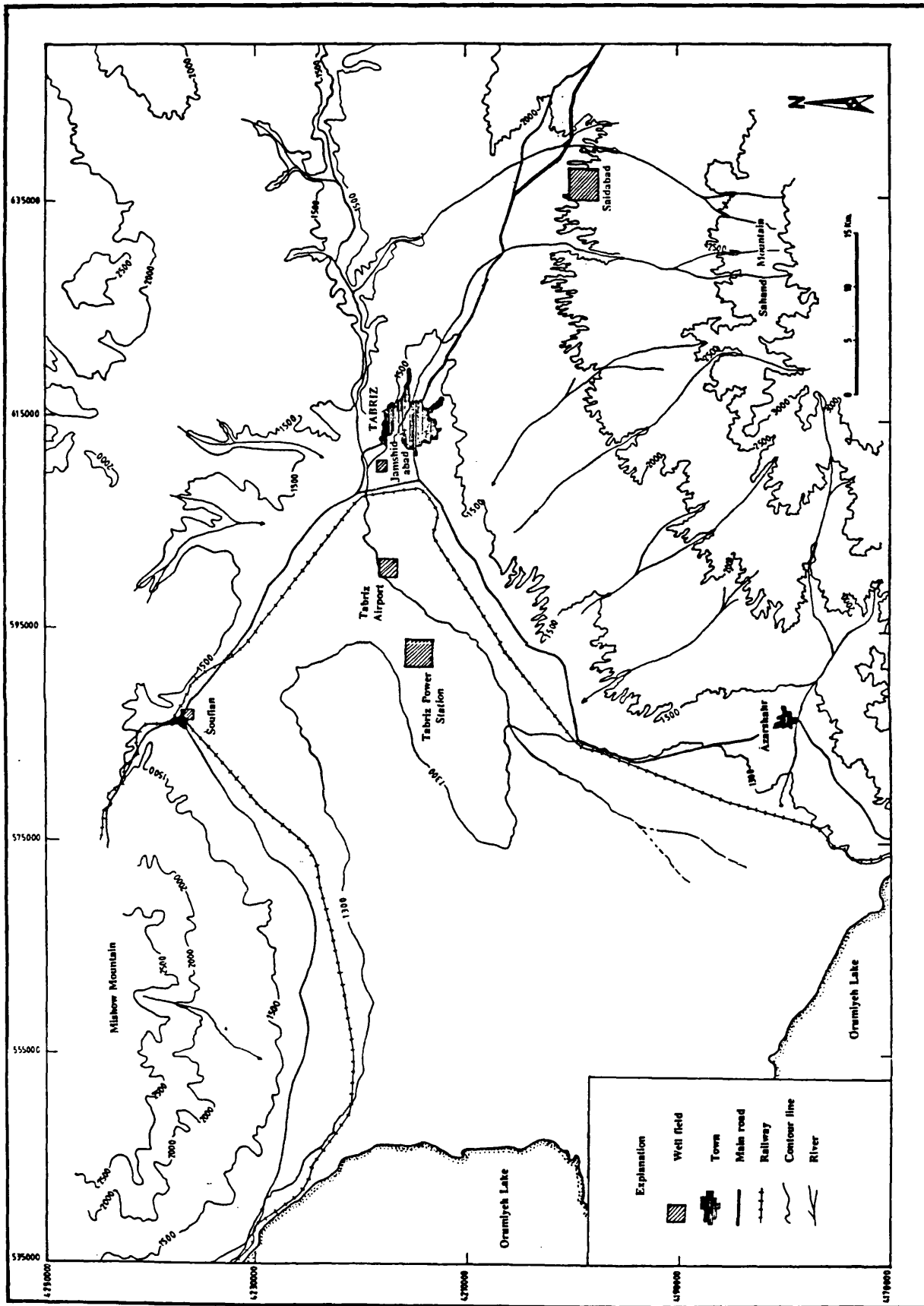
Pumping test data of drawdown and recovery versus time are available from different parts of the project area (see Fig. 5.1). As stated previously, there are two main types of aquifers which supply drinking, domestic, industrial and agricultural water to Tabriz and its surrounding urban and rural areas.

First, the unconfined Sahand alluvial tuff aquifer lies to the south and southwest of Tabriz City. Data representative of this aquifer comes from the Saidabad well field with eight pumping and three observation wells. Actually, there are data recorded for thirteen pumping wells, but five were not analysed because of close distance to other wells in the well-field. Furthermore, time drawdown and recovery data are only available for one of the observation wells (SWP3) and for the other two, they were reconstructed from plots of the responses.

Secondly, the multi-layered aquifer, unconfined aquifer on the top and confined to semi-confined aquifer below, lies to the west of Tabriz City in the Tabriz Plain. These aquifers consist of alluvial material and the data are available from different well fields such as, Jamshidabad, Tabriz Airport, Tabriz Power Station and the Soufian area. Unfortunately, there are no recorded data available for observation wells in the above- mentioned well fields. Therefore the storage coefficient can not be determined for this aquifer directly.

It would appear that the test design and execution was not good in some well fields. The reason was the lack of observation wells or too great distance between pumping and observation wells, and a short duration of pumping with respect to the type of the aquifer.

According to Fetter (1980), as a general rule the location of observation wells



5.1 Well field location map.

should be closer and the duration of a pumping test longer, for a water table aquifer than a confined aquifer. The frequency of time intervals for water level measurements made during the test period have been arranged in a logarithmically increasing fashion, but there are no good early data recorded for pumping wells with respect to high initial drawdowns. Johnson (1987) stated that the early test data are extremely important and as much information as possible should be obtained in the first 10 minutes of pumping for every pumping and observation well. The reason for this is that as the cone of influence moves outwards from the well it may encounter either an acceleration or a deceleration of drawdown with increasing time.

## **5.2. Applied Methods**

Drawdown and recovery data obtained from pumping and observation wells were analysed by conventional and numerical techniques.

### **5.2.1 Analytical Solutions**

#### **5.2.2.1 Drawdown Solution**

Given the different analytical solutions, the Jacob straight line method was preferred, rather than Theis (1935) type curve method. The reason was: (i) the high initial drawdowns in the pumping wells which gave a smooth time drawdown or recovery plots (ii) the high rate of well loss in most of pumping wells which gave incorrect transmissivity values when they are analysed by the Theis type curve method. Therefore the type curve method was only used in a few wells in which there was limited well loss.

Full details of the basic theory and solution of the straight-line method are given by Cooper and Jacob (1946) and Jacob (1964). The semi-log or Jacob's method is based on the Theis non-steady state, ground water solution, involving time and storage. However, the conditions for its application are more restricted than the Theis type curve method. It is more accurate when the value of  $r^2/t$  is relatively small and there is a critical value of  $u < 0.2$  that must be satisfied before the analysis can be applied.

$$[u=r^2S/4Tt]$$

The main advantages of the method are: (i) type curves are not required, (ii)

it does not need good initial drawdown data, (iii) it gives a more distinguishable plot for the high initial drawdown and recovery data, (iv) much easier for application and interpretation, and (v) drawdown due to well loss does not affect transmissivity values. The general procedure and equations which are used in this method are shown in the field data plot and analysis sheets. The main assumptions underlying the analytical methods are summarized below:-

- aquifer is homogeneous and isotropic
- T is constant at all time and in all place
- flow is laminar
- the aquifer has infinite area extent
- the pumping well has infinitesimal diameter
- water removed from aquifer storage is discharged immediately with decline in head (instantaneous response)
- the well fully penetrates the aquifer
- the pumping well is 100 percent efficient.

These assumptions strictly apply only for a confined aquifer condition. Therefore, when the aquifer is leaky or water-table some of them are not satisfied.

### 5.2.1.2 Recovery Solution

When pumping is stopped, the recovery of the water level in both pumping and observation well acts as a 'mirror-image' of the drawdown, regardless of the type of aquifer conditions. Hence it can be used as a check on aquifer properties. The recovery method has the advantage that the rate of recharge (Q) is presumed constant and equal to the mean rate of discharge (Q) during pumping.

Rushton (1981)<sup>\*</sup>, described the recovery phase of pumping as of great value in the interpretation of the test, because the recovery reflects the response of the whole aquifer whereas the abstraction phase tends to be dominated by conditions close to the abstraction well. However, it is not possible to obtain a reliable analysis of the recovery data unless the abstraction phase has been represented correctly.

The recovery data can only be analysed when the test pumping is done at a constant rate. Therefore, the exact time of starting and stopping the pump need to be recorded, along with any changes in pumping rate and the time that they occur.

<sup>\*</sup> Jones and Rushton(1981)

According to Johnson Division (1987 second edition), complete recovery, generally requires a period considerably longer than the previous pumping period, except in cases where recharge to the aquifer has occurred during the pumping and recovery periods.

There are number of methods to analyse the recovery data. In the study area, the data for all sites were analysed by the calculated recovery method with plots on semi-logarithmical paper. A summary of the recovery analysis results are shown in Table 5.2b. The details of the analysis and their agreements with the related time drawdown data will explain in next section.

### **5.2.2. Numerical Solution**

Usually, one or more of the assumptions underlying the analytical solutions is not valid, though the range of problems that can be analysed is impressive (see for example Hantush 1956; Kruseman and de Ridder 1970; Streltsova 1976).

Connorton and Reed (1978) stated that conventional methods based on analytical solutions are not sufficiently versatile for solving long term pumping tests data. Further, according to Rushton and Chan (1976), when there are more than three unknown parameters in the analytical solution, the provision of an exhaustive set of curves is not practicable.

With reference to the above reasons the numerical method was applied for analysing the data obtained from all pumping and observation wells. The analytically deduced results were used in the model data file for the first runs, then they were changed by several trials to obtain an adequate fit.

The numerical technique of analysing pumping tests data has been developed by Rushton, with contributions from Booth (1976), Chan (1977), Redshaw (1979), Rathod (1988), Srivastava (1988) and several others. This method has the advantage that many factors can be included in a single numerical solution. These factors are listed by Jones and Rushton (1981) as:

- (a) well of finite radius.
- (b) free water contained within well
- (c) variations in abstraction rate including zero abstraction rate (recovery)
- (d) outer boundaries either impermeable or zero drawdown

- (e) variable saturated depth
- (f) permeability which varies with radius or depth
- (g) storage coefficient which varies with depth or radius including change between confined and unconfined conditions
- (h) leaky aquifers
- (i) intermittent recharge
- (j) delayed yield from storage
- (k) non-linear well losses.

Full details of the numerical technique are given by Rushton and Redshaw (1979), and only the basic approach is summarized below.

The non-steady state equation describing radial flow in an aquifer is;

$$\frac{\partial}{\partial r} (bK_r \frac{\partial s}{\partial r}) + \frac{b}{r} K_r \frac{\partial s}{\partial r} = S \frac{\partial s}{\partial t} + q \quad (5.1)$$

where  $s$ =drawdown below datum,  $r$ =radial co-ordinate,  $b$ =saturated thickness of aquifer,  $K_r$ =radial permeability,  $t$ =time,  $S$ =storage coefficient (confined and unconfined),  $q$ =recharge per unit area,

This equation has been solved by creating a new variable:

$$a = \log_e r \quad (5.2)$$

Then, substituting this variable in equation 5.1 and multiplying through by  $r^2$ , leads to the equation:

$$bK_r \frac{\partial^2 s}{\partial a^2} = S r^2 \frac{\partial s}{\partial t} + q r^2 \quad (5.3)$$

Solutions to this equation with appropriate boundary and initial conditions, assuming a regular mesh interval  $\Delta a$  and an approximated finite difference can be written:

$$\frac{bK_r}{\Delta a^2} (s_{n-1} - 2s_n + s_{n+1})_{t+\Delta t} = \frac{S r^2}{\Delta t} (s_{n,t+\Delta t} - s_{n,t}) + q_{t+\frac{1}{2}\Delta t} r_n^2 \quad (5.4)$$

The use of mesh spacing with constant increments of  $\Delta a$  results in a fine mesh in the vicinity of the abstraction well and more widely spaced at greater distance. A time increment from  $t$  to  $t+\Delta t$  is also used logarithmically.

It is possible to visualize the equation 5.4 in terms of equivalent hydraulic

resistances which they are defined as;

$$H_n = \Delta a^2 / m k_r \quad (5.5)$$

$$T_n = \Delta v / S r_n^2 \quad (5.6)$$

By substitution into equation 5.4, the equation for node n becomes

$$\frac{(s_{n-1} - 2s_n + s_{n+1})_{t+\Delta t}}{H_n} = \frac{s_{n,t+\Delta t} - s_{n,t}}{T_n} + Q r_n^2 \quad (5.7)$$

The recharge at node n is given by;

$$q = -Q/A_n \quad (5.8)$$

where  $A_n$  = area represented by node 1 and equals  $2r\Delta_r$

Since  $a = \log e_r$ ,  $\Delta_r = r\Delta_a$ .

Then

$$A_n = 2 r^2 \Delta_a$$

and

$$q = -Q/2 r^2 \Delta_a$$

The equations represented in the program (see Appendix 3) are calculated by substituting node N and node 1 in the above mentioned equations associated with some assumptions; where Node 1 represents the whole of the region within the well. the radius is R(2) and the outer boundary R(NMAX). The increment,  $\Delta a = 0.38376$  and there are six mesh intervals for a tenfold increase in radius, with the finite interval ending at R(NMAX).

## Solutions For The Other Factors

### 1) Leakage

If the aquifer is leaky, the leakage can be represented as a recharge which depends on drawdown as;

$$q = k_r m (s_{j,t+\Delta t} - s_{j,w}) / L^2$$

where  $s_{j,t+\Delta t}$  is the current value of the drawdown  $s_{j,w}$  is the position, below datum, of the water surface in the overlying stratum, L is the leakage coefficient.

### 2) Delayed yield:

The concept of delayed yield was explained by Boulton (1964). When the delayed yield is incorporated in the discrete model, the quantity of water per unit area entering a typical node of the aquifer during the nth time interval will be determined.

During the  $n$ th time step the time increases from  $t_n - \Delta t_n$  to  $t_n$  and the drawdown increases by an amount  $\Delta s_n$ . Apart from infiltration there are also the following components:

- i) a quantity arising from the instantaneous storage
- ii) the inflow arising from delayed yield due to previous drawdown
- iii) during the current time step a contribution occurs due to the delayed yield.

Gathering together these three components of flow gives equations for solution of the delayed yield. For more details see Rushton and Chan (1977) and Rushton and Redshaw (1979).

### **3) Well losses**

When well losses occur, additional drawdown results due to turbulent flow and well clogging. This effect can be modelled by reducing the hydraulic conductivity by a multiplication factor for the node closest to the pumping well. For the pumping test analyses from the project area, it was reduced in nodes 2 and 3 of the pumping wells.

### **4) Position of observation well;**

For the exact position of an observation well the mesh can be designed to coincide with desired position. The node ( $r_w$ ) determines the logarithmic spacing. Node 2 represents the edge of the well, and there are 6 nodes for 10 fold increase in radius; i.e if  $r_w=0.15\text{m}$  =node 2 , node 8=1.5m, node 14=15m, and node 20=150m.

## **5.4. Analytical Analysis of Data From Study Area**

### **Saidabad well field area**

This well-field is located to the south-east of Tabriz City. Its total area is about 100 km<sup>2</sup>, being some 2km distant from the village of Saidabad (see Fig. 5.2). It comprises thirteen pumping and three observation wells, which were drilled for purposes of drinking water supply.

Time-drawdown and recovery data from wells SW1, SW3, SW7, and their respective observation wells SWP1, SWP3, and SWP7, as well as single pumping wells SW5, SW8, SW10, SW11, and SW13 were analysed by different analytical methods.



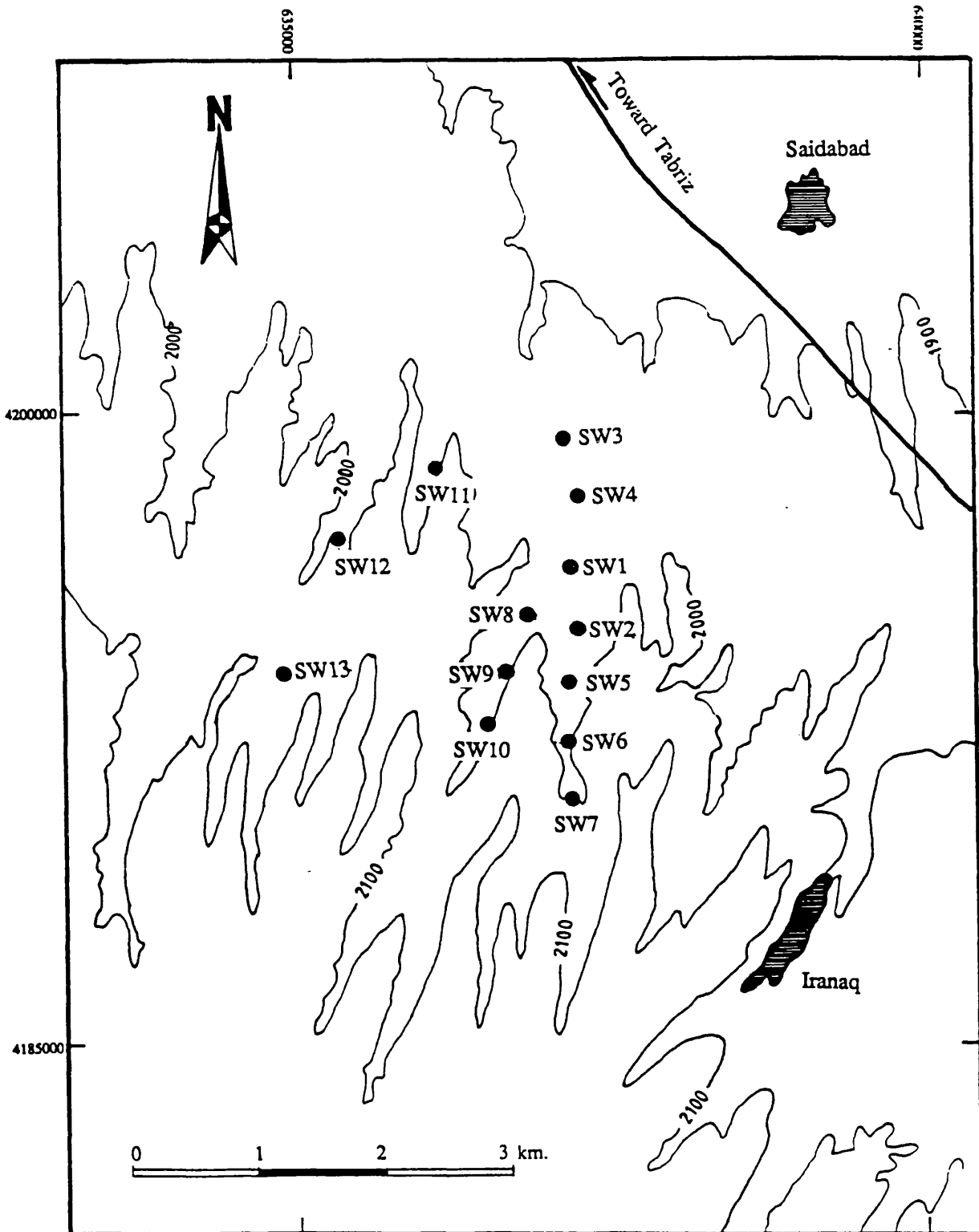


Fig. 5.2 Saidabad well field and location of pumping wells.

All the above-mentioned wells were drilled in 1977 by IRAB Engineering Company Limited, using conventional rotary techniques.

In some wells, particularly in the northern part of the well-field area, the drilled holes fully penetrate the homogeneous alluvial tuff aquifer. A summary of the total and completed depths of wells are listed in Table 5.1. Also technical cross sections of the well diameters, screen and casing lengths are represented in Figure 5.3.

**Table 5.1**

<b><u>Pw/Ow NO.</u></b>	<b><u>Screen Length (m)</u></b>	<b><u>Completed Depth(m)</u></b>	<b><u>Total Depth(m)</u></b>
SW1	131.76	315	370
SWP1	132.00	315	315
SW3	139.08	269	310
SWP3	140.00	269	269
SW5	178.00	340	360
SW7	190.32	352	352
SWP7	190.00	352	352
SW8	168.36	337	345
SW10	175.71	330	350
SW11	219.52	320	333
SW13	88.4	203	242

In this section only the analysed data from pumping wells with observation wells are going to be explained fully and the single pumping well data analyses are included in Appendix 5.

A constant-rate test was carried out in well SW1 in December 1976, with a discharge rate of 7171 m<sup>3</sup>/d for a duration of 3 days. The time-drawdown and recovery data were recorded for the pumping well and the observation well 50 metres away.

The time-drawdown and recovery data for both wells were plotted on single logarithmic paper (see Figs. 5.4 to 5.7). As is clear from the all of these plots, the

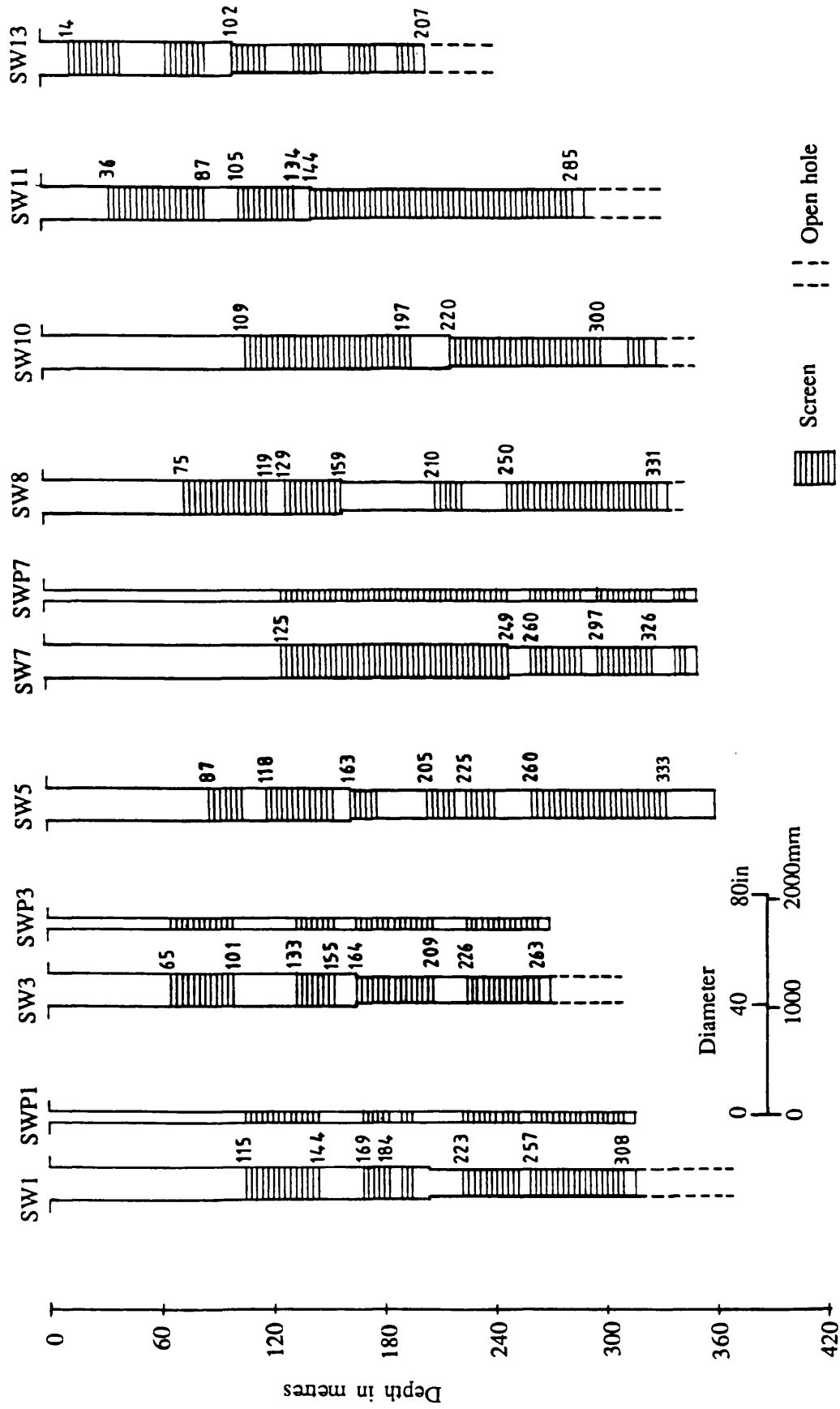


Fig. 5.3 Cross sections showing Saidabad well construction.

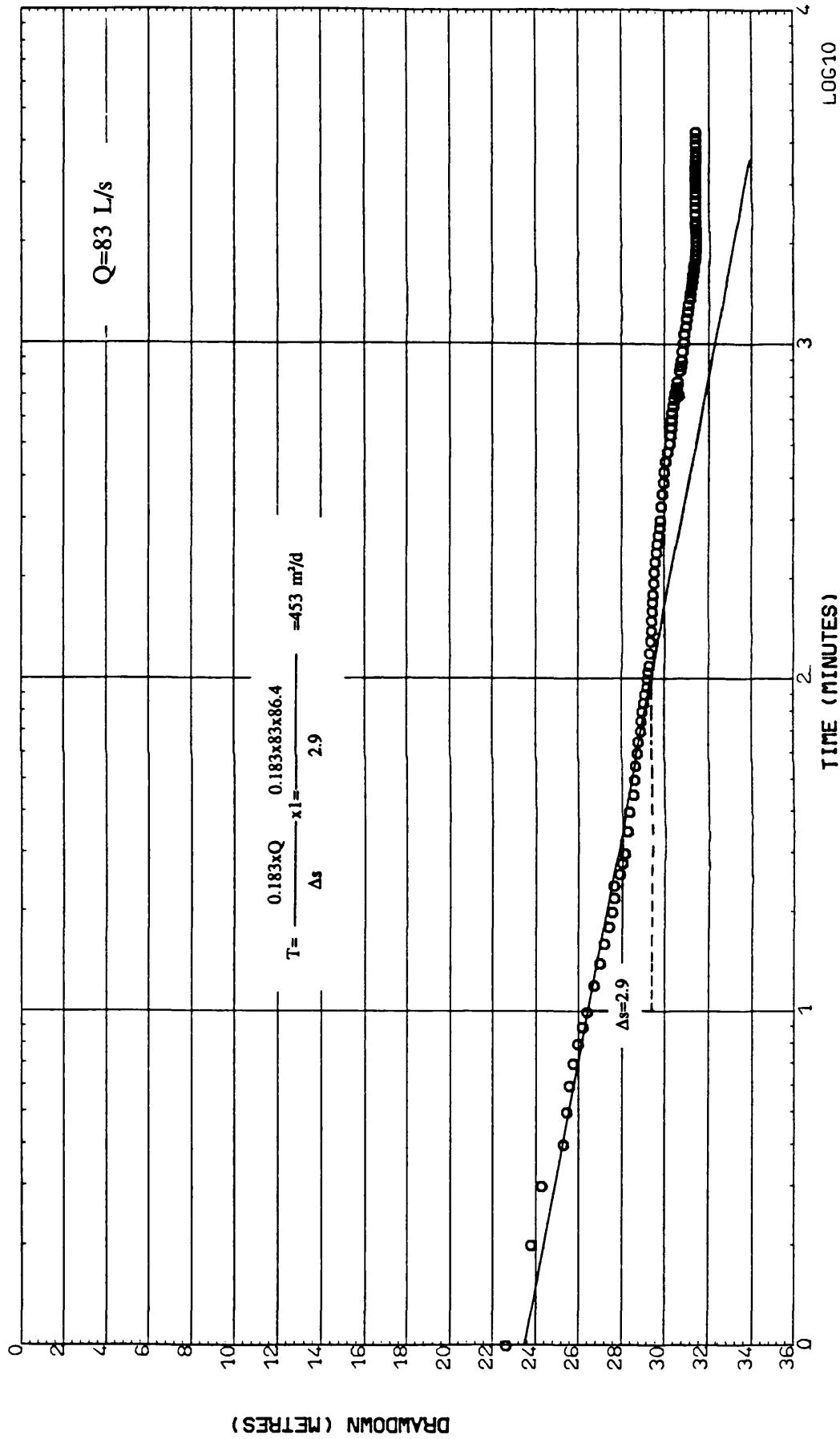


Fig. 5.4 PW SW1, Straight line method: Time-Drawdown plot.

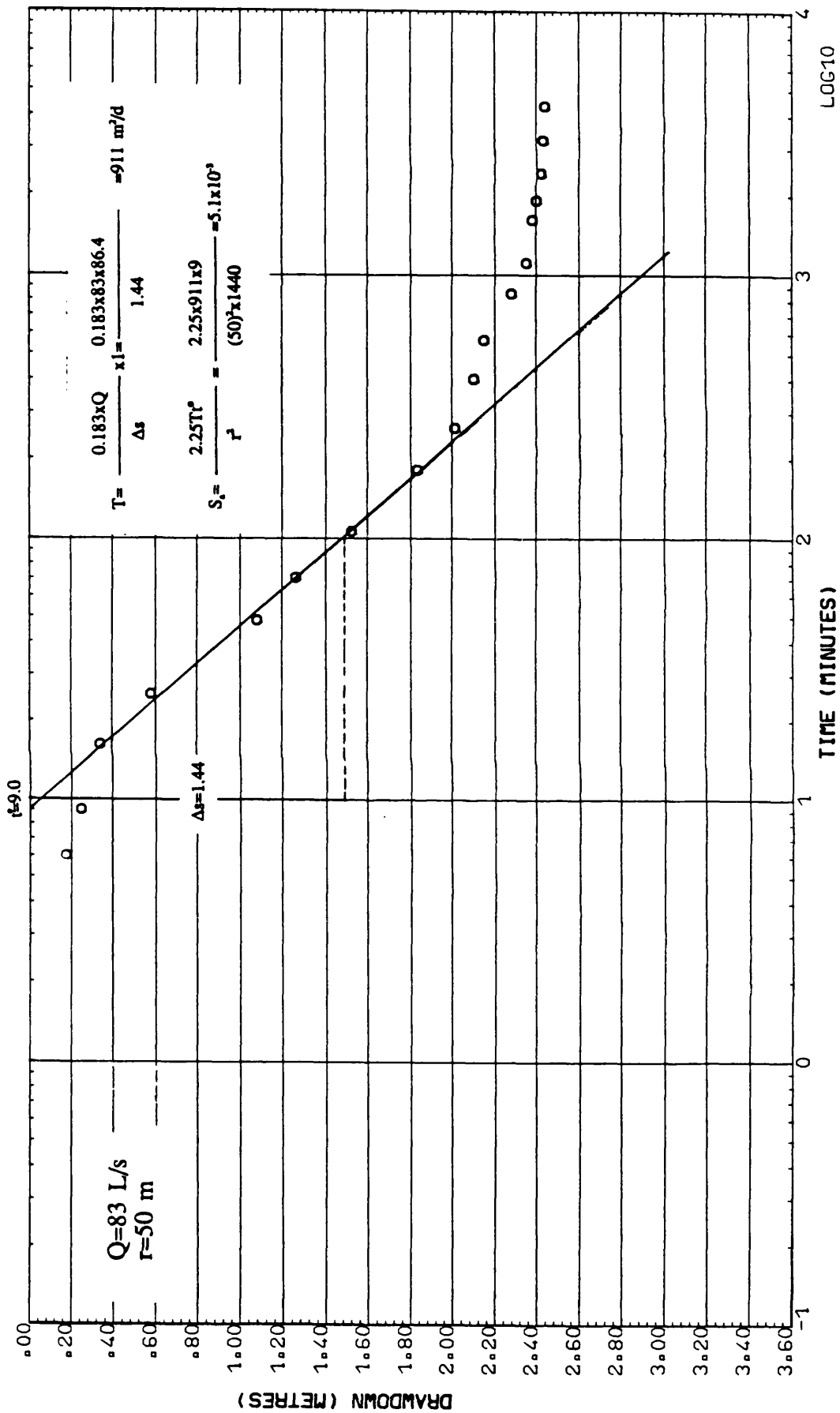


Fig. 5.5 OW SPW1, Straight line method: Time-Drawdown plot.

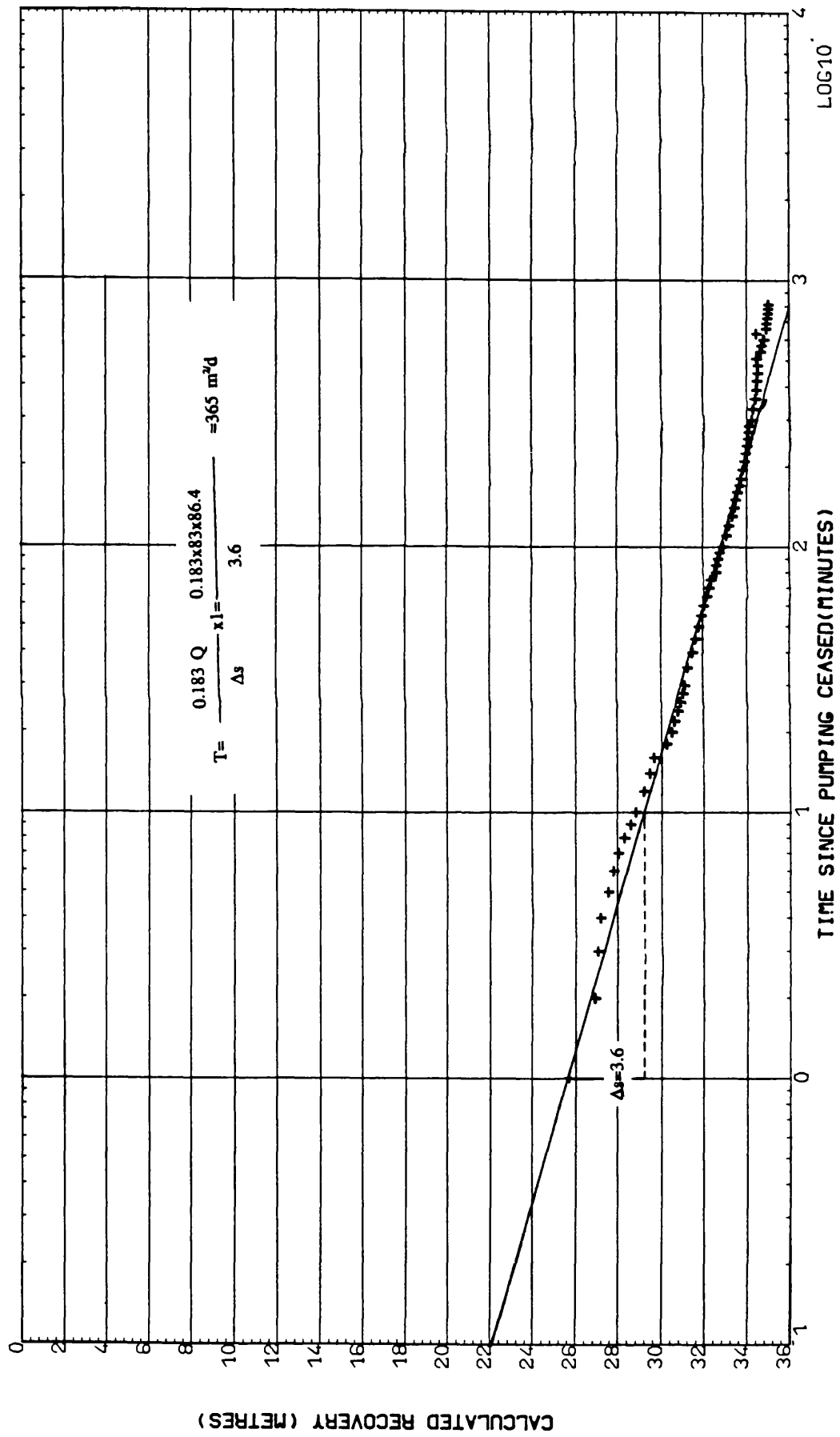


Fig. 5.6 PW SW1, Straight line method: Calculated recovery plot.

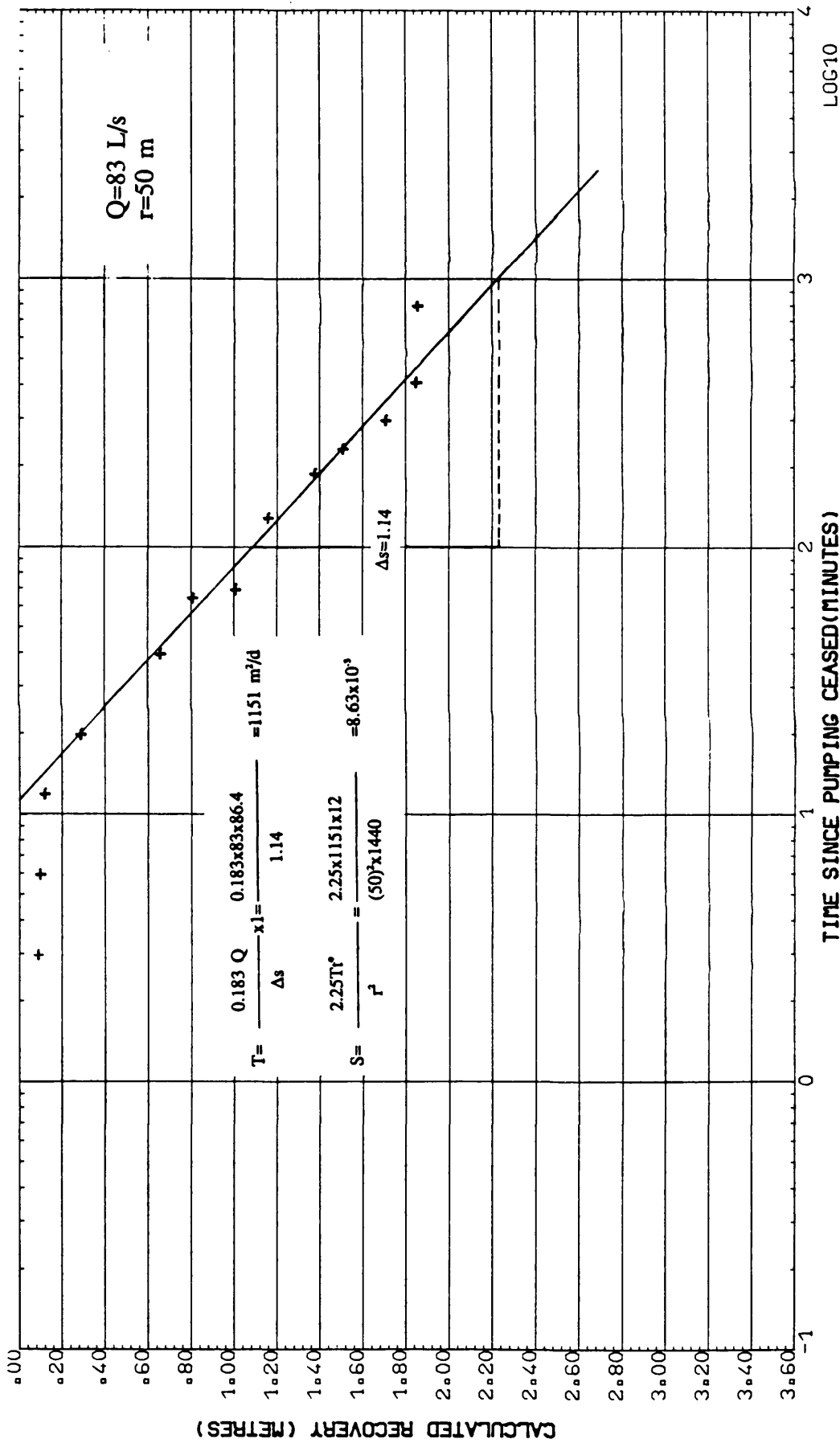


Fig. 5.7 OW SPW1, Straight line method: Calculated recovery plot.

curves drawn through the field data show a leaky confined response, whereas the geological conditions of the water bearing layer (see Fig. 5.8) and the static water levels equally clearly indicate that the aquifer is under unconfined conditions.

Furthermore, all of the conditions which are necessary for confined and/or leaky-confined aquifers are not satisfied. Rushton and Rathod (1988) described that confined conditions occur when an aquifer is underlain and overlain by impermeable strata with piezometric heads above the base of the confining bed. According to them, for confined conditions to apply, the hydraulic conductivity of these impermeable layers must be at least five orders of magnitude less than the aquifer.

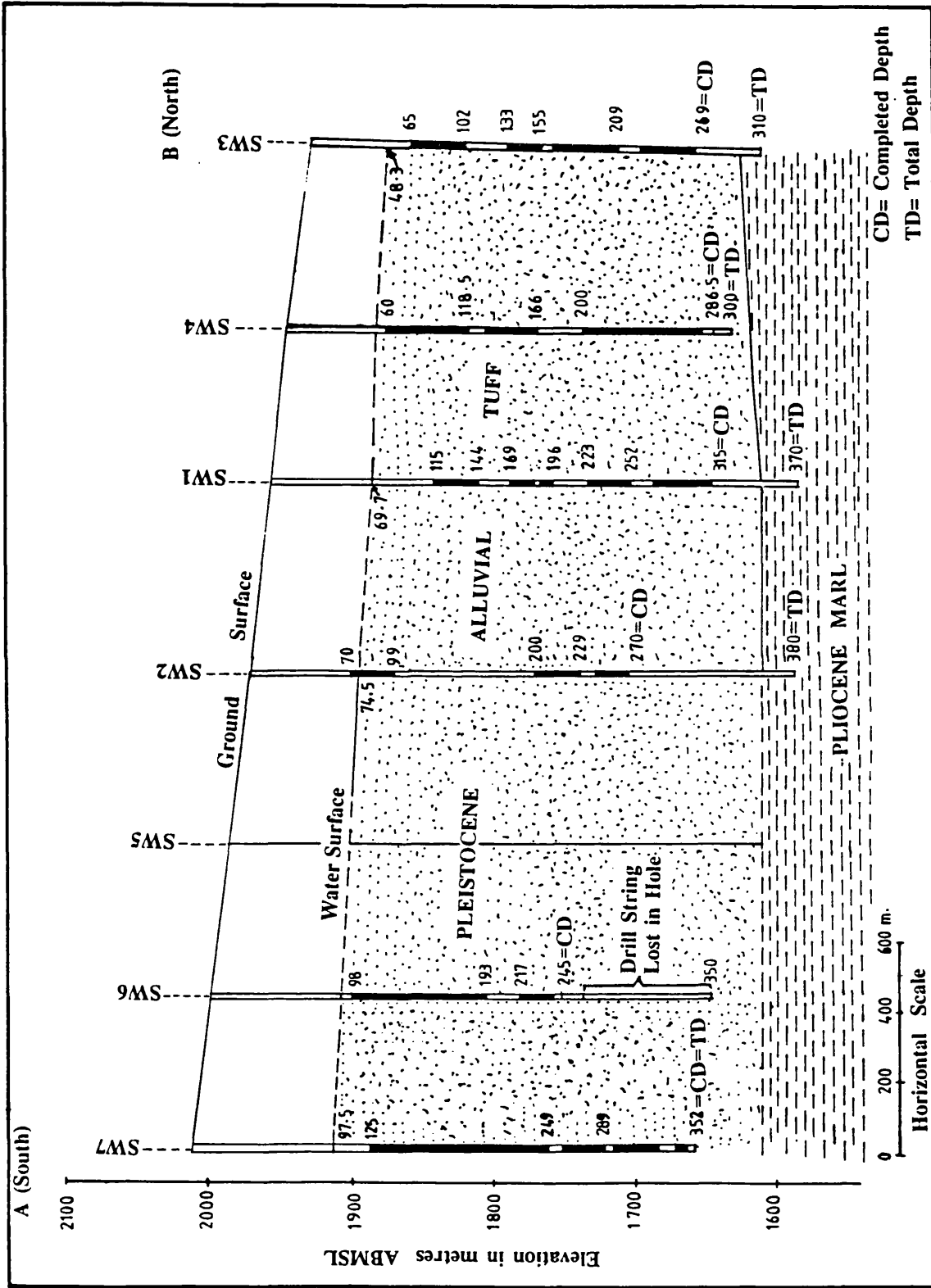
Jacob (1946b) stated that leaky-confined conditions occur when an aquifer is overlain by a semi-pervious layer with a phreatic aquifer above it, in which the hydraulic conductivity of the semi-permeable layer is two to four orders of magnitude less than the leaky aquifer. Therefore, it would appear as if the recorded data were affected by some other factor(s), such as short duration of pumping (which has not allowed gravity drainage to be completed), low delayed yield effect, inhomogeneity and so on.

The average transmissivity (T) value for pumping well SW1 is about 470 m<sup>2</sup>/d whereas, the value for observation well SPW1 is about 910 m<sup>2</sup>/d and storativity (S) is 1.3x10<sup>-1</sup>.

The time-drawdown and recovery analyses for these wells were in very poor agreement with one another. The value of T from the recovery data for the observation well is greater than the drawdown and vice versa for the pumping well. The early storage coefficient for the observation well gave slightly different values for the two sets of data (see Table 5.2a).

Pumping well SW3 (see Fig 5.2.) is the most northerly of the abstraction wells in this well-field. It penetrates the whole thickness of the aquifer which is 222m at this site. The static water levels in the pumping and observation well (r=50m) were 47.80 and 46.87 metres respectively below the ground surface when the pumping test started. The test was carried out for three days in February 1977, with a constant rate discharge of 8294 m<sup>3</sup>/d. The time-drawdown and recovery data were recorded for both the pumping and observation wells and the obtained data was plotted on log-log and semi-log scale (see Figs. 5.9 to 5.12).





*(Ref)*

Fig. 5.8 Geological section through Saidabad exploratory wells.

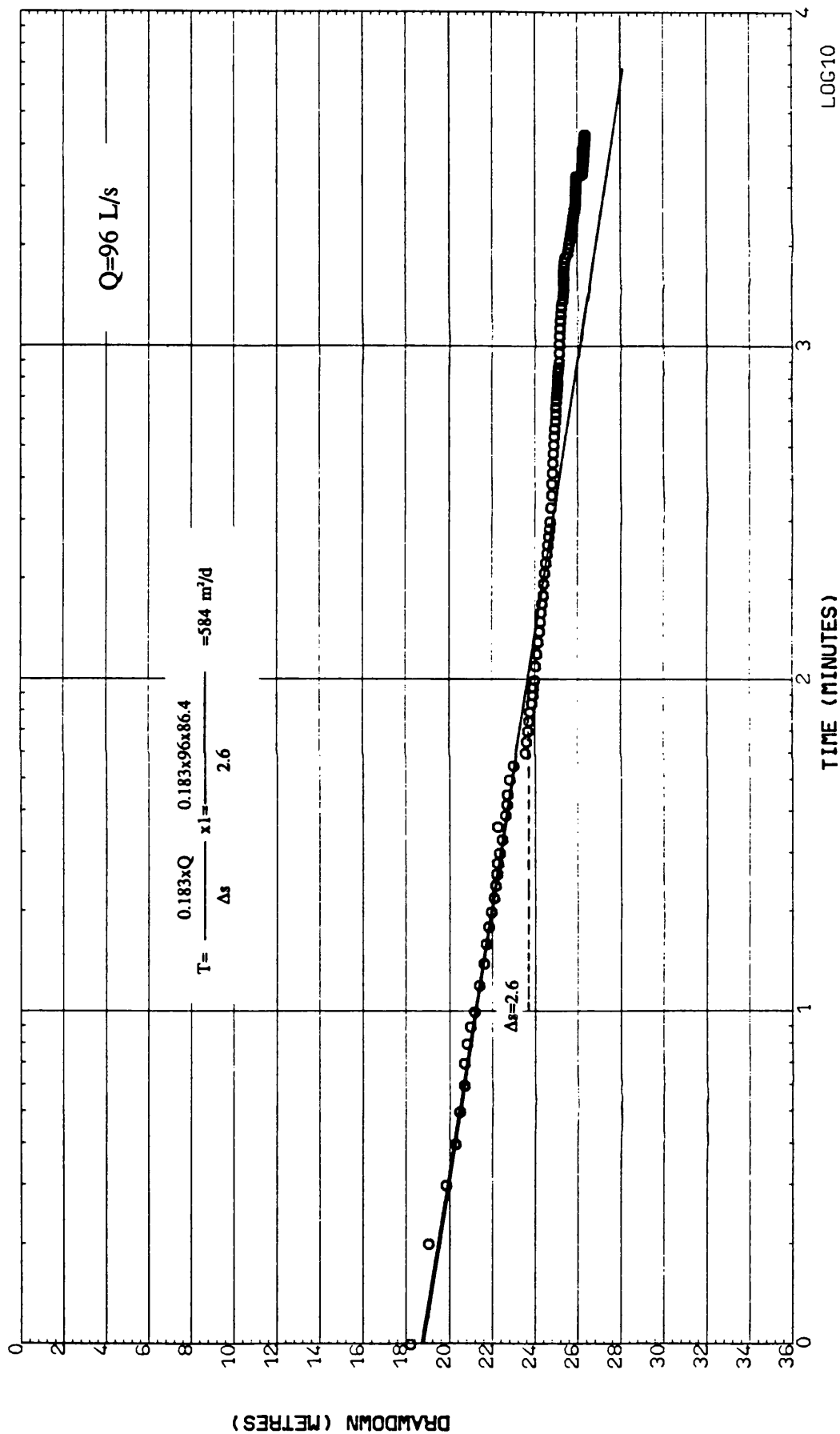


Fig. 5.9 PW SW3, Straight line method: Time-Drawdown plot.

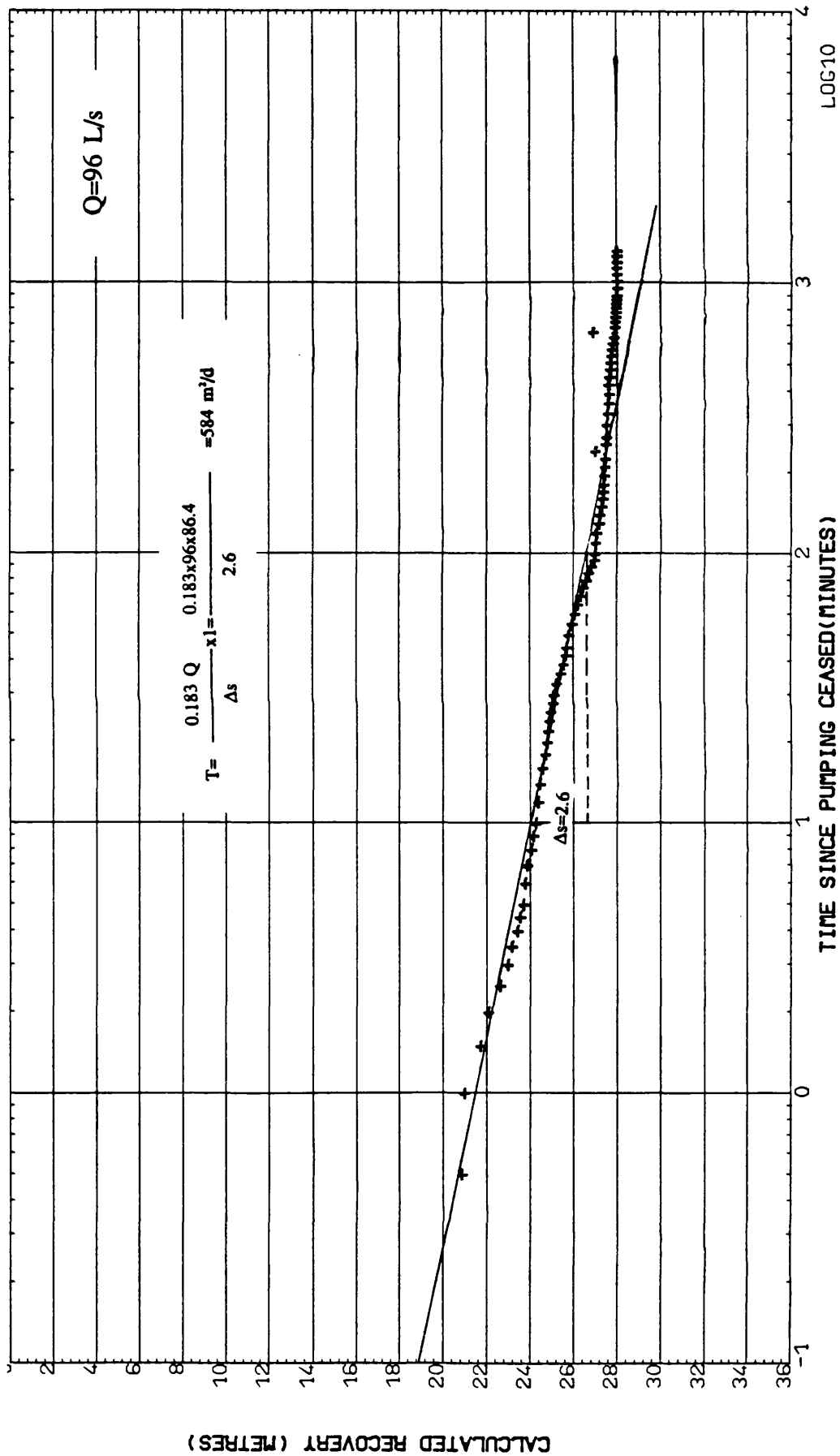


Fig. 5.10 PW SW3, Straight line method: Calculated recovery plot.

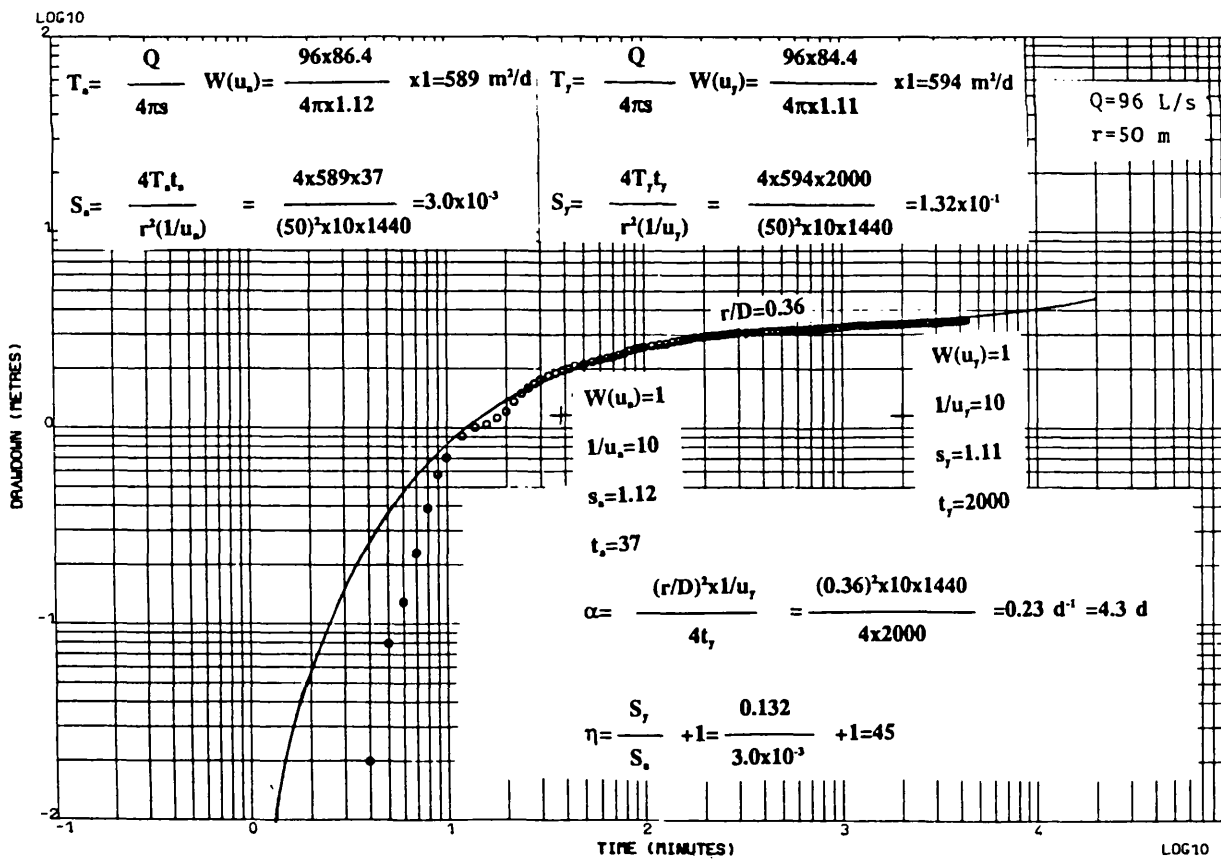
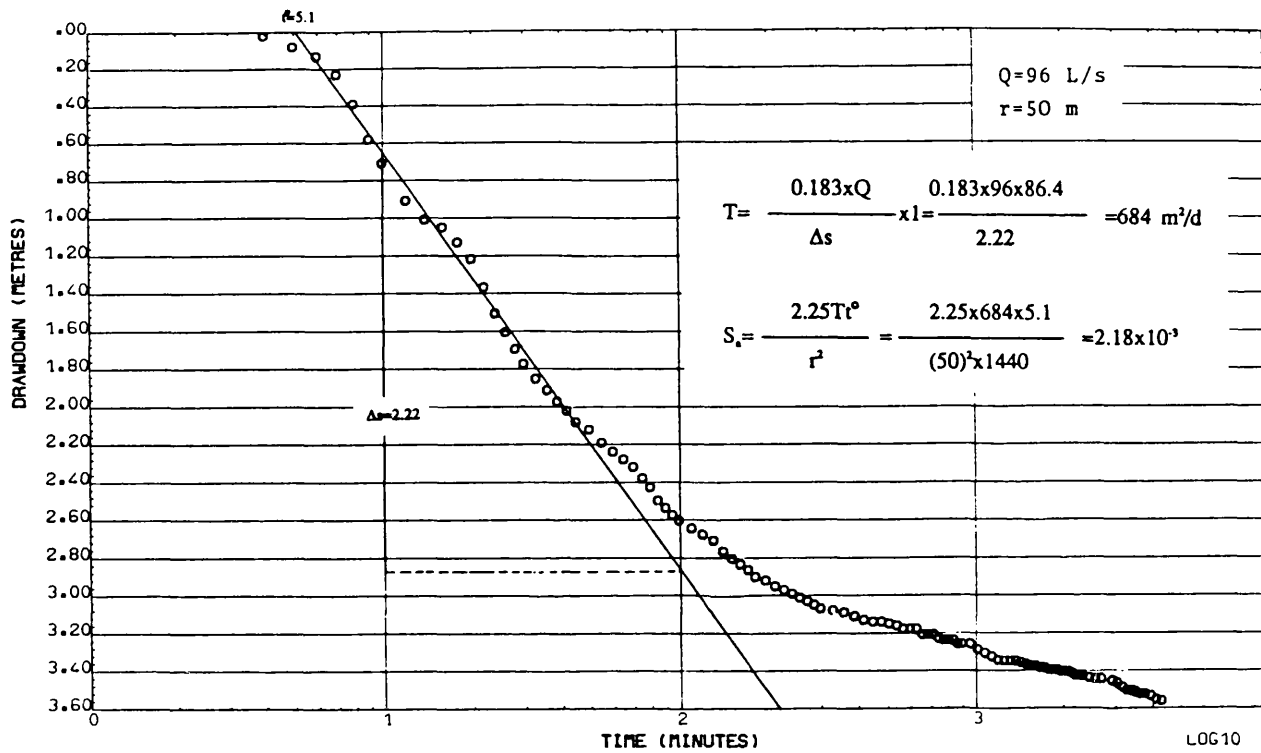


Fig. 5.11 OW SPW3, Time-Drawdown plots: (a) Straight line method, (b) Type curve method.

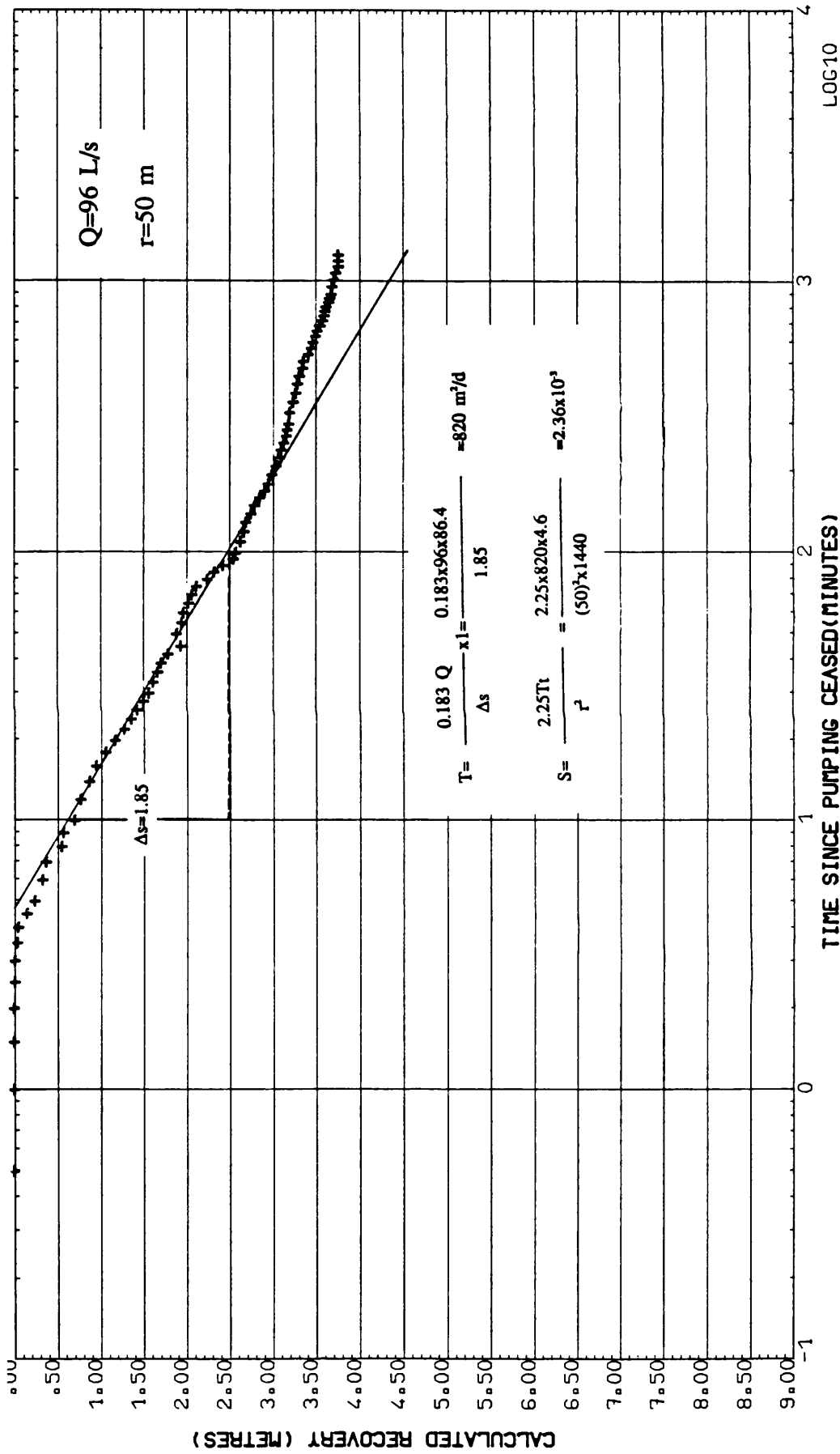


Fig. 5.12 OW SPW3, Straight line method: Calculated recovery plot.

Information derived from the drilling and borehole logging, as well as plotted time-drawdown data for the observation well, shows that the aquifer is under water-table conditions. Therefore, the plotted time-drawdown data was analysed by applying the Boulton type curve solution. However, the early data did not fit the type curve very well, perhaps due to the high rate of the discharge, which makes it very difficult to record the earliest data properly. The T values for the pumping and observation well are in the range of 585 to 678 m<sup>2</sup>/d obtained from use of different methods and the S values for early and late data are 3.0x10<sup>-3</sup> and 1.32x10<sup>-1</sup>, respectively.

The resultant values for transmissivity from the drawdown and recovery data for the pumping well were in very good agreement, whereas, for the observation well they gave different values. The drawdown data analysed by type curve and straight line methods gave slightly different transmissivity values, whereas the early storage coefficient calculated from two sets of data and the alternative methods were in close agreement.

Pumping well SW7 is the most southerly of the abstraction wells in this well field (see Fig. 5.2). The aquifer thickness in this well is greater than at SW3. The full depth of the Pleistocene Alluvial Tuff at this site is estimated to be more than 400 metres, whereas the depths of the abstraction and observation wells are only 352 metres. Therefore the aquifer is not fully penetrated. Lining details of casing and screen for the pumping and observation wells are shown in Figure 5.3.

The pumping test was carried out in this well for 3 days, with a constant discharge rate of 3456 m<sup>3</sup>/d in February 1977. The static water level below the ground surface in pumping and observation wells were 97.28 and 90.10, respectively.

The time-drawdown and recovery data obtained from the test are plotted for pumping and observation wells on semi-logarithmic papers (Figs. 5.13 to 5.16), and analysed by the Jacob straight-line method. The values of T for the pumping and observation well ranged from 350 to 395 and 375 to 575 m<sup>2</sup>/d, respectively and the confined storage coefficient from 2x10<sup>-3</sup> to 8x10<sup>-3</sup>.

The drawdown and recovery analyses for the pumping well are in close agreement. However, the observation well shows a great difference, not only for transmissivity but also for the storage coefficient.

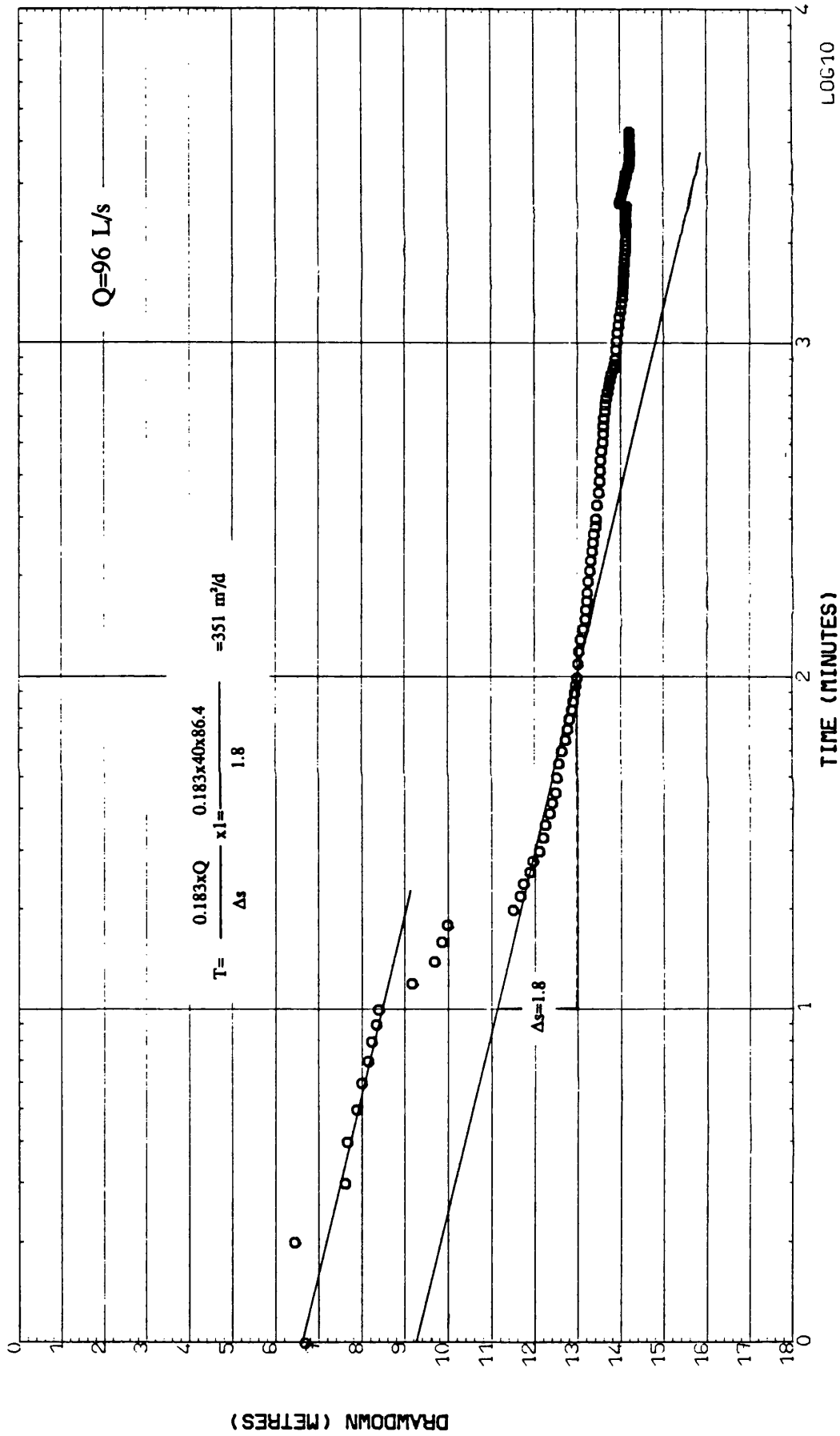


Fig. 5.13 PW SW7, Straight line method: Time-Drawdown plot.

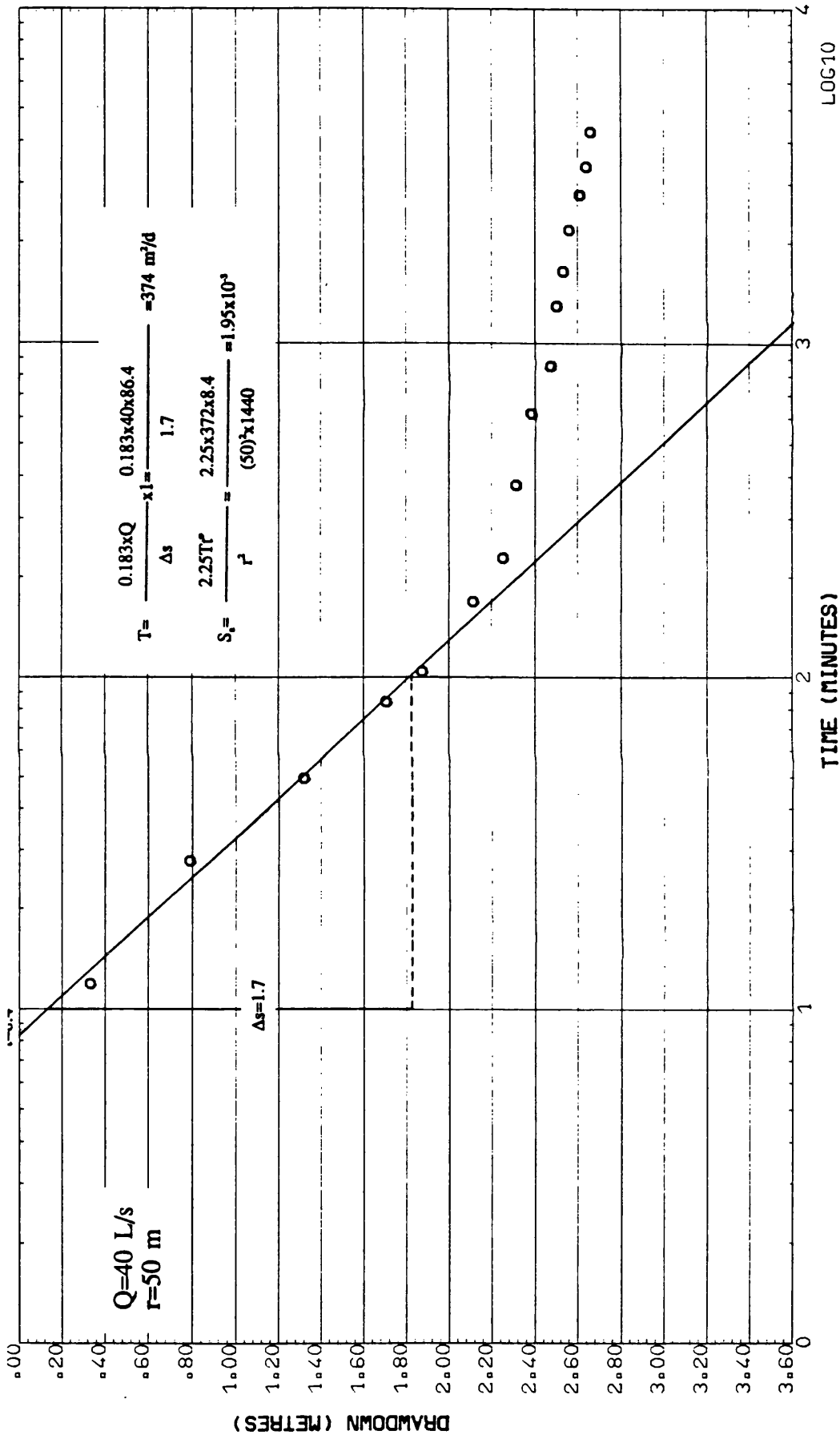


Fig. 5.14 OW SPW7, Straight line method: Time-Drawdown plot.



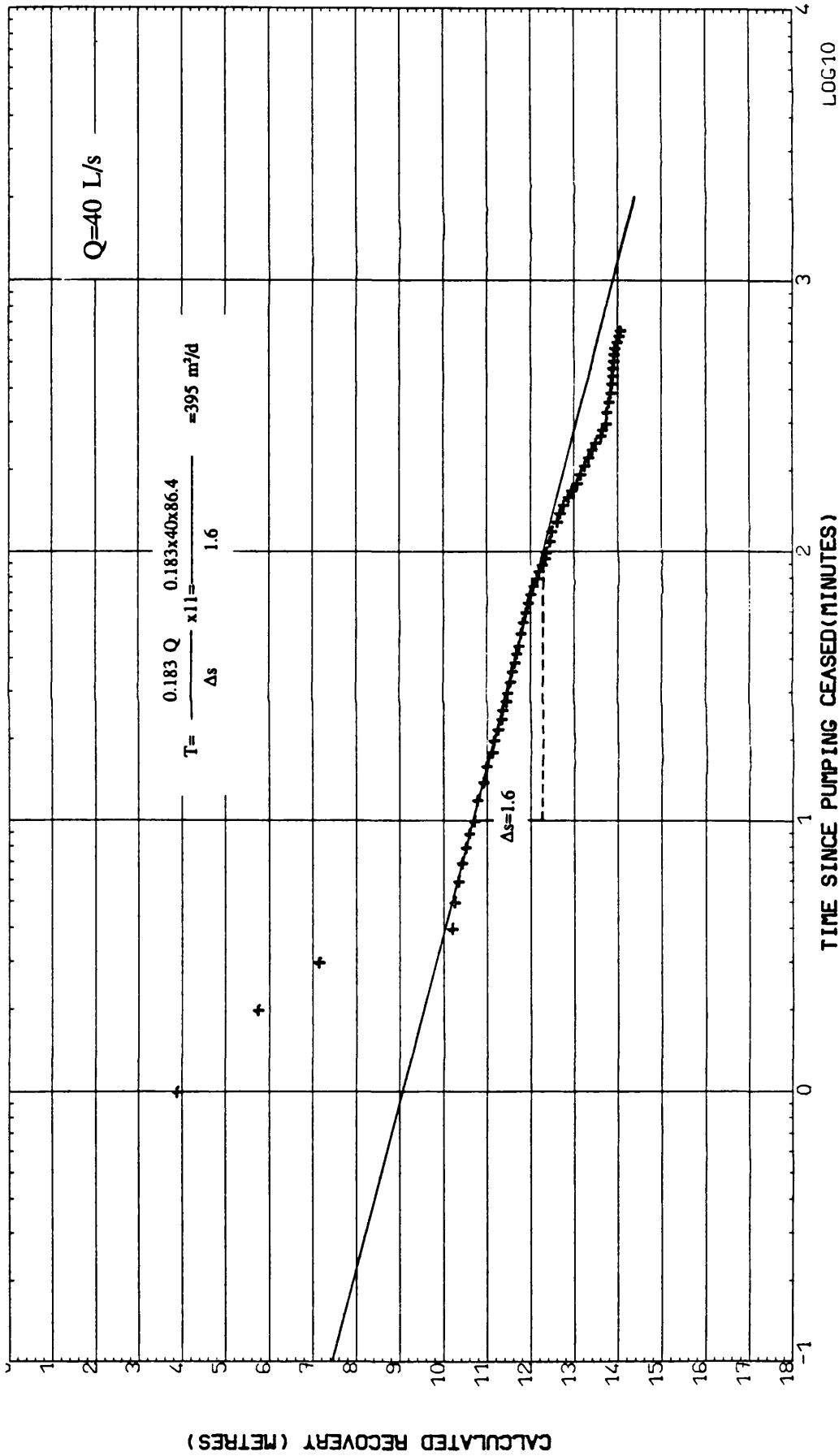


Fig. 5.15 PW SW7, Straight line method: Calculated recovery plot.

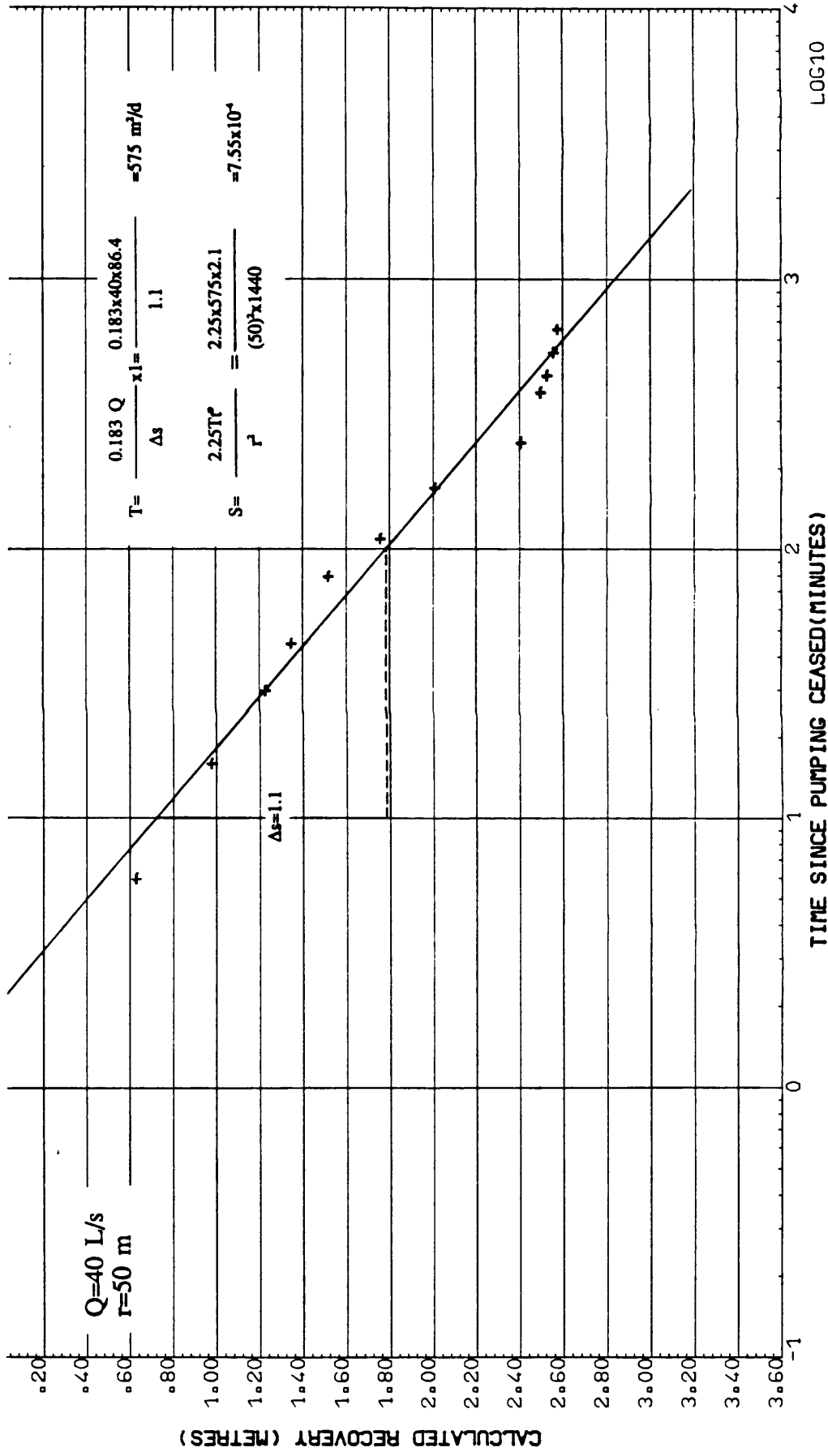


Fig. 5.16 OW SPW7, Straight line method: Calculated recovery plot.

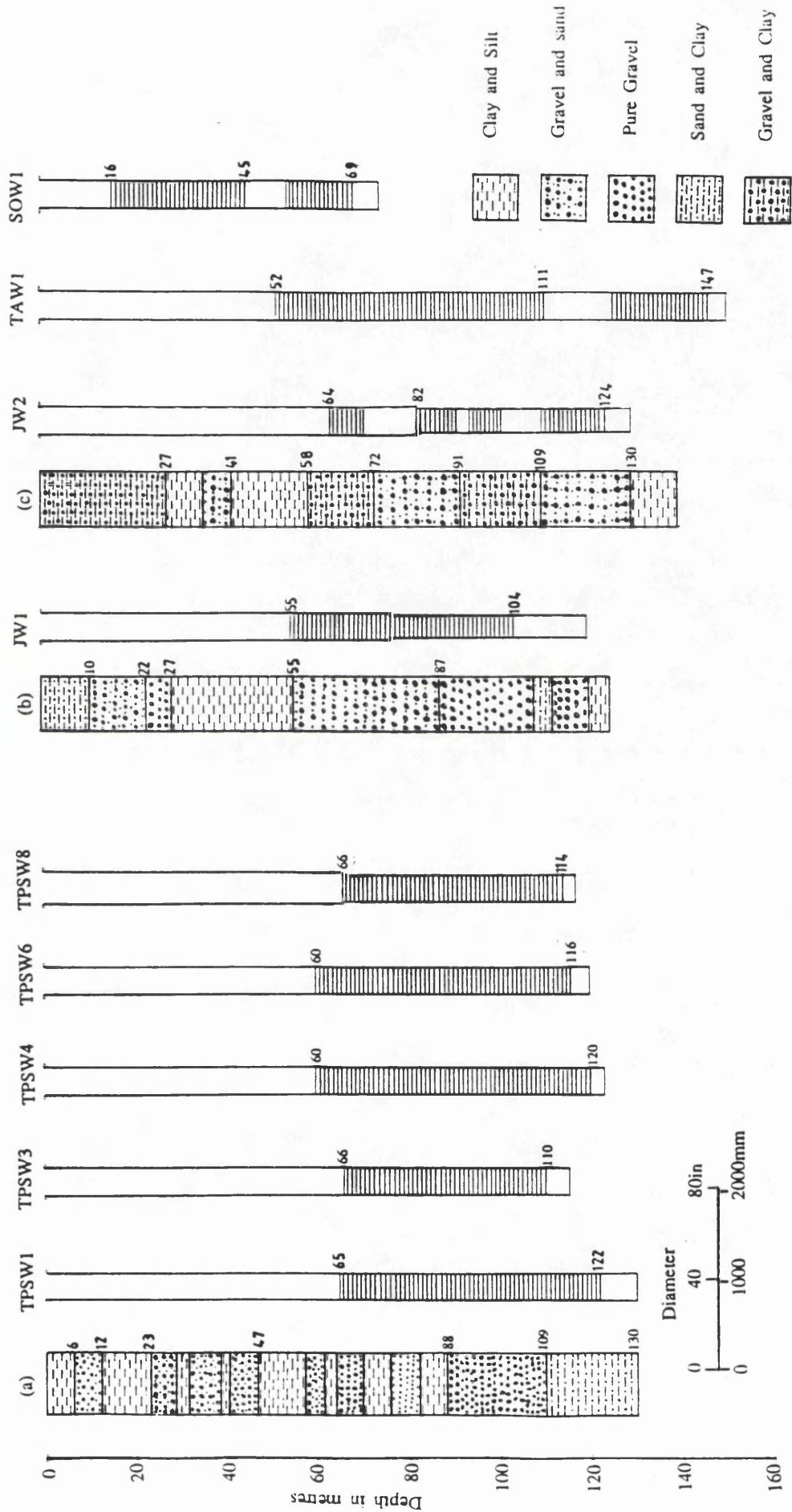


Fig. 5.17 Geological and technical cross sections of the Tabriz Plain wells: (a) Tabriz Power Station well field, (b) Jamshidabad well 1, and (c) Jamshidabad well 2.

*Ref to Rep.*

The time-drawdown and recovery data for the other pumping wells in this well-field area were also plotted and analysed by the Jacob straight-line method (see Appendix 5). The plots and their calculations are shown in Appendix 5 from Figure A5.1 to A5.5 and the results of the analyses are summarised in Table 5.2. A technical cross-section of these wells is represented in Figure 5.3.

The time-drawdown and recovery analyses are in close agreement with one another except for well SW8. The shape of the recovery curve in this well shows a typical water table aquifer condition in a semi-logarithmic plot (see Fig. A5.2 of Appendix 5) which is completely different from the drawdown curve. The value of transmissivity calculated from the first and third segments are exactly the same. However, this well gives different transmissivity values for the two sets of data.

### **Jamshidabad well field**

The Jamshidabad area is located to the north-west of Tabriz City. Two pumping wells were drilled in this area by IRAB Engineering Company in 1976. Wells JW1 and JW2 penetrate the unconfined and confined to semi-confined aquifers to depths of 125 and 140 metres, respectively. A lithological profile and details of casing and screen for these wells are shown in Figure 5.17. As the diagram shows, the water was pumped from the deep confined aquifer.

A constant rate pumping test was run in well JW1 at 5700 m<sup>3</sup>/d from 14th to 16th December, 1976. The recovery of the water level was measured immediately after pumping stopped and continued for 14 hours. The static water level in this well was 10.70 metres below the ground surface when the pumping test started.

The resultant time-drawdown and recovery data were plotted on semi-logarithmic paper and analysed by the Jacob straight line method (see Figs. 5.18 and 5.19). They slightly deviate from straight lines in both sets of data. Since the drilled well log (see Fig. 5.17) shows the supply to depend on the deeper zones, these can be under confined or semi-confined conditions. However, the pumping test data plots and the static water level show a confined condition for the deep aquifer.

The calculated T values for this well range between 580 and 660 m<sup>2</sup>/d and there is no considerable difference between the results of the drawdown and recovery data analyses.

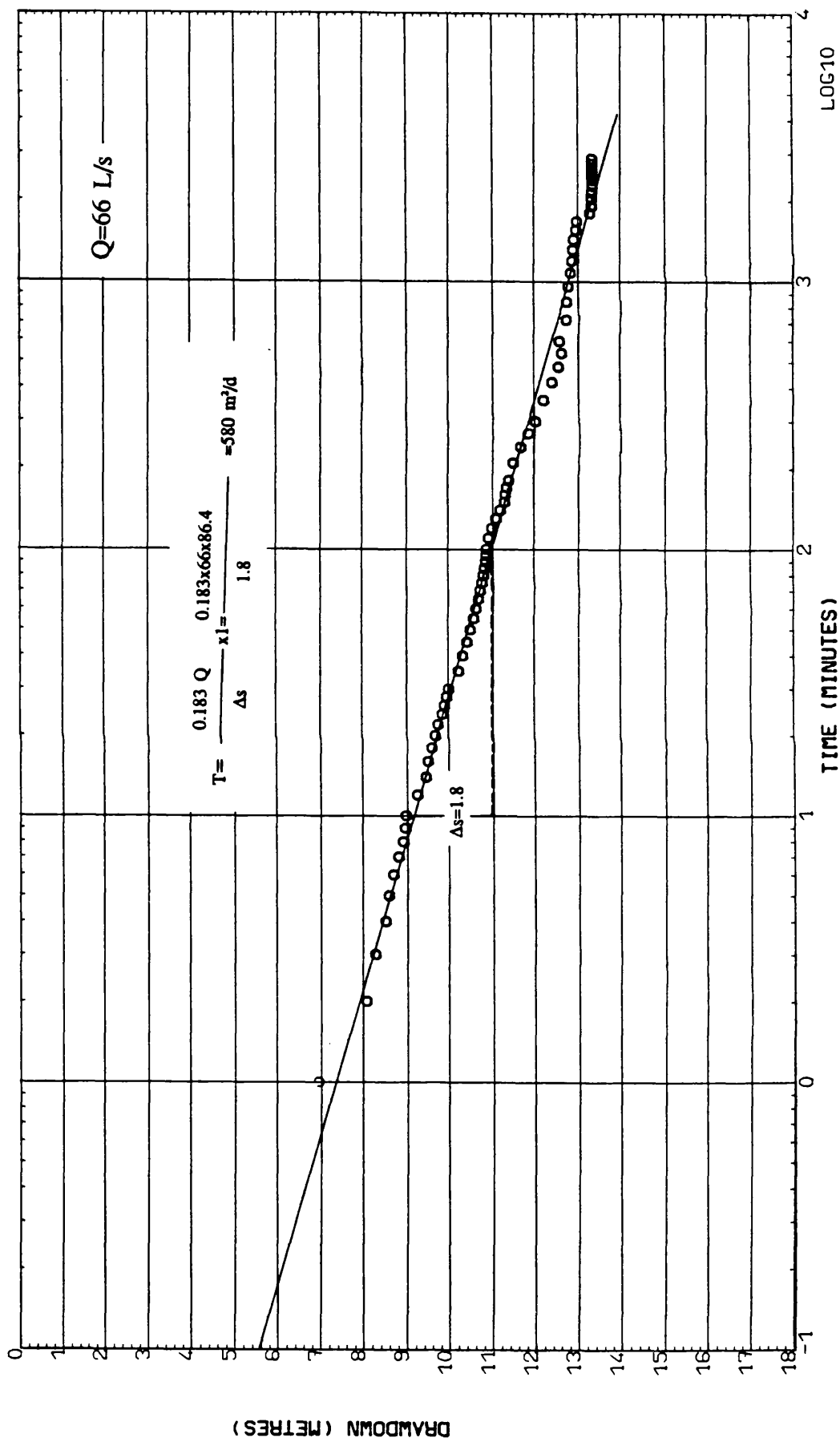


Fig. 5.18 PW JW1, Straight line method: Time-Drawdown plot.

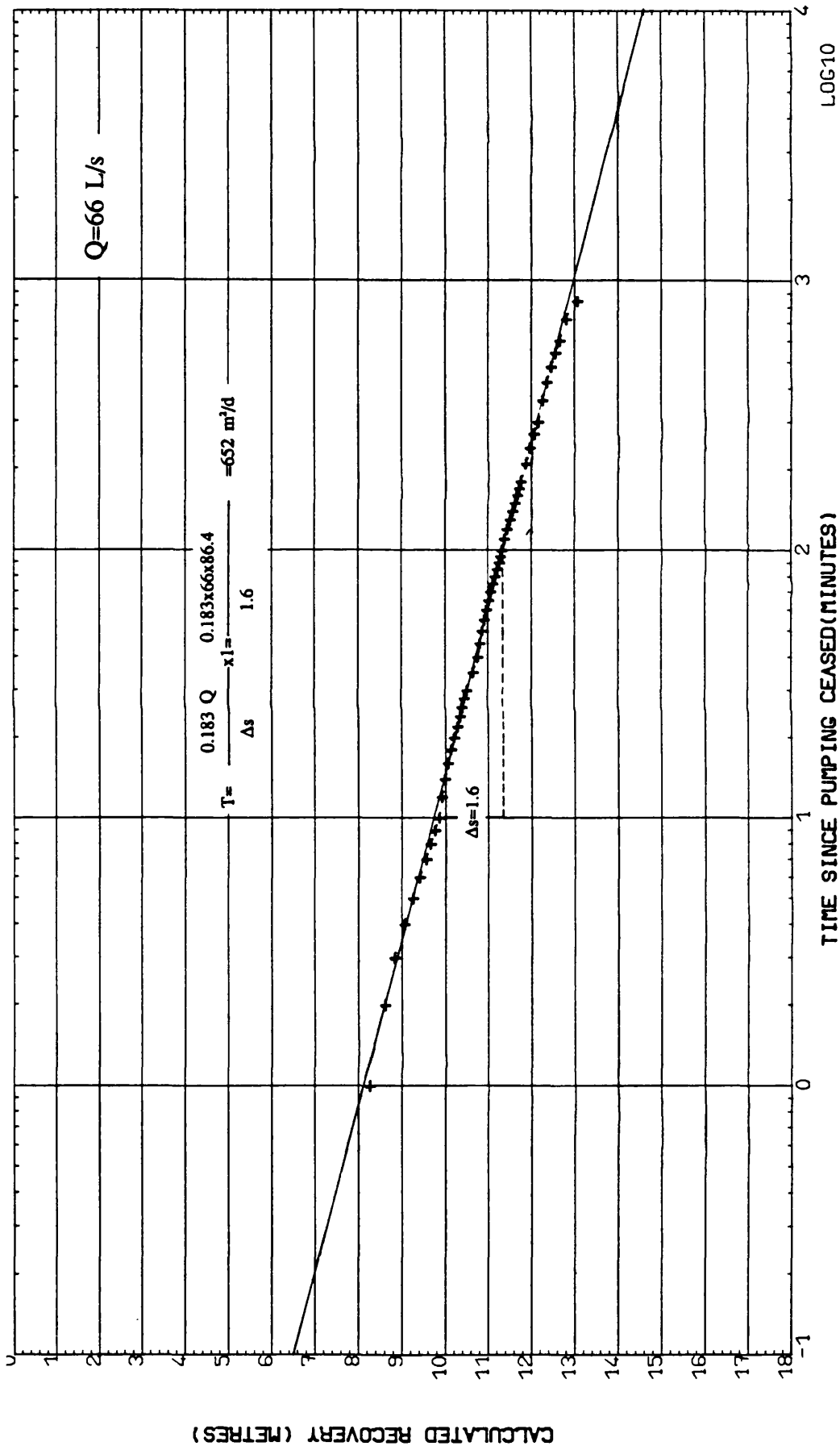


Fig. 5.19 PW JW1, Straight line method: Calculated recovery plot.

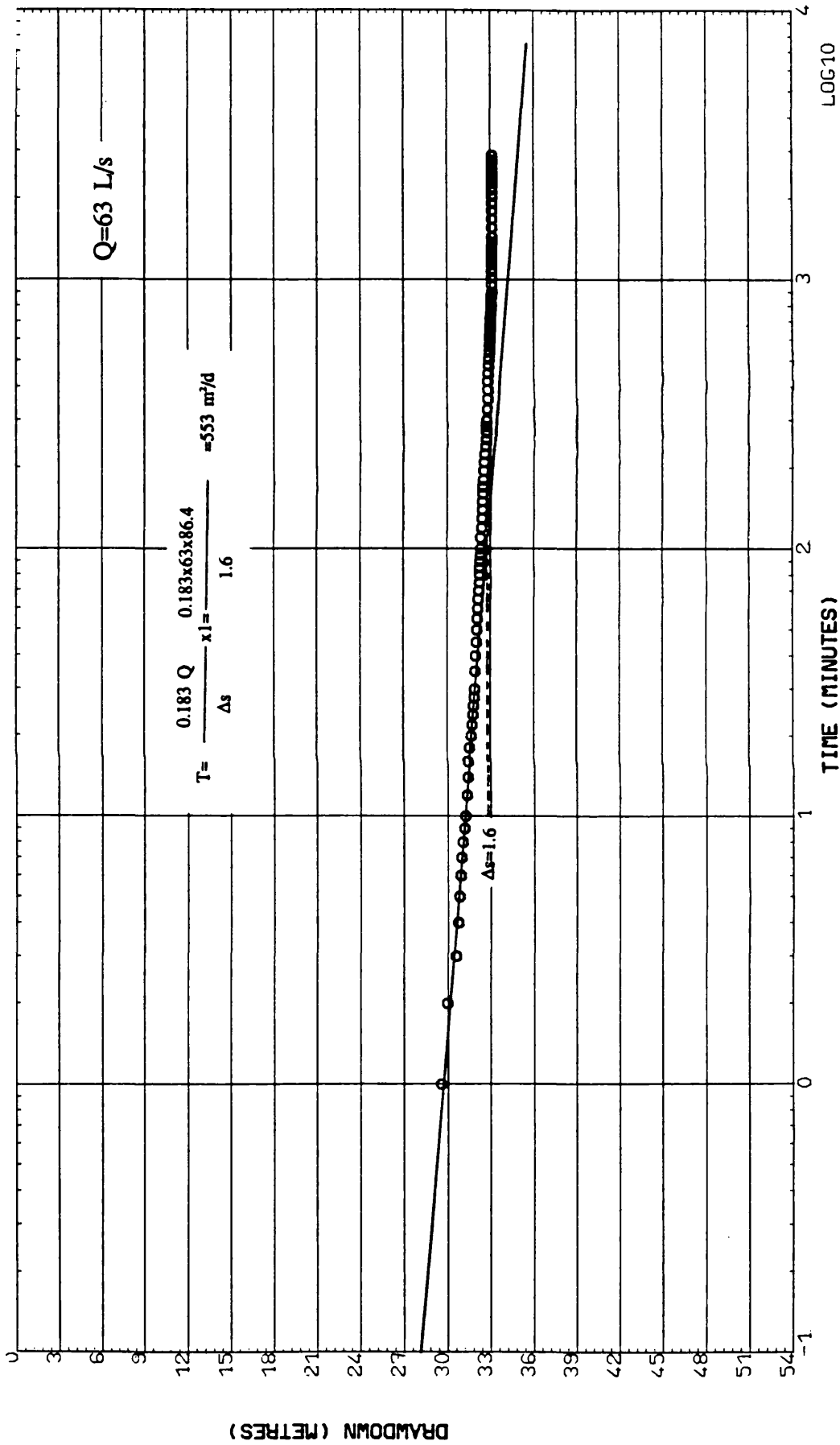


Fig. 5.20 PW JW2, Straight line method: Time-Drawdown plot.

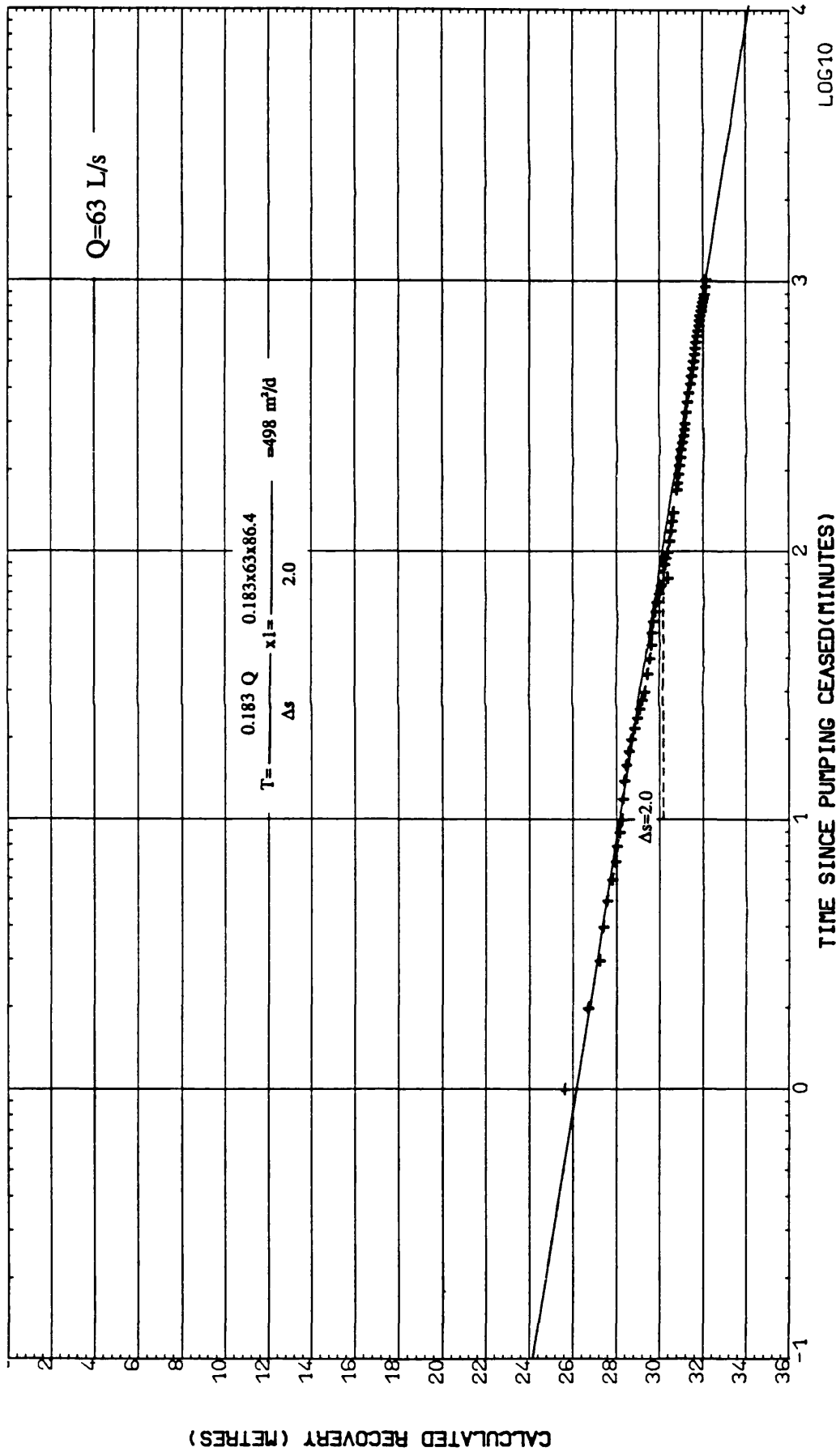


Fig. 5.21 PW JW2, Straight line method: Calculated recovery plot.



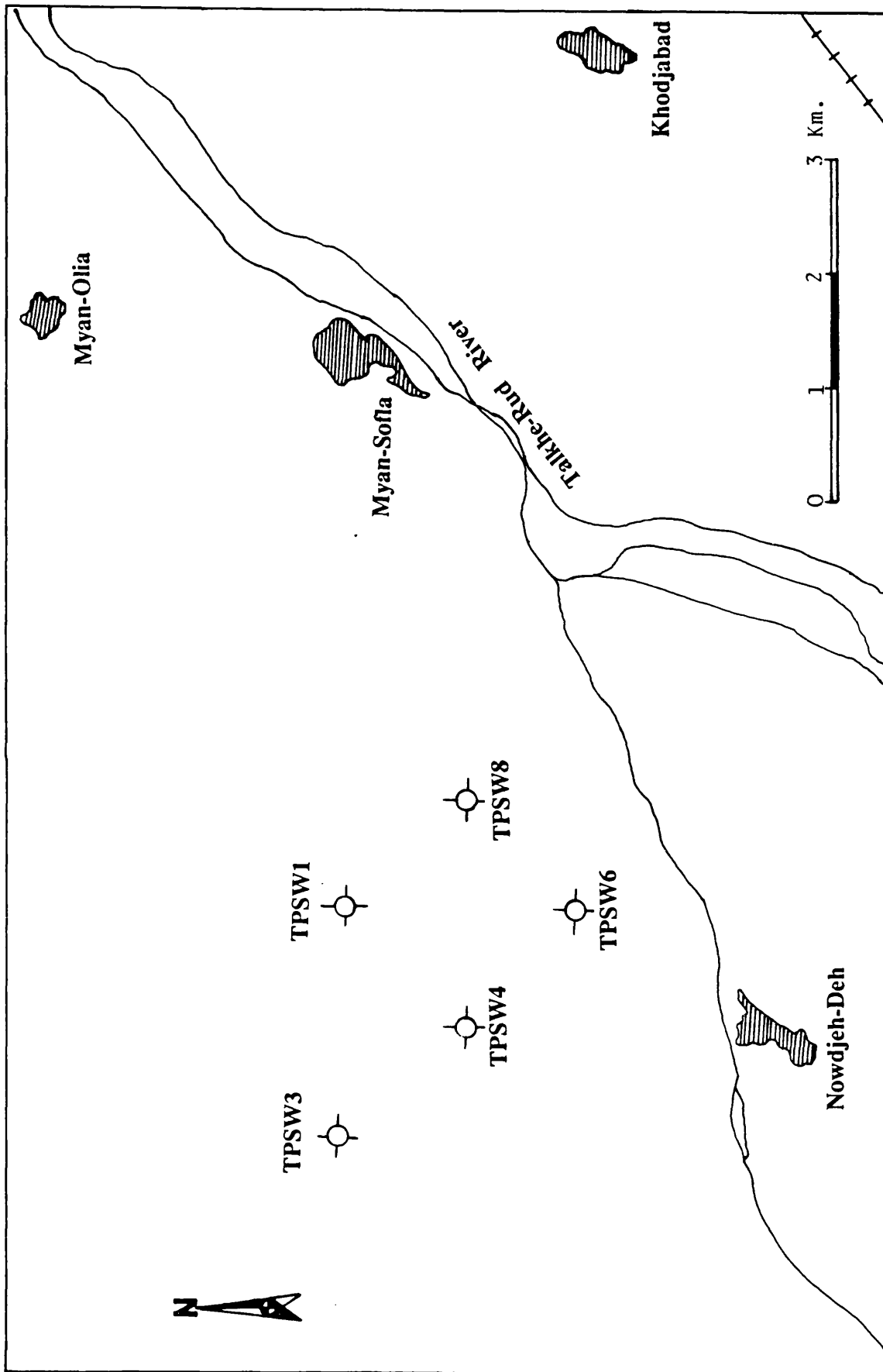


Fig. 5.22 Tabriz Power Station well field and location of pumping wells.

Brief details of the lithological profile and lining details for well JW2 are shown in Figure 5.17. The pumping test in this well was started on December 1967, and continued for 2 days, with a constant rate discharge of 5443 m<sup>3</sup>/d. The static water level was measured at 9.32 metres below the ground surface before the pumping commenced.

The recorded time-drawdown and recovery data, observed for 0.7 days duration, have been plotted on semi-logarithmic paper and analysed by the straight-line method (see Figs. 5.20 and 5.21). The time drawdown data deviate from the straight line after 100 minutes, though the calculated recovery data show a very good fit. It may be that the reason for the difference is the short duration of the observed recovery data. The transmissivity values deduced from both sets of data show a close agreement with a range between 498 and 550 m<sup>2</sup>/d.

### **Tabriz Power Station well field**

The Tabriz Power Station is situated approximately 20km south-west of the city of Tabriz, north of the main asphalt highway (see Fig. 5.1). The well field area lies immediately north of the proposed Power Station site. The area was studied by IRAB Engineering Com. LTD. in 1976, but the original data of this study are not available.

The Azarbijan Regional Water Authority drilled five pumping wells to meet the required power station water demand in 1981. The exact location of these wells can be seen in Figure 5.22. Also brief details of the drilled well logs and lining are shown in Figure 5.17.

The wells were screened in the deep aquifer which lies approximately between 60 and 120 metres depth. The casing and screen pipe inner diameters are 12 inches for all of these wells except well TPSW8 which is 14 inches.

Well TPSW1 was drilled to a total depth of 130 m and screened in the deeper aquifer between 70 and 130 metres. The static water level in this well was 1.02m below the ground surface when the pumping started.

A constant-rate pumping test was carried out in this well for 24 hours at a rate of 8415 m<sup>3</sup>/d in October 1980. The recovery data were recorded immediately after the pumping was stopped, and continued for 7 hours. The observed time

drawdown and recovery data were plotted on log-log and semi-log papers (see Figs 5.23 and 5.24). The time-drawdown data deviate from the straight-line after 100 minutes. However, for the recovery data, this phenomenon happens 50 minutes after the pumping was stopped.

Such behaviour of the field data is due to the leakage of water from the overlying unconfined aquifer. However, the value of this leakage is too small to be analysed with the Hantush and Jacob leaky-confined aquifer solutions (Leaky type curve or inflection methods).

The values of transmissivity deduced from both sets of field data are in good agreement and range between 842 and 856 m<sup>2</sup>/d.

Well TPSW3 penetrated to a depth of 115 metres and is screened in the deep aquifer between 66 and 110 metres. At the time of the pumping test, the piezometric head corresponded with ground level.

A constant rate test was performed in this well at a rate of 8415 m<sup>3</sup>/d, for 24 hours on 23rd October 1980. The recovery phase was measured for only 50 minutes, immediately after the pumping stopped. The semi-log analyses of the observed data are represented in Figures 5.25 and 5.26. The time-drawdown data in the semi-log plot deviate from a straight line after 200 minutes. However, the recovery data show a good fit for the short duration of recorded data.

The above-mentioned methods were also used for data obtained from pumping wells TPSW4, TPSW6 and TPSW8 (see Figures A5.11 to A5.16 in the Appendices). The plotted data for all of these wells show a very good match with the Theis type-curve and Jacob straight-line methods. Good results were obtained from the tests with transmissivities ranging from 2174 (TPSW8) to 820 m<sup>2</sup>/d (TPSW1). The time drawdown and recovery analysis generally are in close agreement with one another with the exception of TPSW1. The results of the tests are shown in Table 5.3.

### **Tabriz Airport well field**

The proposed Tabriz airport water supply wells were located about 12km north-west of the city of Tabriz and about 8km south-west of the Tabriz airport(see Fig. 5.1). Five pumping wells were drilled in this well field by AGRO-Water Consulting engineers in 1977. The well construction and pumping test data are only

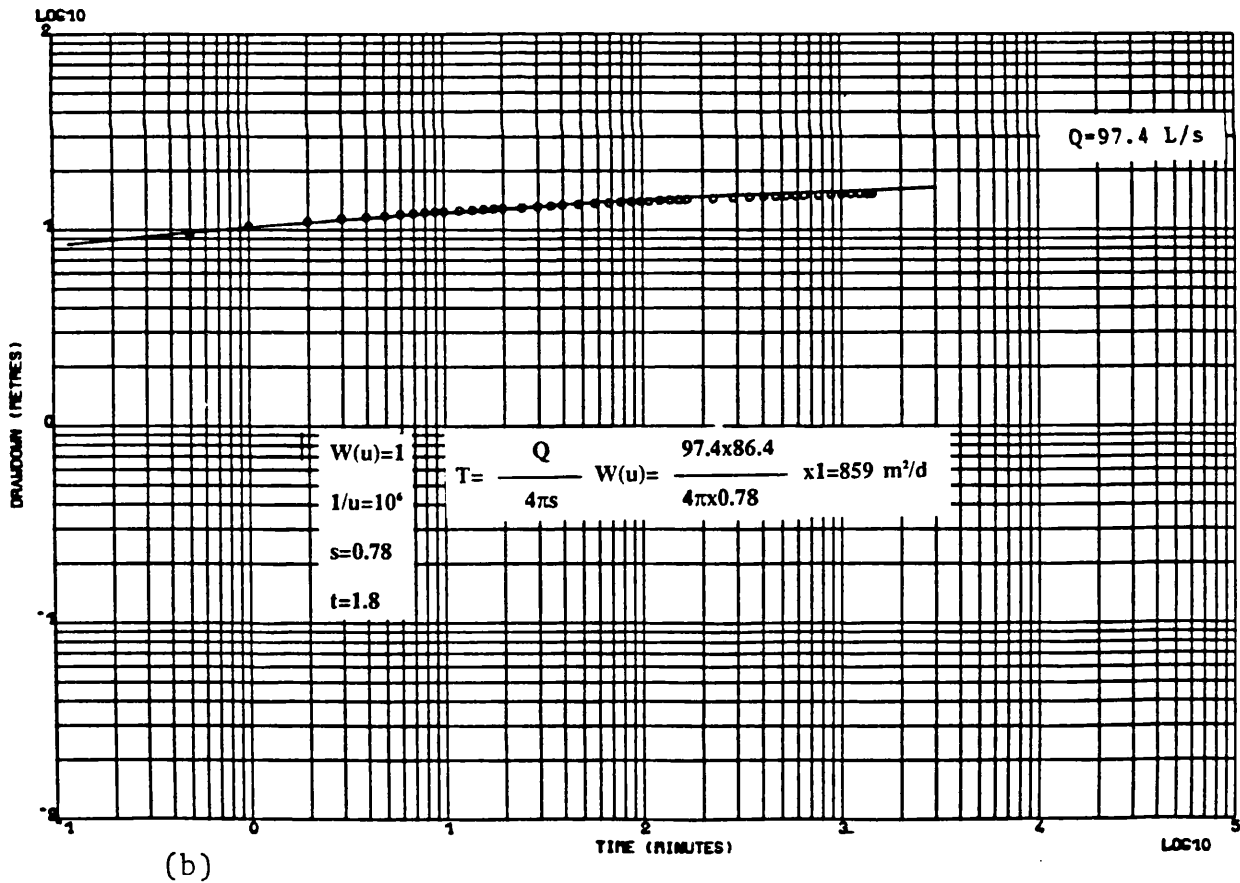
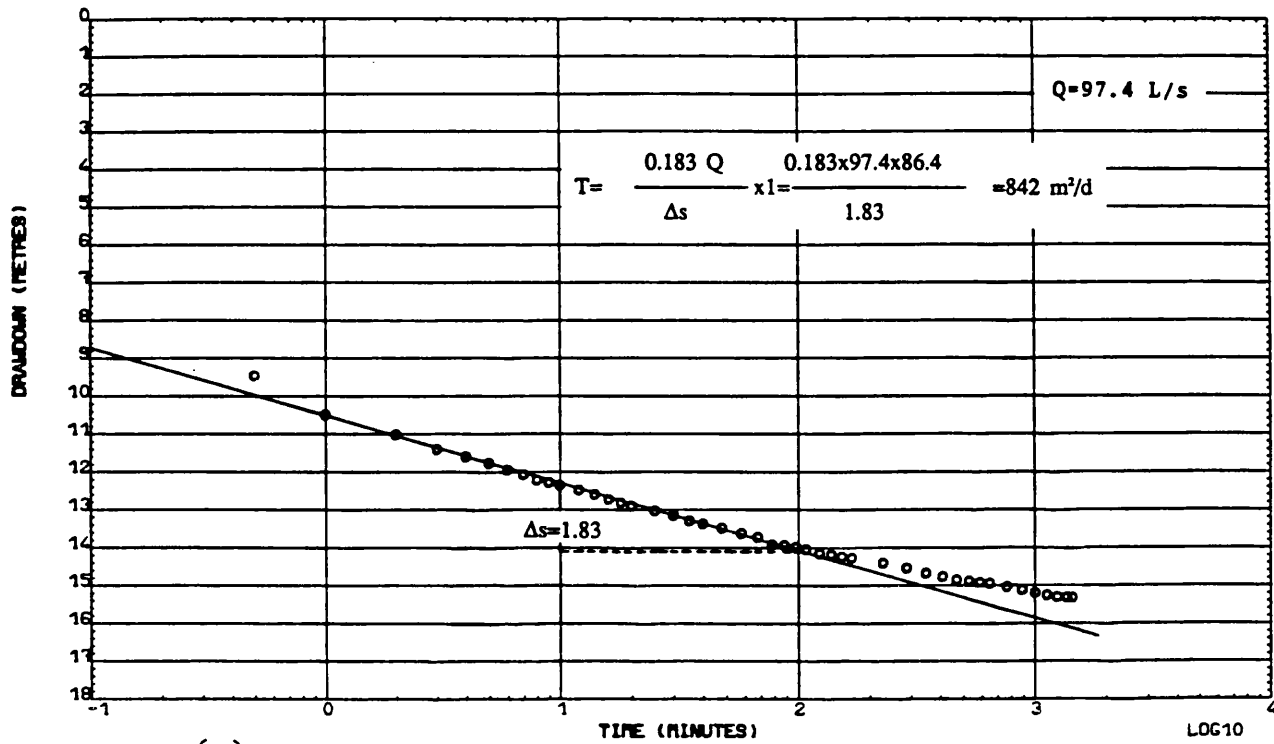
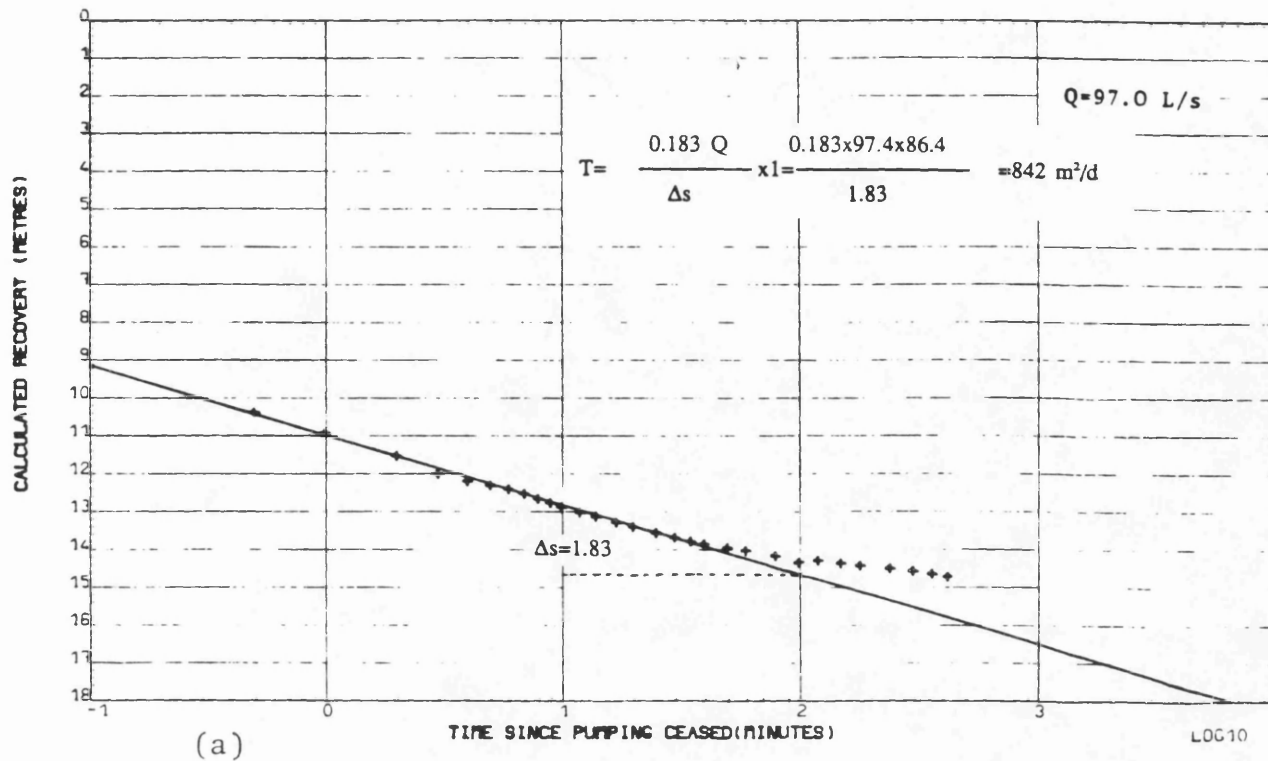
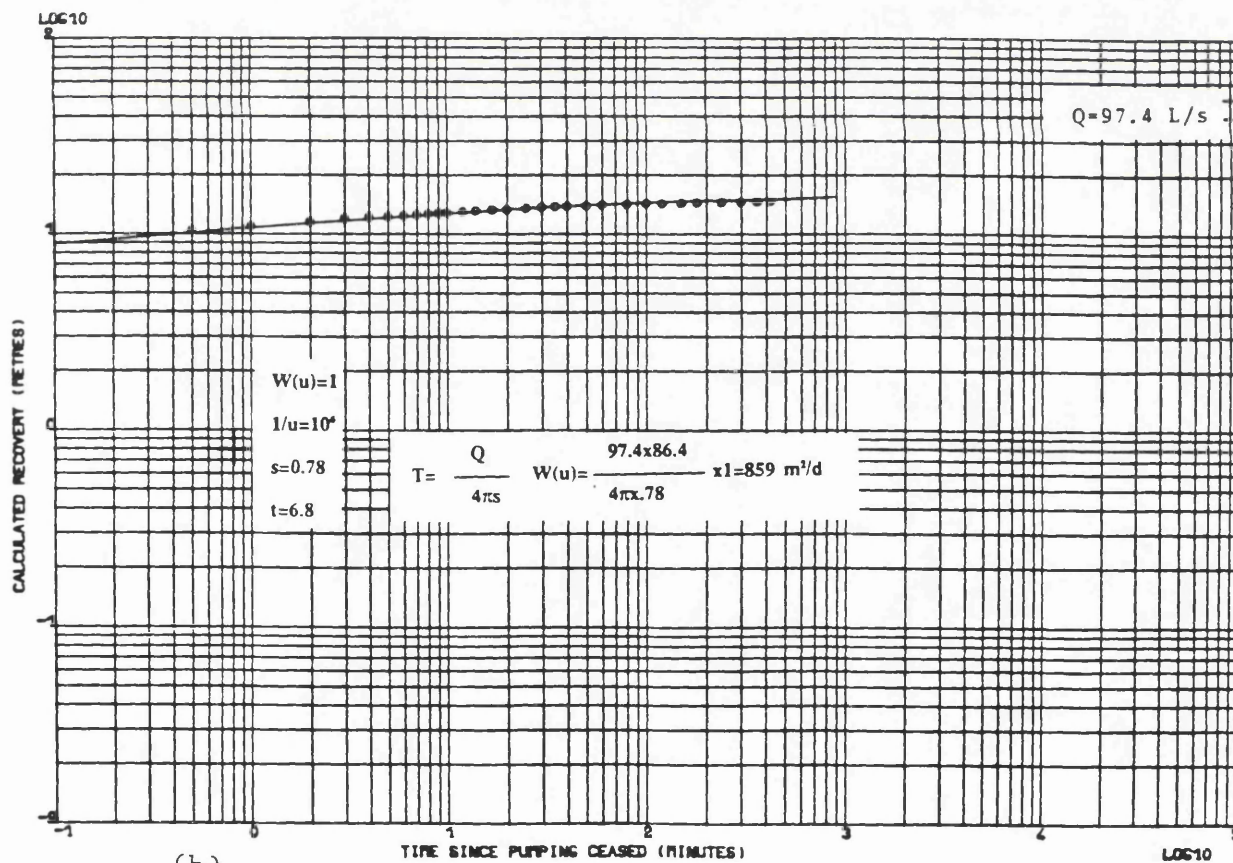


Fig. 5.23 PW TPSW1, Time-Drawdown plots: (a) Straight line method,

(b) Type curve method.



(a)



(b)

Fig. 5.24 PW TPSW1, Calculated recovery plots: (a) Straight line method, (b) Type curve method.

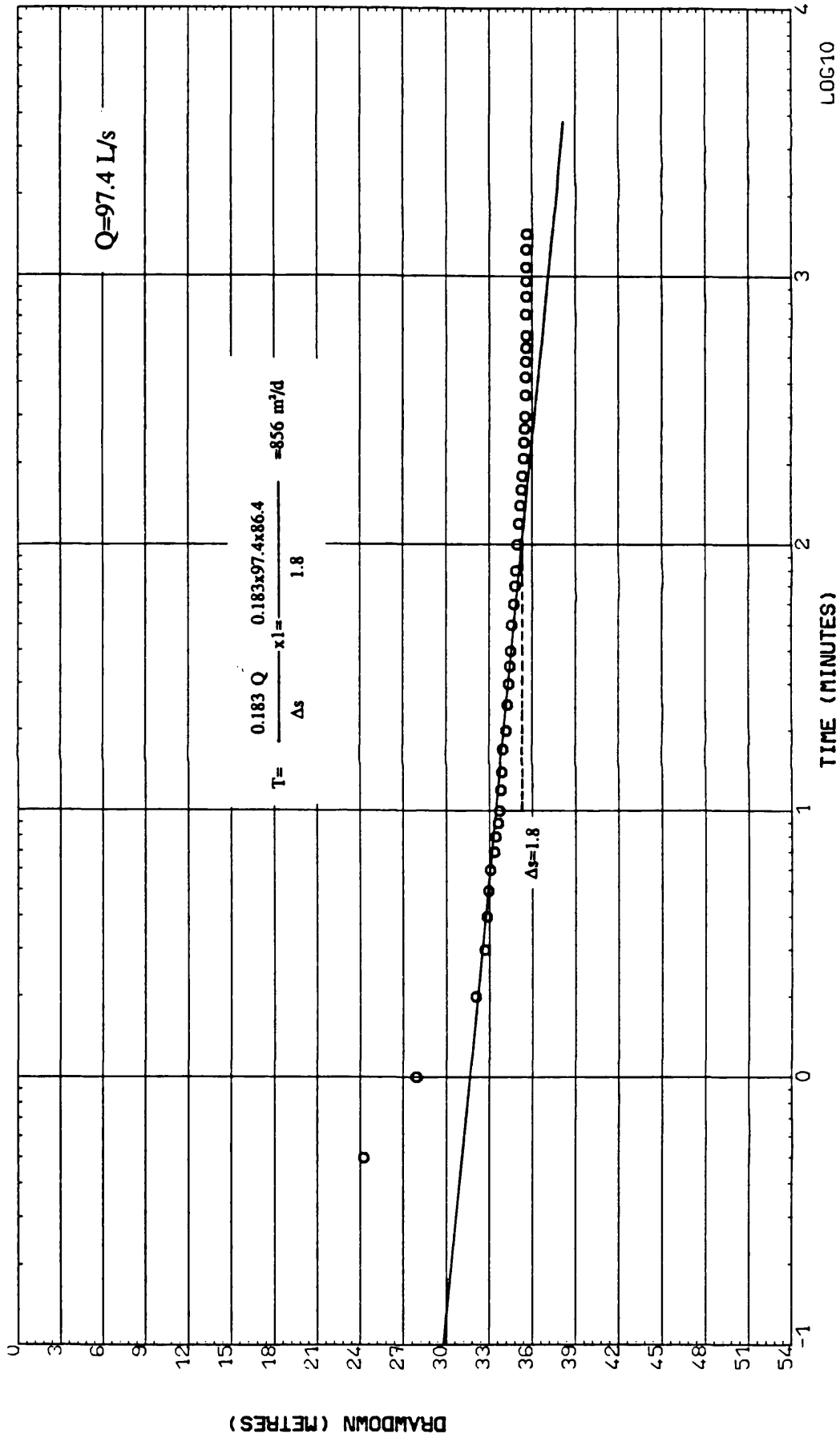


Fig. 5.25 PW TPSW3, Straight line method: Time-Drawdown plot.

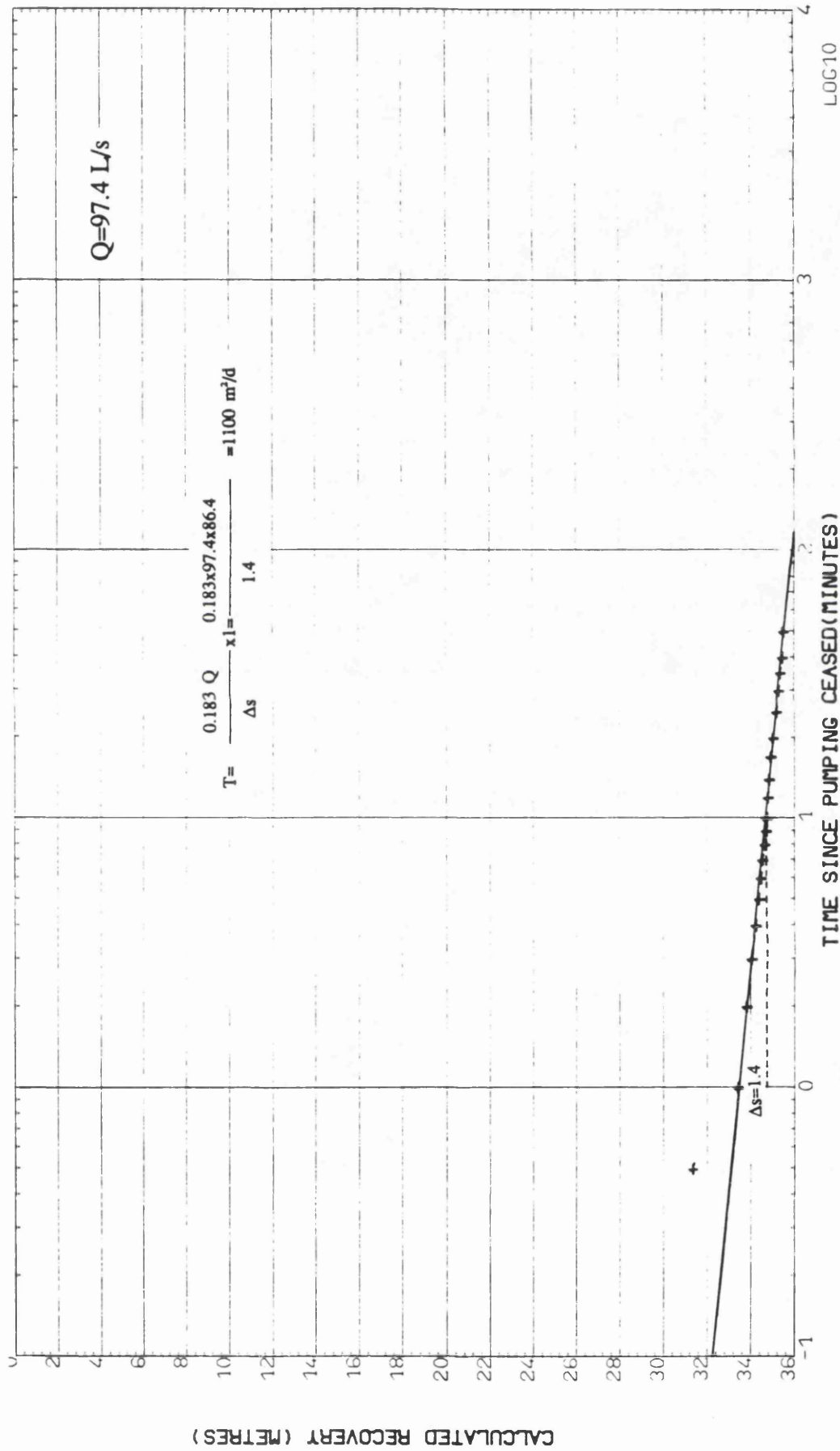


Fig. 5.26 PW TPSW3, Straight line method: Calculated recovery plot.

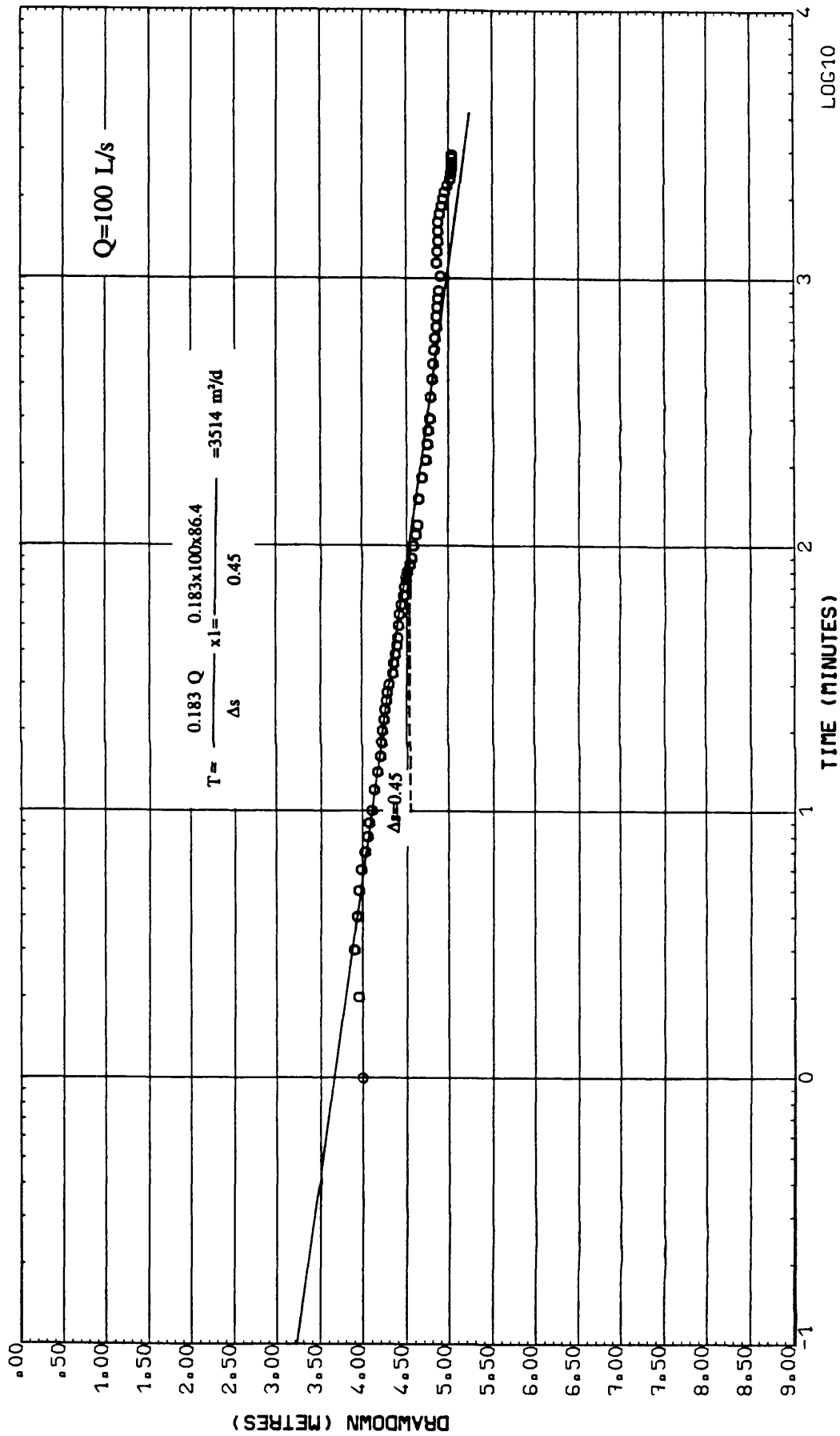


Fig. 5.27 PW TAW, Straight line method: Time-Drawdown plot.



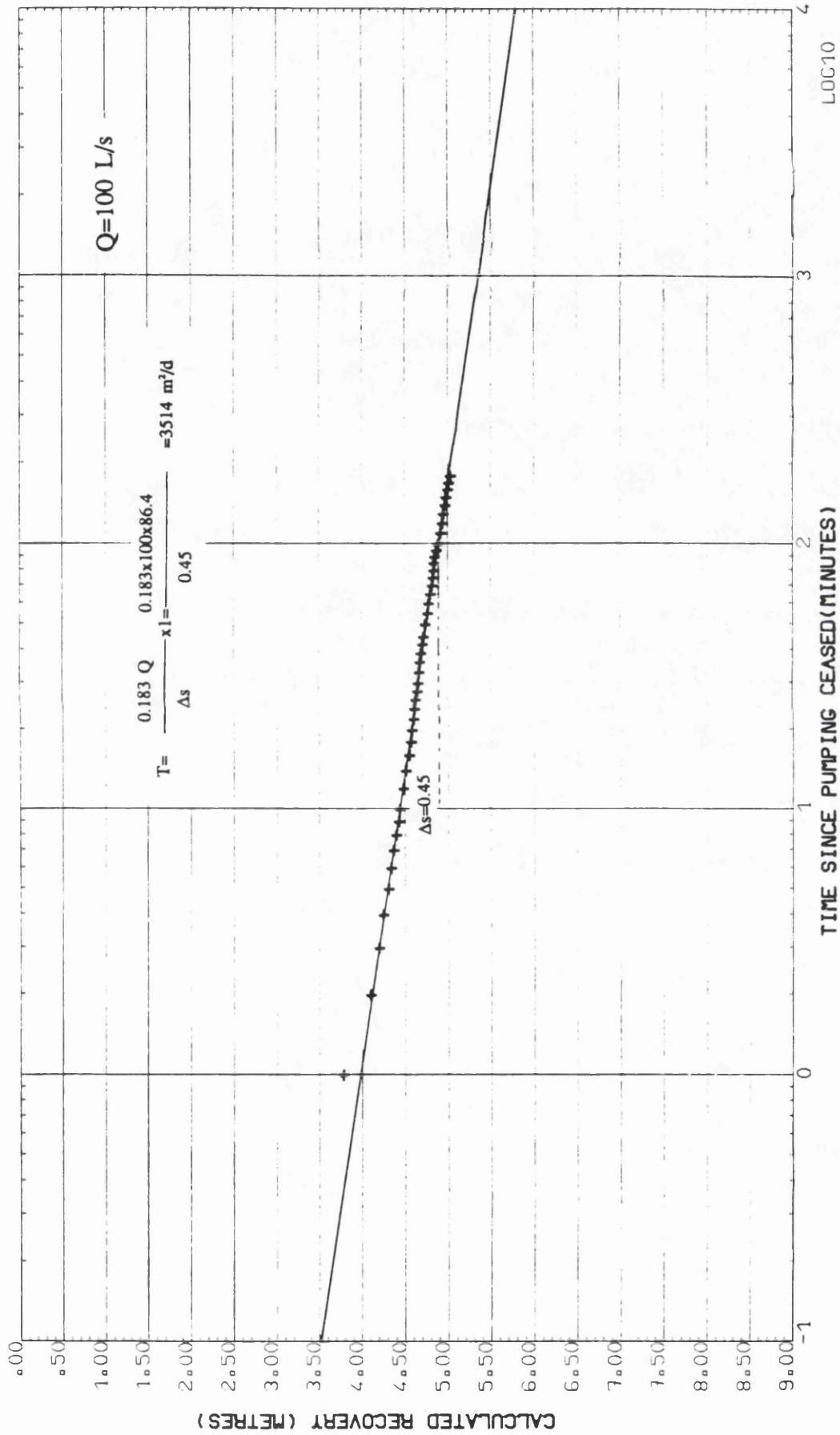


Fig. 5.28 PW TAW, Straight line method: Calculated recovery plot.

available for one of them (TAW) which is investigated in this project. The lithological profile and length of casing and screen are shown in Figure 5.17. Total depth of the well is 151 metres with casing and screen diameter of 12 inches.

A constant rate test at 8600 m<sup>3</sup>/d was performed on 3rd August 1977, and recovery data were recorded immediately after pumping stopped. The static water level was measured at 2.7 metres below the ground surface when the pumping started. Figures 5.27 and 5.28 show the time-drawdown and recovery plots of this well. The Jacob straight-line method was tried and showed good agreement with the plotted data.

An average transmissivity of the order of 3500 m<sup>2</sup>/d was obtained from the analyses. The very high value of the transmissivity for the area is believed to be due to the 'buried river valley' in the vicinity of the pumping well. It should be mentioned that the Tabriz Airport well field area is only a few kilometres distant from the Tabriz Power Station well field.

#### Soufian water supply well

The well tested in this location is 30km north-west of Tabriz City (see Fig. 5.1). The well tapped unconfined alluvial material to a depth of 75 metres with an inner pipe diameter of 12 inches. The well was screened in two sections at depth between 15.72 to 45m and 54.36 to 69 metres.

A pumping test was carried out for 20 hours at a rate of 6394 m<sup>3</sup>/d on 25th September 1977. The recovery data were also recorded for this well following cessation of the pumping. The static water level was measured at 19.3 metres below the ground surface when pumping started.

Time-drawdown and recovery data were plotted on semi-log paper (see Figs. 5.29 and 5.30). The Theis type-curve and straight-line methods were used to analyse the field data. There was some difficulty in obtaining an adequate fit from the Theis type-curve method. This was probably due to the high rate of drawdown which gave smoothed time-drawdown and recovery curves. The straight line method analysis seems to give reasonable results. The transmissivity values range between 1230 and 1260 m<sup>2</sup>/d in this area.

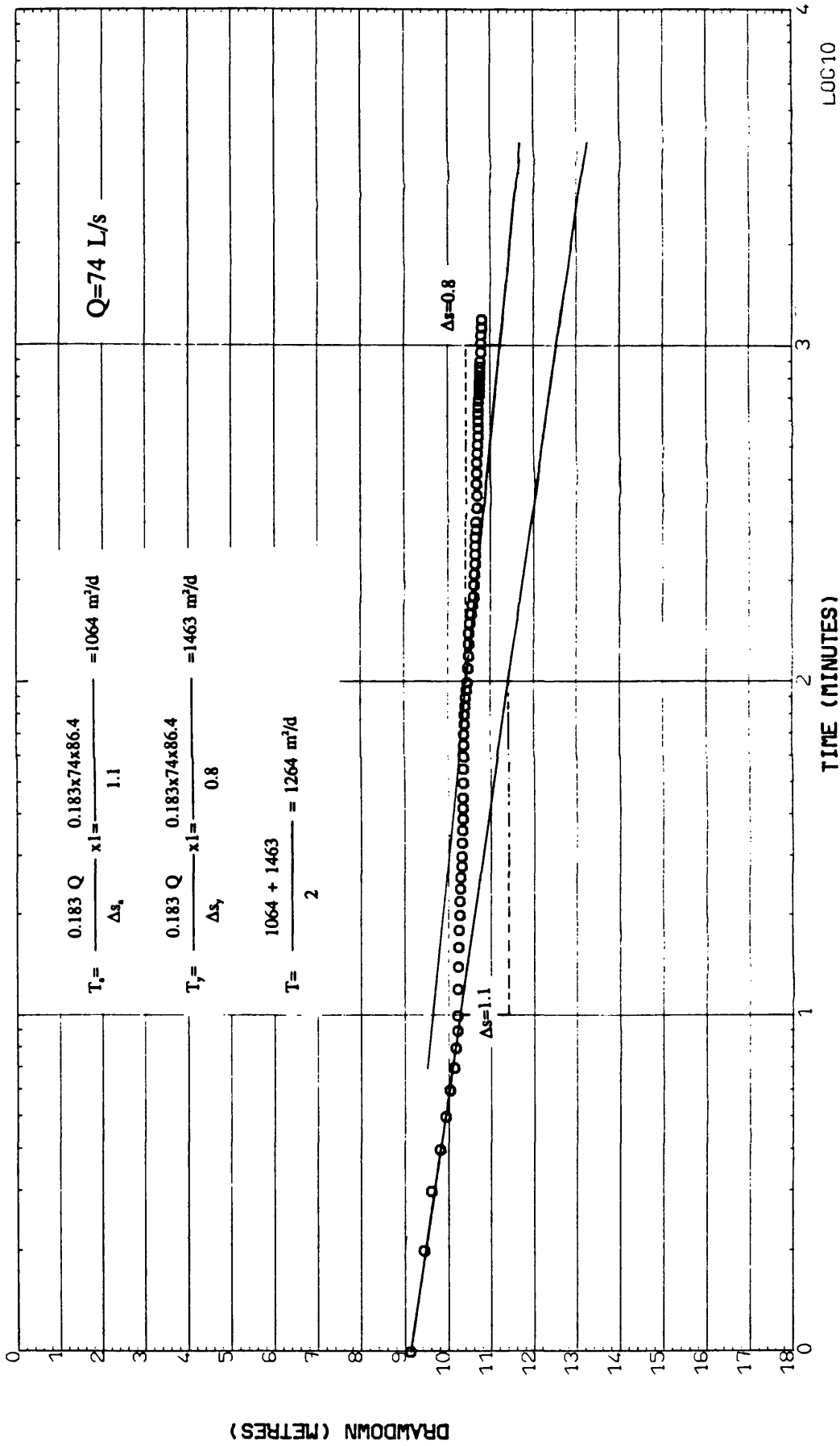


Fig. 5.29 PW SOW, Straight line method: Time-Drawdown plot.

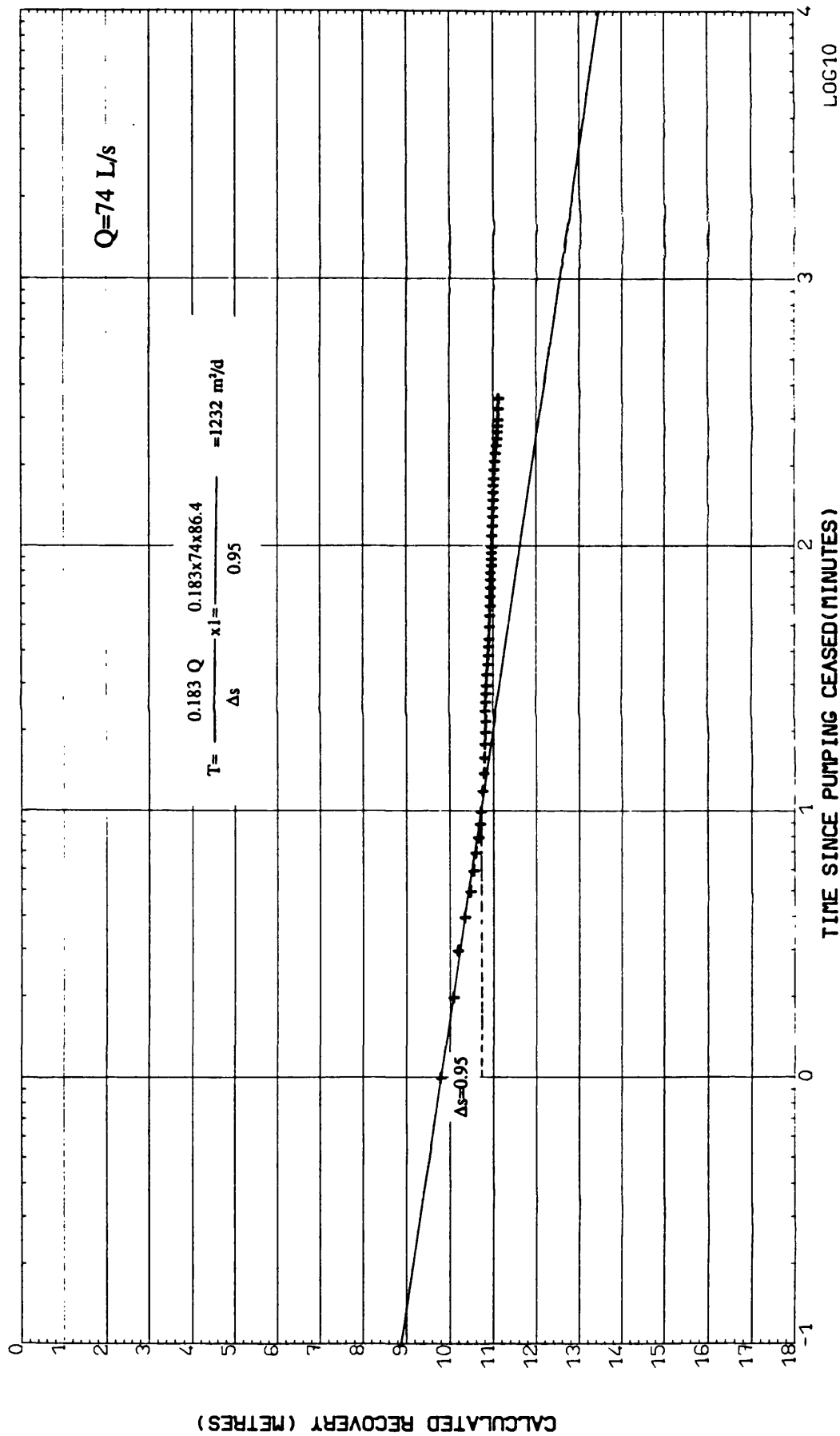
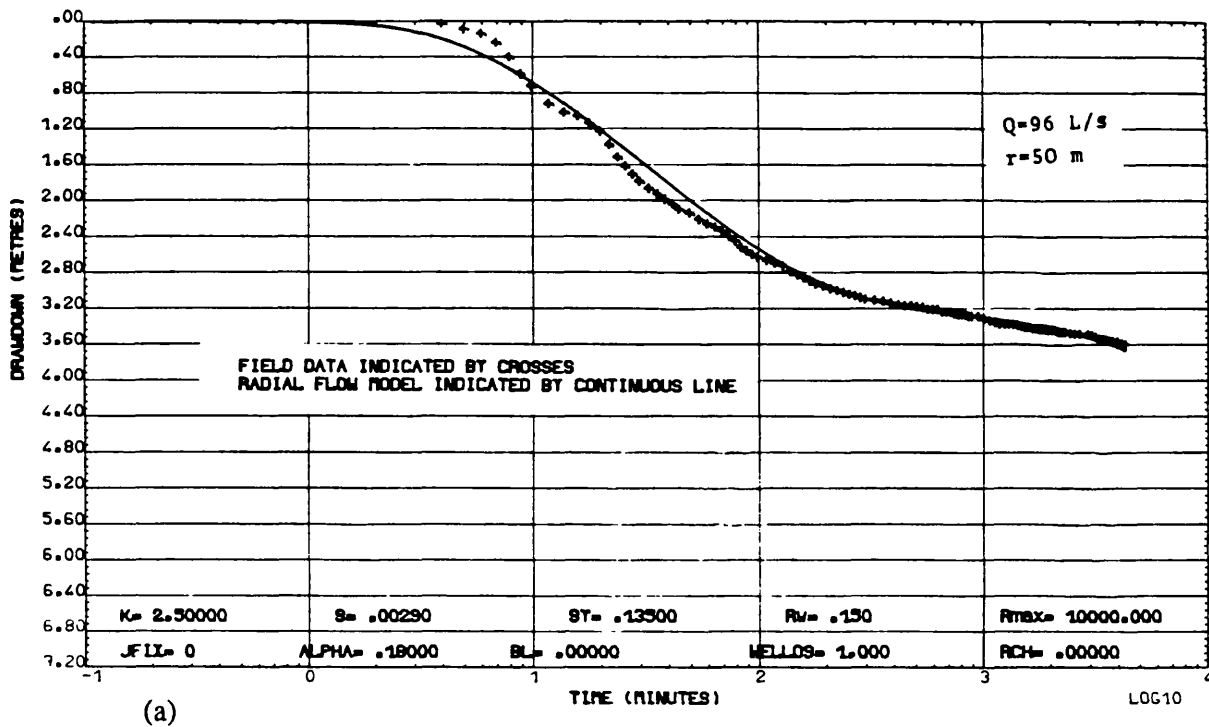
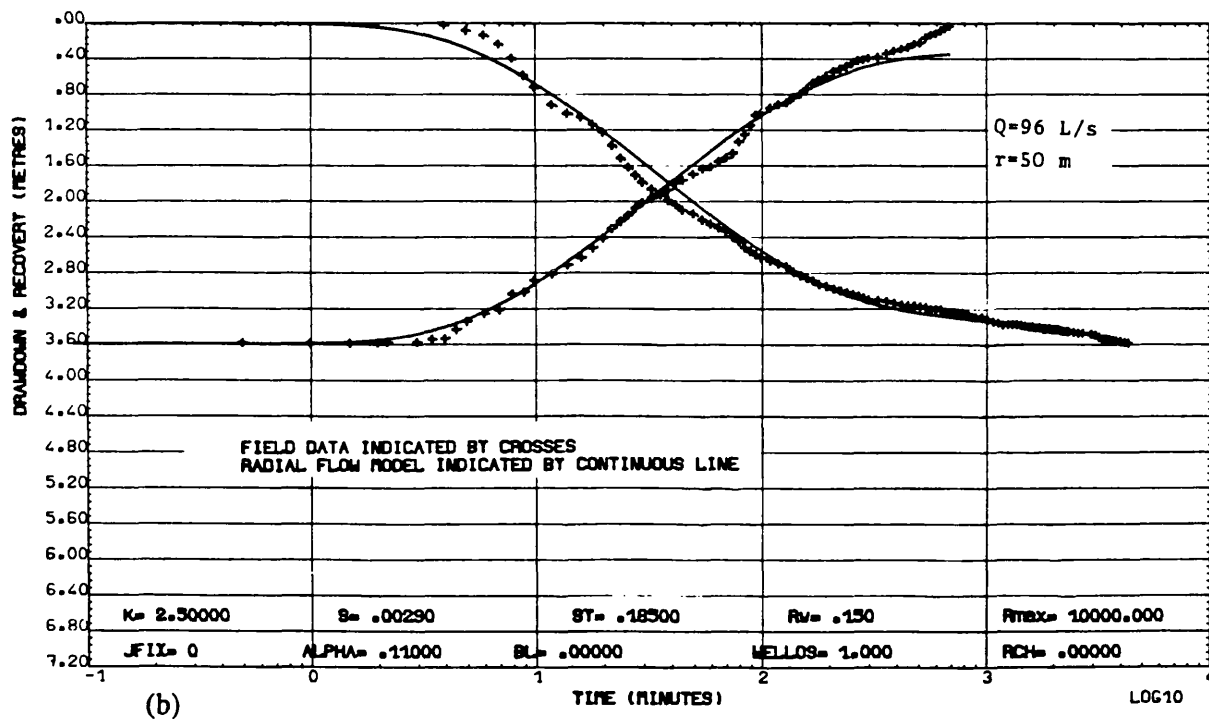


Fig. 5.30 PW SOW, Straight line method: Calculated recovery plot.

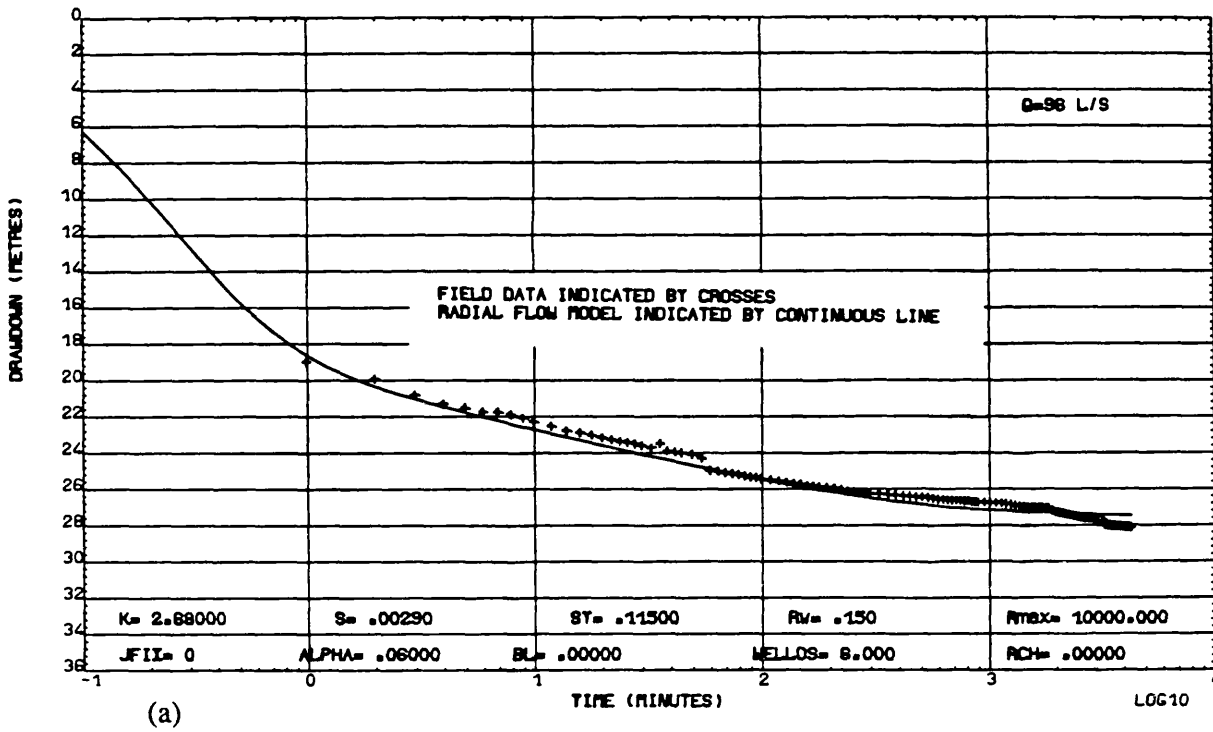


(a)

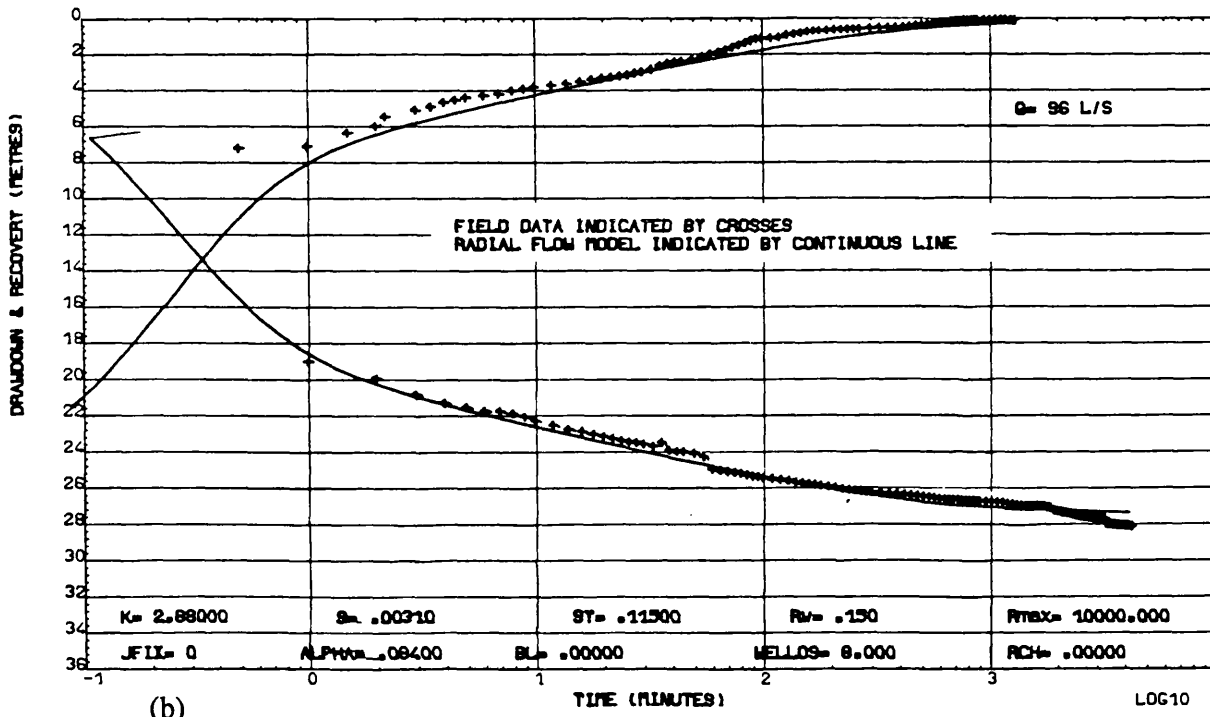


(b)

Fig. 5.31 OW SPW3, Model analysis: (a) Without recovery, (b) With recovery.



(a)



(b)

Fig. 5.32 PW SW3, Model analysis: (a) Without recovery, (b) With recovery.

## **5.5. Numerical Analysis of Data**

Each pumping and observation well that was analysed by analytical methods was also analysed by the numerical technique. As stated earlier, there is no observation well in most of the well fields, so that the calculated storage coefficients from pumping wells are necessarily estimated values, even with the numerical method.

### **Saidabad well field**

Many factors influence drawdown at the abstraction well in an unconfined aquifer. These factors include the transmissivity ( $Kxb$ ), confined and unconfined storage coefficients, delayed yield, modified transmissivity in the vicinity of the abstraction well, the free water contained within the well, the influence of the boundaries as well as the abstraction rates. Some of these are known and constant, whereas others depend on the type of aquifer. The following parameters are variable:- permeability, storage coefficients, delayed yield, and well loss factor.

However, the numerical model can include all these factors in a single numerical analysis but using this, in many cases, it is difficult to distinguish the relative importance of their roles.

As explained previously there is only one observation well (SPW3) in the Saidabad well field for which the originally recorded time-drawdown and recovery data are available. Thus, an attempt was made to identify and quantify as many aquifer parameters as possible by applying the different methods for analysing data from this well.

The position of the observation well and the results of hydraulic properties from the analytical methods were set in the model data file. The theoretical radial flow model curve determined by the numerical technique was fitted to field data plotted on semi-logarithmic paper. Best fit matching was tried by changing the values of the related parameters until the best agreement had been achieved.

Figure 5.31 shows the numerical analysis of field data with and without recovery in observation well SPW3. The aquifer parameters deduced from this simulation are shown in the same figure. The well loss factor for the observation well is equivalent to 1, which means that there is no well loss in the observation wells.

By comparison, this value for the associated pumping well is 6.0 which is equivalent to a horizontal hydraulic conductivity of one sixth of the normal value at a distance of 7cm from the well face.

Fuller details of the modification of hydraulic conductivity in the vicinity of the abstraction well due to turbulent flow or well clogging will be discussed in the next chapter. The numerical method takes into account the well loss factor besides the other parameters for determining the aquifer properties. However, it does not give any percentage of drawdown as a well loss or well efficiency. It seems that percentage of well loss can be determined from this method only by replotting the same deduced aquifer parameters without well loss factor. In this case, the difference between the previous best fitted drawdown curve and new numerical replotted curve will be the value of the well loss.

The observation well SPW3 (see Fig. 5.32) shows only slight differences between the results deduced from the discrete numerical model and those obtained from the Boulton type-curve method, whereas the analytical straight line method leads to results that are inconsistent.

For the pumping well 3 (SW3), the value of the transmissivity from the analytical method shows good agreement with the value deduced from the numerical method. However, the other parameters such as the storage coefficients and delayed yield index are slightly different from the results deduced from the associated observation well.

Supplementary information providing model data for adequate estimation of the aquifer parameters from the abstraction wells was taken from the following sources:-

- the value of transmissivity which is deduced by the analytical solutions ( $T=bxK$ )
- the well loss amount calculated from a step-drawdown test with reference to the discharge rate
- the results deduced from the observation wells located in the same well field or aquifer
- establishment of the Boulton  $\Delta$  value greater than 10 ( $\Delta=1+S_y/S_s$ ).

Then, best fit matching was tried by testing different values for the parameters used in the model until a good agreement had been achieved.



The final trial of the model and field plots matching for the pumping and observation wells 1 (SW1 & SPW1) are shown in Figures 5.33 and 5.34.

The transmissivity values deduced from these wells by numerical analysis are slightly different from the analytical analysis results, especially the observation well which shows a lower value of transmissivity than the analytical method.

The storage coefficients for pumping and observation wells show poor agreement. The confined and unconfined storage coefficients and delayed yield values for the observation well are greater than those of the pumping well. The transmissivity value for the observation well is about twice as great as that for the pumping well. However, there is a well loss multiplication factor of 8 to be taken into account at the pumping well.

The final trial plots for pumping and observation wells 7 (SW7 & SPW7) with an adequate fit between the field and model plots are shown in Figures 5.35 and 5.36. There is close agreement between the analytical analysis and the model results for these wells.

Also, in comparison with well 1, there is good agreement between the aquifer properties deduced from the pumping and observation wells. The storage coefficients are exactly the same and the transmissivity and delayed yield values show very slight differences, with the well loss factor for the pumping well is equal to 2.

The time-drawdown and recovery data for the other pumping wells of this well field area were run and compared with the radial flow model results. There is a good agreement between the transmissivity values deduced from this method and the analytical analyses. The storage coefficients and delayed yield values show a small range of variation. The final trial plot results for the all of these pumping wells are shown in Appendix 5 from Figures A5.11 to A5.15 and the results for the well field are summarised in Table 5.4.

### **Jamshidabad wells**

Both pumping wells from the Jamshidabad area (JW1 & JW2) were analysed by the numerical method. The final trial for pumping well JW1 (see Fig. 5.37) shows a good fit with the field results. The well loss factor for this well is equal to 1 which it means it is very efficient with no well loss.

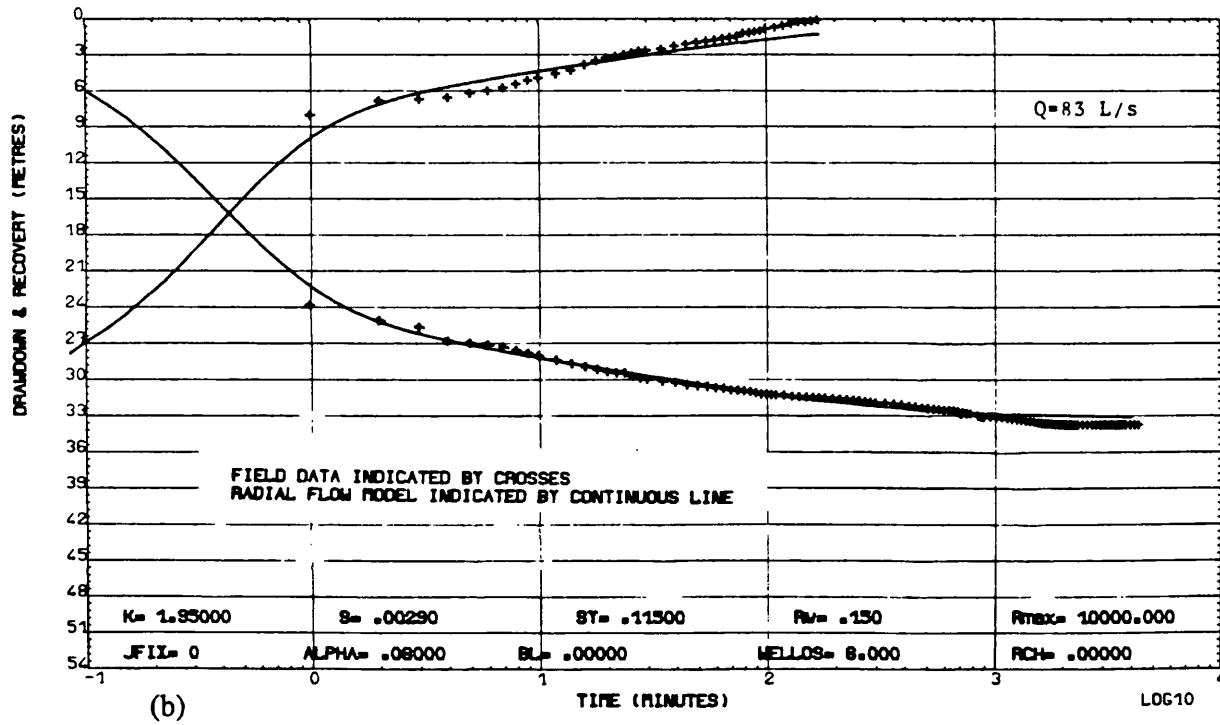
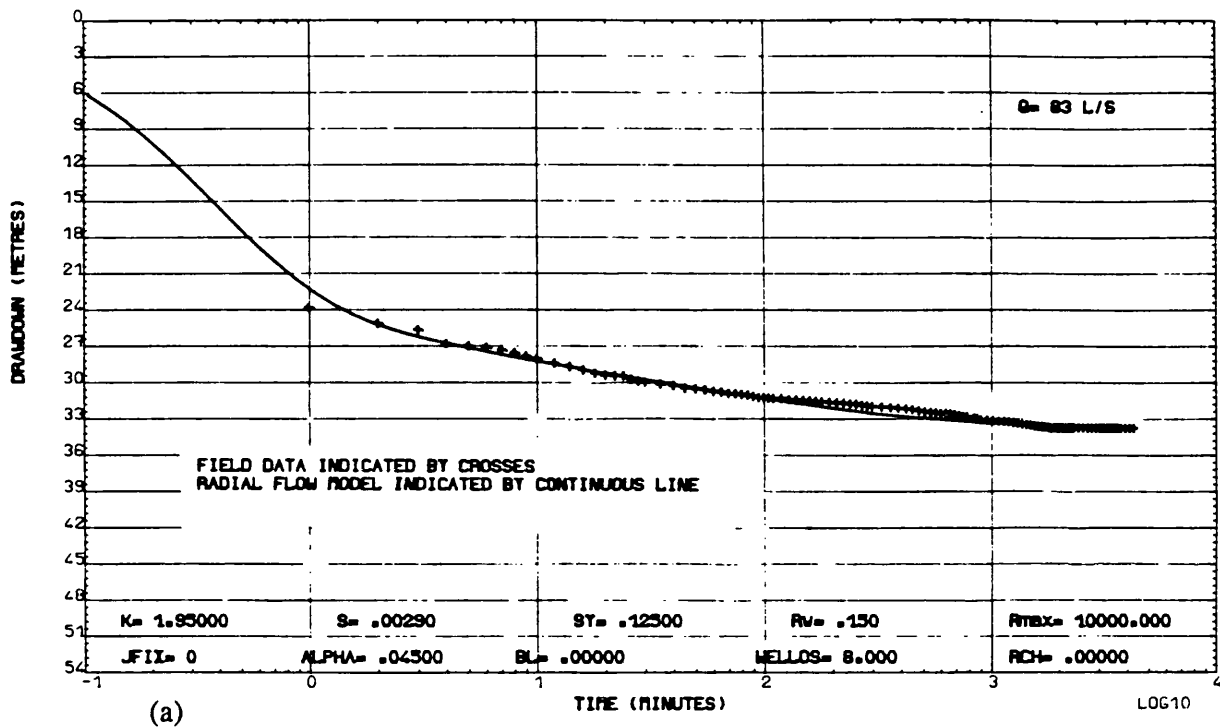


Fig. 5.33 PW SW1, Model analysis: (a) Without recovery, (b) With recovery.

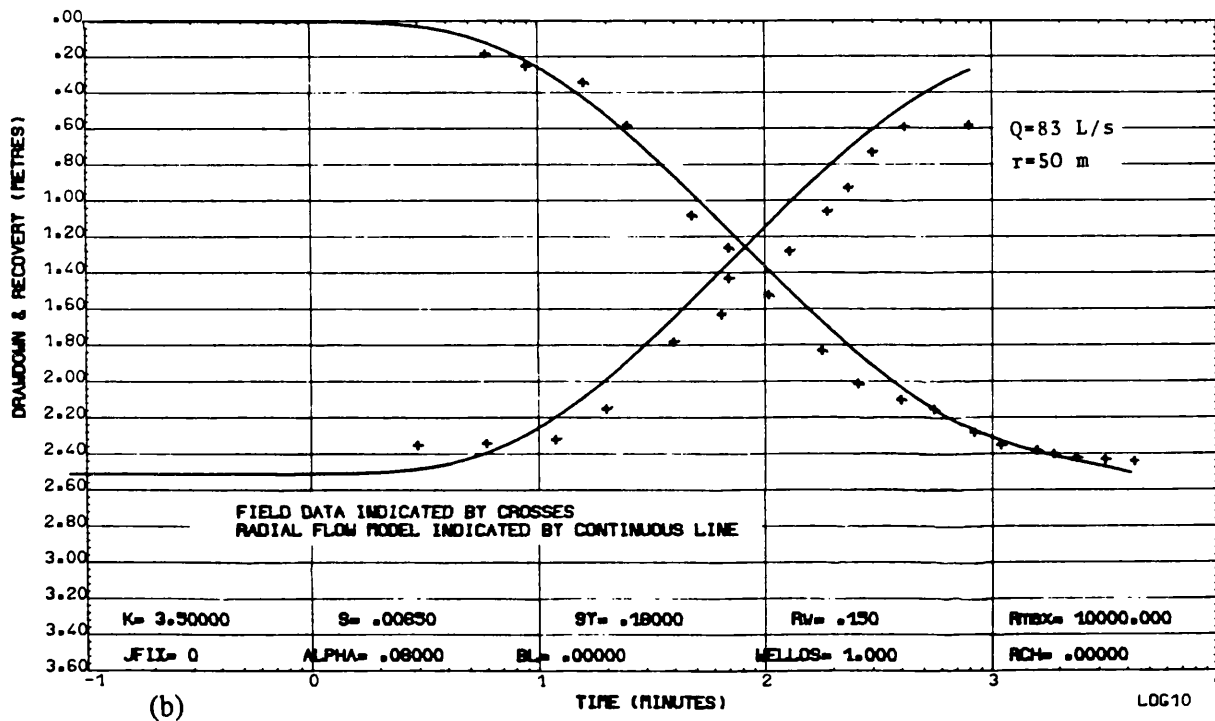
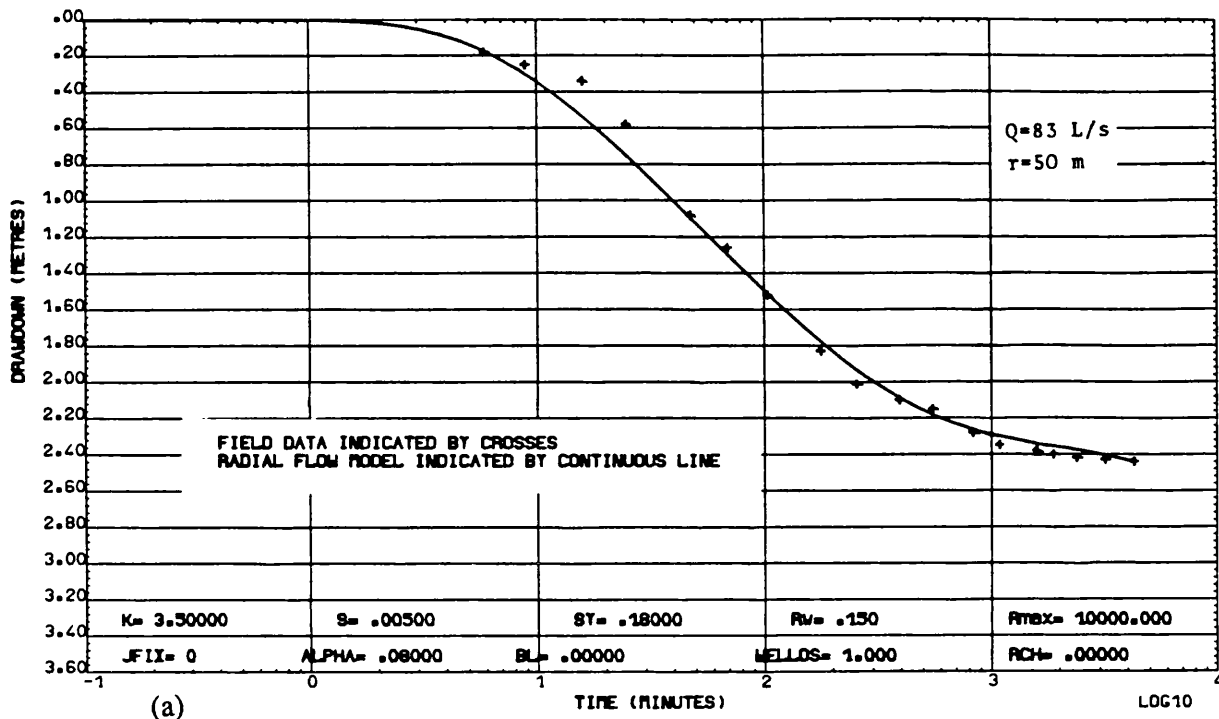


Fig. 5.34 OW SPW1, Model analysis: (a) Without recovery, (b) With recovery.

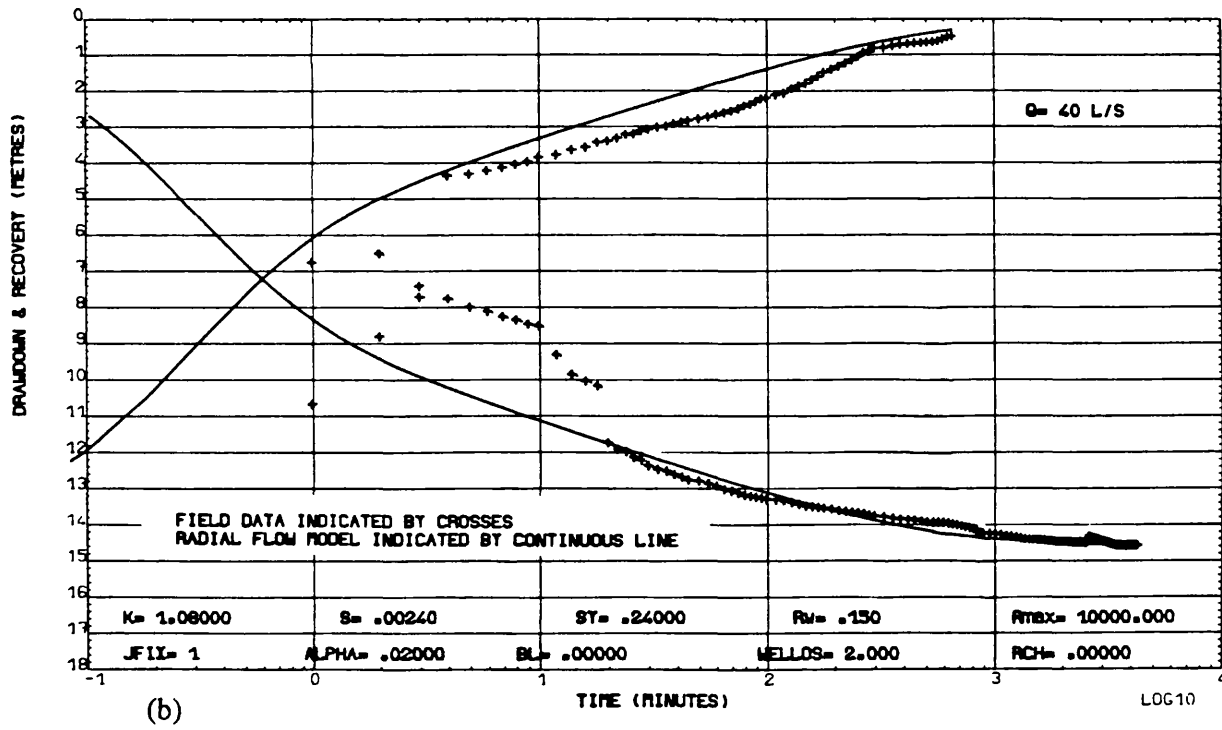
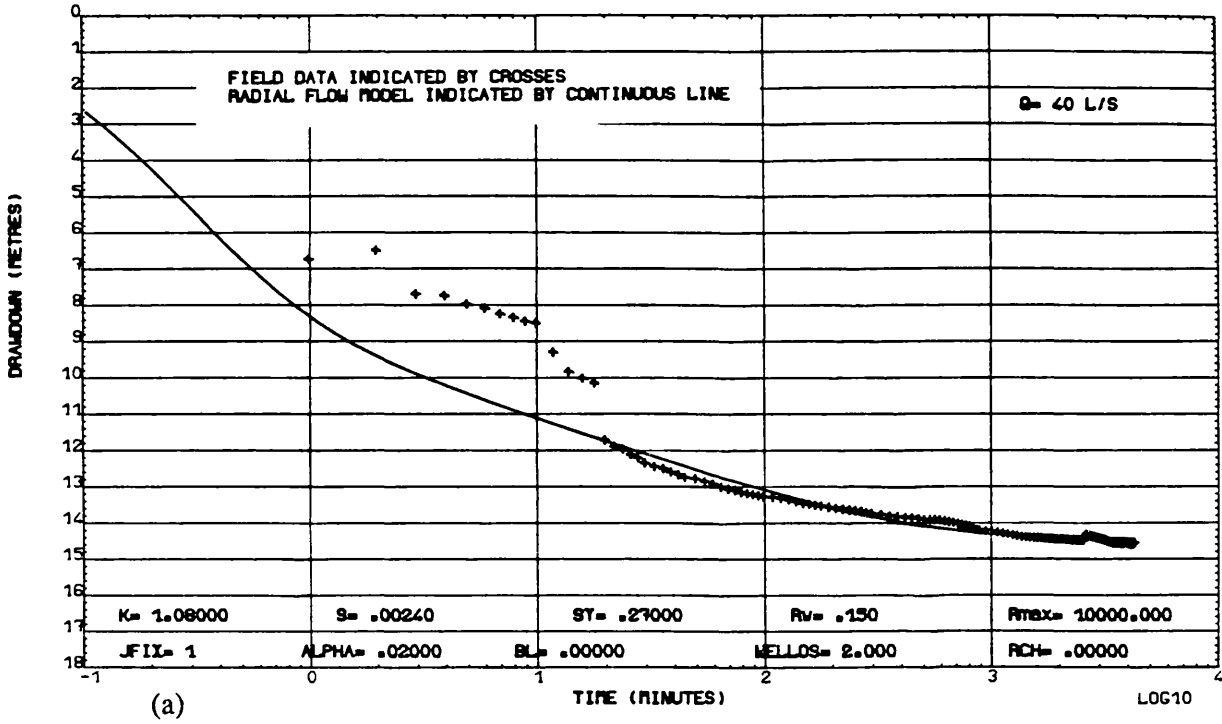


Fig. 5.35 PW SW7, Model analysis: (a) Without recovery, (b) With recovery.

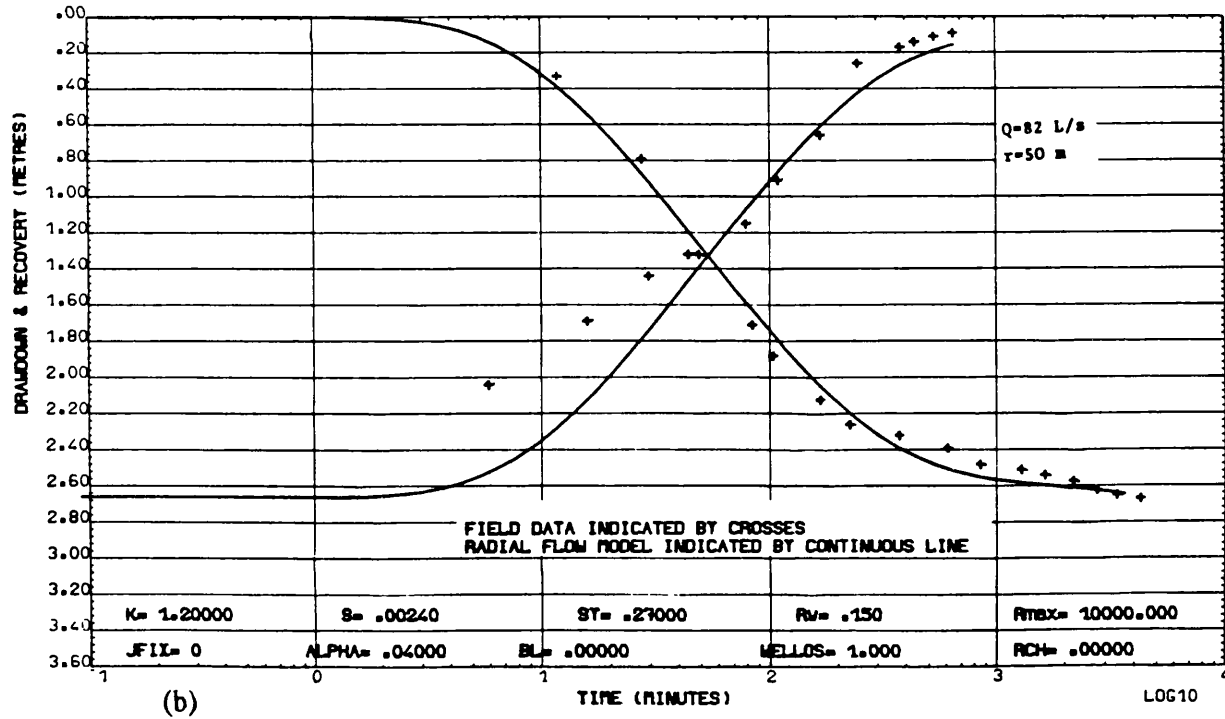
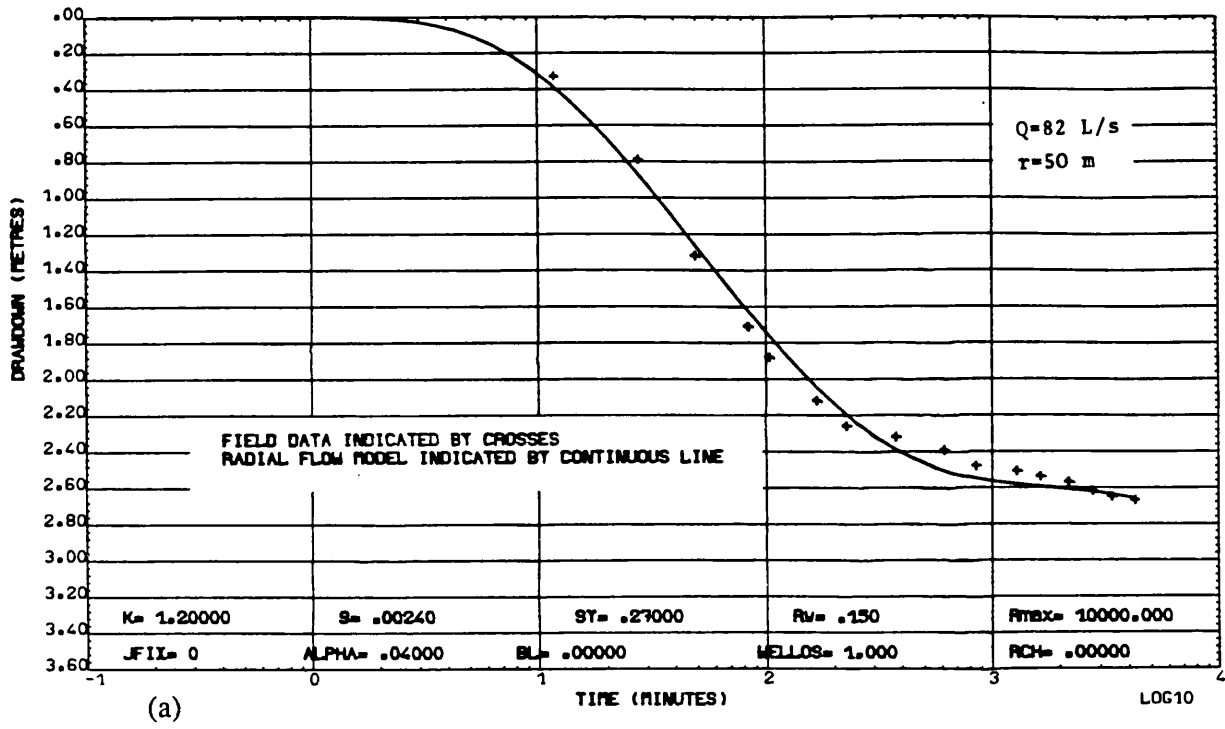


Fig. 5.36 OW SPW7, Model analysis: (a) Without recovery, (b) With recovery.

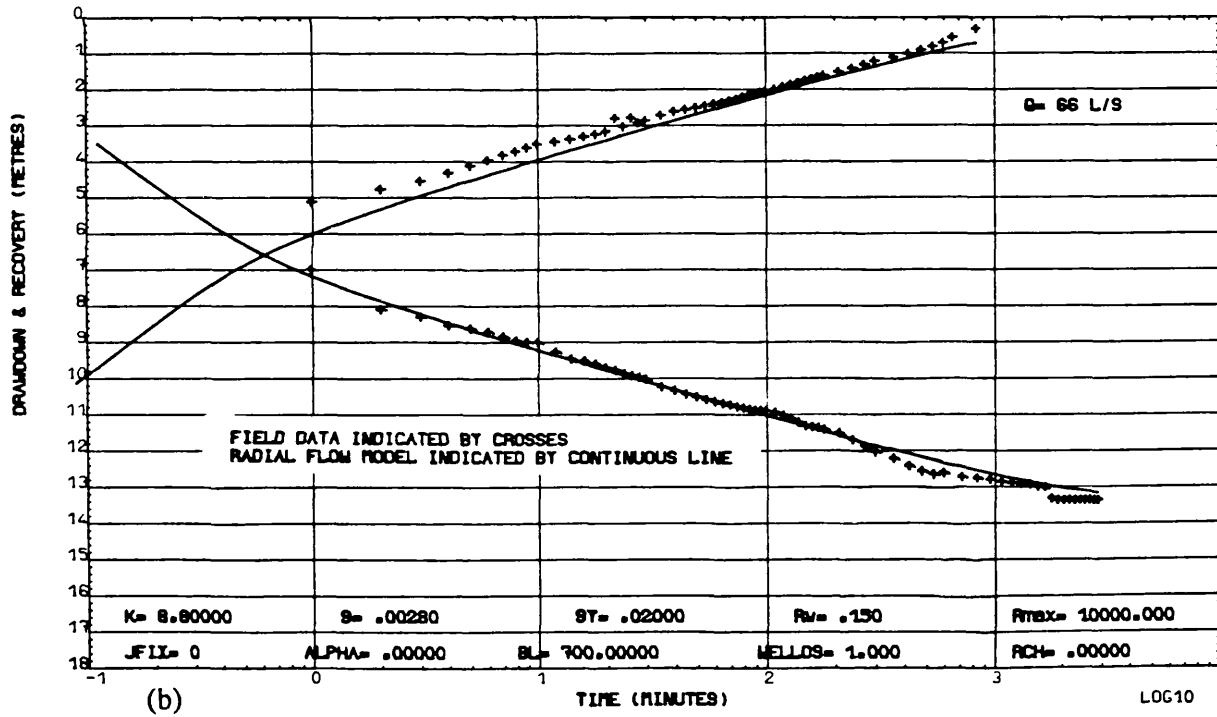
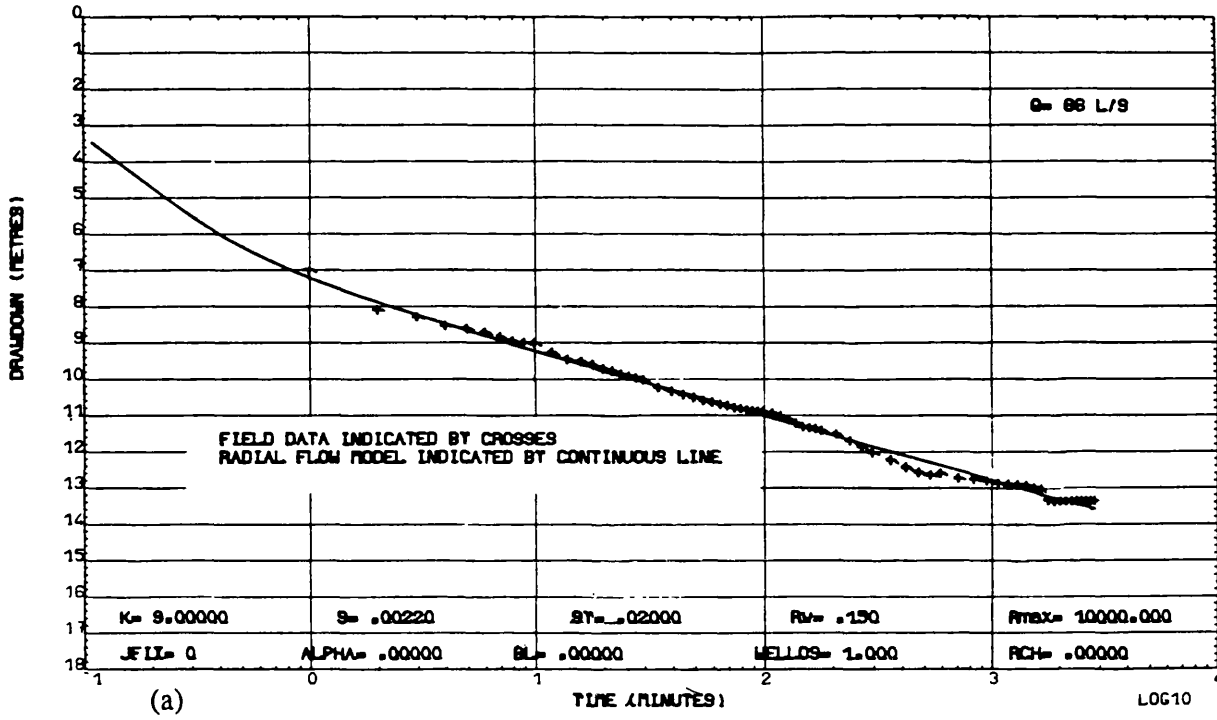


Fig. 5.37 PW JW1, Model analysis: (a) Without recovery, (b) With recovery.

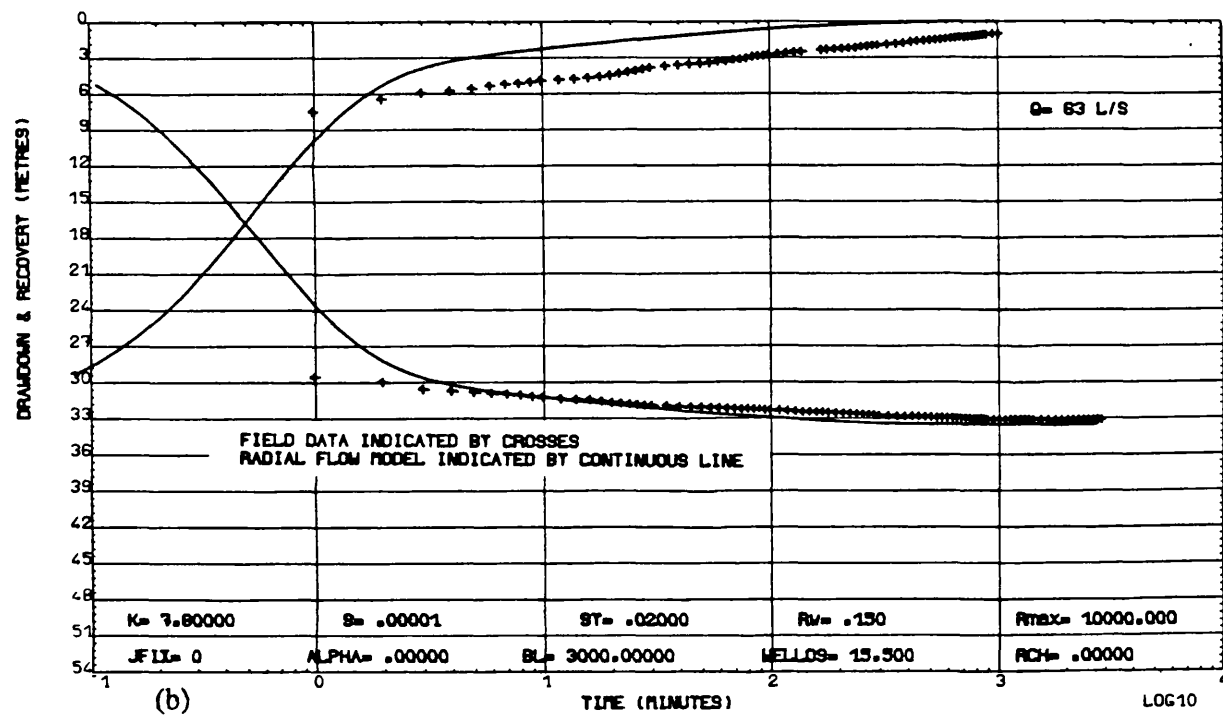
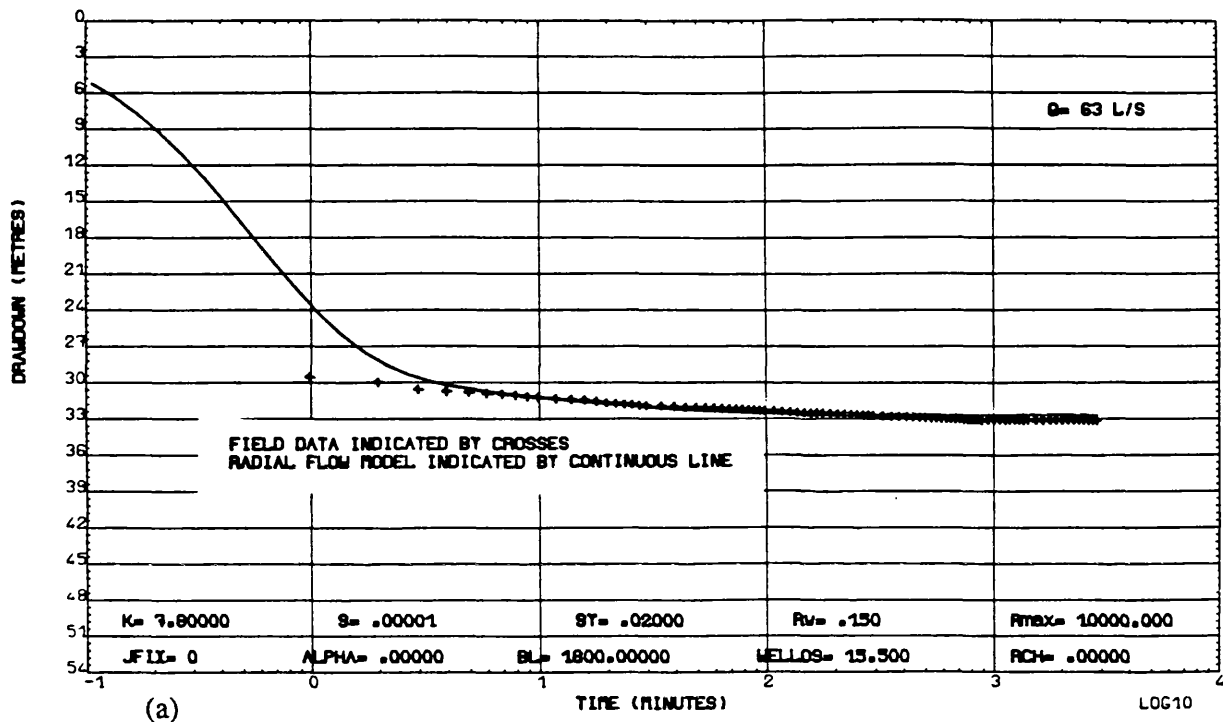


Fig. 5.38 PW JW2, Model analysis: (a) Without recovery, (b) With recovery.

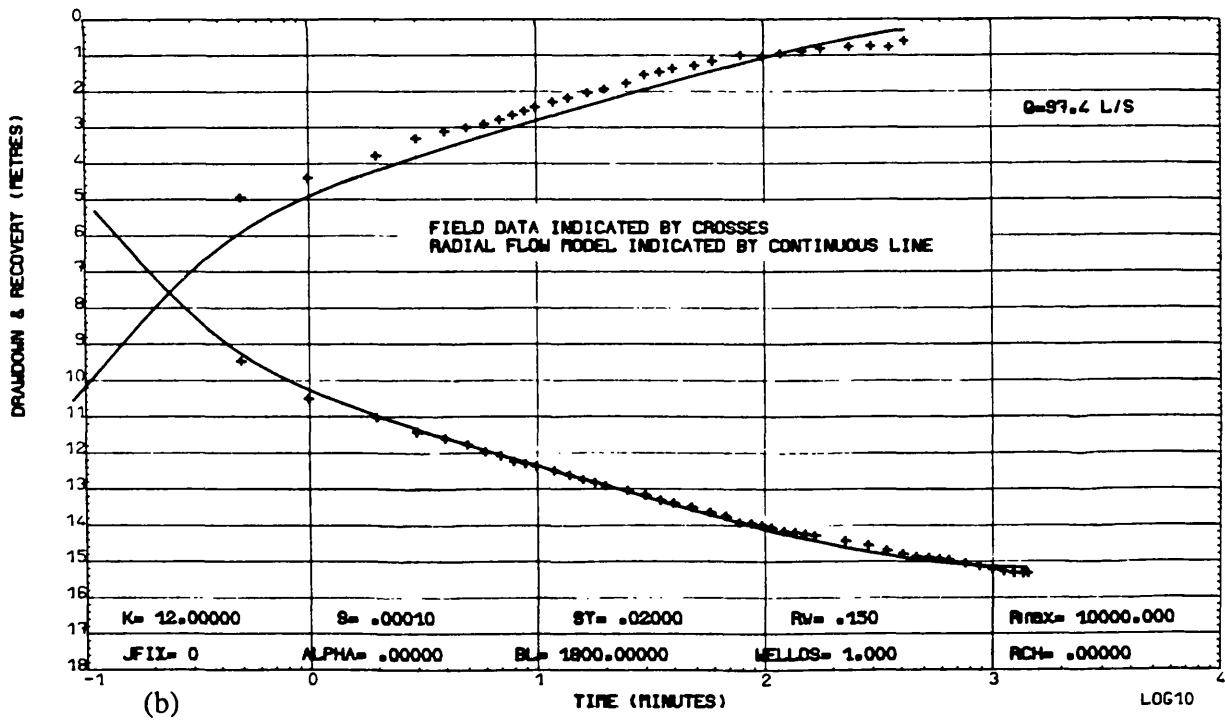
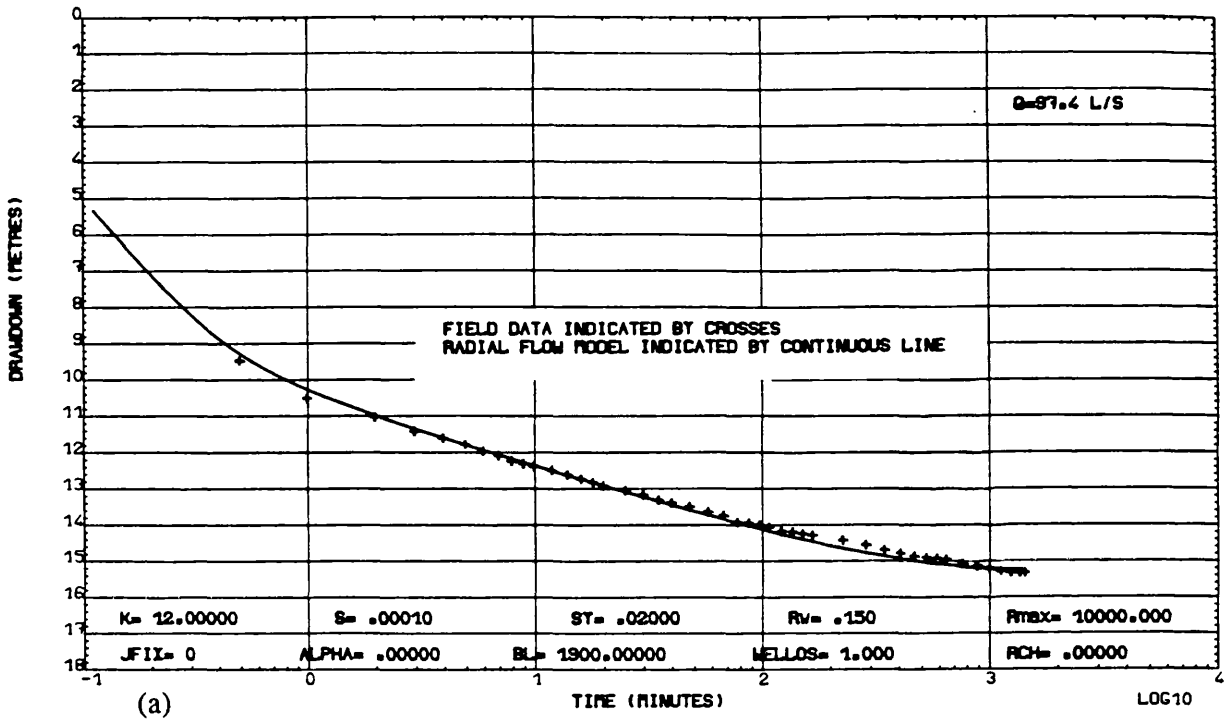


Fig. 5.39 PW TPSW1, Model analysis: (a) Without recovery, (b) With recovery.



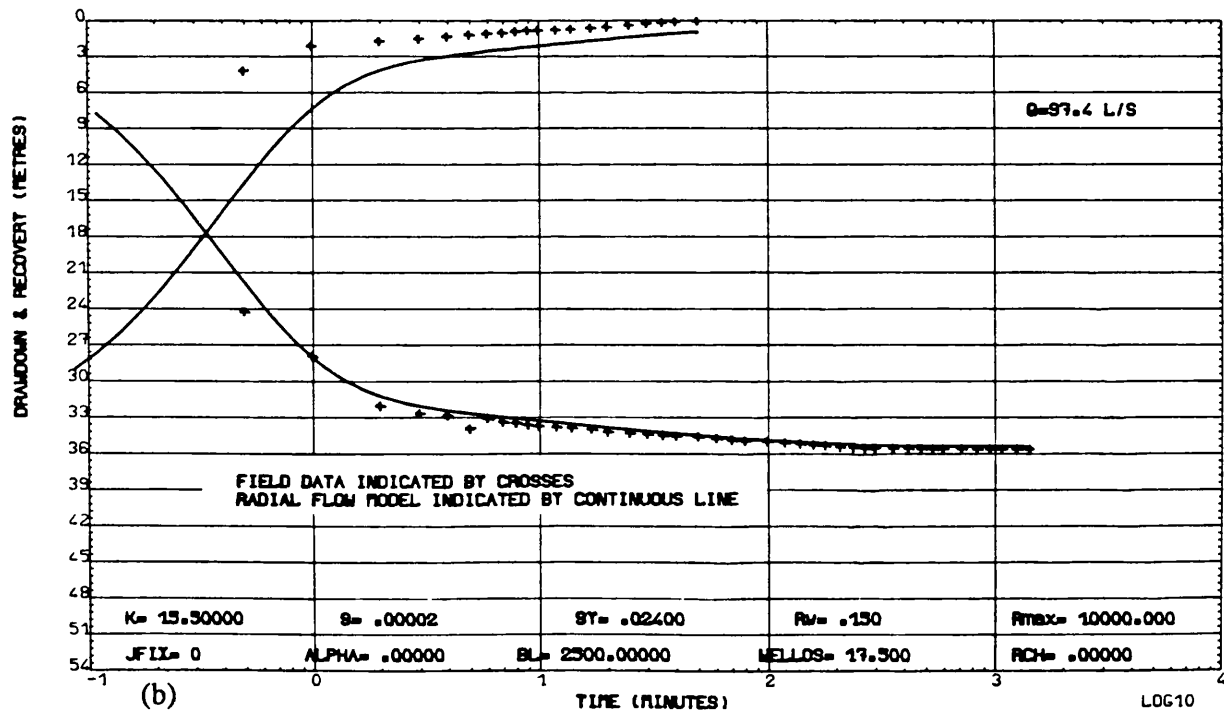
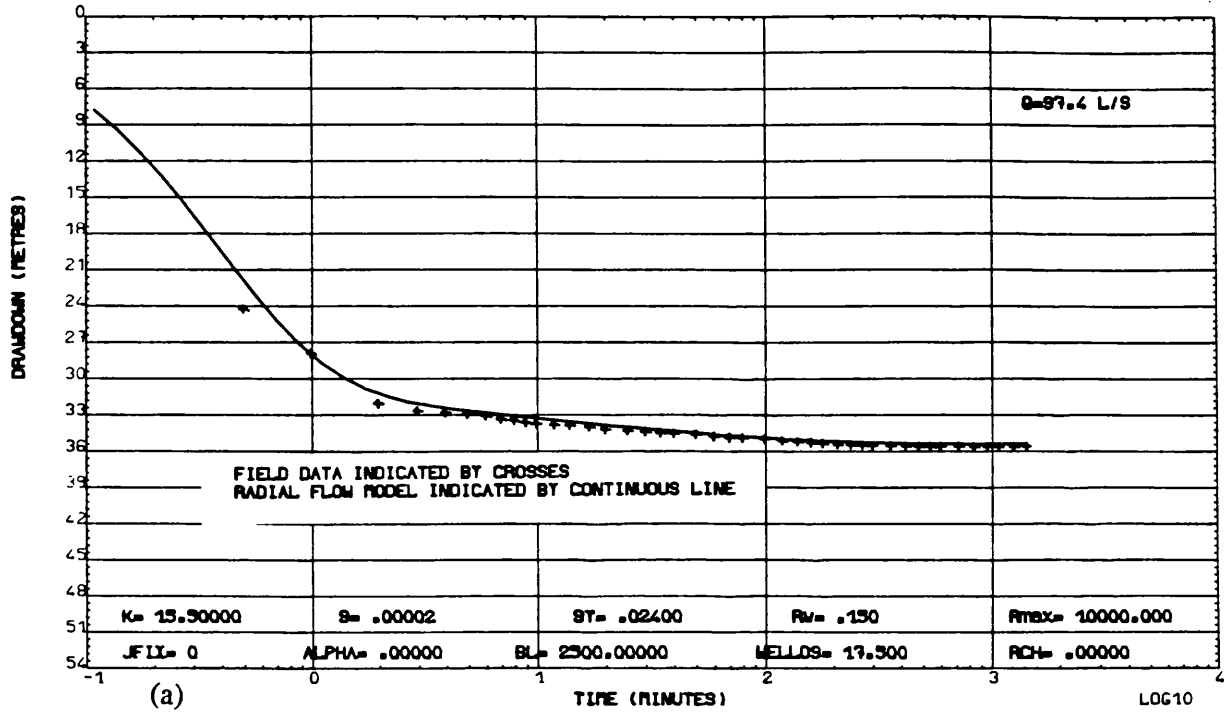


Fig. 5.40 PW TPSW3, Model analysis: (a) Without recovery, (b) With recovery.

The transmissivity value is very close to the value deduced from the analytical analysis. The storage coefficient is  $2.2 \times 10^{-3}$  which is an adequate estimated value. The reason for the better response is that the conditions are more uniform for the parameters used in the model (there is no well loss and the well is under confined condition).

Well JW2 (see Fig. 5.38) in comparison with JW1 has two additional variables as well loss and leakage factors, which reduce the reliability of the results. The well loss factor for this well is equal to 15.5 and leakage factor from the lower conductivity zone is about 1800m.

However, the numerical method only gives the leakage factor of the semi-permeable layer, but the Hantush (1956) third formation constant, 'leakance', which characterizes the ability of the semi- confined bed to transmit upward or downward leakage, can be calculated as;

$$K/b = T/L^2$$

Hence 
$$K/b = 547 / (1800)^2 = 1.69 \times 10^{-1} \text{ day}$$

Knowing the thickness of the overlying confining bed ( $b=17\text{m}$ ) its hydraulic conductivity is;

$$K = bT/L^2 = 17 \times 547 / (1800)^2 = 2.87 \times 10^{-3} \text{ m/d}$$

Thus, the K value is small which may be why it could not be calculated from the analytical analysis.

### **Tabriz Power Station well field**

Full details of the well construction and pumping tests of this well field are explained in Section 5.4 and it was stated earlier that at this location the aquifer type is confined. However, there is evidence of small values of leakage in all wells when the numerical solution is used.

There is no well loss in wells TPSW1, TPSW4 and TPSW8; whereas wells TPSW3 and TPSW6 show large values for well loss factor as deduced from the model simulations.

The estimated storage coefficients for these wells are less than  $1.1 \times 10^{-4}$ , and

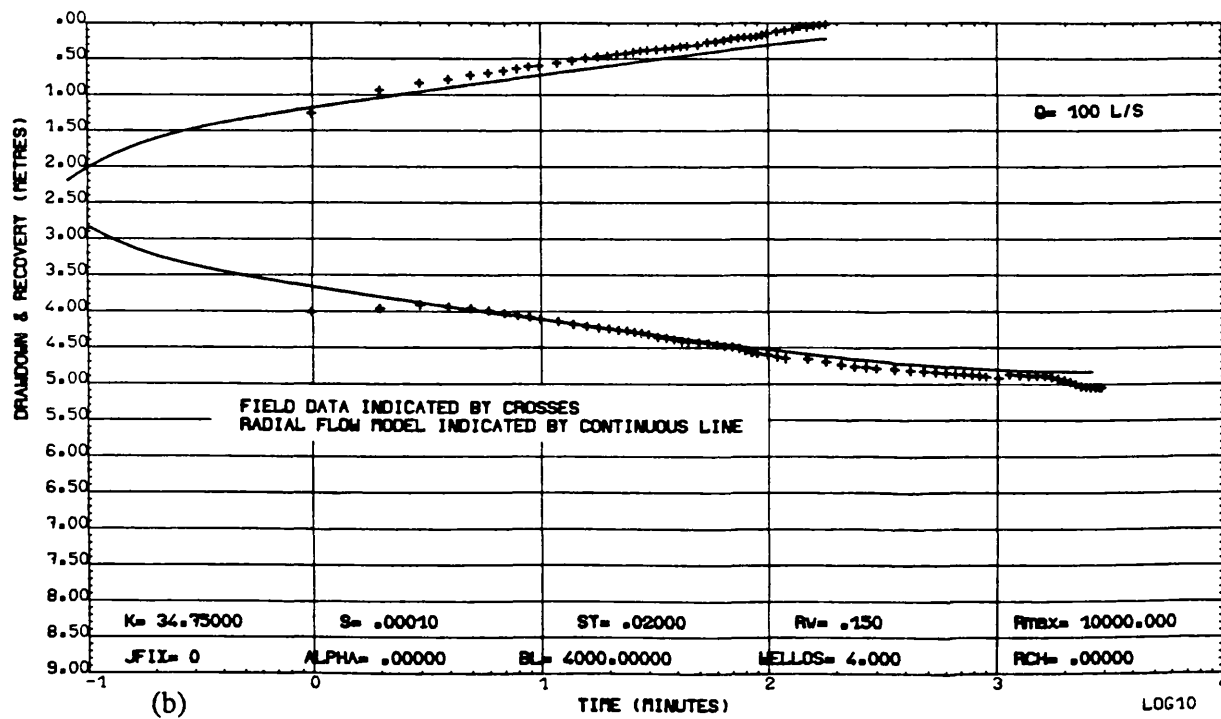
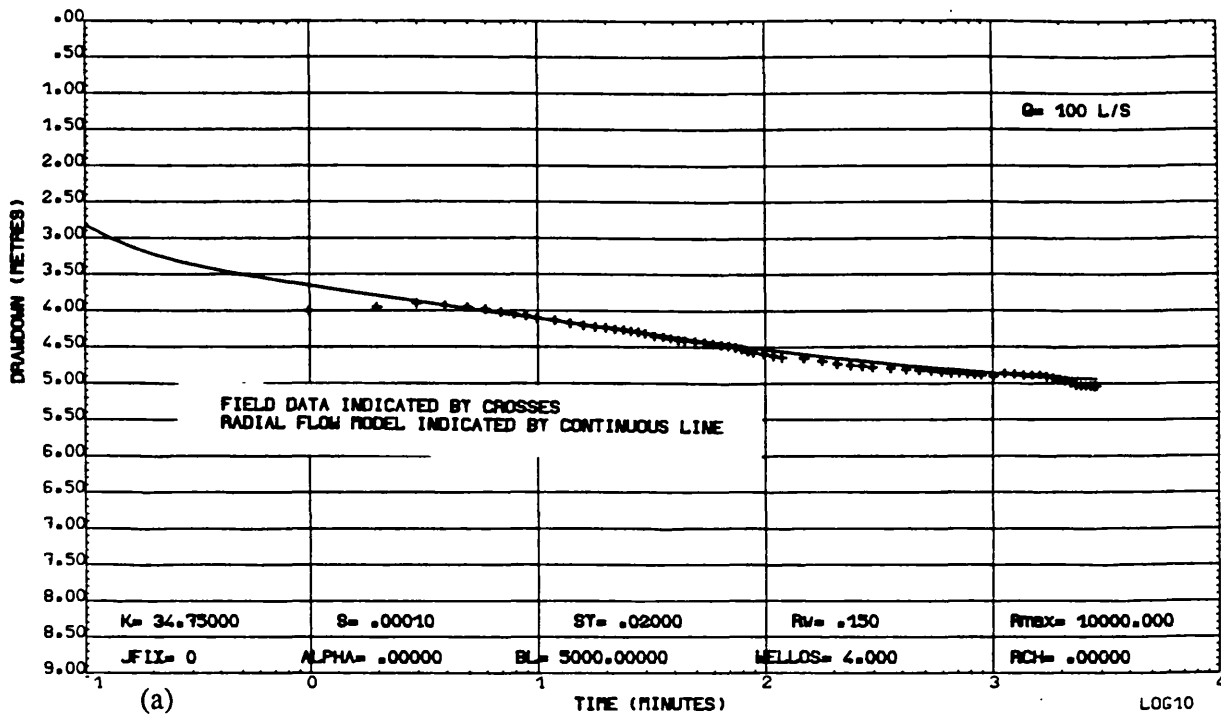


Fig. 5.41 PW TAW, Model analysis: (a) Without recovery, (b) With recovery.

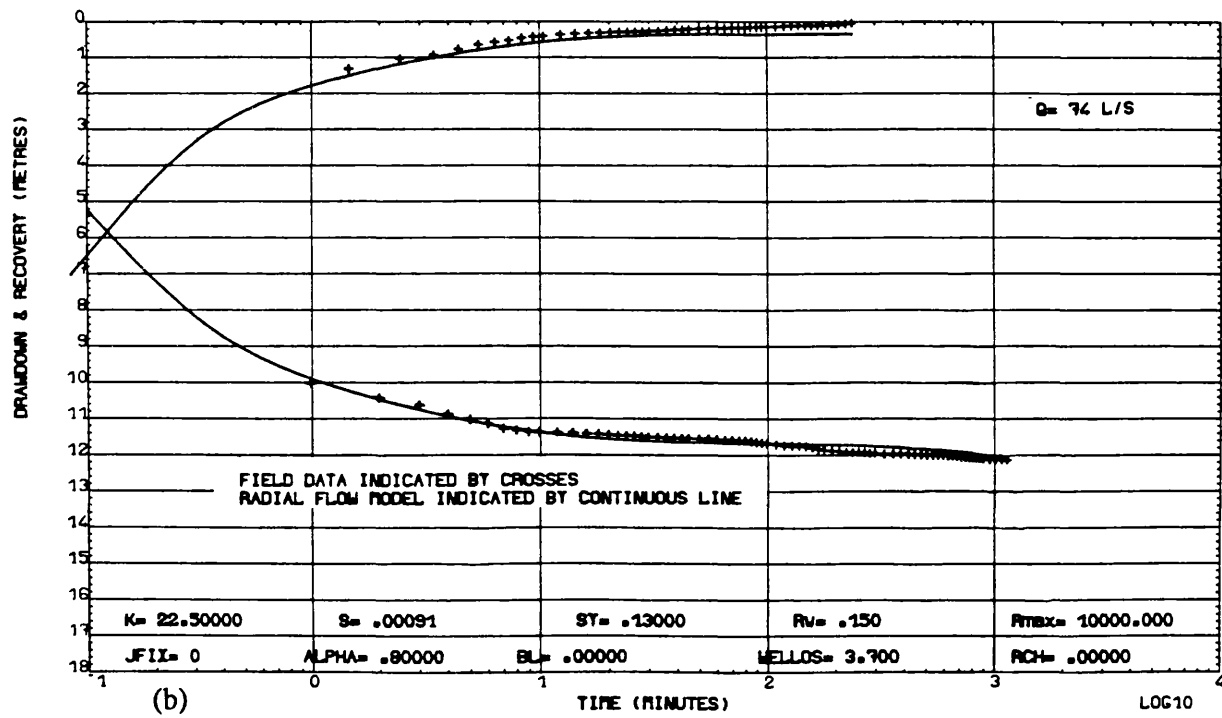
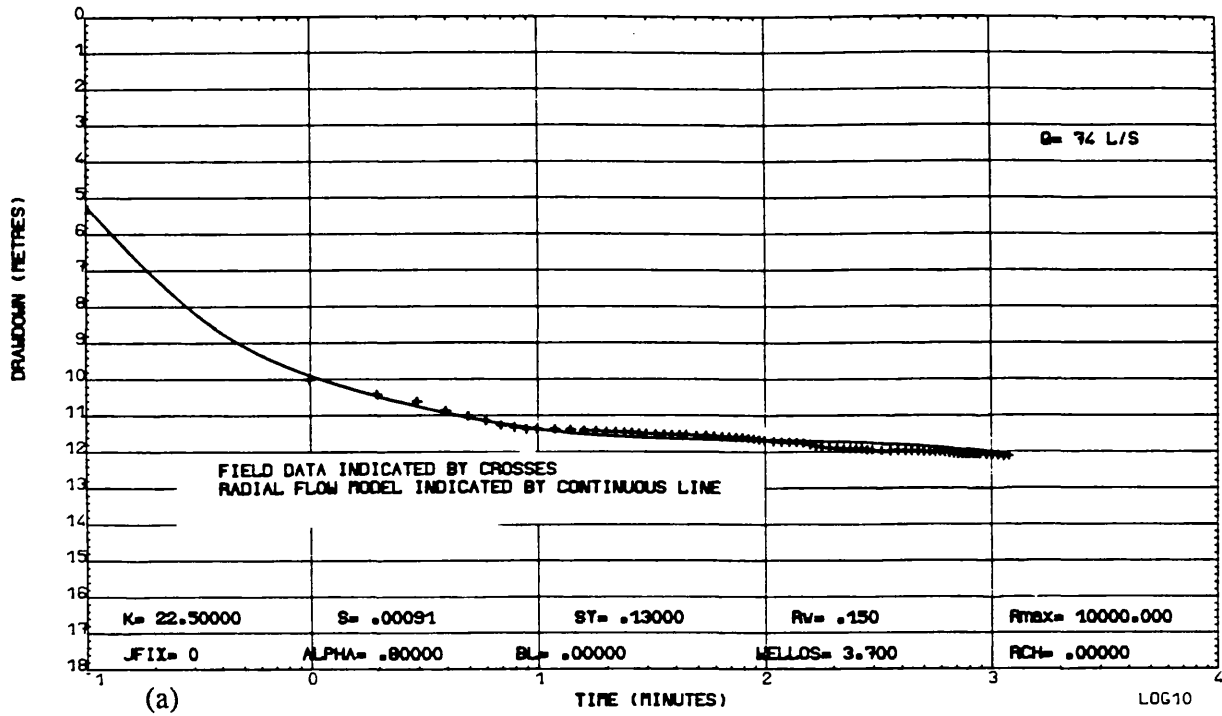


Fig. 5.42 PW SOW, Model analysis: (a) Without recovery, (b) With recovery.

the transmissivity values are in close agreement with the results from the analytical method.

The numerical analysis of wells TPSW1 and TPSW3 and the adequate fit of field and modelled results are shown in Figures 5.39 and 5.40. The model-deduced leakage factor for well TPSW1 is 1900m and the thickness of the semi-permeable layer about 10 metres. The hydraulic conductivity of this layer can be calculated as;

$$K=bT/L^2=10 \times 840 / (1900)^2 = 2.33 \times 10^{-3} \text{ m/d}$$

Thus the value of the hydraulic conductivity of the semi-permeable layer is so small that it can be ignored in analytical analysis. The importance of considering the leakage factor in this well field is due to the salinity of the overlying phreatic aquifer.

Well TPSW3 also shows very small values of leakage from the upper confining bed. It has a large value of well loss factor (17.5), which can only be reduced by decreasing the value of calculated transmissivity. The transmissivity values deduced from the model for the other wells in this well field are in close agreement with the analytical analysis results. The simulations for the field and modelled results are shown in Appendix 5 from Figures A5.16 to A5.18 and the numerical analysis results for the well field are represented in Table 5.5.

#### **Tabriz Airport water supply well**

Well TAW1 from the Tabriz Airport well-field area was also analysed by the radial flow simulation method. The transmissivity value obtained shows good agreement with the analytical analysis results. The leakage factor is extremely small, though the well loss is equal to 4. Thus, the sensitive parameters are the well loss factor and transmissivity; changing one of them will affect the other. The field and modelled results matching plot for this well is represented in Figure 5.41.

#### **Soufian water supply well**

Full details of the well construction and pumping tests for this well were explained in the previous section. The aquifer type was considered to be unconfined. The numerical method of analysis of the well was used and the data and results of the final trial for the best fit between the field and modelled results are shown in

Figure 5.42. The results deduced from this method require a well loss factor of 3.7. Thus, there are at least five variable parameters which can affect the variations of the modelled curve.

The accuracy of the results depends on the reliability of the field data and the supplementary information obtained from the analytical methods. Analysis of the field data with the straight-line and Theis type-curve methods not only gives some idea about the transmissivity but also the great differences between the results from the two methods show the significance of the well loss. The aquifer properties deduced from the numerical method are as below;

<u>b(m)</u>	<u>K(m/d)</u>	<u>T(m<sup>2</sup>/d)</u>	<u>S<sub>con.</sub></u>	<u>S<sub>uncon.</sub></u>	<u>WLF</u>	<u>α(d<sup>-1</sup>)</u>
56	22.5	1250	9.1x10 <sup>-4</sup>	1.3x10 <sup>-2</sup>	3.7	0.8

WLF= Well loss factor

α= delayed yield

### Sensitivity Analysis of Model

The information required for pumping test data analysis with the radial flow model is as follows; aquifer properties, observation well position, top and base of aquifer, well radius, boundary conditions, and rate and duration of abstraction.

It is difficult to record the results of all of the trials which were attempted to obtain satisfactory parameters. Therefore, the general results of the trials and the sensitivity of the parameters are explained below.

Examination of the unconfined aquifer time-drawdown curves showed that for the initial segment, the well radius and confined storage coefficient are most significant. Increasing the well radius or the confined storage coefficient value reduces the drawdowns in pumping and observation wells during the related time (for the first few minutes).

Depending on the aquifer type, the second segment of time drawdown or recovery curves is dominantly controlled by the delayed yield and a little by the unconfined storage coefficient. The greater values of delayed yield and unconfined storage coefficient lead to smaller drawdowns and make the response flatter in the second segment.

Modifications of the unconfined storage controls the third segment of the time-drawdown curves and an increase of this parameter leads to lesser drawdowns in this section of the curve.

Changes in hydraulic conductivity affect the whole curve and this effect increases directly with elapsed time. A high value of hydraulic conductivity leads to smaller drawdown. Changes of the well loss factor also leads to the same effects but it does not vary with elapsed time. It should be noted that the high well loss factor increases the drawdown.

The effects of barrier or recharge boundaries which depend on their distance from the abstraction well can increase or decrease the drawdowns respectively when the cone of influence reaches these boundaries. The recharge case can easily be mistaken for the leakage phenomenon.

Therefore, it is possible that by varying other parameters, an equally good agreement could be obtained with the field results. Additional and reliable information about the aquifer is needed before it can be stated with certainty that the parameters deduced in the foregoing analysis are the correct parameters.

**Table:5.2**

**PUMPING TEST ANALYSIS RESULTS**

**PUMPING TEST ANALYSIS RESULTS**

Well Field: Saidabad

Solution: Analytical

Well Field: Saidabad

Solution: Analytical

(a) Time-Drawdown

(b) Time-Recovery

Type of Aquifer: Unconfined

Type of Aquifer: Water Table

Well No.	Method of Solution	T(m <sup>2</sup> /d)	S <sub>e</sub>	S <sub>y</sub>	α(d <sup>-1</sup> )
SW1	SL	453	-	-	-
SPW1	SL	911	5.5x10 <sup>-3</sup>	-	-
SW3	SL	584	-	-	-
SPW3	SI	684	2.18x10 <sup>-3</sup>	-	-
SPW3	TC	590	3.0x10 <sup>-3</sup>	1.32x10 <sup>-1</sup>	0.32
SW5	SL	654	-	-	-
SW7	SI	351	-	-	-
SPW7	SL	374	1.95x10 <sup>-3</sup>	-	-
SW8	SL	498	-	-	-
SW10	SL	489	-	-	-
SW11	SL	518	-	-	-
SW13	SL	233	-	-	-

Well No.	Method of Solution	T(m <sup>2</sup> /d)	S <sub>e</sub>	S <sub>y</sub>	α(d <sup>-1</sup> )
SW1	SL	365	-	-	-
SPW1	SL	1151	8.63x10 <sup>-3</sup>	-	-
SW3	SL	584	-	-	-
SPW3	SI	820	2.36x10 <sup>-3</sup>	-	-
SW5	SL	576	-	-	-
SW7	SI	395	-	-	-
SPW7	SL	575	7.55x10 <sup>-4</sup>	-	-
SW8	SL	282	-	-	-
SW10	SL	514	-	-	-
SW11	SL	553	-	-	-
SW13	SL	231	-	-	-



Table :5.3

PUMPING TEST ANALYSIS RESULTS

Well fields Location: Tabriz PLain

Solution: Analytical

Type of Aquifer: Confined

Well No.	Method of Solution	Time-Drawdown	Time-Recovery
		T (m <sup>2</sup> /d)	T (m <sup>2</sup> /d)
JW1	SL	580	652
JW2	SL	553	498
TAW	SL	3514	3514
TPSW1	SL	842	856
TPSW1	TC	859	859
TPSW3	SL	856	1100
TPSW4	SL	2045	2045
TPSW4	TC	2021	2021
TPSW6	SL	1185	1925
TPSW8	SL	2046	2174
TPSW8	TC	1990	2100

**Table: 5.4**

**PUMPING TEST ANALYSIS RESULTS**

**Well Field: Saidabad**

**Solution: Numerical**

**Type of Data: Time-Drawdown**

**Type of Aquifer: Unconfined**

Well No.	b(m)	K(m/d)	T(m <sup>2</sup> /d)	S <sub>con.</sub>	S <sub>subcon.</sub>	WLF	α(d <sup>-1</sup> )
SW1	245	1.95	478	2.9x10 <sup>-3</sup>	1.25x10 <sup>-1</sup>	8.0	0.045
SPW1	245	3.50	858	5.0x10 <sup>-3</sup>	1.8x10 <sup>-1</sup>	1.0	0.08
SW3	222	2.68	595	2.9x10 <sup>-3</sup>	1.15x10 <sup>-1</sup>	6.0	0.06
SPW3	222	2.50	555	2.9x10 <sup>-3</sup>	1.35x10 <sup>-1</sup>	1.0	0.16
SW5	277	2.37	656	1.5x10 <sup>-3</sup>	1.25x10 <sup>-1</sup>	11.0	0.12
SW7	300	1.08	324	2.4x10 <sup>-3</sup>	2.7x10 <sup>-1</sup>	2.0	0.02
SPW7	300	1.20	360	2.4x10 <sup>-3</sup>	2.7x10 <sup>-1</sup>	1.0	0.04
SW8	267	1.80	481	3.0x10 <sup>-3</sup>	1.65x10 <sup>-1</sup>	6.0	0.10
SW10	253	1.85	468	3.0x10 <sup>-3</sup>	1.1x10 <sup>-1</sup>	6.0	0.04
SW11	289	1.65	477	3.0x10 <sup>-3</sup>	1.6x10 <sup>-1</sup>	6.5	0.10
SW13	230	1.05	242	6.0x10 <sup>-3</sup>	2.4x10 <sup>-1</sup>	8.4	0.10

**WLF= Well Loss Factor**

**Table: 5.5**

**PUMPING TEST ANALYSIS RESULTS**

**Area of Well Fields: Tabriz Plain**

**Solution: Numerical**

**Type of Data: Time-Recovery**

**Type of Aquifer: Confined to semi-confined**

Well No.	b(m)	K(m/d)	T(m <sup>2</sup> /d)	S <sub>con.</sub>	WLF	L(m)
JW1	66	9.00	594	2.2x10 <sup>-3</sup>	1.0	-
JW2	72	7.60	547	1.0x10 <sup>-5</sup>	15.5	1800
TAW	101	34.75	3510	1.0x10 <sup>-4</sup>	4.0	5000
TPSW1	70	12.00	840	1.0x10 <sup>-4</sup>	1.0	1900
TPSW3	55	15.50	853	2.0x10 <sup>-5</sup>	17.5	2500
TPSW4	67	29.60	1983	1.1x10 <sup>-4</sup>	1.0	4000
TPSW6	61	18.80	1147	2.0x10 <sup>-5</sup>	12.5	4000
TPSW8	61	33.20	2025	7.0x10 <sup>-5</sup>	1.0	4800

WLF= Well Loss Factor

## **CHAPTER 6**

### **STEP-DRAWDOWN TESTS**

#### **6.1) General**

#### **6.2) Planning a Step-Drawdown Test**

#### **6.3) Step-Drawdown Test Analysis Methods**

##### **6.3.1) Jacob arithmetic method**

##### **6.3.2) Bruin & Hudson method**

##### **6.3.3) Eden & Hazel method**

##### **6.3.4) Rorabaugh graphical method**

#### **6.4) Use of Step-Drawdown Test Analysis**

##### **6.4.1) Determination of well characteristics**

##### **6.4.2) Estimating aquifer properties**

#### **6.5) Data Analysis of Project Area**

## CHAPTER 6

### STEP-DRAWDOWN TEST

#### 6.1. General

Step-drawdown tests are frequently used to examine the performance of wells. It is usually assumed that the drawdown in a pumped well has two main components. The first, arising from the resistance of the aquifer formation to laminar flow, is termed "aquifer loss" and the second, resulting from the resistance to turbulent flow in the vicinity of the well and through the screen, is known as "well loss".

According to Clark (1977) an additional component of well loss can arise from the frictional resistance during flow up the well, which may be important in deep wells. Rushton and Rathod (1988) demonstrated that the actual response due to step pumping is often more complex. They considered various conditions in the vicinity of the pumped well, such as changes in hydraulic conductivity with discharge rate, a seepage face forming in the well, zones of lower or higher conductivity within the aquifer, the aquifer changing from the confined to unconfined state in the vicinity of the well, and a reduction in the effective depth of penetration due to the collection of sediment in the well. Results from numerical model simulations indicate that there are distinctive discharge-drawdown relationships for each situation.

Jacob (1946) indicated that the well loss is approximately proportional to the square of the discharge rate and the relationship between the two main components of drawdown is;

*Check  
in Refs*

$$s_w = BQ + CQ^2 \quad (6.1)$$

where  $s_w$  = total drawdown within the pumping well,  $BQ$  = aquifer loss, and  $CQ^2$  = well loss.

He suggested the step drawdown test to determine the well loss in the above relationship and the effective radius of a pumping well. However, the step drawdown test is now rarely used to determine the effective radius of a pumping well, but it is widely used to determine well losses.

Bruin and Hudson (1955), Bierschenk and Wilson (1961), and Eden and Hazel (1973) based their interpretations of the step test on Jacob's assumption. However,

Rorabaugh (1953), in a further study of the step test, noted that flow in the vicinity of the pumping well can be laminar if pumping rates are sufficiently low and, under laminar flow conditions, the well loss component is directly proportional to the pumping rate. He also observed that turbulent flow well loss is commonly more accurately described as being proportional to the pumping rate raised to some power greater than two.

The step-drawdown test data for the project area are available from all abstraction wells which were considered for constant rate test analysis plus another well-field at Tabriz Park with five pumping wells (see Fig. 5.1). The data are analysed with the different methods which will be explained in next sections.

## **6.2. Planning a Step-Drawdown Test**

The step-drawdown test consists of pumping the well at various discharges and is usually undertaken by incremental increases either in stepwise fashion without recovery or in what amounts to a series of short tests with full recovery after each stage. The alternative types of plot and results are illustrated in Figure 6.1.

The accuracy of step-drawdown test analysis results depends on the number and the length of steps and the accuracy of the equipment and observed data. The data comprise measurements of discharge rates and water levels. The accuracy of the plot of specific drawdown ( $s/Q$ ) versus discharge rate ( $Q$ ) will depend on the number of data points on the graph; that is, the number of steps in the test. Clark (1977), recommended that at least four steps should be used to ensure accuracy and he noted that three steps in a test may be insufficient. Also, it is important that the discharge rates chosen in the step-drawdown test should extend to cover the maximum discharge range of the well and the increments of discharge rate should be of equal duration.

The length of the steps in a test can be varied to fit local conditions. It is commonly difficult to stabilize the discharge rate in the first few minutes of a test. Therefore, a minimum step of 100 minutes duration was recommended to allow adequate stable data to be obtained for each step. Steps longer than three hours can not really be justified on a practical basis.

### 6.3. Step-Drawdown Test Analysis Methods

The aim of step-drawdown test analysis was originally to evaluate the well loss factor C and effective radius of well (Jacob 1964). Now it is widely used to evaluate the unknown parameters B and C in the Jacob equation, a, b and C in that of Eden and Hazel and B, C, C', and n in Rorabaugh method.

Check  
Ref

#### 6.3.1. Jacob arithmetic method

Jacob developed the following general equation for calculating the well loss factor C;

$$C = \frac{(\Delta s_w^i / \Delta Q^i) - (\Delta s_w^{i-1} / \Delta Q^{i-1})}{(\Delta Q^{i-1} + \Delta Q^i)} \quad (6.2)$$

The increments of drawdown in a test are determined by plotting the test data on semi-log scale with time on the log scale (see Fig. 6.1a). The line of best fit through the data is extended to the end of the succeeding step. Then the increment of drawdown for a chosen value is determined for each step. Therefore a value of C for each step can be calculated by substituting the values of incremental drawdown and discharge rate for adjacent steps into the general equation.

In the Jacob arithmetic analysis, measurements of increments of drawdown and discharge rate are open to error. A faulty reading on one step will affect the well loss calculation for that step and the one following, and commonly leads to a wide spread in the calculated values for C. The values of C calculated by the Jacob arithmetic method are presented in Table 6.1.

#### 6.3.2 Bruin & Hudson method

Bruin & Hudson (1955) and Bierschenk & Wilson (1969) simplified the Jacob equation by dividing throughout by Q to give:-

$$s_w/Q = B + CQ \quad (6.3)$$

They derived a graphical procedure to determine the increments of drawdown, where the total drawdown for each discharge rate is the sum of the incremental drawdown of that step plus all previous steps. Thus, the parameters B & C can be determined from a graphical method by plotting  $s_w/Q$  against Q as represented in Figure 6.1. In

this method, C is determined from the slope of the line of best fit through the data points, with B being calculated from the intercept of that line with the  $s_w/Q$  axis at zero discharge rate. The well characteristics calculated from this method are shown in Table 6.2a.

### 6.3.3. Eden & Hazel method

The basic assumption in all step-drawdown test analyses is that the increase in discharge rate at the beginning of each step is equivalent to a new pump in the well with a discharge rate equal to the increase in the discharge rate i.e. the discharge increment. The total drawdown in a step drawdown test is equal to the sum of the drawdown caused by the theoretical pumps responsible for each discharge step in the test.

The equation for the drawdown throughout a step-drawdown test in a confined aquifer has been modified from the Cooper and Jacob approximate equation by Sternberg (1968), and later by Eden and Hazel (1973). Jacob had noted that for values of  $u=r^2s/4\pi T$  less than 0.01, Theis's solution for a well pumping a constant discharge can be expressed as:

$$s=(Q/4\pi T) \log_{10}(2.25Tt/r_w^2 S) \quad (6.4)$$

This equation can be written:

$$s=(a + b \log t)Q \quad (6.5)$$

where  $a=(2.3/4\pi T) \log_{10} 2.25T/r_w^2 S$  (6.5a)

and  $b=2.3/4\pi T$  (6.5b)

Combining equations 1 and 3, the expression for a pumped well with well losses will be:

$$s_{wt}=(a + b \log t)Q + CQ^2 \quad (6.6)$$

The drawdown in the well at the end of the step-drawdown test presented in Figure 6.2 is the sum of the effects of all the steps, that is:

$$s_{wt} = (a+b \log(t_5 - t_1))Q_1 + (a+b \log(t_5 - t_2))(Q_2 - Q_1) + (a+b \log(t_5 - t_3))(Q_3 - Q_2) \\ + (a+b \log(t_5 - t_4))(Q_4 - Q_3) + CQ_4^2$$

For the general case of a step commencing at time  $t_x$  with a discharge rate increment of  $Q_x - Q_{x-1} = \Delta Q_x$ , the head loss at any time  $t$  due to the discharge increment  $\Delta Q_x$  will



be:

$$s_{wt} = \Delta Q_x (a + b \log(t - t_x)) + CQ_x^2 \quad (6.7)$$

The total drawdown due to all the steps will be:

$$s_{wt} = \sum_{x=1}^{x=n} \Delta Q_x (a + b \log(t - t_x)) + CQ_n^2 \quad (6.8)$$

$$s_{wt} = \sum_{x=1}^{x=n} a \Delta Q_x + \sum_{x=1}^{x=n} b \Delta Q_x \log(t - t_x) + CQ_n^2 \quad (6.9)$$

$$s_{wt} = aQ_n + b \sum_{x=1}^{x=n} \Delta Q_x \log(t - t_x) + CQ_n^2 \quad (6.10)$$

$$H = \sum_{x=1}^{x=n} \Delta Q_x \log(t - t_x)$$

A value of  $H_x$  (recalculated time summed) should be obtained for each drawdown value.

An arithmetic plot of drawdown versus  $H$  gives a family of parallel straight lines, each line corresponding to a particular value of discharge rate. The slope of the line(s) is  $b$  and the intercept of each line on the drawdown axis is the drawdown at unit time (see Fig. 6.2).

These drawdown values at unit time are used with their respective discharge rates to construct a specific drawdown-discharge graph. The slope of this graph will be  $C$ , and the intercept on the specific drawdown axis will be  $a$ . The computations involved in this method are tedious when done by hand but a computer program has been developed to handle the calculations.

Eden & Hazel outlined following assumptions for their method of analysis:

- 1) the aquifer is isotropic, homogeneous and infinite in area extant.
- 2) in the case of an unconfined aquifer, water release from storage instantaneously and drawdown is small compared to the total thickness of the aquifer.

- 3) field data lie in the region within which the Cooper-Jacob straight line approximation is valid.
- 4) the discharge measured at each observation has been constant since the time of the previous observation.
- 5) turbulent head loss is proportional to  $Q^2$ .

#### 6.3.4. Rorabaugh graphical method

As stated earlier, Jacob assumed well loss to be proportional to the square of the pumping rate but it sometimes happens that such a choice fails to produce satisfactory results. Thus, Rorabaugh (1953) described a method of analysis suitable for differentiating between laminar flow and turbulent flow and for determining the constants necessary to describe flow in other case (Lennox, 1966).

Rorabaugh indicated that if the exponent for turbulent flow is expressed as an unknown constant (i.e. 'n') a similar analysis to that of Jacob may be used. Hence, the equation can be written as:

$$s_w = BQ + CQ^n \quad (6.10)$$

which rearranges to:

$$(s_w/Q - B) = CQ^{n-1}$$

or

$$\log(s_w/Q - B) = \log C + (n-1)\log Q$$

The term  $(s_w/Q - B)$  can be plotted against the discharge rate on log-log paper. B is unknown therefore a series of values are assumed for it, and from trial and error the true value is obtained which gives a straight line plot. The slope of this line is then  $(n-1)$  and the intercept on the  $(s_w/Q - B)$  axis at unit discharge rate ( $Q=1$ ) will equal value of C (see Fig. 6.3).

The graphical method needs accurate data because small errors in discharge or drawdown measurements will cause relatively large errors in n, B, and C values. This sensitivity is present in Jacob's method but is not nearly so apparent as in the log-log graphical method. The Rorabaugh method also requires more time to complete than the Jacob method. For this reason, only data from one well of each well field was analysed by this method (see Table 6.2b).

## 6.4. Use of Step-Drawdown Test Analysis

### 6.4.1 Determination of well characteristics

The step-drawdown test may be useful in choosing a pumping rate for an existing well or predicting the specific capacity at some rate of discharge other than those measured during the test. For wells reaching equilibrium conditions in each step, it can be a true specific capacity, otherwise specific capacity at any one discharge rate must vary with time. For this reason, it is important to state the duration of the pumping period for which a particular value of specific capacity is computed.

The calculation of transmissivity from single well data by ignoring the well losses leads to an underestimation of its value. Therefore, knowledge of the well loss component of drawdown allows correction of discharge test in such a well.

The step-drawdown test has commonly been used to determine a factor called 'well efficiency' defined as the ratio of the aquifer loss to the total drawdown .

$$\text{Well efficiency} = \frac{BQ}{(BQ + CQ^2)} \times 100 = \frac{BQ}{s_{wt}} \times 100 \quad (6.11)$$

The lower percentage of well efficiency in comparisons between wells of similar depths in the same well field might suggest that the wells are badly designed. However, Mogg (1968), in a critical review, stated that the step drawdown test can not determine well efficiency because it is merely a means of discovering if there is a change in specific capacity with change in discharge.

### 6.4.2. Estimating Aquifer Properties

#### a) Transmissivity

The step-drawdown test data can be used to estimate the transmissivity of the aquifer. A very simple approach is to analyse the data obtained from the first step, after correction for well losses, with the Theis, Jacob or other applicable methods.

The specific-drawdown - discharge-rate plot can also be used to estimate transmissivity in those tests reaching equilibrium in each step. The equations suggested by Logan (1964) which has been derived from the Thiem (1906)

equilibrium formula can be used for this analysis. The Logan simplified equations are:

$$\text{For confined conditions} \quad T = \frac{1.22Q}{s} \quad (6.12)$$

$$\text{For unconfined conditions} \quad T = \frac{2.43Qb}{s(2b-s)} \quad (6.13)$$

where  $s$  is drawdown and  $b$  is the thickness of the aquifer. Thus, for confined conditions, transmissivity may be estimated from the specific capacity (or the reciprocal of specific drawdown) obtained from the above mentioned plot. However, for unconfined conditions the records of the thickness of the aquifer and the drawdown in the well is essential. The accuracy of this determination will depend on the accuracy of the estimated constant derived from the  $\log r/r_w$ .

Eden & Hazel graphical analysis enables one to calculate the transmissivity from each step. For the arithmetic plot of  $H$  versus drawdown as shown in Figure 6.2, the slope of the line for each step is  $b$ . The values of  $b$  from all steps are averaged and then substituted in the equation:

$$b = 2.3/4\pi T \text{ or } T = 2.3/4\pi b$$

#### b) Storage coefficient

The storage coefficient can be estimated from the Eden & Hazel equation (6.4a) but, unfortunately the effective radius of the well ( $r_w$ ) is not known and must be estimated. Errors in this estimation will be squared in the calculation. Therefore, it should be remembered that the results may be greatly in error.

### 6.5. Data Analysis for Project Area

The data for step-drawdown testing is available from six well fields situated in the project area. The aquifer conditions and well constructions, as well as lithological conditions for five of them were explained in previous chapters. However, the necessary information for the Tabriz Park well-field will be considered in the following sections.

### Saidabad well field

The results of 8 step-drawdown tests conducted at this well field in 1978 were analysed using the above-mentioned methods. The cross sections of well construction and lithological conditions in this well field were shown in Figures 5.2 and 5.8, respectively. Their discharge rates and resultant calculated data are tabulated on the related figures. For the Jacob arithmetic and Bruin and Hudson graphical methods of analysis, the increments of drawdown are determined by plotting the test data on semi-log paper with time on the log axis (see Fig. 6.1). The handled data for well SW1 is as follows:-

<u>Steps</u>	<u>Q(m<sup>3</sup>/d)</u>	<u>ΔQ(m<sup>3</sup>/d)</u>	<u>Δs(m)</u>	<u>Δs/ΔQ(d/m<sup>2</sup>)</u>	<u>ΣΔs/ΔQ(d/m<sup>2</sup>)</u>
1	4665.6	4665.6	23.4	5.02x10 <sup>-3</sup>	5.02x10 <sup>-3</sup>
2	5702.4	1036.8	5.6	5.40x10 <sup>-3</sup>	5.09x10 <sup>-3</sup>
3	6825.6	1123.2	6.5	5.79x10 <sup>-3</sup>	5.36x10 <sup>-3</sup>

Actually, the step-drawdown test for well SW1 was conducted in 4 steps, but the drawdowns in the 4th step are too small to make any difference between this and the previous step. Therefore the data for step 4 were ignored in all methods of analysis. The low increment of discharge or/and a change in the hydraulic conductivity or some other conditions around the well can cause this behaviour in the test.

For steps 1 and 2, equation (6.2) may be rewritten as:

$$C = \frac{\Delta s_2 / \Delta Q_2 - \Delta s_1 / \Delta Q_1}{\Delta Q_1 + \Delta Q_2}$$

Then

$$C_{1,2} = \frac{5.40 \times 10^{-3} - 5.02 \times 10^{-3}}{4665.6 + 1036.8} = 6.77 \times 10^{-8} \text{ d}^2/\text{m}^5$$

and for steps 2 and 3 is

$$C_{2,3} = \frac{5.79 \times 10^{-3} - 5.40 \times 10^{-3}}{1036.8 + 1123.2} = 1.79 \times 10^{-7} \text{ d}^2/\text{m}^3$$

Thus, the apparent average  $C = 1.23 \times 10^{-7} \text{ d}^2/\text{m}^3$

Equation (6.2) assumes that the well is stable that  $C$  does not change during the step test. However, some wells are sometimes unstable and the value of  $C$  is affected by changes in pumping rate. The calculated values of  $C$  from Jacob arithmetic method for all of the wells were shown in Table 6.1.

The Bruin & Hudson and Eden & Hazel methods of analysis of data for this well (see Figs. 6.1 and 6.2) showed well loss factors of  $7.85 \times 10^{-8}$  and  $2.55 \times 10^{-7} \text{ d}^2/\text{m}^3$ , respectively. The Rorabaugh method was also tried to analyse the derived data (see Fig. 6.3). The resultant values of  $C$ ,  $B$ , and  $n$  are  $3.6 \times 10^{-9} \text{ m}(\text{s/l})^{4.6}$ ,  $0.427 \text{ ml}^{-1}\text{s}$  and  $4.6$  respectively. The value of  $n$  is greater than the value suggested by Jacob or Rorabaugh but less than those reported by Lennox.

Well efficiency can be calculated at any discharge rate from the equation (6.11) i.e. at  $Q=6000 \text{ m}^3/\text{d}$ , with  $B$  and  $C$  obtained from the Bruin and Hudson method, well efficiency ( $E$ ):

$$E = \frac{4.66 \times 10^{-3} \times 6000}{4.66 \times 10^{-3} \times 6000 + 7.85 \times 10^{-8} \times (6000)^2} \times 100 = 90\%$$

The theoretical drawdown-yield curve calculated from this method is shown in Figure 6.4a.

The value of transmissivity calculated from the Eden and Hazel method is  $520 \text{ m}^2/\text{d}$  which is greater than the result for the constant test result. The Logan equilibrium equation was also tried but the resultant value was smaller than expected. The calculated storage coefficient has not yielded a reasonable value.

Values of well loss factor ( $C$ ), for wells SW3, SW5, SW7, SW10, SW11, and SW13 decrease in step fashion which indicates that the development during the pumping period is large and solution using equation (6.2) or other methods are impossible.

The available step-drawdown test data for well SW8 were also analysed by

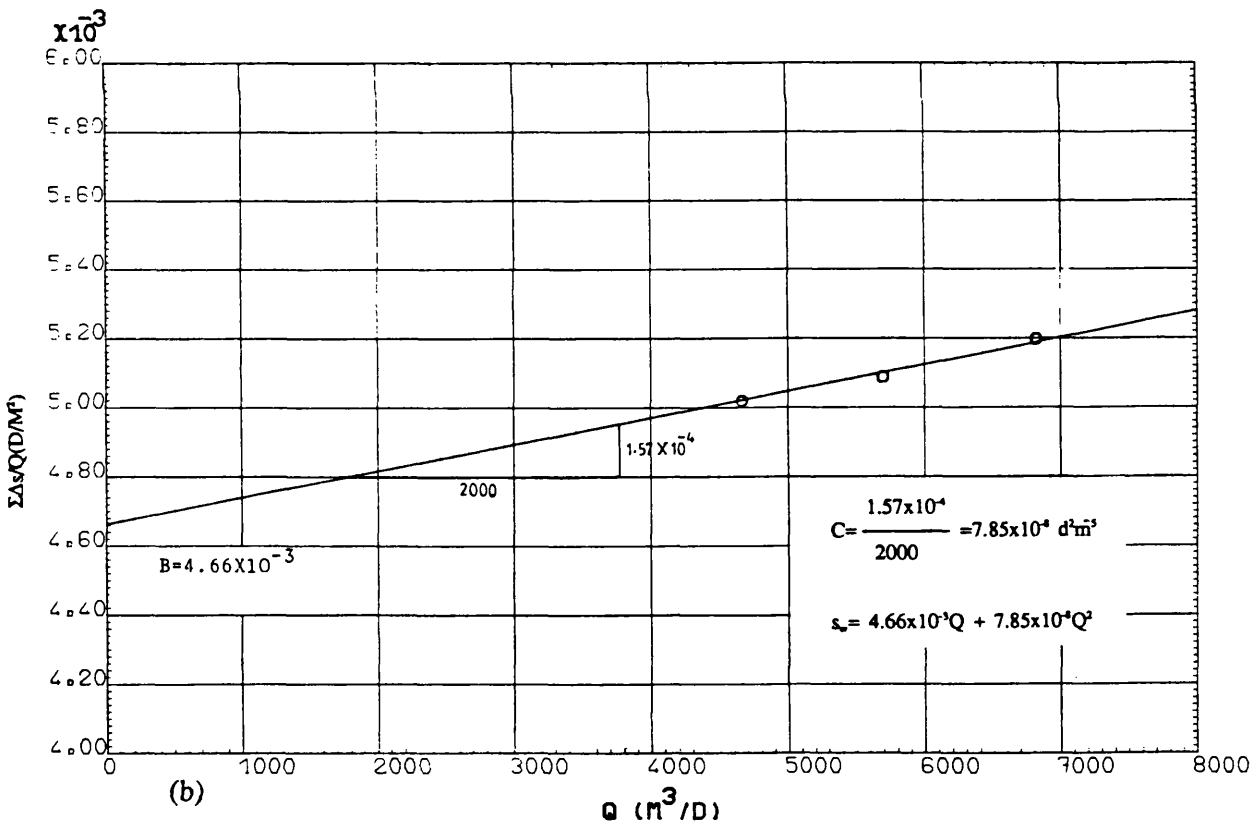
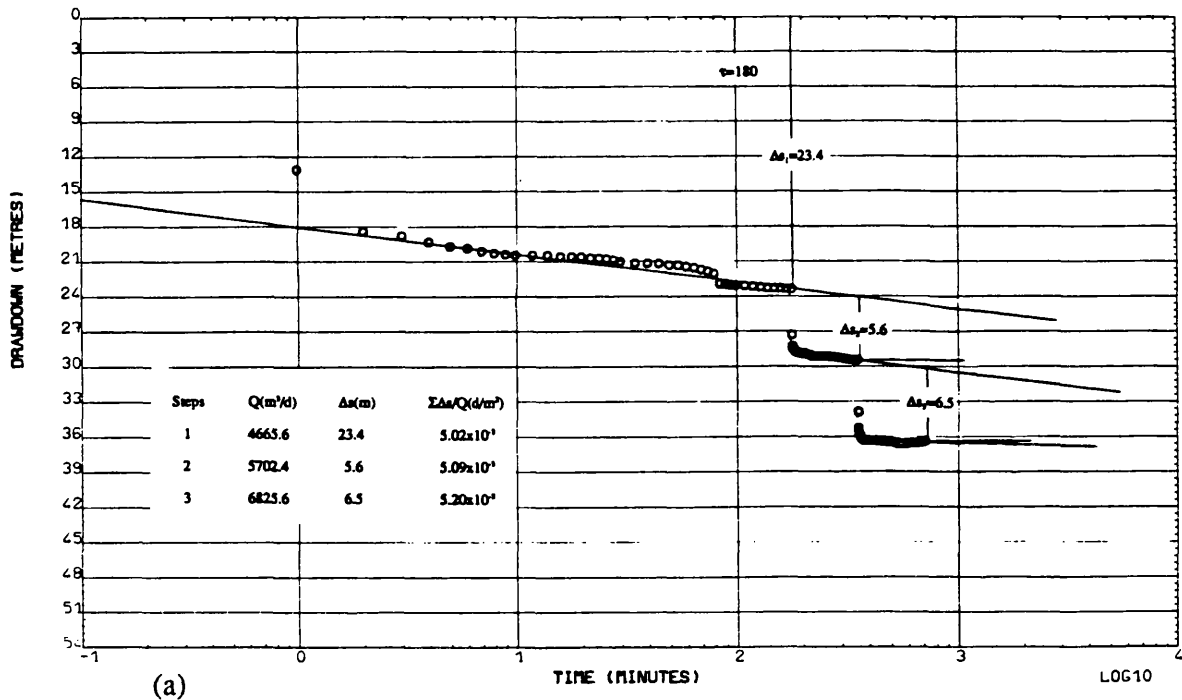
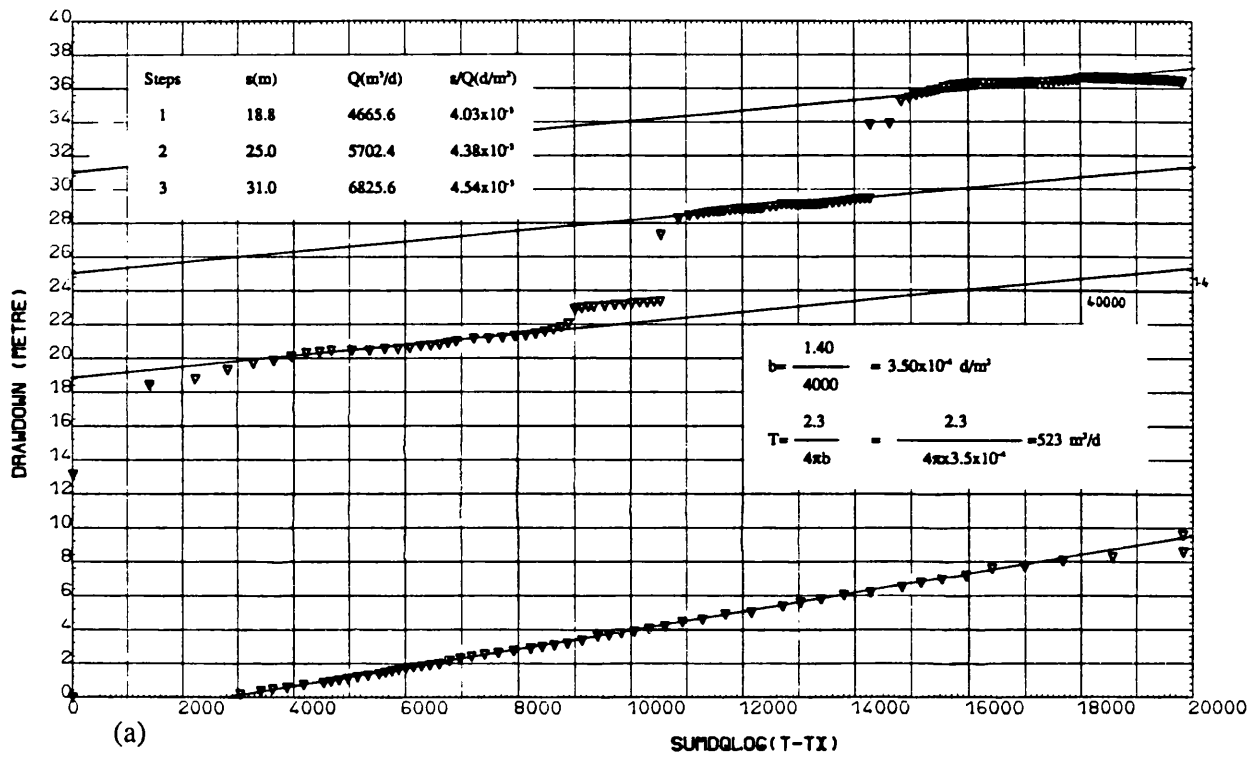
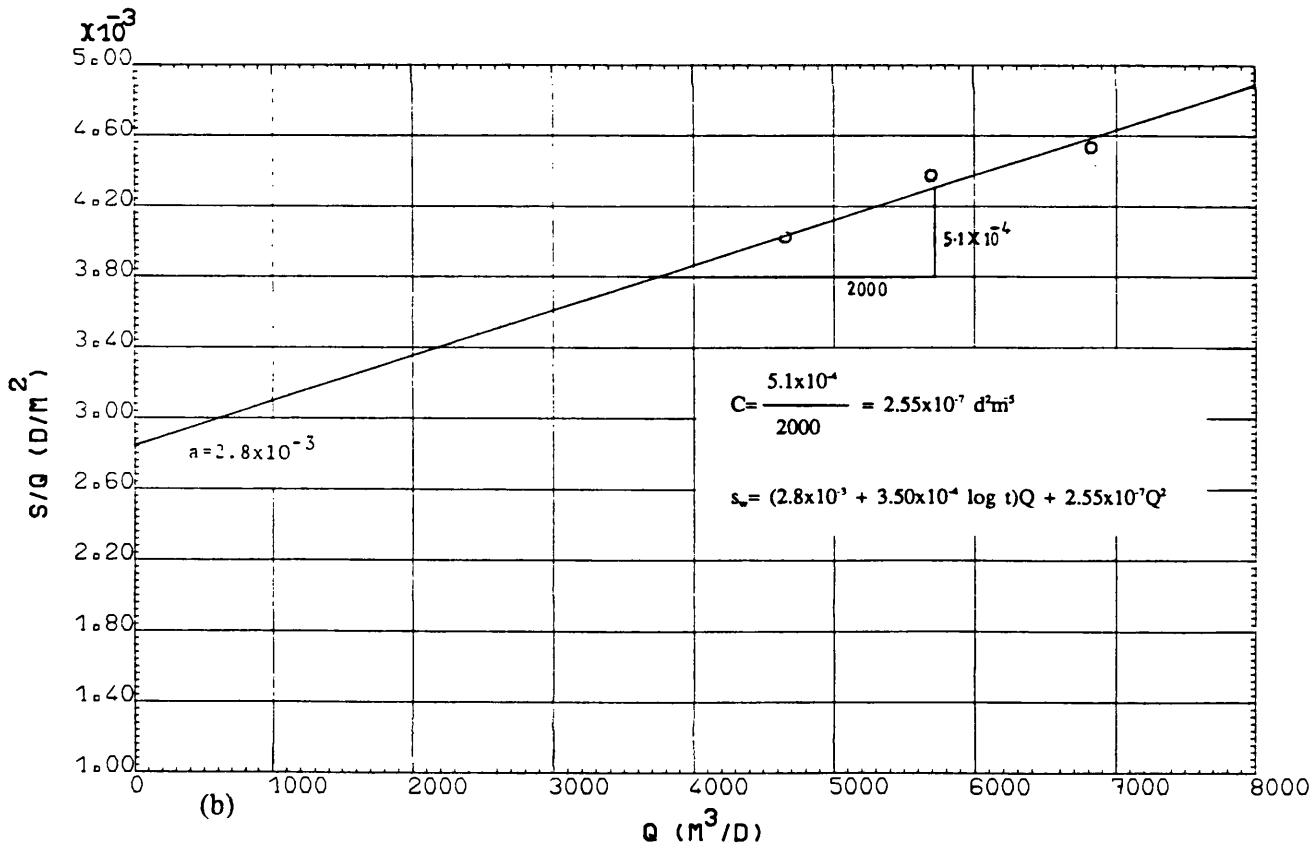


Fig. 6.1 PW SW1, Step-Drawdown test: Bruin & Hudson method, (a) data handling, (b) data plot.



(a)



(b)

Fig. 6.2 PW SW1, Step-Drawdown test: Edén & Hazel method, (a) data handling, (b) data plot.



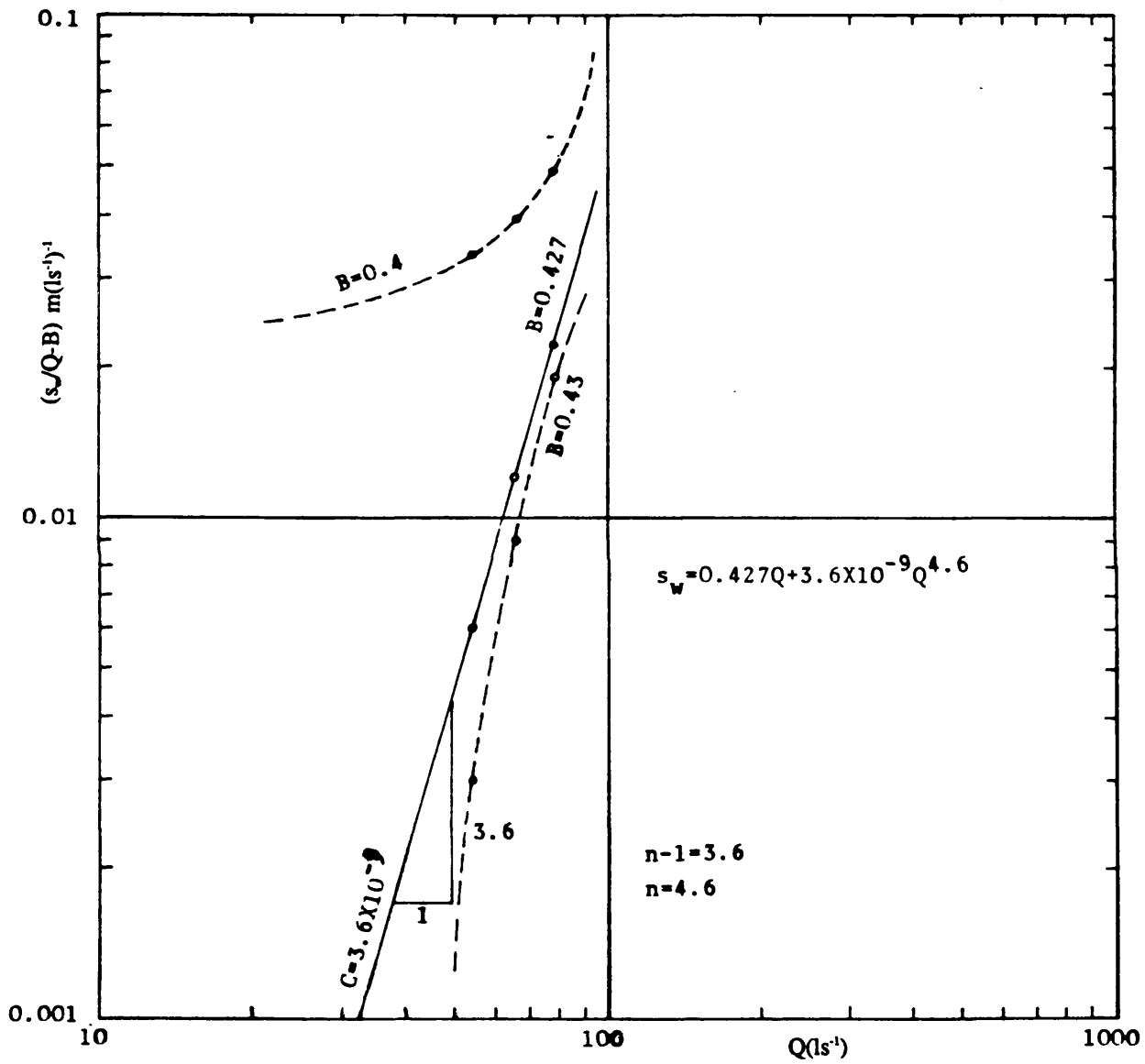


Fig. 6.3 PW SW1, Step-Drawdown test: Rorabaugh method.

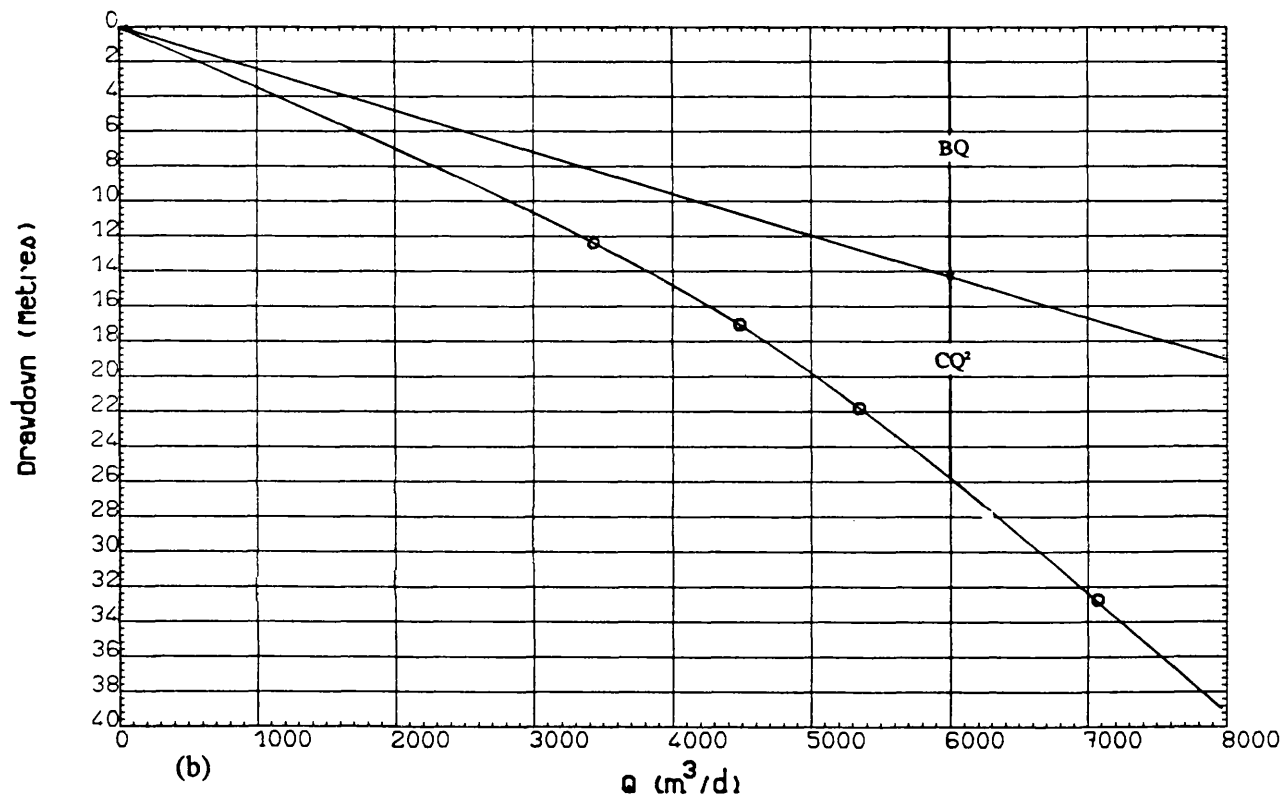
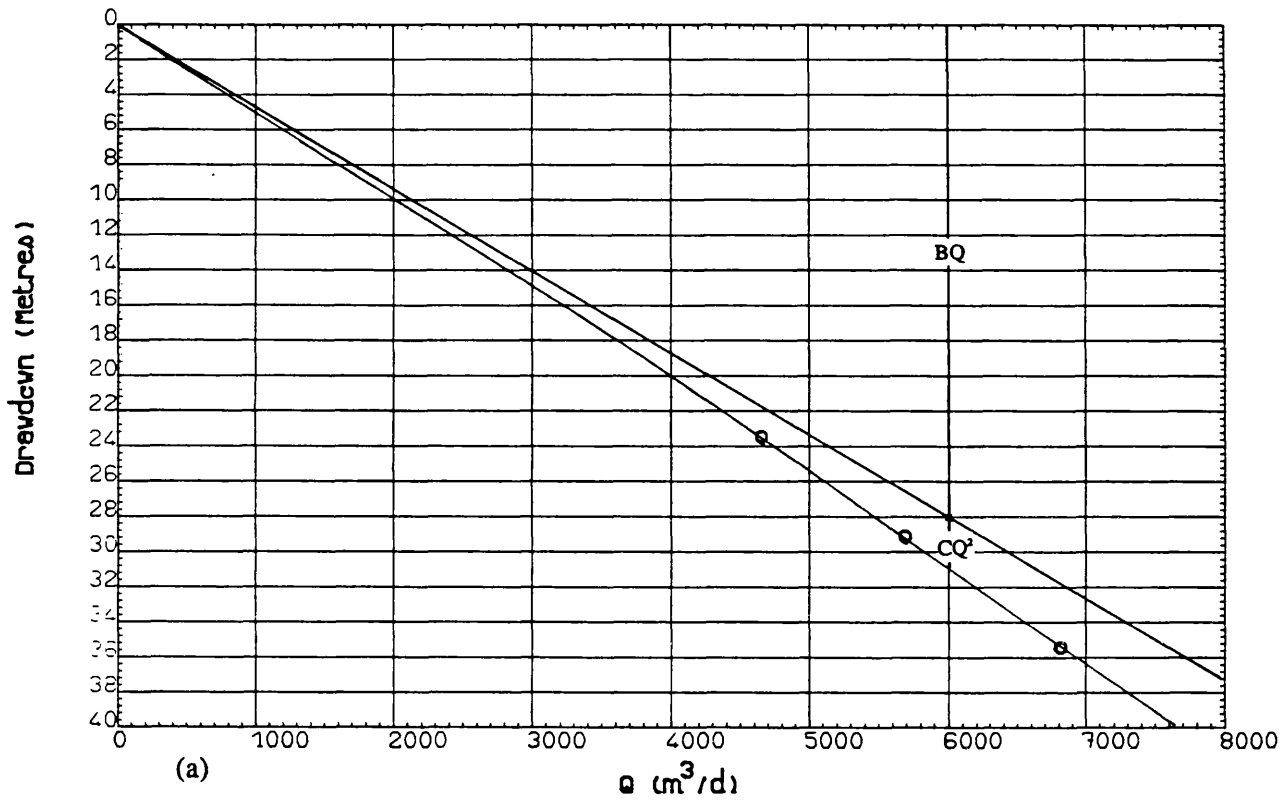


Fig. 6.4 Step-Drawdown test: Theoretical drawdown - yield curve, (a) PW SW1,  
(b) PW SW8.

different methods ( see Figs. A6.1 and A6.2 of Appendix 6). With the Jacob arithmetic method of analysis, the values of C for steps 1 to 3 show positive values, whereas for step 4 it gives a negative value suggestive of change in the well condition. (see Table 6.1). In the graphical method also, this data point does not fit the line passing through the other three points. Therefore, the results of analysis from the first three steps are shown on the same figures.

A well efficiency of 55% at  $Q=6000 \text{ m}^3/\text{d}$  was calculated from the Bruin and Hudson method of analysis and the relationship between theoretical drawdown and discharge is shown in Figure 6.4b. The value of transmissivity was calculated by the Eden and Hazel method and is close to the value previously deduced from the constant rate test.

In general, the results of step-drawdown test data from this well field were not satisfactory. This behaviour can result from various conditions in the vicinity of the wells as well as the condition of the aquifer itself.

### **Jamshidabad area**

The results of two step-drawdown tests conducted in this area in 1978 were analysed by the general procedures outlined above. The well cross sections and lithological profiles were shown in Figure 5.17.

The plots and calculated well and aquifer loss factors, as well as governing drawdown equations from the graphical methods, for well JW2 are illustrated in Figures 6.5 to 6.7 and for JW1 in Figures A6.3 and A6.4 of Appendix 6. The results of the Jacob method of analysis of well loss factor are shown in Table 6.1.

In well JW1, the well loss factors resulting from the graphical methods are in very close agreement (see Table 6.2), whereas the Jacob method result shows a greater value.

The tests comprise four steps with sufficient duration of time, and the lines drawn through the data points show a good fit for both methods. Therefore the accuracy of the results seems to be reasonable.

The theoretical drawdown-yield curve, which is a plot of the governing drawdown equation, is shown in Figure 6.8a. A well efficiency of 82% was calculated at  $Q=5000 \text{ m}^3/\text{d}$  which means the well design was satisfactory.

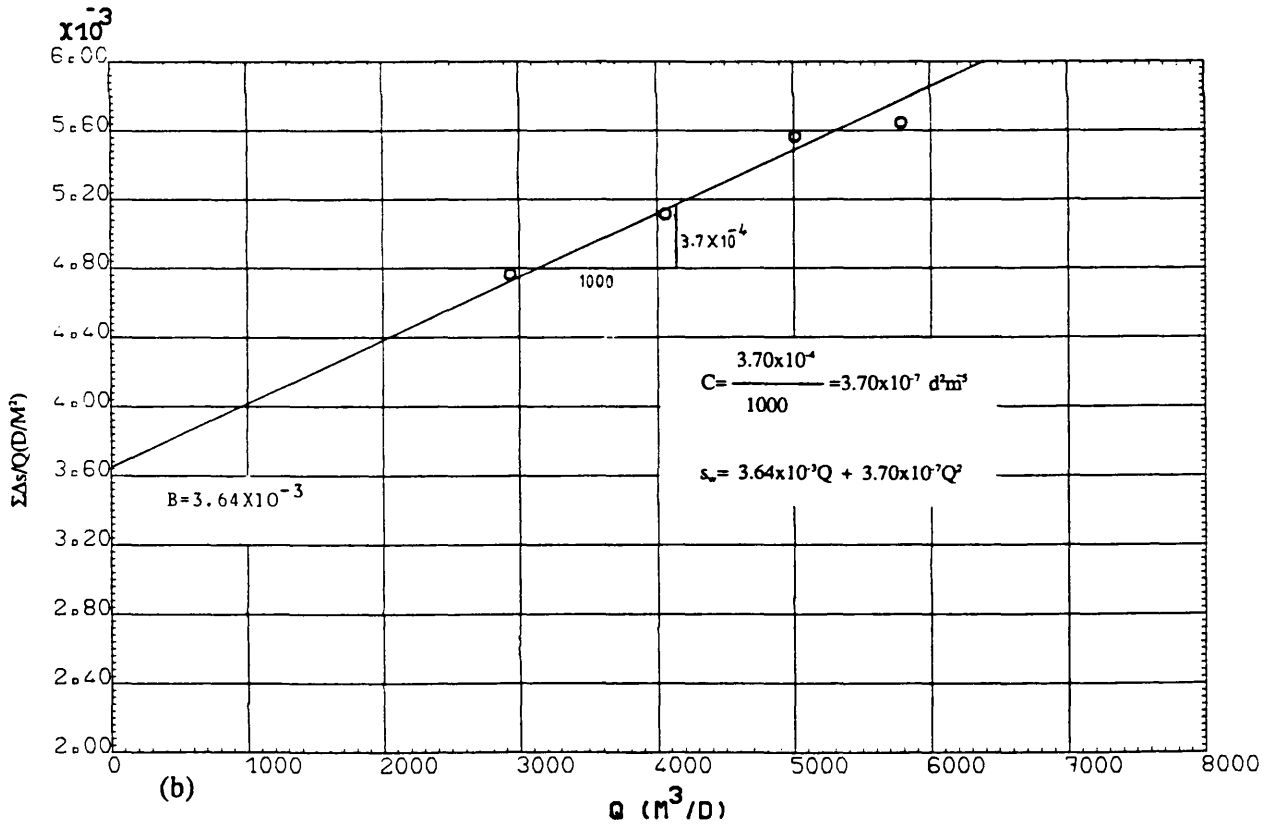
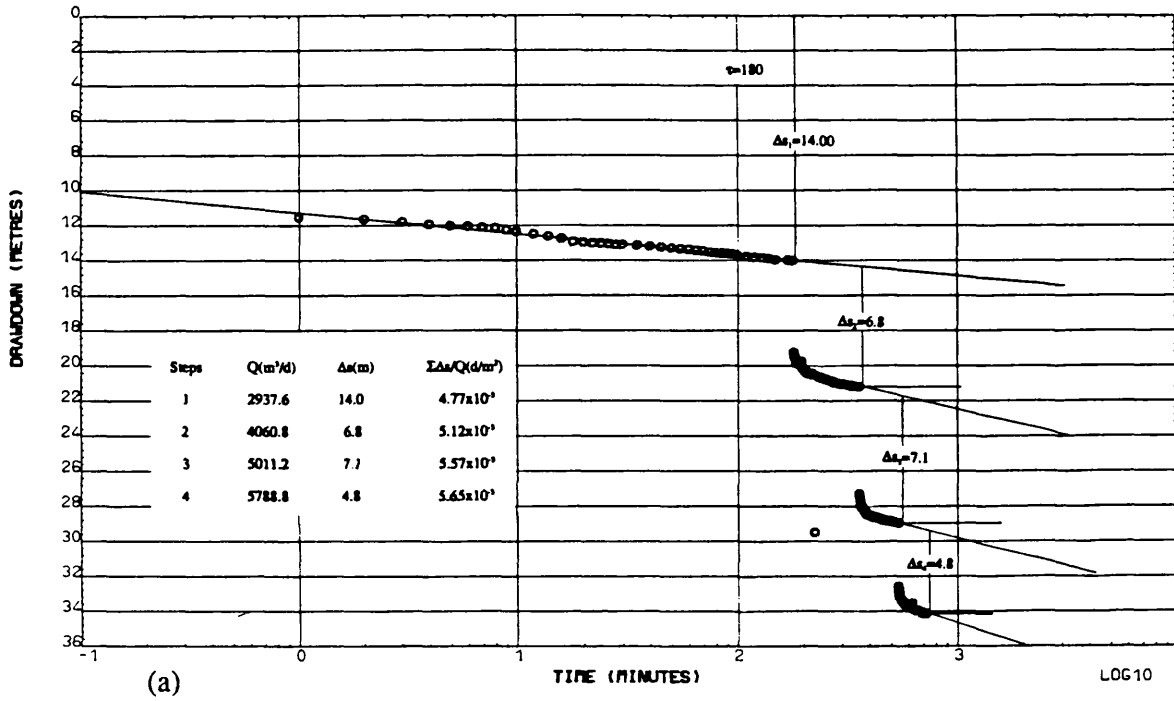


Fig. 6.5 PW JW2, Step-Drawdown test: Bruin & Hudson method, (a) data handling, (b) data plot.

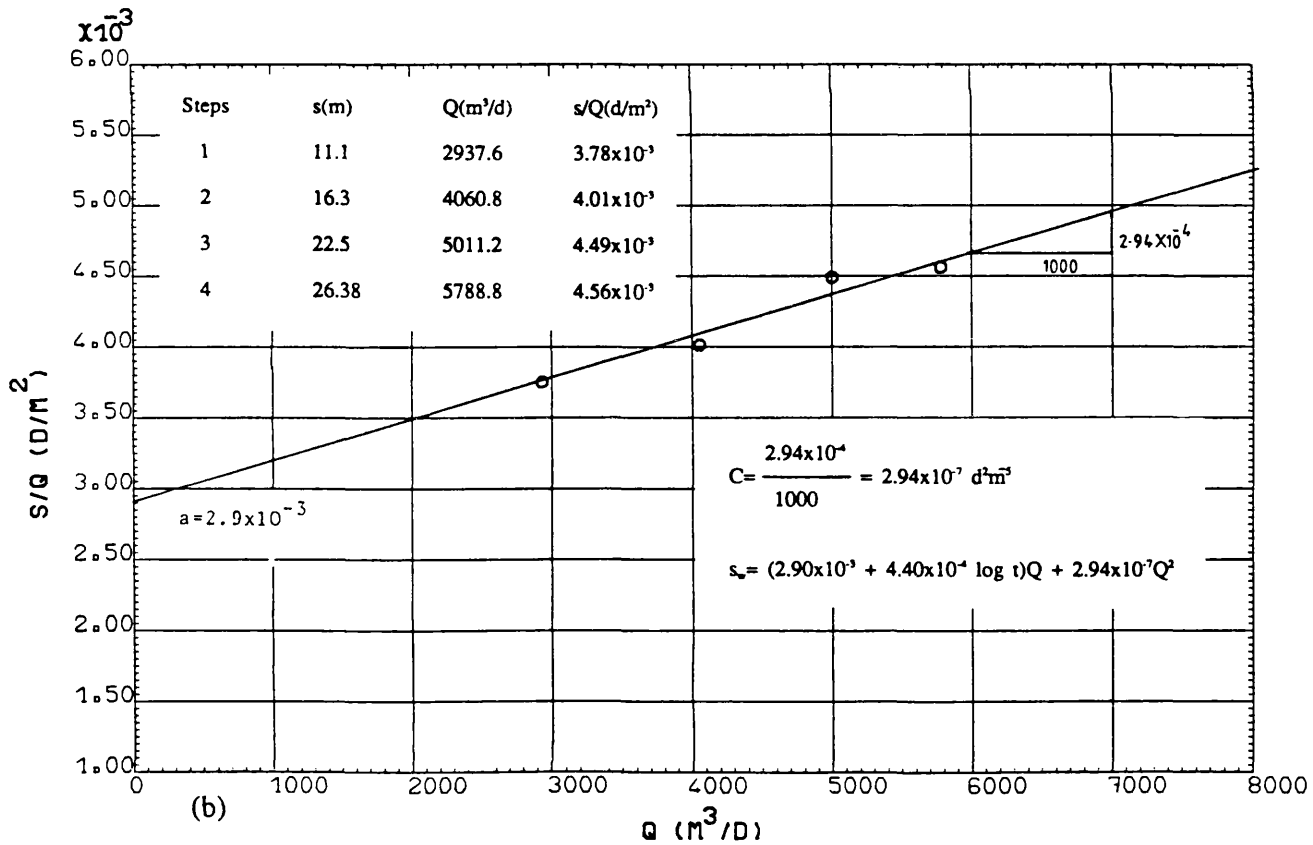
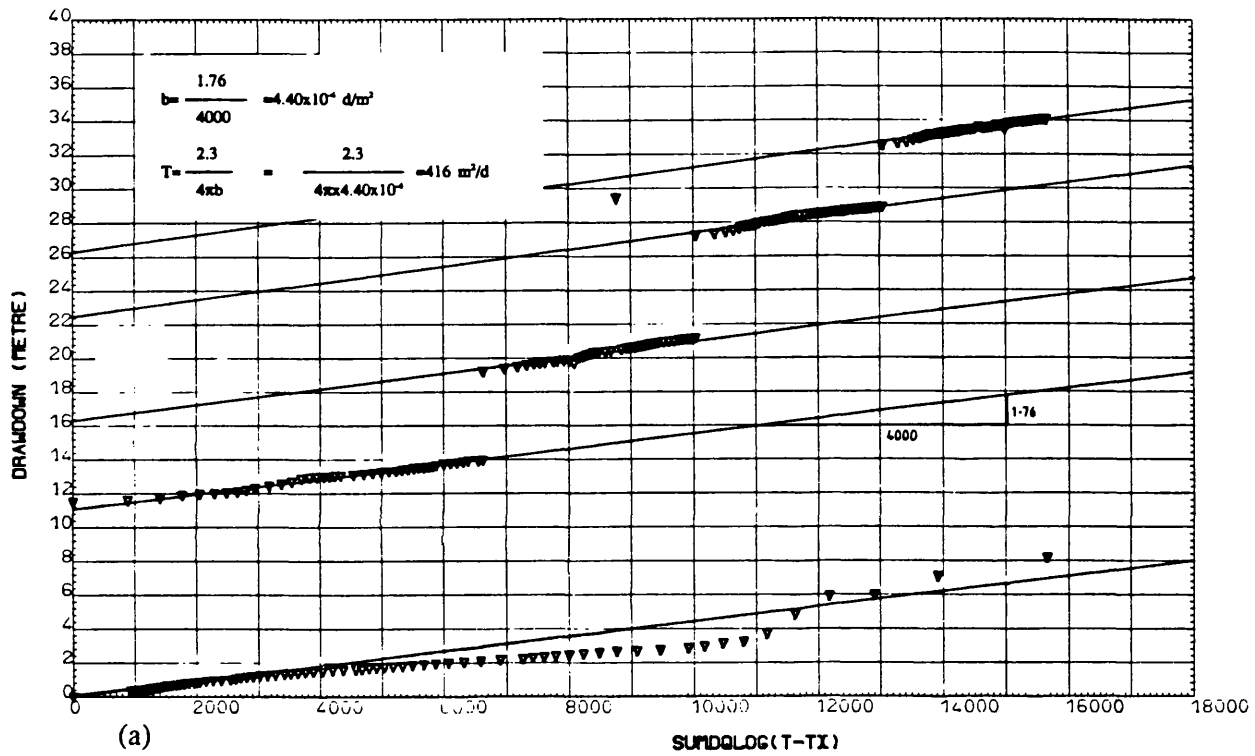


Fig. 6.6 PW JW2, Step-Drawdown test: Eden & Hazel method, (a) data handling, (b) data plot.

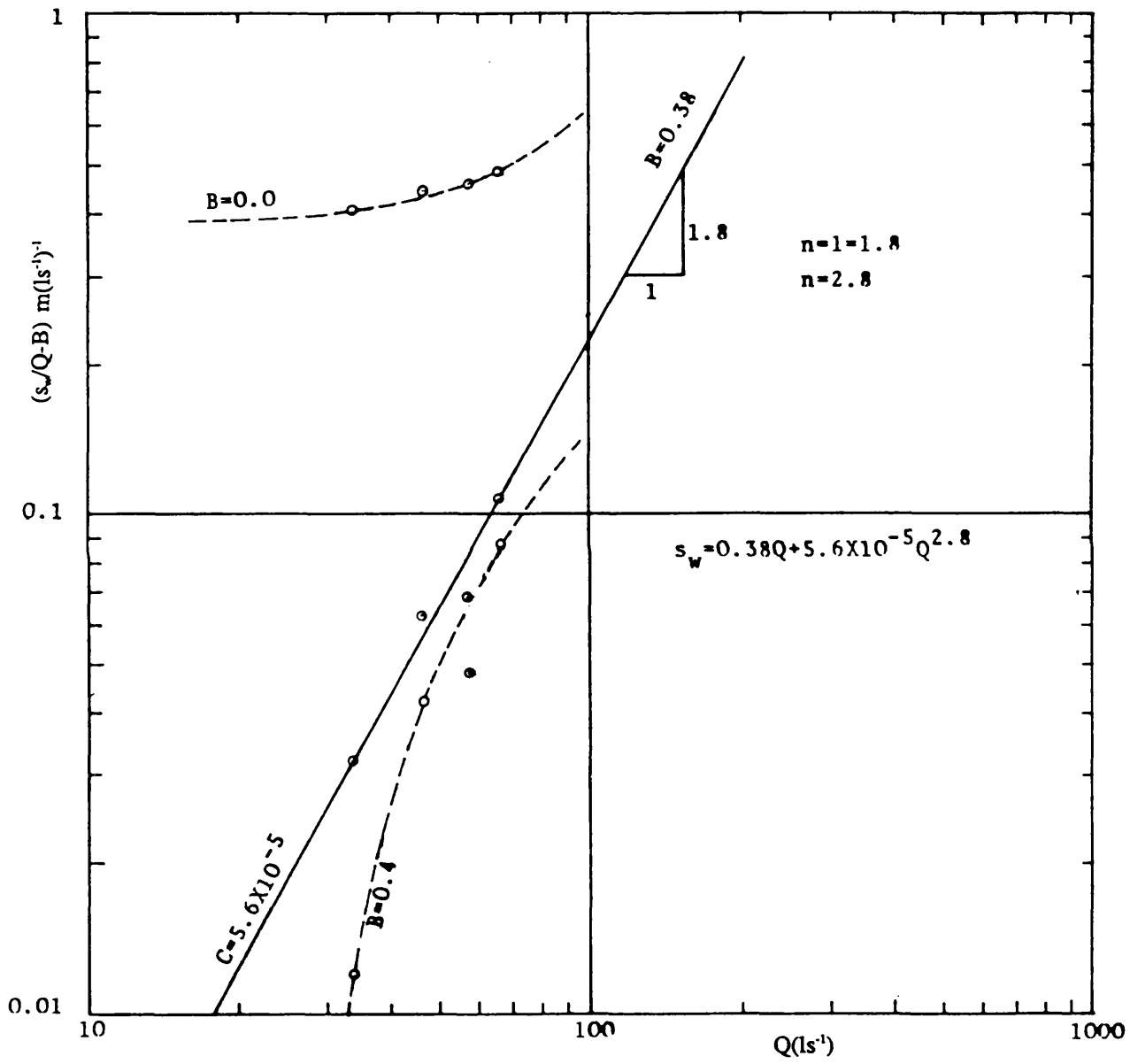


Fig. 6.7 PW JW2, Step-Drawdown test: Rorabaugh method.

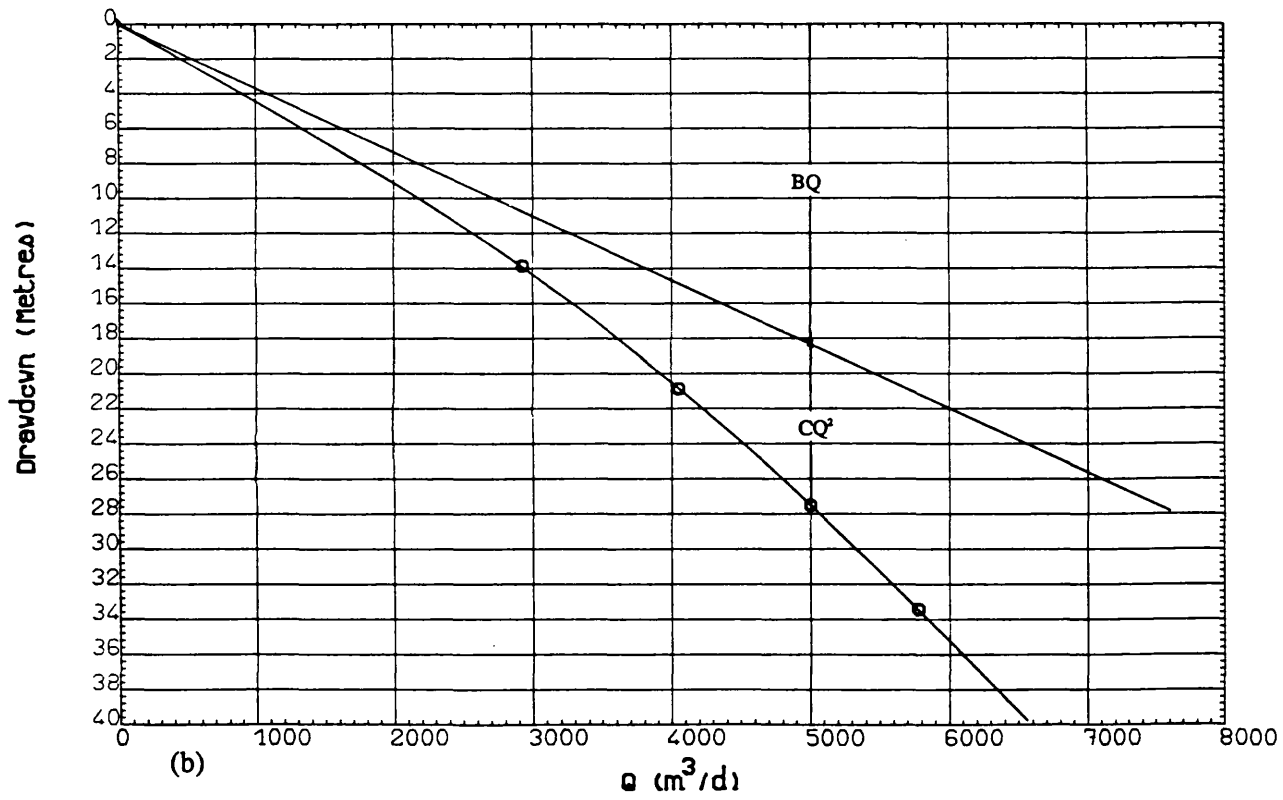
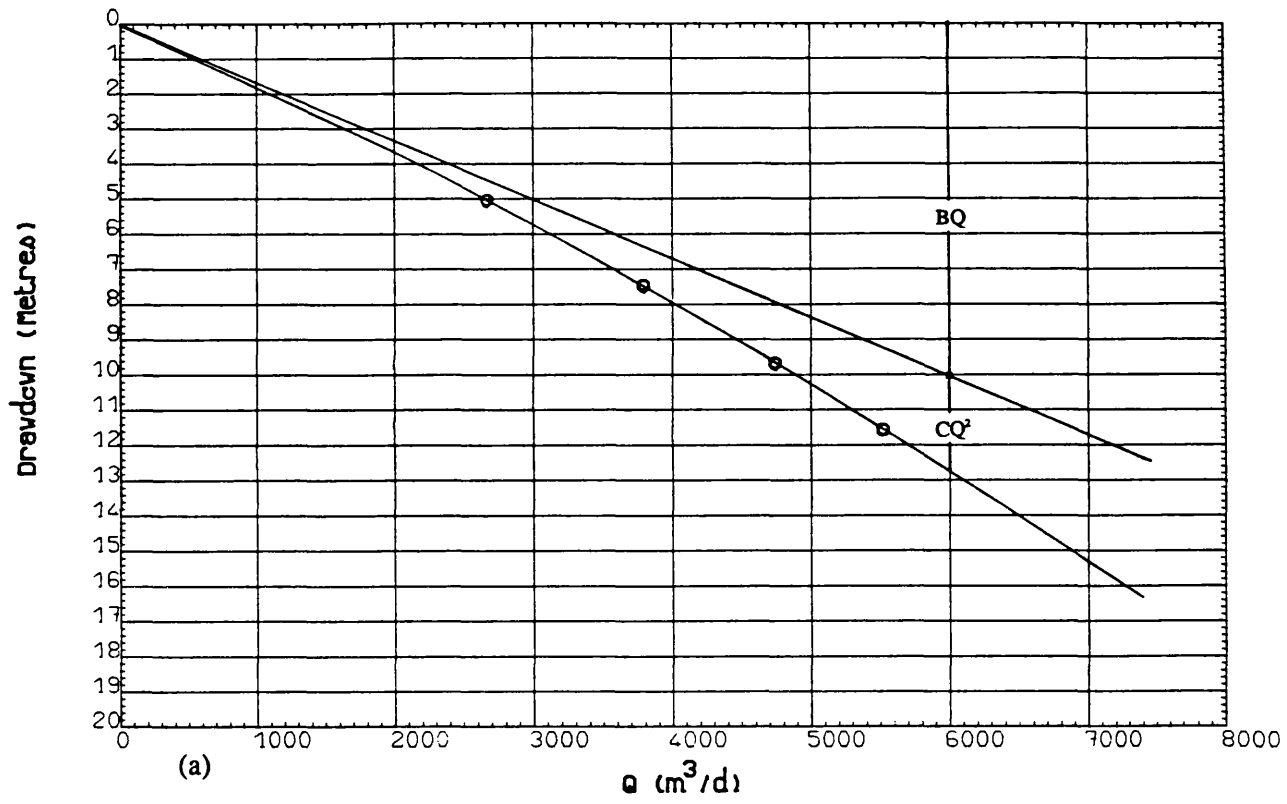


Fig. 6.8 Step-Drawdown test: Theoretical drawdown - yield curve, (a) PW JW1,  
(b) PW JW2.

The value of transmissivity calculated from the Eden & Hazel method (Table 6.2) is very close to the values deduced from the constant rate test. However, the value of storage coefficient calculated from this method ( $2.21 \times 10^{-2}$ ) with respect to the aquifer condition is greater than the expected value.

The number of steps and their duration in well JW2 is the same as in well JW1 and the straight line through the data points shows good agreement (see Fig. 6.6) A well efficiency of 66% at  $Q=5000 \text{ m}^3/\text{d}$  was calculated in this well, which in comparison with the well JW1 is low. The relationship between well and aquifer losses is illustrated in Figure 6.8b as a theoretical drawdown-yield curve. The value of transmissivity determined from this test ( $416 \text{ m}^2/\text{d}$ ) is less than the value determined from the constant-rate test. The resultant value of  $n$  is 2.8 (Fig. 6.7) and the estimated value of storage coefficient is not satisfactory.

### Tabriz Power Station well field

The results of five step-drawdown tests conducted in this well field in 1980 were analysed in similar fashions to the tests on the Jamshidabad wells. The tests were carried out in three steps with 180 minutes for each step; the accuracy of the analyses with respect to the number of steps should be borne in mind.

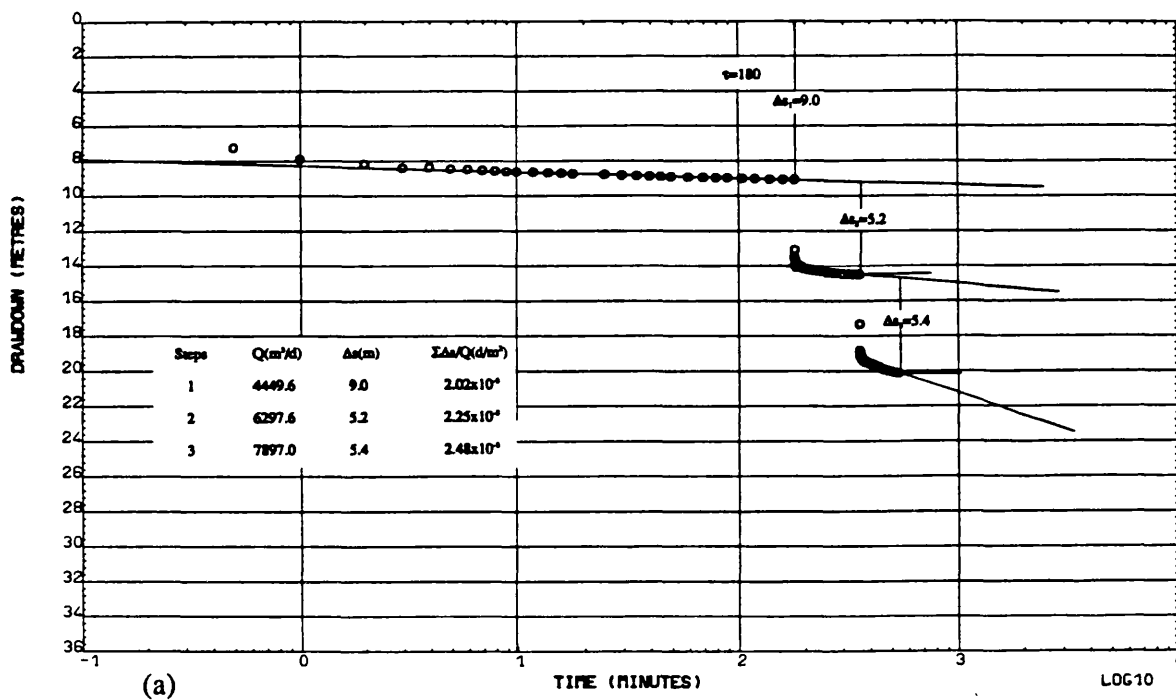
The general plots of the analyses and resultant values of  $B$ ,  $C$ ,  $n$ , and governing drawdown equations for well TPSW6 are shown in Figures 6.9 to 6.11 and the theoretical drawdown-yield curve derived from Bruin and Hudson method equation is illustrated in Figure 6.12b. The above-mentioned methods of analyses for the other wells of this well-field are shown in Appendix 6 (see Figs. A6.5 to A6.14).

The well efficiencies for these wells at  $Q=5000 \text{ m}^3/\text{d}$  were calculated as follows:

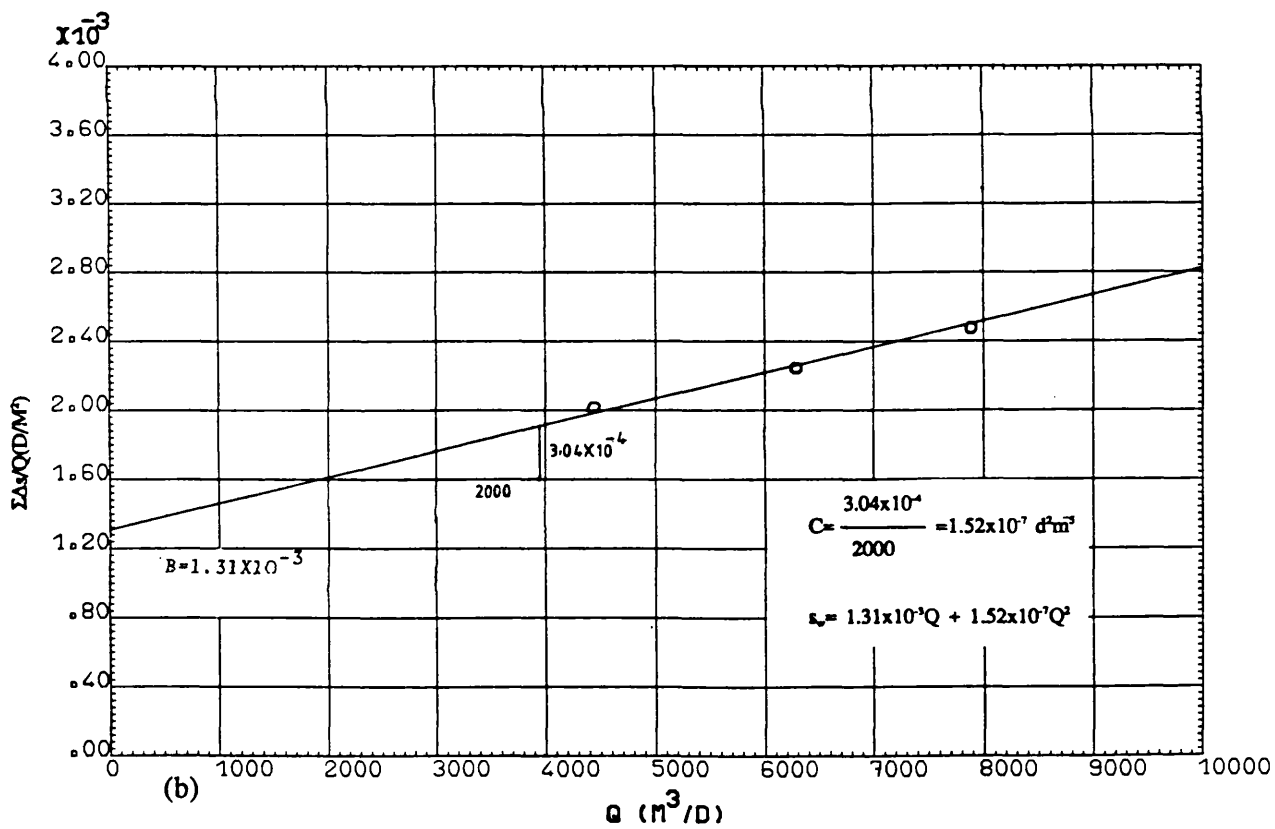
Well No.	TPSW1	TPSW3	TPSW4	TPSW6	TPSW8
Well eff. (%)	77	22	96	63	93

The minimum percentage of well efficiency is for well TPSW3 which is believed to have been damaged during well construction (the well sections were shown in Fig. 5.17). It shows a sharp decline in specific capacity as the discharge rate increases.





(a)



(b)

Fig. 6.9 PW TPSW6, Step-Drawdown test: Bruin & Hudson method, (a) data handling,

(b) data plot.

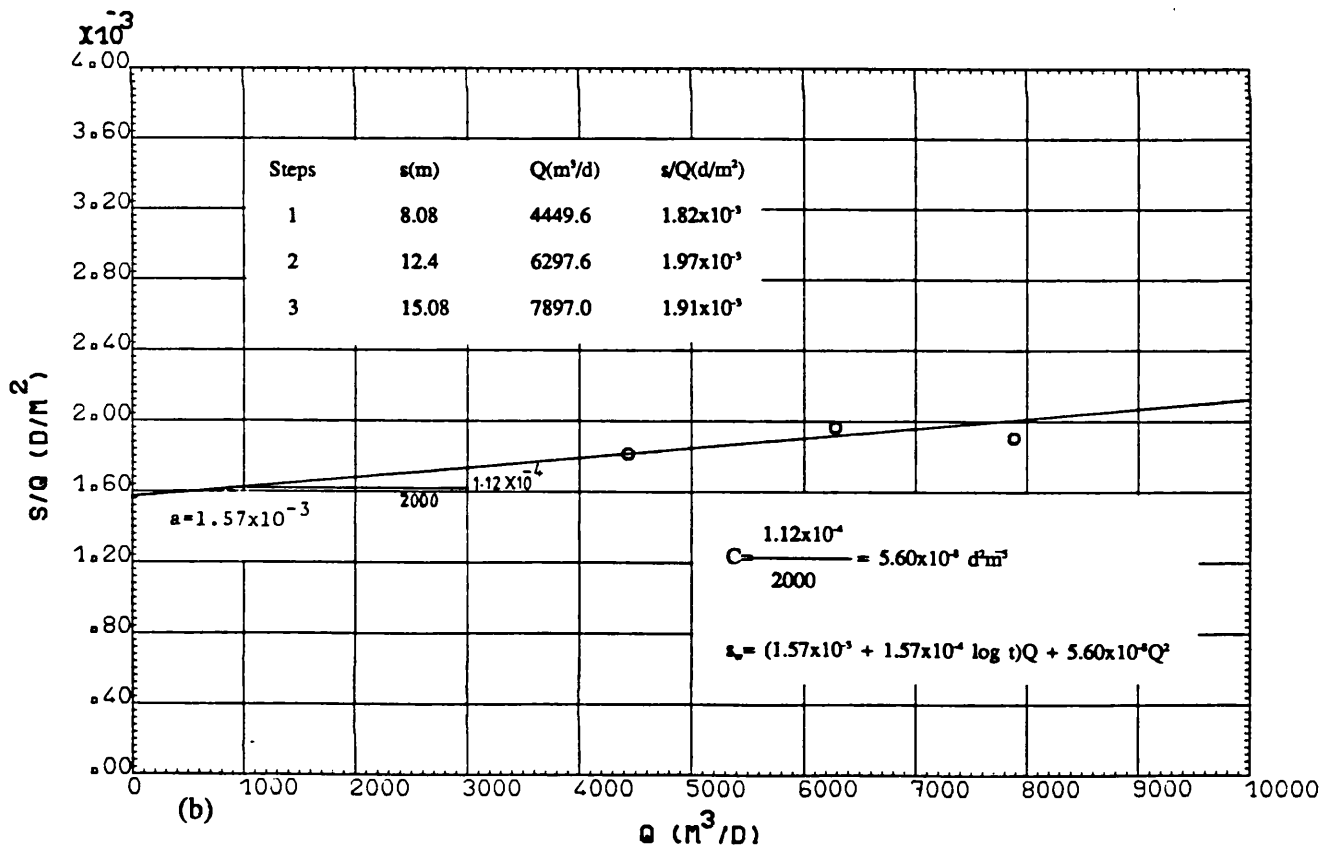
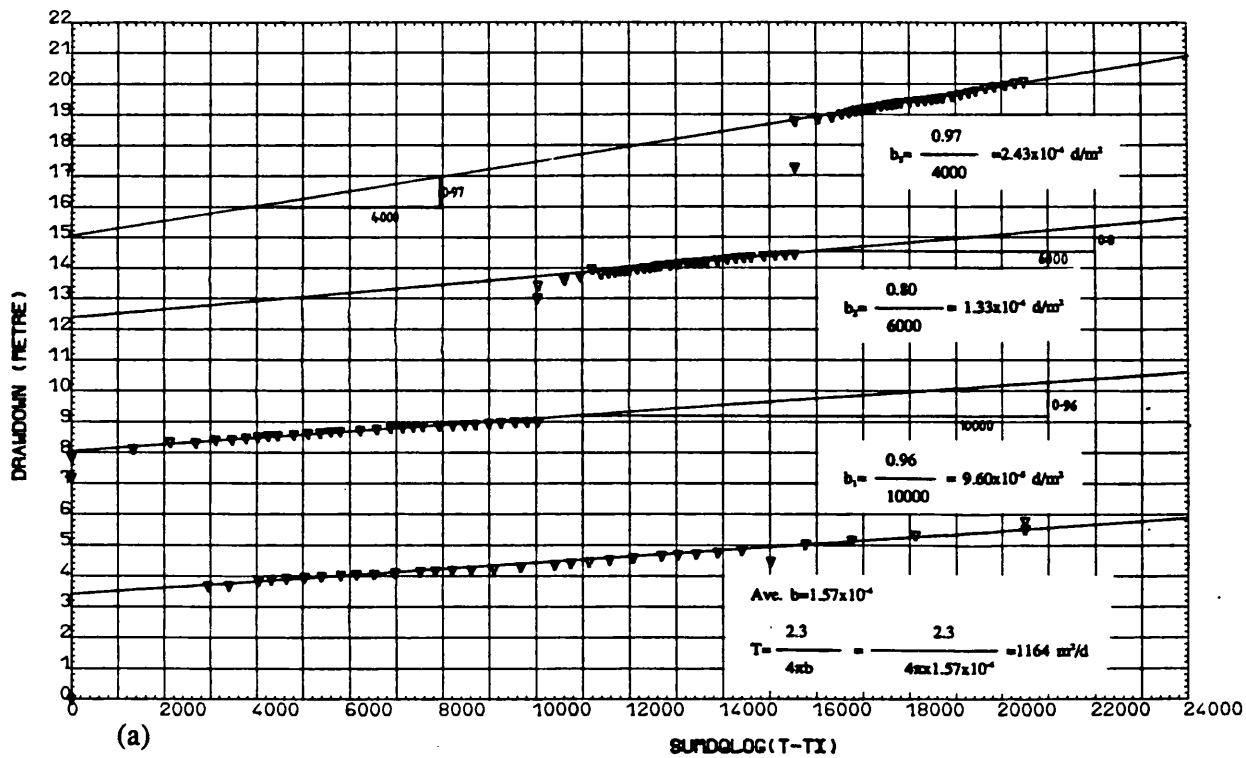


Fig. 6.10 PW TPSW6, Step-Drawdown test: Eden & Hazel method, (a) data handling, (b) data plot.

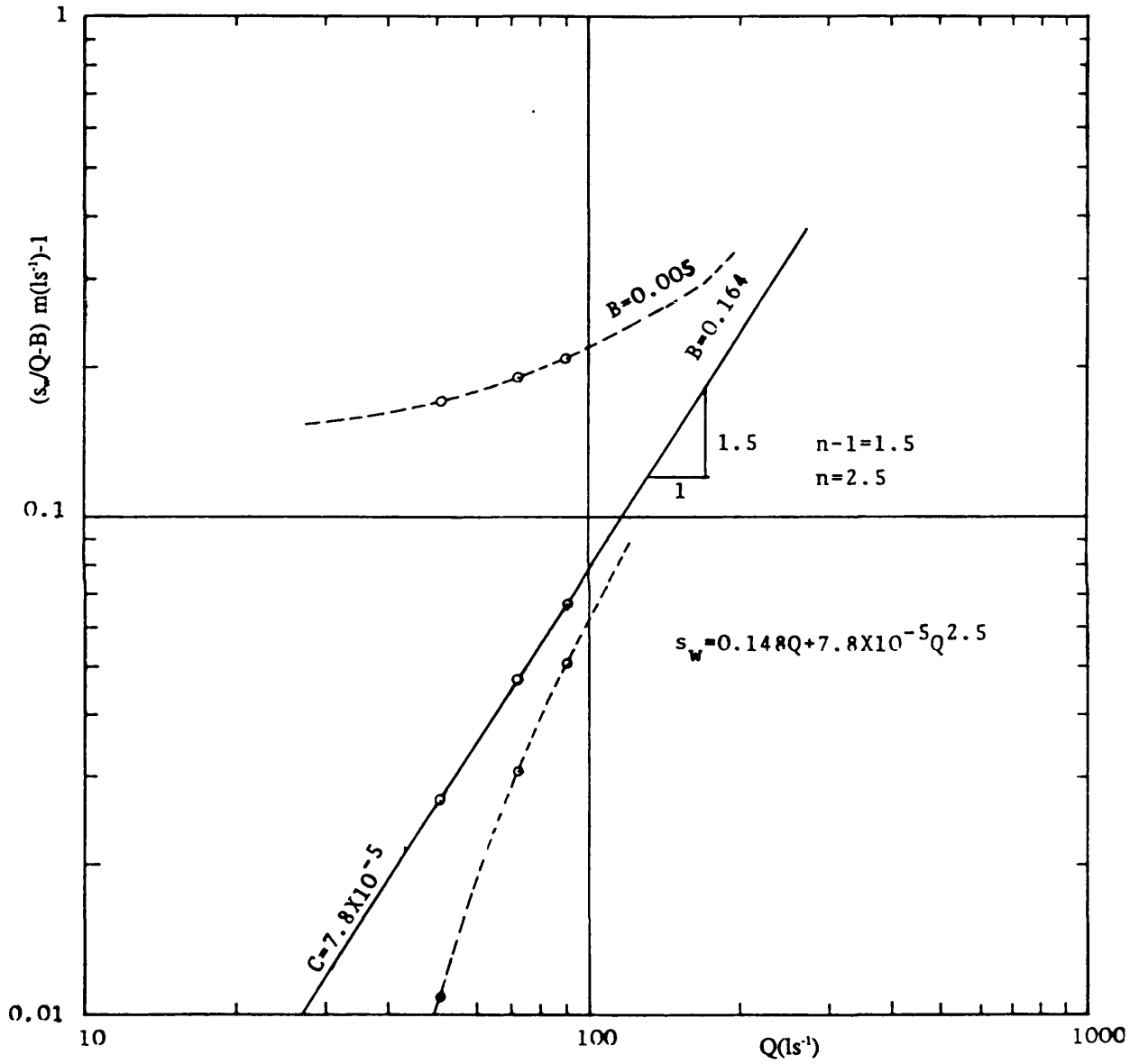


Fig. 6.11 PW TPSW6, Step-Drawdown test: Rorabaugh method.

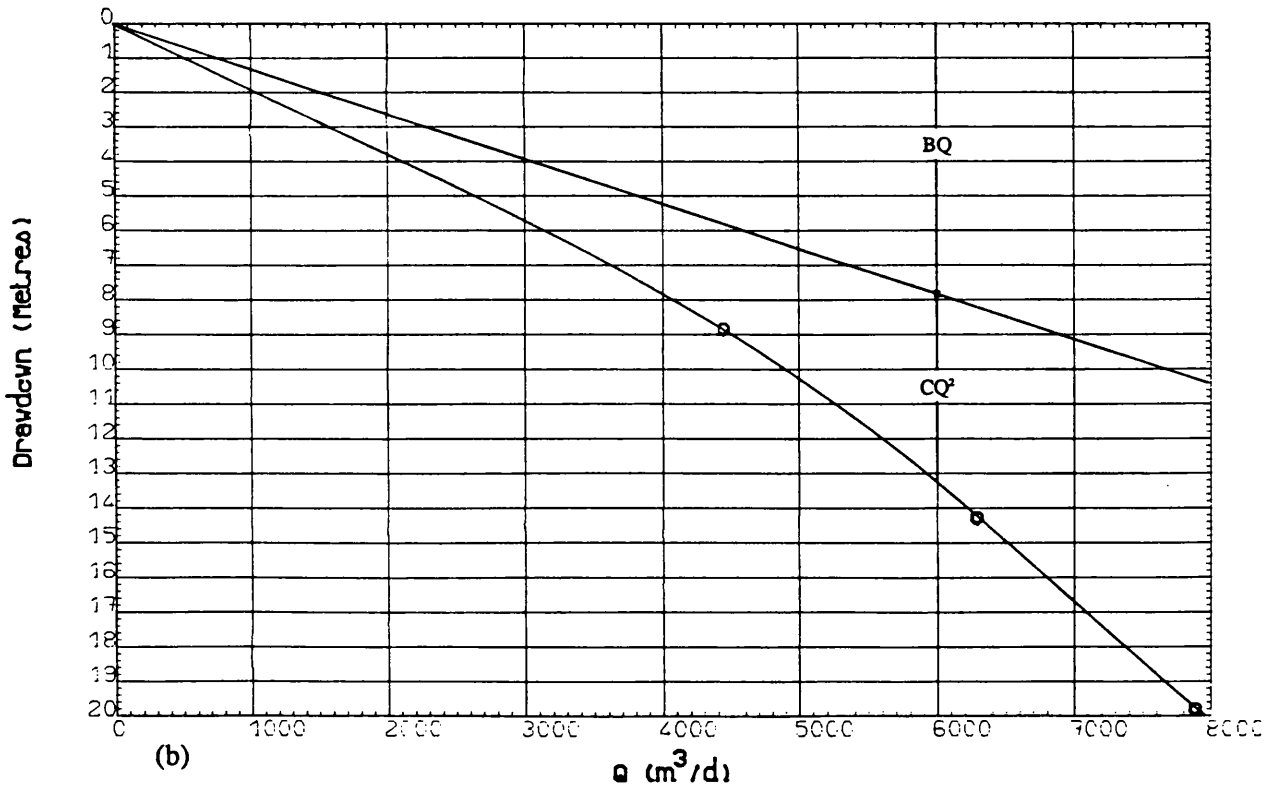
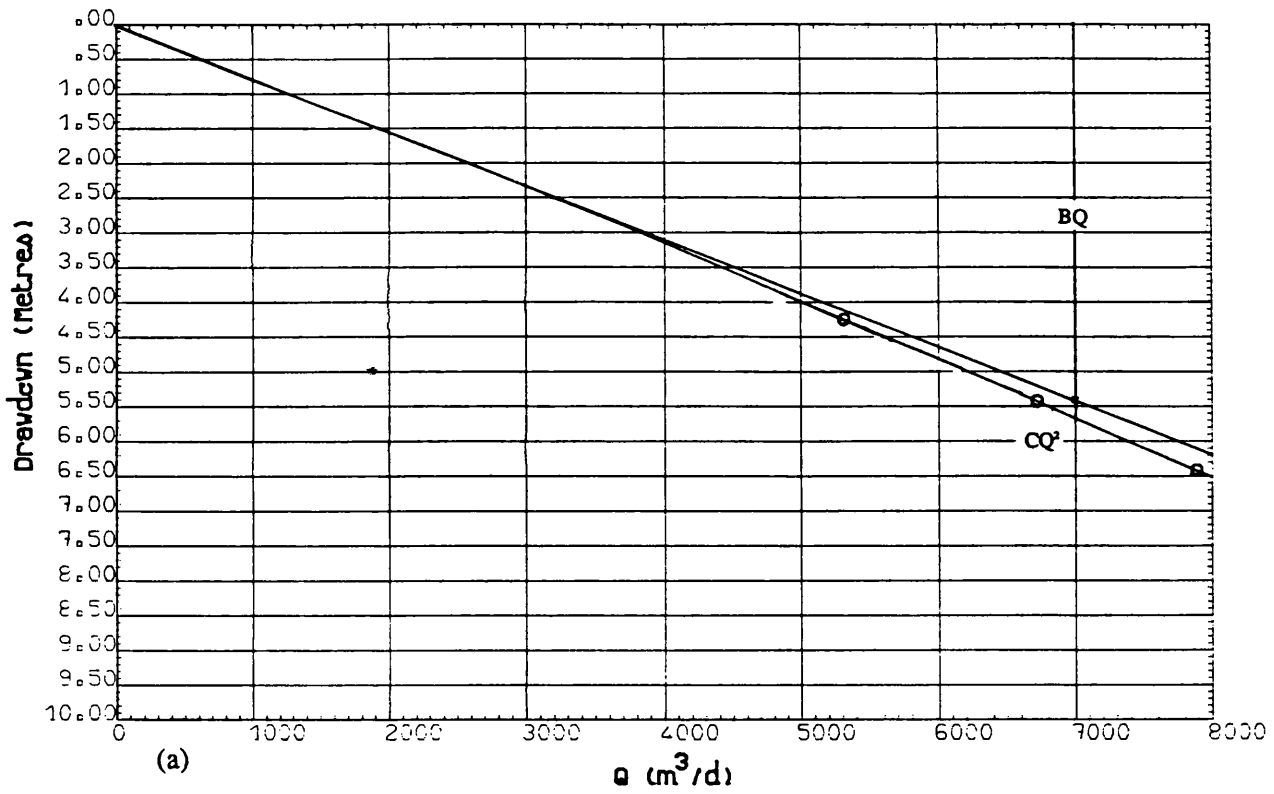


Fig. 6.12 Step-Drawdown test: Theoretical drawdown - yield curve, (a) PW TPSW4,  
(b) PW TPSW6.

The resultant values of C from the Jacob method are given in Table 6.1. The calculated value of C for the well TPSW3 by this method is very high because the calculated value of well loss component is greater than the actual total drawdown. This is unacceptable, and demonstrates the limitations of the method.

The calculated values of transmissivity from the Eden & Hazel method are shown on the related Eden and Hazel diagrams. All these values are in close agreement with the values deduced from the constant-rate tests (see Table 6.2), with the exception of well TPSW1 which shows a higher value. The calculated values for storage coefficient are not satisfactory. The Bruin & Hudson, Eden & Hazel, and Rorabaugh methods of data of well TPSW6 showed well loss factors of  $1.52 \times 10^{-7} \text{ d}^2\text{m}^{-5}$ ,  $5.6 \times 10^{-8} \text{ d}^2\text{m}^{-5}$ , and  $7.8 \times 10^{-5} \text{ m}(\text{s/l})^{2.5}$ , respectively. The resultant values of B and n from Rorabaugh method are 0.165 ml/s and 2.5, respectively.

### Tabriz airport well

Figures 6.13 and 6.14 are plots of the data obtained during the step-drawdown test in 1979 on well TAW. The calculated specific drawdown-discharge data and plots and resultant values of B and C, as well as the governing theoretical drawdown equations, are shown in the same figures. In both methods the data points more or less lie in a straight line. The theoretical drawdown-yield curve derived from the governing drawdown equation is illustrated in Fig. 6.16.

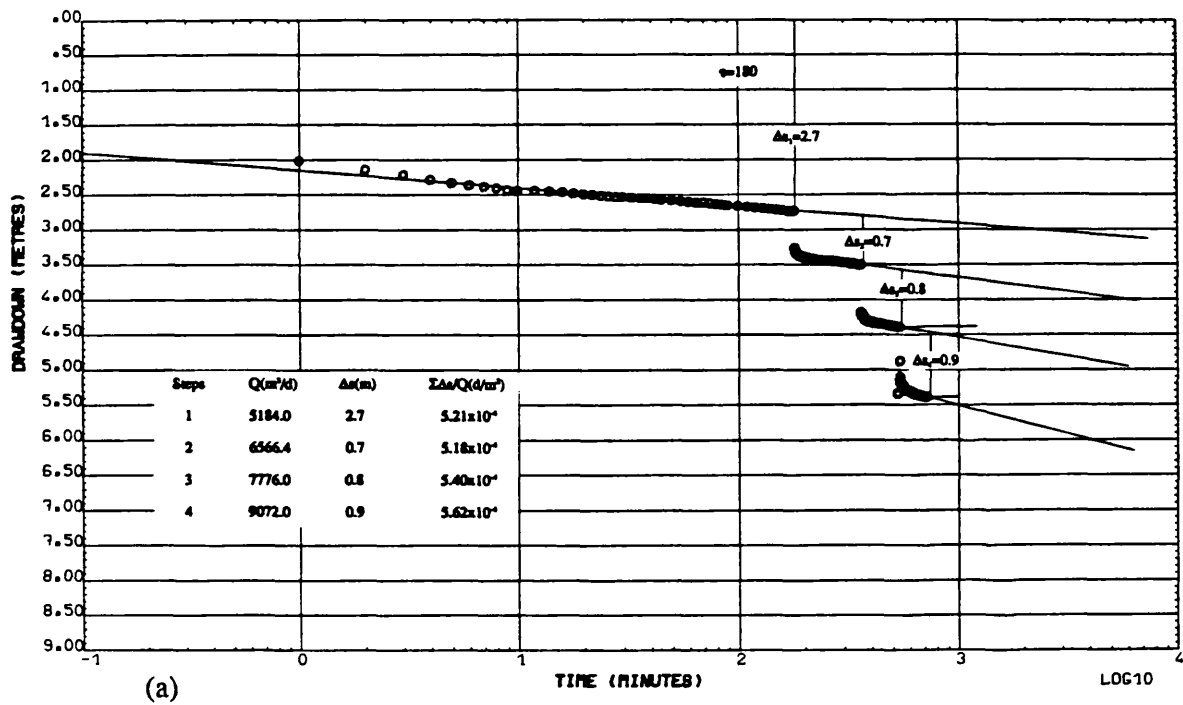
For the Rorabaugh method, the data is plotted on log-log paper (Fig. 6.15). The first two points plotted as a horizontal line (slope=0) indicating laminar flow. Since three further points are available for higher rates of discharge, it is possible to evaluate the test. The data was interpreted from the equations:

$$\text{for } Q < QC, s_w = BQ + C'Q \text{ (for laminar flow)}$$

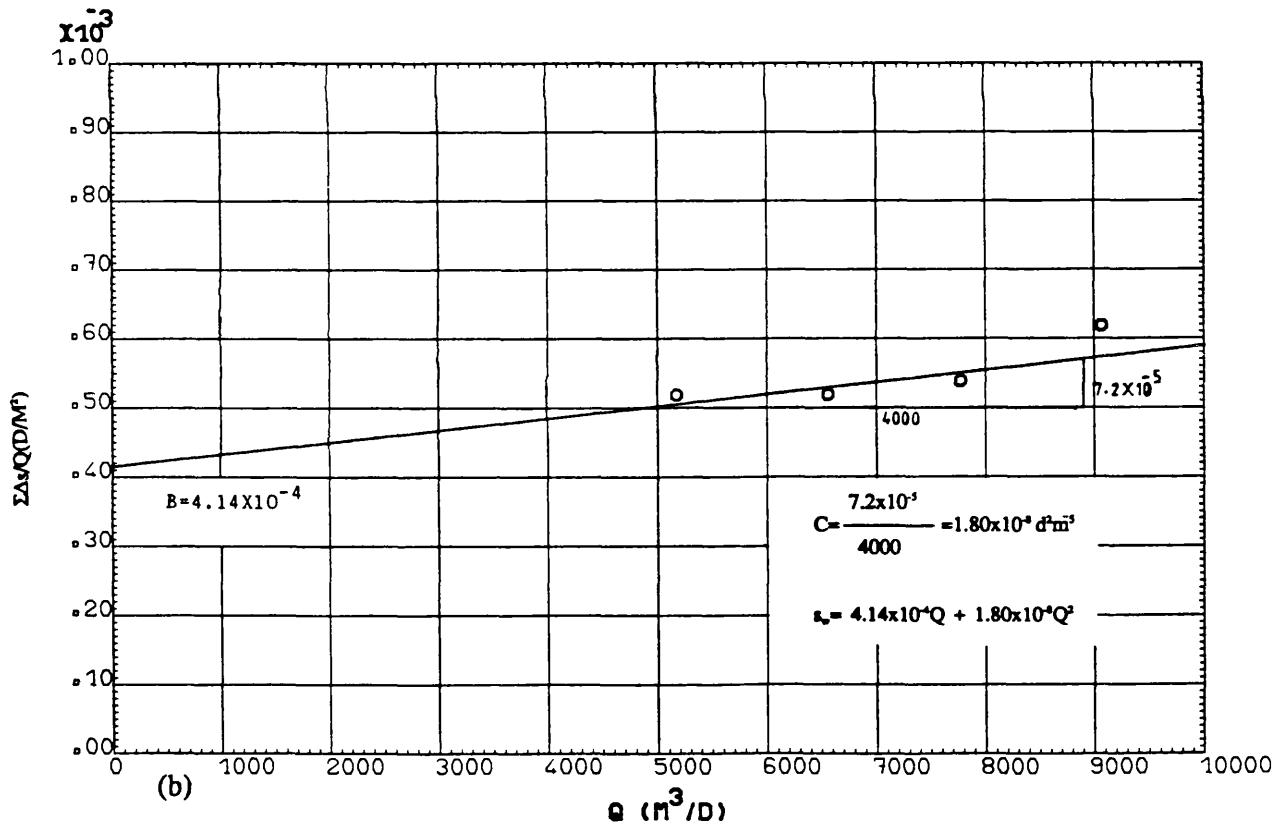
$$\text{for } Q > QC, s_w = BQ + CQ^2 \text{ (for turbulent flow)}$$

where  $C'$  is the well loss constant for laminar flow, and  $QC$  is the critical discharge below which laminar flow prevails.

The critical discharge,  $QC$  was determined as 79 l/sec from the intersection of the two straight lines. B, C,  $C'$  and n were determined to be 0.0345,  $1.36 \times 10^{-4}$ ,  $1.02 \times 10^{-2}$ , and 2 respectively. Therefore, the above mentioned theoretical equations can be written as:



(a)



(b)

Fig. 6.13 PW TAW, Step-Drawdown test: Bruin & Hudson method, (a) data handling,

(b) data plot.

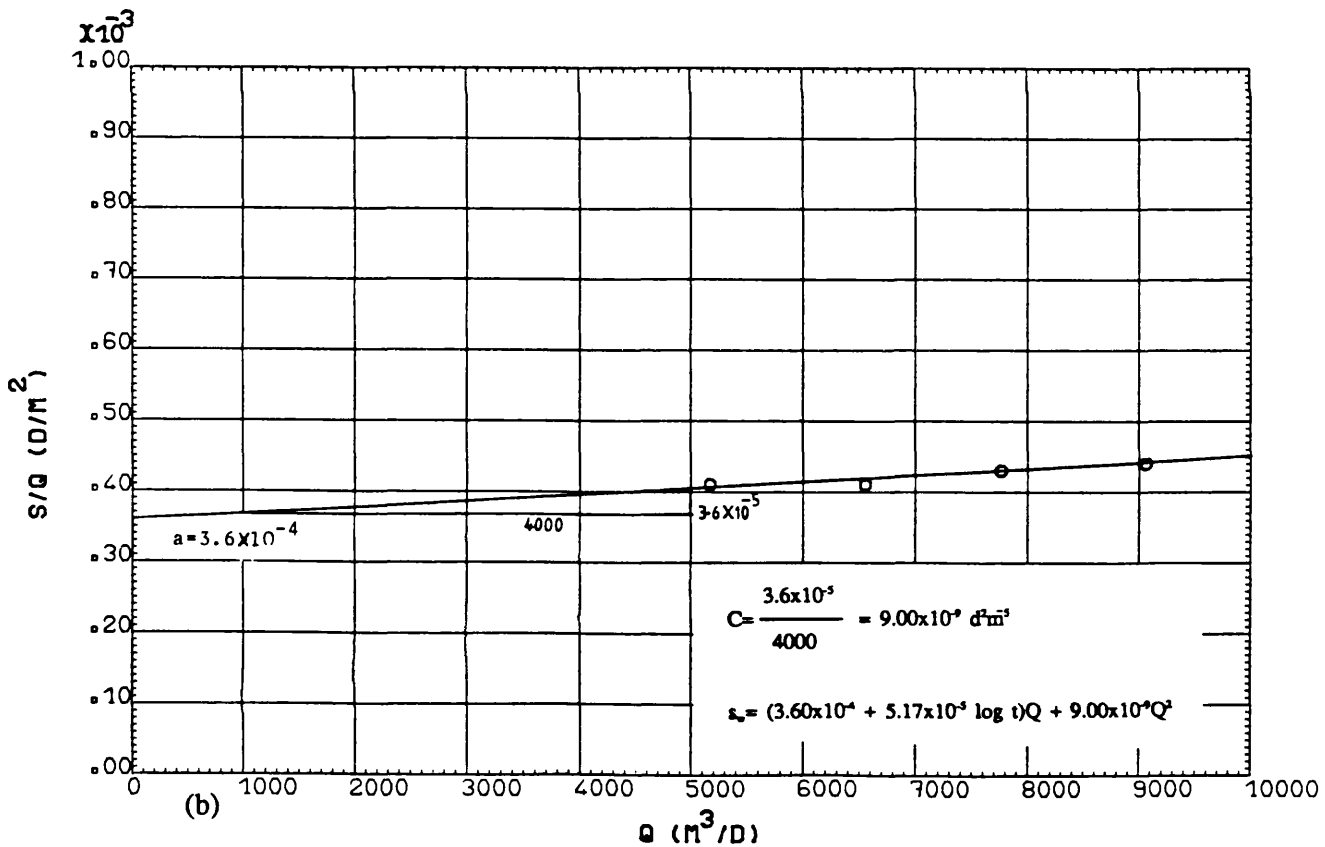
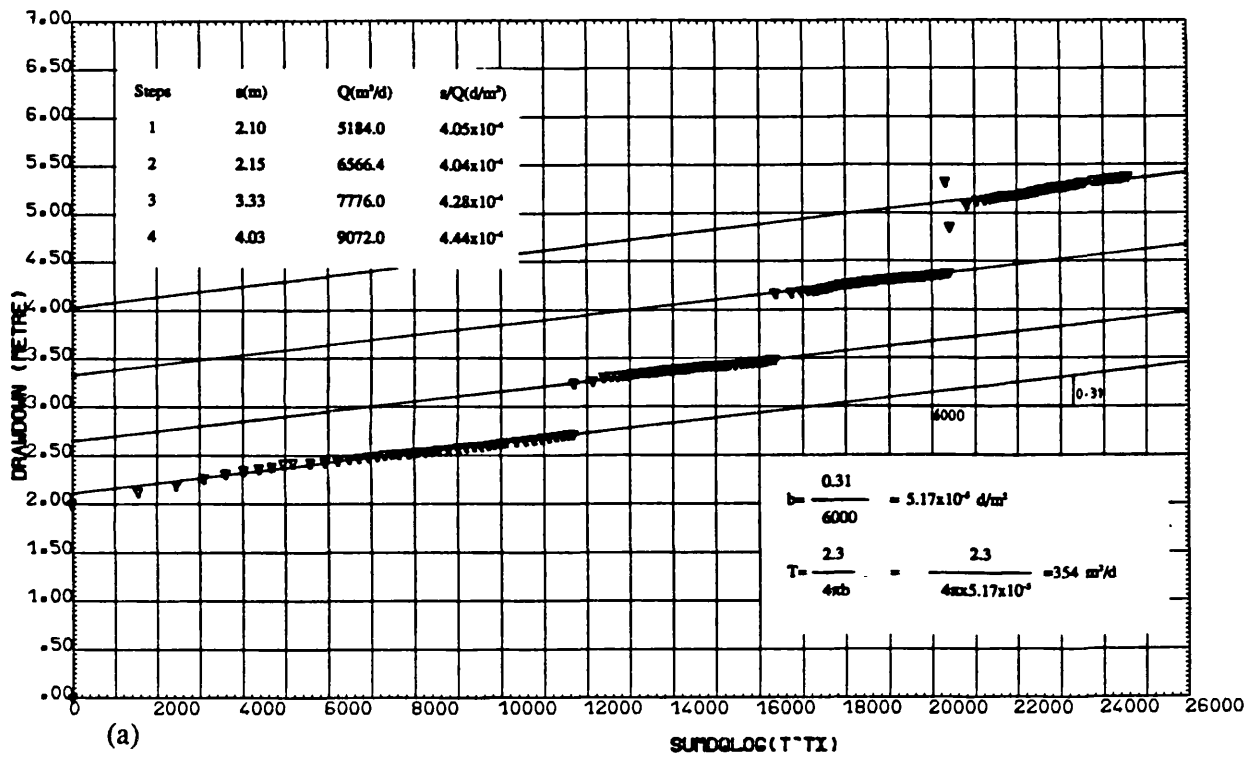


Fig. 6.14 PW TAW, Step-Drawdown test: Eden & Hazel method, (a) data handling, (b) data plot.

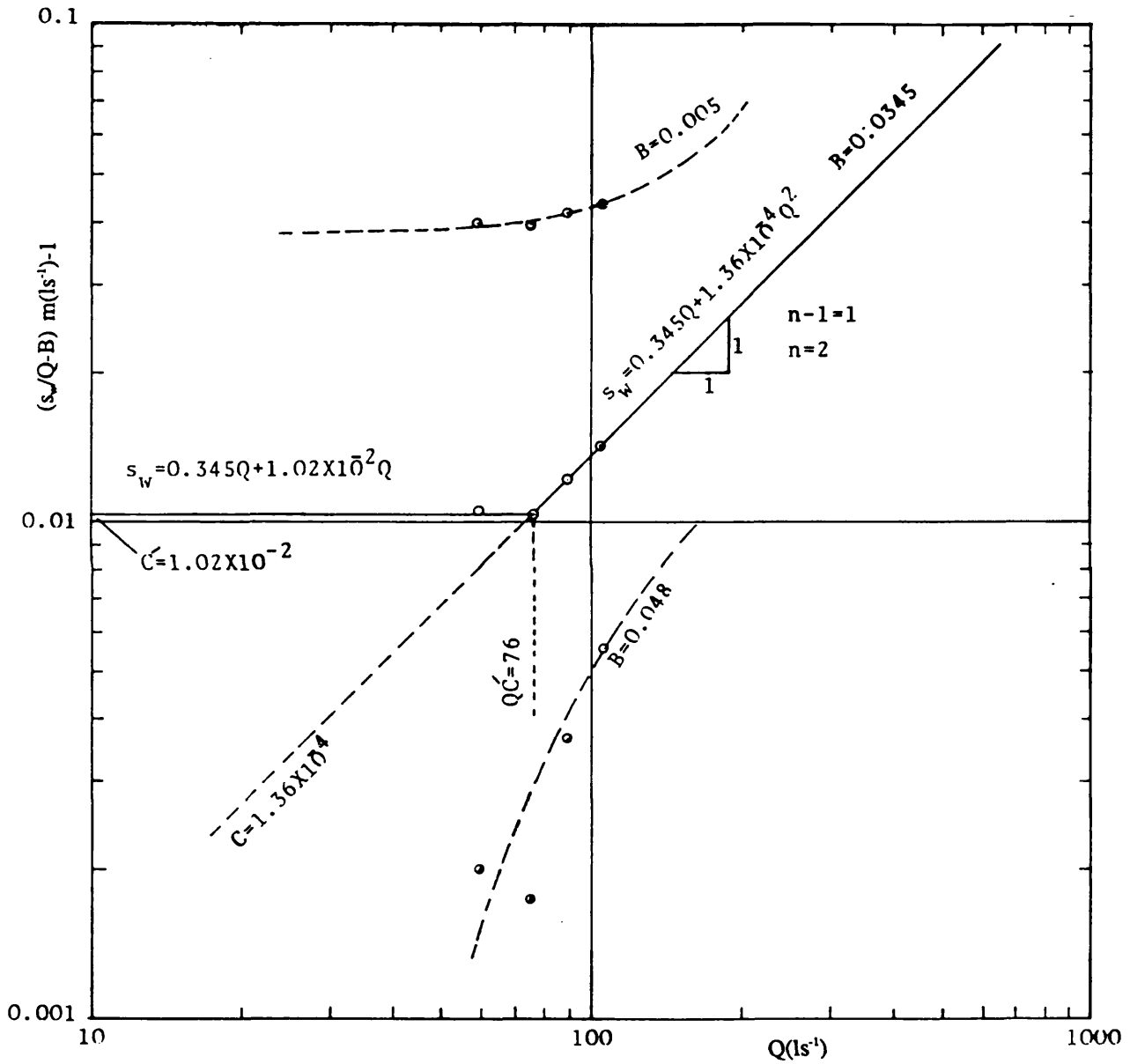


Fig. 6.15 PW TAW, Step-Drawdown test: Rorabaugh method.



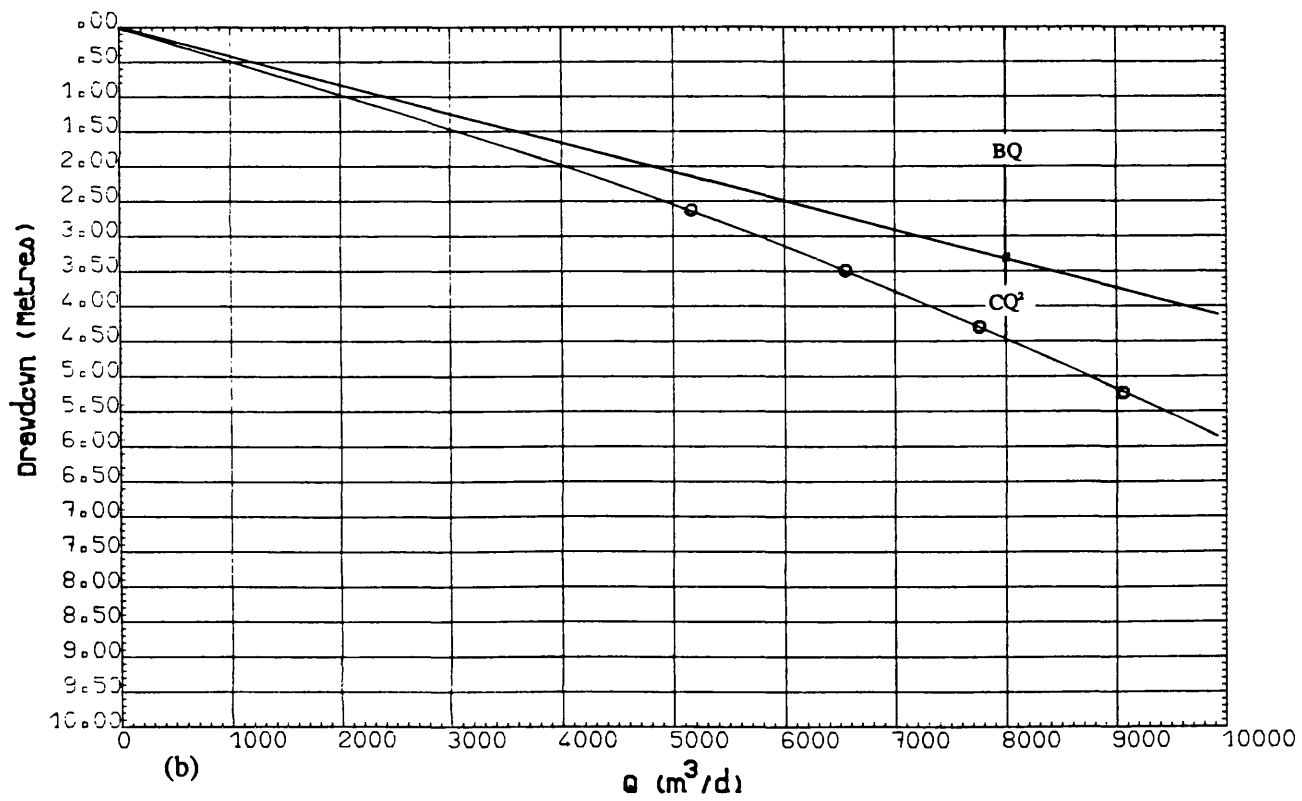
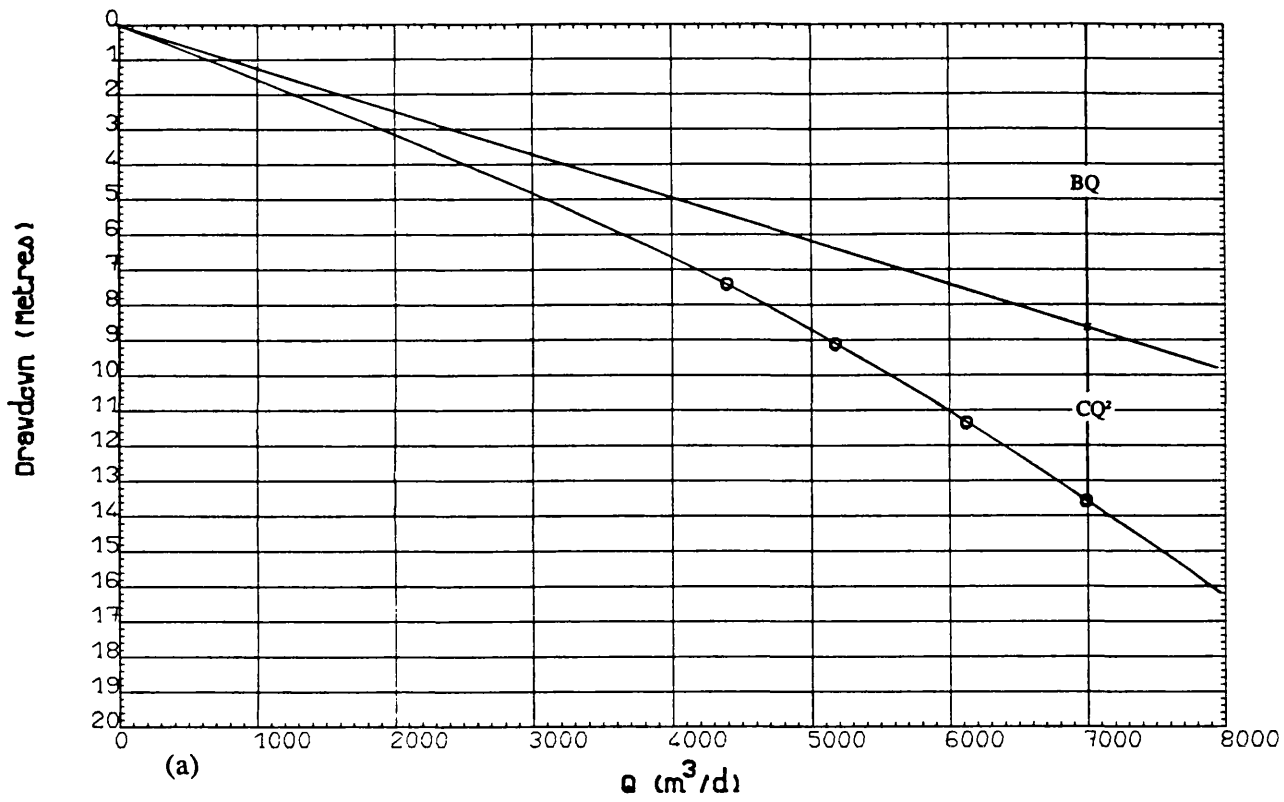


Fig. 6.16 Step-Drawdown test: Theoretical drawdown -yield curve, (a) PW TAW, (b) PW SOW.

for  $Q < Q_C$ ,  $s_w = 0.0345Q + 1.02 \times 10^{-2}Q$  (for laminar flow)

for  $Q > Q_C$ ,  $s_w = 0.0345Q + 1.36 \times 10^{-4}Q^2$  (for turbulent flow)

A well efficiency of 72% at  $Q=9000 \text{ m}^3/\text{d}$  was calculated for this well which with respect to the high value of discharge is satisfactory. The value of transmissivity calculated from the test is in close agreement with the values deduced from the constant rate test and the resulting value of  $n$  is exactly equal to the value suggested by Jacob ( $n=2$ ).

### Soufian water supply well

Figures 6.17 and 6.18 are plots of data obtained during the step drawdown test as well as specific drawdown-discharge data which have been calculated from the original test data. All the calculations and results are shown on the same diagrams. The specific drawdown-discharge data have also been analysed by the Rorabaugh method and the resultant plot and values of  $B$ ,  $C$ , and  $n$  are shown in Figure 6.19.

The test was carried out in four steps and all data points are covered by the straight line drawn through the data. The value of  $C$  obtained from the different methods has a small range.

A well efficiency of 64% at  $Q=7000 \text{ m}^3/\text{d}$  was calculated from the Bruin & Hudson method results and the theoretical drawdown discharge curve is shown in Figure 6.16b. The calculated value of transmissivity from the Eden and Hazel method is in very close agreement with the values deduced from the constant rate test.

### Tabriz Park well-field

The Tabriz Park well-field area was situated in the western part of the city of Tabriz where the River Liguwan Chay joins the Aji Chay (see Fig 5.1). The IRAB Engineering Company drilled five pumping wells in 1978 to meet the required water demand for the planned park in this area.

The wells were screened in the deep aquifer which lies approximately between 60 and 135 metres depth. The casing and screen inner diameters are 12 inches for all these wells. Technical sections of the wells are shown in Figure 6.20.

Four step tests were carried out in these wells, except for well PTW3 which

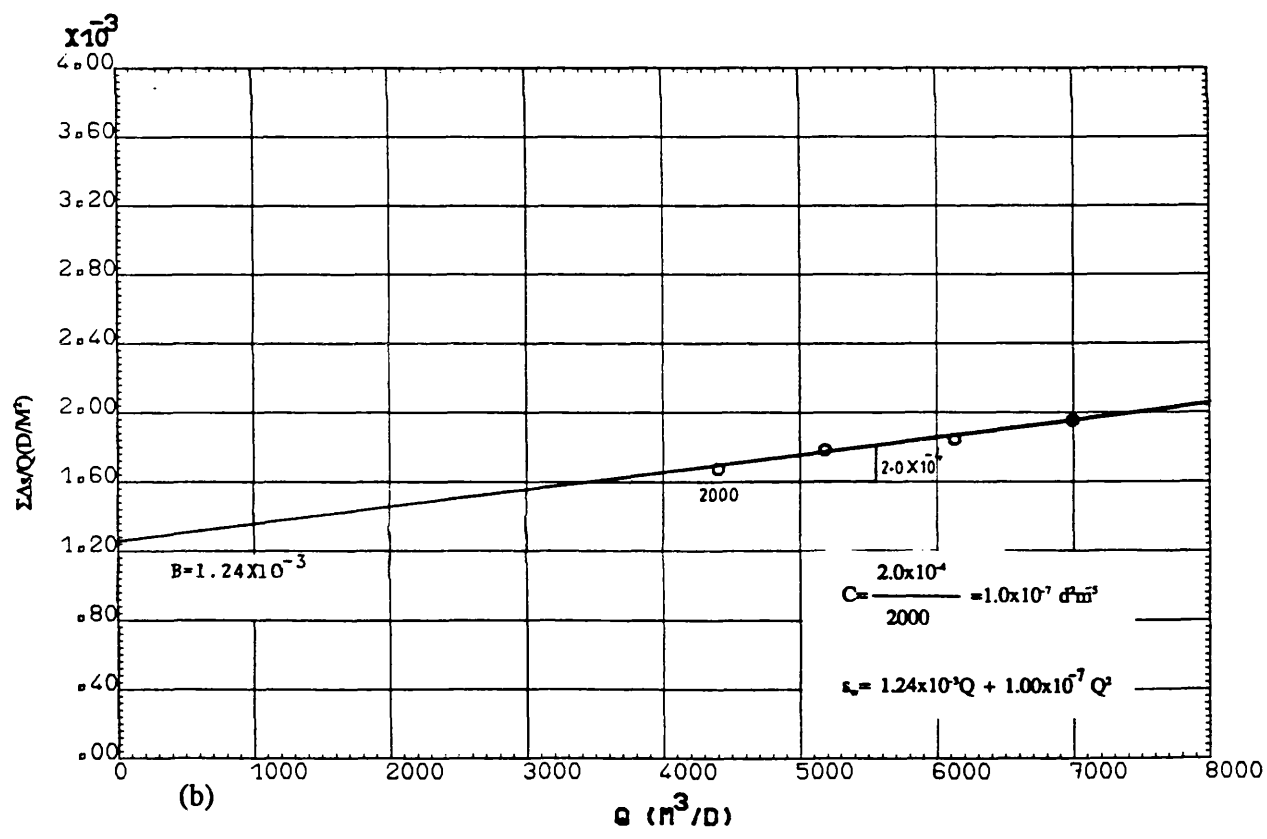
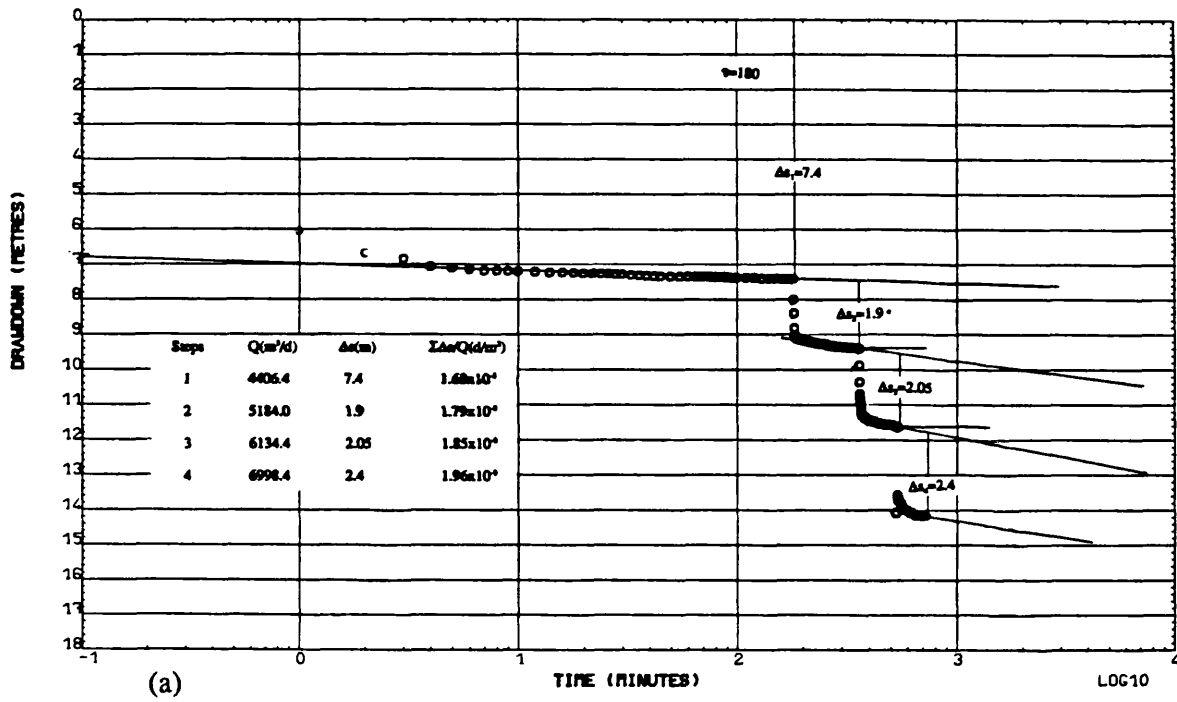


Fig. 6.17 PW SOW, Step-Drawdown test: Bruin & Hudson method, (a) data handling, (b) data plot.

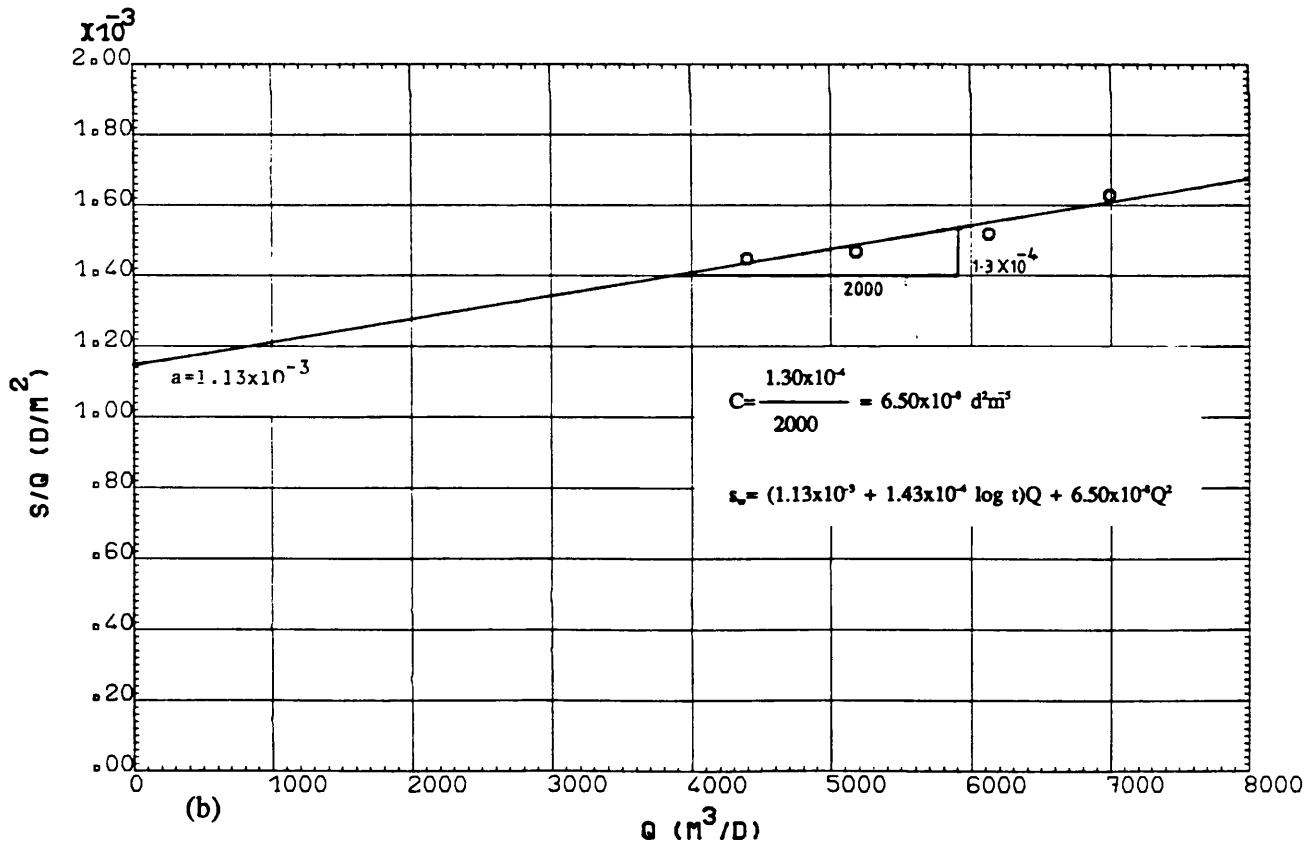
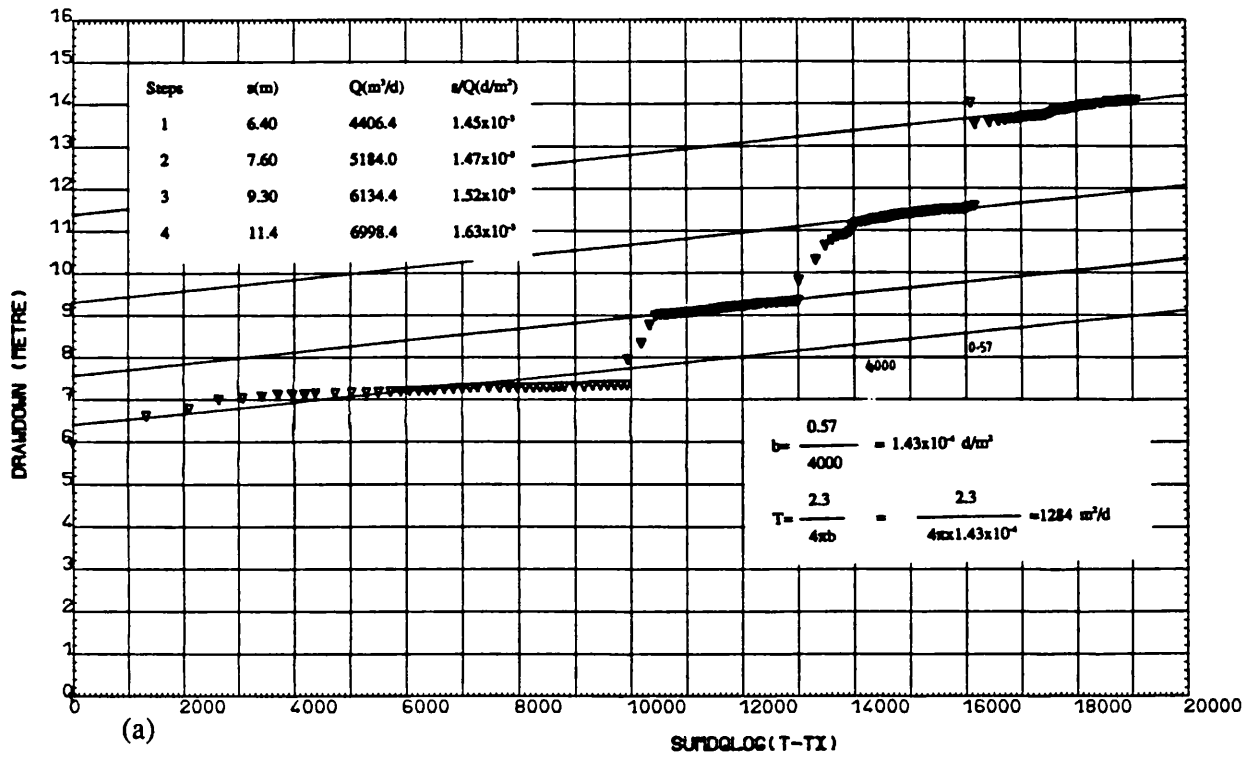


Fig. 6.18 PW SOW, Step-Drawdown test: Eden & Hazel method, (a) data handling, (b) data plot.

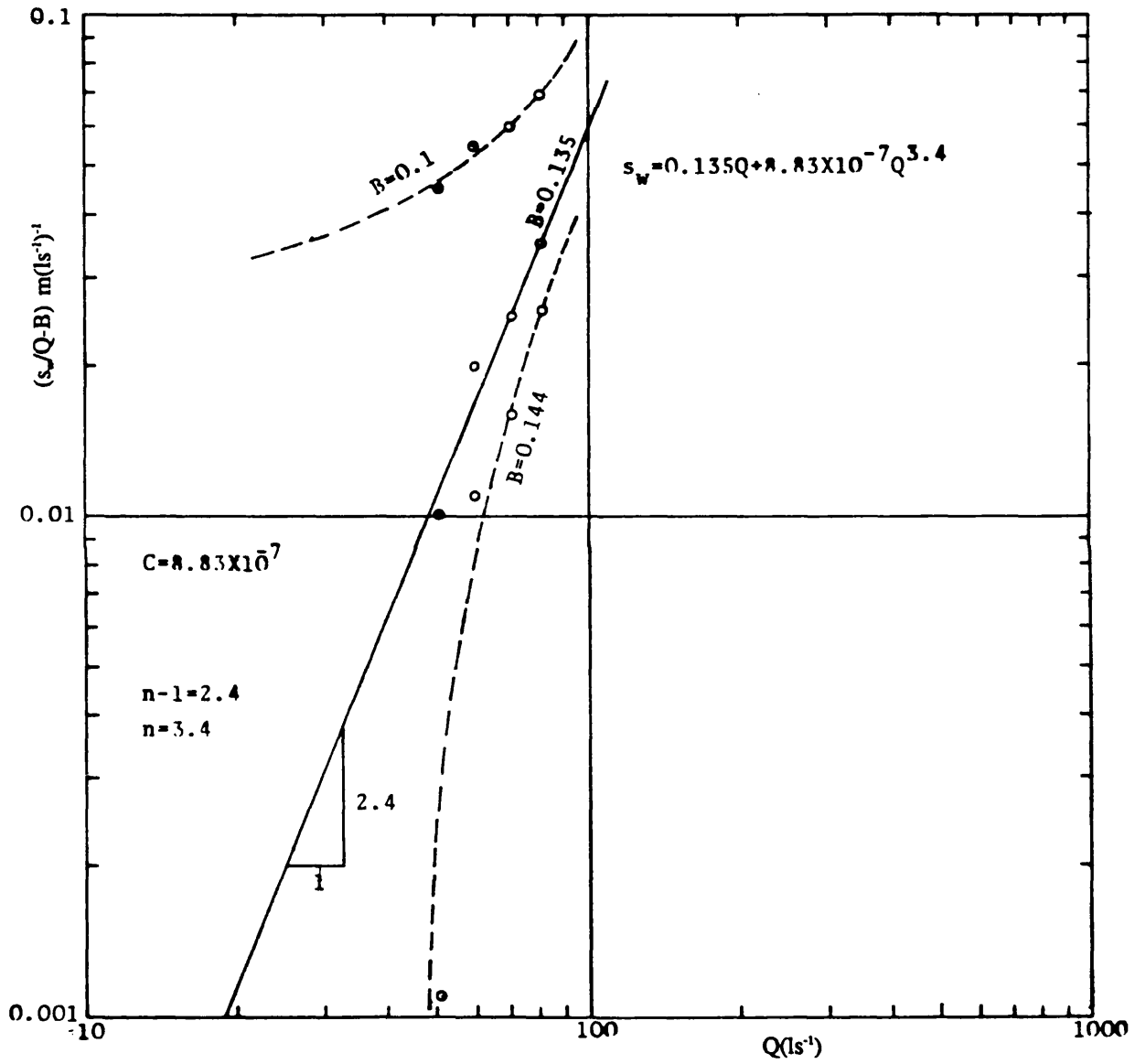


Fig. 6.19 PW SOW, Step-Drawdown test: Rorabaugh method.

was run in three steps.

Wells PTW1 and PTW2 were drilled to a total depth of 133m and screened in the deeper aquifer between 65 and 130 metres depth. The static water levels were 9.3 and 8.8 metres, respectively below the ground surface when the step test started.

The data obtained from these two wells were analysed in similar fashion to the other well fields. The plots of the data and the calculated values of B, C, and n, and the governing drawdown equations for each method are shown in Figures 6.21 to 6.25. The value of n calculated from the Rorabaugh method (see Fig. 6.23) for well PTW1 is very close (2.2) to the value suggested by the Jacob method.

The calculated well efficiency for wells PTW1 and PTW2 at  $Q=7000 \text{ m}^3/\text{d}$  are 86% and 73%, respectively. The theoretical well and aquifer loss components, as well as the total loss, are shown in Figures A5.14 and A5.15 of Appendix 6 as theoretical drawdown yield curves. The values of transmissivity calculated from the Eden and Hazel method are 842 and 458  $\text{m}^2/\text{d}$ , respectively. The accuracy of the results, with respect to the number of steps and best fit of data points to the straight line drawn through them, is satisfactory.

The total drilled depth and screen length in wells PTW3, PTW4, and PTW5 were 150 and 90 metres, respectively, and the static water level ranged from 11 to 14 metres below the ground surface. The data resulting from the step drawdown tests carried out in these wells in March 1978 were analysed by all the above-mentioned methods. The plots of the data and the calculated values of B and C, and the governing drawdown-discharge equations were shown in Appendix 6 (see Figs. A6.16 to A6.22).

The values of C calculated by the Jacob arithmetic method are presented in Table 6.1. Well PTW3 was tested in three steps and the first point of the specific drawdown discharge data does not fit to the straight line. Thus, the accuracy of the resultant values is not satisfactory, whereas the other two wells have been tested in four steps with more or less a good fit. The values of well efficiency at  $Q=5000 \text{ m}^3/\text{d}$  were calculated for wells PTW3, PTW4, and PTW5 in which the results were 96%, 85% and 69%, respectively, and the theoretical drawdown-yield curves derived from the governing drawdown equation are shown in Figure A6.20 of Appendix 6.

The values of transmissivity and well characteristics calculated by the Eden and

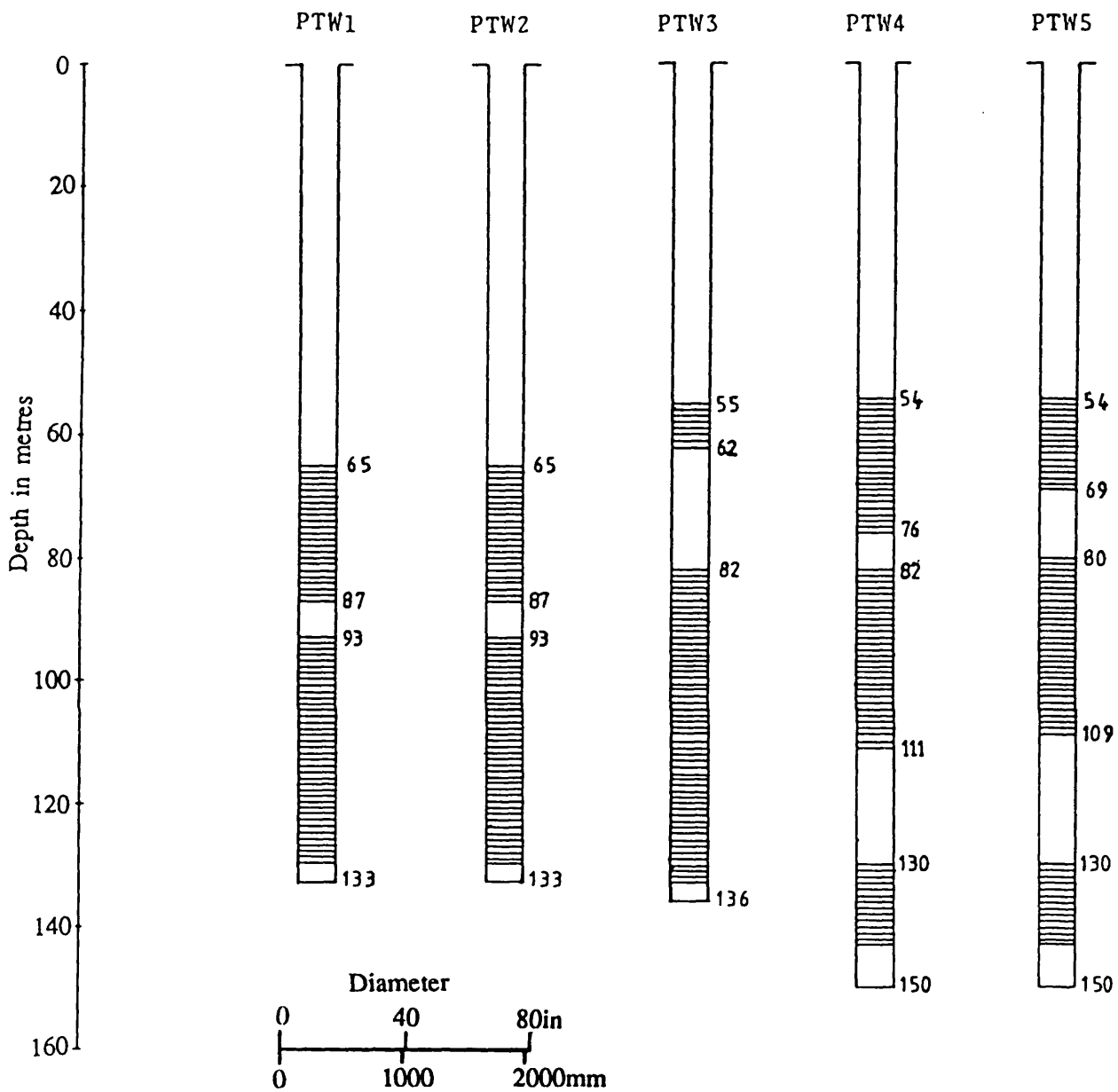


Fig. 6.20 Technical cross sections of the Park, Tabriz wells.

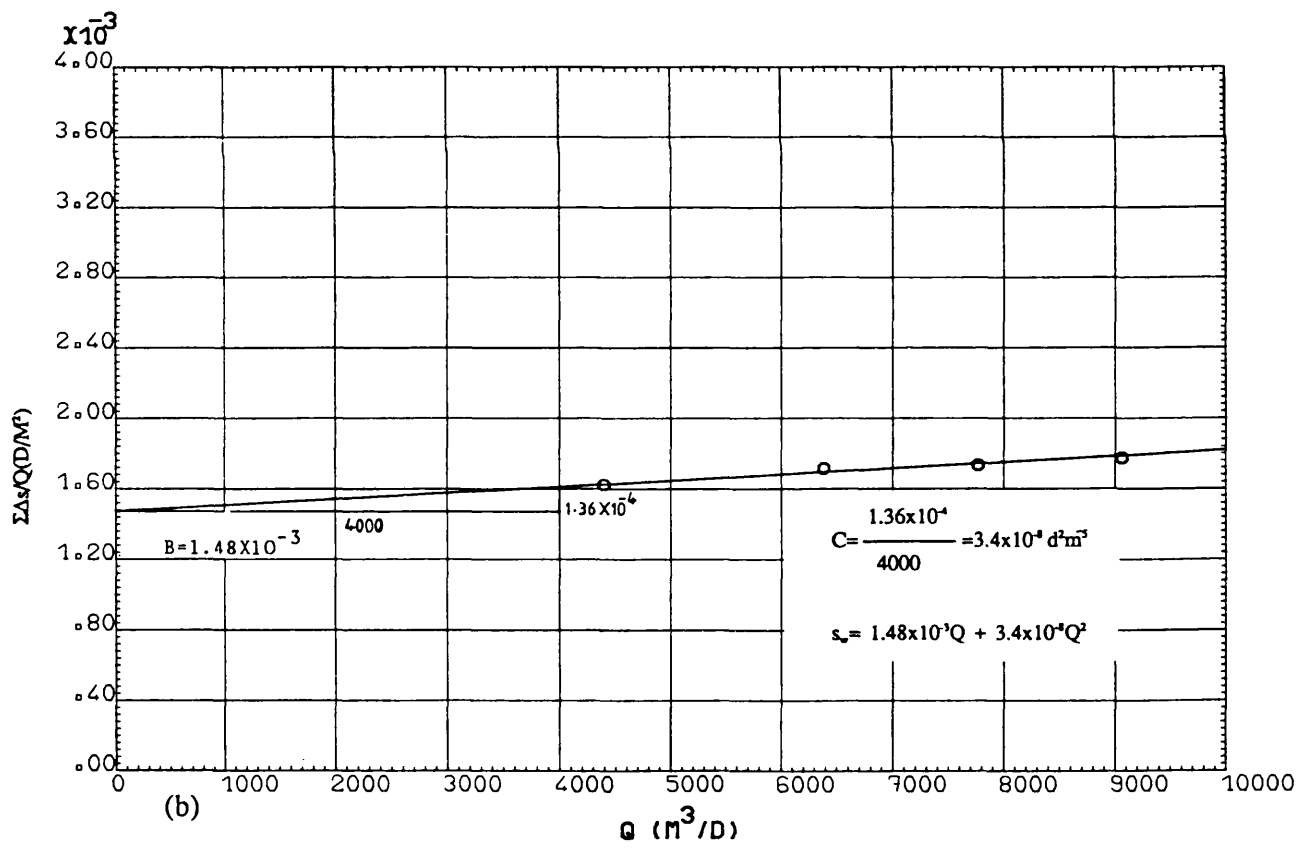
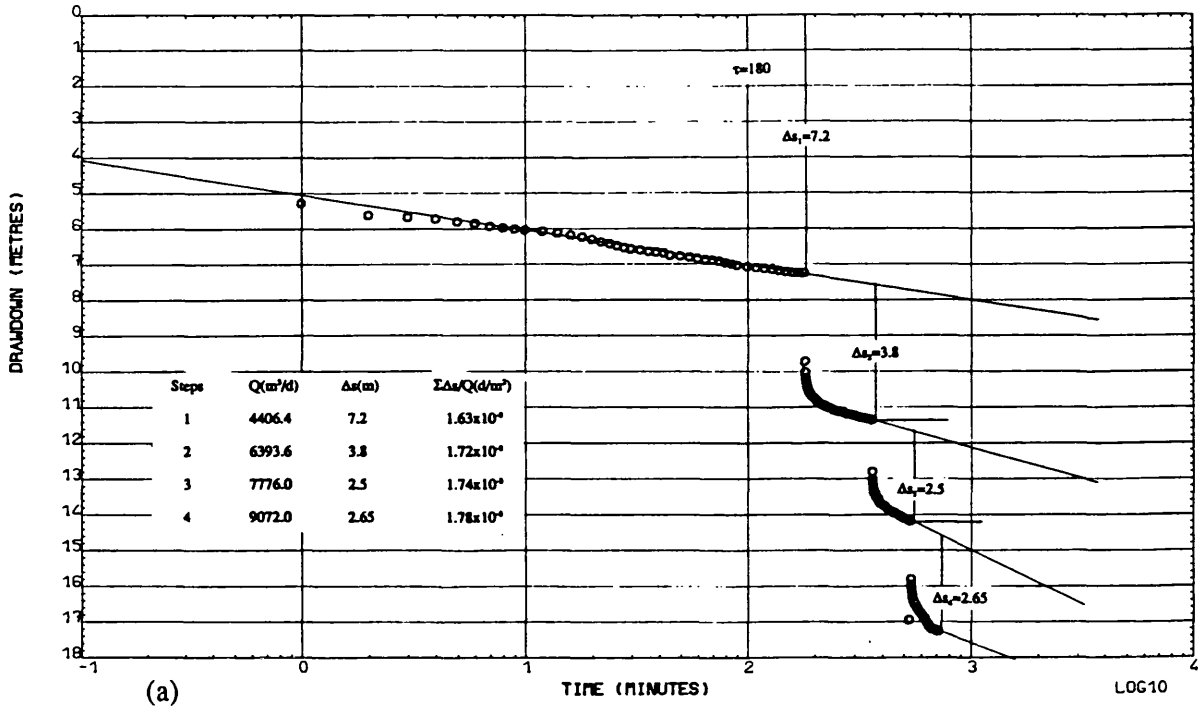


Fig. 6.21 PW PTW1, Step-Drawdown test: Bruin & Hudson method, (a) data handling, (b) data plot.



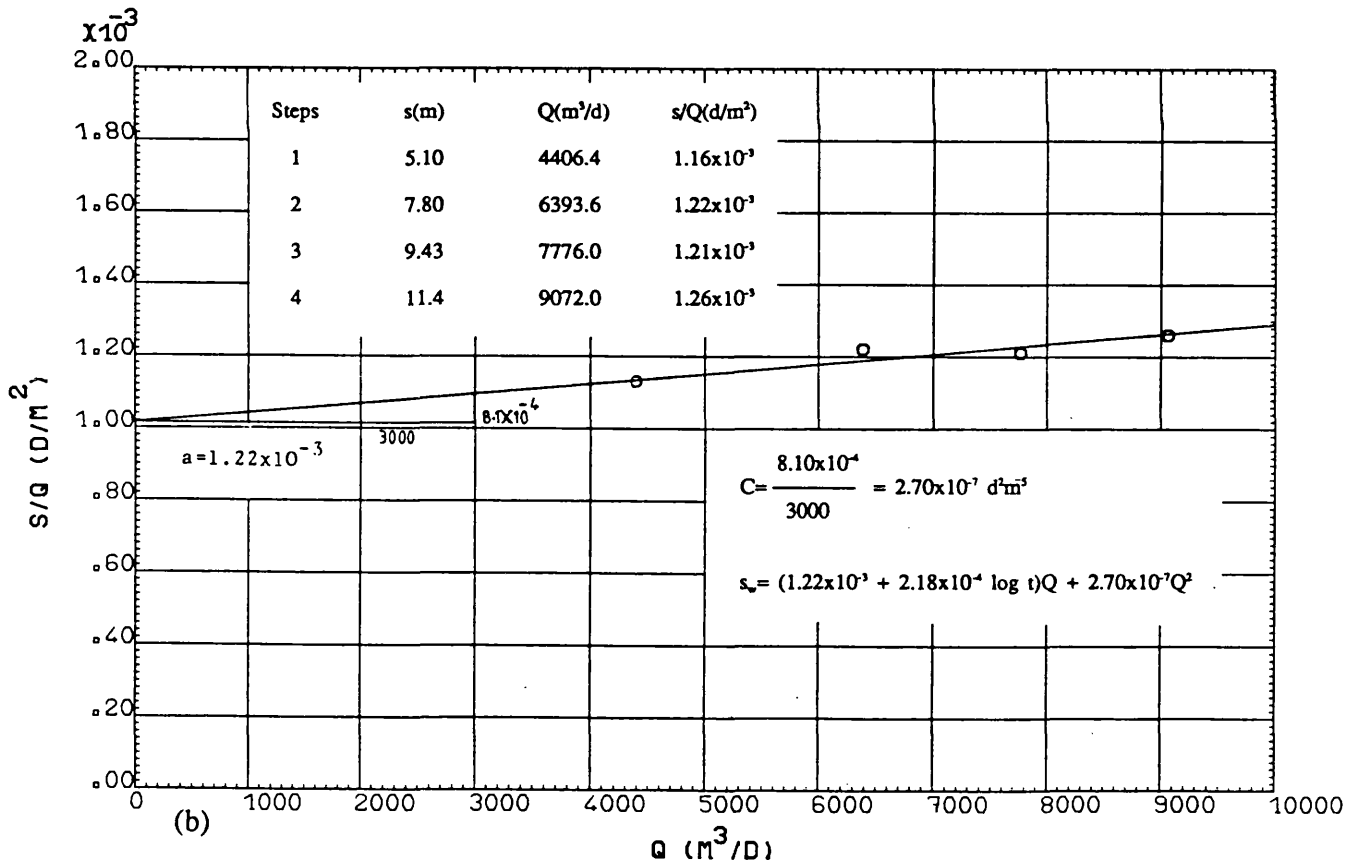
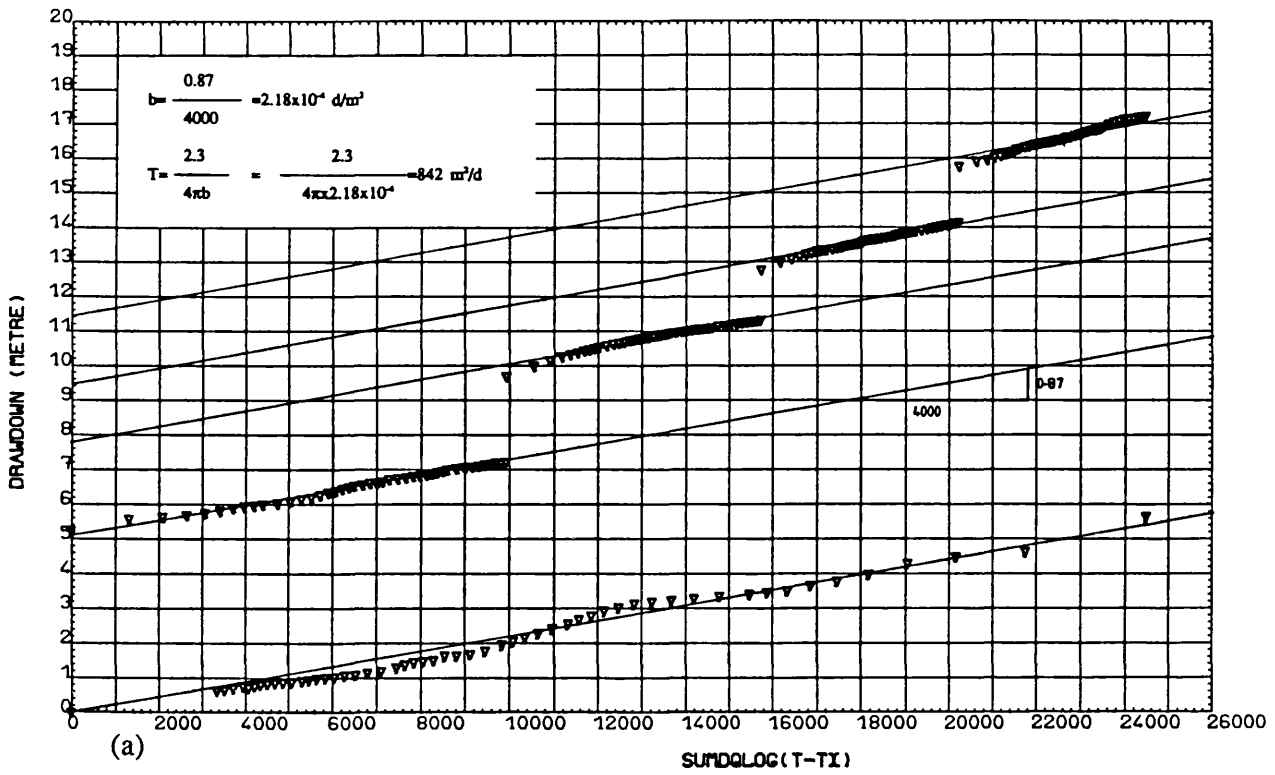


Fig. 6.22 PW PTW1, Step-Drawdown test: Eden & Hazel method, (a) data handling, (b) data plot.

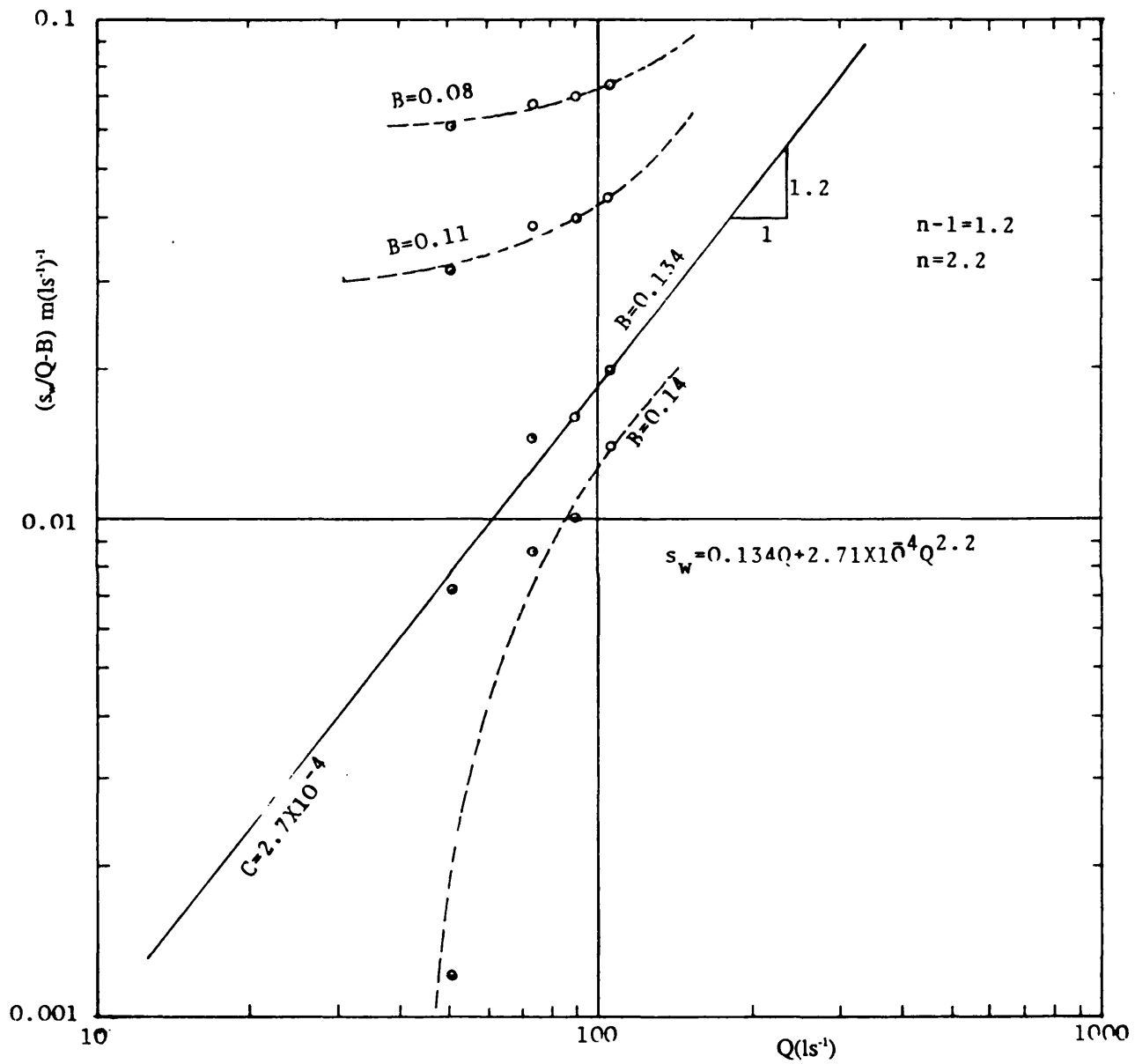


Fig. 6.23 PW PTW1, Step-Drawdown test: Rorabaugh method.

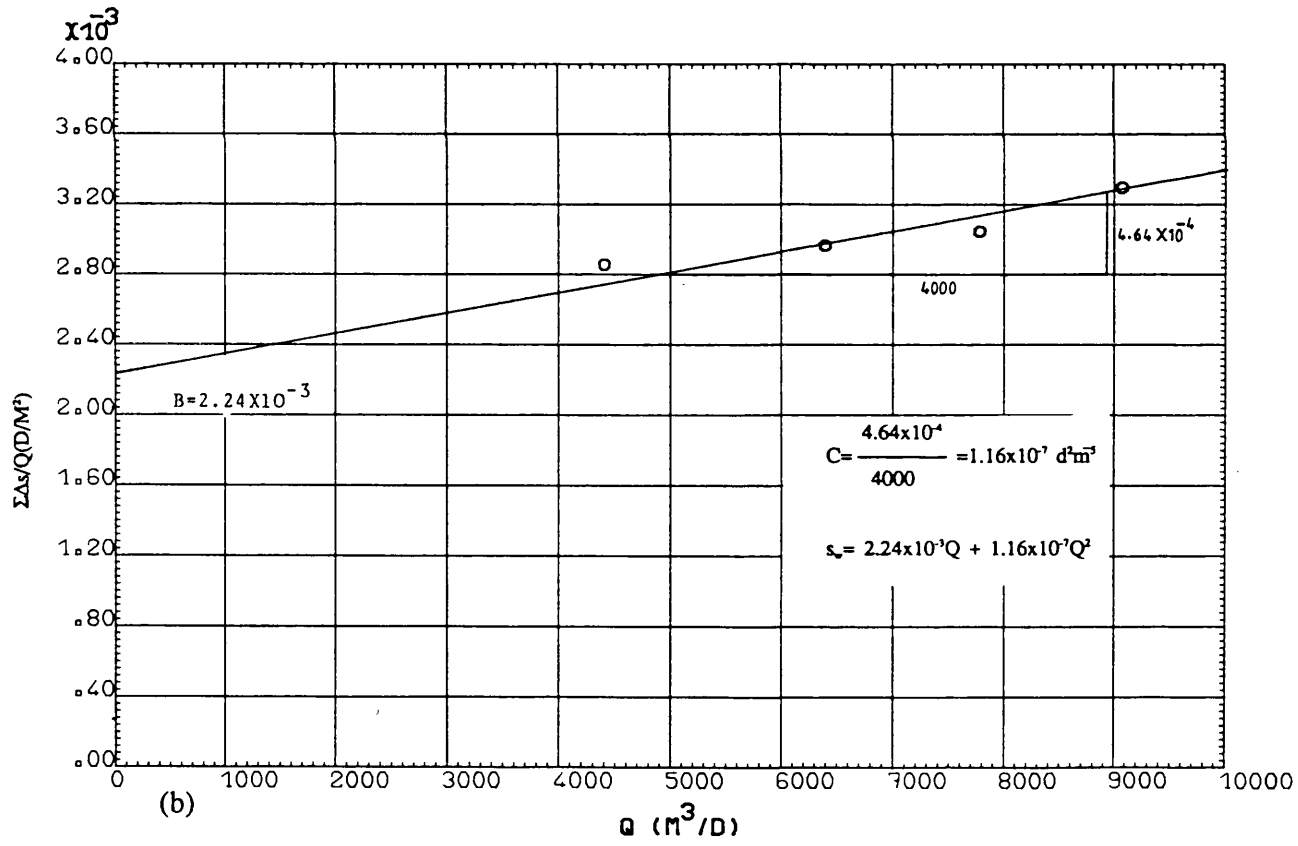
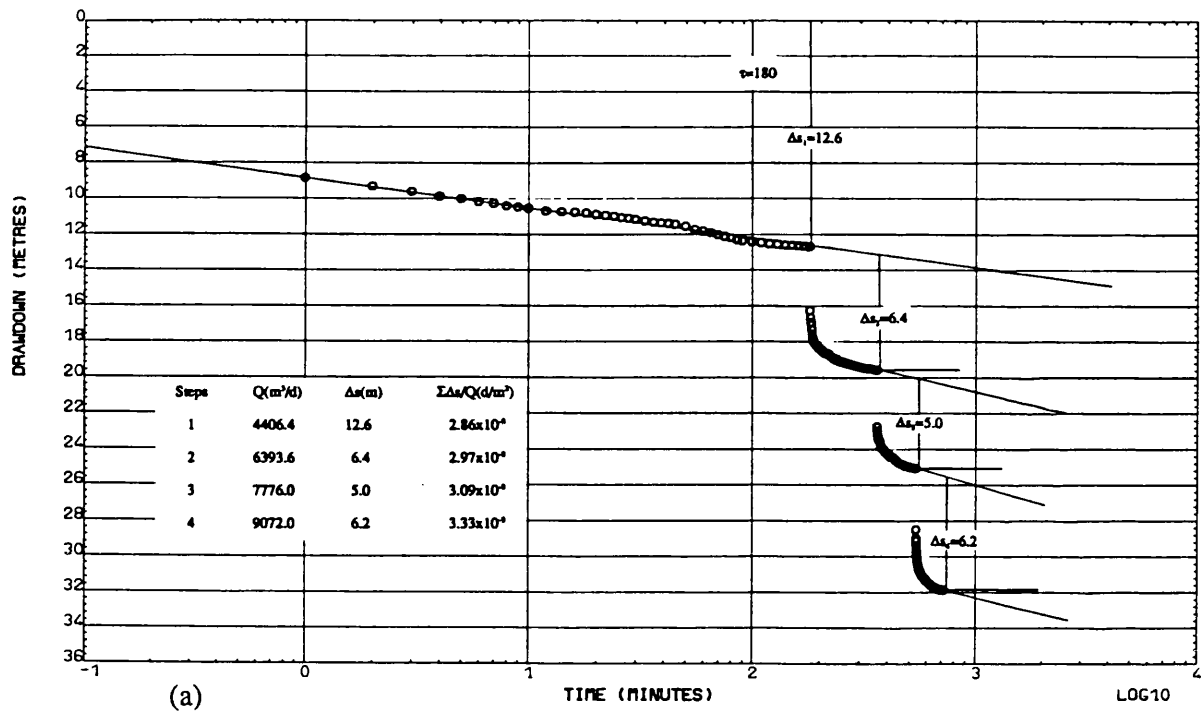


Fig. 6.24 PW PTW2, Step-Drawdown test: Bruin & Hudson method, (a) data handling, (b) data plot.

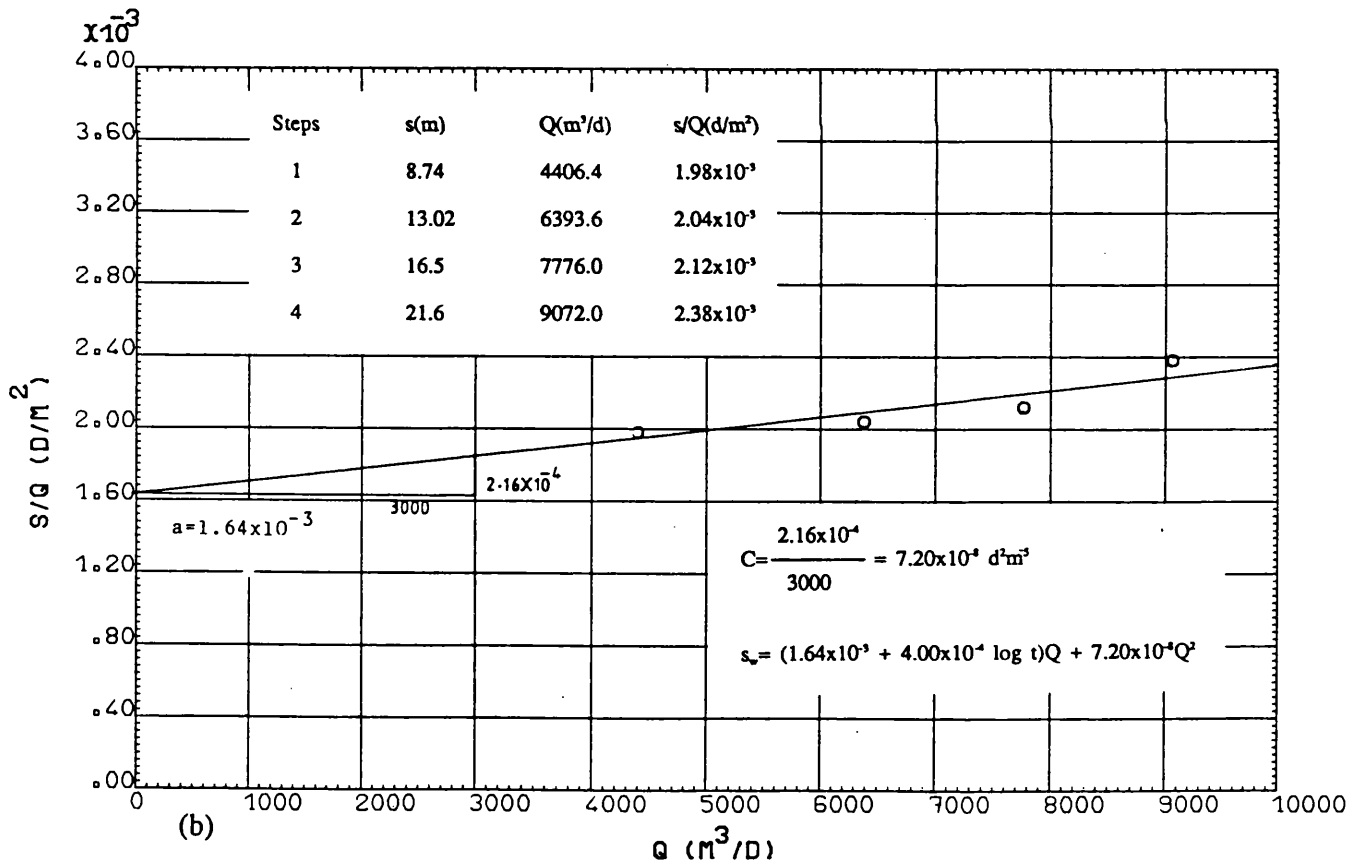
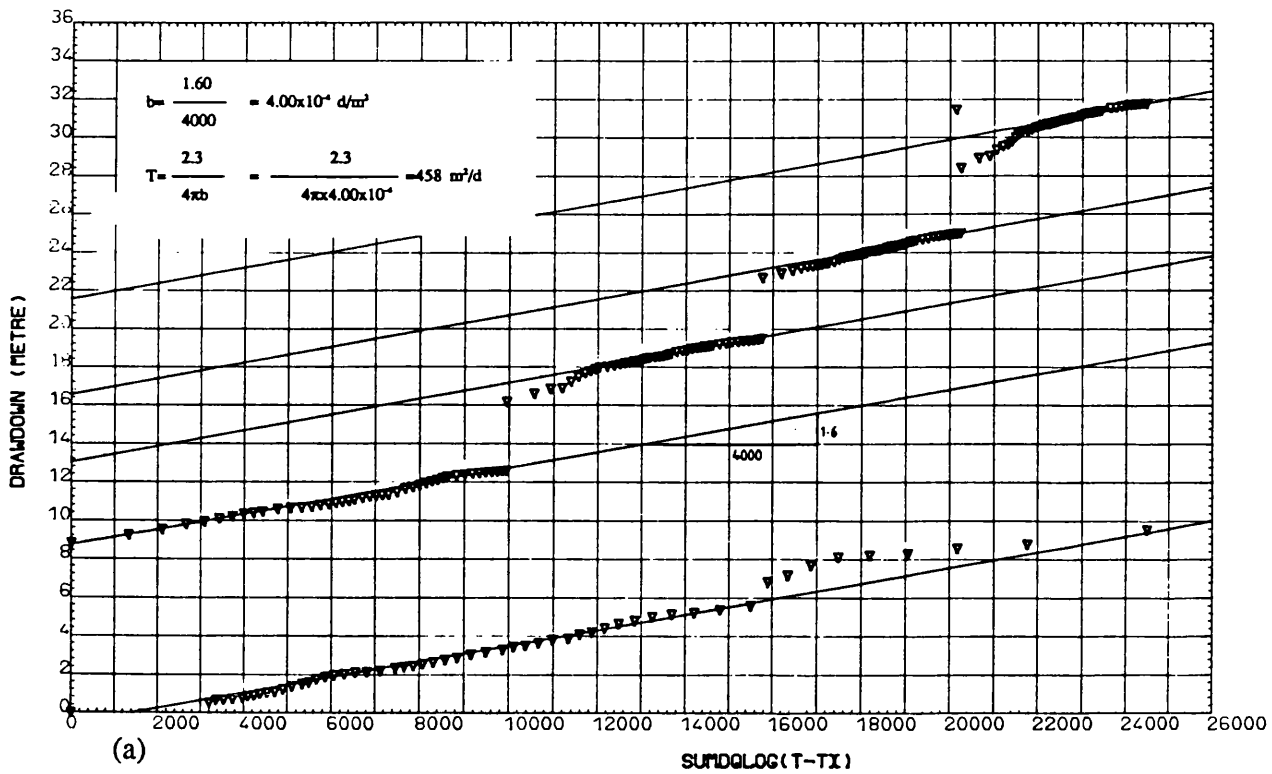


Fig. 6.25 PW PTW2, Step-Drawdown test: Eden & Hazel method, (a) data handling, (b) data plot.

Hazel, and Bruin and Hudson methods are shown in the related figures as well as in Table 6.2.

### **Comparison of Results With the Numerical Solution**

As stated in previous chapter, the Rushton radial-flow model is able to take into account a range of conditions, as well as well losses, in a single numerical solution. When constant rate test data obtained from pumping well are analysed with a numerical model, the value of transmissivity reduces by a multiplication factor due to the well loss effect at some distance from the well face. Actually, in this method, the calculated value of well loss factor is not a real value of well loss.

However, it would appear as if the well loss component can be determined if the same calculated parameters which have been run for a best fit with a particular value of well loss, are re-run without the well loss factor (well loss factor=1) as in Figure 6.26. There the difference between the best-fit drawdown curve and the zero well loss replotted curve will be the value of the well loss. Dividing this well loss value by the square of the discharge will give the value of C. The accuracy of the result depends on the accuracy of the parameters used in the model data file such as aquifer properties and well radius.

This method can be used in conjunction with a step drawdown test to obtain the maximum information on well and aquifer conditions as well as supplementary information for their analysis.

The well loss values deduced from the Rushton numerical model for some pumping wells in the project area were compared with the well loss values deduced from the step drawdown tests in Table 6.3. In brief it may be seen that there is close agreement between the results determined by the model and multi-step drawdown test methods.

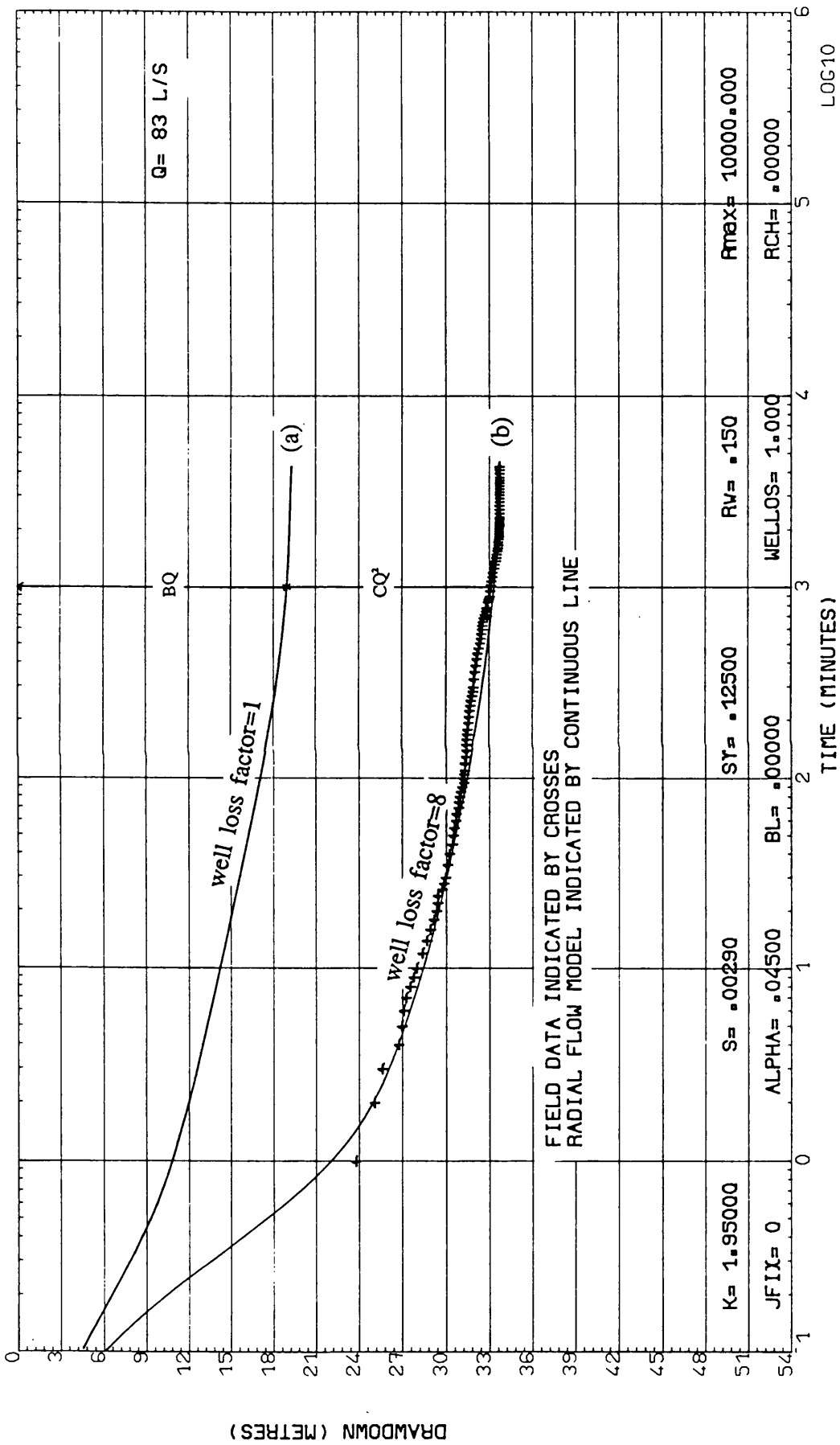


Fig. 6.26 PW SW1, Model analysis: (a) without well loss, (b) with well loss.

**Table 6.1** Well loss factor values (C) calculated by Jacob arithmetic method.

Well No.	C <sub>1,2</sub> (d <sup>2</sup> m <sup>-5</sup> )	C <sub>2,3</sub> (d <sup>2</sup> m <sup>-5</sup> )	C <sub>3,4</sub> (d <sup>2</sup> m <sup>-5</sup> )	Ave. C (d <sup>2</sup> m <sup>-5</sup> )
SW1	6.77x10 <sup>-8</sup>	1.79x10 <sup>-7</sup>	-	1.23x10 <sup>-7</sup>
SW8	4.51x10 <sup>-7</sup>	-2.72x10 <sup>-7</sup>	-1.07x10 <sup>-6</sup>	-2.98x10 <sup>-7</sup>
SOW	1.47x10 <sup>-7</sup>	-1.62x10 <sup>-7</sup>	3.42x10 <sup>-7</sup>	1.09x10 <sup>-7</sup>
TAW	-2.28x10 <sup>-9</sup>	5.98x10 <sup>-8</sup>	1.32x10 <sup>-8</sup>	2.36x10 <sup>-8</sup>
JW1	1.84x10 <sup>-7</sup>	-1.88x10 <sup>-7</sup>	3.47x10 <sup>-7</sup>	1.14x10 <sup>-7</sup>
JW2	3.15x10 <sup>-7</sup>	6.85x10 <sup>-7</sup>	-7.52x10 <sup>-7</sup>	8.27x10 <sup>-8</sup>
TPSW1	2.37x10 <sup>-7</sup>	-2.12x10 <sup>-7</sup>	-	1.26x10 <sup>-8</sup>
TPSW3	3.18x10 <sup>-7</sup>	8.25x10 <sup>-7</sup>	-	5.71x10 <sup>-7</sup>
TPSW4	2.67x10 <sup>-9</sup>	1.55x10 <sup>-8</sup>	-	9.10x10 <sup>-9</sup>
TPSW6	1.25x10 <sup>-7</sup>	1.65x10 <sup>-7</sup>	-	1.45x10 <sup>-7</sup>
TPSW8	-1.77x10 <sup>-9</sup>	4.86x10 <sup>-8</sup>	-	4.68x10 <sup>-8</sup>
PTW1	4.38x10 <sup>-8</sup>	-3.75x10 <sup>-8</sup>	8.59x10 <sup>-8</sup>	3.07x10 <sup>-8</sup>
PTW2	5.63x10 <sup>-8</sup>	1.88x10 <sup>-7</sup>	4.33x10 <sup>-7</sup>	2.26x10 <sup>-7</sup>
PTW3	-8.80x10 <sup>-8</sup>	9.84x10 <sup>-8</sup>	-	5.19x10 <sup>-9</sup>
PTW4	4.22x10 <sup>-8</sup>	5.94x10 <sup>-9</sup>	7.39x10 <sup>-7</sup>	2.62x10 <sup>-7</sup>
PTW5	2.35x10 <sup>-8</sup>	2.17x10 <sup>-7</sup>	1.46x10 <sup>-7</sup>	1.29x10 <sup>-7</sup>

**Table 6.2** The estimated values of transmissivity and well characteristics (a) Bruin and Hudson, and Eden and Hazel methods, and (b) Rorabaugh method.

(a)

Well No.	Bruin and Hudson method		Eden and Hazel method			
	B(d/m <sup>2</sup> ) x10 <sup>-3</sup>	C(d <sup>2</sup> m <sup>-5</sup> ) x10 <sup>-8</sup>	T(m <sup>2</sup> /d)	b(d/m <sup>2</sup> ) x10 <sup>-4</sup>	a(d/m <sup>2</sup> ) x10 <sup>-3</sup>	C(d <sup>2</sup> m <sup>-5</sup> ) x10 <sup>-8</sup>
SW1	4.66	7.85	523	3.50	2.80	25.5
SW8	2.36	32.0	456	4.00	2.08	19.4
JW1	1.68	7.5	626	2.93	0.97	8.5
JW2	3.64	37.0	416	4.40	2.90	29.4
TPSW1	1.36	8.0	1126	1.63	1.30	3.5
TPSW3	0.53	36.5	915	2.00	0.76	30.4
TPSW4	0.77	0.55	2153	0.85	0.57	0.64
TPSW6	1.31	15.2	1164	1.57	1.57	5.60
TPSW8	0.68	1.1	2219	0.53	0.51	0.85
TAW	0.41	1.8	354	0.52	0.36	0.90
SOW	1.24	10.0	1284	1.43	1.13	6.50
PTW1	1.48	3.4	842	2.18	1.22	27.0
PTW2	2.24	11.6	458	4.00	1.64	7.2
PTW3	2.08	2.5	475	3.85	1.14	3.70
PTW4	1.35	4.6	608	3.00	-	-
PTW5	0.66	6.0	861	2.13	0.41	2.43

(b)

well No.	B(ms/l)	C m(s/l) <sup>a</sup> x10 <sup>-6</sup>	n
SW1	0.427	0.0036	4.6
JW2	0.38	56.0	2.8
TPSW6	0.164	78.0	2.5
TAW	0.035	1360.0	2
SOW	0.135	0.880	3.4
PTW1	0.134	270.0	2.2



**Table 6.3** Comparison of well loss values (CQ<sup>2</sup>) calculated by radial flow model and step-test methods

Well No.	Q m <sup>3</sup> /d	<u>Calculated CQ<sup>2</sup> values from model and step test</u>				
		model (m)	Jacob (m)	B & H (m)	E & H (m)	R (m)
SW1	7171.2	14.1	6.33	4.04	13.11	2.42
SW8	7084.8	9.8	8.98	16.06	9.74	-
JW1	5702.4	*	3.71	2.44	2.76	-
JW2	5443.2	17.4	2.45	10.96	8.71	6.11
TPSW1	8415.3	*	0.89	5.67	2.48	-
TPSW3	8415.3	20.1	40.44 <sup>?</sup>	25.85	21.53	-
TPSW4	8380.8	*	0.64	0.39	0.45	-
TPSW6	8415.3	10.4	10.27	10.76	3.97	7.30
TPSW8	9504	*	4.22	0.99	0.77	-
TAW	8640	0.9	1.76	1.34	0.67	-
SOW	6393.6	2.85	4.45	4.09	2.66	2.0

\* well loss factor is one

- data was not analysed

<sup>?</sup> well loss is more than total drawdown

## **CHAPTER 7**

### **HYDROCHEMISTRY**

#### **7.1 Introduction**

#### **7.2 Sample Collection and Analysis**

#### **7.3 Evaluation and Accuracy Check of Data**

#### **7.4 Presentation and Interpretation of Data**

##### **7.4.1 Numerical Classification**

##### **7.4.2 Graphical Representation and Interpretation**

#### **7.5 TDS and Their Relation to Electrical Conductivity**

#### **7.6 Ground Water Contamination in the Tabriz Area**

#### **7.7 Factors and Processes Controlling Ground Water Compositions**

##### **7.7.1 Major constituents**

#### **7.8 Ground Water Quality Evaluation**

##### **7.8.1 Suitability of Ground Water for Drinking Purposes**

##### **7.8.2 Suitability of Ground Water for Agriculture**

## **CHAPTER 7**

### **HYDROCHEMISTRY**

#### **7.1 Introduction**

The chemical and biological characteristics of ground water determine its usefulness for industry, agriculture and the home. The study of ground water chemistry provides important clues on the geological history of the water bearing layers, gives some indication of ground water recharge, and the velocity and direction of flow patterns and storage. Chemical processes in the subsurface can influence the strength of geological materials and in situations where they are not recognized can cause failure of artificial slopes, dams, mining excavations and other features of importance to man.

The water quality considered in this study involves the type and amount of dissolved solids in ground water as well as the factors controlling its chemical composition such as aquifer materials, recharge water characteristics, and climatic and hydrological conditions. Also considered, are the major changes in water chemistry that commonly occur as ground water moves along its flow paths.

The hydrochemical parameters requiring determination in any study depend on the study objectives. The general chemical analysis of ground water should include well-head measurements for the purposes of convenient rapid assessment and to provide control for laboratory measurements and determinations of the concentrations of the major inorganic substances dissolved in the water. The major ions provide the opportunity for initial interpretation. Where no distinguishing major ions are present, as for example in some brackish and saline ground waters, minor ions can be sampled for analysis and interpretation.

#### **7.2 Sample Collection and Analysis**

Sampling is an important part of the study of ground water composition and could be the major source of error in the whole process of obtaining water quality information. The extent of a small sample as a reliable representative of a large volume of water depends on the homogeneity of the water being sampled, the manner

of collection and the number of the samples.

The aim of many ground water quality investigations is to evaluate the resource as thoroughly as possible, and its variations in time and space. However, this usually requires numerous samples and field observations from repeated visits.

Ground water sampling is more crucial than that of surface water because the physical factors which promote mixing in surface water are absent, or are less effective in ground water systems, which gives rise to poor mixing in ground water even in uniform permeable strata. In most sediments, the horizontal permeability is greater than the vertical permeability, which allows the chemical characteristics of water in a particular stratum to develop a different type of water from that above or below. Mixing of water from different strata in a well, and in some instances exposure of the water to the atmosphere, may bring about chemical instability. This chemical instability may cause changes in certain constituents.

Ground water samples have been collected twice a year from about 180 selected points including 100 deep well, 21 shallow wells, and 59 qanats (see Fig 7.1) distributed over the study area, during May and October by the Azarbijan Regional Water Authority (ARWA), using tightly closed bottles of one litre capacity. All the samples collected from the qanats and shallow wells represent ground water within the water table aquifer system. Some of the samples collected from deep wells, especially in the central part of the Tabriz Plain, represent ground water within the multi-layered aquifer system with individual hydrochemical characteristics for each water-bearing layer.

Lloyd and Heathcote (1985) presented a hydrochemical data sheet listing comprehensive parameters for the measurement and analysis during hydrochemical studies. Some field test parameters such as pH, Temp, EH, and dissolved oxygen are properties of the water which are likely to be altered by sampling and storage. Despite the acknowledged importance of field testing of water in hydrochemical studies, no well-head measurements were carried out in the study area.

Analyses of all the collected samples were carried out in the analytical laboratory of the ARWA. They used the standard methods of analysis for the major ions; potassium, nitrate and other minor and trace constituents were not analysed in this laboratory.

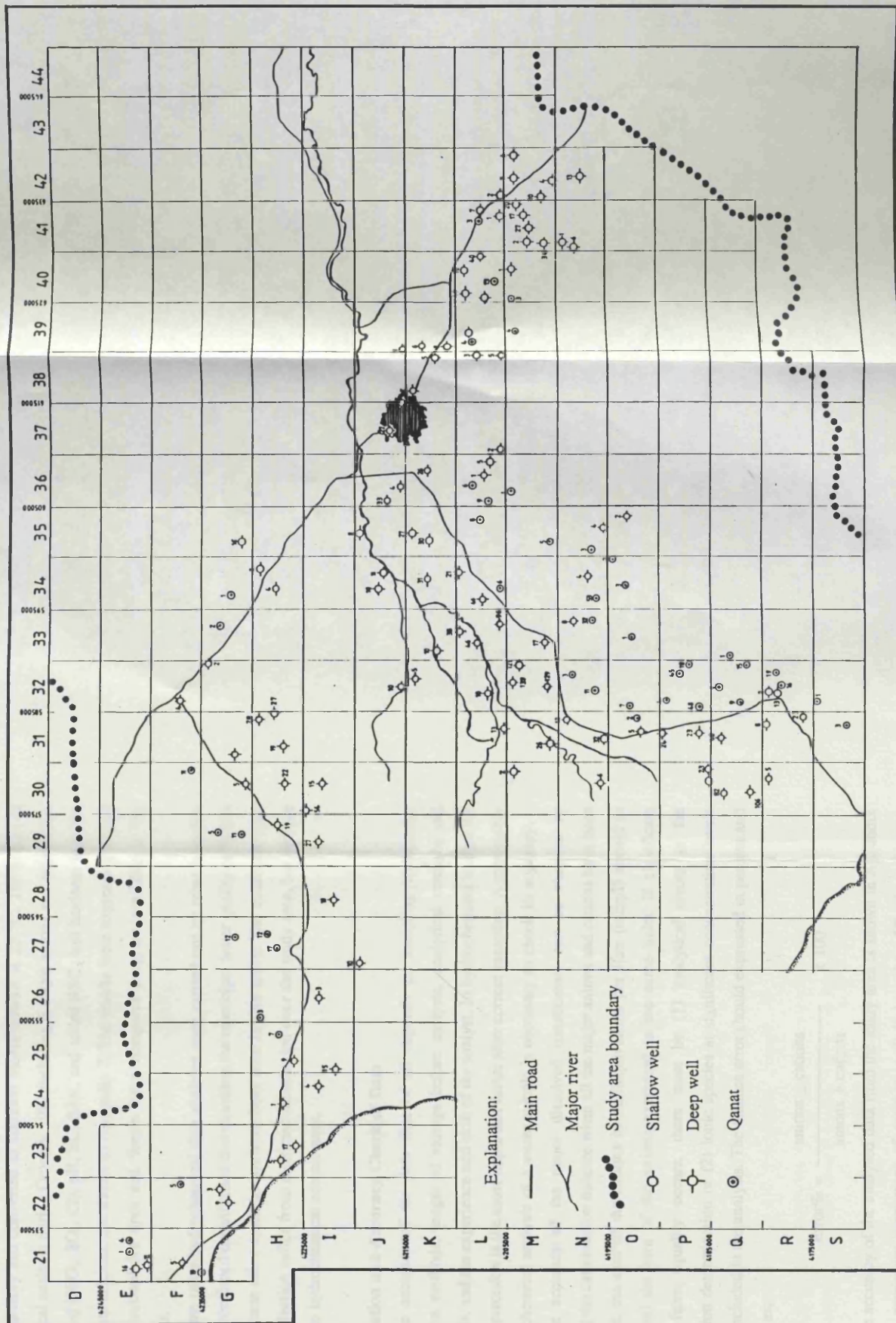


Fig. 7.1 Map showing location of hydrochemical samples.

The amount of total dissolved solid (TDS) was determined by multiplying the EC value by a conversion factor (0.66). pH and EC measurements were carried out in the laboratory and converted to standard measurements at 25 °C. The results of the chemical analysis during October 1987 including 6 major anions and cations (Ca, Mg, Na and HCO<sub>3</sub>, SO<sub>4</sub>, Cl), pH, EC, SAR, and added  $\overline{RSC}$ , and hardness in terms of carbonate calcium, are shown in Appendix 7. The results were expressed in mg/l and re-calculated for epm and %epm by a computer program available in the department.

Some other hydrochemical data analyses were carried out by other branches of above-mentioned organization that considers the municipal water quality of Tabriz City and some other small towns have been used in this study. The additional data from this Section suffer from restricted distribution over the study area, but include many more hydrochemical constituents.

### 7.3 Evaluation and Accuracy Check of Data

The accuracy of the data first of all depends on sampling techniques, preservation methods, length of storage before analysis, analytical methods and instruments, and the experience and skill of the analyst. In hydrochemical studies the analytical precision is the most important factor after correct sampling. A reasonably complete chemical analysis of a water sample is necessary to check its accuracy.

The accuracy of the major dissolved constituents can be checked by calculating the cation-anion balance when all the major anions and cations have been determined, the sum of the cations in milliequivalents per litre (mEq/l) should in theory equal the sum of the anions expressed in the same units. If significant deviation from equality occurs, there must be (1) analytical errors in the concentration determination or (2) ionic species at significant concentration levels were not included in the analysis. The balance error should be expressed in percent and calculated as;

$$\text{Error\%} = \frac{\text{anions} - \text{cations}}{\text{anions} + \text{cations}} \times 100$$

The accuracy of the analysed data from the study area is shown in Appendix 7, and the maximum percentage of error over-all is less than 5%. According to

Freeze and Cherry (1980) and Hem (1985), an error less than about 5% is acceptable for scientific studies. The consistently low values for error indicate either very good analytical procedures or some manipulation of the data.

#### 7.4 Presentation and Interpretation of Data

Handling and presentation of the chemical data in a convenient manner for visual inspection is an important tool in ground water investigations. A considerable number of techniques and methods are available to classify, compare, and summarise large amounts of data. In particular, the computerized methods are most effective in converting units, storing, retrieving, and manipulating large volumes of data and can minimize mistakes in calculation, as well as plotting these large volumes as tables, graphs and maps.

Zaporoze(1972) reviewed the methods of presentation and interpretation of hydrochemical data and divided the applications into four major sections as: (1) classification, (2) correlation, (3) analytical, and (4) illustrative, with further subsections for each method.

In this study, the routinely measured and recorded hydrochemical data for October 1987, and in some cases for previous years, were represented and interpreted by numerical classification and graphical methods.

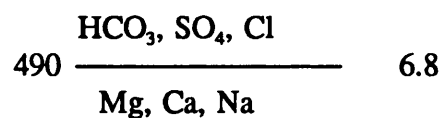
##### 7.4.1 Numerical Classification

Classification methods are useful for initial characterization of the chemical composition of ground water. Such methods differentiate chemical types of water and help identify dominant types. Two methods of classification were used to classify the water types in the study area.

(a) Kurlov formulae (1928): In this method the constituents which comprise more than 25 percent of the total mEq/l are expressed by a quasi-fraction with anions and cations in the numerator and denominator, respectively. Analyses are shown in descending order of concentration, and the sums of anions and cations are each taken as 100 percent of mEq/l. The sample number 1 from the Appendix 7 can be written:

$$\text{TDS} \frac{\text{anions}}{\text{cations}} \quad \text{pH}$$

e.g.



The Kurlov formulae for all the samples studied are given in Appendix 7. The total dissolved solids (expressed in mg/l) precede the fraction and the pH values follows the fraction. The basic water type can be rapidly recognized from the diminishing arrangement of ions in the formulae.

(b) **Vostroknutov classification**: This method is similar to the above-mentioned numerical classification method, in as much as it considers only those constituents which exceed 25 percent of the total mEq/l. In this method small volumes of data can be plotted as points in appropriate boxes of a tabulation shown in Table 7.1a. The tabulation is particularly useful for statistical purposes when large volumes of data are to be compared.

The data for the Tabriz area were analysed by this method as displayed in Tables 7.1a, 7.2a and 7.3a. The Tabriz area was divided into three hydrochemical zones namely (1) Alluvial Tuff aquifer, (2) northern part of the Tabriz Plain (Soufian-Shabestar- Tassoij zone) and, (3) southern and central part of the Tabriz Plain. The tabulation represents the number of occurrences reflecting the frequency of water types for the above-mentioned hydrochemical zones.

Tables 7.1b, 7.2b and 7.3b provide a summary of four major bicarbonate, sulphate, chloride and mixed water type groups. These groups of waters may be dominated by Ca, Mg, Na or mixed cations, when the concentration of each cation exceeds 25 percent. According to this classification, the bicarbonate water group dominates the Alluvial Tuff aquifer and the northern part of the Tabriz Plain. For the Alluvial Tuff aquifer, of the 63 water samples, 44 (70%) are rich in bicarbonate, 13 (20%) are mixed and 6 (10%) rich in sulphate. There is no chloride type water in this aquifer. In the northern part of the Plain from 45 water analyses, 30 (67%) are rich in bicarbonate, 8 (18%) in chloride, 6 (13%) are mixed and only 1 (2%) is rich in sulphate. The Alluvial Tuff aquifer is rich in Ca+Na and very poor in Mg, whereas the northern part of plain is rich in Ca+Mg which reflects the difference in the water bearing-layers in the area. The southern and central part of the Plain represents a saline type of water in most cases. From 70 water analyses, 28 (40%) are rich in



		HCO <sub>3</sub>				SO <sub>4</sub>				Cl			
		HCO <sub>3</sub>	SO <sub>4</sub>	Cl		SO <sub>4</sub>	HCO <sub>3</sub>	Cl		CL	SO <sub>4</sub>	HCO <sub>3</sub>	
				Cl	SO <sub>4</sub>			Cl	HCO <sub>3</sub>			HCO <sub>3</sub>	SO <sub>4</sub>
Ca	Ca												
	Na	4		1		2				2	3		
	Mg	2	2		1							1	
Mg	Na	1					1						
	Mg						3				1		
Mg	Mg												
	Ca		3			1							
	Na					1							
Na	Ca		1										
	Na	1											
	Mg												
Na	Na						1			12	1		1
	Mg		1					1		3			
	Ca	2							1		1		
Ca	Mg		1		1					1			
	Ca		1			1	1	1	2	2	1	2	1

(a)

Dominant 25 %	HCO <sub>3</sub>		SO <sub>4</sub>		Cl		Mixed		Total	
	No. of Samples	%	No. of Samples	%	No. of Samples	%	No. of Samples	%	No. of Samples	%
Ca	15	(33.3)	-		1	(2.2)	1	(2.2)	17	(37.8)
Mg	5	(11.1)	-		-		-		5	(11.1)
Na	1	(2.2)	1	(2.2)	4	(8.9)	1	(2.2)	7	(15.5)
Mixed	9	(20.0)	-		3	(6.7)	4	(8.9)	16	(35.6)
Total	30	(66.6)	1	(2.2)	8	(17.8)	6	(13.3)	45	(100.0)

(b)

Table 7.2 a) Tabular graph of the northern part of Tabriz Plain ground water type frequency, b) combinations of cations and anions in ground water of the northern part of Tabriz Plain aquifers (expressed as numbers & percentages of the total).

		HCO <sub>3</sub>				SO <sub>4</sub>				Cl			
		HCO <sub>3</sub>		SO <sub>4</sub>		Cl		SO <sub>4</sub>		HCO <sub>3</sub>		Cl	
		HCO <sub>3</sub>	SO <sub>4</sub>	Cl	SO <sub>4</sub>	HCO <sub>3</sub>	Cl	HCO <sub>3</sub>	Cl	Cl	SO <sub>4</sub>	HCO <sub>3</sub>	SO <sub>4</sub>
Ca	Ca	2	1										
	Na	11	5	3		4		1	2	2		4	
	Mg	1	5					1					
	Na	1	2			1							
	Mg	4	1	1				1					
Mg	Mg												
	Ca												
	Na												
	Ca												
Na	Na												
	Mg							1					
	Ca												
	Mg												
Ca	Mg												
	Ca	3	3					2	1				

(a)

Dominant 25 %	HCO <sub>3</sub> No. of % Samples		SO <sub>4</sub> No. of % Samples		Cl No. of % Samples		Mixed No. of % Samples		Total No. of % Samples	
Ca	28	(4.7)	3	(4.7)	-	-	11	(17.2)	42	(66.7)
Mg	-	-	-	-	-	-	-	-	-	-
Na	6	(9.5)	2	(3.2)	-	-	1	(1.6)	9	(14.3)
Mixed	10	(15.9)	1	(1.6)	-	-	1	(1.5)	12	(19.0)
Total	44	(69.8)	6	(9.5)	-	-	13	(20.6)	63	(100.0)

(b)

Table 7.1 a) Tabular graph of Alluvial Tuff aquifer ground water type frequency, b) combinations of cations and anions in ground water of Alluvial Tuff aquifer (expressed as numbers & percentages of the total).

		HCO <sub>3</sub>				SO <sub>4</sub>				Cl			
		HCO <sub>3</sub>	SO <sub>4</sub>	Cl		SO <sub>4</sub>	HCO <sub>3</sub>	Cl		Cl	SO <sub>4</sub>	HCO <sub>3</sub>	
				Cl	SO <sub>4</sub>			Cl	HCO <sub>3</sub>			HCO <sub>3</sub>	SO <sub>4</sub>
Ca	Ca		2										
	Na	2	1										
	Mg	1	2										
	Na	2	1										
	Mg	5	5									1	1
Mg	Mg		1										
	Ca	3	1										
	Na		1							1			1
	Ca		1	1									
Na	Na					1				1			
	Mg				1					1	1		1
	Ca			1								1	
	Mg			1	1								1
Ca										1			

(a)

Dominant 25 %	HCO <sub>3</sub>		SO <sub>4</sub>		Cl		Mixed		Total	
	No. of Samples	%	No. of Samples	%	No. of Samples	%	No. of Samples	%	No. of Samples	%
Ca	6	(8.6)	5	(7.1)	4	(5.7)	1	(1.4)	16	(22.9)
Mg	4	(5.7)	1	(1.4)	-	-	-	-	5	(7.1)
Na	2	(2.9)	3	(4.3)	21	(30.0)	6	(8.6)	32	(45.7)
Mixed	9	(12.9)	3	(4.3)	3	(4.3)	2	(2.9)	17	(24.3)
Total	21	(30.0)	12	(17.1)	28	(40.0)	9	(12.9)	70	(100.0)

(b)

Table 7.3 a) Tabular graph of the south-east part of the Tabriz Plain ground water type frequency, b) combinations of cations and anions in ground water of the south-east part of the Plain aquifers ( expressed as numbers & percentages of the total).

chloride, 21 (30%) in bicarbonate, 12 (17%) in sulphate, and 9 (13%) are mixed with dominant Na and Ca cations.

## **7.4.2 Graphical Representation and Interpretation**

### **Distribution Maps**

As ground water moves along its flow paths in the saturated zone, increases of total dissolved solids (TDS) and some of the major ions normally occur. Thus, there may be a close relationship between TDS and ground water potential maps. Such maps provide useful preliminary information about a system, together with indication of water quality.

In Figure 7.2 the distribution of TDS is compared with ground water levels for the Tabriz Plain. Ground water flow in the area is partly influenced by large withdrawals from the ground water, but this effect is not reflected by the hydrochemistry.

The values of TDS for the Alluvial Tuff aquifer range from 150 to 800 mg/l, whereas the values for the southern and central part of the Plain are 1000 to 5000 mg/l. In the northern part of the Plain such as the Tassoji- Soufian area, the TDS distributions coincide with the ground water potential lines and indicate lower with a TDS range from 200 to 1200 mg/l compared with the southern and central part of the Plain.

Ground water flow in the central part of the Plain reaches a partial barrier boundary attributed to a low permeability zone on the Aji Chay river flank. Consequently, the ground water levels rise and as a result the evaporation from the ground water increases the concentration of TDS. The Aji Chay river saline water itself is another main source of high salinity and TDS in the area, which is clearly reflected in TDS map.

### **Hydrochemical Diagrams**

**Pattern diagram analysis:** Pattern diagrams have long been used to represent analyses in distinctive graphical shapes. One such example suggested by Stiff (1952) is to plot concentrations of anions and cations on three or four horizontal axes extending either side of a vertical zero axis (see Fig. 7.3). A main advantage of this

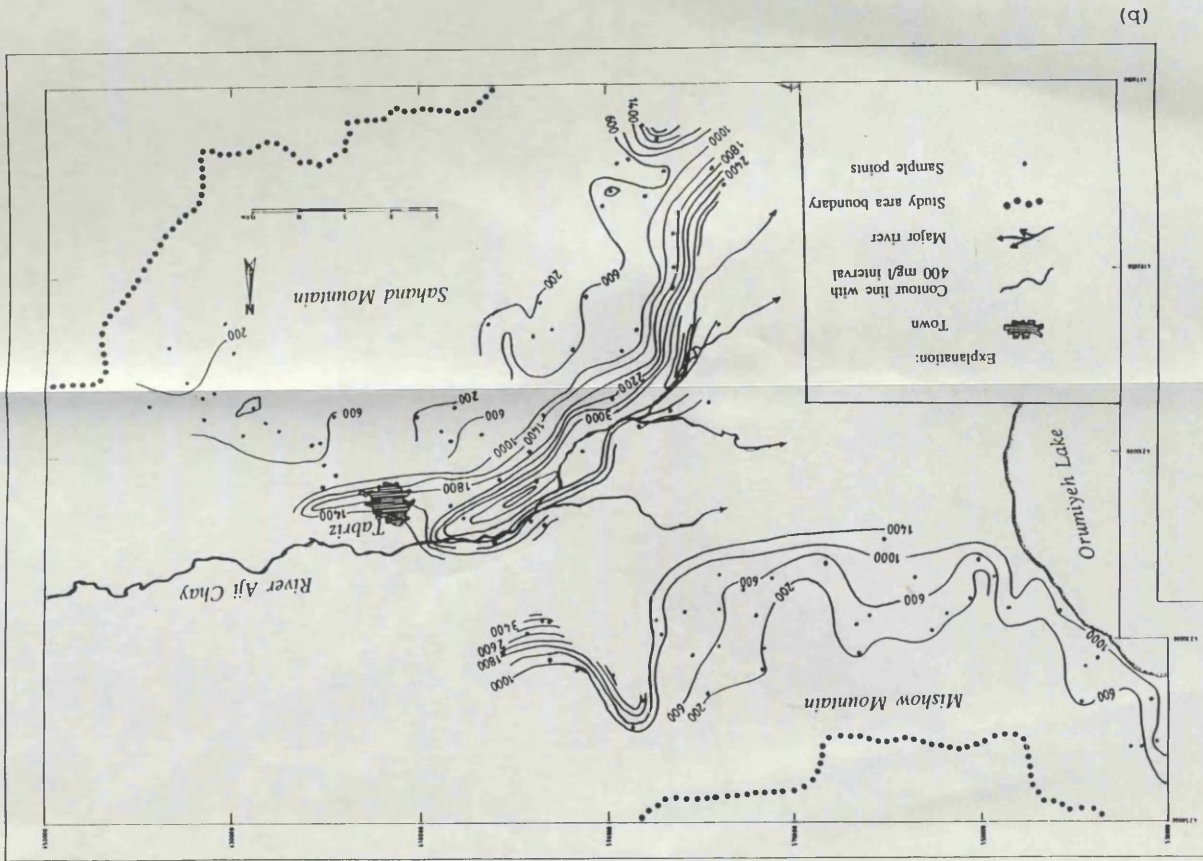
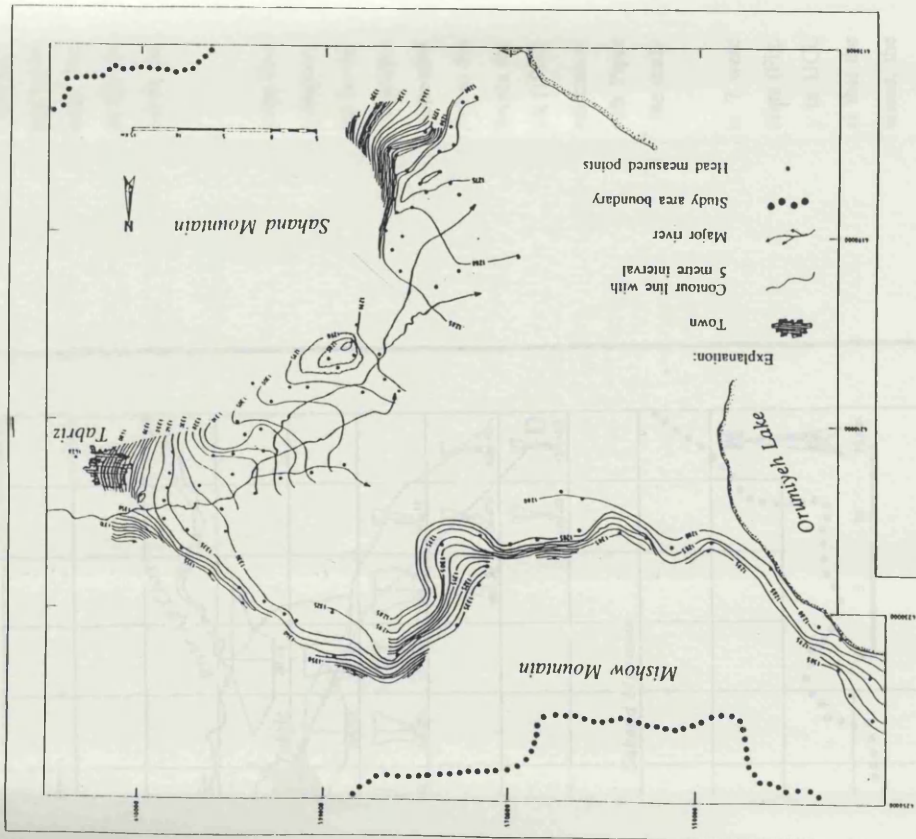


Fig. 7.2 Relationship between (a) ground water levels (1987) and (b) TDS (1987) in the Tabriz area.

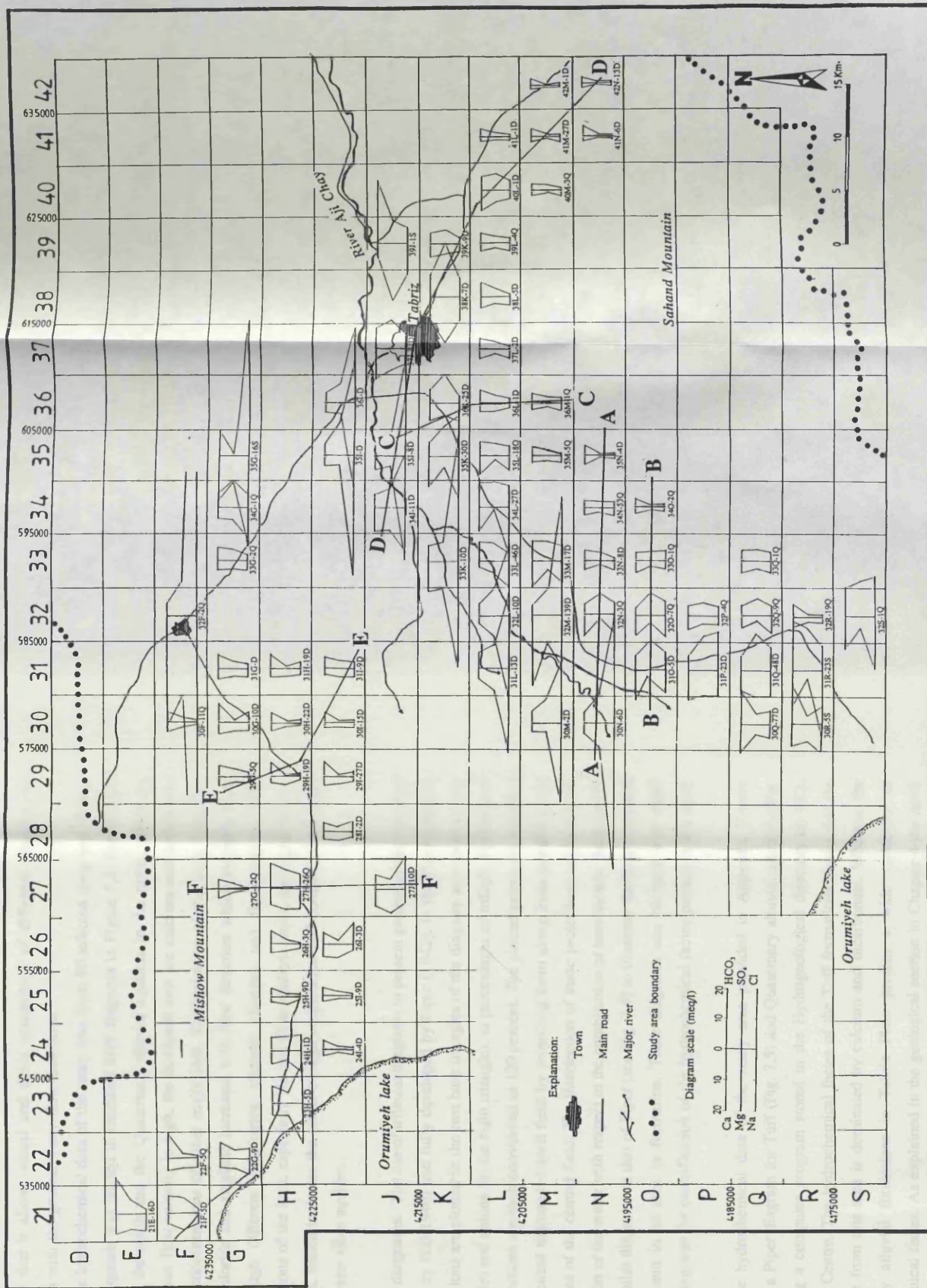


Fig. 7.3 Pattern diagrams for the major ions of ground water of the Tabriz area.



method is that it allows visual and direct comparison of different samples and correlation with the ground water flow directions.

The hydrochemical data of the study area from 80 selected deep and shallow wells and qanats was plotted in modified Stiff diagrams in Figure 7.3. For the Tuff aquifer in the south and the Quaternary alluvial aquifers in the north, where the ground water flow velocity is high, the dominant ions are calcium and bicarbonate with low concentrations of other major ions. Concentration of the ions, especially sodium, chloride and sulphate increases with flow direction which suggests water flow through different lithologies, climatic changes and flow regimes. The concentrations of the ions, especially Na and Cl in shallow wells, are higher than in deep wells, which indicates the effect of high evaporation and contamination in the shallow water table aquifer.

**Trilinear diagrams:** The use of trilinear diagrams to present ground waters was first attempted by Hill(1940) and fully developed by Piper (1942). In the Piper diagram, the major ions are plotted in the two base triangles of the diagram as cations (in the left triangle) and anions (in the right triangle), as percentages of mEq/l. Total anions and total cations are each considered as 100 percent. The plotted points are extended into the central diamond-shaped field by projecting them along lines parallel to the upper edges of the central field. The intersection of these projections represents the composition of the water with respect to the combination of ions shown. Back (1966) used a similar diagrams to that of Piper (see Fig. 7.4) to illustrate the hydrochemical facies present in an area or formation. These diagrams can be used with Piper trilinear diagrams for classification of the hydrochemical facies present in the study area.

The hydrochemical data of the study area provided in Appendix 7 were plotted as a Piper diagram for Tuff (Fig. 7.5) and Quaternary alluvial aquifers (Fig. 7.6), using a computer program stored in the Hydrogeological directory in UCL Computer Centre. The hydrochemical facies of the Tuff formations shows that the water type from this area is dominated by calcium and bicarbonate. Whereas, the Quaternary alluvial formations in Tabriz Plain present a wide variability of hydrochemical facies. As explained in the geological section in Chapter 4 the north

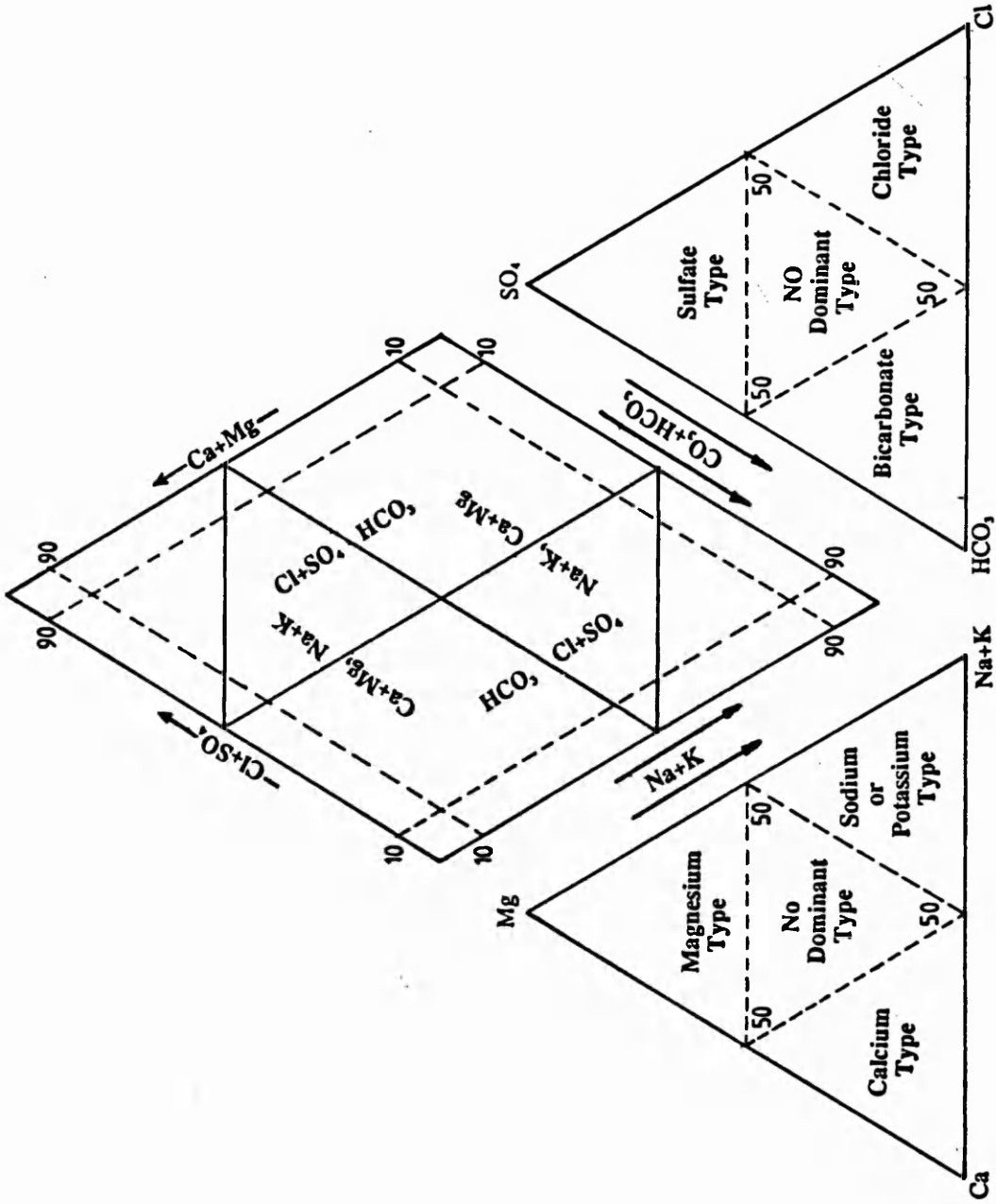


Fig. 7.4 Water analysis diagram showing hydrochemical facies, in percent of total equivalent per million (after Back, 1966).



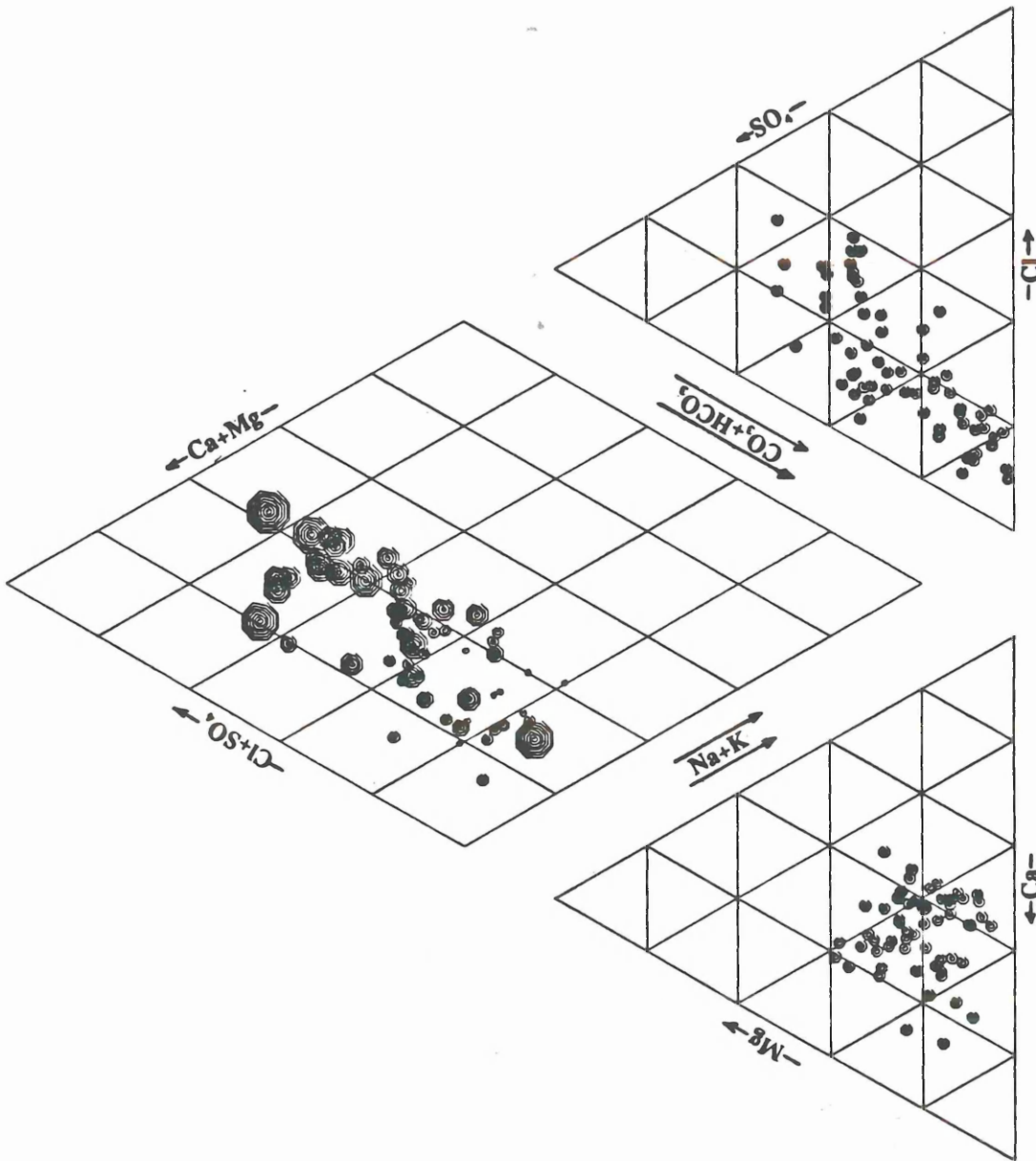


Fig. 7.5 Alluvial Tuff aquifer; ground water chemical analysis by Piper diagrams.

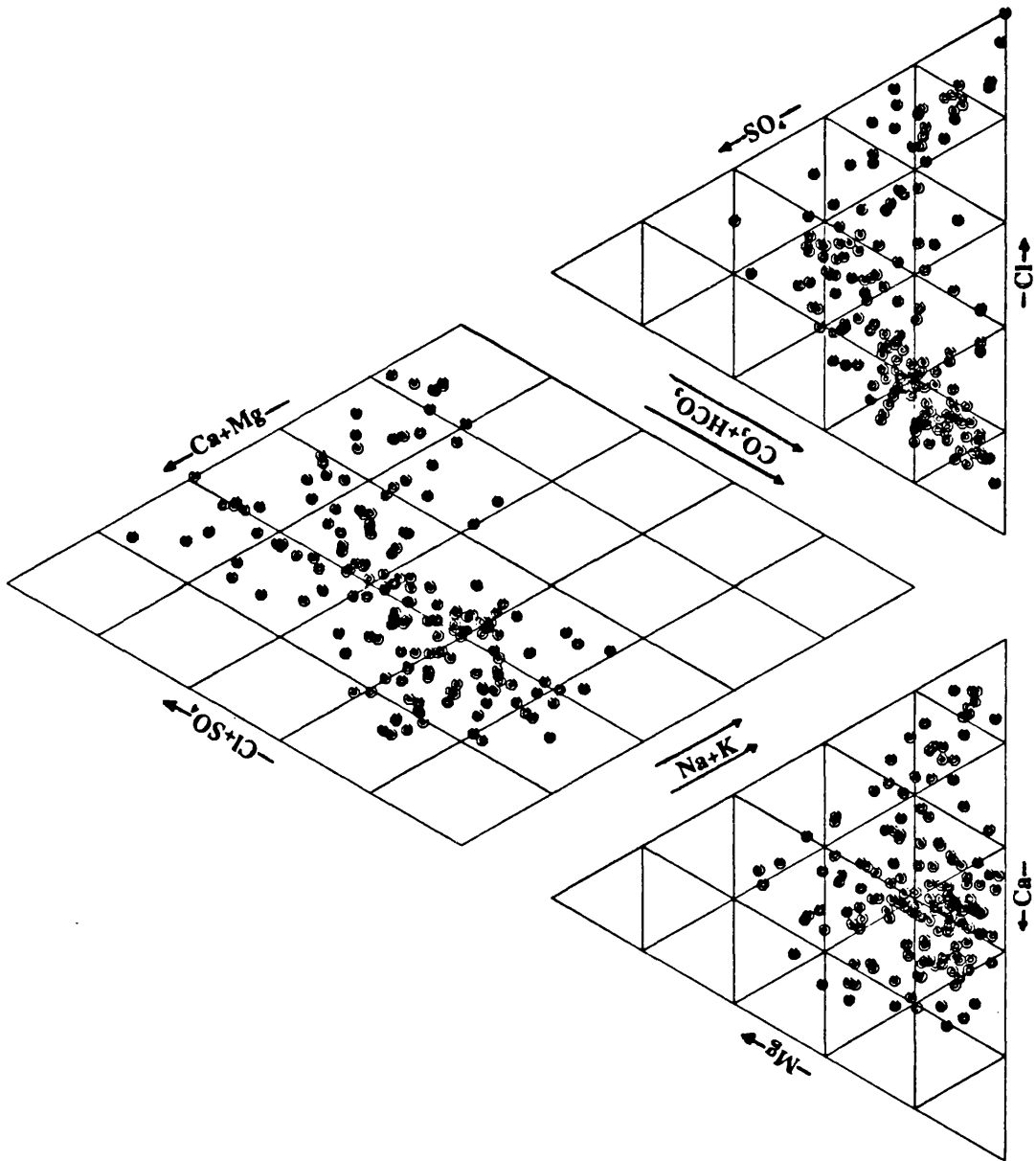


Fig. 7.6 The Tabriz Plain aquifers; ground water chemical analysis by Piper diagrams.

and north-east part of the Tabriz plain is dominated by Devonian to Cretaceous marine sediments and thick calcareous system which includes schists and quartzite and intruded, gabbro and granite, as well as major Miocene marl, sandstone, gypsum and salt formations. As a result, the water recharging the above-mentioned geological formations and/or their alluvial fans created different types of water. In the north and north-west parts of the area, in calcareous and intruded facies the primary water type of calcium and bicarbonate is the dominant facies. In the general discharge area along the low land in middle part of the plain, the sodium chloride facies is dominant.

An alternative diagram to that of Piper has been suggested by Durov (1948) and was elaborately expanded and developed by Burdon and Mazloum (1958), Lloyd (1965), and Lloyd and Heathcote (1985), as shown in Figure 7.7. The diagram based on percentage major ion milliequivalent values, but in this case the anions and cations together are considered as comprising 100 percent.

In the expanded diagram, the cation and anion triangles are recognized and are separated along the 25 percent axes, so that the main square is conveniently divided into 9 fields. The anion and cation values are plotted in the appropriate triangles and projected into the main fields.

The expanded Durov diagram has the distinct advantage over the Piper diagram in that it provides a better display of hydrochemical types and some processes, and in practical terms has less line work in the main field.

In Burdon and Mazloum (1958), the anions  $\text{HCO}_3$ ,  $\text{SO}_4$  and Cl being the most mobile constituents of ground water as well as the main indicators for genetic and metasomatic investigations, are used as the basis for classification of ground water. The cations Ca, Mg and Na+K are considered secondary. Therefore, four major groups of ground water emerge:

- 1) Bicarbonate group,  $\text{HCO}_3 > 50\%$  of total anions, with either Ca, Mg or Na+K as the dominant cation
- 2) Sulphate group,  $\text{SO}_4 > 50\%$  of total anions with either Ca, Mg or Na+K as the dominant cation
- 3) Chloride group, Cl  $> 50\%$  of total anions with either Ca, Mg or Na+K as the dominant cation

4) Mixed group, with no one anion exceeding 50 percent.

40 analyses of 65 water analyses from the Alluvial Tuff aquifer were plotted in the expanded Durov diagram shown in Figure 7.7. Of the 40 samples, 23 contain more than 50% bicarbonate anions; from these 23, in 10 cases Ca exceeds 50%. In the 13 remaining samples, no cation exceeds 50%. Only in one analysis did the value of  $\text{SO}_4$  exceed 50% and the concentration of chloride in all the analyses is less than 40%. The concentrations of Na and Mg are less than 20% and 40%, respectively. Consequently, these waters belong almost completely to the bicarbonate and mixed groups of water and contain a predominant amount of the Ca cation.

The Alluvial Tuff aquifer is moderately porous and permeable with higher hydraulic gradients, consequently the water transmitted acquires small quantities of dissolved solids. The TDS ranges between 300 to 1000 mg/l, with an average value about 410 mg/l. However, the mineralization of water passing through the aquifer increases in proportion with increasing distance from the recharge area, which was clearly demonstrated by the line of simple dissolution or mixing in Figure 7.7. The main recharge area lies in the higher altitude Sahand mountain with an average 500mm of annual rainfall and snow.

Figure 7.8 shows plots of 38 water sample analyses from the north and north-west parts of the Tabriz Plain, known as the TassoJ-Soufian area. From the 38 samples, 22 of them contain more than 25% bicarbonate anions; in 8 of the 22, Ca is more than 25% and only in one case does Mg exceed 25%. The  $\text{SO}_4$  and Cl comprise more than 25% of anions in one and 5 samples respectively. The percentage of Mg and Na exceeded 25% of cations in 4 samples, and for the other samples they range between 15 to 25% and 5 to 25% respectively. The predominant geological formations affecting these waters are Devonian to Cretaceous, calcareous and flysch-type sediments and their Quaternary terraces and gravel fans. The results show a distinct water type differing from the central part of the Plain, whereas it shows some similarity with the plot of Figure 7.7 for the Alluvial Tuff aquifer, as both areas are dominated by bicarbonate and mixed group water types rich in Ca. The average percentage concentrations of Mg and Na in the northern part of the Plain are much more than in the Tuff aquifer. This is due to the lithological differences of the two aquifers and to the presence of dolomite and in some cases other evaporite material

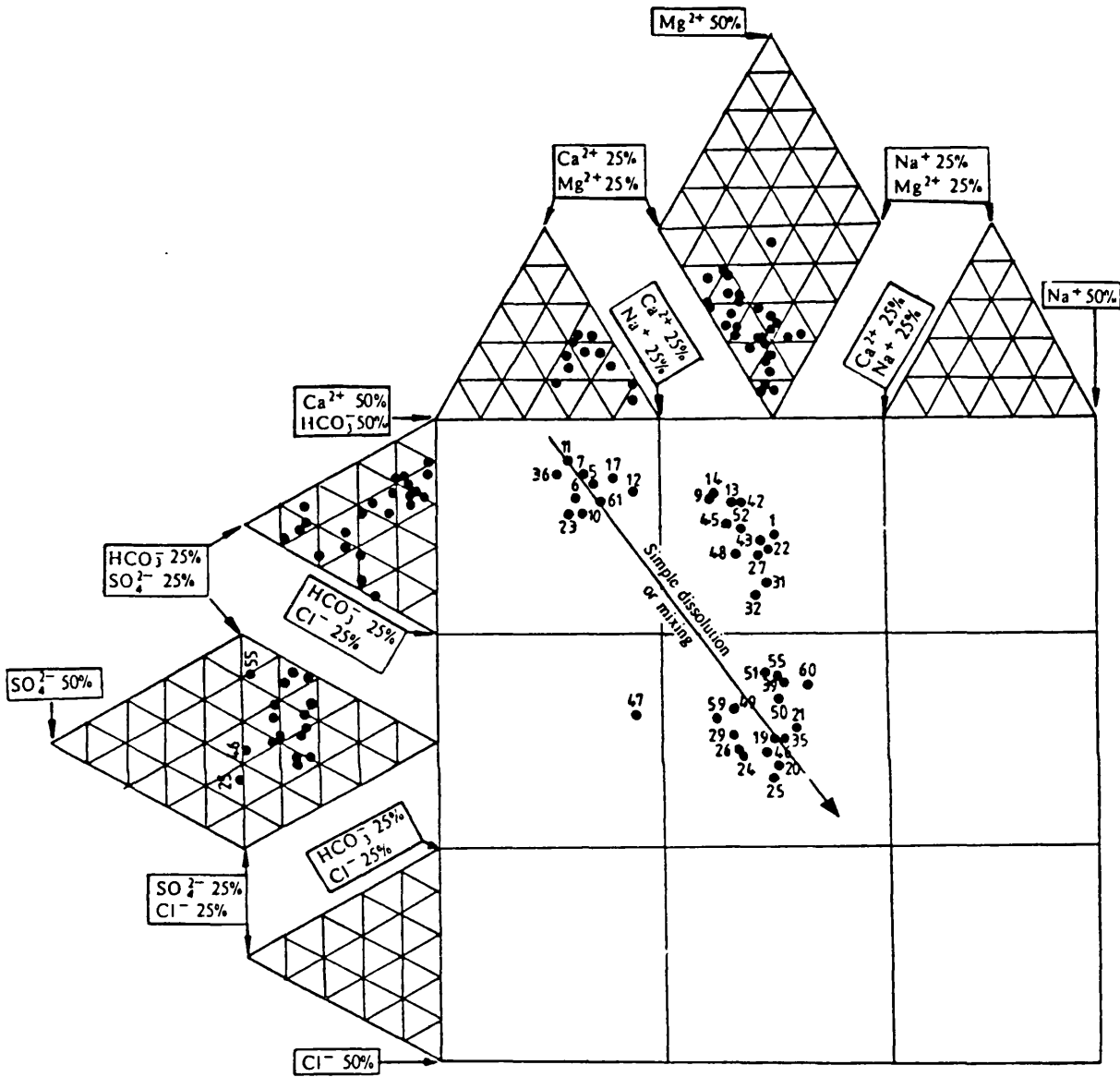


Fig. 7.7 Expanded Durov diagrams, demonstrating major ions in ground water of alluvial tuff aquifer (Oct. 1987).

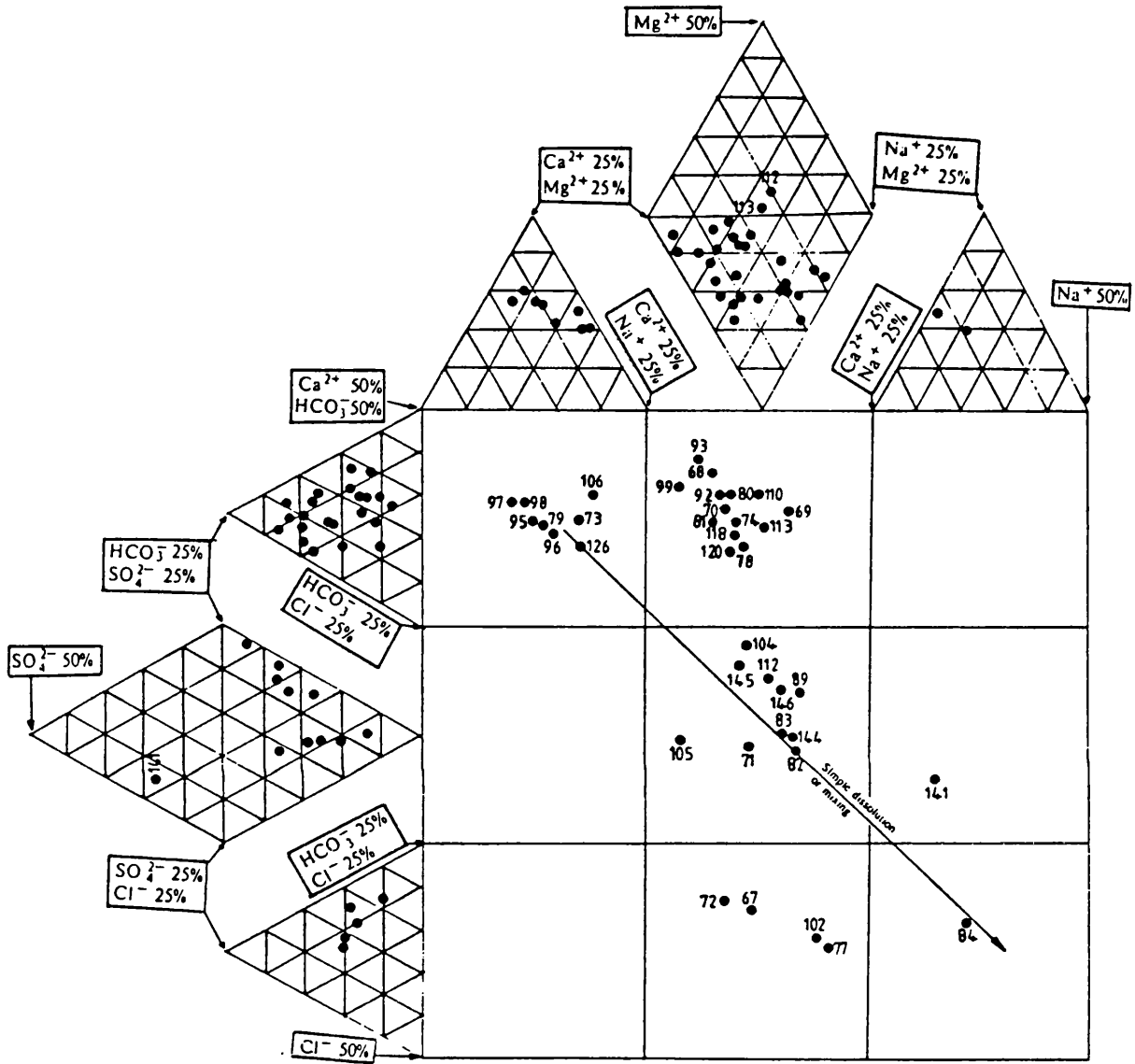


Fig. 7.8 Expanded Durov diagrams, demonstrating major ions in ground water of the northern part of the Plain (Oct. 1987).

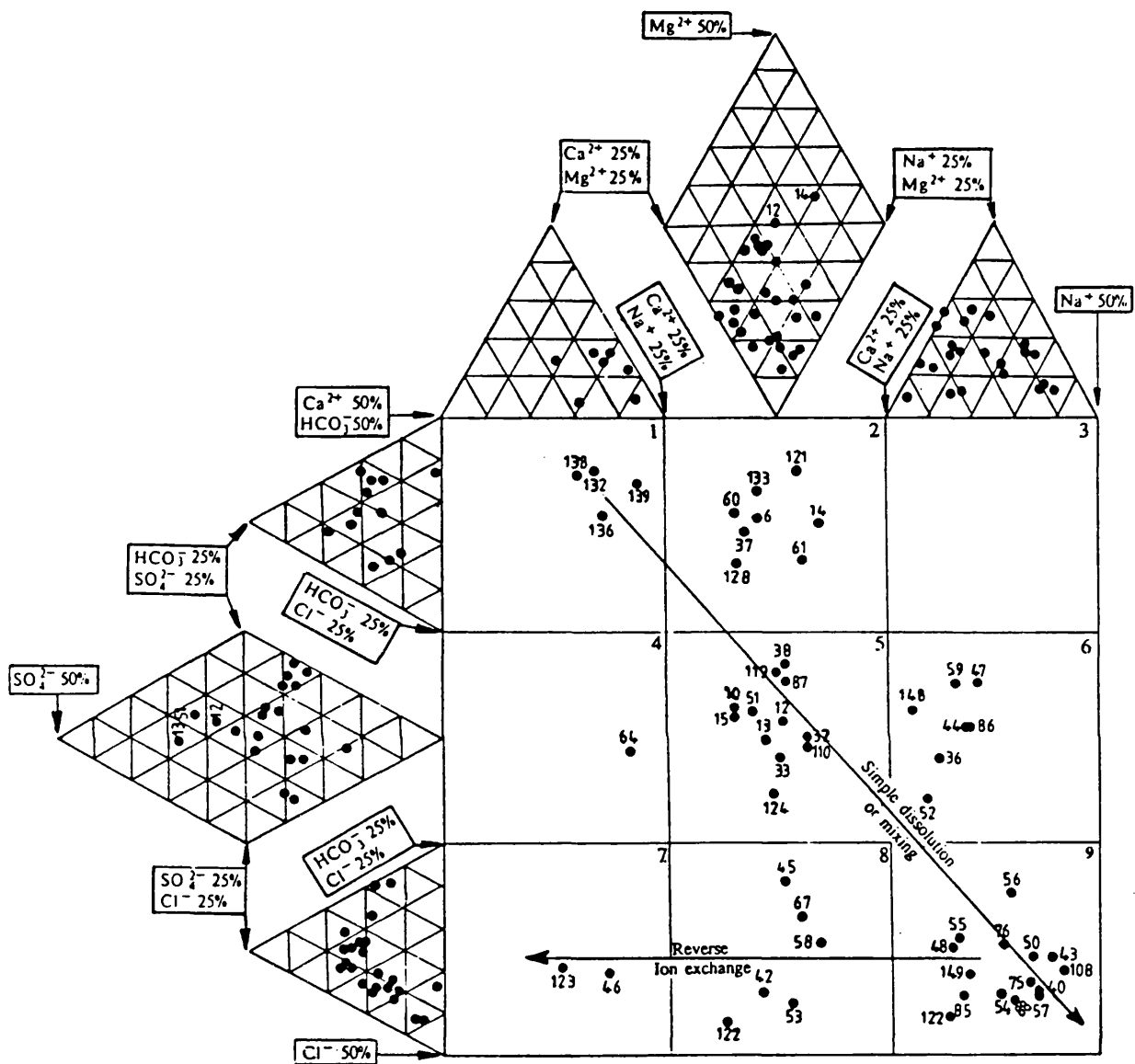


Fig. 7.9 Expanded Durov diagrams, demonstrating major ions in ground water of the southern and central parts of the Plain (Oct. 1987).

in the northern part of the Plain.

Figure 7.9 represents waters obtained from the southern and central parts of the Plain which lies to the west and south-west of Tabriz (around the river Aji Chay) and the area between Tabriz and Soufian. The 55 water analyses from this area show a variety of types of water, but dominantly in the chloride group. From 55 samples, 23 contain more than 25% chloride; in 15 of these 23 the Na is more than 25%, and in 2 cases the Ca exceeded 25% which suggests that reverse ion exchange occurs. The  $\text{HCO}_3$  and  $\text{SO}_4$  comprise more than 25% of all anions in 12 and 3 samples respectively. In the 9 remaining samples, no anion exceeded 25%.

The area between Tabriz and Soufian is mainly covered by the Miocene sandstones, salt domes and Cretaceous limestone, but all waters in the area were contaminated with saline water draining from the Miocene formations.

The waters obtained from the vicinity of the River Aji Chay also show high salinity, which changes with depth, especially where the multi-layer aquifer system is dominant. The deep aquifers are less saline than the shallow aquifers, but the average salinity is high. Throughout the southern part of the Plain, especially in the Azarshahr area, the salinity decreases towards the Alluvial Tuff aquifer.

### **7.5 TDS and Their Relation to Electrical Conductivity**

Total dissolved solids (TDS), as defined by Freeze and Cherry (1980), are the solid residue obtained by evaporating a measured volume of filtrated water sample to dryness. Hence, the solid residue consists of dissociated and undissociated substances, exclusive of suspended material, colloids, and dissolved gases.

Figure 7.2 shows the distribution of the TDS in the waters of the Tabriz area, for October 1987 expressed in mg/l. The TDS distribution map shows a gradual increase from the recharge areas in the Sahand and Mishow mountains towards the central part of the Plain. This increase is thought to be due to mineral dissolution or leakage of highly mineralized waters occurring along the flow path. The increase in dissolved solids is greater in the low lands of the Plain due to a reduction in flow velocity of the ground water and high evaporation from the shallow water table aquifers. The areas around the rivers Aji Chay , Gomanab Chay and Sinekh Chay show higher values of dissolved solids because of the infiltration of saline water to



the water table.

According to Todd (1980), and Freeze & Cherry (1980), the classification of the ground water with respect to the dissolved solids concentration, and the percentage of the samples in each class was considered for the Tabriz area as shown in Table 7.4.

**Table 7.4**

<u>Water Type</u>	TDS (mg/l)	<u>numbers and percentages of the frequency</u>		
		<u>Alluvial Tuff</u>	<u>northern part of the Plain</u>	<u>central part of the Plain</u>
Fresh	0-10 <sup>3</sup>	63 (100%)	37 (77%)	22 (32%)
Brackish	10 <sup>3</sup> -10 <sup>4</sup>	-	11 (23%)	46 (67%)
Saline	10 <sup>4</sup> -10 <sup>5</sup>	-	-	1 (1%)
Brine	>10 <sup>5</sup>	-	-	-

The classification shows that 100% of the water samples from the Alluvial Tuff aquifer, 77% from the northern part of the Plain, and 32% from southern and central parts of the Plain, are classified as fresh water, with 23% samples from the northern part of the Plain, and 67% from the southern and central parts of the Plain, are brackish water. There is only one sample in the central part of Plain which has a TDS of more than 10,000 mg/l.

The presence of charged ionic species in solution makes the solution conductive. As ion concentrations increase, electrical conductance of the solution increases; therefore the conductance measurements provides an indication of ion concentration.

It should be mentioned that natural waters contain a variety of both ionic and uncharged species in various amounts so the conductance determinations can not be used to obtain accurate values of ion concentrations or total dissolved solids. For convention, between EC values and TDS, the following relationship is used:

$$\text{TDS} = A \cdot \text{EC}$$

where EC is the electrical conductance in micromhos, TDS is expressed in mg/l and A is a conversion factor, whose values depends on the ionic composition of the solution.

The TDS values of the hydrochemical data which was used in this study were originally determined from the TDS and EC relationship by ARWA without direct measurement of TDS values. However, some hydrochemical data which were analysed by an other branch of the same organization have been used to derive the correlation between TDS and EC in the area (see Fig. 7.10). The factor used by ARWA for the conversion factor was 0.66, which in comparison with the value deduced from Figure 7.10 (0.8) is on the small side.

## **7.6 Ground Water Contamination in the Tabriz Area**

Todd (1980) defined ground water contamination as the artificially induced degradation of natural ground water. Thus, a large number of sources and causes which are closely associated with human use of water can modify ground water quality. The city of Tabriz with its high population and heavily industrial centres, and without sewage treatment systems, together with some other small towns in the area can cause municipal, industrial and agricultural sources of ground water contamination in the Tabriz area. In addition, the rivers Aji Chay and Sinekh Chay which contribute to ground water recharge in this area act as natural contamination sources of ground water. Hence, in the Tabriz Plain, the ground water is thought to be contaminated by municipal, industrial and miscellaneous sources and causes.

### **1 Municipal and industrial sources and causes**

Sewage and waste waters resulting from municipal and industrial sources can introduce high concentrations of nitrate, Biological Oxygen Demand (BOD), (Chemical Oxygen Demand (COD), organic chemical and possibly bacteria and viruses into ground water. There is no data available for the biological health aspects of the ground water. However, there is some monitoring of shallow and deep wells inside and around Tabriz which are sampled for consideration of ground water quality. Table 7.5 shows the concentrations of nitrate, COD and BOD in these wells. The concentrations of nitrate in shallow wells are above the permissible limit for drinking water and the values of COD and BOD are also higher than the values

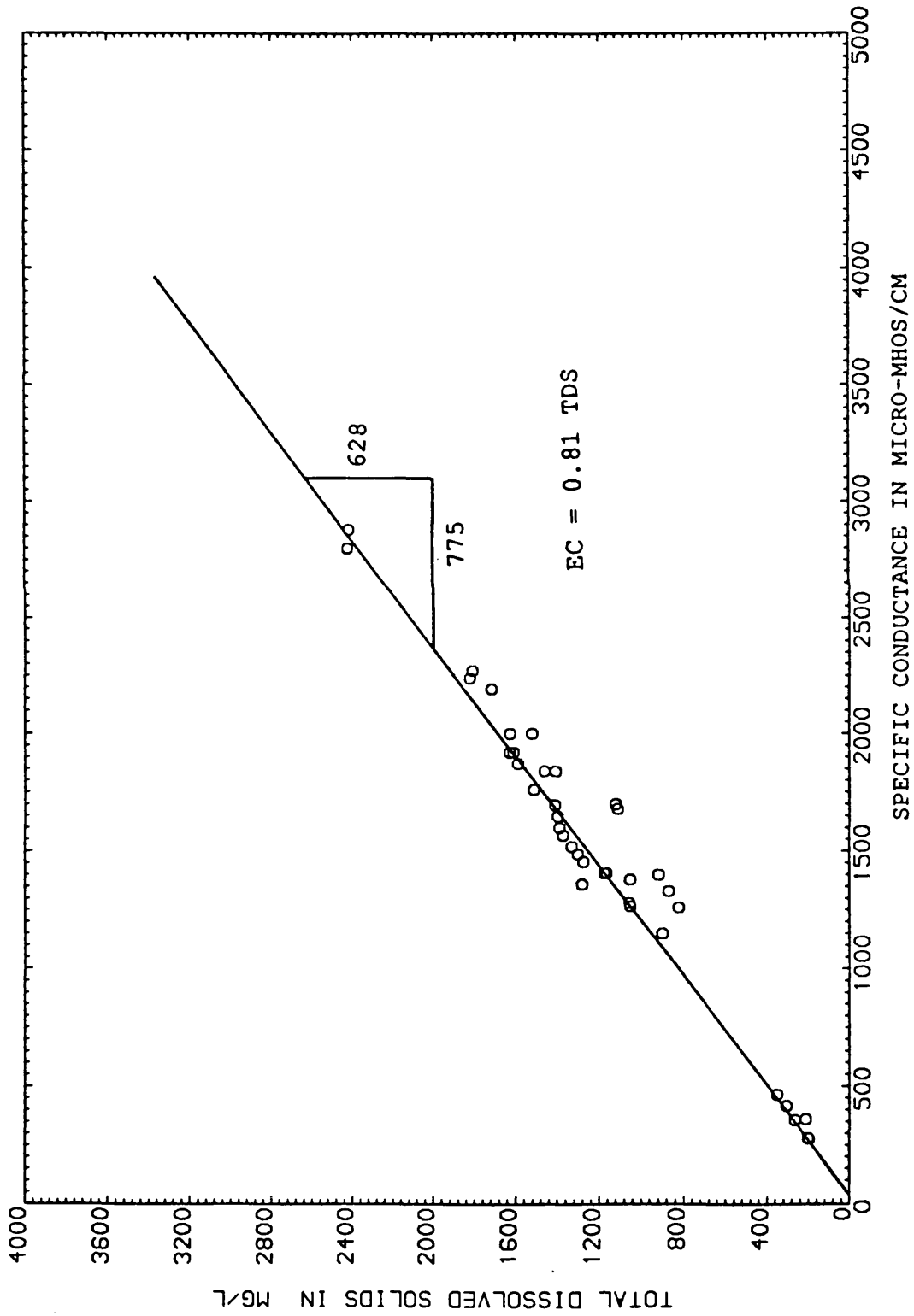


Fig. 7.10 The relation between TDS and EC in the ground water of the Tabriz area.

found in the Alluvial Tuff aquifer. The concentration of the nitrate in the area seems to result from contamination of the ground water with sewage and waste water as well as agricultural activities.

**Table 7.5**

<u>area</u>	<u>well No.</u>	<u>NO<sub>3</sub>(mg/l)</u>	<u>BOD(mg/l)</u>	<u>COD(mg/l)</u>
<i>Alluvial</i>	<i>41M-7D</i>	<i>3.0</i>	<i>0.9</i>	<i>6.1</i>
<i>Tuff</i>	<i>41M-50D</i>	<i>2.1</i>	<i>0.8</i>	<i>2.1</i>
Tabriz	37J-M.D	132	1.1	9.0
City	37K-Kh.D	99	0.9	9.0
	37K-F.D	136	0.9	8
	37J-B.G.D	104	1.4	8
	37J-B.M.D	109	1.3	8

## **2 Miscellaneous Sources and Causes**

The rivers Aji Chay, Sinekh Chay and some other small rivers are contaminated by natural point or line sources of contamination where they cross the salt domes of the Miocene formation, in the north and north-west of the Tabriz area. All these rivers become losing streams when they reach the southern and central parts of the Plain. The monthly variations of the TDS content in the rivers Aji Chay and Sinekh Chay and the variations in the river discharge rates for the Aji Chay are shown in Figures 7.11 and 7.12, respectively. As the figures demonstrate, the concentrations of TDS values for both rivers are above 1000 mg/l for the whole of the year.

Pumping from unconfined fresh-water aquifers which hydraulically are connected with the saline-water aquifers causes intrusion of saline water towards these wells. In addition, pumping from deep, fresh, confined aquifers in this area induces some leakage of contaminated water into these aquifers. For example, the TDS values from wells PB3 and PB4 on the west side of Tabriz City for a three year period indicate increasing contamination of the confined aquifer (see Table 7.6).

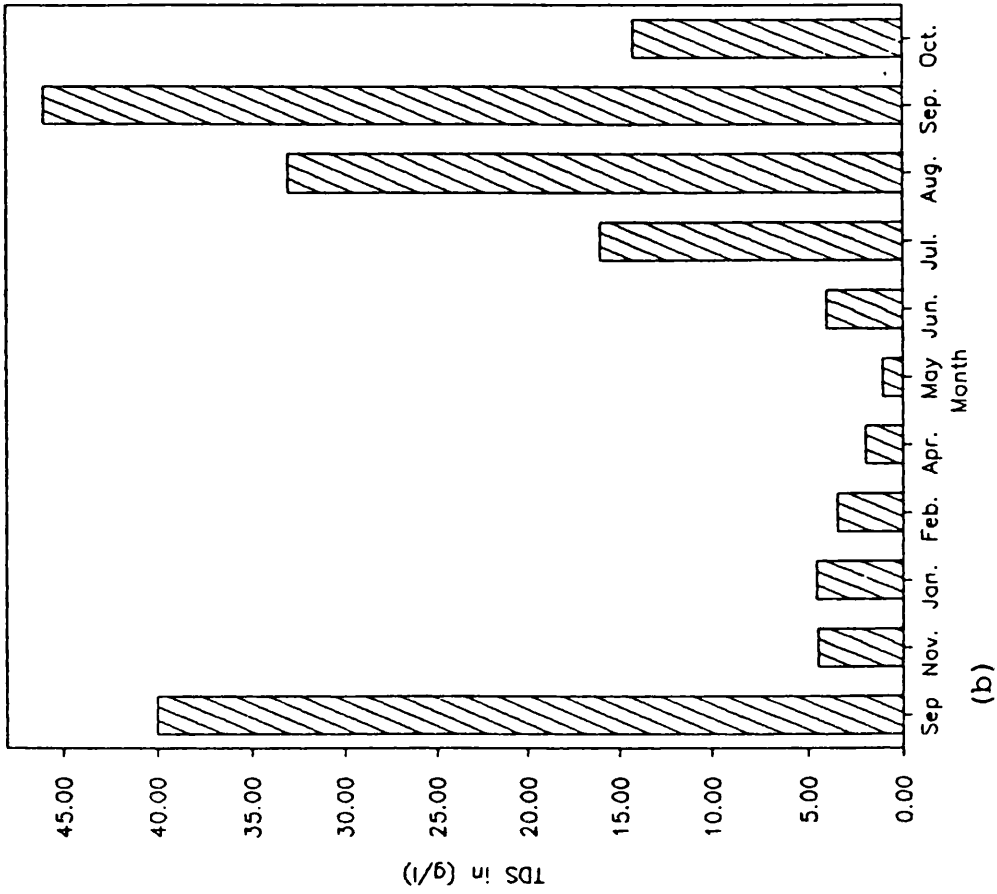
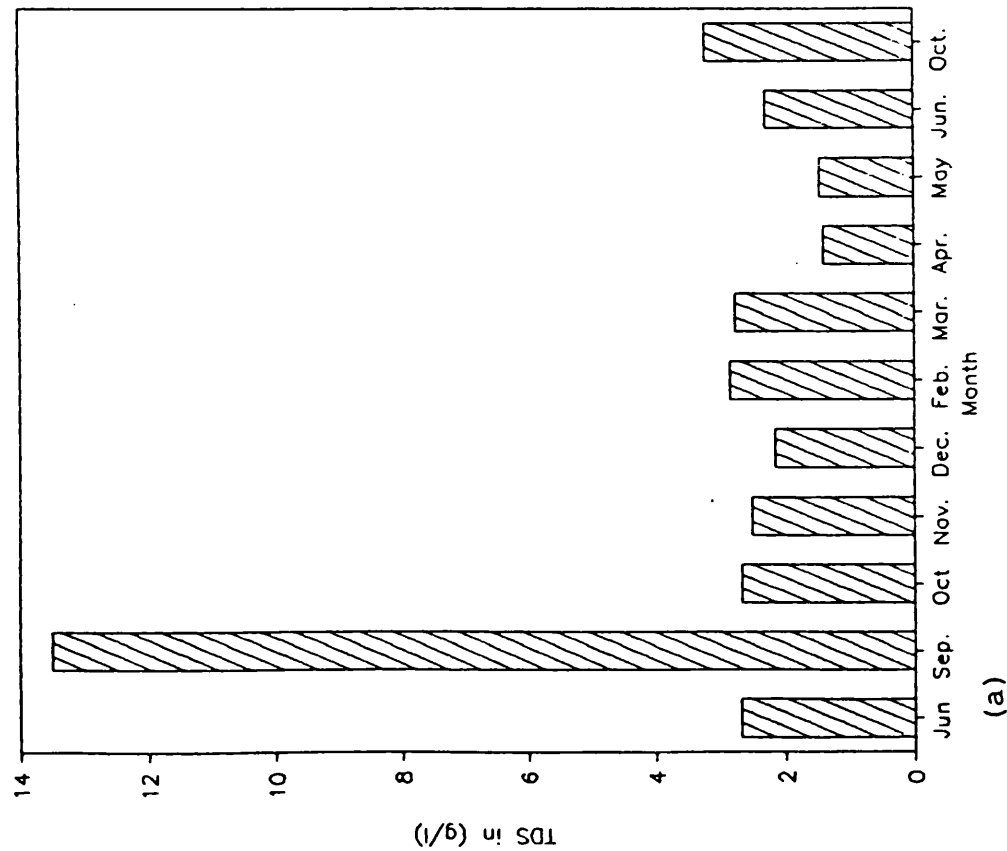


**Fig. 7.11 The monthly variations of TDS (a) in water of the River Gomanab Chay, and (b) in the River Aji Chay (1986-87).**

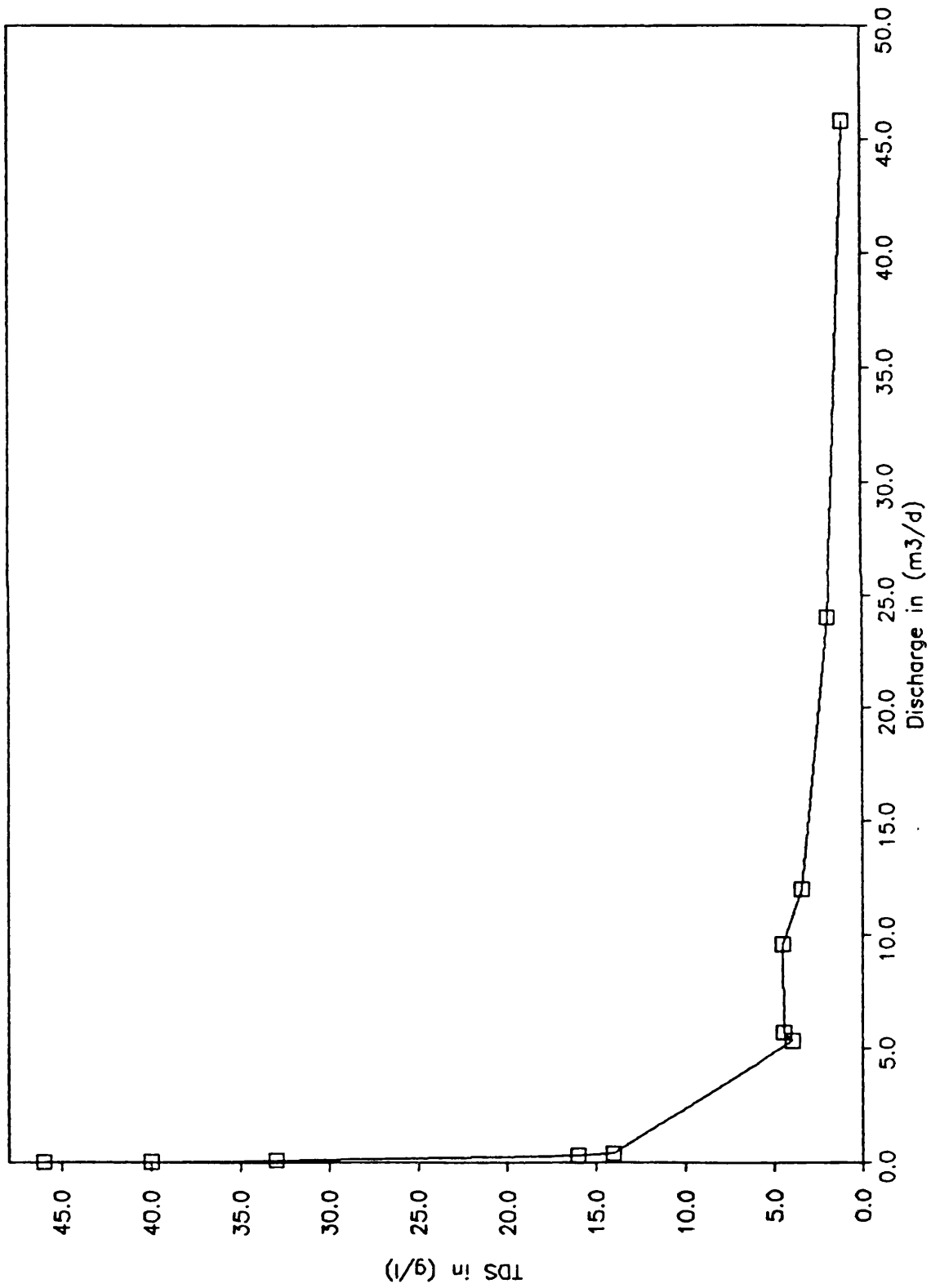


Fig. 7.12 The variations of TDS of river Aji-Chay by discharge rate (1986-1987).

**Table 7.6**

<u>Well</u>	<u>Date</u>	<u>TDS(mg/l)</u>	<u>Well</u>	<u>Date</u>	<u>TDS(mg/l)</u>
PB3	87.09.7	1120	PB4	87.7.21	1072
PB3	88.08.20	1281	PB4	88.08.20	1484
PB3	89.08.25	1357	PB4	89.07.1	2412

A very clear illustration of the contamination of the ground water around the river Aji Chay was shown by the TDS concentration contour map in Figure 7.2.

### **7.7 Factors and Processes Controlling Ground Water Compositions**

All existing ground water in the study area, with the possible exception of ground water in some deep aquifers of the central part of the Plain, originates from atmospheric precipitation. As a result, the ground water in the area is part of the hydrological cycle. In most parts of the area, the general relationships between the chemical composition of the ground water and the amount of the precipitation and evaporation indicate that bicarbonate waters are predominant in the regions of higher precipitation and lower evaporation. However, the role of the lithology of the aquifer is more important and effective than these climatic factors.

The effect of the lithology on the composition of the ground water along the flow paths from the recharge to discharge areas divides the study area at least into three different major hydrochemical zones. However, the geology of the area especially that of the northern part of the Plain is more complicated. On the other hand, it is possible that the diversity of composition of the top soil which covers the water bearing layers introduces a varied influence on the chemical composition of the existing water.

In this section, an attempt has made to explain the process and source of the main ionic constituents of the ground waters analysed and classified in the previous sections.

#### **7.7.1 Major constituents**

**Calcium:** Ground waters in contact with sedimentary rocks derive their calcium from

the solution of limestone, dolomite, aragonite, anhydride, and gypsum. In igneous and metamorphic rocks, it comes from the weathering of minerals, such as apatite, wollastonite, fluorite and various members of feldspar, amphibole and pyroxene groups (Davis and DeWiest, 1966).

The presence of volcano-sedimentary beds of ignimbrite, tephra, pumice and dacite and dacitoid fragments which are rich in amphibole, feldspar, pyroxene, and apatite minerals provide the source of calcium for the Alluvial Tuff aquifers (Moinvaziri and Aminsobhani, 1975). The concentration of calcium in waters of the Tuff aquifer ranged from 20 to 140 mg/l with an average of about 60 mg/l. It generally increases along the principal flow paths from recharge to discharge areas (see Figs. 7.13 and 7.14). As these diagrams show, in some areas, where the flow lines pass through the Tabriz Central Plain the values of calcium concentration decrease. It is believed that this is due to the ion-exchange reactions of calcium and the other cations, where the ground water comes in contact with marls and clays which are saturated with sodium.

Calcium in the Tabriz Plain is largely derived from the sedimentary rocks, such as limestone, dolomite and gypsum. The highest value for calcium concentration is 1142 mg/l from well 30Q-82S located in the south-western part of the Azarshahr. The concentration of calcium in the northern part of the plain ranges from 36 to 130 mg/l with an average of about 80 mg/l.

**Magnesium:** The main sources of the magnesium in the ground water of the Alluvial Tuff aquifer are thought to be biotite, hornblende, and augite which are abundant in the volcano-sedimentary formations of the Sahand area. Concentrations of magnesium in ground water of the Tuff aquifer ranged from 1.2 to 48 mg/l, with an average of 19 mg/l. In general, the concentrations increase in the direction of ground water flow (see Figs.7.13 and 7.14). However, the concentration of magnesium in this aquifer is much less than that of calcium.

Magnesium in the Tabriz Plain is possibly derived from the solution of dolomite and limestone. According to Davis and DeWiest (1966), most calcareous strata contain some magnesium, so the solution of limestone commonly yields some magnesium as well as calcium. The concentrations of magnesium in the Tabriz Plain aquifers are higher than in the Tuff aquifer and because of the geological complexity



of the former area, there are large regional changes in this cation (see Fig.7.15).

**Sodium:** Sodium is the most abundant member of the alkali-metal group of the periodic table. It is, unlike calcium and magnesium, not found as an essential constituent of many of the common rock-forming minerals. Thus, the amounts of sodium held in evaporite sediments and in solution in oceans are an important part of the total. When sodium has been brought into solution, it tends to remain in that state. There are no important precipitation reactions that can maintain low sodium concentrations in solution.

Sodium is retained by adsorption on mineral surfaces, specially by minerals having high cation-exchange capacities, such as clay. However, the interaction between surface sites and sodium is much weaker than the interaction with divalent ions.

Sodium ion concentrations, shown in Figures 7.13 and 7.14, demonstrate a sharp increase in value where the ground water flow lines come in contact with high capacity cation-exchange minerals, with a concurrent decrease in calcium and in some cases magnesium concentrations. The primary source of the sodium ions in ground water of Sahand area are believed to be from the weathering of plagioclase feldspars. The concentration of sodium in ground water of the Alluvial Tuff aquifer ranged from 10 to 150 mg/l with an average of 62 mg/l.

Concentrations of sodium in Tabriz Plain ground waters show a very wide range from 7 to 800 mg/l, which indicates the variations of geological conditions in the area. The high concentration of sodium is likely to be derived from the Miocene and Recent evaporite sediments.

**Bicarbonate and Carbonate:** The quantity of strong acid required to titrate a water sample to an endpoint of pH 4.5 is a measure of the alkalinity of the water. Alkalinity is produced almost exclusively by bicarbonate and carbonate ions. Carbonate ions are present in water only if the pH is greater than 8.3. Below this pH, most of the carbonate ions react with hydrogen to become bicarbonate ions. Most carbonate and bicarbonate ions in ground water are derived from the carbon dioxide in the atmosphere and in the soil, and the solution of carbonate rocks.

The pH values of the ground water of the Tabriz area were measured in the laboratory as being below 8.3 (see Appendix 7). So in this study, the bicarbonate ions

represent the principal ions for alkalinity measurements. The concentration of bicarbonate ions in ground water of this area (ranged from 100 to 1000 mg/l) is dominant in or near the ground water recharge areas. As Figures 7.13 to 7.15 show, the bicarbonate ion concentration along the ground water flow direction increases very slowly in comparison with the other ions. It is actually a dominant ion in or near the recharge areas but the opposite in the discharge areas.

**Sulphate:** The common sources of the sulphate at present are largely recycling from the atmosphere and the solution of sulphates in sedimentary rocks. However, early in the history of the hydrosphere, most sulphates probably originated from the oxidation of sulphide from igneous rocks and volcanic sources.

Concentration of sulphate ions in ground water of the Tabriz area shows some variation depending on the lithological differences of the water bearing layers. As Figures 7.13 and 7.14 demonstrate, the concentration of sulphate in ground water of the Alluvial Tuff aquifer gradually increases along the ground water flow directions, but sharply increases where the ground water comes in contact with the Pleistocene, fine grained, clastic sediments with diatomite, fish and carbonate sulphate beds, to the east and south-east of the city of Tabriz, as well as in some areas between the Tuff and Tabriz Plain Quaternary formations ( Tabriz- Mamagan-Azarshahr zone).

**Chloride:** Chloride is a minor constituent of the earth's crust, but a major dissolved constituent of most natural waters. Chloride ions do not enter into oxidation or reduction reactions, they do not form important solute complexes with other ions unless the chloride concentration is extremely high, and are not adsorbed on mineral surfaces.

The common sources of chloride in ground water comes from four different sources, (1) chloride from ancient sea water entrapped in sediments, (2) solution of halite and related minerals in evaporite deposits, (3) concentration by evaporation of chloride contributed by rain or snow, and (4) solution of dry fallout from the atmosphere, particularly in arid regions (Davis and DeWiest, 1966).

Chloride ions in the ground water of the Alluvial Tuff aquifer are thought to be derived from the alteration of minerals such as apatite and hornblende, as well as solution of dry fallout from the atmosphere. Therefore, the concentration (ranging from 10 to 120 mg/l) in the ground water of this area increases along the ground

water flow direction from recharge to discharge areas (Figs. 7.13 and 7.14).

The main natural source of the chloride in ground water of the Tabriz Plain is the exposed evaporite sediments in the area and some saline streams, which carry saline waters and allow them to infiltrate into the ground water. According to Hem (1985), the differential permeability of clay and shale layers holds back chloride, while water molecules pass through them and accumulate until high concentrations are reached. It was thought possible that the clay and shale beds in some areas of the Plain affect the chloride concentrations in ground water in this way.

Man's activity is thought to be another important source for chloride through irrigation processes, since the water used for irrigation becomes concentrated by evapotranspiration. The concentration of chloride in the ground water of the Plain ranged from 20 to 3600 mg/l with high concentrations in low lying water-table aquifers.

**Hardness:** Hardness of water is defined as the content of metallic ions which react with sodium to produce solid soaps (Freeze & Cherry, 1980). The hardness is normally expressed as total concentration of calcium and magnesium, the most abundant divalent metallic cations, as milligrams per litre of equivalent  $\text{CaCO}_3$ .

Then:

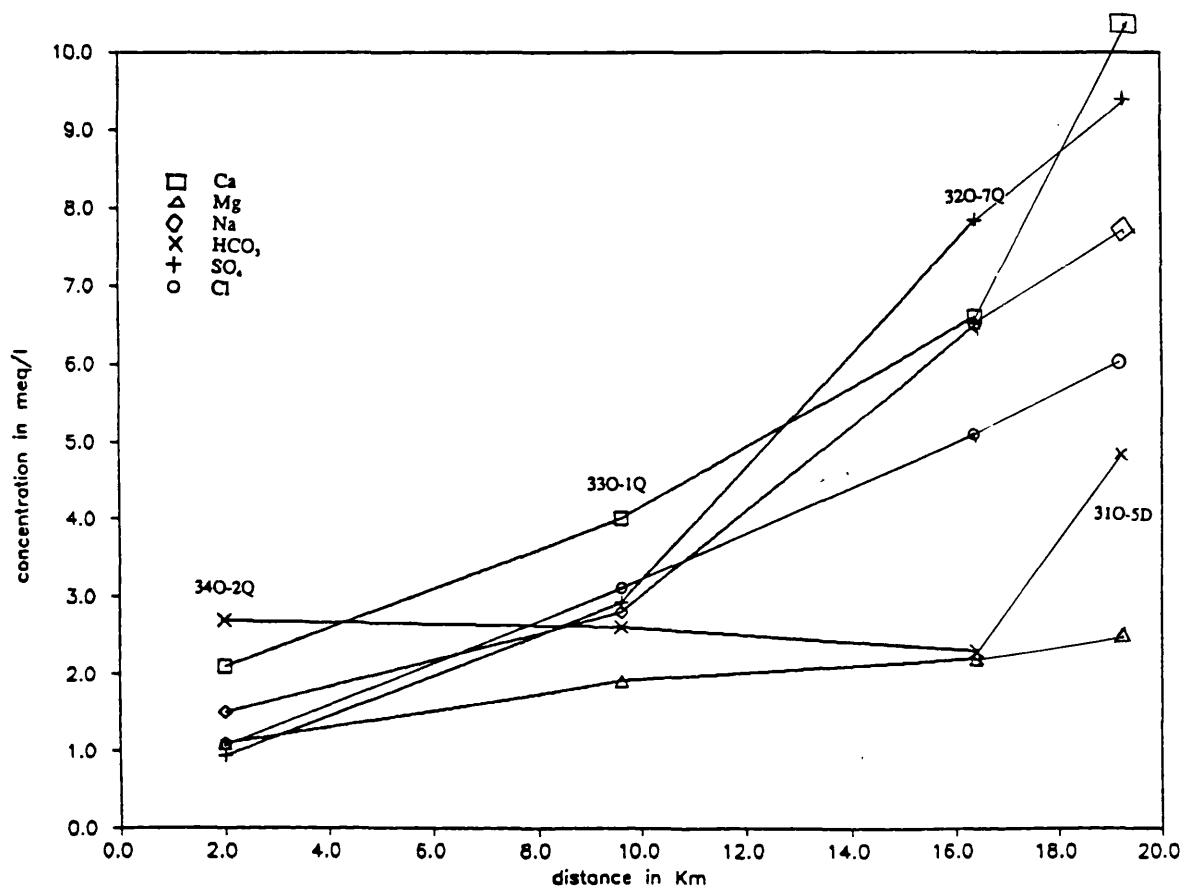
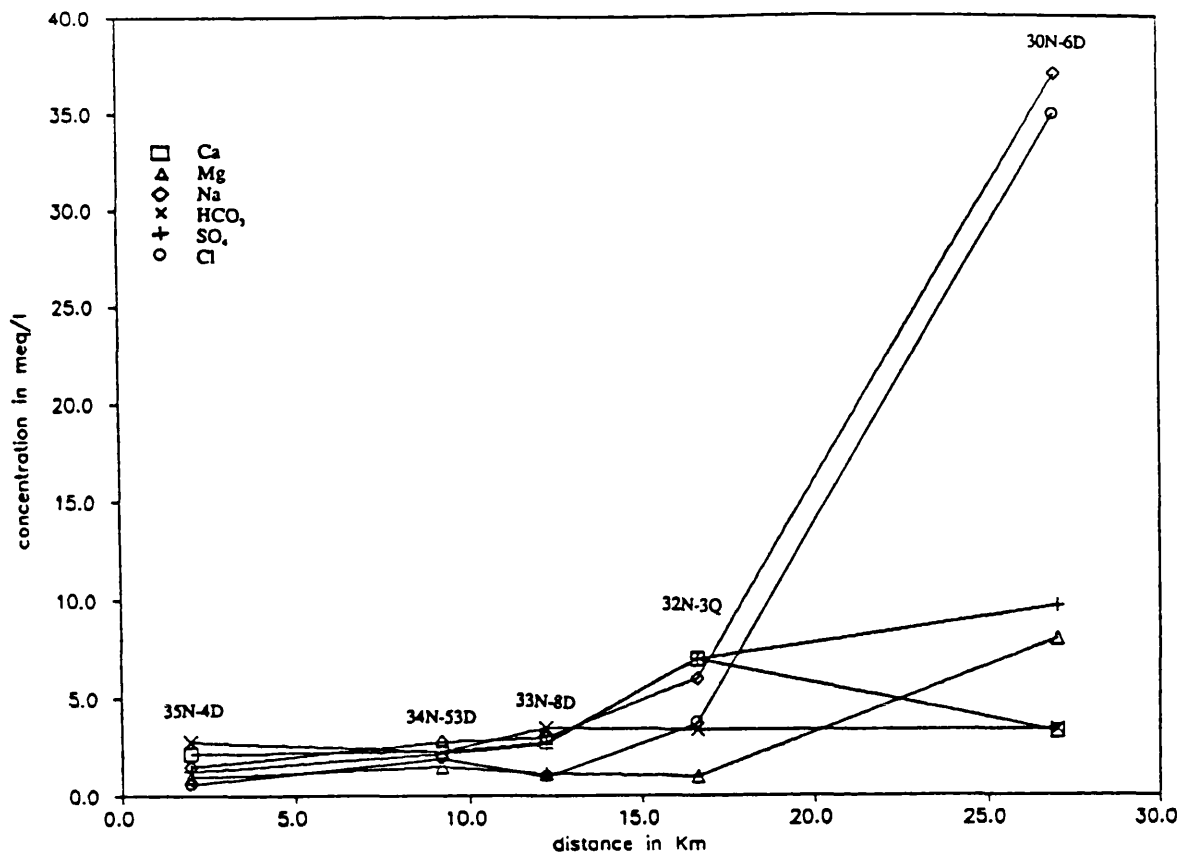
$$\text{total hardness} = 2.5(\text{Ca}) + 4.1(\text{Mg})$$

or in practice it can be computed by multiplying the sum of milliequivalent per litre of calcium and magnesium by 50.

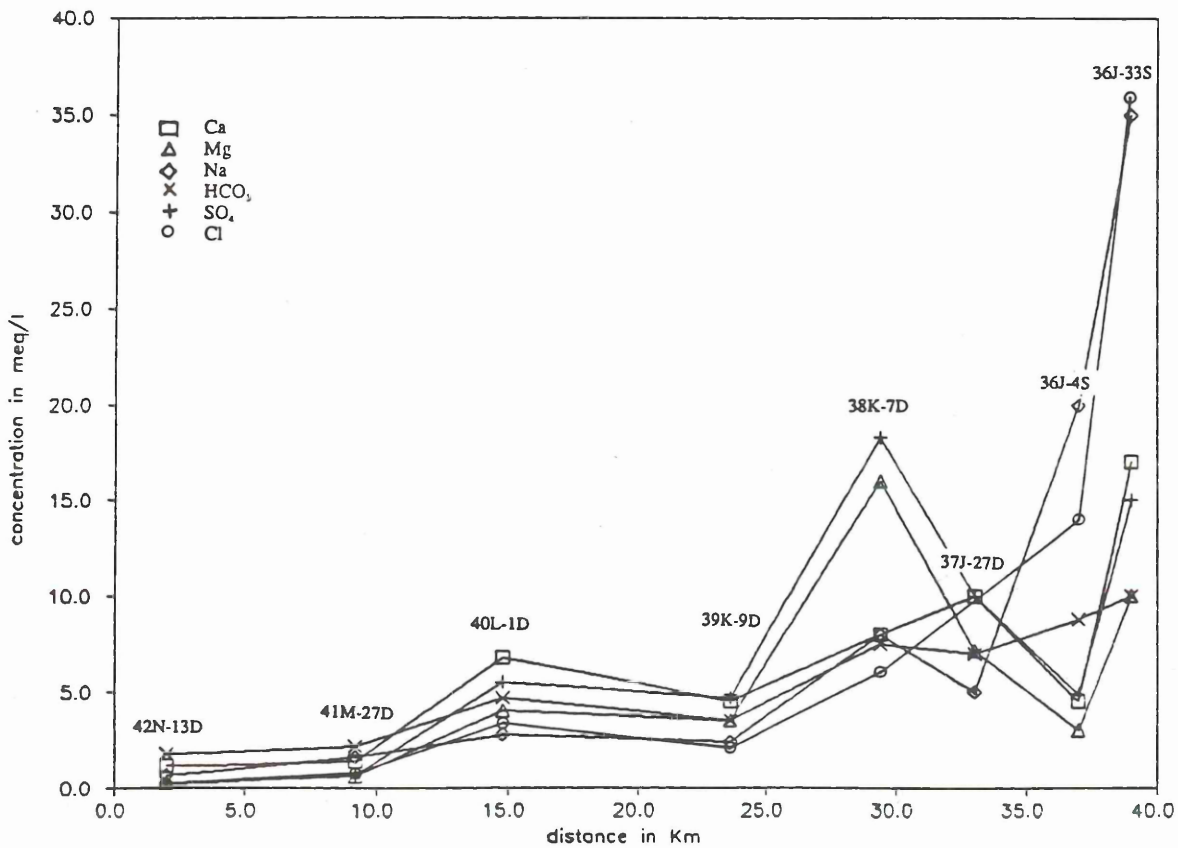
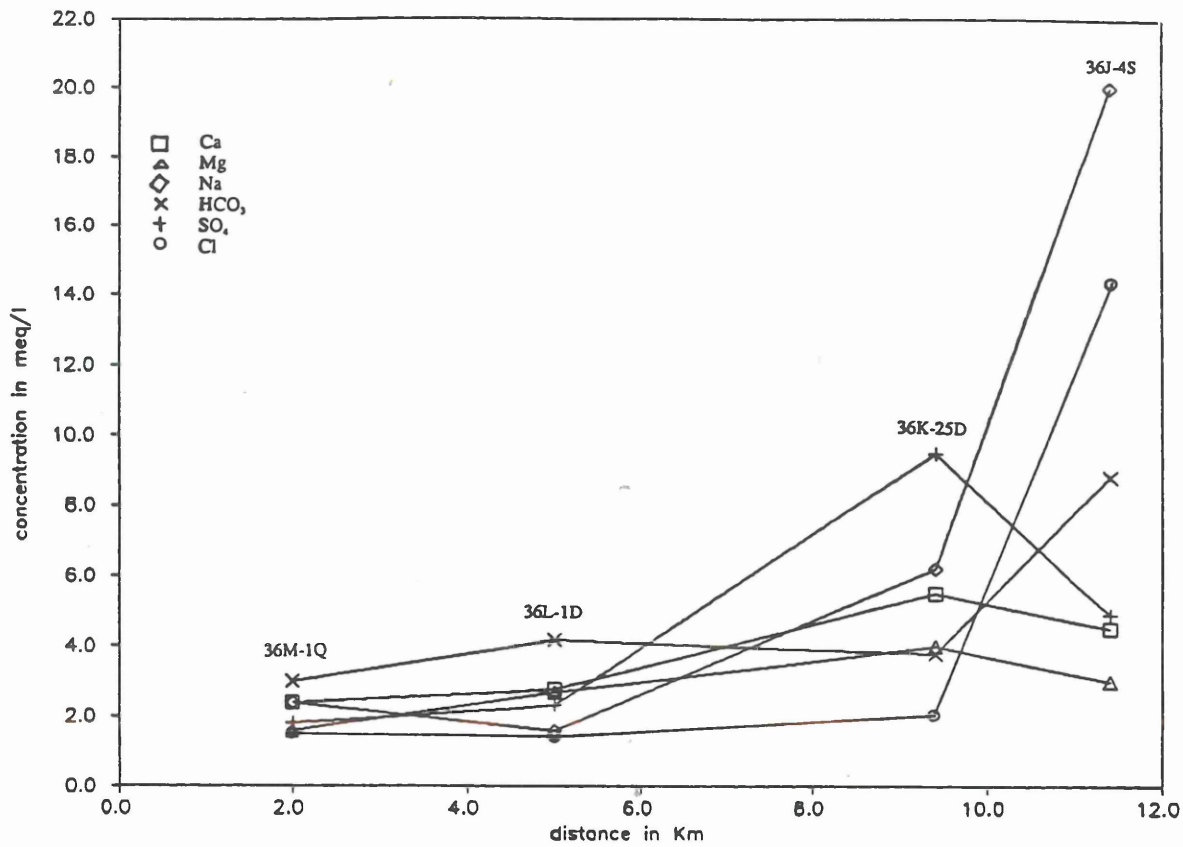
Calculated hardness values for the ground water samples of the study area are given in Appendix 7; and based on the Todd (1980) classification of the hardness (see Table 7.7) the majority of the samples (79%) are classified as very hard, 17% as hard and 4% as moderately hard waters.

**Table 7.7**

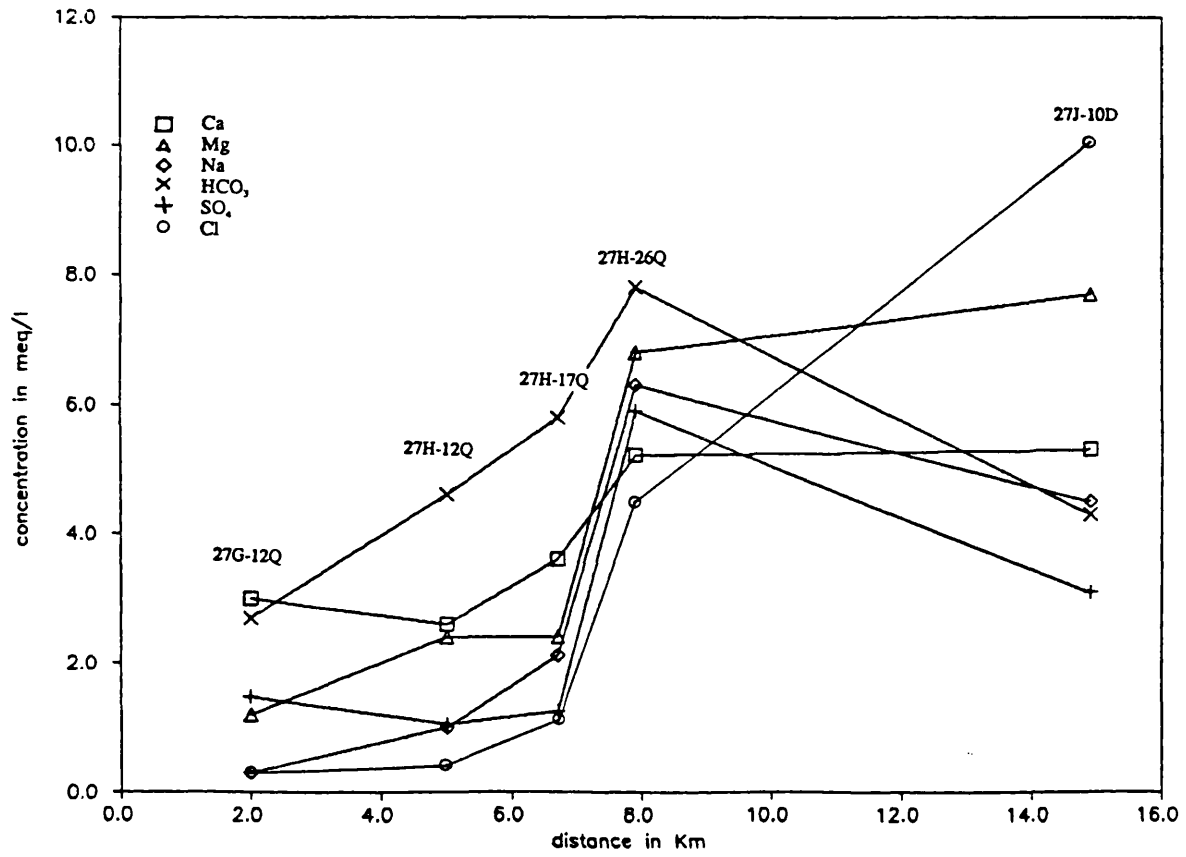
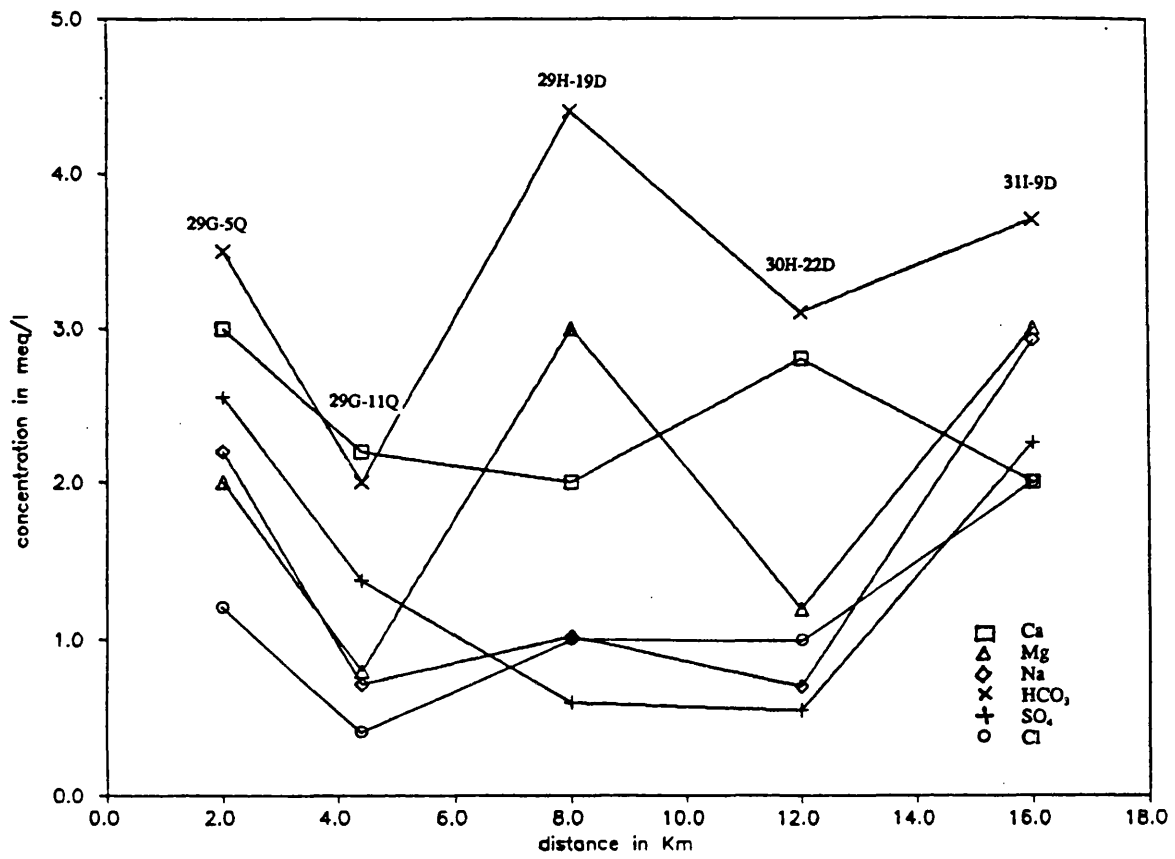
<u>hardness</u> <u>mg/l as <math>\text{CaCO}_3</math></u>	<u>Todd water</u> <u>class</u>	<u>sample</u> <u>(%)</u>
soft	0-75	0
moderately hard	75-150	4
hard	150-300	17
very hard	over 300	79



7.13 Hydrochemical sections along the ground water principal flow directions (a) along the A-A and (b) along the B-B (see Fig. 7.3 for the lines of sections).



7.14 Hydrochemical sections along the ground water principal flow directions (a) along the C-C, and (b) along the D-D (see Fig. 7.3 for the lines of sections).



7.15 Hydrochemical sections along the ground water principal flow directions a) along the E-E, and b) along the F-F (see Fig. 7.3 for the lines of sections).

## **7.8 Ground Water Quality Evaluation**

An immediate objective of any water quality study is to determine whether the water is suitable for the proposed use. Accordingly, reliable standards and tolerances are essential for consideration of water that is to be used for various purposes. In this study, the assessment of quality of ground water is based mainly on the data which was collected and analysed by ARWA. Those analyses are limited, and minor constituents and toxic elements have not been considered. Only some limited samples from potable water wells have been analysed by the Laboratories and Water Treatment Administration section of this organization and these analyses include some additional hydrochemical parameters.

### **7.8.1 Suitability of Ground Water for Drinking Purposes**

Water that is to be used in the home should be free of undesirable physical properties such as colour or turbidity and also should have no unpleasant taste or odour. In addition to these specifications, the water must be chemically safe for human consumption, and harmful micro-organisms must be absent.

Acceptable standards for drinking water vary from country to country depending upon economic prosperity, experience, climate and geographical location. The main standards used are those recommended by the World Health Organization, the United States Environmental Protection Agency and the European Economic Community. The standards tend to change with time as medical information becomes available so that any set of standards can only be considered as a guide.

In Table 7.8 drinking water from wells 41M-7D and 41M-50D as representatives of the Alluvial Tuff aquifer ground water are compared with the EEC standards (European Economic Community, 1975; in Lloyd,1985) for inorganic parameters.

**Table 7.8**

Parameter	GL (mg/l)	MAS (mg/l)	MRC (mg/l)	Well 41M-7D	Well 41M-50D
pH	6.5-8.5	9.5	6.0	6.5	6.6
Dis. O <sub>2</sub>	1	5	-	11	11.2
EC	400	1250	-	390	410
TDS	-	1500	-	290	316
TH	35	-	10	144	168
Ca	100	-	10	43	43
Mg	30	50	5	9	14
Na	20	100	-	32	35
K	10	12	-	7	8
HCO <sub>3</sub>	30	-	-	171	171
SO <sub>4</sub>	5	250	-	32	36
Cl	25	200	-	25	30
NO <sub>3</sub>	-	50	-	4	3
NO <sub>2</sub>	-	0.1	-	0	0
As	-	0.05	-	0	0
P	0.3	2.0	-	0.1	0.1

GL= Guide level      MAS= Maximum admissible concentration

MRC= Minimum required concentration      Dis. O<sub>2</sub> = Dissolved oxygen

TH= Total Hardness

As Table 7.8 shows, ground water from the Alluvial Tuff aquifer is very suitable for drinking in comparison with the EEC guides level for those parameters which have been measured. There are no data available for the minor elements and hardness is also higher than the guide level concentration. The ground water quality data from the Tabriz Plain (Appendix 7) is varied, in the high lands as well as where they come from the non evaporite formations, the quality shows good agreement with the standards, but in low lands and in evaporite deposits the quality is very poor and the standards never can be met.

### 7.8.2 Suitability of Ground Waters for Agriculture

Waters required for agricultural purposes include all the requirements for the non-domestic purposes on farms, water consumed by livestock, and waters used for



irrigation. Standards for livestock are not readily available, so that for the most part drinking standards for humans are applied. However, most animals can tolerate higher concentrations of total dissolved solids. The upper limits of the TDS in water for the different kinds of livestock were given by McKee and Wolf (1963, in Hem 1985) listed in Table 7.9.

**Table 7.9**

<u>Stock</u>	<u>Concentration (mg/l)</u>
Poultry	2,860
Horses	6,435
Dairy Cattle	7,150
Beef Cattle	10,100
Sheep (adult)	12,900

So far as the total dissolved solids are concerned, it seems that ground waters in the Tabriz area are suitable for livestock purpose.

The most extensive use of ground water in the area is for the irrigation of crops. As a result, a considerable study of the susceptibility of plants and their growth to the quality of the water used for irrigation is necessary. The suitability of ground water for irrigation depends on the types of plants and the soil.

Salt concentration in water may harm plant growth by changing the osmotic condition in the root zone which can automatically change the rate of water flow to the plants. Normally, osmotic effects are caused by total salt concentrations and the osmotic pressure of soil waters relates directly to the electrical conductivity. According to Shainbery and Oster (1978), for the range of EC that will permit plant growth, the osmotic pressure has the relation:

$$OP = 0.36 \text{ EC mS cm}^{-1}$$

Further, the effects of salts on soils, creating changes in soil structure, permeability and aeration potential, can affect plant growth indirectly.

Soil type, climatic conditions and management of irrigation and drainage may

influence the reactions of a given crop to the salt constituents. A guideline for relative tolerances of crops to salt concentration is given in Table 7.10 (after Todd, 1980). According to this table the concentrations of salt in the alluvial tuff and fans are suitable for most type of crops, whereas in the central part of the Plain it is mainly restricted to very high salt tolerance crops.

In addition to salt concentration, most classification systems include specific ion effects such as sodium and boron concentrations. Sodium concentration is important in classifying an irrigation water because it reacts with soil to reduce its permeability. The Salinity Laboratory of the United States Department of Agriculture (1954) recommended the sodium adsorption ratio (SAR) and EC for classifying irrigation water.

This graphical classification was used to evaluate the ground waters of Tabriz area for irrigation purposes. The plotted data for SAR and EC (Appendix 7) in the diagram (Fig. 7.16) indicates that most of the ground waters from the Alluvial Tuff aquifer fall within C2S1 class or in general ranges between C1S1 to C3S1, which reveals low to high salinity hazard and low sodium hazard. Data from the northern part of the Tabriz Plain ranges between medium to very high salinity hazards and low to very high sodium hazards. However, data from the central Tabriz Plain, except in a few cases, lies in high and very high salinity hazards and low to very high sodium hazards classes.

Excessive boron concentrations can be toxic for some plants, despite very small quantities being necessary for normal growth of all plants. Unfortunately, there is no data available for boron concentrations from the Tabriz area.

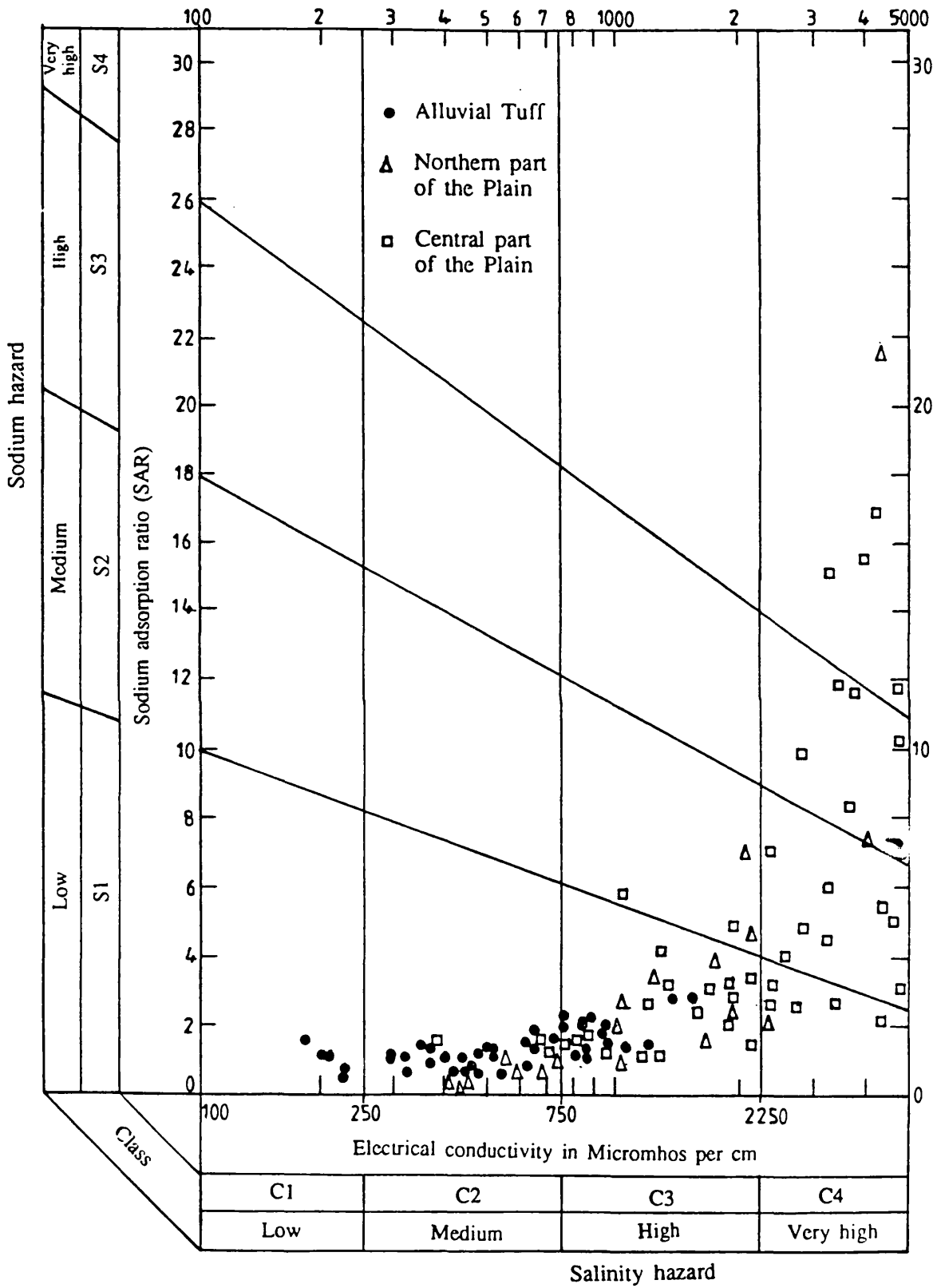


Fig. 7.16 Classification of ground waters of the Tabriz area for irrigation purposes.

Crop Division	Low Salt Tolerance	Medium Salt Tolerance	High Salt Tolerance	
Fruit crops	Avocado	Cantaloupe	Date palm	
	Lemon	Date		
	Strawberry	Olive		
	Peach	Fig		
	Apricot	Pomegranate		
	Almond			
	Plum			
	Prune			
	Grapefruit			
	Orange			
	Apple			
	Pear			
	Vegetable crops	3000 $\mu\text{S}/\text{cm}$	4000 $\mu\text{S}/\text{cm}$	10,000 $\mu\text{S}/\text{cm}$
Green bean		Cucumber	Spinach	
Celery		Squash	Asparagus	
Radish		Peas	Kale	
4000 $\mu\text{S}/\text{cm}$		Onion	Garden beet	
		Carrot	12,000 $\mu\text{S}/\text{cm}$	
		Potato		
		Sweet corn		
		Lettuce		
		Cauliflower		
		Bell pepper		
		Cabbage		
		Broccoli		
		Tomato		
		10,000 $\mu\text{S}/\text{cm}$		
Forage crops		2000 $\mu\text{S}/\text{cm}$	4,000 $\mu\text{S}/\text{cm}$	12,000 $\mu\text{S}/\text{cm}$
		Burnet	Sickle milkvetch	Bird's-foot trefoil
	Ladino clover	Sour clover	Barley (hay)	
	Red clover	Cicer milkvetch	Western wheat grass	
	Alsike clover	Tall meadow oat grass	Canada wild rye	
	Meadow foxtail	Smooth brome	Rescue grass	
	White Dutch clover	Big trefoil	Rhodes grass	
	4000 $\mu\text{S}/\text{cm}$	Reed canary	Bermuda grass	
		Meadow fescue	Nattali alkali grass	
		Blue grame	Salt grass	
		Orchard grass	Alkali sacaton	
		Oats (hay)	18,000 $\mu\text{S}/\text{cm}$	
		Wheat (hay)		
		Rye (hay)		
		Tall fescue		
		Alfalfa		
		Hubam clover		
		Sudan grass		
		Dallis grass		
		Strawberry clover		
		Mountain brome		
		Perennial rye grass		
		Yellow sweet clover		
	White sweet clover			
	12,000 $\mu\text{S}/\text{cm}$			
Field crops	4000 $\mu\text{S}/\text{cm}$	6000 $\mu\text{S}/\text{cm}$	10,000 $\mu\text{S}/\text{cm}$	
	Field bean	Castor bean	Cotton	
		Sunflower	Rape	
		Flax	Sugar beet	
		Corn (field)	Barley (grain)	
		Sorghum (grain)	16,000 $\mu\text{S}/\text{cm}$	
		Rice		
		Oat (grain)		
		Wheat (grain)		
		Rye (grain)		
	10,000 $\mu\text{S}/\text{cm}$			

NOTE: Electrical conductance values represent salinity levels of the saturation extract at which a 50 percent decrease in yield may be expected as compared to yields on nonsaline soil under comparable growing conditions. The saturation extract is the solution extracted from a soil at its saturation percentage.

Table 7.10 Relative tolerances of crops to salt concentrations (after Richards, in Todd, 1980).

## **CHAPTER 8**

### **GROUND WATER RESOURCES**

#### **8.1 Introduction**

#### **8.2 Estimation of Resources**

##### **8.2.1 Introduction**

##### **8.2.2 Ground Water Recharge**

###### **8.2.2.1 Infiltration from Precipitation**

###### **8.2.2.2 Irrigation and Municipal Return Flow**

###### **8.2.2.3 Infiltration from Losing Streams**

##### **8.2.3 Ground Water Discharge**

###### **8.2.3.1 Artificial Withdrawal by Wells and Qanats**

###### **8.2.3.2 Natural Spring Discharge**

###### **8.2.3.3 Actual Evaporation and Transpiration**

##### **8.2.4 Ground Water Budget**

#### **8.3 Ground Water Management**

## CHAPTER 8

### GROUND WATER RESOURCES

#### 8.1 Introduction

Ground water resources in Iran, especially in the Tabriz area where surface water sources are inadequate, have been recognised and used from ancient times. About 980 qanats in the study area testify to the fact that ground water was the main source of water for domestic, municipal and agricultural purposes.

Following the growth in the population in recent years, demands for water substantially increased and new wells were utilised for the necessary rapid development. As a result, ground water levels declined and some of the qanats dried up. In 1976, the Azarbijan Regional Water Authority (ARWA) announced that the usage of ground water from the Liquvan and Saidabad areas (part of the alluvial tuff aquifer to the south and south-east of Tabriz City) was to be only for municipal purposes and farmers were not allowed to put down any new well in this area (Nowtash et al., 1984).

Ground water now makes up 100 percent of the municipal and industrial requirements and about 80 percent of agricultural water supply demands in the study area. Therefore, the authorised planning for usage of ground water resources require careful assessment, protection, and management, which has been neglected to some extent in the past.

Determination of the available water within a basin requires evaluation of those active elements of the hydrological cycle which make significant contributions to water balance computations from both potable and non-potable sources.

#### 8.2 Estimation of Resources

##### 8.2.1 Introduction

Ideally, before any large scale development of ground water takes place in a basin, an estimation of ground water inputs and outputs is very important in order to prevent future reduction of yields and/or deterioration of ground water quality. However, this estimation is not an easy practice, because so many parameters are involved and direct or indirect measurements of them are very difficult. There are

various methods available to assess the ground water resources in an area (see Williamson et al., 1981). But the hydrological budget (water balance) method is preferred because (a) it has the advantage of providing a fuller understanding of the hydrology in its wider context and (b) there were inadequate data available for the other methods.

The simple water balance equation that considers the interrelationship of ground and surface waters is:

**Inputs = Outputs + Change in Storage**

the inputs include those components that regulate the flow into the ground water resources (recharge) and outputs are those that take water from the basin.

The acceptable balance of water depends on the proper identification and calculation of the various components of the hydrological cycle that control the natural and artificial inputs and outputs. The following are the most important components of input or recharge in the study area; (a) direct infiltration from precipitation (b) irrigation return flow and infiltration from sewage water (c) infiltration from losing streams. The components of outputs are; (a) evapotranspiration (b) spring discharge (c) artificial withdrawal by pumping wells and qanats.

As it is clear from Chapter 4, inputs and outputs to ground water resources in the area operate on a closed system. In other words, there is no ground water inflow and outflow across the boundaries of the study area and the only major river that crosses the border of the area is the Aji Chay river which has daily flow measurements at two points, one where it enters the area (at Vanyar station) and the other some 40km downstream at Akhole.

## **8.2.2 Ground Water Recharge**

The ground water recharge for the southern (southern alluvial fans and tuff) and northern parts of the area is estimated separately. The recharge to ground water in these areas can take place from different sources as outlined above.

### **8.2.2.1 Infiltration from precipitation**

**(a) Infiltration in Southern Part of the Area:** For estimating direct recharge from

precipitation, identification of the following factors is essential; (i) the area of ground over which direct recharge of precipitation takes place and (ii) the amount of effective infiltration.

The first factor is the area of the unconfined aquifer and it can be computed easily. But the second factor needs more consideration. There is no direct and accurate method to determine the effective infiltration from precipitation for a catchment. Also the well known indirect approach in the form of a water balance computation (see Chapter 2) which calculates the actual evapotranspiration is not applicable for this study area. Therefore, in these circumstances, it seems that two approaches can be used to establish the amount of effective infiltration in different parts of the area.

The first approach uses the values that were mentioned in literature and previous works with respect to geological formations. For example Kuros (1978) considered the water balance for the Sahand area and he assumed the amount of direct effective infiltration to the aquifer to be 100mm with reference to Bentz's (1969) assumptions of infiltration to ground water in different climate and geological conditions. This value gives about 25 to 30 percent of total precipitation which is a relatively high value in semi-arid regions.

The second applies a water balance for a small area within the region and generalizes the resultant actual evapotranspiration to the whole study area taking into account the other hydrological conditions. According to the following equation:

$$P = R + E_a + \Delta s$$

where P is precipitation,  $R = R_1 + R_o + R_i$  where  $R_1$  is river discharge and  $R_o$  and  $R_i$  are overland flow and interflow, respectively,  $E_a$  is actual evapotranspiration and  $\Delta s$  is the storage change. The  $\Delta s$  value may be taken as constant for long durations of time (5 to 10 years).

As explained in Chapter 4, the Sahand mountain is formed of two types of formation (a) a permeable alluvial tuff extending over 1400 km<sup>2</sup> area that actually lies between elevations 1500 and 2400m and (b) lowly permeable or impermeable andesitic rocks above 2400m elevation having 500 km<sup>2</sup> area (see Fig. 4.1). However,



in some areas the superficial weathered andesitic rocks can store and transmit some interflow into the alluvial tuff aquifer downslope.

The river discharge analysis results from some stations in the upper part of the Sahand mountain such as Liquvan, Zinjanab and Germezi-Gol (see Fig. 2.1) indicate that the water flow from the andesitic rocks provides an average total streamflow of 298 mm/year and baseflow of 150 mm/year for the overall area (see Table 2.4). These values represent 60 and 30 percent of total precipitation, respectively. If we assume that only 10 percent of the precipitation from this area crosses the border of the aquifer as overflow and interflow, the sum of this and total run-off will exceed 70 percent of the total precipitation.

As a result, the quota of actual evapotranspiration should be only 30 percent of the total precipitation. Thus if this case is generalized to the alluvial tuff formation as a whole, it may be concluded that the direct effective infiltration of 120 mm/year is not an overestimated value.

Consequently, the total volume of water which directly infiltrates (from precipitation) into the alluvial tuff aquifer can be calculated as:

$$v_w = A \times I_e \quad (8.1)$$

where  $v_w$  = volume of water in  $m^3$ ,

$A$  = area in  $m^2$  and

$I_e$  = effective infiltration.

Then,  $1400 \times 10^6 \times 0.12 = 288 \times 10^6 \text{ m}^3$

and the interflow and overflow from the andesitic rocks as:

$$500 \times 10^6 \times 0.05 = 25 \times 10^6 \text{ m}^3 .$$

The area of the southern alluvial fans is  $250 \text{ km}^2$  and the amount of direct effective infiltration into this aquifer is assumed to be 100 mm/year due to higher actual evapotranspiration and lower precipitation in comparison with the alluvial tuff. Therefore, it can be calculated from the equation (8.1) as:

$$250 \times 10^6 \times 0.1 = 25 \times 10^6 \text{ m}^3/\text{year}$$

**(b) Infiltration in Northern Part of the Area:** The above-mentioned method of estimating the direct effective infiltration into the aquifer can be used for the northern part of the area. The general topographical conditions in this part are more or less the same as in the southern part but the amount of precipitation as well as the geological conditions especially in the mountainous area are quite different.

The amount of river discharge from the mountainous aquitard is measured at Daryan station (see Fig. 2.1). According to these measurements, the average six-year total river discharge in this area is about 60 percent of the total precipitation (precipitation 400 mm/year). The average pan evaporation in the northern alluvial fans is more than in the southern part. Hence, the amount of effective infiltration is assumed to be 100 mm/year and the direct infiltration to the alluvial fans aquifer with 470 km<sup>2</sup> area is:

$$470 \times 10^6 \times 0.10 = 47 \times 10^6 \text{ m}^3$$

The interflow and overland flow from the mountainous area to the aquifer (downslope) is assumed to be 10 percent of the total precipitation from all over the area (940 km<sup>2</sup>), hence it can be calculated:

$$940 \times 10^6 \times 0.04 = 37.6 \times 10^6 \text{ m}^3$$

#### **8.2.2.2 Irrigation and Municipal Return Flow**

Water returned from irrigation activities to the ground water resources is not easily estimated. It depends on the type of soil, irrigation method etc. Irrigation in the area is carried out during June to October when the precipitation is insignificant and the weather is suitable for the growing of crops. Throughout this period, soil moisture deficits are high and most of the crops need to be irrigated. During the irrigation period any water in excess of field capacity infiltrates down to the ground water resources as irrigation return flow.

The irrigation water required for crop growing in the area mainly comes from ground water via qanats, deep and shallow pumping wells and, depending on the time, from surface water (20 percent).

However, the water demands for drinking, domestic, municipal and industrial uses all come from ground water resources. The large city of Tabriz, with 2 million population and highly industrial areas, consumes the highest amount of ground water in the area. The daily water used in this city is about 260,000 m<sup>3</sup> (3 m<sup>3</sup> /s). There are no modern sewage network facilities for collecting sewage and municipal waste waters in the area, and all used water (after evaporation of part) infiltrates into the ground. As a result, the ground water storage around this city and other towns rises during the high water demand period.

According to the ARWA (Azarbijan Regional Water Authority), the amount of water that is withdrawn from ground water resources during the year (1987) is 670 million m<sup>3</sup>. Therefore, if it is assumed that 40 percent of this water returns to ground water storage, the total annual return flow should be:-

$$670 \times 10^6 \times 0.4 = 286 \times 10^6 \text{ m}^3$$

It should be mentioned that the main disadvantage of the qanat is that water continues to flow throughout the year, whereas demand for irrigation water is concentrated during the above-mentioned period.

### 8.2.2.3 Infiltration from Losing Streams

During the winter and spring seasons, the flow of the rivers increases due to a large amount of precipitation and melting of snow. As explained in Chapter 2, the stream network in the area can be divided into three main systems: (1) River Aji Chay, (2) northern rivers, and (3) southern rivers.

**Aji Chay**: This river enters the area at its eastern boundary (see Fig. 2.1), passes through the Vanyar gorge and after some 100km joins the Orumiyeh Lake. In this part of its course, daily flow measurements are made at Vanyar and Akhole stations (some 40km apart). The average total streamflow for the three years 1984 to 1986 is shown in Table 2.4. The average total streamflow decreased from 5310 cumec-

days at Vanyar station to 4545 cumec-days at Akhole station, a loss of 14 percent of the total flow. It seems, that most of the losses are as evaporation rather than infiltration because of the flatness of the area, the low permeability of the material, and the high evaporation rate. However, some infiltration takes place to buried channels and the water table aquifer from this river. But due the poor quality of this water, the abstraction from the recharge area does not take place and the fluctuations of water level depend on the evaporation rate.

**Southern rivers:** From the five main rivers in the southern part of the area, the rivers Liquvan and Saidabad join the River Aji Chay only during the wettest seasons. The other three dry up in the lower part of their courses due to infiltration and evaporation losses and diversion of their water for irrigation.

Two of these rivers (Liquvan and Sardrud) were gauged at upstream and downstream locations and provide a good opportunity to consider the river behaviour during its course. The average seven-year total streamflows (1980 to 1986) measured at the Liquvan station, with a 76 km<sup>2</sup> catchment and at the Hervi station with a 186.3 km<sup>2</sup> catchment indicate an 8 percent reduction in total flow along this length. Hence, there is no significant contribution to the river flow after the Liquvan station and in the case of low flow, most of the water losses are due the infiltration and evapotranspiration processes. After the Hervi station these losses become very high and only a small part of river flow can reach the Aji Chay river, and even that is restricted to very wet seasons.

Therefore, it can be concluded that the water contributed to the southern rivers comes from the andesitic mountainous area (500 km<sup>2</sup>) and is lost through the alluvial tuff and fans due to infiltration and evapotranspiration processes.

If it is assumed that 50 percent of this water infiltrates to the aquifers, the total recharged water from the southern rivers can be estimated as:

$$500 \times 10^6 \times 0.298 \times 0.5 = 74.75 \times 10^6 \text{ m}^3$$

**Northern rivers:** There are seven rivers in the northern part of the area, and they also very seldom reach to the Aji Chay river. The general topographical conditions in this part are more or less the same as in the southern part. However, the amount

of precipitation is less than the southern part especially in the north-east which receives the minimum amount in the area. The evapotranspiration varies in the opposite sense and it is higher in the northern part.

The method that was used for estimating the amount of infiltration into ground water from the southern rivers can also be used in this part, if the change in climatic conditions is taken into account. Hence, it may be assumed that the contribution from the mountainous area to the river discharge is about 200 mm/year all over the area and infiltration from the rivers accounts for 40 percent of the total river discharge. Then:

$$940 \times 10^6 \times 0.2 \times 0.4 = 75.2 \times 10^6 \text{ m}^3$$

### 8.2.3 Ground Water Discharge

#### 8.2.3.1 Artificial Withdrawal by Wells and Qanats

It has been mentioned previously that the ground water is used for drinking, domestic, industrial and irrigation purposes. The most extensive use is made for irrigation during the spring and summer seasons, whereas for the other purposes withdrawal from ground water is more evenly spread during the whole year. The qanats, owing to the nature of their construction, take out ground water throughout the year.

According to the ARWA (1987), 800 shallow and 1300 deep wells and 982 qanats operate in the study area. The total withdrawal from all these artificial discharge points was measured during August 1987 and generalised for the whole year by the ARWA as Table 8.1.

**Table 8.1**

Discharge Point	Number	Total Annual Discharge (Mm <sup>3</sup> )
Shallow wells	800	94.751
Deep wells	1300	409.713
Qanats	980	150.273
Total	3080	654.7376

**8.2.3.2 Natural Spring Discharge:** in addition to the pumping wells and qanats the area contains 147 springs where ground water flows at the surface. The three principal variables which determine spring discharge are aquifer permeability, contributing catchment area and amount of ground water recharge. The average total flow of  $17.335 \times 10^6 \text{ m}^3$  per year was recorded from these springs by ARWA (1987) which brings the total ground water discharge in the area to  $672.072 \times 10^6 \text{ m}^3$  /year.

### **8.2.3.3 Actual Evaporation and Transpiration**

Actual evapotranspiration is the most complex meteorological parameter and its direct measurement is impossible. Potential and actual evapotranspiration, the availability of data and methods for their estimation, and geological and climatic conditions effects were discussed in Chapter 2, where it was concluded that the calculation of actual evapotranspiration with respect to the available data is impossible for this study area.

Hence, it seems that the above-mentioned application of a water balance for a small area in the region and its generalization to the whole of the study area, taking into account the other hydrological conditions, is the only approach that can help in the estimation of realistic actual evapotranspiration rates.

**Actual Evaporation:** The actual evaporation in the small sub-catchment in the mountainous areas (in southern and northern parts of the study area) was determined by subtracting the total run-off and interflow plus overland flow from the total precipitation. The resultant value is about 30 percent of the total precipitation, but it increases toward the plain and it was assumed to be 60 percent in the southern alluvial tuff and fans and 65 percent for the northern alluvial fans, reflecting the higher average annual temperature in this part. The evaporation rate for the other parts of the area ( $3940 \text{ km}^2$ ), such as the north-east (Miocene formation) and the Central Plain, is assumed to be more than 95 percent of the total precipitation ( $200 \text{ mm/year}$ ), due to the prevailing hydrogeological conditions in this area.

Evaporation in the Tabriz Central Plain is more than the total rainfall falling on the area because the spread of the Aji Chay river water in this area during the wet season makes more water available for evaporation. The percentage and volumetric evaporation amounts from these areas are shown in Table 8.2.

**Table 8.2.**

Location	Area (km <sup>2</sup> )	Precipitation (mm/year)	Evaporation (%)	Evaporation (Mm <sup>3</sup> /year)
Southern upper M.	500	500	30	75
Alluvial tuff	1400	300	60	252
Southern All. fans	250	230	60	34.5
Northern upper M.	940	400	30	112.8
Northern All. fans	470	250	65	76.4
Other areas	3940	200	95	748.6
Total	7500	-	-	1,230

**Transpiration:** Actual transpiration is related to the water movement through plants and it is defined as the water exchange between soil and atmosphere through the root system (Balek, 1989). The mechanism of transpiration is well understood but difficult to quantify or present in mathematical terms.

The amount of water loss from the catchment due to transpiration depends on the availability of water, degree and type of vegetation, along with climatic factors.

In some parts of the study area, water is only available during the spring, whereas in some other areas, where surface and ground waters are used for irrigation purposes, it lasts until the end of the summer season. It is assumed that average transpiration for the study area is about 15 mm per year which is only 5 percent of total average precipitation (average precipitation = 300 mm/year). Thus, it can be calculated as:

$$7500 \times 10^6 \times 0.015 = 112.5 \times 10^6 \text{ m}^3/\text{year}$$

Figure 8.1 represents components of the hydrological cycle in three adjacent areas.

#### 8.2.4 Ground Water Budget

For a given period of time, the total incoming ground water is balanced by the total outgoing ground water plus or minus changes in ground water storage. This balance expresses a ground water budget and may be stated as:

$$I = O + \Delta s$$

where I is total recharge to ground water, O= total outputs and  $\Delta s$  = change in storage.

Among the recharge elements, the irrigation and municipal used-water return flow, the effective infiltration from precipitation and influent seepage from rivers, as well as the overland and interflow originating from the higher mountains are the most important sources of recharge in the area. Artificial withdrawal and ground water evapotranspiration make up the larger components of ground water discharge. Nearly all the effective components of ground water recharge and discharge were estimated, except evaporation from the shallow aquitards such as the central plain and the alluvial fans. This value is assumed to be the same as the transpiration rate ( $90 \times 10^6$  m<sup>3</sup>/year)

In the case of the Tabriz area, a sound knowledge of the ground water occurrence and the continuity of the mountain and plain regions is essential. The hydrological components of the adjacent areas and the behaviour of ground water in these areas are shown in Figure 8.1.

There is no significant effective infiltration in the higher mountains and the high amounts of precipitation losses from these areas as runoff, overland flow and interflow, as well as the gains by lower mountains and plain intake areas, have been explained in previous sections.

The ground water budget is similar to a surface water balance and requires proper identification and determination of different components of recharge and discharge. These components can only function where there is a permeable geological stratum capable of containing and transmitting ground water under natural field conditions.

Therefore the ground water budget in the lower mountains and Tabriz plain



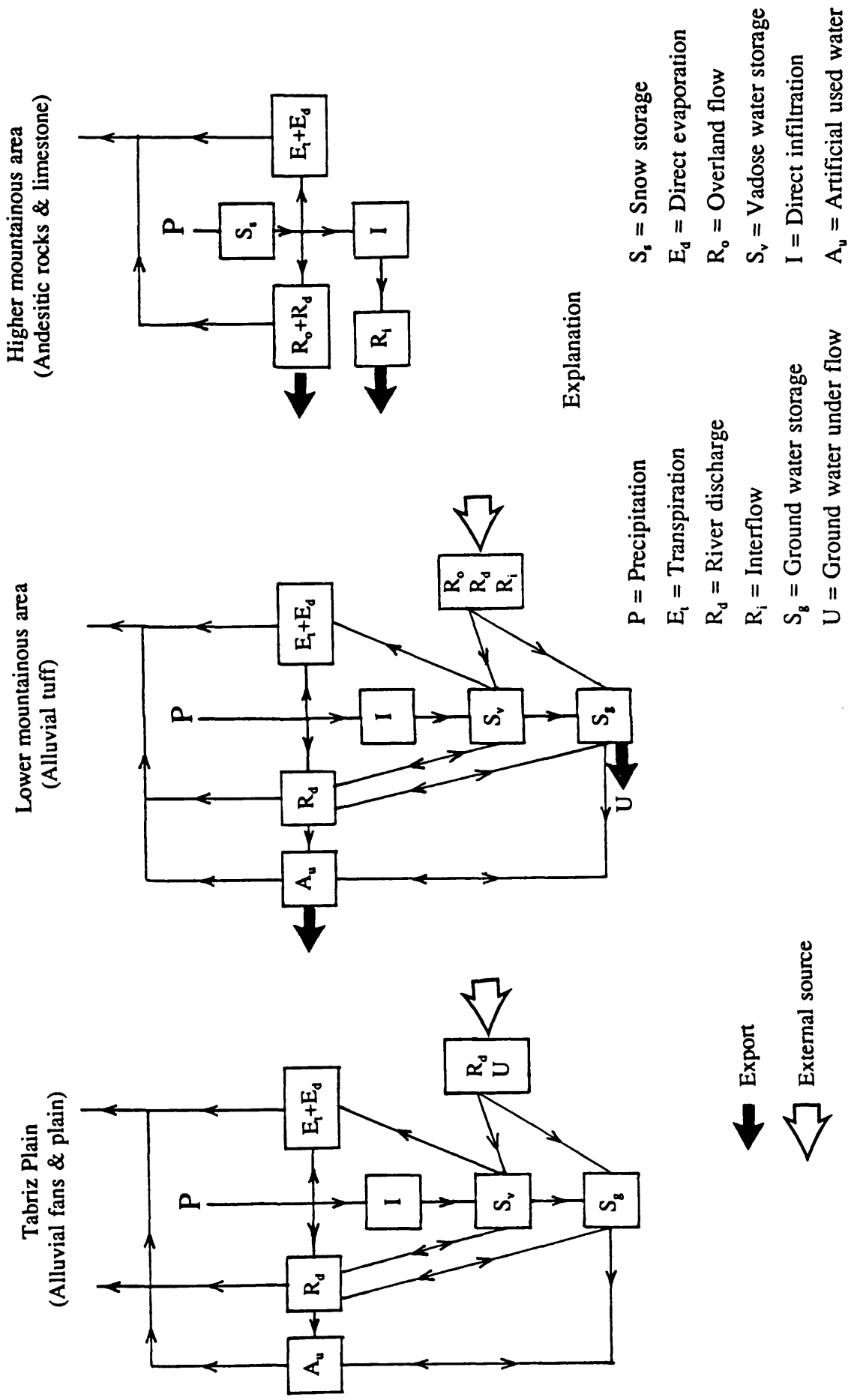


Fig. 8.1 The hydrological components of the adjacent areas and the behaviour of the groundwater in these areas.

aquifers can be considered as in Table 8.3.

**Table 8.3**

<u>Input Components</u>	<u>Input Amounts (Mm<sup>3</sup>/year)</u>	<u>Output Components</u>	<u>Output Amounts (Mm<sup>3</sup>/year)</u>
Direct Effective Infiltration	360	Shallow Wells	95
Irrigation and Municipal Return Flow	286	Deep Wells	410
Influent Seepage from Rivers	150	Qanats	150
Overland & Interflow from Higher Mountains	63	Springs	17
		Evapotranspiration	113
Total	859	Total	785

### **8.3 Ground Water Management**

**a) Concept and Practice:** Ground water management was defined by Todd (1980) as "a program of development and utilization of sub-surface water for some stated purpose, usually of a social and economic nature, or in other words, the desired goal to obtain a maximum quantity of water to meet predetermined quality requirements at least cost". Bear and Verruijt (1989) state that "management is making such decisions as to the total quantity of water to be withdrawn annually, the location of wells for pumping and conditions at aquifer boundaries". With respect to these definitions, management needs to pay as much attention to the artificial as to the natural aspects of the hydrological cycle.

According to Jones (1972), during a youthful state of ground water development, management practice is unappreciated but desirable. Effective management practice becomes increasingly necessary when a mature state of ground

water development operates, while highly sophisticated management becomes essential during the old age and rejuvenation states of development, if the resources are to be prevented from further damage. During these stages, great care and manipulation of resources is required with critical assessment of both permanent and temporary storage and perennial yield for the conjunctive use of surface water, ground water, and consideration of artificial recharge to ground water.

As explained in Chapter 4, the ground water levels are declining in those parts of the aquifers in which fresh water is available and the annual replenishment is known to be less than the total water withdrawal (see Figs 4.8 to 4.9). Following the criteria of Jones (1972) in the approach to management, and the previous discussions of water balance and ground water resources, the state of development in most part of the study area has passed into the phase of 'old age' when management of resources is an essential requirement.

**b) Demands and supply methods:** Demands on any scheme of water management in the study area would include the following items: (i) public water supply, (ii) agricultural water supply, (iii) industrial water supply, (iv) waste water control and (v) recreational usage water.

To meet these demands, precipitation is the ultimate source of water and in the high mountain area largely becomes surface run-off, whereas in lower mountain and plain areas this run-off water and most of the direct precipitation infiltrates into high permeability strata and becomes a sub-surface resource.

The management or selection of the best policies that will lead to satisfying of these demands can be considered by a variety of methods which include constraint, re-use, waste-water control, and artificial recharge.

**c) Perennial Yield:** The modern concept of 'optimal yield' and 'safe yield' is expressed in terms of perennial yield. Todd (1980) defines the perennial yield of ground water as "the amount of water can be withdrawn from it perennially under specified operating conditions without producing an undesired result such as progressive reduction of water resources, development of uneconomic pumping conditions, degradation of ground water quality and interference with prior water rights."

The perennial yield in a basin is governed by the recharge criteria and any

water development operates, while highly sophisticated management becomes essential during the old age and rejuvenation states of development, if the resources are to be prevented from further damage. During these stages, great care and manipulation of resources is required with critical assessment of both permanent and temporary storage and perennial yield for the conjunctive use of surface water, ground water, and consideration of artificial recharge to ground water.

As explained in Chapter 4, the ground water levels are declining in those parts of the aquifers in which fresh water is available and the annual replenishment is known to be less than the total water withdrawal (see Figs 4.8 to 4.9). Following the criteria of Jones (1972) in the approach to management, and the previous discussions of water balance and ground water resources, the state of development in most part of the study area has passed into the phase of 'old age' when management of resources is an essential requirement.

**b) Demands and supply methods:** Demands on any scheme of water management in the study area would include the following items: (i) public water supply, (ii) agricultural water supply, (iii) industrial water supply, (iv) waste water control and (v) recreational usage water.

To meet these demands, precipitation is the ultimate source of water and in the high mountain area largely becomes surface run-off, whereas in lower mountain and plain areas this run-off water and most of the direct precipitation infiltrates into high permeability strata and becomes a sub-surface resource.

The management or selection of the best policies that will lead to satisfying of these demands can be considered by a variety of methods which include constraint, re-use, waste-water control, and artificial recharge.

**c) Perennial Yield:** The modern concept of 'optimal yield' and 'safe yield' is expressed in terms of perennial yield. Todd (1980) defines the perennial yield of ground water as "the amount of water can be withdrawn from it perennially under specified operating conditions without producing an undesired result such as progressive reduction of water resources, development of uneconomic pumping conditions, degradation of ground water quality and interference with prior water rights."

The perennial yield in a basin is governed by the recharge criteria and any

quantitative determination of it is based on specified conditions. Any changes in these conditions will modify the perennial yield. For the present ground water regime in the study area, the factors that produce undesired results are (1) a sharp decline of ground water levels in some areas, (2) drawing in of saline ground water from nearby areas into the confined and unconfined aquifers due to excessive pumping from these aquifers in the Tabriz plain, (3) very shallow aquifer water evaporation from the Tabriz urban area due to large returns of municipal and sewage waters to the ground, and (4) saline water intrusion from some rivers which cross the Miocene formations.

The quantitative determination of perennial yield with respect to the above-mentioned conditions, and consequent results indicate that a "mining" conditions exist in parts of the study area at the present time, with artificial outputs exceeding natural inputs.

## CHAPTER 9

### GROUND WATER MODELLING

#### 9.1 Introduction

A ground water model may be defined as a simplified version of the real system that approximately simulates the operation of the system and allows manipulation of the results. The simplification is introduced in the form of a set of assumptions that expresses our understanding of the nature of the system and its behaviour. The ground water model, if properly constructed, can be a valuable predictive tool for understanding ground water flow through an aquifer, ground water development and water resource management. However, the validity of the predictions will depend on how well the model approximates field conditions and how good are the field data. Mercer and Faust (1981) concluded that the use of models should not be considered as a step-by-step procedure. Actually, it is an iterative process from which one never achieves a fully satisfactory conclusion. The reason for this is that the models can never duplicate real systems, for which complete data are never available.

Various types of models have been used for simulating ground water flow systems. These types can be divided into four broad classes such as (a) analytical, (b) numerical, (c) analogue and (d) physical models (Fetter, 1988). The numerical model was selected in this study, because of the availability of a 'user-friendly' package and its ability to handle large amounts of data.

It should be stressed that the data available from the study area are not ideal for the modelling of the ground water system. However, it was felt that an attempt to model this inadequate data would be useful to identify those areas where detailed field data are critical to the success of a model and to indicate the types of information that need to be obtained. Furthermore, it provided the author with the opportunity to familiarise himself with numerical model procedures.

This study will explain the sensitivity of the model response to different values of the parameters, measure the relative importance of the various parameters and reasonable amounts of inputs and outputs to and from the ground water. But due to the lack of suitable data, the calibration and predictive stages of the model work

can not be carried out for the modelled area.

## 9.2 Conceptual Model

The first step in the procedure of modelling is the construction of a conceptual model of the aquifer system and the ground water problem. The conceptual model includes a set of assumptions that reduces the real system to a simplified version that is acceptable from the objective point of view of the modelling. In the study area, these assumptions can be related to (a) the type of aquifer formation, (b) the geometry and boundaries of the aquifer, (c) the conditions of the boundaries, (d) the flow type in the aquifer, and (e) sources and sinks.

Only the alluvial tuff and the southern part of the Tabriz Plain aquifers are included in the model area due to some restrictions of the available model code. In the modelled area, the main water-bearing formations consist of the Plio-Pleistocene Sahand alluvial tuff and the Quaternary Tabriz plain alluvial fans. The alluvial tuff and fans are unconfined, whereas in the central part of the Tabriz Plain, the alluvial aquifer is covered by silt and clay materials and has a confined condition. The aquifers are heterogenous and anisotropic and the geometry of these formations was defined from the topographical and aquifer thickness contours (resulting from geophysical investigation) for the alluvial tuff aquifer and by the data points and well logs for the Tabriz Plain alluvial fans.

In considering the boundary conditions, it should be mentioned (as explained in chapters 4 and 8) that the Sahand mountain is formed from two types of formation (a) the alluvial tuff aquifer which actually lies between elevations 1500m and 2400m amsl, and (b) the low permeability or impermeable andesitic rocks above 2400m elevation (see Fig. 9.1). The boundary conditions between these two formations were considered in two alternative assumptions. The first assumption supposes that there is no flow from the andesitic rocks into the aquifer, and the second assumption presumes that there is a constant-head boundary between these two formations. The reason for the first assumption relates to the geological conditions in the area. However, the second assumption considers the higher mountain as a main recharge area with a huge amounts of snow storage and possibly with a high amount of inter-flow from the superficial weathered zone into the aquifer.

The western, north-western and north-eastern boundaries are barrier boundaries and there are no-flow boundary conditions on these sides. Only a small part of the northern boundary is considered to be a variable head boundary (see Table 9.1).

The main source of recharge to the aquifers is from direct rainfall infiltration, irrigation return flow and losing rivers. The recharge amount in the higher elevations (upper mountain) is greater than in the lower elevation areas, which have less precipitation but receive some water as overland flow and interflow.

Discharge from the ground water takes place by pumping from deep and shallow wells for irrigation purposes during the spring, summer and autumn seasons, and for drinking, domestic and industrial purposes during the whole year. Qanats and natural springs are active during the year, unless the ground water level falls below the spring and qanat mother well levels.

### 9.3 Numerical Model

The next step in the modelling procedure is to translate the physical components into mathematical terms which simulate the natural behaviour of a system through the solution of mathematical equations. A mathematical model itself can be solved with either analytical or numerical models, but in this chapter the numerical solution will be considered. The numerical solution normally involves approximating continuous partial-differential equations with boundary and initial conditions by a set of discrete equations in time and space. These equations are combined to form a system of algebraic equations that can be solved for the desired time steps.

One numerical approach which has been applied successfully to ground water flow equations is the finite difference approximation technique (see Mercer and Faust, 1981; Wang and Anderson, 1976). In using the finite-difference method to solve partial differential equations, a grid should be established throughout the modelling region. There are two main types of grids, mesh-centred and block-centred: with the mesh-centred grid the nodes are located on the intersection of grid lines, whereas in the block-centred grid the nodes are centred between the grid lines.



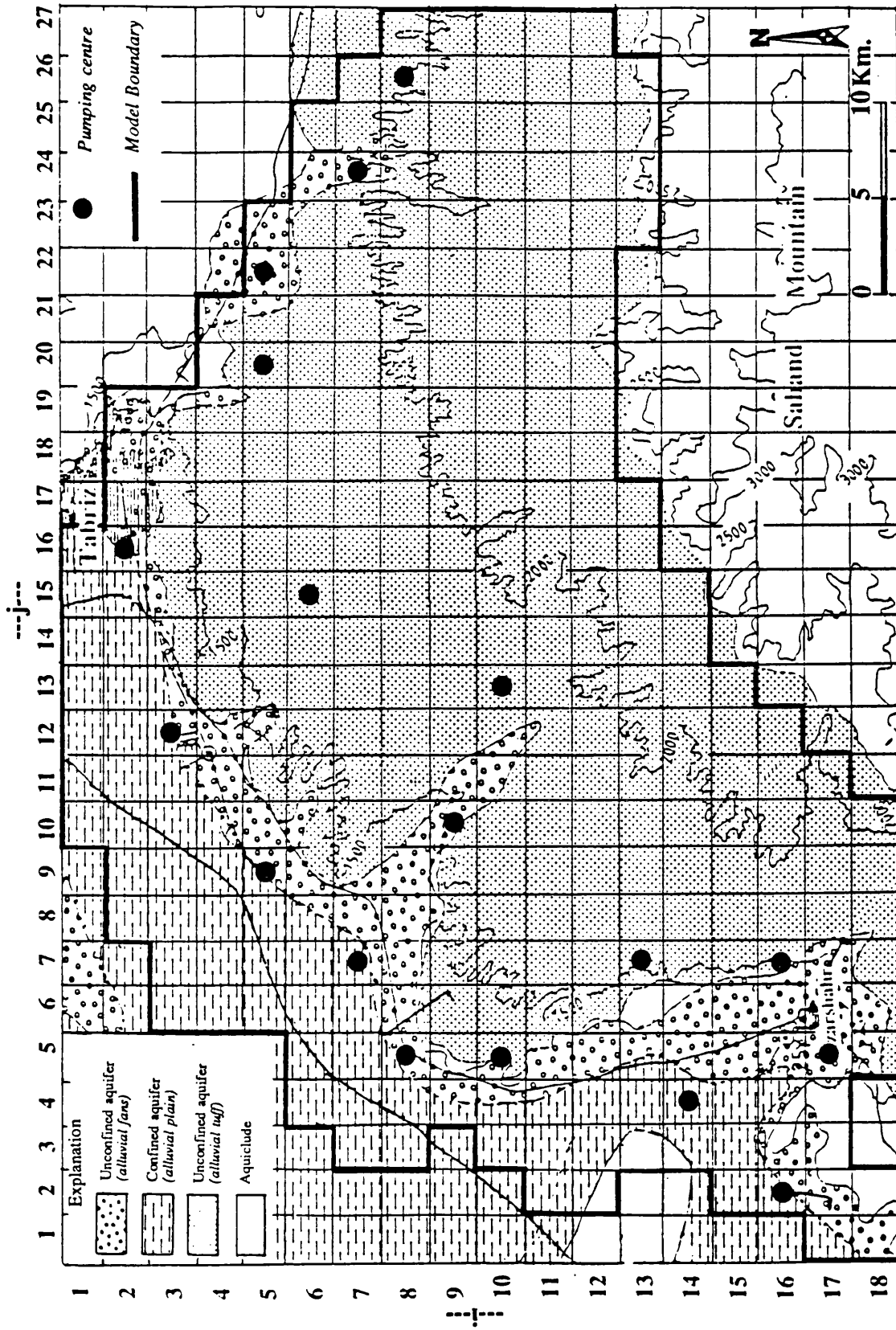


Fig. 9.1 Map showing the aquifer types, model boundaries and pumping centres.

Table 9.1 The model boundary conditions

	1	2	3	4	5	6	7	8	9	10	11	12	13	14	15	16	17	18	19	20	21	22	23	24	25	26	27	28	
1	0	0	0	0	0	0	0	0	0	1	1	1	1	1	1	1	0	0	0	0	0	0	0	0	0	0	0	0	0
2	0	0	0	0	0	1	1	1	1	1	1	1	1	1	1	1	1	1	1	0	0	0	0	0	0	0	0	0	0
3	0	0	0	0	0	1	1	1	1	1	1	1	1	1	1	1	1	1	1	0	0	0	0	0	0	0	0	0	0
4	0	0	0	0	0	1	1	1	1	1	1	1	1	1	1	1	1	1	1	1	1	1	0	0	0	0	0	0	0
5	0	0	0	0	0	1	1	1	1	1	1	1	1	1	1	1	1	1	1	1	1	1	1	1	0	0	0	0	0
6	0	0	0	1	1	1	1	1	1	1	1	1	1	1	1	1	1	1	1	1	1	1	1	1	1	1	0	0	0
7	0	0	1	1	1	1	1	1	1	1	1	1	1	1	1	1	1	1	1	1	1	1	1	1	1	1	1	0	0
8	0	0	1	1	1	1	1	1	1	1	1	1	1	1	1	1	1	1	1	1	1	1	1	1	1	1	1	1	0
9	0	0	0	1	1	1	1	1	1	1	1	1	1	1	1	1	1	1	1	1	1	1	1	1	1	1	1	1	0
10	0	0	1	1	1	1	1	1	1	1	1	1	1	1	1	1	1	1	1	1	1	1	1	1	1	1	1	1	0
11	0	1	1	1	1	1	1	1	1	1	1	1	1	1	1	1	1	1	1	1	1	1	1	1	1	1	1	1	0
12	0	1	1	1	1	1	1	1	1	1	1	1	1	1	1	1	1	1	1	1	1	1	1	1	1	1	1	1	0
13	0	0	1	1	1	0	1	1	1	1	1	1	1	1	1	1	1	1	1	1	1	1	1	1	1	1	1	1	0
14	0	0	1	1	1	1	0	1	1	1	1	1	1	1	1	1	1	1	1	1	1	1	1	1	1	1	1	1	0
15	0	1	1	1	1	1	1	1	1	1	1	1	1	1	1	1	1	1	1	1	1	1	1	1	1	1	1	1	0
16	0	1	1	1	1	1	1	1	1	1	1	1	1	1	1	1	1	1	1	1	1	1	1	1	1	1	1	1	0
17	1	1	1	1	1	1	1	1	1	1	1	1	1	1	1	1	1	1	1	1	1	1	1	1	1	1	1	1	0
18	1	1	0	0	1	1	1	1	1	1	1	1	1	1	1	1	1	1	1	1	1	1	1	1	1	1	1	1	0
19	0	0	0	0	0	0	0	0	0	0	0	0	0	0	0	0	0	0	0	0	0	0	0	0	0	0	0	0	0

- 0 For non-active cells
- 1 For active cells and variable head boundary conditions
- 1 For constant head boundary conditions

### 9.3.1 Model Code

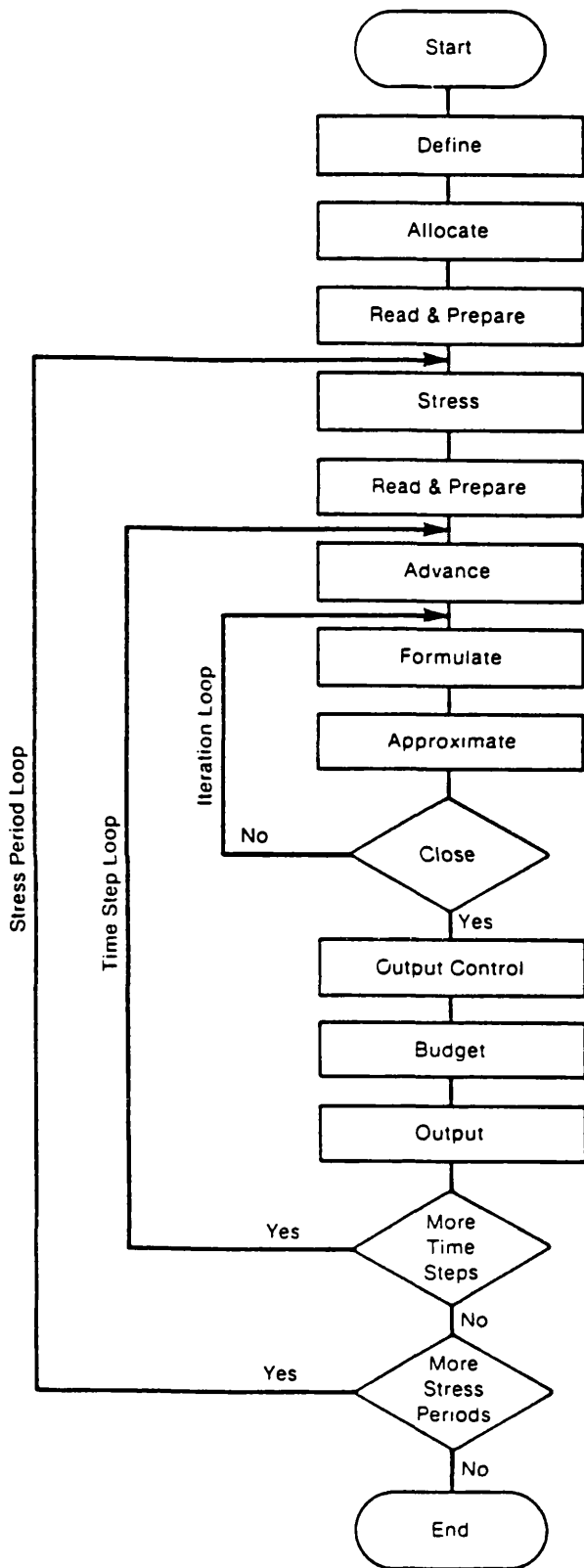
Following the understanding of the simulated aquifer(s) and the definition of the boundaries, the Modflow package written by McDonald and Harbaugh (U.S. Geological Survey, 1987) was selected as a most suitable model to use. The Modflow program has been written in Fortran 77 language and consists of a main routine and a series of independent subroutines called modules. It is a finite-difference, ground-water model that can simulate two- and three-dimensional, transient flow in an anisotropic, heterogenous, layered aquifer system. The finite-difference approach is block-centred and layers may be simulated as confined, unconfined, or convertible between the two conditions. The model has been grouped into packages with each package dealing with a single aspect of the simulation. For example, the well package simulates the effect of wells, and the river, recharge, drain and evapotranspiration packages simulate the effects of rivers, recharge, drains and evapotranspiration, respectively. Table 9.2 lists the various packages used in this model with a brief description of their operation. Solution techniques for the finite-difference equations are either the Strongly Implicit Procedure (SIP) or the Slice Successive Over-relaxation procedure (SSOR).

Figure 9.2 shows the functions which must be performed for typical simulation. Prior to entering the stress loop, the program executes the three first steps which pertain to the simulation as a whole. In the first step (Define), the problem to be simulated is defined: then successively the size of the model, the type of simulation (transient or steady-state), the number of stress periods, the hydrological options, and the solution scheme to be used are specified. In the second step (Allocate), the memory space required by the program is allocated. In the third step (Read and Prepare), all data that are not functions of time are read. These data include boundary conditions, initial heads, transmissivity, hydraulic conductivity, specific yield, storage coefficient, elevations of layer tops and bases, and parameters required by the specified solution scheme. In the other steps, the number of time steps, pumping rates, areal recharge and budget are processed. Therefore, this figure provides a flow chart for the overall program structure.

The conceptualization and implementation, input instructions for the package and documentation of the individual module contained in the package are explained

Table 9.2 List of the various packages used in Modflow.

<u>Package Name</u>	<u>Abbreviation</u>	<u>Package Description</u>		
Basic	BAS	Handles those tasks that are part of the model as a whole. Among those tasks are specification of boundaries, determination of time-step length, establishment of initial conditions, and printing of results.		
Block-Centered Flow	BCF	Calculates terms of finite-difference equations which represent flow within porous medium; specifically, flow from cell to cell and flow into storage.		
Well	WEL	Adds terms representing flow to wells to the finite-difference equations.		
Recharge	RCH	Adds terms representing areally distributed recharge to the finite-difference equations.		
River	RIV	Adds terms representing flow to rivers to the finite-difference equations.		
Drain	DRN	Adds terms representing flow to drains to the finite-difference equations.		
Evapotranspiration	EVT	Adds terms representing ET to the finite-difference equations.		
General-Head Boundaries	GHB	Adds terms representing general-head boundaries to the finite-difference equations.		
Strongly Implicit Procedure	SIP	Iteratively solves the system of finite-difference equations using the Strongly Implicit Procedure.		
Slice-Successive Overrelaxation	SOR	Iteratively solves the system of finite-difference equations using Slice-Successive Overrelaxation.		



**DEFINE** — Read data specifying number of rows, columns, layers, stress periods, and major program options.

**ALLOCATE** — Allocate space in the computer to store data.

**READ AND PREPARE** — Read data which is constant throughout the simulation. Prepare the data by performing whatever calculations can be made at this stage.

**STRESS** — Determine the length of a stress period and calculate terms to divide stress periods into time steps.

**READ AND PREPARE** — Read data which changes from one stress period to the next. Prepare the data by performing whatever calculations can be made at this stage.

**ADVANCE** — Calculate length of time step and set heads at beginning of a new time step equal to heads calculated for the end of the previous time step.

**FORMULATE** — Calculate the coefficients of the finite difference equations for each cell.

**APROXIMATE** — Make one cut at approximating a solution to the system of finite difference equations.

**OUTPUT CONTROL** — Determine whether results should be written or saved on disk for this time step. Send signals to the BUDGET and OUTPUT procedures to indicate exactly what information should be put out.

**BUDGET** — Calculate terms for the overall volumetric budget and calculate and save cell-by-cell flow terms for each component of flow.

**OUTPUT** — Print and save heads, drawdown and overall volumetric budgets in accordance with signals from OUTPUT CONTROL procedure.

Fig. 9.2 Flow chart of program structure.

for all the above-mentioned packages in the main manual.

As indicated earlier, the ground water flow model was originally written for a mainframe computer system (McDonald and Harbaugh) as Modflow and then implemented to microcomputer by the Holcomb Research Institute (HRI) as the Modflow-PC. The summarized Modflow Pre-Processor flow chart for Microcomputers is shown on Figure 9.3 and more details may be seen in the manual of Modflow (Hall Ground Water Consultant Inc. 1987). The main menu of the model provides the following options:

- (1) set the data drive/pathname,
- (2) change the default system of units, field widths, precision, and multiplication factor for the data set arrays,
- (3) retrieve an existing file or create a new set of input files to the Modflow program,
- (4) convert Pre-Processor files to the Fortran format acceptable to Modflow.

The PC version of the Modflow package is restricted to 18 pumping centres as well as 18 river reaches.

### **9.3.2 Model Inputs**

In order to apply a selected model formulation, depending on the type of model and problem, certain model inputs are required. These include boundary conditions which may be no-flow boundary, constant-head or variable-head boundary, initial head, well data such as abstraction rates and locations, river data with river stage elevations and river-bed permeabilities, transmissivity, permeability, aquifer thickness, top and base elevations of aquifers, vertical permeability and recharge matrix.

Before entering data into the model, the setting up of the grid for the model area (maximum 40 by 40) and selection of the approach for solving the finite-difference equation are necessary. Therefore, a uniform 2.5 by 2.5 km square grid with a grid size of 28 by 19 was setting up to represent the model area (see Fig. 9.1). Also, for solving the finite-difference equation, the Strongly Implicit Procedure (SIP) was selected.

The initial head data for the Tabriz Plain area were obtained from the ground

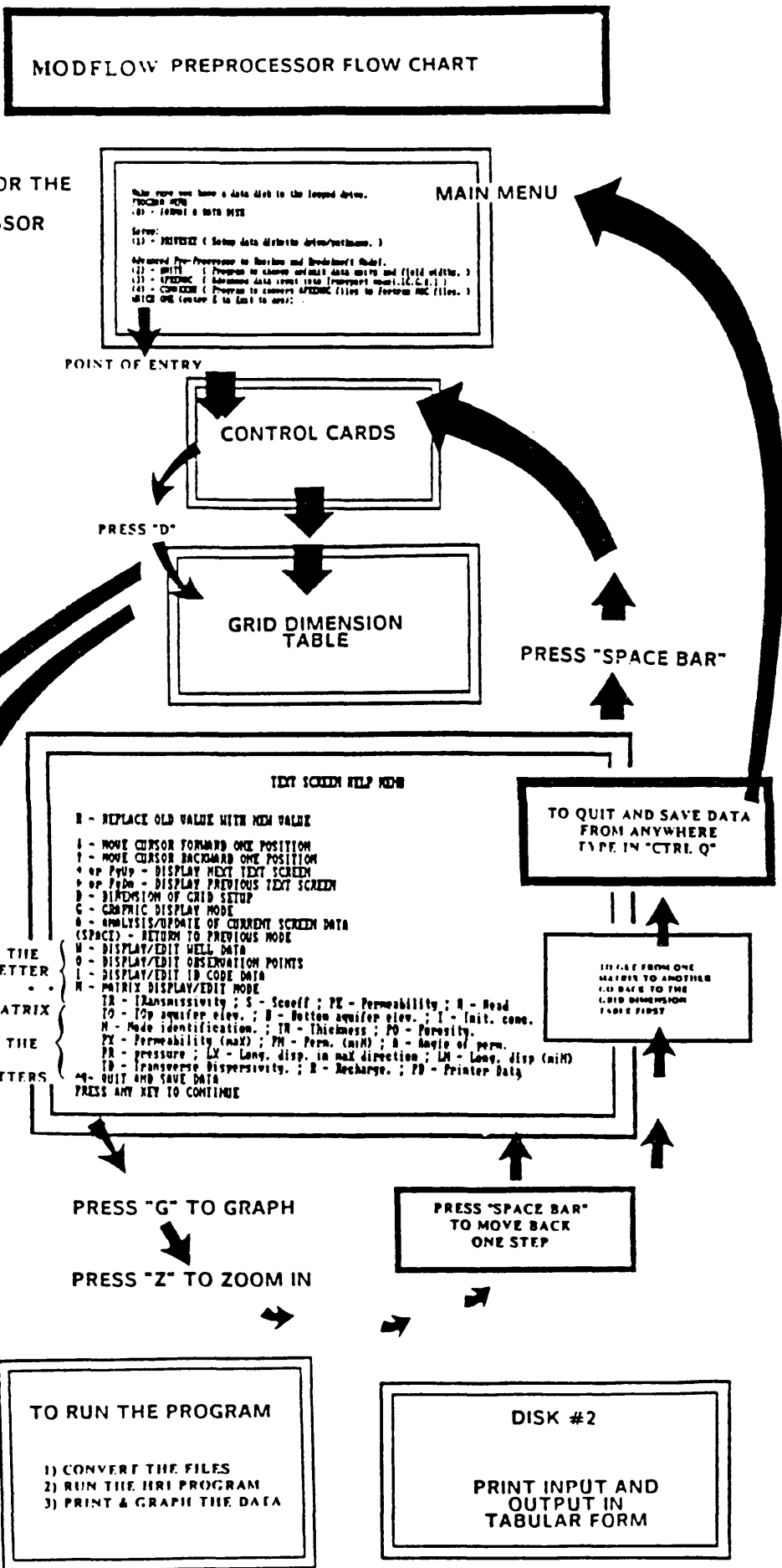


Fig. 9.3 Pre-processor chart for Modflow.

water level contour map for the wet season period (see Fig. 9.4a and Tables 9.3). But for the alluvial tuff aquifer, the equivalent data were estimated from the topographical map of the area assuming that the water level is a subdued reflection of the ground surface. It was also assumed that the depth to ground water level increases towards the mountainous area from 10m at the lowest elevation to 100m at the highest elevation. This estimation is based on the data obtained from the Saidabad well-field (see Fig. 5.8 in Chapter five).

The aquifer thickness in the Tabriz Plain was obtained from the well log data, whereas for the alluvial tuff it was deduced from the surface geophysical survey results as well as well logs. Table 9.4 shows the thickness input data to the model.

The recharge and discharge to and from the ground water were estimated from the results explained in Chapter 8. It should be mentioned that in Chapter 8 the amount of discharge over all the study area was considered, whereas the model input data require the discharge rates from each pumping centres to be individually determined. These estimations of abstraction rates are based on the number and type of wells grouped in the pumping centre, and duration and rate of pumping during the year. Table 9.5 (b) shows the estimated abstraction rates from the pumping centres for no-flow and constant-head boundary conditions. The areal recharge for both boundary conditions were shown on Tables 9.6 and 9.7.

The river input data were entered for three main rivers, where their seepage significantly increases the ground water recharge rate. For the other small rivers, the amounts of areal recharge were assumed to be higher for those river cells. The tabulated river input data is shown in Table 9.5 (a). All the above-mentioned data were converted from metric (m) to Imperial (ft) units to meet the model requirements.

An initial estimation of permeability or transmissivity was made based on the pumping test analysis results and the geological information. Many trial and error computer runs were made varying aquifer parameters, recharge, and discharge rates until a satisfactory final head distribution was obtained. The final transmissivity distributions used in no-flow and constant-head boundary conditions are shown in Tables 9.8 and 9.9, respectively. In general, the transmissivity values finally used were less than those obtained from the pumping test analysis. However, the values for the Tabriz Plain are comparable, while in the alluvial tuff aquifer the model



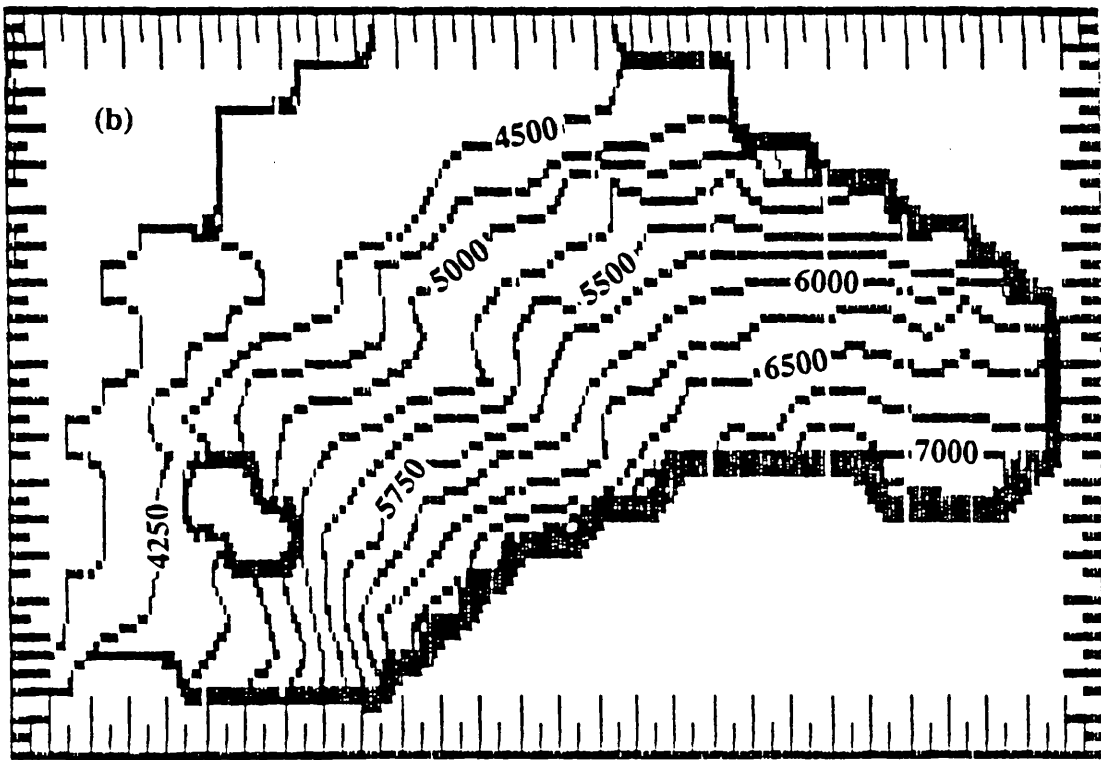
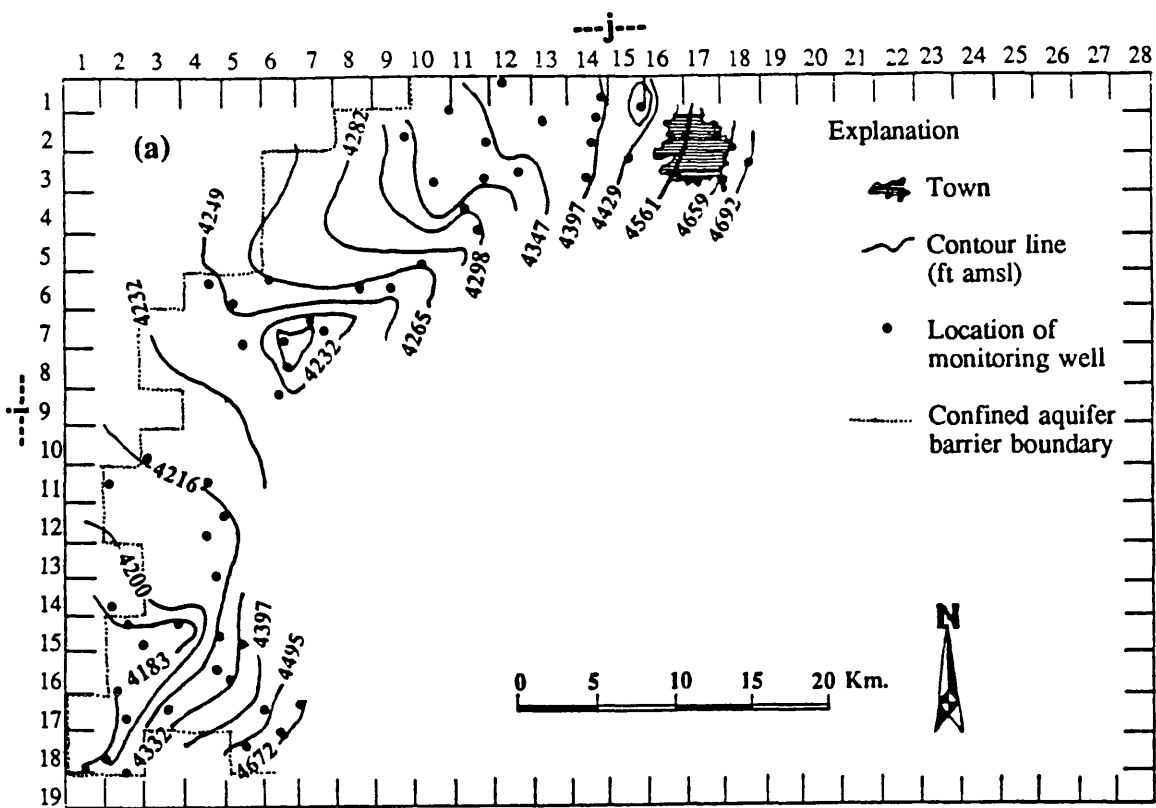


Fig. 9.4 (a) Ground water levels for wet season (1987) and (b) initial head in model from measured data and topographical extrapolation.

**Table 9.3 Initial head data distribution (ft amsl)**

	1	2	3	4	5	6	7	8	9	10	11	12	13	14	15	16	17	18	19	20	21	22	23	24	25	26	27	28								
1	0	0	0	0	0	0	0	0	0	4330	4344	4364	4370	4380	4410	4430	0	0	0	0	0	0	0	0	0	0	0	0	0							
2	0	0	0	0	0	4260	4269	4280	4305	4320	4340	4360	4385	4385	4420	4480	4590	4610	4670	0	0	0	0	0	0	0	0	0	0	0						
3	0	0	0	0	0	4262	4272	4285	4305	4320	4325	4335	4356	4390	4445	4510	4615	4675	4715	0	0	0	0	0	0	0	0	0	0	0	0					
4	0	0	0	0	0	4267	4278	4288	4290	4295	4298	4470	4500	4570	4630	4720	4770	4890	4930	4960	5180	0	0	0	0	0	0	0	0	0	0					
5	0	0	0	0	0	4270	4278	4278	4282	4282	4350	4670	4700	4720	5125	5260	5125	5080	5350	4970	4990	5170	5180	0	0	0	0	0	0	0	0					
6	0	0	0	4245	4250	4255	4260	4262	4262	4265	4560	4840	4990	5080	5080	5260	5530	5530	5530	5440	5440	5440	5440	5460	5460	5670	0	0	0	0	0					
7	0	0	4235	4240	4240	4242	4250	4300	4500	4750	4830	4990	5170	5150	5420	5440	5620	5800	5800	5800	5800	5800	5800	5800	5800	5620	5710	5890	0	0	0	0				
8	0	0	4230	4235	4235	4235	4235	4400	4470	4700	5050	5125	5260	5510	5440	5700	5900	5980	6100	6160	6160	6160	6160	6200	5980	6250	6070	6000	0	0	0	0				
9	0	0	4220	4223	4230	4550	4870	4540	4580	4700	4970	5150	5400	5620	5800	5880	6000	6160	6200	6340	6340	6340	6430	6430	6260	6430	6290	6300	0	0	0	0	0			
10	0	0	4208	4212	4220	4500	4700	4870	5080	5170	5170	5440	5550	5750	5980	6120	6220	6510	6480	6570	6610	6610	6610	6610	6550	6610	6540	6600	0	0	0	0	0	0		
11	0	4208	4212	4220	4500	4700	4870	5080	5170	5170	5440	5550	5750	5980	6120	6220	6510	6480	6570	6610	6610	6610	6610	6610	6550	6610	6540	6600	0	0	0	0	0	0		
12	0	4205	4208	4212	4270	4600	4890	5170	5310	5440	5710	5710	5980	6050	6100	6300	6610	6610	6880	6900	7100	7100	7000	7000	7000	7000	6990	6990	0	0	0	0	0	0		
13	0	0	4206	4210	4347	0	4900	5260	5440	5710	5980	6070	6250	6400	6450	6600	7200	0	0	0	0	0	0	7400	7300	7240	7300	0	0	0	0	0	0	0	0	
14	0	0	4200	4206	4345	4470	0	5400	5620	5710	6070	6340	6610	6790	7000	0	0	0	0	0	0	0	0	0	0	0	0	0	0	0	0	0	0	0	0	0
15	0	4175	4175	4216	4350	4570	4800	5200	5710	5980	6250	6430	6800	0	0	0	0	0	0	0	0	0	0	0	0	0	0	0	0	0	0	0	0	0	0	0
16	0	4183	4195	4250	4350	4470	4700	5080	5710	6250	6520	6800	0	0	0	0	0	0	0	0	0	0	0	0	0	0	0	0	0	0	0	0	0	0	0	0
17	4183	4190	4315	4350	4395	4560	4620	4980	5530	6160	6600	0	0	0	0	0	0	0	0	0	0	0	0	0	0	0	0	0	0	0	0	0	0	0	0	0
18	4183	4265	0	0	4530	4620	4900	5100	5450	5900	0	0	0	0	0	0	0	0	0	0	0	0	0	0	0	0	0	0	0	0	0	0	0	0	0	0
19	0	0	0	0	0	0	0	0	0	0	0	0	0	0	0	0	0	0	0	0	0	0	0	0	0	0	0	0	0	0	0	0	0	0	0	0

Data in italics obtained from the ground water contour map and non-italic data from topographical map

Table 9.4 Aquifer thicknesses (ft)

	1	2	3	4	5	6	7	8	9	10	11	12	13	14	15	16	17	18	19	20	21	22	23	24	25	26	27	28	
1	0	0	0	0	0	0	0	0	0	200	200	200	200	200	200	200	0	0	0	0	0	0	0	0	0	0	0	0	
2	0	0	0	0	0	0	0	200	200	200	200	200	200	200	200	200	200	230	230	0	0	0	0	0	0	0	0	0	0
3	0	0	0	0	0	200	200	200	200	200	200	230	230	230	230	230	230	230	100	0	0	0	0	0	0	0	0	0	0
4	0	0	0	0	0	200	200	200	200	230	230	100	100	80	240	260	260	80	80	80	0	0	0	0	0	0	0	0	0
5	0	0	0	0	0	200	200	200	230	230	100	100	80	240	360	650	410	500	320	320	360	240	0	0	0	0	0	0	0
6	0	0	0	200	200	200	200	230	230	80	240	160	160	240	400	650	500	580	650	580	580	650	500	320	0	0	0	0	
7	0	0	160	200	200	200	200	230	80	164	240	320	410	410	500	500	500	650	700	650	700	650	700	720	650	410	0	0	
8	0	0	160	160	160	140	80	140	240	320	580	650	500	530	650	650	670	690	670	650	650	670	650	670	650	410	650	0	
9	0	0	130	120	100	130	130	160	240	410	650	650	650	670	690	700	720	720	720	720	720	700	700	680	660	600	720	0	
10	0	0	130	130	120	100	130	160	160	500	500	550	500	500	500	600	680	700	720	720	700	680	660	650	650	700	720	0	
11	0	130	130	130	100	160	250	410	650	600	500	500	500	600	650	650	650	700	700	700	650	620	580	580	800	820	800	0	
12	0	130	130	130	100	100	230	410	500	540	660	660	620	660	660	660	620	410	500	240	330	410	330	500	600	660	660	0	
13	0	0	140	140	80	0	240	410	680	650	680	720	720	680	320	160	80	0	0	0	0	0	240	410	420	240	0	0	
14	0	0	160	160	100	60	0	590	650	670	650	700	650	450	80	0	0	0	0	0	0	0	0	0	0	0	0	0	
15	0	230	230	230	200	160	160	100	570	500	570	570	250	0	0	0	0	0	0	0	0	0	0	0	0	0	0	0	
16	0	230	230	230	200	160	120	500	500	460	240	0	0	0	0	0	0	0	0	0	0	0	0	0	0	0	0	0	
17	260	260	350	400	450	400	400	340	340	460	230	0	0	0	0	0	0	0	0	0	0	0	0	0	0	0	0	0	
18	260	260	0	0	80	80	80	160	80	0	0	0	0	0	0	0	0	0	0	0	0	0	0	0	0	0	0	0	
19	0	0	0	0	0	0	0	0	0	0	0	0	0	0	0	0	0	0	0	0	0	0	0	0	0	0	0	0	

**Table 9.5 (a) River input data (b) pumping centre locations and abstraction rates**

(a)

<u>River location No.</u>	<u>i</u>	<u>j</u>	<u>Water Level Elevation</u>	<u>Permeability (ft/s x 10<sup>-3</sup>)</u>	<u>River Bed Elevation</u>
1	17	5	6402.0	0.800	6400.0
1	17	6	6202.0	0.800	6200.0
1	17	7	5802.0	0.800	5800.0
1	16	4	5601.0	0.800	5600.0
1	16	5	5101.0	0.800	5100.0
1	11	17	4981.0	0.800	4980.0
1	10	16	4921.0	0.800	4920.0
3	9	6	6252.0	0.800	6250.0
3	9	24	5982.0	0.800	5980.0
3	8	15	5712.0	0.800	5710.0
3	8	24	5442.0	0.800	5440.0
3	7	14	5081.0	0.800	5080.0
3	7	24	4901.0	0.800	4900.0
2	6	13	4702.0	0.800	4700.0
2	6	23	4602.0	0.800	4600.0
2	5	23	4432.0	0.800	4430.0
2	4	20	4332.0	0.800	4331.0
2	4	21	4221.0	0.800	4220.0

(b)

<u>Well No.</u>	<u>i</u>	<u>j</u>	<u>Pumping rates(ft<sup>3</sup>/s)</u>	
			<u>No-flow boundary</u>	<u>Constant head boundary</u>
1	8	26	-26.400	-21.400
2	7	24	-32.800	-32.200
3	5	22	-33.000	-32.800
4	5	20	-32.000	-34.000
5	6	15	-22.000	-26.000
6	10	13	-30.400	-44.000
7	9	10	-28.000	-38.200
8	2	16	-36.390	-34.000
9	3	12	-28.000	-26.000
10	5	9	-26.800	-34.600
11	7	7	-28.000	-36.200
12	8	5	-16.000	-16.200
13	10	5	-16.000	-21.000
14	13	7	-14.000	-17.000
15	14	4	-26.800	-26.800
16	16	7	-14.000	-15.000
17	16	2	-22.000	-23.000
18	17	5	-17.200	-17.000

Table 9.6 Estimated areal recharges for no-flow boundary conditions (ft/sec x 10<sup>-10</sup>)

	1	2	3	4	5	6	7	8	9	10	11	12	13	14	15	16	17	18	19	20	21	22	23	24	25	26	27	28	
1	0	0	0	0	0	0	0	0	0	0	0	0	0	0	0	190	0	0	0	0	0	0	0	0	0	0	0	0	0
2	0	0	0	0	0	0	0	0	0	0	0	0	0	0	0	0	190	190	0	0	0	0	0	0	0	0	0	0	0
3	0	0	0	0	0	0	0	0	0	0	0	0	0	0	0	0	0	190	190	190	220	228	0	0	0	0	0	0	0
4	0	0	0	0	0	0	0	0	0	0	0	0	0	0	0	0	0	0	190	190	220	228	200	200	0	0	0	0	0
5	0	0	0	0	0	0	0	0	0	0	0	0	0	0	0	0	0	0	0	190	228	228	200	200	0	0	0	0	0
6	0	0	0	0	0	0	0	0	0	0	0	0	0	0	0	0	0	0	0	0	190	228	228	200	200	0	0	0	0
7	0	0	0	0	0	0	0	0	0	0	0	0	0	0	0	0	0	0	0	0	0	190	228	228	200	200	0	0	0
8	0	0	0	0	0	0	0	0	0	0	0	0	0	0	0	0	0	0	0	0	0	0	190	228	228	200	200	0	0
9	0	0	0	0	0	0	0	0	0	0	0	0	0	0	0	0	0	0	0	0	0	0	0	190	228	228	200	200	0
10	0	0	0	0	0	0	0	0	0	0	0	0	0	0	0	0	0	0	0	0	0	0	0	0	0	0	0	0	0
11	0	0	0	0	0	0	0	0	0	0	0	0	0	0	0	0	0	0	0	0	0	0	0	0	0	0	0	0	0
12	0	0	0	0	0	0	0	0	0	0	0	0	0	0	0	0	0	0	0	0	0	0	0	0	0	0	0	0	0
13	0	0	0	0	0	0	0	0	0	0	0	0	0	0	0	0	0	0	0	0	0	0	0	0	0	0	0	0	0
14	0	0	0	0	0	0	0	0	0	0	0	0	0	0	0	0	0	0	0	0	0	0	0	0	0	0	0	0	0
15	0	0	0	0	0	0	0	0	0	0	0	0	0	0	0	0	0	0	0	0	0	0	0	0	0	0	0	0	0
16	0	0	0	0	0	0	0	0	0	0	0	0	0	0	0	0	0	0	0	0	0	0	0	0	0	0	0	0	0
17	220	220	220	228	360	360	360	360	360	360	360	0	0	0	0	0	0	0	0	0	0	0	0	0	0	0	0	0	0
18	220	220	0	0	228	300	320	360	300	360	0	0	0	0	0	0	0	0	0	0	0	0	0	0	0	0	0	0	0
19	0	0	0	0	0	0	0	0	0	0	0	0	0	0	0	0	0	0	0	0	0	0	0	0	0	0	0	0	0

**Table 9.7 Estimated areal recharges for constant head boundary conditions (ft/sec x 10<sup>-10</sup>)**

	1	2	3	4	5	6	7	8	9	10	11	12	13	14	15	16	17	18	19	20	21	22	23	24	25	26	27	28				
1	0	0	0	0	0	0	0	0	0	0	0	0	0	0	0	100	0	0	0	0	0	0	0	0	0	0	0	0	0			
2	0	0	0	0	0	0	0	0	0	0	0	0	0	0	0	0	190	190	0	0	0	0	0	0	0	0	0	0	0	0		
3	0	0	0	0	0	0	0	0	0	0	0	0	190	190	190	190	190	220	190	0	0	0	0	0	0	0	0	0	0	0		
4	0	0	0	0	0	0	0	0	0	0	190	190	190	190	220	220	220	220	228	190	190	0	0	0	0	0	0	0	0	0		
5	0	0	0	0	0	0	0	0	190	190	220	220	220	220	220	220	220	220	228	228	190	190	190	0	0	0	0	0	0	0		
6	0	0	0	0	0	0	0	0	220	220	220	220	220	220	220	220	220	220	300	300	228	228	228	228	190	0	0	0	0	0		
7	0	0	0	0	0	0	0	190	220	220	220	220	220	220	220	220	221	220	300	300	300	300	300	228	228	228	228	0	0	0		
8	0	0	0	0	0	0	190	190	220	220	220	220	220	220	220	222	222	300	300	300	300	300	300	300	300	300	300	300	300	0	0	
9	0	0	0	0	0	190	220	220	220	220	220	220	220	220	220	300	300	300	300	300	300	300	300	300	300	300	300	300	300	0	0	
10	0	0	0	0	190	220	220	220	228	228	220	220	220	220	221	300	300	300	300	300	300	300	300	300	300	300	300	300	300	0	0	
11	0	0	0	0	220	220	220	220	228	228	228	300	300	300	300	300	300	300	300	300	300	220	220	220	300	300	300	300	300	0	0	
12	0	0	0	0	220	220	220	220	228	228	300	300	300	300	300	300	300	300	300	300	300	300	300	300	300	300	300	300	300	0	0	
13	0	0	0	0	228	0	220	220	220	220	300	300	300	300	300	300	300	300	0	0	0	0	0	360	360	360	0	0	0	0	0	
14	0	0	0	0	228	300	0	220	220	300	300	300	300	300	300	0	0	0	0	0	0	0	0	0	0	0	0	0	0	0	0	
15	0	0	0	0	220	220	312	312	312	32	300	300	300	0	0	0	0	0	0	0	0	0	0	0	0	0	0	0	0	0	0	
16	0	0	0	0	220	300	300	312	312	320	300	320	300	0	0	0	0	0	0	0	0	0	0	0	0	0	0	0	0	0	0	0
17	220	220	220	228	300	300	312	320	300	300	320	0	0	0	0	0	0	0	0	0	0	0	0	0	0	0	0	0	0	0	0	
18	220	220	0	0	228	300	320	320	300	320	0	0	0	0	0	0	0	0	0	0	0	0	0	0	0	0	0	0	0	0	0	
19	0	0	0	0	0	0	0	0	0	0	0	0	0	0	0	0	0	0	0	0	0	0	0	0	0	0	0	0	0	0	0	

Table 9.8 Final transmissivity distribution for no-flow boundary conditions (ft<sup>2</sup>/sec x 10<sup>-3</sup>)

	1	2	3	4	5	6	7	8	9	10	11	12	13	14	15	16	17	18	19	20	21	22	23	24	25	26	27	28		
1	0	0	0	0	0	0	0	0	0	120	120	120	124	128	124	120	0	0	0	0	0	0	0	0	0	0	0	0	0	
2	0	0	0	0	0	0	0	120	80	120	120	120	120	130	124	120	120	138	115	0	0	0	0	0	0	0	0	0	0	
3	0	0	0	0	0	120	120	120	120	120	120	143	141	141	138	138	138	60	0	0	0	0	0	0	0	0	0	0	0	
4	0	0	0	0	0	120	120	120	120	120	138	138	8	10	6	19	21	21	40	32	0	0	0	0	0	0	0	0	0	
5	0	0	0	0	0	130	130	120	120	138	138	60	8	8	10	29	52	33	30	29	128	144	96	0	0	0	0	0	0	
6	0	0	0	120	120	120	120	150	150	48	22	13	13	19	32	39	30	35	39	35	35	39	39	30	64	0	0	0		
7	0	0	96	120	120	120	150	32	10	14	19	25	25	25	30	20	15	20	21	20	26	28	29	39	25	0	0	0	0	
8	0	0	96	96	96	87	50	87	20	19	35	39	30	32	39	26	27	21	20	20	26	27	27	26	25	65	0	0	0	
9	0	0	0	65	60	60	78	78	99	144	16	26	26	26	27	41	35	36	36	22	22	21	21	41	40	36	43	0	0	
10	0	0	78	78	72	4	5	5	96	96	30	30	22	20	20	24	20	21	22	22	21	20	33	33	39	42	43	0	0	
11	0	78	78	78	10	4	6	10	12	20	24	30	30	40	36	13	20	20	21	21	20	12	35	23	48	41	40	0	0	
12	0	78	78	78	40	40	14	25	15	16	20	20	25	40	40	26	19	12	15	7	7	8	13	15	24	26	26	0	0	
13	0	0	84	84	32	0	19	33	20	20	20	22	22	7	10	6	2	0	0	0	0	0	5	8	13	4	0	0	0	0
14	0	0	96	96	40	12	0	47	20	20	20	21	7	5	2	0	0	0	0	0	0	0	0	0	0	0	0	0	0	0
15	0	138	138	138	40	32	10	8	23	8	11	11	3	0	0	0	0	0	0	0	0	0	0	0	0	0	0	0	0	0
16	0	138	138	138	92	40	32	10	15	5	5	2	0	0	0	0	0	0	0	0	0	0	0	0	0	0	0	0	0	0
17	156	156	28	32	180	160	160	31	10	7	9	0	0	0	0	0	0	0	0	0	0	0	0	0	0	0	0	0	0	0
18	156	156	0	0	80	8	8	6	13	5	0	0	0	0	0	0	0	0	0	0	0	0	0	0	0	0	0	0	0	0
19	0	0	0	0	0	0	0	0	0	0	0	0	0	0	0	0	0	0	0	0	0	0	0	0	0	0	0	0	0	0

**Table 9.9 Final transmissivity distribution for constant head boundary conditions ( $\text{ft}^2/\text{sec} \times 10^{-3}$ )**

	---j---																												
	1	2	3	4	5	6	7	8	9	10	11	12	13	14	15	16	17	18	19	20	21	22	23	24	25	26	27	28	
1	0	0	0	0	0	0	0	0	0	120	120	120	124	128	124	120	0	0	0	0	0	0	0	0	0	0	0	0	0
2	0	0	0	0	0	120	120	120	120	120	120	120	120	130	124	120	120	138	115	0	0	0	0	0	0	0	0	0	0
3	0	0	0	0	0	120	120	120	120	120	120	120	143	143	138	138	138	60	0	0	0	0	0	0	0	0	0	0	0
4	0	0	0	0	0	120	120	120	120	120	138	138	12	8	6	14	21	21	40	40	32	0	0	0	0	0	0	0	0
5	0	0	0	0	0	120	120	120	120	138	138	60	8	48	19	14	52	33	30	34	128	144	96	0	0	0	0	0	0
6	0	0	0	120	120	120	120	120	150	149	48	22	13	13	19	16	13	15	17	39	87	116	130	40	128	0	0	0	
7	0	0	96	120	120	120	120	150	48	13	19	29	33	33	33	30	30	25	26	21	13	20	14	58	52	25	0	0	
8	0	0	96	96	96	98	87	50	87	20	26	52	52	40	42	39	39	27	21	17	20	13	54	33	25	26	0	0	
9	0	0	0	65	60	60	78	78	99	144	33	59	52	52	54	41	49	43	58	29	29	14	68	33	48	29	0	0	
10	0	0	78	78	72	8	10	10	96	96	50	50	44	40	40	36	41	21	29	29	21	14	40	65	39	63	29	0	
11	0	78	78	78	10	8	13	20	41	65	48	45	45	75	54	39	20	13	21	42	13	12	58	58	56	66	32	0	
12	0	78	78	78	40	60	23	49	50	54	53	59	56	99	99	66	12	16	20	10	13	16	33	50	30	20	26	0	
13	0	0	84	84	48	0	36	62	102	52	27	29	29	54	26	13	3	0	0	0	0	0	10	16	21	10	0	0	
14	0	0	96	96	60	36	0	36	98	67	39	28	20	36	6	0	0	0	0	0	0	0	0	0	0	0	0	0	
15	0	138	138	138	40	32	10	10	23	8	11	46	20	0	0	0	0	0	0	0	0	0	0	0	0	0	0	0	
16	0	138	138	138	92	40	32	12	15	8	9	19	0	0	0	0	0	0	0	0	0	0	0	0	0	0	0	0	
17	156	156	28	32	180	160	160	31	10	7	18	0	0	0	0	0	0	0	0	0	0	0	0	0	0	0	0	0	
18	156	156	0	0	80	8	8	12	24	7	0	0	0	0	0	0	0	0	0	0	0	0	0	0	0	0	0	0	
19	0	0	0	0	0	0	0	0	0	0	0	0	0	0	0	0	0	0	0	0	0	0	0	0	0	0	0	0	



values used are much smaller than the test results.

#### **9.4 Model results**

Estimation of the regional aquifer parameters and a check on the ground water balance was the main objective of the modelling of the Tabriz area. As explained previously, due to the lack of input and historical data, the non-steady state simulation and calibration of the model were not carried out. Therefore, the model simulated only steady-state conditions and the resultant final versions of the contour maps of head are shown in Figure 9.5. In these figures, the results of the two boundary conditions are compared, but due to the small sized graphical output of the model and very steep slope conditions in the study area their differences are not clear. Therefore, the resultant final heads are also shown numerically in Tables 9.10 and 9.11. These tables can also be compared with initial heads in Table 9.2.

The volumetric ground water budgets resulting from the model for both above-mentioned boundary conditions are shown in Table 9.12. The model has calculated all areal, river and constant head boundary recharge and discharge rates to and from the ground water ( $\text{ft}^3/\text{sec}$ ) and volume of water during the first stress period (one day).

Identification of the position and nature of the external boundaries of the model is reasonably straightforward, but the identification of the hydraulic condition on these boundaries is difficult. Therefore, two types of boundary conditions were selected which yielded different values of output and input parameters. When constant-head conditions are used, smaller values of areal recharge or higher values of abstraction rate are required to meet the extra water provided by this particular boundary condition (compare Tables 9.5 to 9.7). Also in this condition, higher values of transmissivity are required near the boundary to transmit the ground water to the recharge area (see Tables 9.8 and 9.9). Thus it may be seen that great care must be taken in the selection of boundary conditions in any type of numerical modelling.

##### **9.4.1 Sensitivity analysis**

There will always be some uncertainty about the aquifer parameters, the position and nature of the boundaries, and recharge rates. Sensitivity analysis

provides a useful way to identify the effect of these uncertainties by varying each of the parameters in turn and determining their effects on the heads and flows.

For the aquifer parameters, the variations in transmissivity ( $K \times b$ ) play an important role in changing the model results. A uniform increase of transmissivity values leads to higher values of drawdown in the higher elevations and consequently an overflow in the lower elevation areas. The effect of vertical permeability is negligible and the storage coefficient is only active when the non-steady state simulation of model is carried out.

The recharge and discharge values are also very important and any changes in these values cause an immediate response of the model results. The effects of change in the boundary conditions were explained in the previous section.

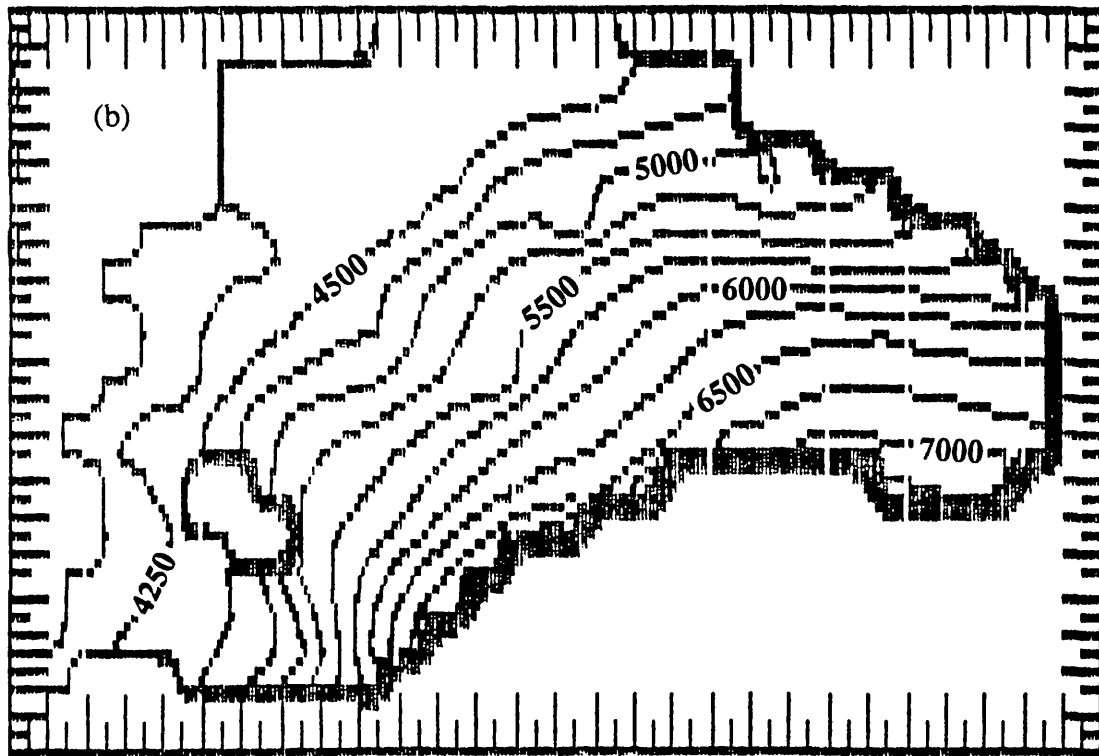
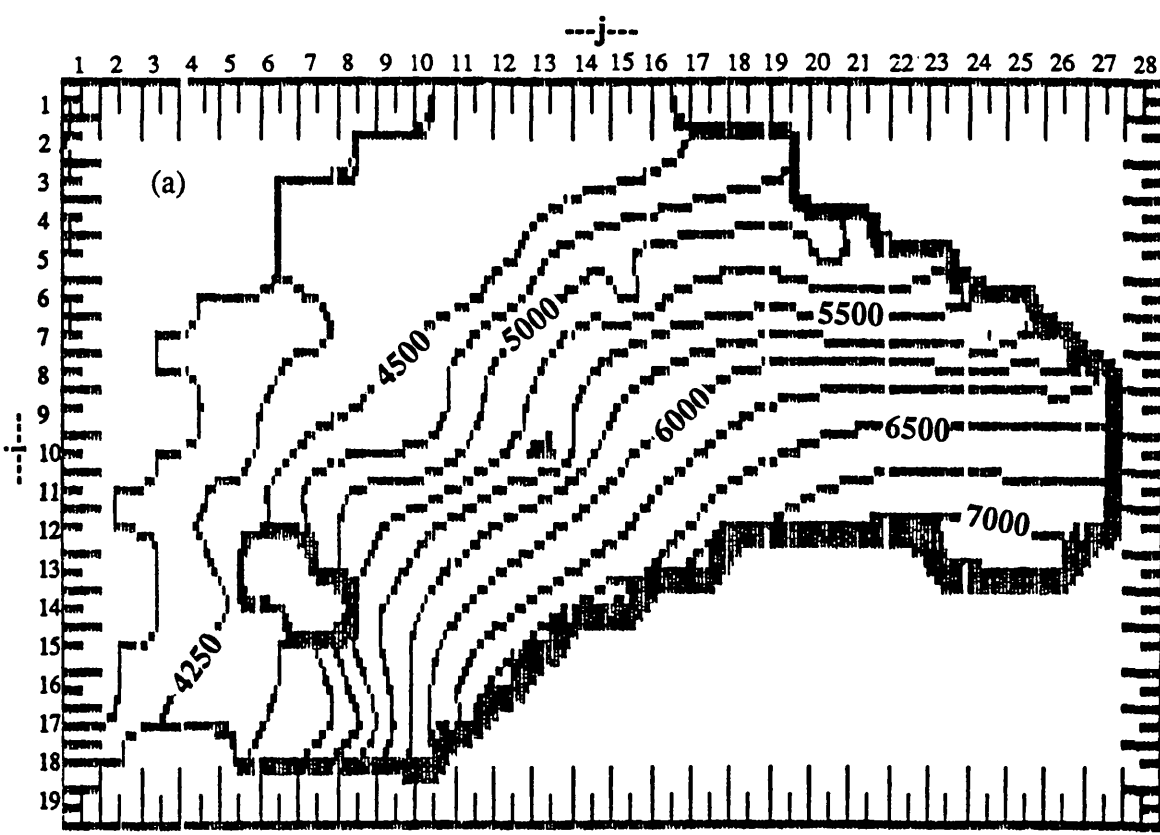


Fig. 9.5 Map showing the resultant final heads (a) for no-flow boundary conditions and (b) for constant head boundary conditions.

**Table 9.10 Final head under no-flow boundary conditions at end of time step 1 in stress period 1 (ft AMSL)**

	---j---																														
	1	2	3	4	5	6	7	8	9	10	11	12	13	14	15	16	17	18	19	20	21	22	23	24	25	26	27	28			
1	0	0	0	0	0	0	0	0	0	4339	4347	4362	4388	4414	4429	4432	0	0	0	0	0	0	0	0	0	0	0	0	0		
2	0	0	0	0	0	0	0	4304	4314	4331	4340	4349	4388	4423	4442	4425	4379	4669	4713	0	0	0	0	0	0	0	0	0	0	0	
3	0	0	0	0	0	4277	4283	4295	4309	4328	4336	4308	4390	4445	4488	4543	4634	4704	4768	0	0	0	0	0	0	0	0	0	0	0	
4	0	0	0	0	0	4271	4277	4287	4299	4336	4366	4377	4520	4637	4740	4809	4880	4916	4941	4983	5062	0	0	0	0	0	0	0	0	0	
5	0	0	0	0	0	4259	4267	4277	4293	4328	4349	4401	4462	4748	4923	4992	5102	5152	5161	5111	4911	5092	5067	5185	0	0	0	0	0	0	
6	0	0	0	0	4211	4219	4240	4254	4293	4328	4379	4480	4673	4972	5113	4950	5264	5334	5376	5377	5324	5312	5328	5407	5557	5691	0	0	0	0	
7	0	0	0	0	4199	4202	4205	4227	4214	4308	4408	4549	4744	4978	5192	5338	5411	5539	5622	5704	5719	5699	5696	5691	5658	5493	5778	5886	0	0	
8	0	0	0	0	4195	4191	4169	4248	4306	4412	4533	4662	4913	5138	5301	5490	5657	5791	5917	6027	6075	6082	6087	6061	6041	6028	6063	5957	6261	0	
9	0	0	0	0	4197	4200	4292	4386	4500	4616	4641	4947	5206	5346	5611	5824	5972	6107	6222	6306	6365	6394	6388	6395	6384	6397	6392	6430	0	0	
10	0	0	0	0	4214	4201	4134	4422	4637	4763	4810	5082	5280	5207	5725	5986	6137	6290	6412	6508	6588	6631	6645	6659	6626	6631	6625	6623	0	0	
11	0	4231	4229	4239	4300	4597	4859	5030	5045	5146	5375	5557	5713	5957	6127	6310	6470	6586	6684	6755	6811	6855	6842	6831	6808	6789	6773	0	0	0	
12	0	4232	4233	4255	4362	4551	4832	5136	5307	5481	5668	5829	5974	6108	6249	6421	6574	6707	6809	6930	7024	7066	7062	7045	6986	6933	6887	0	0	0	
13	0	0	0	4216	4221	4297	0	4752	5215	5454	5695	5892	6046	6150	6322	6424	6616	7033	0	0	0	0	0	7338	7259	7194	7259	0	0	0	
14	0	0	0	4195	4156	4286	4444	0	5372	5570	5830	6054	6211	6406	6589	7000	0	0	0	0	0	0	0	0	0	0	0	0	0	0	
15	0	4180	4210	4241	4348	4494	4769	5313	5627	5955	6232	6398	6713	0	0	0	0	0	0	0	0	0	0	0	0	0	0	0	0	0	0
16	0	4148	4221	4291	4391	4507	4578	5097	5579	6033	6410	6742	0	000.	0	0	0	0	0	0	0	0	0	0	0	0	0	0	0	0	0
17	4208	4199	4256	4350	4428	4542	4652	4962	5516	6045	6376	0	0	0	0	0	0	0	0	0	0	0	0	0	0	0	0	0	0	0	0
18	4214	4210	0	0	4464	4633	4857	5244	5632	6009	0	0	0	0	0	0	0	0	0	0	0	0	0	0	0	0	0	0	0	0	0
19	0	0	0	0	0	0	0	0	0	0	0	0	0	0	0	0	0	0	0	0	0	0	0	0	0	0	0	0	0	0	0

Data in italics obtained from the ground water contour map and non-italic data from topographical map

**Table 9.11 Final head under constant head boundary conditions at end of time step 1 in stream period 1 (ft amsl)**

	1	2	3	4	5	6	7	8	9	10	11	12	13	14	15	16	17	18	19	20	21	22	23	24	25	26	27	28			
1	0	0	0	0	0	0	0	0	0	4346	4354	4367	4391	4413	4427	4428	0	0	0	0	0	0	0	0	0	0	0	0	0		
2	0	0	0	0	0	4292	4296	4305	4318	4337	4348	4357	4392	4423	4440	4424	4574	4665	4710	0	0	0	0	0	0	0	0	0	0	0	
3	0	0	0	0	0	4287	4291	4300	4313	4334	4345	4321	4396	4444	4482	4531	4626	4700	4768	0	0	0	0	0	0	0	0	0	0	0	
4	0	0	0	0	0	4277	4282	4289	4299	4341	4376	4390	4506	4661	4731	4776	4860	4907	4949	5022	5134	0	0	0	0	0	0	0	0	0	
5	0	0	0	0	0	4262	4268	4276	4251	4354	4413	4476	4733	4884	4910	5043	5105	5135	5102	4958	5179	5177	5286	0	0	0	0	0	0	0	
6	0	0	0	0	4207	4238	4251	4298	4336	4392	4506	4705	4968	5034	4844	5250	5392	5450	5433	5333	5307	5321	5388	5571	5690	0	0	0	0	0	
7	0	0	4195	4198	4202	4223	4202	4319	4425	4571	4783	5013	5198	5319	5390	5570	5709	5775	5786	5723	5696	5638	5650	5616	5772	5855	0	0	0	0	
8	0	0	4191	4187	4167	4253	4319	4446	4583	4732	4973	5168	5307	5469	5617	5769	5904	6014	6094	6127	6159	6113	6100	6041	6028	5903	6000	0	0	0	
9	0	0	0	4194	4198	4307	4424	4568	4712	4747	5025	5236	5359	5580	5761	5925	6065	6192	6304	6391	6437	6473	6476	6387	6372	6351	6300	0	0	0	
10	0	0	4222	4201	4116	4397	4635	4818	4907	4977	5176	5318	5283	5703	5915	6073	6191	6339	6479	6586	6647	6723	6730	6648	6633	6599	6600	0	0	0	0
11	0	4242	4239	4249	4325	4603	4863	5063	5126	5217	5389	5566	5727	5955	6091	6211	6342	6524	6684	6739	6852	6918	6886	6844	6810	6752	6690	0	0	0	0
12	0	4242	4241	4268	4397	4618	4902	5180	5309	5420	5591	5783	5973	6137	6225	6315	6515	6610	6880	6900	7100	7100	7052	7022	7007	6981	6990	0	0	0	0
13	0	0	4219	4230	4304	0	4911	5258	5420	5554	5771	6011	6219	6375	6450	6600	7200	0	0	0	0	0	7400	7300	7240	7300	0	0	0	0	
14	0	0	4190	4157	4284	4389	0	5393	5512	5665	5940	6271	6538	6790	0	0	0	0	0	0	0	0	0	0	0	0	0	0	0	0	0
15	0	4162	4195	4226	4327	4457	4759	5289	5563	5896	6283	6560	6800	0	0	0	0	0	0	0	0	0	0	0	0	0	0	0	0	0	0
16	0	4129	4201	4268	4365	4479	4556	5070	5559	6058	6527	6800	0	0	0	0	0	0	0	0	0	0	0	0	0	0	0	0	0	0	0
17	4203	4188	4238	4324	4399	4513	4625	4949	5493	6103	6600	0	0	0	0	0	0	0	0	0	0	0	0	0	0	0	0	0	0	0	0
18	4208	4203	0	0	4435	4604	4850	5192	5527	5872	0	0	0	0	0	0	0	0	0	0	0	0	0	0	0	0	0	0	0	0	0
19	0	0	0	0	0	0	0	0	0	0	0	0	0	0	0	0	0	0	0	0	0	0	0	0	0	0	0	0	0	0	0

Data in italics obtained from the ground water contour map and non-italic data from topographical map

**Tabel 9.12 Volumetric budget for entire model at end of time step 1 in stress period 1 (a) under no-flow boundary conditions and (b) under constant-head boundary conditions.**

(a)

<u>Cumulative volumes (ft<sup>3</sup>)</u>	<u>Rates for this time step (ft<sup>3</sup>/sec)</u>
In:	In:
Storage = .00000	Storage = .00000
Constant head = .00000	Constant head = .00000
Wells = .00000	Wells = .00000
Recharge = .38874E+08	Recharge = 449.93
River leakage = 2350.1	River leakage = .27200E-01
Total in = .38876E+08	Total in = 449.96
Out:	Out:
Storage = .00000	Storage = .00000
Constant head = .00000	Constant head = .00000
Wells = .38862E+08	Wells = 449.79
Recharge = .00000	Recharge = .00000
River leakage = 15038.	River leakage = .17406
Total out = .38877E+08	Total out = 449.96
In - Out = -564.00	In - Out = -.65002E-02
Percent discrepancy = .00	Percent discrepancy = .00

(b)

<u>Cumulative volumes (ft<sup>3</sup>)</u>	<u>Rates for this time step (ft<sup>3</sup>/sec)</u>
In:	IN:
Storage = .00000	Storage = .00000
Constant head = .98377E+07	Constant head = 113.86
Wells = .00000	Wells = .00000
Recharge = .33356E+08	Recharge = 386.07
River leakage = 2350.1	River leakage = .27200E-01
Total in = .43196E+08	Total in = 499.96
Out:	Out:
Storage = .00000	Storage = .00000
Constant head = .38733E+06	Constant head = 4.4829
Wells = .42803E+08	Wells = 495.40
Recharge = .00000	Recharge = .00000
River leakage = 6233.3	River leakage = .72144E-01
Total out = .43196E+08	Total out = 499.96
In - Out = .00000	In - Out = -.30518E-04
Percent discrepancy = .00	Percent discrepancy = .00

## CHAPTER 10

### CONCLUSIONS AND RECOMMENDATIONS

#### 10.1 Conclusions

The study area is bordered to the north and north-west by the Morov and Mishow mountains, to the south by the volcanic Sahand mountain and to the west by the Orumiyeh Lake. The prevailing climate of the area has semi-arid characteristics. The precipitation varies from about 200mm in the lowlands to about 500mm in the higher mountainous areas. The average mean monthly temperatures in Tabriz vary from -2 °C in January up to 28 °C in July, with a total annual corrected pan-evaporation of about 1000mm for the area.

Within the study area of approximately 7500 km<sup>2</sup> only about 42 percent contains good water-bearing strata. The pre-Quaternary rocks, with the exception of the Plio-pleistocene alluvial tuff, generally have the nature of aquicludes or very poor aquifers. There are two types of aquifers in the area, the first is unconfined and includes the southern alluvial tuff and northern and southern alluvial fans, as well as some parts of the central part of the Plain. The second is a multi-layer aquifer system that lies in the central Plain, and the Aji Chay and Mehran Chay river terraces and buried channel formations.

According to the results of geophysical investigations and drilled well logs, the thicknesses of the above-mentioned aquifers are as follows; (a) the fresh water, confined aquifer of the Tabriz Plain lies between about 58 and 120 m depth, (b) the average thickness of alluvial fans adjacent to the Plain is about 50 m, and (c) the thickness of the alluvial tuff aquifer ranges between a minimum of 10m and a maximum of 500m, with an average of 200m.

Monthly ground water levels have been recorded in the confined and unconfined aquifers of the Plain for a long time. Long-term decline of such levels is indicated in wells 28I-4S, 26I-1S, 32M-3D, 30R-1S and 24I-1S which are located in the alluvial fans of the northern and southern parts of the Plain. The maximum decline of water levels occurs in wells 26I-1D and 28I-4S, being about 6 to 8 metres over the 4 to 5 year period.

Seasonal fluctuations of ground water level operate in most of the monitoring wells. However, the maximum seasonal fluctuations (averaging 10m over a period of 6 years) occur in the most south-western part of the area, at well 30Q-2D located in the Azarshahr sub-basin. The total annual replenishment to the Plain aquifers calculated from the ground water level fluctuations is about  $4.1 \times 10^8 \text{ m}^3$ .

Ground water hydraulic gradients are subdued replicas of the land surface, though in the heavily pumped area in the south-western part of the Plain, reverse flow of ground water has occurred with resultant contamination of fresh water by saline water intrusion.

Drawdown and recovery data obtained from different parts of the area have been analysed by analytical and numerical methods to determine aquifer properties for the above-mentioned water-bearing layers. The resultant transmissivity values from both methods range from 500 to 3500  $\text{m}^2/\text{d}$  and 240 to 1000  $\text{m}^2/\text{d}$  for the Plain and alluvial tuff aquifers, respectively.

There are no observation well data available from the Plain area, therefore the storage coefficient could not be determined directly for this part of the area. However, the storage coefficient values resulting from the numerical method range between  $2.2 \times 10^{-3}$  and  $2.0 \times 10^{-5}$  for this area and between  $2.7 \times 10^{-1}$  and  $1.1 \times 10^{-1}$  for the alluvial tuff aquifer.

The step-drawdown test data have been analysed by the Bruin & Hudson, Eden & Hazel, Rorabaugh, and Jacob methods for most of the pumping wells in the study area. The resultant values suggest that some of the test wells were not properly designed and/or developed. The well loss (C) and aquifer loss (B) factors calculated by the Bruin and Hudson method range from  $1.0 \times 10^{-7}$  to  $1.1 \times 10^{-8} \text{ d}^2\text{m}^{-5}$  and  $4.66 \times 10^{-3}$  to  $4.14 \times 10^{-4} \text{ dm}^2$ , respectively.

The Tabriz area was divided into three hydrochemical zones, i.e. alluvial tuff, northern part of the Plain, and southern and central parts of the Plain. The values of total dissolved solids (TDS) in these zones range from 150 to 800 mg/l, 200 to 1200 mg/l, and 1000 to 5000 mg/l respectively. This higher value of TDS in the central part of the Plain resulted from (a) flatness of the ground surface, (b) shallow depth of ground water, (c) a boundary of silt and clay at the outlet of ground water flow from the aquifer, and (d) leakage of saline water from the River Aji Chay into the



aquifer.

Bicarbonate water is dominant in the alluvial tuff aquifer and higher elevation parts of the northern Plain. In this northern part, only 18 percent of water analyses have shown chloride type waters, whereas in the alluvial tuff such chloride type water is absent. The alluvial tuff water is rich in Ca and Na, whereas water in the northern part of the Plain is rich in Ca and Mg which reflect differences in the water bearing-layers in the area. The southern and central parts of the Plain represent a saline type of water in most cases, with 40 percent of the water samples from this area being rich in chloride.

Direct infiltration from precipitation, return flow from irrigation and sewage water, and seepage from losing rivers are the main components of the recharge, with evapotranspiration, spring discharge and artificial withdrawal from pumping wells and qanats being the main components of discharge in the area. The amount of total recharge from the above-mentioned components are calculated to be  $859 \times 10^6$  m<sup>3</sup>/year and the total artificial and spring discharges were measured by ARWA during August 1987 and generalised as  $763 \times 10^6$  m<sup>3</sup>/year.

The numerical ground water model was used to gain some understanding of the nature of ground water flow through the aquifers, to estimate regional aquifer parameters, and provide a check on the ground water balance. The model was run for a steady-state situation with assumed constant-head and no-flow boundary conditions. The aquifer parameters and recharge and discharge values were compared for both boundary conditions. The model was very sensitive to variations of the recharge and discharge rates as well as the transmissivity. The values of transmissivity resulting from the model were less than those deduced from the pumping test analysis.

## 10.2 Recommendations

The following recommendations are suggested on the basis of the problems that were encountered during the collection and analysis of the data.

A systematic data-bank section (archive and skilled people) is needed to collect and store all available data and provide a back up to replace those that are missing. Greater care should be taken to preserve all collected data, especially those

step-drawdown and constant rate tests that are very costly exercises.

The data from most of the climatological stations have not been recorded regularly. As a result, such irregularly collected data do not allow analysis of the data from all stations over the same suitable long-term period. It is recommended that any failed equipment and/or other obstacles in stations should be removed as soon as possible and regular and adequate data collected.

The withdrawal of ground water and the drilling of new wells in the southwestern part of the Plain (in Taimorly Village) should be strictly controlled in order to prevent the occurrence of reverse ground water flow and saline water intrusion into the fresh water aquifer.

A long-term rise of ground water levels was indicated in the western part of the Tabriz City due to intensive use and recharge of domestic and industrial water into the aquifer. Considerable ground water can be abstracted from this area for industrial and agricultural purposes subject to biochemical treatments.

The alluvial tuff aquifer supplies the major proportion of drinking and domestic water for Tabriz and its surrounding urban and rural areas. Hence, the measurement of ground water levels in such an aquifer is essential in order to detect long-term variations of water levels in the area.

The possibility of leakage from the uppermost saline water table aquifer of Tabriz Plain into the underlying multi-layered fresh water aquifers was determined in wells TPSW1 and TPSW3. The resultant values of hydraulic conductivity of the semi-permeable strata are very small. However, great care is essential when screen and casing are placed in new drilled wells.

The chemical analysis of ground water samples should include the analysis of potassium and nitrate along with the other major ions in order to make the analysis complete. This is essential for checking the validity of data quality, as a meaningful interpretation of existing hydrochemical evolution can only be obtained from reliable sets of data.

For the present ground water regime, the factors that produce undesired results are (a) sharp decline of ground water levels in some areas, (b) movement of saline ground water from nearby areas into the confined and unconfined aquifers due to excessive pumping from these aquifers in the Tabriz Plain, (c) high shallow-aquifer,

water evaporation from the Tabriz urban area due to high recharge of the municipal used and sewage water, and (d) saline water intrusion from some rivers which cross the Miocene formations.

Further hydrogeological data collection from the alluvial tuff aquifer will provide an opportunity to develop a regional ground water flow model. The model would provide a better understanding of ground water flow through the aquifer, ground water development possibilities and the testing of various management schemes.

## REFERENCES

- Abkav Consulting Engineers, 1976. Geo-electrical and seismic refraction survey in Azarshahr, Mamaghan, Khosrowshahr, Sardrud, Basmenj, and Bostanabad areas.
- AGRO-Water Consulting Engineers, 1977. Ground water Resources of Saidabad area and vicinity.
- Back, W., 1966. Hydrochemical facies and ground water flow patterns in northern part of Atlantic Coastal Plain. U.S. Geol. Surv. Prof. Paper 498-A, 42 pp.
- Balek, J., 1989. Groundwater resources assessment. Development in water science, Amsterdam, 249 pp.
- Bear, J. and Verruijt, A., 1990. Modelling groundwater flow and pollution. D. Reidel, Holland, 413pp.
- Beaumont, P., Blake, G. H. and Wagstaff, J. M., 1976. The Middle East: a geographical study, Wiley, London.
- Bengtsson, L., 1982. Groundwater and meltwater in the snowmelt induced runoff. Hydrological Sciences -Journal des Sciences Hydrologiques, 27, 2, 6.
- Bentz, A. and Martini, M. J., 1969. Lehrbuch der angewandten geologie und geowissenschaftlich methoden, second volume.
- Berberian, M., 1976. Contribution to the seismo-tectonics of Iran Part II. Geological Surv. Iran, Rep. No. 39, Tehran.
- Bierschenk, W. H. and Wilson, G. R., 1961. The exploration and development of groundwater resources in Iran. In symposium of Athen, Internat. Assoc. Sci. Hydrology. Vol. 2, pp. 607-27.
- Boulton, N. S., 1964. Analysis of data from non-equilibrium pumping tests allowing for delayed yield from storage. Proc. Instn. Civ. Engrs, Vol. 26, pp. 469-82.
- Bruin, J. and Hudson, H. E., 1955. Selected methods for pumping test analysis. Illinois State Water Survey. Rept. of Investigations. 25 pp.
- Burdon, D. J. and Mazloum, S. 1958. Some chemical types of groundwater from Syria. UNESCO SYMP. Teheran, pp. 73-90, UNESCO, Paris.
- CITRA-SOGREAH-CGG-HYDRA, 1965. Development and utilization of the ground water resources in the Tabriz area and vicinity (report in French).

- Clark, Lewis., 1977. The analysis and planning of step-drawdown tests. Q. Jl. Eng. Geol., Vol. 10, pp. 125-143.
- Cooper, H. H. and Jacob, C. E., 1946. A generalised graphical method for evaluating formation constants and summarizing well-field history. Trans. Amer. Geophys. Union, Vol. 27, No. IV, pp. 526-534.
- Connorton, B. J., and Reed, R. N., 1978. A numerical model for the prediction of long-term well yield in an unconfined chalk aquifer, Quart. Jour. Eng. Geol., Vol. II pp. 127-38.
- Davis, S. N. and DeWiest, R. J. M., 1966. Hydrogeology. John Wiley, New York, 463 pp.
- Dewan, M. L. and Famouri, J., 1947. The soils of Iran, FAO United Nations, Rome, 319 pp.
- Doorenbos, J. and Pruitt, W. O., 1977. Crop water requirements. Irrigation and Drainage paper 24. Food and Agriculture Organization, Rome, 144 pp.
- Durov, S. A., 1948. Natural water and graphic representation of their composition. Dokl. Akad. Nauk. SSSR 59, pp. 87-90.
- Eden, R. N. and Hazel, C. P., 1973. Computer and graphical analysis of variable discharge pumping tests of wells. Civil Engng. Trans. Inst. Eng. Austr.pp. 5-10.
- Eftekharneshad, J., 1975. Brief description of tectonic history and structural development of Azarbijan. Geol. Surv. Iran, Int. Rep.
- ELC-Electroconsult of Millano Company, 1969. Tabriz Plain water development. First Report.
- European Economic Community, 1975. Proposal for a council directive, relating to the quality of water for human consumption. Off. J. European Communities no. C214.
- Fetter, C. W., 2d. ed., 1988. Applied hydrogeology. Charles E. Merrill Pub. Co., London, 592 pp.
- Fetter, C. W., 1980. Applied hydrogeology. Charles E. Merrill Pub. Co., London, 488 pp.
- Fletcher, G. D., 2d. ed., 1987. Groundwater and Wells. Johnson Division, St. Pauls, Minnesota 55112, U.S.A., 1089 pp.
- Freeze, R. A. and Cheery, J. A., 1979. Groundwater. Prentice-hall, Inc., Englewood Cliffs, N. J. 07632, U.S.A., 604 pp.

- Ganji, M. H., 1968. Climate in the Cambridge History of Iran, Vol. 1: The land of Iran ed. by W. B. Fisher. Cambridge: Cambridge University Press, pp 212-249.
- Geophysical Institute of Israel, 1964. Geo-electrical survey of the Tabriz area.
- Grindley, J., 1970. Estimation and mapping of evaporation. IASH Pub. No. 92. World Water Balance, Vol. 1, pp. 200-213.
- Hantush, M. S., 1956. Analysis of data from pumping tests in leaky aquifers. Trans. Amer. Geophys. Union, Vol. 37, No. 6, pp. 702-714.
- Hem, J. D., 1985. Study and Interpretation of the Chemical Characteristics of Natural water (third edition). U. S. Geol. Surv. water supply paper 2254, 264 pp.
- Hill, R. A., 1940. Geochemical patterns in Coachella Valley California. American Geophysical Union Transactions, Vol. 21 pp. 46-49.
- Institute of Hydrology (IH), 1980. Low flow study, Report 1, London.
- IRAB Engineering Co., 1977. Final report on drilling and testing of deep wells for water supply to Tabriz Power Station.
- Issar, A., 1969. The groundwater provinces of Iran. Bulletin of the International Association of Scientific Hydrology, XIV, 1.
- Jacob, C. E., 1964. Drawdown test to determine effective radius of artesian well. Proc. Amer. Soc. Civ. Engrs., 72, pp. 629-646.
- Jensen, M. E. ed., 1974. Consumptive use of water and irrigation water requirements. Report for American Society of Civil Engineers. New York. 215p.
- Jones, G. P. and Rushton, K. R., 1981. Pumping test analysis. Lloyd, J. W.(Ed), Case studies in Ground Water resources evaluation. Clarendon Press, Oxford, pp. 65-86.
- Jones, G. P., 1972. Management of underground water resources, Q. Jl Engng. Geol. Volume 4, pp. 317-328.
- Kruseman, G. P. and De Ridder, N. A., 1970. Analysis and evaluation of pumping test data. Int. Inst. Land Reclam. and Improv. Wageningen, The Netherland., Bulletin. 11; 200 pp.
- Kurlov, M. G. 1928. Classification of mineral waters of Siberia. Tomsk, U.S.S.R.
- Kuros, G.H., 1977. Ground water study for Tabriz, Vol. 7, Tehran-Iran.

- Lennox, D. H., 1966. Analysis and application of step-drawdown tests. Proc. Amer. Soc. Civ. Engrs. Jl., Hydraulics Division. HY6. pp. 25-47.
- Lloyd, J. W., (Ed), 1981. Case-studies in groundwater resources evaluation. Clarendon press, Oxford, 206 pp.
- Lloyd, J. W. and Heathcote, J. A., 1985. Natural inorganic hydrochemistry in relation to ground water-An introduction, Clarendon Press, Oxford, 296 pp.
- Logan, J., 1964. Estimating transmissibility from routine production tests of water wells. Ground water Vol. 2, pp. 35-37.
- Mcdonald, M. G., and Harbaugh, A. W., 1988. A modular three-dimensional finite-difference ground-water flow model. Tech. Water-Resources Inv., Bk. 6, Chap. A1
- McKee, J. E. and Wolf, H. W., 1963. Water quality criteria, California State Water Quality Control Board Publications 3-A, 548 pp.
- Mercer, J. M. and Faust, C. R., 1981. Ground-Water modelling. Worthington, Ohio, National Water Works Association, 60 pp.
- Ministry of Agriculture, Fisheries and Food (MAFF), 1967. Potential Transpiration. Tech. Bull. 16, HMSO.
- Mogg, J. L., 1968. Step-drawdown test needs critical review. Ground water, vol. 7, No. 1, pp 28-34
- Moinvaziri, H. and Aminsobhani, I., 1975. Volcanological and Volcano-sedimentological study of Sahand Mountain. University of Tarbeyat Moallim, Tehran, Report in Persian.
- National Iranian Oil Company, 1978. Geological maps and sections of Iran, sheet 1, north-west of Iran. Tehran, Iran.
- Nowtash, H. et al., 1984. Water resources development of Sahand area, Artificial recharge investigations. Azarbijan Regional Water Authority. Report in Persian.
- Penman, H. L., 1948. Natural evaporation from open water, bar soil and grass. Proc. R. Soc. London, ser. A, 193 pp. 120-45.
- Penman, H. L., 1950. The water balance of the Stour catchment area. J. Inst. Water Eng., Vol. 4 pp. 457-469.
- Perrin de Brichambant, G. and Wallen, C. C., 1963. A study of Agroclimatology in Semi-arid and Arid zones of Near East. World Meteorological Organisation. Technical Note No. 56, Geneva, 64 pp.

- Piper, A. M., 1944. A graphical procedure in the geochemical interpretation of water analysis. Trans. Amer. Geophys. Union, Vol. 25, pp. 914-923.
- Rorabaugh, M. I., 1953. Graphical and theoretical analysis of step-drawdown tests of artesian wells. Proc. Amer. Soc. Civ. Engrs. Vol. 79. Separate No. 362, pp. 1-23.
- Rushton, K. R., 1978. Estimating transmissivity and storage co-efficient from abstraction well data. Groundwater Vol. 16, No. 2 pp. 81-85.
- Rushton, K. R. and Redshaw, S. C., 1979. Seepage and Ground Water Flow. John Wiley and Sons. Chichester, Inc. 332 pp.
- Rushton, K. R. and Srivastava, N. K., 1988. Interpreting injection well tests in an alluvial aquifer. Journal of Hydrology Vol. 99, pp. 49-60.
- Rushton, K. R. and Booth, S. J., 1975. Pumping test analysis using a discrete time-discrete space numerical method. Journal of Hydrology. Vol. 28, pp. 13-27.
- Rushton, K. R. and Chan, Y. K., 1976. A numerical model for pumping test analysis. Proc. Inst. Civ. Engrs., Part 2, pp. 281-296.
- Shainberg, I. and Oster, J. D., 1978. Quality of irrigation water. International Irrigation Centre, Israel, Publ. No. 2.
- Shaw, E. M., 1988. Hydrology in Practice. Van Nostrand Reinhold (UK) Co. Ltd. Workingham, Berkshire, England, 569 pp.
- Speen, W. C., 1947. A determination of the effect of topography upon precipitation. Trans. Amer. Geophys. Un. 28, pp 285-90
- Stephenson, G. R. and Freeze, R. A., 1974. Mathematical simulation of subsurface flow contributions to snowmelt runoff Reynolds Greek watershed, Idaho. Water Research Vol. 10, No. 2.
- Sternberg, Y. M., 1968. Simplified solution for variable rate pumping tests. Proc. Amer. Soc. Civ. Engrs. Jl. Hydraulics Division, HY 1, pp. 177-180.
- Stiff, H. A., 1951. The interpretation of chemical water analysis by means of patterns. Journal of Petroleum Technology, Vol. 3, No. 10, pp. 15-17.
- Streltsova, T. D., 1973. Flow near a pumped well in an unconfined aquifer under non-steady conditions. Water Resources Research, Vol. 9 No. 1 pp. 227-235.
- Theis, C. V., 1935. The relation between the lowering of the piezometric surface and the rate and duration of discharge of a well using ground water storage. Trans. Amer. Geophys. Union, Vol. 2, pp. 519-524.

\* Searcy, J. K., 1959. Flow duration curves. U.S.G.S. Wat. Sup. Pap. 1542a.



- Thornthwaite, C. W., 1948. An approach toward a rational classification of climate. Geogr. Rev., Vol. 38, pp 55-94.
- Todd, D. K., 2d. ed., 1980. Groundwater Hydrology. John Wiley & Sons Inc. New York, U.S.A., 535 pp.
- Walton, W. C., 1970. Groundwater Resources Evaluation. McGraw-Hill Inc. New York. 664 pp.
- Wang, H. F. and Anderson, M. P., 1982. Introduction to ground water modelling. W. H. Freeman, San Francisco, 236 pp.
- Ward, R. C., 1975. Principles of Hydrology. Second Edition, Mcgraw-Hill Book Company (UK) Ltd. Maidenhead, Berkshire, England, 367 pp.
- Water Science and Technology Board, 1990. Groundwater models, Scientific and regulatory applications. National Academy Press, Washington, D. C., 303 pp.
- Williamson, R. J. and Lawrence, C.R., 1980. Review of methods for estimating recharge in Australia. Proceeding of the groundwater recharge conference.
- Wilson, E. M., 3rd. ed., 1983. Engineering hydrology. Macmillan, London, 310 pp.
- Zaporozec, A., 1972. Graphical interpretation of water quality data. Ground Water Vol. 10, pp. 32-43.

## **Appendix 1 Constant Rate Test and Calculated Recovery Data**

## Appendix 1: Constant Rate Test Data

Drawdown and Recovery Data from Saidabad Pumping Well 1 (SW1) Q = 7171 (m<sup>3</sup>/d)

Time(min)

1	2	3	4	5	6	7	8	9	10
12	14	16	18	20	22	24	26	28	30
35	40	45	50	55	60	65	70	75	80
85	90	95	100	105	110	120	130	140	150
160	170	180	195	210	225	240	255	270	285
300	330	360	390	420	450	480	510	540	570
600	630	660	690	720	750	780	710	840	870
900	960	1020	1080	1140	1200	1260	1320	1380	1440
1500	1560	1620	1680	1740	1800	1860	1920	1980	2040
2100	2160	2220	2280	2340	2460	2580	2700	2820	2940
3060	3180	3300	3420	3540	3660	3780	3960	4140	4320
4321	4322	4323	4324	4325	4326	4327	4328	4329	4330
4332	4334	4336	4338	4340	4342	4344	4346	4348	4350
4355	4360	4365	4370	4375	4380	4385	4390	4395	4400
4405	4410	4415	4420	4430	4440	4450	4460	4470	4480
4490									

Drawdown and Calculated Recovery (m)

23.77	25.05	25.59	26.74	26.93	27.05	27.25	27.50	27.75	27.97
28.34	28.65	28.88	29.14	29.30	29.40	29.39	29.70	29.82	29.93
30.09	30.21	30.42	30.48	30.53	30.66	30.70	30.83	30.87	30.92
30.99	31.08	31.19	31.19	31.24	31.27	31.27	31.34	31.38	31.41
31.45	31.48	31.51	31.55	31.58	31.61	31.68	31.72	31.79	31.85
31.88	31.91	31.98	32.05	32.09	32.16	32.24	32.35	32.40	32.44
32.48	32.50	32.53	32.58	32.66	32.72	32.77	32.81	32.89	32.93
32.99	33.02	33.09	33.12	33.18	33.22	33.29	33.33	33.41	33.45
33.48	33.53	33.56	33.60	33.61	33.64	33.66	33.67	33.67	33.67
33.68	33.68	33.68	33.68	33.69	33.69	33.69	33.69	33.69	33.69
33.69	33.69	33.70	33.70	33.70	33.70	33.70	33.70	33.70	33.70
7.98	6.77	6.65	6.51	6.15	5.94	5.69	5.40	5.11	4.89
4.52	4.25	3.77	3.45	3.20	3.07	2.92	2.79	2.65	2.58
2.45	2.22	2.08	1.92	1.81	1.70	1.59	1.49	1.40	1.15
1.12	1.03	0.95	0.78	0.63	0.52	0.35	0.20	0.20	0.12
0.03									

Q = discharge rate

**Drawdown and Recovery Data from Saidabad Observation Well 1(SWP1)**

**r = 50m**

**Q = 7171 (m<sup>3</sup>/d)**

**Time (min)**

6	9	16	25	48	70	105	180	260	400
560	840	1100	1600	1900	2400	3200	4320		
4323	4326	4332	4340	4360	4385	4390	4450	4510	4555
4620	4735	5120							

**Drawdown and Calculated Recovery (m)**

0.18	0.25	0.34	0.58	1.08	1.26	1.52	1.83	2.01	2.10
2.15	2.28	2.35	2.38	2.40	2.42	2.43	2.44		
2.35	2.34	2.32	2.15	1.78	1.63	1.43	1.28	1.06	0.93
0.73	0.59	0.58							

**Drawdown and Recovery Data from Saidabad Observation Well 7 (SWP7)**

**r = 50m**

**Q= 3456 (m<sup>3</sup>/d)**

**Time (min)**

12	28	50	85	105	170	230	380	620	860
1300	1650	2200	2800	3400					
4320	4326	4336	4350	4365	4400	4430	4490	4570	4705
4765	4860	4980							

**Drawdown and Recovery (m)**

0.33	0.79	1.32	1.71	1.88	2.12	2.26	2.32	2.39	2.48
2.51	2.54	2.57	2.62	2.65					
2.57	2.04	1.69	1.44	1.32	1.15	0.91	0.66	0.26	0.17
0.14	0.11	0.09							

**r = distance between the observation well and pumping well centre**

Drawdown and Recovery Data from Saidabad Pumping Well 3 (SW3)

Q= 8294 (m<sup>3</sup>/d)

Time (min)

1	2	3	4	5	6	7	8	9	10
12	14	16	18	20	22	24	26	28	30
33	36	39	42	45	50	55	60	65	70
75	80	85	90	95	100	110	120	130	140
150	160	170	180	195	210	225	240	255	270
285	300	330	360	390	420	450	480	510	540
570	600	630	660	690	720	750	780	810	840
870	900	960	1020	1080	1140	1200	1260	1320	1380
1440	1500	1560	1620	1680	1740	1800	1860	1920	1980
2040	2100	2160	2220	2280	2340	2400	2460	2520	2580
2640	2700	2760	2820	2880	2940	3000	3060	3120	3180
3240	3300	3360	3420	3480	3540	3600	3660	3720	3780
3840	3900	3960	4020	4080	4140	4200	4260	4320	
4320.5	4321	4321.5	4322	4322	4323	4323.5	4324	4324.5	4325
4326	4327	4328	4329	4330	4332	4334	4336	4338	4340
4342	4344	4346	4348	4350	4353	4356	4359	4362	4365
4370	4375	4380	4385	4390	4395	4400	4405	4410	4415
4420	4430	4440	4450	4460	4470	4480	4490	4500	4515
4530	4545	4560	4575	4590	4620	4650	4680	4710	4740
4770	4800	4830	4860	4890	4920	4950	4980	5010	5040
5070	5100	5130	5160	5190	5220	5280	5340	5400	5460
5520	5580	5640							

Drawdown and Calculated Recovery (m)

18.99	19.92	20.80	21.29	21.51	21.74	21.75	21.87	22.05	22.28
22.52	22.77	22.88	23.01	23.15	23.27	23.37	23.43	23.48	23.57
23.71	23.48	23.89	23.95	23.98	24.08	24.28	24.95	25.01	25.08
25.14	25.19	25.28	25.34	25.36	25.44	25.48	25.55	25.61	25.68
25.72	25.78	25.82	25.88	25.92	25.95	26.03	26.10	26.14	26.18
26.22	26.25	26.28	26.32	26.34	26.38	26.40	26.44	26.45	26.47
26.50	26.54	26.56	26.58	26.60	26.61	26.63	26.66	26.67	26.69
26.70	26.72	26.73	26.75	26.77	26.79	26.82	26.85	26.87	26.89
26.91	26.95	26.96	26.97	26.99	27.00	27.03	27.06	27.20	27.25
27.28	27.32	27.34	27.38	27.41	27.45	27.48	27.51	27.54	27.56
27.60	27.61	27.61	27.62	27.62	27.63	27.64	27.65	27.65	27.66
27.67	27.95	27.96	27.98	27.98	28.00	28.01	28.02	28.03	28.05
28.04	28.05	28.07	28.08	28.09	28.10	28.10	28.11	28.12	
7.20	7.10	6.35	5.99	5.45	5.10	4.90	4.65	4.53	4.38
4.28	4.20	4.00	3.90	3.80	3.70	3.62	3.52	3.38	3.30
3.25	3.20	3.14	3.02	2.96	2.84	2.64	2.52	2.40	2.38
2.28	2.13	2.00	1.88	1.74	1.62	1.49	1.37	1.26	1.12
1.10	1.08	1.05	0.90	0.87	0.79	0.71	0.69	0.67	0.65
0.62	0.60	0.58	0.57	0.55	0.53	0.50	0.48	0.47	0.45
0.41	0.38	0.35	0.32	0.30	0.25	0.20	0.18	0.16	0.14
0.13	0.11	0.10	0.09	0.08	0.07	0.07	0.07	0.06	0.06
0.06	0.05	0.05							

**Drawdown and Recovery Data from Saidabad Observation Well 3 (SWP3)**

$r = 50\text{m}$        $Q = 8294 \text{ (m}^3/\text{d)}$

Time (min)

4	5	6	7	8	9	10	12	14	16
18	20	22	24	26	28	30	33	36	39
42	45	50	55	60	65	70	75	80	85
90	95	100	110	120	130	140	150	160	170
180	195	210	225	240	255	270	285	300	330
360	390	420	450	480	510	540	570	600	630
660	690	720	750	780	810	840	870	900	960
1020	1080	1140	1200	1260	1320	1380	1440	1500	1560
1620	1680	1740	1800	1860	1920	1980	2040	2100	2160
2220	2280	2340	2460	2580	2700	2940	3060	3180	3300
3420	3540	3660	3780	3960	4140	4320			
4320.5	4321	4321.5	4322	4322	4323	4323.5	4324	4324.5	4325
4326	4327	4328	4329	4330	4332	4334	4336	4338	4340
4342	4344	4346	4348	4350	4353	4356	4359	4362	4365
4370	4375	4380	4385	4390	4395	4400	4405	4410	4415
4420	4430	4440	4450	4460	4470	4480	4490	4500	4515
4530	4545	4560	4575	4590	4605	4620	4650	4680	4710
4740	4770	4800	4830	4860	4890	4920	4950	4980	5010

Drawdown and Calculated Recovery (m)

0.02	0.08	0.13	0.23	0.39	0.58	0.71	0.91	1.01	1.05
1.13	1.22	1.37	1.51	1.61	1.70	1.78	1.86	1.92	1.98
2.03	2.09	2.13	2.20	2.25	2.29	2.33	2.39	2.44	2.51
2.55	2.59	2.62	2.66	2.69	2.72	2.78	2.82	2.85	2.88
2.92	2.94	2.97	2.99	3.01	3.03	3.05	3.07	3.09	3.10
3.11	3.13	3.15	3.16	3.16	3.17	3.18	3.20	3.20	3.20
3.23	3.23	3.23	3.25	3.26	3.26	3.26	3.28	3.28	3.28
3.31	3.33	3.35	3.37	3.37	3.37	3.37	3.38	3.39	3.40
3.40	3.41	3.41	3.42	3.42	3.42	3.43	3.43	3.43	3.44
3.45	3.45	3.45	3.46	3.47	3.47	3.48	3.49	3.51	3.53
3.53	3.54	3.55	3.55	3.56	3.57	3.58	3.58	3.58	3.58
3.58	3.57	3.57	3.54	3.53	3.43	3.34			
3.25	3.21	3.03	3.01	2.88	2.81	2.71	2.63	2.52	2.41
2.30	2.22	2.15	2.07	2.01	1.96	1.91	1.87	1.79	1.76
1.69	1.63	1.61	1.55	1.51	1.46	1.33	1.25	1.15	1.03
1.01	0.95	0.91	0.89	0.83	0.79	0.73	0.67	0.63	0.59
0.54	0.51	0.48	0.45	0.42	0.41	0.39	0.38	0.34	0.31
0.29	0.27	0.23	0.22	0.16	0.13	0.11	0.08	0.06	0.03

Drawdown and Recovery Data from Saidabad Pumping Well 7 (SW7) Q= 3456 (m<sup>3</sup>/d)

Time (min)

1	2	3	4	5	6	7	8	9	10
12	14	16	18	20	22	24	26	28	30
33	36	39	42	45	50	55	60	65	70
75	80	85	90	95	100	110	120	130	140
150	160	170	180	195	210	225	240	255	270
285	300	330	360	390	420	450	480	510	540
570	600	630	660	690	720	750	780	810	840
870	900	960	1020	1080	1140	1200	1260	1320	1380
1440	1500	1560	1620	1680	1740	1800	1860	1920	1980
2040	2100	2160	2220	2280	2340	2400	2460	2520	2580
2640	2700	2760	2820	2880	2940	3000	3060	3120	3180
3240	3300	3360	3420	3480	3540	3600	3660	3720	3780
3840	3900	3960	4020	4080	4140	4200	4260	4320	
4321	4322	4323	4324	4325	4326	4327	4328	4329	4330
4332	4334	4336	4338	4340	4342	4344	4346	4348	4350
4353	4356	4359	4362	4365	4370	4375	4380	4385	4390
4395	4400	4405	4410	4415	4420	4430	4440	4450	4460
4470	4480	4490	4500	4515	4530	4545	4560	4575	4590
4605	4620	4650	4680	4710	4740	4770	4800	4830	4860
4890	4920	4950	4980						

Drawdown and Calculated Recovery (m)

6.75	6.50	7.70	7.75	7.98	8.10	8.25	8.34	8.45	8.50
9.30	9.84	10.02	10.15	11.72	11.90	11.97	12.12	12.20	12.35
12.45	12.50	12.60	12.67	12.75	12.78	12.85	12.91	13.00	13.05
13.10	13.16	13.19	13.22	13.25	13.28	13.30	13.33	13.37	13.42
13.47	13.49	13.52	13.54	13.56	13.60	13.62	13.65	13.67	13.69
13.73	13.75	13.77	13.81	13.83	13.84	13.85	13.87	13.90	13.91
13.91	13.92	13.95	13.97	13.99	14.02	14.05	14.07	14.10	14.15
14.19	14.20	14.22	14.24	14.26	14.29	14.31	14.34	14.36	14.39
14.40	14.41	14.41	14.42	14.42	14.44	14.44	14.44	14.45	14.45
14.45	14.45	14.46	14.46	14.48	14.47	14.47	14.47	14.48	14.49
14.30	14.33	14.35	14.36	14.38	14.40	14.42	14.43	14.45	14.47
14.49	14.51	14.53	14.54	14.56	14.56	14.56	14.56	14.57	14.57
14.57	14.56	14.56	14.56	14.56	14.56	14.56	14.56	14.56	
10.66	8.80	7.40	4.34	4.29	4.20	4.12	4.03	3.95	3.83
3.76	3.62	3.55	3.42	3.38	3.30	3.20	3.19	3.10	3.06
3.00	2.97	2.90	2.86	2.81	2.76	2.71	2.65	2.59	2.54
2.48	2.40	2.36	2.28	2.20	2.18	2.09	2.05	1.92	1.84
1.78	1.67	1.59	1.47	1.39	1.30	1.21	1.13	1.05	0.92
0.89	0.80	0.79	0.74	0.70	0.68	0.66	0.65	0.63	0.62
0.60	0.55	0.50	0.47						

**Drawdown and Recovery Data from Jamshidabad Pumping Well 1 (JW1) Q= 5702 (m<sup>3</sup>/d)**

**Time(mim)**

1	2	3	4	5	6	7	8	9	10
12	14	16	18	20	22	24	26	28	30
35	40	45	50	55	60	65	70	75	80
85	90	95	100	110	120	130	140	150	160
170	180	210	240	270	300	360	420	480	540
600	720	840	960	1080	1200	1320	1440	1560	1680
1800	1920	2040	2160	2280	2400	2520	2640	2760	2880
2881	2882	2883	2884	2885	2886	2887	2888	2889	2890
2892	2894	2896	2898	2900	2902	2904	2906	2908	2910
2915	2920	2925	2930	2935	2940	2945	2950	2955	2960
2965	2970	2975	2980	2990	3000	3010	3020	3030	3040
3050	3060	3090	3120	3150	3180	3240	3300	3360	3420
3480	3540	3720							

**Drawdown and Calculated Recovery (m)**

6.97	8.08	8.28	8.52	8.60	8.70	8.82	8.93	8.98	8.99
9.25	9.45	9.50	9.58	9.68	9.75	9.85	9.90	9.95	10.00
10.22	10.32	10.42	10.50	10.58	10.63	10.68	10.72	10.77	10.80
10.83	10.86	10.87	10.88	10.92	11.00	11.10	11.20	11.30	11.32
11.35	11.40	11.50	11.68	11.85	12.00	12.20	12.40	12.55	12.63
12.58	12.72	12.75	12.79	12.85	12.88	12.90	12.92	12.98	13.00
13.30	13.34	13.34	13.34	13.35	13.35	13.35	13.35	13.35	13.35
5.10	4.75	4.53	4.30	4.10	3.95	3.80	3.70	3.60	3.50
3.44	3.37	3.30	3.23	3.16	2.78	3.02	2.77	2.91	2.85
2.71	2.60	2.55	2.50	2.45	2.40	2.35	2.30	2.25	2.20
2.15	2.10	2.07	2.04	1.98	1.92	1.85	1.80	1.75	1.70
1.65	1.60	1.50	1.40	1.30	1.20	1.10	1.00	0.90	0.80
0.70	0.55	0.30							



Drawdown and Recovery Data from Jamshidabad Pumping Well 2 (JW2) Q= 5443 (m<sup>3</sup>/d)

Time (min)

1	2	3	4	5	6	7	8	9	10
12	14	16	18	20	22	24	26	28	30
35	40	45	50	55	60	65	70	75	80
85	90	95	100	110	120	130	140	150	160
170	180	195	210	225	240	255	270	285	300
330	360	390	420	450	480	510	540	570	600
630	660	690	720	750	780	810	840	870	900
960	1020	1080	1140	1200	1260	1320	1380	1440	1560
1680	1800	1920	2040	2160	2280	2400	2520	2640	2760
2880									
2881	2882	2883	2884	2885	2886	2887	2888	2889	2890
2892	2894	2896	2898	2900	2902	2904	2906	2908	2910
2915	2920	2925	2930	2935	2940	2945	2950	2955	2960
2965	2970	2975	2980	2990	3000	3010	3020	3050	3060
3075	3090	3105	3120	3135	3150	3165	3180	3210	3240
3270	3300	3330	3360	3390	3420	3450	3480	3510	3540
3570	3600	3630	3660	3690	3720	3750	3780	3840	3900

Drawdown and Calculated Recovery (m)

29.53	29.93	30.55	30.68	30.78	30.86	30.93	31.2	31.15	31.20
31.32	31.37	31.42	31.53	31.64	31.71	31.77	31.81	31.85	31.89
31.93	31.96	32.0	32.5	32.8	32.10	32.13	32.16	32.18	32.20
32.23	32.25	32.27	32.30	32.32	32.36	32.39	32.42	32.43	32.45
32.47	32.49	32.53	2.55	32.57	32.60	32.63	32.66	32.68	32.70
32.72	32.75	32.78	32.80	32.83	32.85	32.88	32.91	32.92	32.93
32.95	32.96	32.97	32.98	33.0	33.3	33.3	33.4	33.4	33.8
33.6	33.6	33.6	33.7	33.7	33.7	33.7	33.8	33.8	33.8
33.8	33.8	33.8	33.8	33.8	33.9	33.9	33.9	33.9	33.9
33.9									
7.48	6.43	5.91	5.73	5.54	5.31	5.16	5.9	4.97	4.86
4.80	4.75	4.66	4.55	4.44	4.29	4.16	4.4	3.90	3.78
3.66	3.58	3.51	3.47	3.41	3.30	3.26	3.15	3.8	3.3
2.92	2.86	2.83	2.73	2.65	2.58	2.53	2.46	2.31	2.28
2.26	2.23	2.18	2.15	2.8	2.3	1.98	1.94	1.88	1.82
1.76	1.68	1.63	1.58	1.55	1.50	1.47	1.44	1.39	1.36
1.30	1.28	1.26	1.19	1.16	1.13	1.8	1.5	1.0	0.98

Drawdown and Recovery Data from Tabriz Airport Pumping Well (TAW) Q= 8640 (m<sup>3</sup>/d)

Time (min)

1	2	3	4	5	6	7	8	9	10
12	14	16	18	20	22	24	26	28	30
33	36	39	42	45	50	55	60	65	70
75	80	85	90	100	110	120	150	180	210
240	270	300	360	420	480	540	600	660	720
780	840	900	1020	1140	1260	1380	1500	1620	1740
1860	1980	2100	2220	2340	2460	2580	2700	2820	2880
2881	2882	2883	2884	2885	2886	2887	2888	2889	2890
2892	2894	2896	2898	2900	2902	2904	2906	2908	2910
2913	2916	2919	2922	2925	2930	2935	2940	2945	2950
2955	2960	2965	2970	2975	2980	2990	3000	3010	3020
3030	3040	3050	3060						

Drawdown and Calculated Recovery (m)

4.00	3.95	3.90	3.93	3.95	3.98	4.02	4.05	4.07	4.10
4.13	4.17	4.20	4.22	4.23	4.25	4.26	4.28	4.29	4.31
4.35	4.36	4.38	4.40	4.41	4.42	4.43	4.45	4.47	4.48
4.50	4.52	4.55	4.57	4.59	4.62	4.64	4.65	4.69	4.73
4.75	4.76	4.78	4.79	4.81	4.82	4.83	4.84	4.86	4.86
4.87	4.88	4.89	4.91	4.86	4.87	4.88	4.88	4.88	4.90
4.92	4.94	4.96	4.99	5.02	5.03	5.04	5.04	5.04	5.04
1.25	0.93	0.83	0.78	0.72	0.69	0.66	0.63	0.60	0.59
0.55	0.52	0.48	0.46	0.45	0.43	0.42	0.40	0.38	0.37
0.36	0.35	0.34	0.32	0.31	0.30	0.26	0.25	0.23	0.21
0.20	0.19	0.19	0.18	0.16	0.14	0.11	0.09	0.08	0.04
0.05	0.03	0.02	0.01						

Drawdown and Recovery Data from Soufian Pumping Well (SOW) Q= 6394 (m<sup>3</sup>/d)

Time (min)

1	2	3	4	5	6	7	8	9	10
12	14	16	18	20	22	24	26	28	30
33	36	39	42	45	50	55	60	65	70
75	80	85	90	95	100	110	120	130	140
150	160	170	180	195	210	225	240	255	270
285	300	330	360	390	420	450	480	510	540
570	600	630	660	690	720	750	780	810	840
870	900	960	1020	1080	1140	1200			
1201	1202	1203	1204	1205	1206	1207	1208	1209	1210
1212	1214	1216	1218	1220	1222	1224	1226	1228	1230
1233	1236	1239	1242	1245	1250	1255	1260	1265	1270
1275	1280	1285	1290	1295	1300	1310	1320	1330	1340
1350	1360	1370	1380	1395	1410	1425	1440		

Drawdown and Calculated Recovery (m)

10.00	10.40	10.60	10.85	11.00	11.12	11.25	11.30	11.35	11.35
11.36	11.37	11.39	11.40	11.42	11.43	11.44	11.45	11.47	11.48
11.49	11.50	11.51	11.51	11.51	11.53	11.53	11.55	11.56	11.56
11.58	11.58	11.60	11.62	11.64	11.66	11.69	11.72	11.72	11.72
11.74	11.78	11.82	11.85	11.87	11.88	11.90	11.91	11.91	11.91
11.93	11.93	11.95	11.95	11.95	11.96	11.96	11.97	11.98	11.99
11.99	11.99	12.00	12.00	12.01	12.03	12.03	12.03	12.04	12.04
12.04	12.06	12.08	12.08	12.08	12.10	12.10			
1.30	1.01	0.91	0.75	0.62	0.55	0.50	0.44	0.40	0.38
0.34	0.31	0.30	0.29	0.28	0.27	0.27	0.26	0.26	0.25
0.24	0.22	0.21	0.20	0.19	0.18	0.17	0.16	0.16	0.15
0.15	0.15	0.13	0.13	0.13	0.12	0.12	0.11	0.10	0.10
0.09	0.09	0.09	0.08	0.08	0.06	0.04	0.02		

## **Appendix 2 Step-Drawdown Test Data**

**Appendix 2: Step-Drawdown Test Data**

Step-Drawdown Tests Data from Saidabad Pumping Well 1 (SW1) Time Steps=180 (min)

Q1=4666 (m<sup>3</sup>/d) Q2=5702 (m<sup>3</sup>/d) Q3=6826 (m<sup>3</sup>/d) Q4=7171 (m<sup>3</sup>/d)

Time (min)

0	1	2	3	4	5	6	7	8	9
10	12	14	16	18	20	22	24	26	28
30	35	40	45	50	55	60	65	70	75
80	85	90	95	100	110	120	130	140	150
160	170	180							
181	182	183	184	185	186	187	188	189	190
192	194	196	198	200	202	204	206	208	210
215	220	225	230	235	240	245	250	255	260
265	270	275	280	290	300	310	320		
330	340	350	360						
361	362	363	364	365	366	367	368	369	370
372	374	376	378	380	382	384	386	388	390
395	400	405	410	415	420	425	430	435	440
445	450	455	460	470	480	490	500	510	520
530	540								
541	542	543	544	545	546	547	548	549	550
552	554	556	558	560	562	564	566	568	570
575	580	585	590	595	600	605	610	615	620
625	630	635	640	650	660	670	680	690	700
710	720								

Drawdown (m)

0.00	13.12	18.42	18.77	19.32	19.70	19.87	20.12	20.32	20.4
20.46	20.46	20.46	20.57	20.57	20.62	20.72	20.75	20.82	20.92
21.02	21.17	21.17	21.22	21.32	21.37	21.47	21.57	21.72	21.87
22.07	22.92	22.99	23.05	23.07	23.11	23.17	23.21	23.27	23.32
23.32	23.37	23.39							
27.32	28.29	28.44	28.52	28.62	28.65	28.71	28.72	28.74	28.75
28.77	28.82	28.85	28.87	28.87	28.87	28.87	28.89	28.89	28.91
28.98	29.02	29.12	29.12	29.12	29.12	29.12	29.12	29.12	29.14
29.16	29.16	29.18	29.20	29.22	29.27	29.32	29.37	29.42	29.44
29.47	29.47								
33.87	33.92	35.27	35.45	35.62	35.72	35.77	35.85	35.88	35.92
36.07	36.14	36.22	36.24	36.26	36.28	36.30	36.32	36.32	36.32
36.32	36.32	36.32	36.32	36.32	36.32	36.32	36.34	36.34	36.36
36.38	36.39	36.39	36.40	36.40	36.42	36.44	36.46	36.48	36.50
36.52	36.52								
36.62	36.64	36.65	36.65	36.65	36.65	36.65	36.65	36.66	36.66
36.66	36.66	36.65	36.64	36.64	36.62	36.62	36.63	36.63	36.63
36.63	36.62	36.62	36.62	36.60	36.60	36.58	36.58	36.58	36.56
36.56	36.54	36.54	36.54	36.54	36.54	36.54	36.52	36.52	36.48
36.46	36.42								

Step-Drawdown Test Data from Jamshidabad Pumping Well 2 (JW2) Time Steps=180 (min)

Q1=2938 (m<sup>3</sup>/d) Q2=4061 (m<sup>3</sup>/d) Q3=5011 (m<sup>3</sup>/d) Q4=5789 (m<sup>3</sup>/d)

Time(min)

0	1	2	3	4	5	6	7	8	9
10	12	14	16	18	20	22	24	26	28
30	35	40	45	50	55	60	65	70	75
80	85	90	95	100	110	120	130	140	150
170	180								
181	182	183	184	185	186	187	187	189	190
192	194	196	198	200	202	204	206	208	210
215	220	225	230	235	240	245	250	255	260
265	270	275	280	290	300	310	320	330	340
350	360								
361	362	363	364	365	366	367	368	369	370
372	374	376	378	380	382	384	386	388	390
395	400	405	410	415	420	425	430	435	440
445	450	455	460	470	480	490	500	510	520
530	540								
541	542	543	544	545	546	547	548	549	550
552	554	556	558	560	562	564	566	568	570
575	580	585	590	595	600	605	610	615	620
625	630	635	640	650	660	670	680	690	700
710	720								

Drawdown (m)

0.00	11.50	11.60	11.75	11.90	11.98	12.00	12.05	12.10	1220
12.30	12.45	12.57	12.70	12.90	12.93	12.96	12.98	13.00	1305
13.06	13.10	13.15	13.20	13.25	13.30	13.32	13.38	13.42	1348
13.52	13.54	13.56	13.58	13.64	13.71	13.76	13.80	13.85	1390
13.92	13.95								
19.20	19.40	19.50	19.61	19.68	19.72	19.75	19.77	19.78	1981
19.85	19.89	19.69	20.03	20.10	20.18	20.24	20.30	20.32	2036
20.38	20.42	29.47	20.51	20.58	20.61	20.64	20.68	20.72	2076
20.80	20.85	20.88	20.91	20.96	20.98	21.01	21.06	21.10	2112
21.15	21.17								
27.24	27.35	27.47	27.52	27.65	27.78	27.83	27.87	27.92	2798
28.04	28.06	28.10	28.13	28.20	28.22	28.25	28.30	28.34	2837
28.40	28.43	28.48	28.50	28.51	28.54	28.56	28.57	28.60	2863
28.65	28.67	28.69	28.72	28.75	28.77	28.79	28.82	28.85	2888
28.89	28.92								
32.54	32.66	32.74	32.84	32.97	32.99	33.08	33.15	33.18	3321
33.23	33.26	33.28	33.31	33.33	33.37	33.38	33.42	33.46	3347
33.49	33.51	33.64	33.56	33.58	33.62	33.65	33.69	33.72	3374
33.49	33.81	33.84	33.87	33.90	33.92	33.98	34.01	34.04	3408
34.09	34.10								

Step-Drawdown Test Data from Tabriz Airport Pumping Well(TAW) Time Steps=180 (min)

Q1=5184 (m<sup>3</sup>/d) Q2=6566 (m<sup>3</sup>/d) Q3=7776 (m<sup>3</sup>/d) Q4=9072 (m<sup>3</sup>/d)

Time (min)

0	1	2	3	4	5	6	7	8	9
10	12	14	16	18	20	22	24	26	28
30	33	36	39	42	45	50	55	60	65
70	75	80	85	90	100	110	120	130	140
150	160	170	180						
181	182	183	184	185	186	187	188	189	190
192	194	196	198	200	202	204	206	208	210
213	216	219	222	225	230	235	240	245	250
255	260	265	270	280	290	300	310	320	330
340	350	360							
361	362	363	364	365	366	367	368	369	370
372	374	376	378	380	382	384	386	388	390
393	396	399	402	405	410	415	420	425	430
435	440	445	450	460	470	480	490	500	510
520	530	540							
541	542	543	544	545	546	547	548	549	550
552	554	556	558	560	562	564	566	568	570
573	576	579	582	585	590	595	600	605	610
615	620	625	530	640	650	660	670	680	690
700	710	720							

Drawdown

0.00	2.00	2.13	2.20	2.27	2.32	2.35	2.37	2.39	2.42
2.43	2.43	2.44	2.45	2.47	2.48	2.49	2.50	2.51	2.52
2.52	2.53	2.54	2.54	2.55	2.56	2.57	2.58	2.59	2.60
2.60	2.61	2.62	2.63	2.64	2.65	2.66	2.67	2.68	2.69
2.70	2.71	2.72	2.72						
3.25	3.27	3.31	3.32	3.32	3.33	3.33	3.34	3.35	3.35
3.36	3.36	3.37	3.37	3.38	3.38	3.39	3.39	3.39	3.40
3.40	3.40	3.40	3.41	3.41	3.42	3.42	3.43	3.43	3.43
3.43	3.43	3.43	3.44	3.44	3.45	3.46	3.46	3.47	3.47
3.48	3.49	3.49							
4.17	4.18	4.19	4.20	4.20	4.21	4.22	4.23	4.23	4.24
4.25	4.26	4.26	4.27	4.27	4.28	4.28	4.28	4.29	4.29
4.30	4.30	4.30	4.30	4.31	4.32	4.32	4.32	4.32	4.33
4.33	4.33	4.34	4.34	4.34	4.35	4.35	4.36	4.36	4.37
4.37	4.38	4.38							
4.86	5.09	5.13	5.14	5.15	5.16	5.17	5.18	5.18	5.18
5.19	5.19	5.20	5.21	5.21	5.22	5.23	5.23	5.24	5.25
5.25	5.26	5.27	5.27	5.28	5.28	5.28	5.29	5.30	5.30
5.31	5.32	5.32	5.33	5.34	5.34	5.35	5.36	5.36	5.37
5.37	5.38	5.38							

Step-Drawdown Test Data from Soufian Pumping Well(SOW) Time Steps=180 (min)

Q1=4406 (m<sup>3</sup>/d) Q2=5184 (m<sup>3</sup>/d) Q3=6134 (m<sup>3</sup>/d) Q4=6998 (m<sup>3</sup>/d)

Time (min)

0	1	2	3	4	5	6	7	8	9
10	12	14	16	18	20	22	24	26	28
30	33	36	39	42	45	50	55	60	65
70	75	80	85	90	95	100	110	120	130
140	150	160	170	180					
181	182	183	184	185	186	187	188	189	190
192	194	196	198	200	202	204	206	208	210
213	216	219	222	225	230	235	240	245	250
255	260	265	270	275	280	290	300	310	320
330	340	350	360						
361	362	363	364	365	366	367	368	369	370
372	374	376	378	380	382	384	386	388	390
393	396	399	402	405	410	415	420	425	430
435	440	445	450	455	460	470	480	490	500
510	520	530	540						
541	542	543	544	545	546	547	548	549	550
552	554	556	558	560	562	564	566	568	570
573	576	579	582	585	590	595	600	605	610
615	620	625	530	635	640	650	660	670	680
690	700	710	720						

Drawdown (m)

0.00	6.01	6.65	6.82	7.04	7.08	7.12	7.16	7.16	7.17
7.18	7.19	7.21	7.21	7.22	7.23	7.23	7.24	7.24	7.25
7.26	7.28	7.29	7.30	7.31	7.32	7.32	7.32	7.32	7.32
7.32	7.32	7.33	7.33	7.33	7.35	7.35	7.35	7.35	7.38
7.38	7.38	7.39	7.39	7.39					
7.98	8.37	8.80	9.03	9.05	9.06	9.06	9.07	9.07	9.08
9.09	9.10	9.11	9.11	9.12	9.13	9.14	9.15	9.15	9.16
9.17	9.18	9.19	9.20	9.21	9.22	9.23	9.24	9.25	9.25
9.25	9.29	9.29	9.29	9.31	9.31	9.31	9.33	9.33	9.35
9.35	9.36	9.36	9.38						
9.85	10.33	10.67	10.80	10.89	10.93	10.95	11.00	11.11	11.20
11.23	11.25	11.27	11.30	11.31	11.32	11.33	11.34	11.35	11.36
11.38	11.40	11.41	11.42	11.43	11.44	11.44	11.45	11.47	11.47
11.49	11.49	11.51	11.51	11.52	11.52	11.54	11.54	11.54	11.55
11.55	11.58	11.60	11.62						
13.55	13.60	13.63	13.65	13.68	13.69	13.70	13.71	13.73	13.74
13.75	13.75	13.77	13.77	13.77	13.80	13.82	13.84	13.87	13.89
13.90	13.90	13.91	13.92	13.94	13.96	13.97	13.99	14.01	14.01
14.03	14.03	14.03	14.06	14.06	14.06	14.10	14.10	14.10	14.12
14.13	14.13	14.13	14.13						



**Step-Drawdown Test Data from Tabriz Power Station Pumping Well 6 (TPSW6)**

**Time Steps=180 (min) Q1=4449 (m<sup>3</sup>/d) Q2=6298 (m<sup>3</sup>/d) Q3=7897 (m<sup>3</sup>/d)**

**Time (min)**

0	0.5	1	2	3	4	5	6	7	8
9	10	12	14	16	18	20	25	30	35
40	45	50	60	70	80	90	105	120	140
160	180								
180.5	181	182	183	184	185	186	187	188	189
190	192	194	196	198	200	205	210	215	220
225	230	240	250	260	270	280	300	320	340
360									
360.5	361	362	363	364	365	366	367	368	369
370	372	374	376	378	380	385	390	395	400
405	410	420	430	440	450	465	480	500	520
540									

**Drawdown (m)**

0.00	7.20	7.85	8.13	8.35	8.32	8.41	8.43	8.48	8.52
8.55	8.57	8.59	8.63	8.65	8.69	8.70	8.73	8.78	8.81
8.83	8.85	8.86	8.89	8.90	8.92	8.93	8.96	8.98	9.01
9.02	9.02								
13.03	13.45	13.63	13.74	13.99	13.82	13.86	13.89	13.91	13.92
13.94	13.98	14.00	14.02	14.05	14.08	14.10	14.14	14.17	14.19
14.20	14.22	14.26	14.30	14.32	14.35	14.36	14.40	14.42	14.43
14.44									
17.28	18.79	18.88	18.93	19.03	19.08	19.14	19.17	19.20	19.22
19.24	19.29	19.33	19.35	19.38	19.40	19.42	19.46	19.48	19.51
19.54	19.56	19.62	19.67	19.72	19.78	19.88	19.92	19.97	20.03
20.08									

Step-Drawdown Test Data from Tbriz Park Pumping Well 1 (PTW1)

Time Steps=180(min) Q1=4406 (m<sup>3</sup>/d) Q2=6394 (m<sup>3</sup>/d) Q3=7776 (m<sup>3</sup>/d)

Q4=9072 (m<sup>3</sup>/d)

Time (min)

0	1	2	3	4	5	6	7	8	9
10	12	14	16	18	20	22	24	26	28
30	33	36	39	42	45	50	55	60	65
70	75	80	85	90	100	110	120	130	140
150	160	170	180						
181	182	183	184	185	186	187	188	189	190
192	194	196	198	200	202	204	206	208	210
213	216	219	222	225	230	235	240	245	250
255	260	265	270	280	290	300	310	320	330
340	350	360							
361	362	363	364	365	366	367	368	369	370
372	374	376	378	380	382	384	386	388	390
393	396	399	402	405	410	415	420	425	430
435	440	445	450	460	470	480	490	500	510
520	530	540							
541	542	543	544	545	546	547	548	549	550
552	554	556	558	560	562	564	566	568	570
573	576	579	582	585	590	595	600	605	610
615	620	625	530	640	650	660	670	680	690
700	710	720							

Drawdown (m)

0.00	5.25	5.59	5.65	5.70	5.77	5.82	5.90	5.95	5.98
6.01	6.05	6.10	6.16	6.21	6.28	6.35	6.40	6.46	6.51
6.55	6.58	6.62	6.64	6.66	6.73	6.75	6.78	6.82	6.84
6.86	6.89	6.93	6.97	7.01	7.05	7.08	7.10	7.12	7.15
7.18	7.21	7.22	7.22						
9.70	10.00	10.16	10.28	10.34	10.39	10.45	10.48	10.52	10.55
10.60	10.65	10.67	10.70	10.74	10.76	10.79	10.81	10.83	10.85
10.88	10.91	10.92	10.94	10.96	10.98	11.00	11.02	11.05	11.07
11.08	11.09	11.10	11.12	11.17	11.18	11.20	11.23	11.26	11.27
11.29	11.31	11.33							
12.78	13.00	13.11	13.17	13.23	13.27	13.32	13.33	13.35	13.37
13.39	13.41	13.45	13.48	13.50	13.52	13.54	13.55	13.58	13.62
13.65	13.67	13.68	13.70	13.71	13.73	13.75	13.78	13.81	13.84
13.86	13.87	13.89	13.91	13.93	13.97	14.00	14.02	14.06	14.08
14.10	14.14	14.15							
15.78	15.93	15.97	16.03	16.08	16.13	16.17	16.22	16.27	16.30
16.34	16.37	16.41	16.44	16.45	16.47	16.48	16.49	16.51	16.53
16.56	16.57	16.60	16.63	16.64	16.68	16.72	16.75	16.79	16.82
16.83	16.85	16.87	16.92	17.00	17.07	17.12	17.15	17.17	17.18
17.20	17.22	17.23							

**Appendix 3 Basic Program Used in Numerical analysis  
for Pumping Test Data of the Tabriz Area.**

Appendix 3 : Basic Program Used in Numerical analysis for Pumping Test Data  
of the Tabriz Area.

```

C  RUSHTON NUMERICAL TEST PUMPING MODEL
C  CONFINED OR WATER TABLE AQUIFER
C  NO VERTICAL FLOW
C  LINES 93 AND 222 DETERMINE WHICH NODAL DRAWDOWN IS
C  PLOTTED USING THE PLOTTING PROGRAM (RUSHPLOT). DDN(I)
C  MEANS DRAWDOWNS FOR THE I TH NODE IN THE LIST OF NODES
C  SUPPLIED IN YOUR DATA FILE ARE PLOTTED.
C  D(1) PLOTS DRAWDOWNS FOR THE ABSTRACTION WELL
C  NODE.
C  SPECIFY DOUBLE PRECISION
    IMPLICIT DOUBLE PRECISION(A-H),DOUBLE PRECISION(O-Z)
    DIMENSION R(100),RR(100),D(100),OLDD(100),T(100),H(100),
    1RECH(100),A(100),B(100),C(100),E(100),U(100),V(100),NODE(6),
    2X(100),Y(100),RDIST(6),DDN(6),LINE(20),
    3XPLOT(300),YPLOT(300)
C  READ IN TITLES AND PARAMETERS
    READ(5,5999)LINE
5999 FORMAT(20A4)
    WRITE(6,6105)LINE
6105 FORMAT(' RUSHTON NUMERICAL TEST PUMPING MODEL'/
    11X,20A4//)
    READ (5,*)PERM,SCON,SUNCON,ALPHA
    READ (5,*)WELLOS,BL
    BL2=BL*BL
    WRITE(6,6000)PERM,SCON,SUNCON,ALPHA,BL,WELLOS
6000 FORMAT(' PERMEABILITY',11X,F12.1/ ' S(CONFINED)',12X,F12.7/
    1' S(UNCONFINED)',12X,F10.5/ ' ALPHA',20X,F10.5/
    2' LEAKAGE FACTOR',11X,F10.5/ ' WELL LOSS',16X,F10.2)
    READ (5,*) RWELL,RMAX
    WRITE(6,6010)RWELL,RMAX
6010 FORMAT(' R(WELL)',16X,F12.3/ ' R(MAX)',17X,F12.1)
C
C  SET UP RADIAL MESH
    DO 10 N=1,100
    AN=0.16666666667*FLOAT(N-2)
    R(N)=RWELL*10.0**AN
    IF(R(N).LT.RMAX) GO TO 10
    R(N)=RMAX
    RR(N)=RMAX*RMAX
    NMAX=N
    NMONE=N-1
    GO TO 20
10 RR(N)=R(N)*R(N)
20 DELA=0.383765

```

```

DELA2=DELA*DELA
C
C NOTE THAT ALL LEVELS MEASURED DOWNWARDS FROM DATUM
READ(5,*) TOP,BASE,WLEVEL,RCH
WRITE(6,6020) TOP,BASE,WLEVEL,RCH
6020 FORMAT(' TOP OF AQUIFER',9X,F12.3/' BASE OF AQUIFER',8X,F12.3/
1' STARTING WATERLEVEL',3X,F12.3/' RECHARGE',15X,F12.3)
C
C SET INITIAL CONDITIONS
DO 30 N=1,NMAX
RECH(N)=RCH
Y(N)=0.000
D(N)=WLEVEL
X(N)=0.0
30 OLDD(N)=WLEVEL
READ(5,*) JFIX
READ(5,*) NNODES
IF(JFIX.EQ.1)WRITE(6,6030)
IF(JFIX.EQ.1) GOTO 32
WRITE(6,6031)
6030 FORMAT(22H ** FIXED BOUNDARY** )
6031 FORMAT(22H ** FREE BOUNDARY ** )
32 READ(5,*) (NODE(J),J=1,NNODES)
WRITE(6,6040) (NODE(J),J=1,NNODES)
6040 FORMAT(' NODES CHOSEN',5X,6I3/)
TSTART=0.0
READ(5,*)QPUMP,TSTOP
WRITE(6,6050)QPUMP,TSTOP
6050 FORMAT('/ PUMPING RATE =',F12.3,' M3/DAY FOR',F12.3,' DAYS'/)
C
C CONVERT ABSTRACTION TO QABST
PI=4.0*ATAN(1.0)
QABST=0.5*QPUMP/(PI*DELA)
IND=0
C
C INITIAL TIME AND DELT
TIME=0.0
DELI=0.025*RR(1)*SCON/(PERM*(BASE-TOP))
DELT=DELI
DO 35 I=1,NNODES
I1=NODE(I)
35 RDIST(I)=R(I1)
WRITE(6,6100)(NODE(J),J=1,NNODES)
6100 FORMAT(' TIME (DAYS)',6X,' TIME (MINS)',15X,
1'DRAWDOWN AT NODE/DISTANCE',/43X,'R(WELL)',6I9,' R(MAX)')
WRITE(6,6111)R(1),(RDIST(J),J=1,NNODES),R(NMAX)
6111 FORMAT(' CUM PUMP CUM PUMP ',
18F9.2/)

```

```

C
C   CALC FOR A SPECIFIC TIME, IND=0 FOR LAST STEP
  ICOUNT=0
40 IF(ICOUNT.EQ.0) GO TO 42
  XPLOT(ICOUNT)=SSTIME
  YPLOT(ICOUNT)=DDN(4)
42 CONTINUE
  TIME=TIME+DELT
  TPLOT=TSTART+(0.1/1440.0)
  IF(TIME.GE.TPLOT) ICOUNT=ICOUNT+1
  IF(TIME.LT.TSTOP) GO TO 50
  DELT=TSTOP-TIME+DELT
  TIME=TSTOP
  IND=100
50 CONTINUE
C
C   DELAYED YIELD
  FACA=0.0
  FACB=1.0
  FACC=0.0
  IF(ALPHA.EQ.0.0)GO TO 15
  F=ALPHA*DELT
  IF(F.GT.100.0) GO TO 45
  FACA=EXP(-F)
45 FACB=1.0-FACA
  FACC=FACB/(ALPHA*DELT)
  DO 55 N=1,NMAX
  X(N)=FACA*Y(N)
55 RECH(N)=ALPHA*SUNCON*X(N)+RCH
15 CONTINUE
C
C   CALC. REPEATED 4 TIMES FOR CONVERGANCE
  DO 60 NUM=1,4
  DO 70 N=1,NMONE
C
C   TAKE AV. SAT. DEPTH BETWEEN N AND N+1
  SD=BASE-0.5*(D(N)+D(N+1))
  STOR=SCON+FACB*SUNCON
  IF(SD.LT.(BASE-TOP)) GO TO 80
  SD=BASE-TOP
  STOR=SCON
80 H(N)=DELA2/(SD*PERM)
  IF(BL.NE.0.0)RECH(N)=PERM*SD*(OLDD(N)-WLEVEL)/BL2
70 T(N)=DELT/(STOR*RR(N))
C
C   WELL LOSS ADJUSTMENT,CLOSEST 6 NODES
  DO 300 N=2,3
  H(N)=H(N)*WELLOS

```

```

300 CONTINUE
C
C   REPRESENT WATER IN WELL
H(1)=0.0001*H(1)
T(1)=2.0*DELT*DELA/RR(2)
T(2)=2.0*T(2)
H(NMAX-1)=DLOG(R(NMAX)
1-DLOG(R(NMAX-1)))*(DLOG(R(NMAX))-DLOG
1(R(NMAX-1)))/(SD*PERM)
H(NMAX)=1.0E+10
T(NMONE)=2.0*DELT*DELA/((R(NMAX)
1-R(NMONE-1))*STOR*R(NMONE))
T(NMAX)=1.0*DELT*DELA/((R(NMAX)-R(NMONE))*STOR*R(NMAX))
IF (JFIX.EQ.1) T(NMAX)=1.0E-10*T(NMAX)
C
C   GAUSSIAN ELIMINATION
C   COEFFICIENTS
C   EQUATION IS-A(N)*D(N-1)+B(N)*D(N)-C(N)*D(N+1)=E(N)...
B(1)=1.0/H(1)+1.0/T(1)
C(1)=1.0/H(1)
E(1)=OLDD(1)/T(1)+QABST
DO 90 N=2,NMONE
A(N)=1.0/H(N-1)
B(N)=1.0/H(N-1)+1.0/H(N)+1.0/T(N)
C(N)=1.0/H(N)
90 E(N)=OLDD(N)/T(N)-RR(N)*RECH(N)
A(NMAX)=1.0/H(NMONE)
B(NMAX)=1.0/H(NMONE)+0.5/T(NMAX)
E(NMAX)=0.5*OLDD(NMAX)/T(NMAX)-0.5*RR(NMAX)*RECH(NMAX)
C
C   ELIMINATION
U(1)=B(1)
V(1)=E(1)
DO 100 N=2,NMAX
U(N)=B(N)-(A(N)*C(N-1))/U(N-1)
100 V(N)=E(N)+(A(N)*V(N-1))/U(N-1)
D(NMAX)=V(NMAX)/U(NMAX)
DO 110 NN=1,NMONE
N=NMONE-NN+1
110 D(N)=(V(N)+C(N)*D(N+1))/U(N)
C
C   DELAYED YIELD
DO 115 N=1,NMAX
115 Y(N)=X(N)+FACC*(D(N)-OLDD(N))
C
C   TEST FOR EXCESSIVE DRAWDOWNS
DRAWMX=0.9*BASE+0.1*TOP
IF(D(1).LT.DRAWMX) GO TO 60

```

```

WRITE(6,580)
580 FORMAT(' EXCESSIVE DRAWDOWN')
STOP
60 CONTINUE
C
C OUTPUT AND THEN CHANGE PARAMETER
TIMIN=TIME-TSTART
STIMIN=TIMIN*1440
SSTIME=TIME*1440
DO 120 I=1,NNODES
I1=NODE(I)
120 DDN(I)=D(I1)
IF(TIME.LT.TPLOT) GO TO 44
WRITE(6,560) TIME,TIMIN,SSTIME,STIMIN,D(1),(DDN(J),J=1,NNODES),
1D(NMAX)
560 FORMAT(' ',F9.6,1X,F9.6,1X,F9.3,1X,F9.3,1X,8F9.4)
44 CONTINUE
DO 130 N=1,NMAX
130 OLDD(N)=D(N)
IF(ALPHA.EQ.0.0) GO TO 6
DELT=TIMIN*0.21143
GO TO 7
6 DELT=TIMIN*0.25892
7 CONTINUE
IF(IND.EQ.0) GO TO 40
C
C END OF CALC FOR A SPECIFIC TIME
DELT=DELI
IND=0
TSTART=TIME
C
C INPUT NEW PUMPING PHASE
READ(5,*)QPUMP,TSTOP
QABST=0.5*QPUMP/(PI*DELA)
IF(QPUMP.LT.0.0) GO TO 41
WRITE(6,6050) QPUMP,TSTOP
WRITE(6,6100)(NODE(J),J=1,NNODES)
WRITE(6,6111)R(1),(RDIST(J),J=1,NNODES),R(NMAX)
GO TO 40
41 XPLOT(ICOUNT)=SSTIME
YPLOT(ICOUNT)=DDN(4)
WRITE(4,595)ICOUNT
595 FORMAT(I3)
WRITE(4,*)(XPLOT(J),J=1,ICOUNT)
WRITE(4,*)(YPLOT(J),J=1,ICOUNT)
WRITE(4,600) PERM,SCON,SUNCON,RWELL,RMAX,JFIX
WRITE(4,605) ALPHA,BL,WELLOS,RCH
600 FORMAT(3(1X,F10.5),2(1X,F10.3),1X,I1)

```



605 FORMAT(4(1X,F10.5))

STOP

END

**Appendix 4 Ground Water Level Fluctuations from some Selected  
Monitoring Wells.**

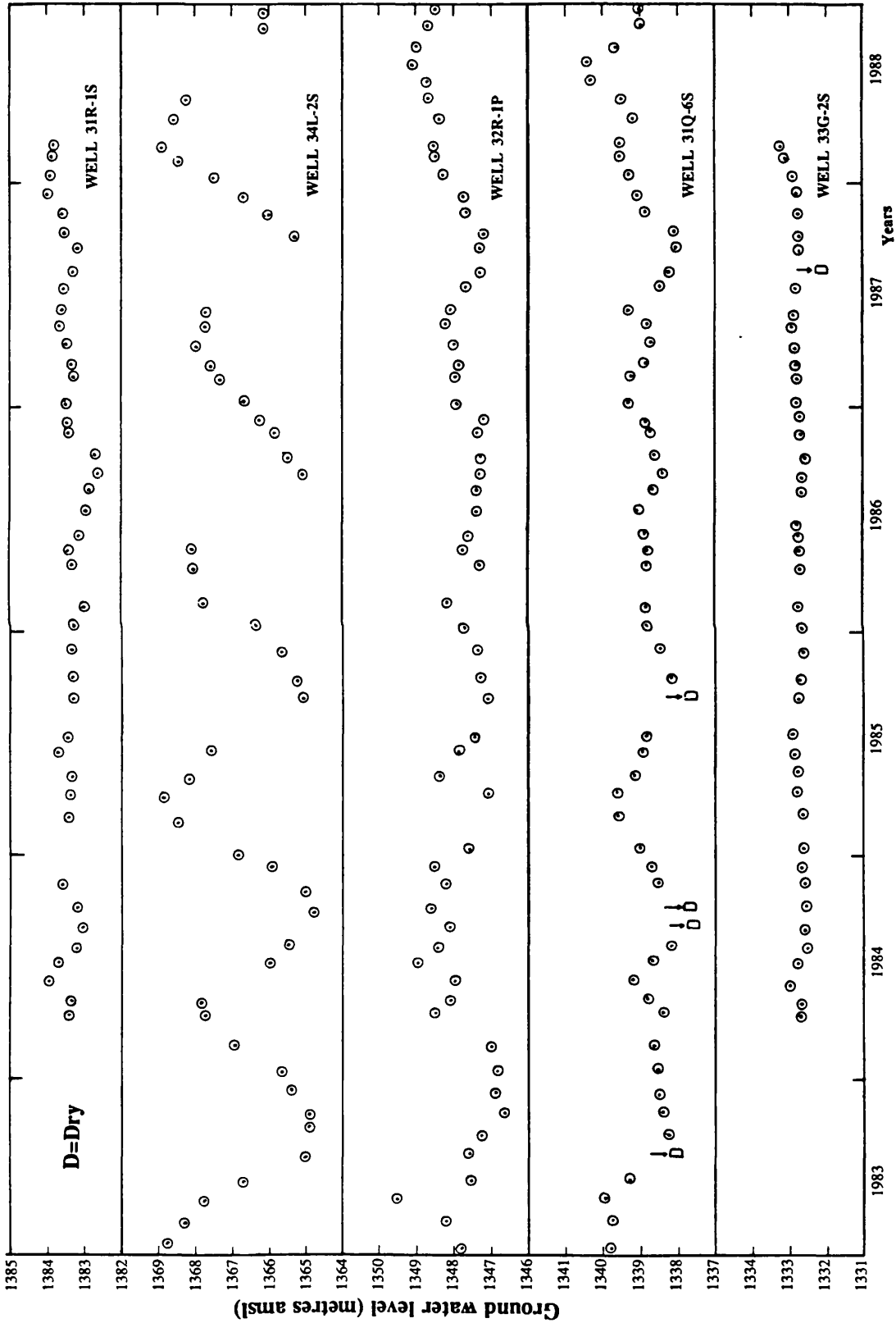


Fig. A4.1 Ground water level fluctuations in selected monitoring wells.

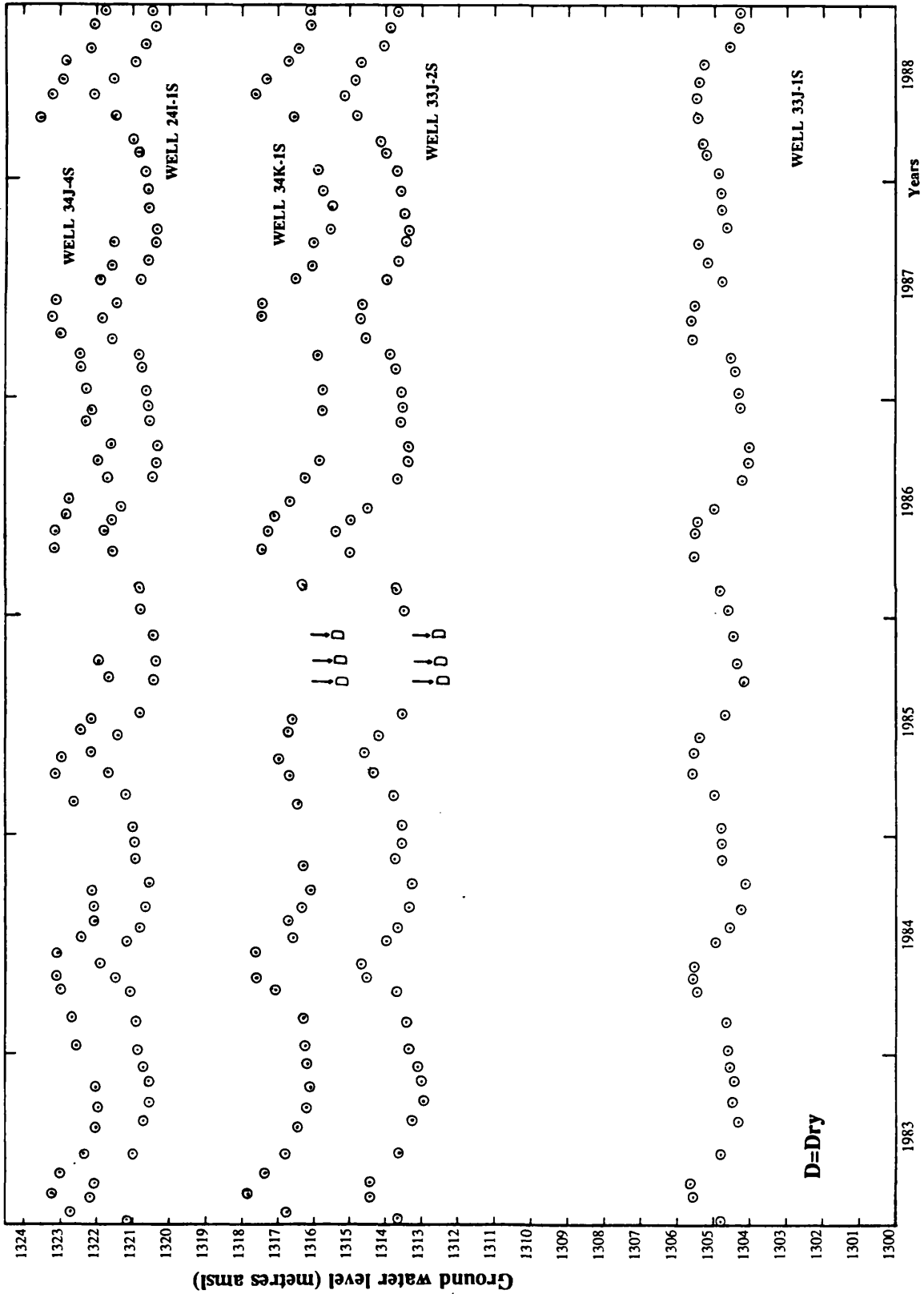


Fig. A4.2 Ground water level fluctuations in selected monitoring wells.

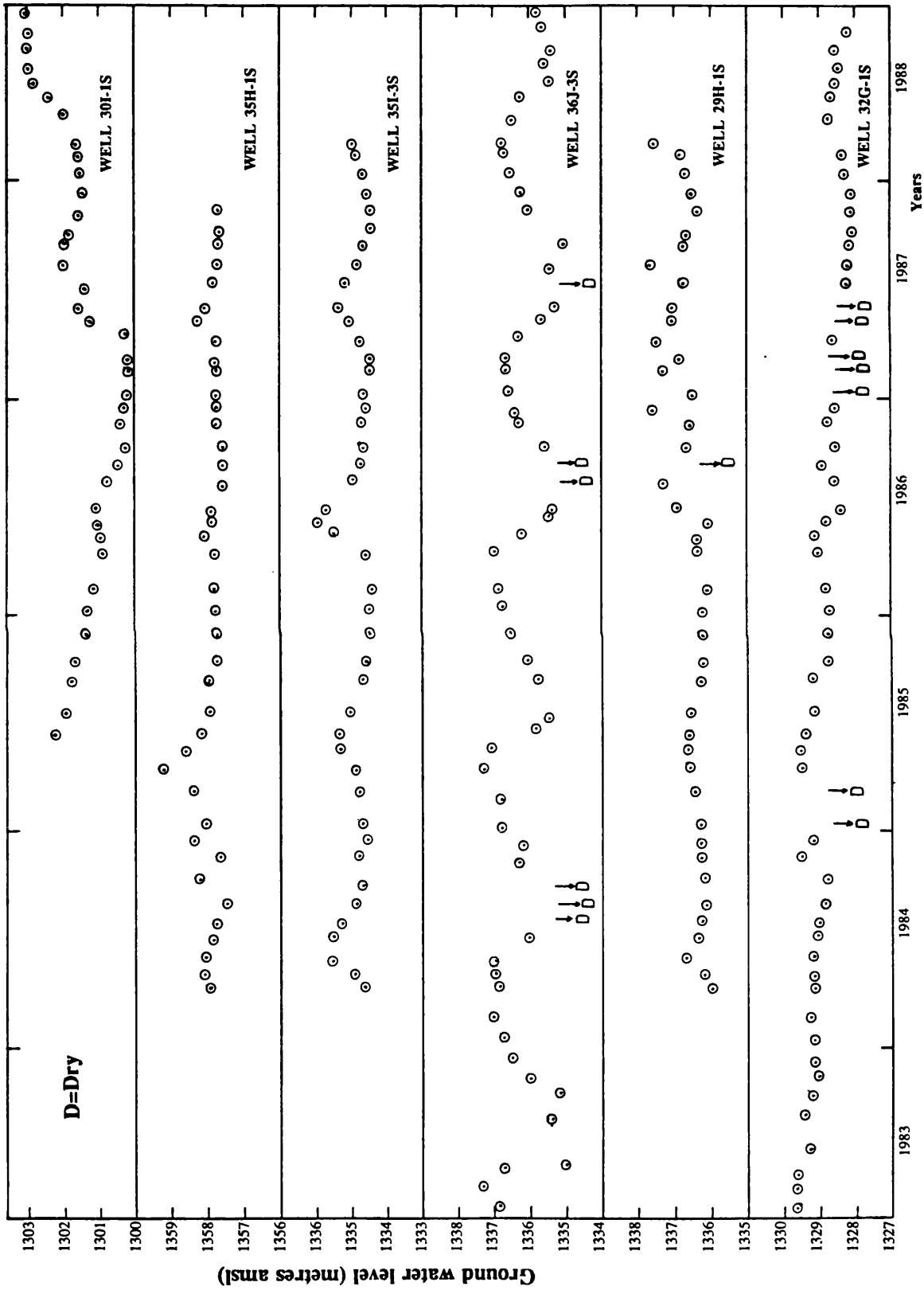


Fig. A4.3 Ground water level fluctuations in selected monitoring wells.

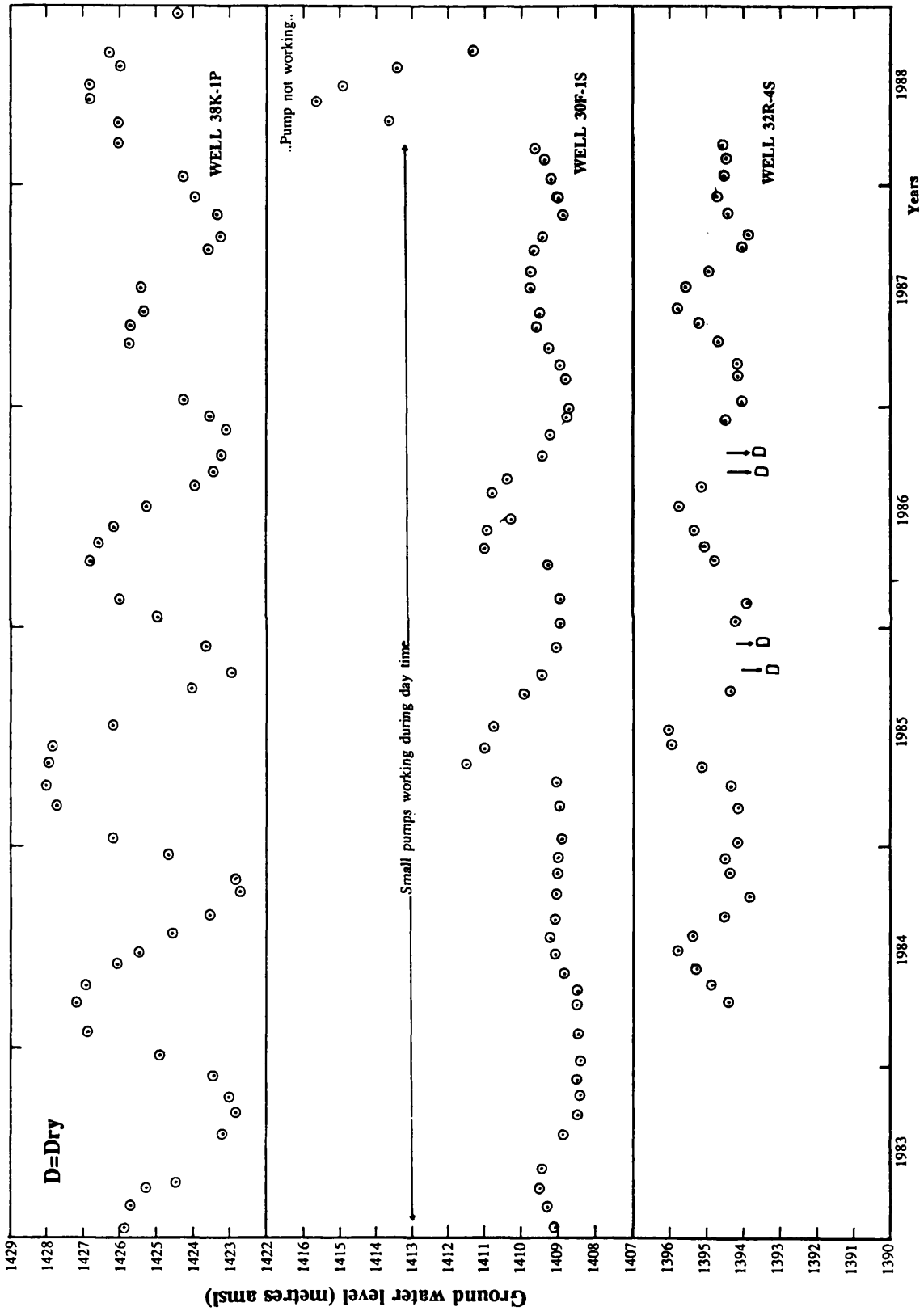


Fig. A4.4 Ground water level fluctuations in selected monitoring wells.

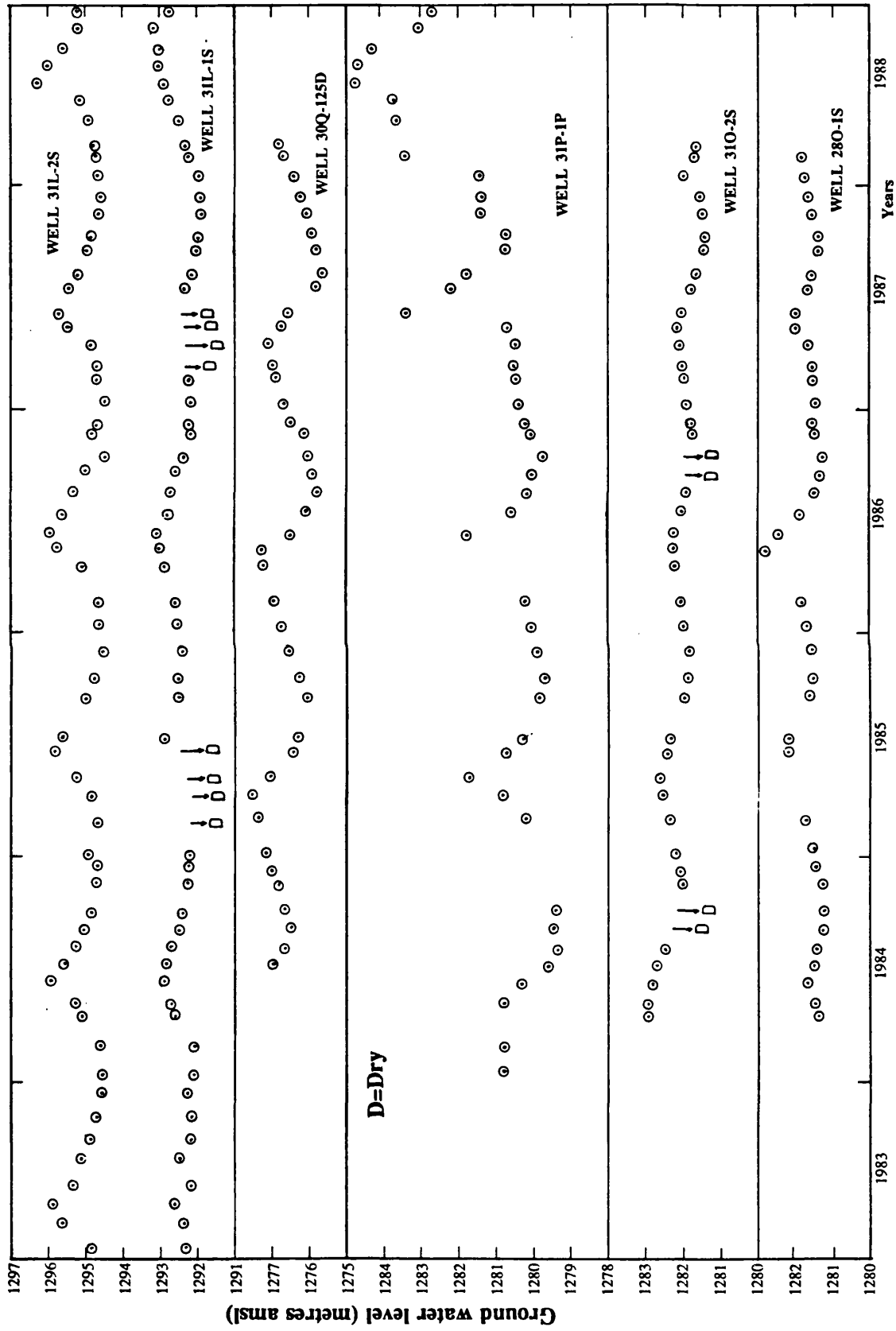


Fig. A.4.5 Ground water level fluctuations in selected monitoring wells.

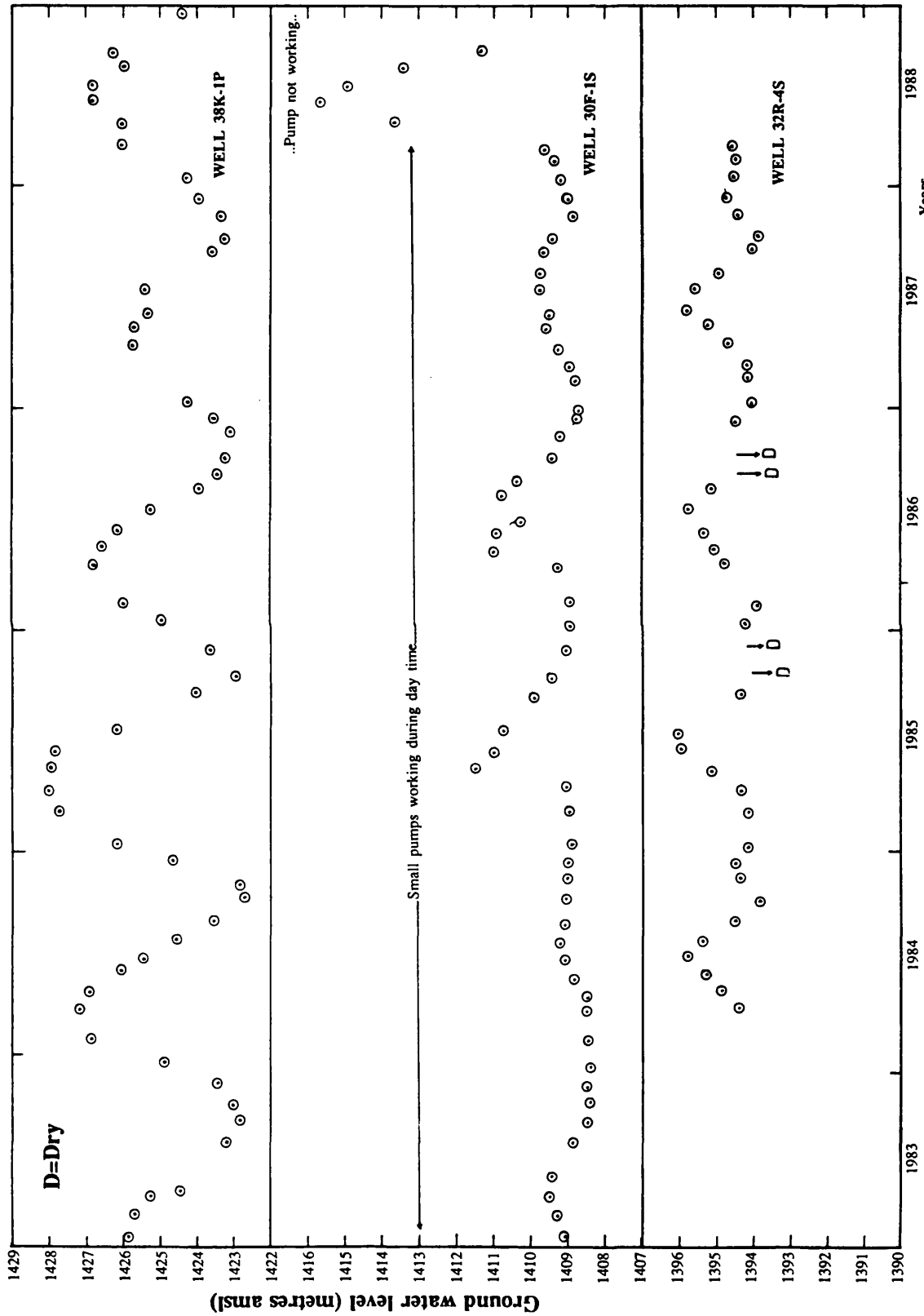


Fig. A4.6 Ground water level fluctuations in selected monitoring wells.



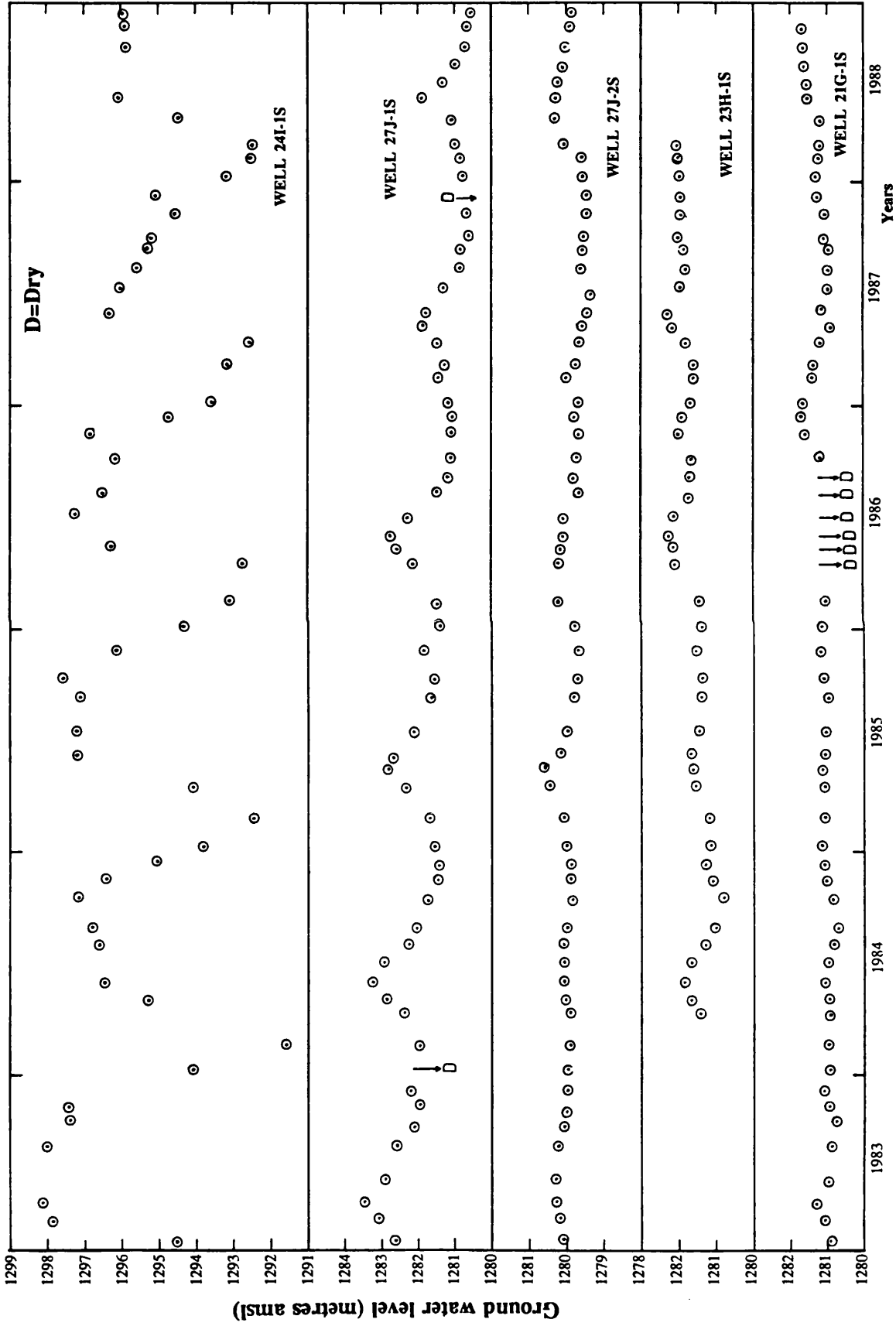


Fig. A4.7 Ground water level fluctuations in selected monitoring wells.

**Appendix 5 Plots of Constant Rate Test Analyses.**

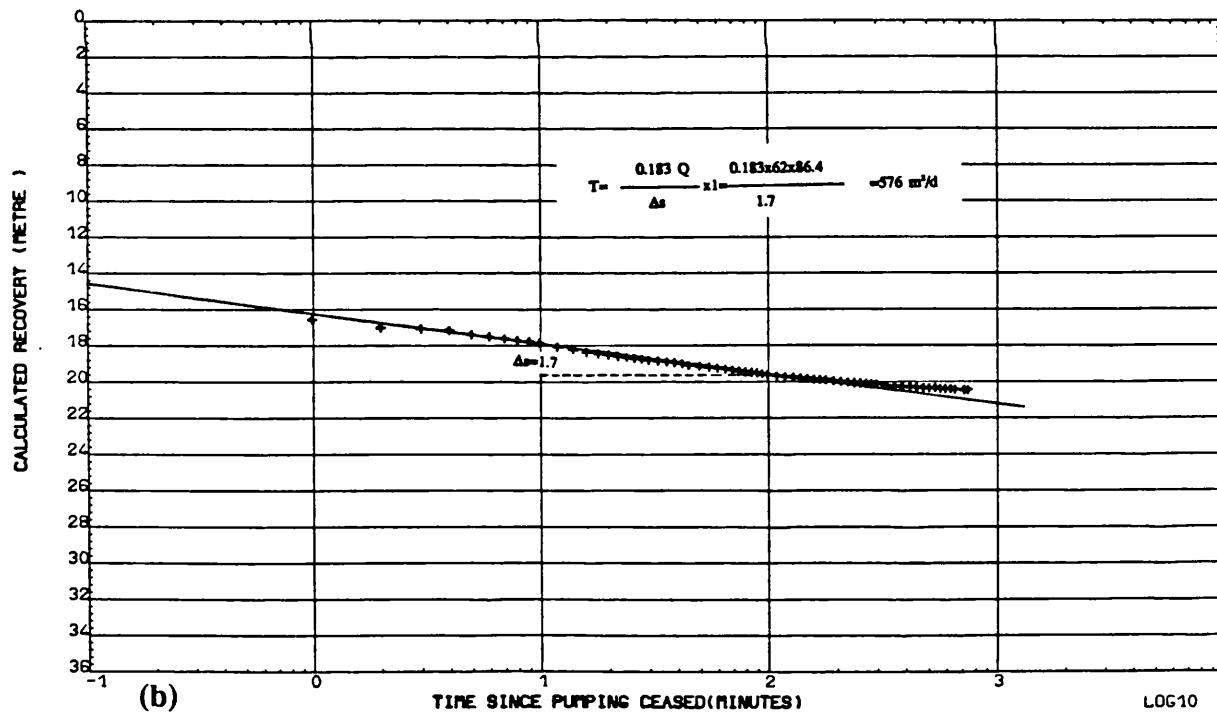
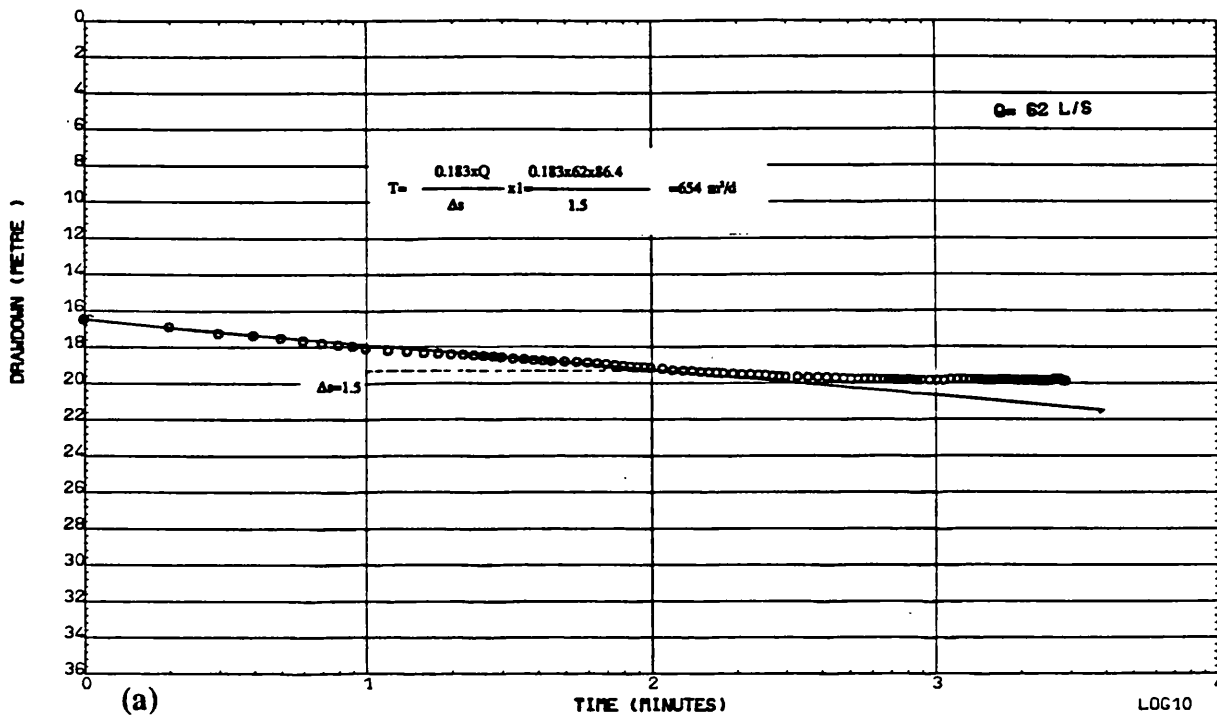


Fig. A5.1 PW SW5, Straight line method: (a) Time-Drawdown plot (b) Calculated Recovery plot.

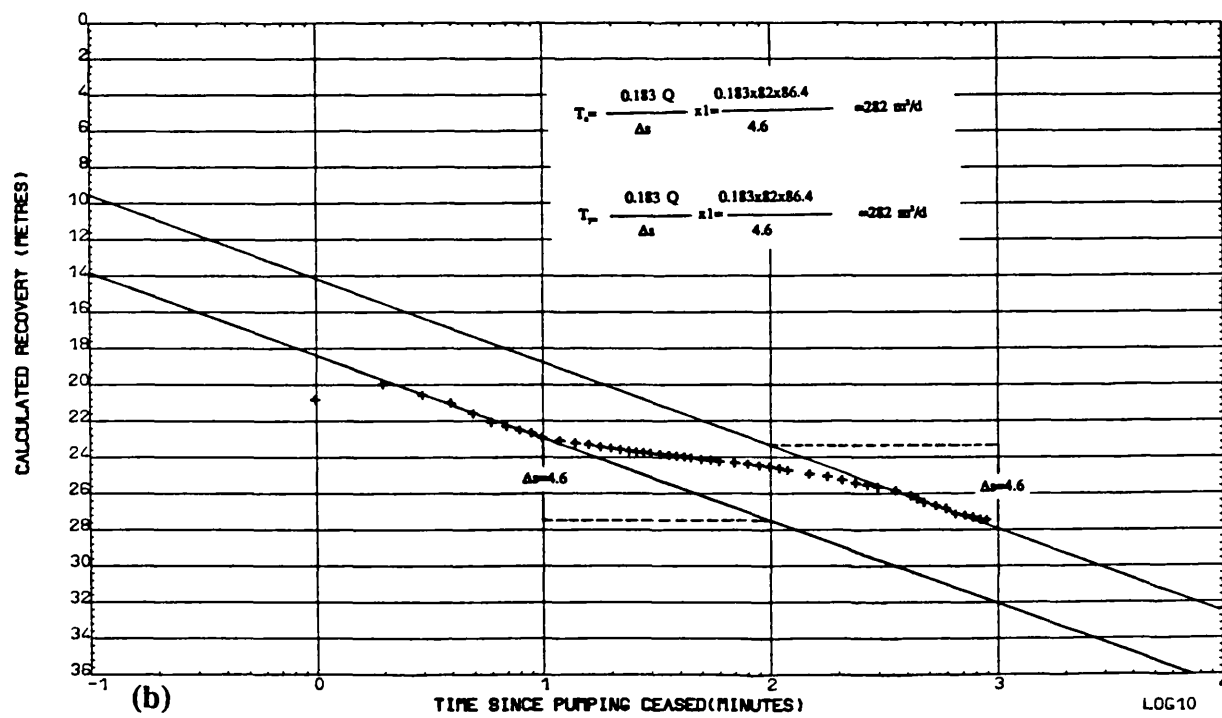
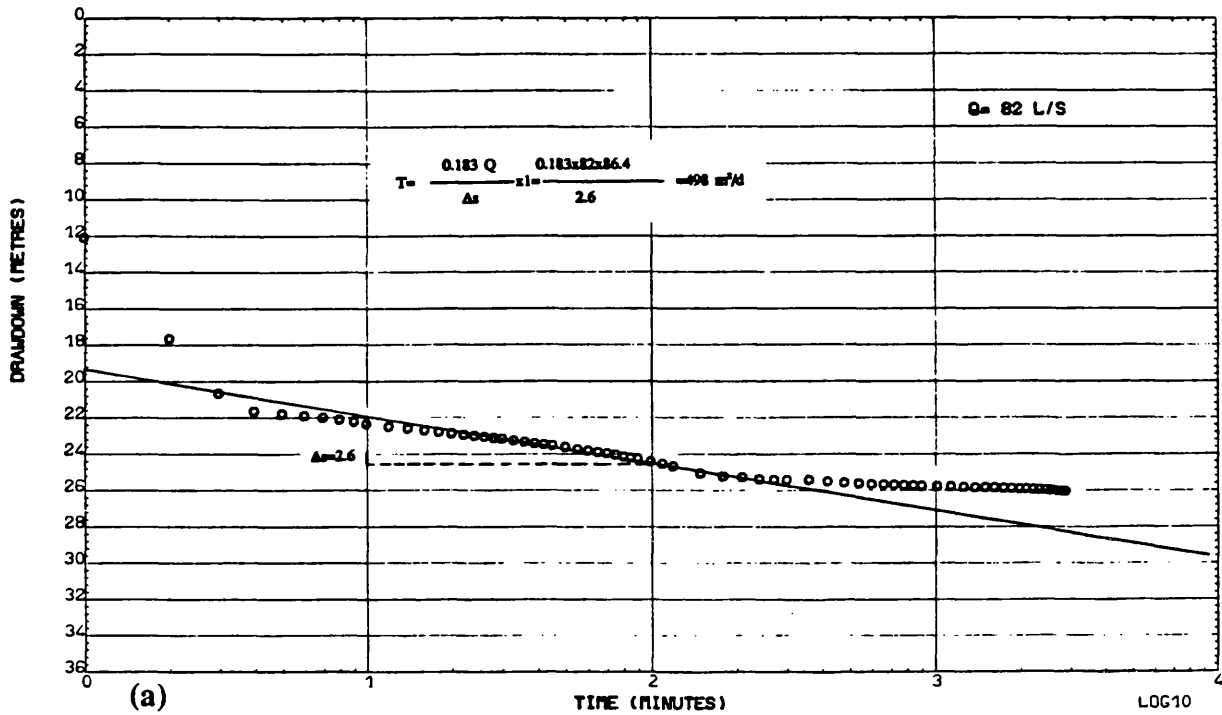


Fig. A5.2 PW SW8, Straight line method: (a) Time-Drawdown plot (b) Calculated Recovery plot.

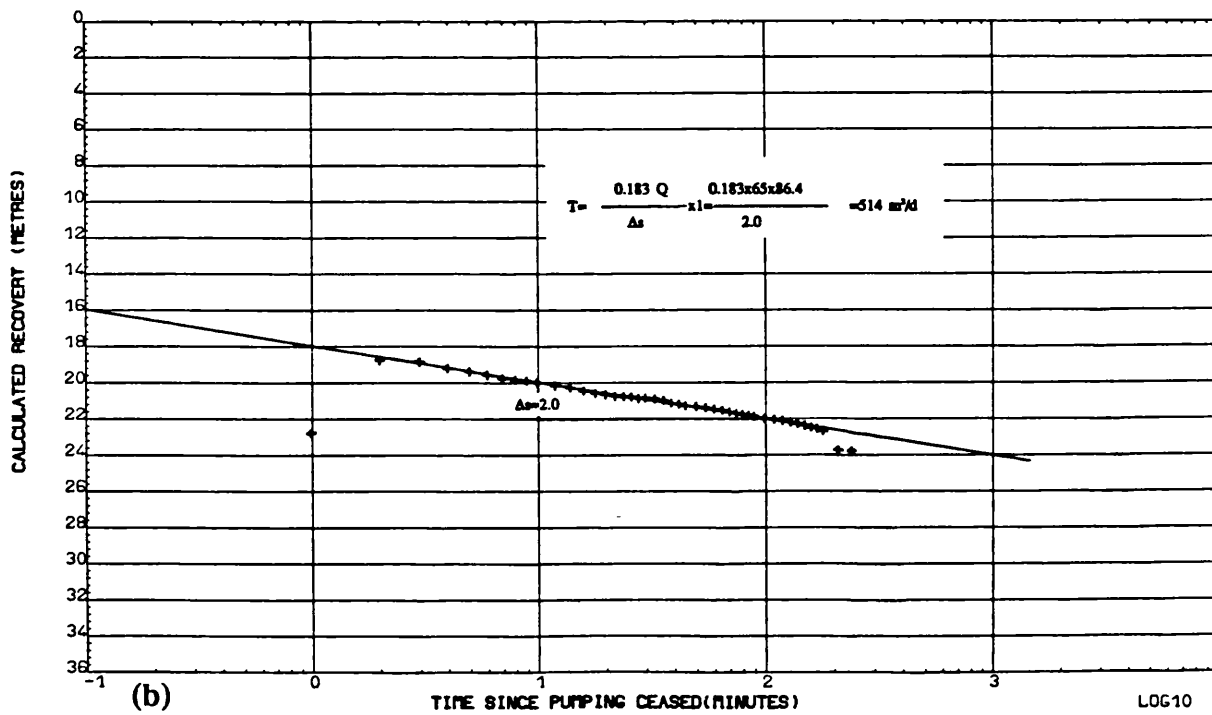
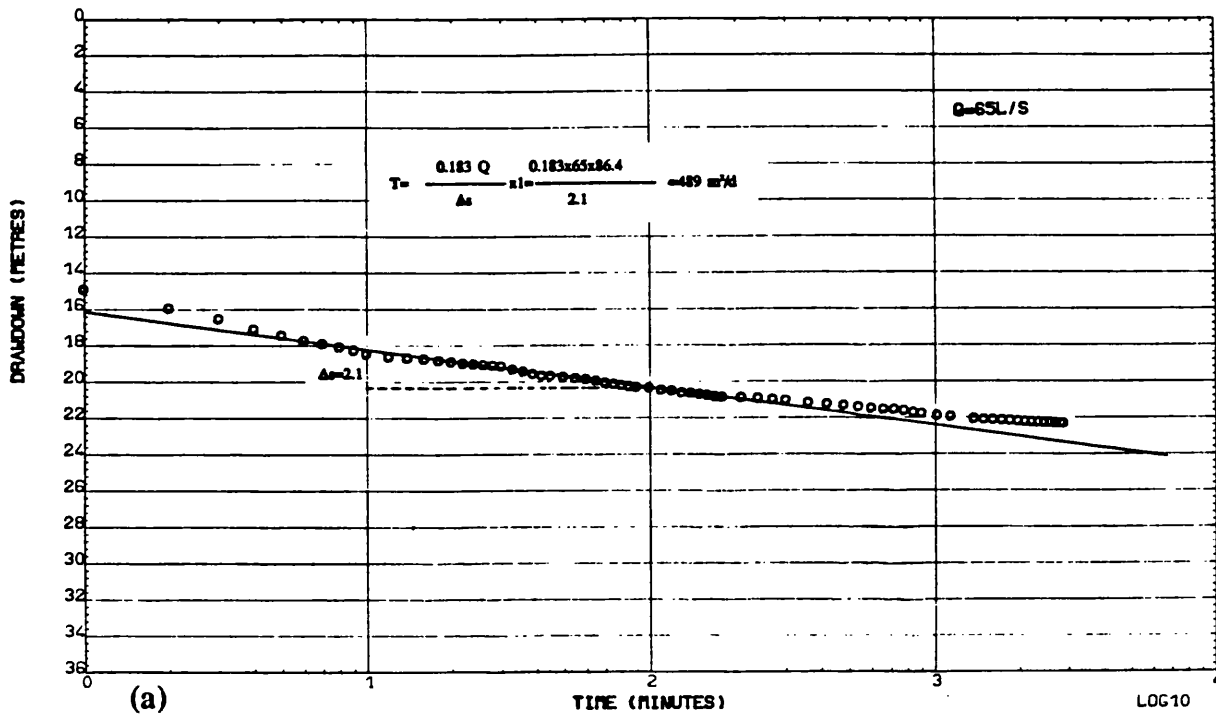


Fig. A5.3 PW SW10, Straight line method: (a) Time-Drawdown plot (b) Calculated Recovery plot.

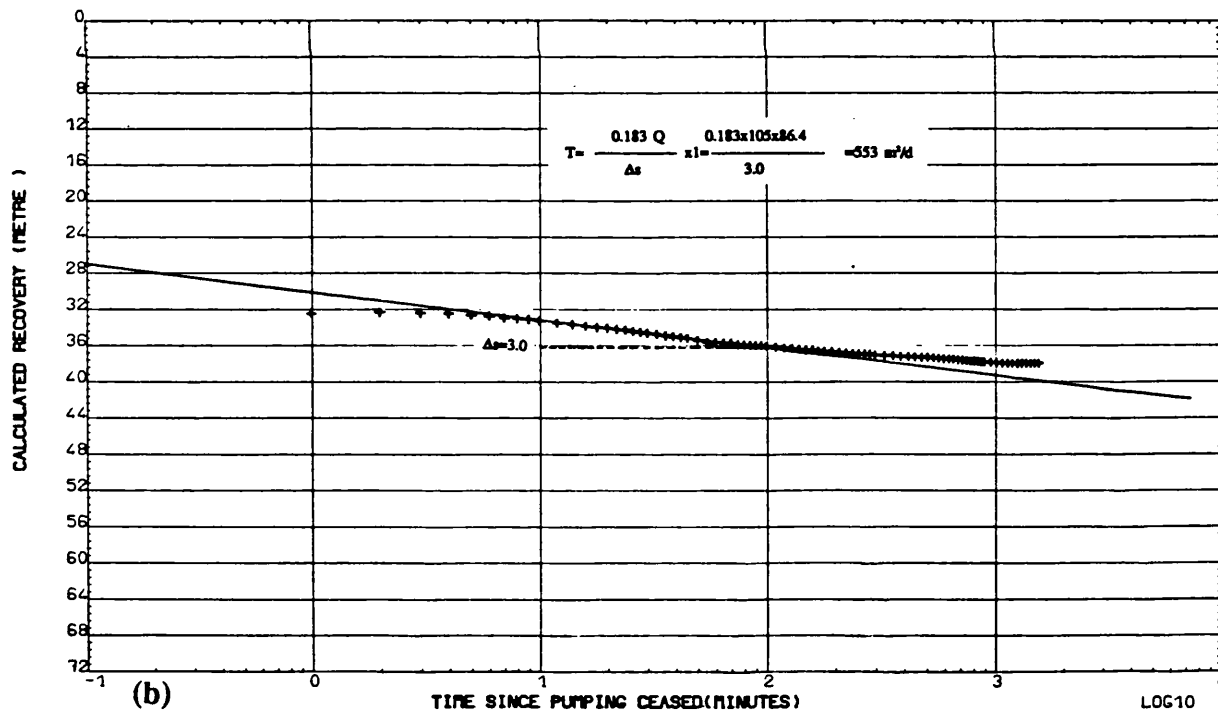
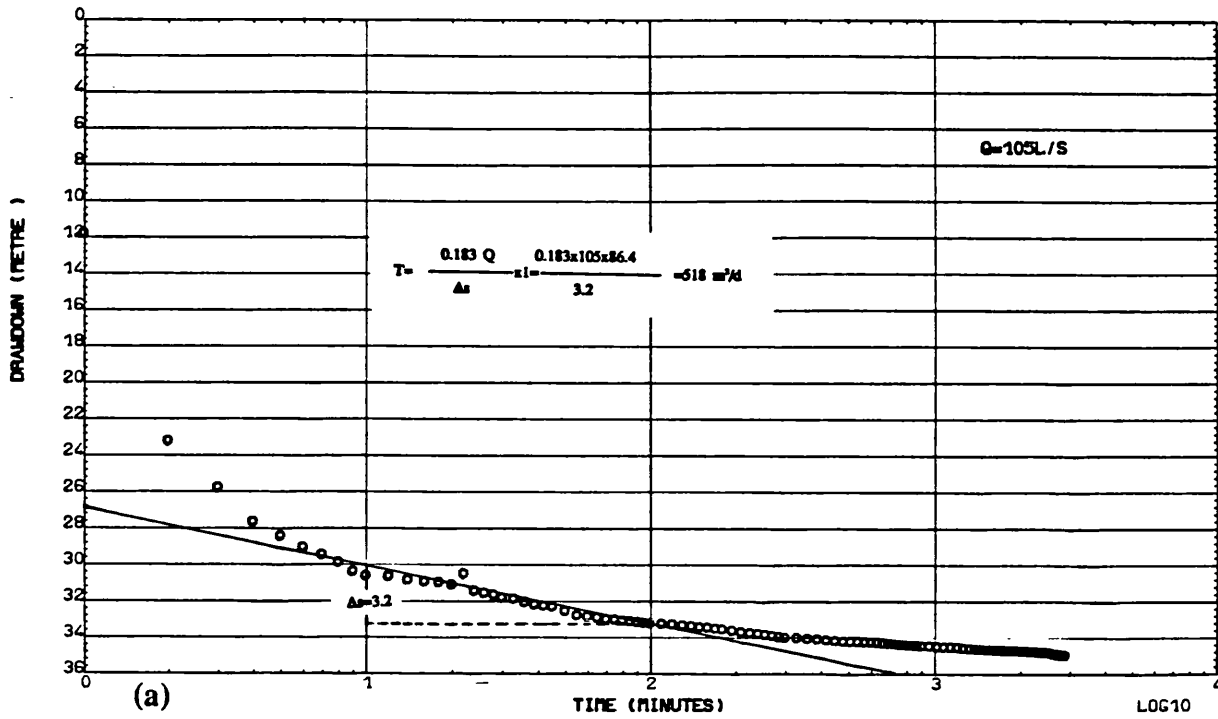


Fig. A5.4 PW SW11, Straight line method: (a) Time-Drawdown plot (b) Calculated Recovery plot.

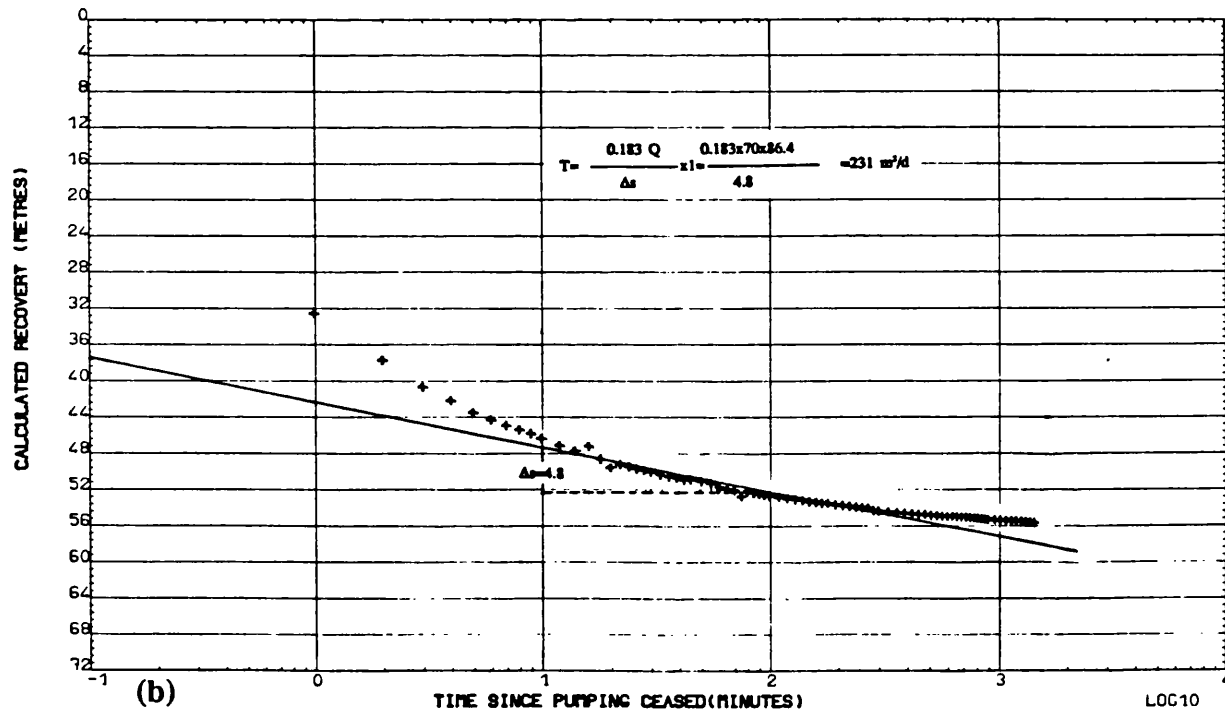
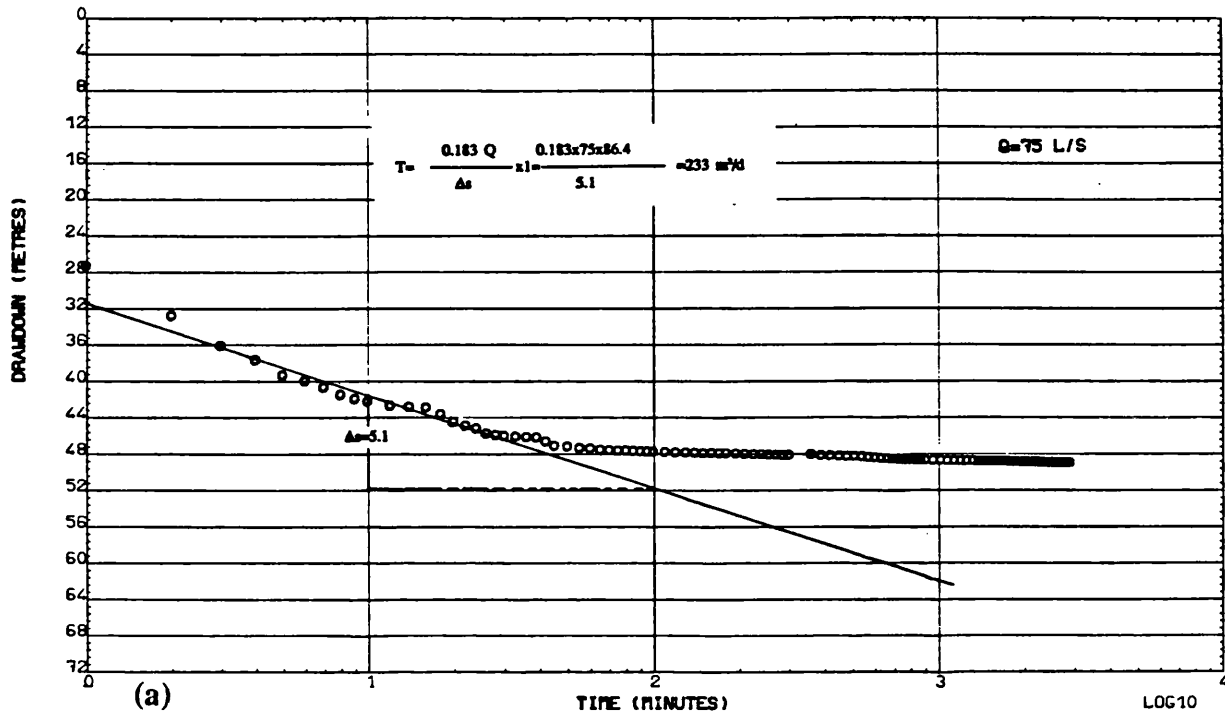


Fig. A5.5 PW SW13, Straight line method: (a) Time-Drawdown plot (b) Calculated Recovery plot.

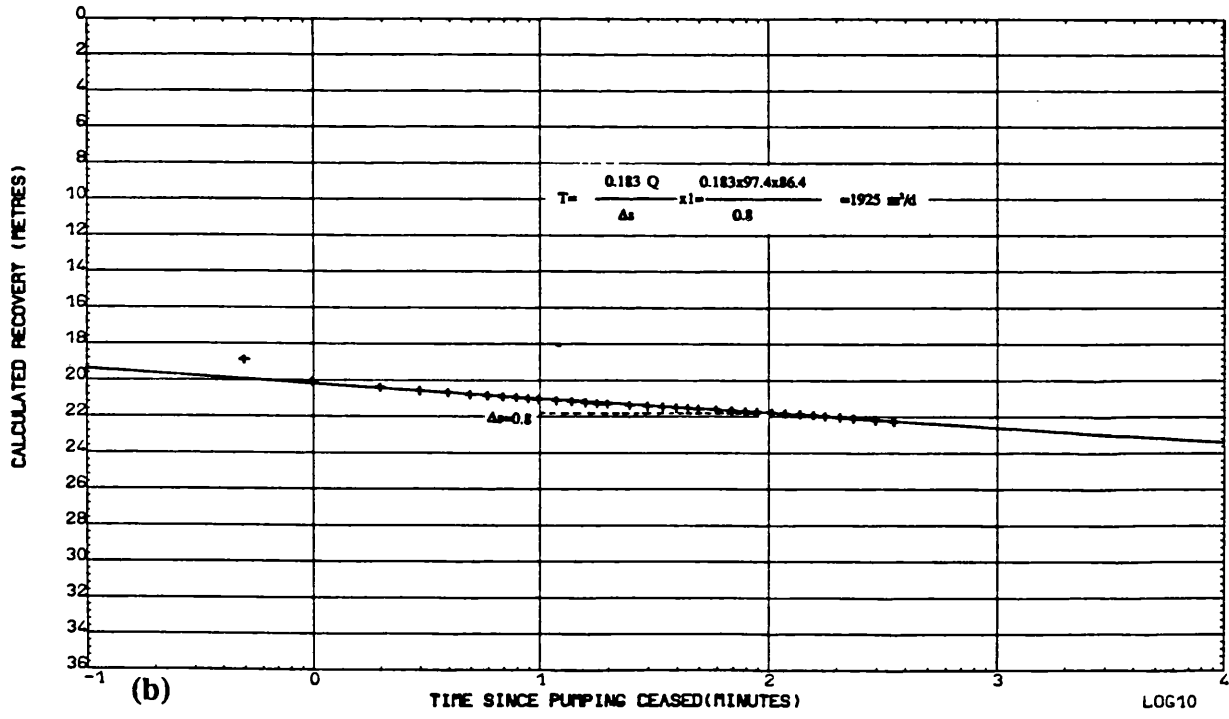
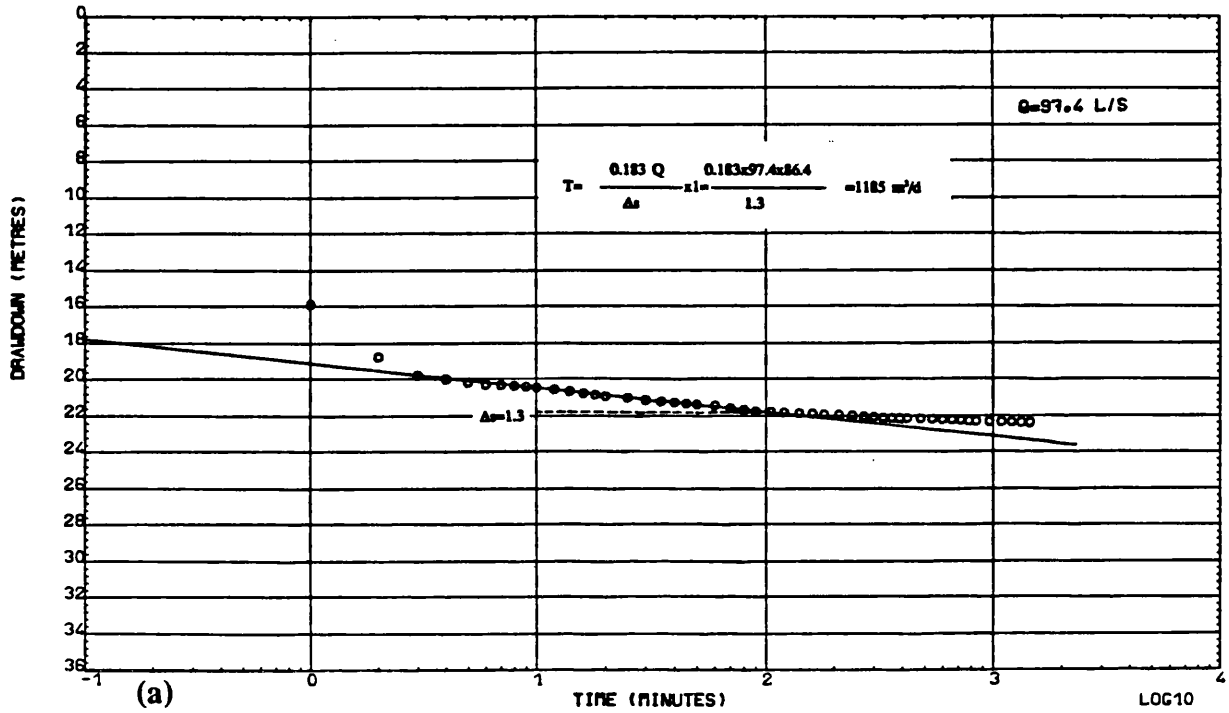


Fig. A5.6 PW TPSW6, Straight line method: (a) Time-Drawdown plot (b) Calculated Recovery plot.



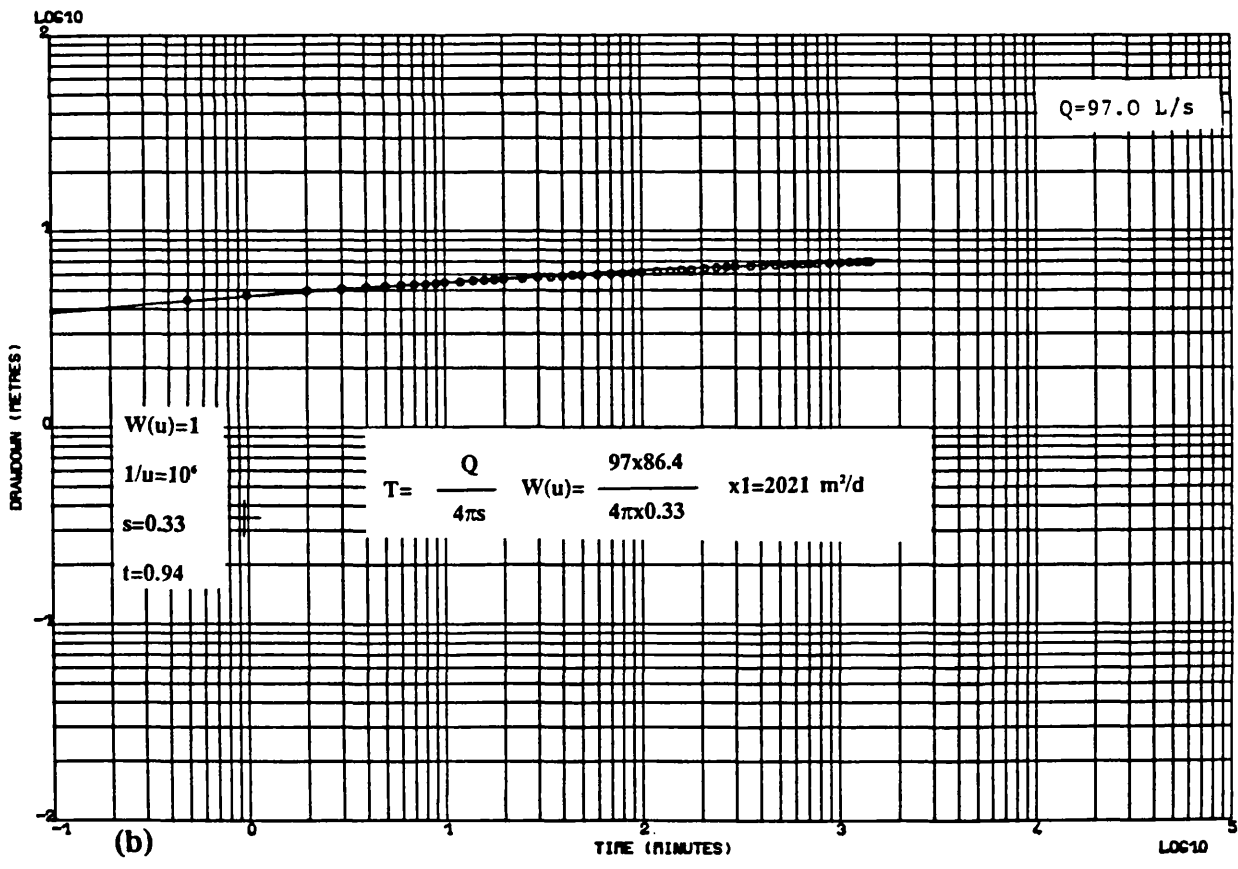
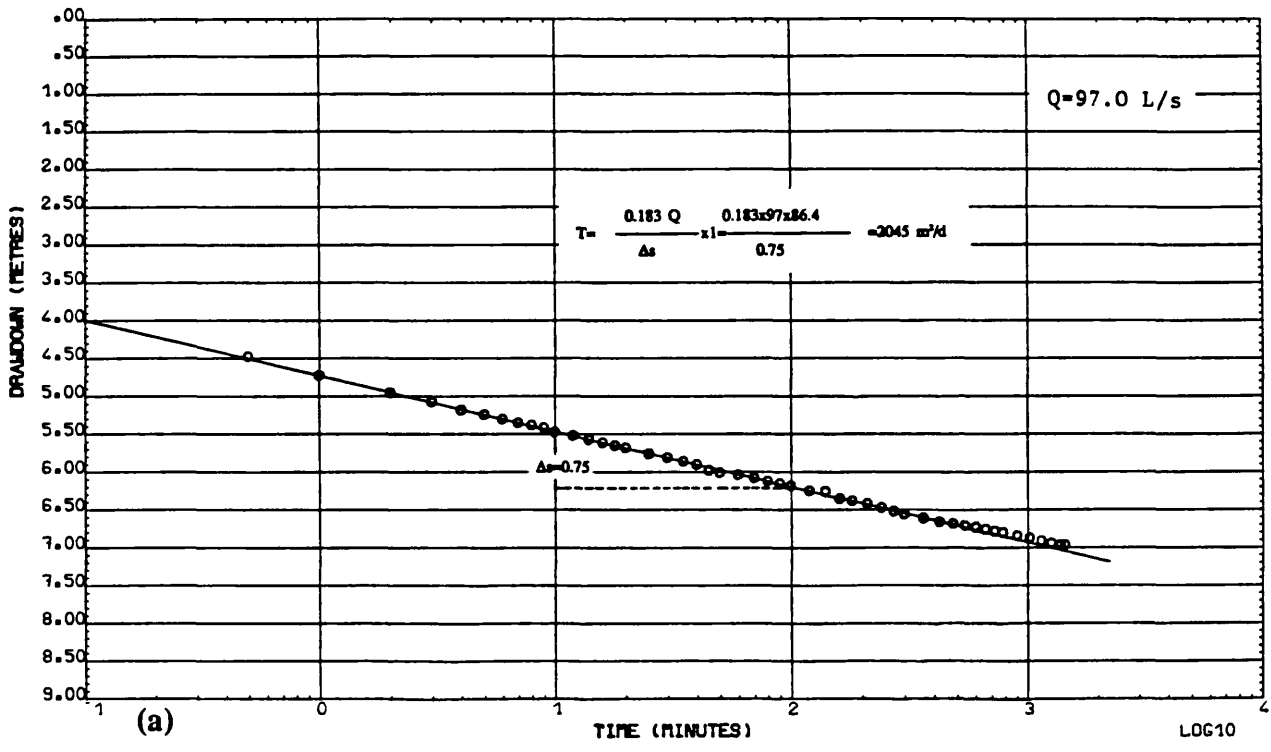
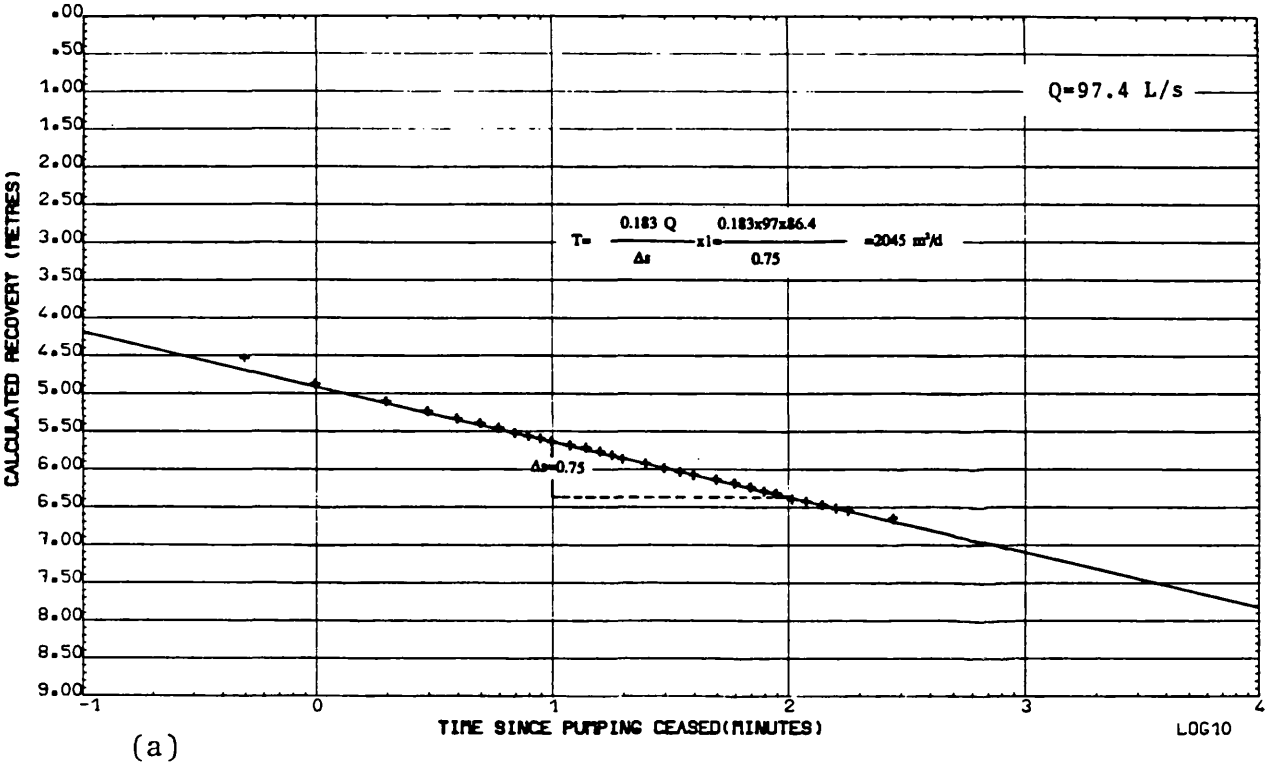
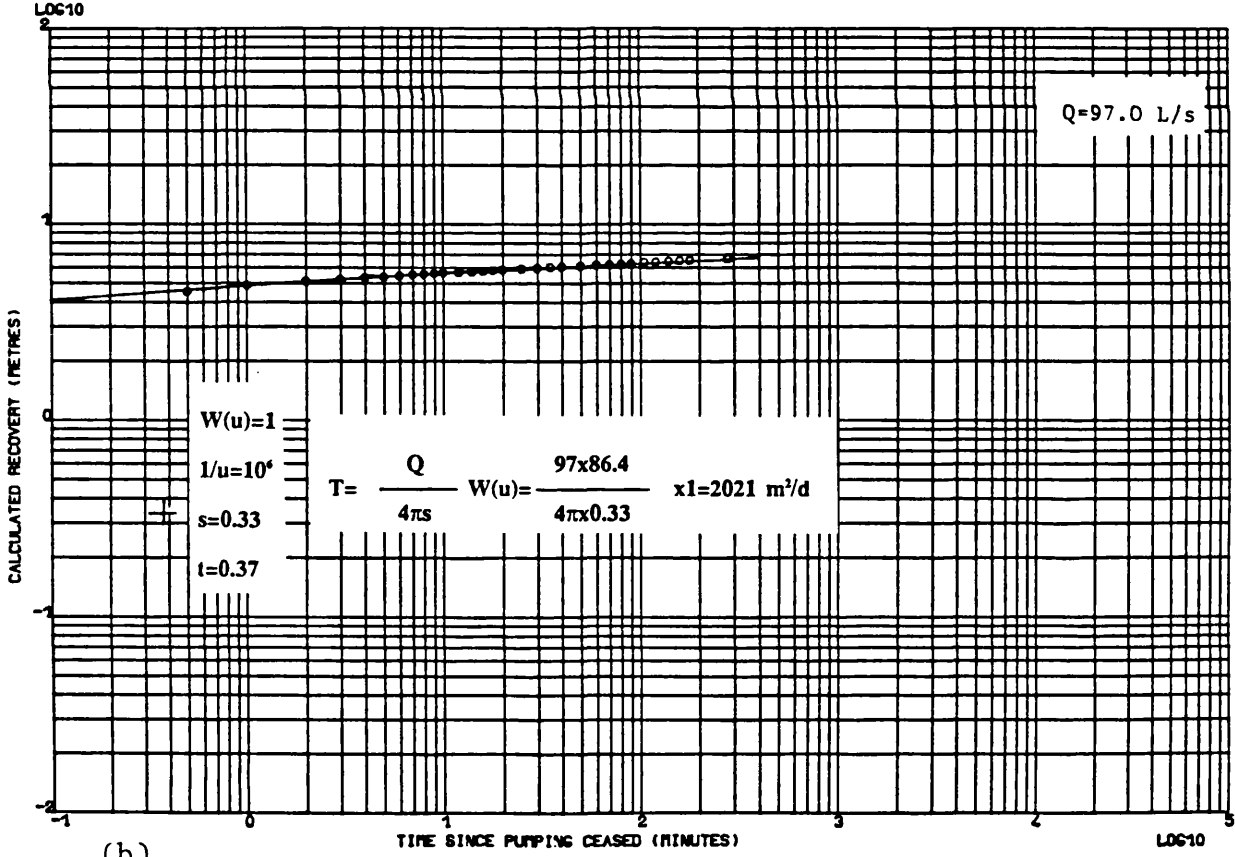


Fig. A5.7 PW TPSW4, Time-Drawdown plots: (a) Straight line method, (b) Type curve method.



(a)



(b)

Fig. A5.8 PW TPSW4, Calculated Recovery plots: (a) Straight line method, (b) Type curve method.

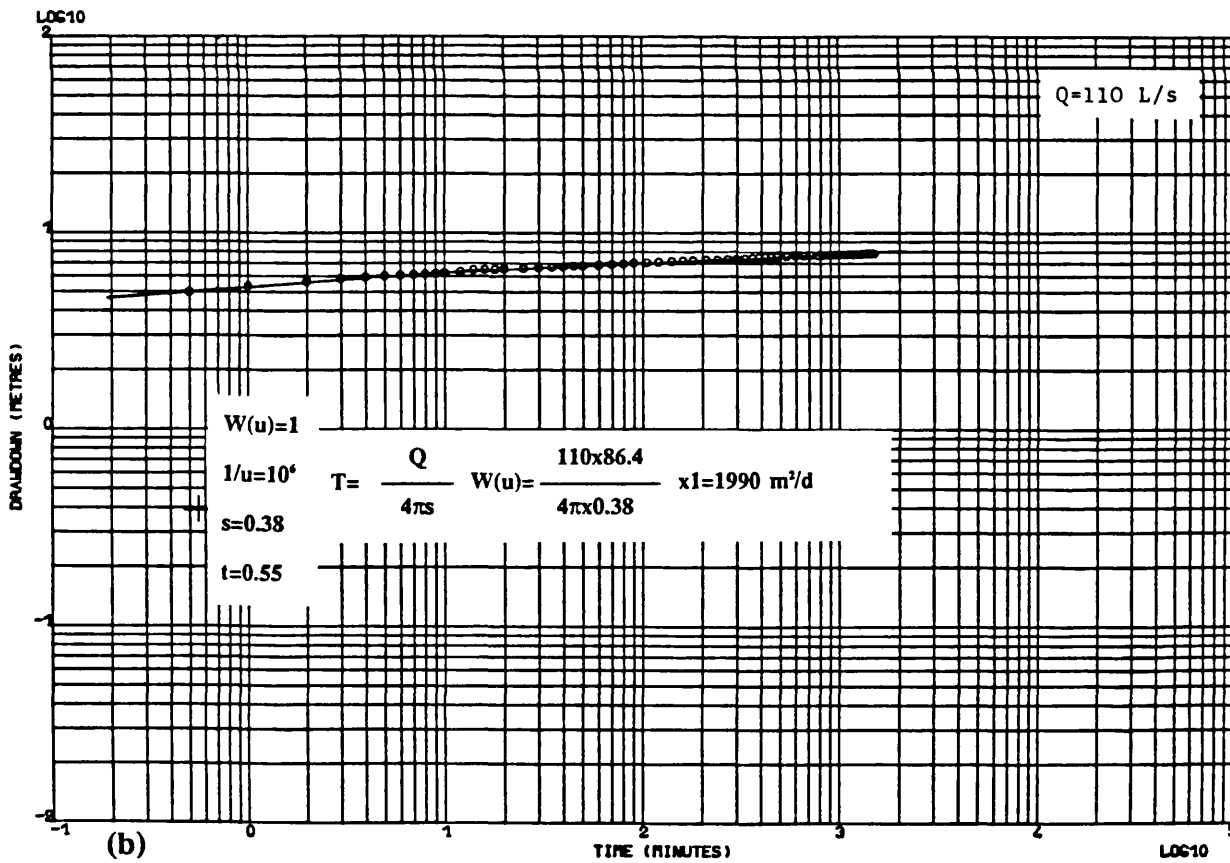
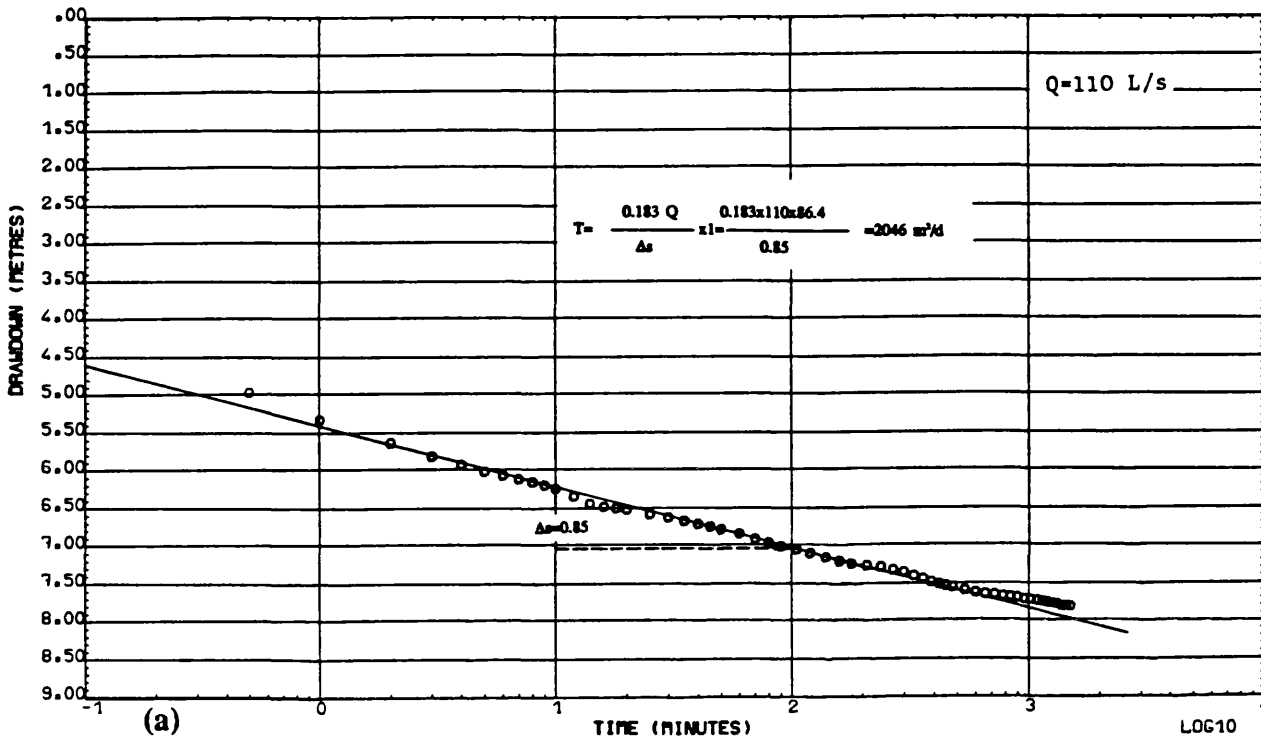


Fig. A5.9 PW TPSW8, Time-Drawdown plots: (a) Straight line method, (b) Type curve method.

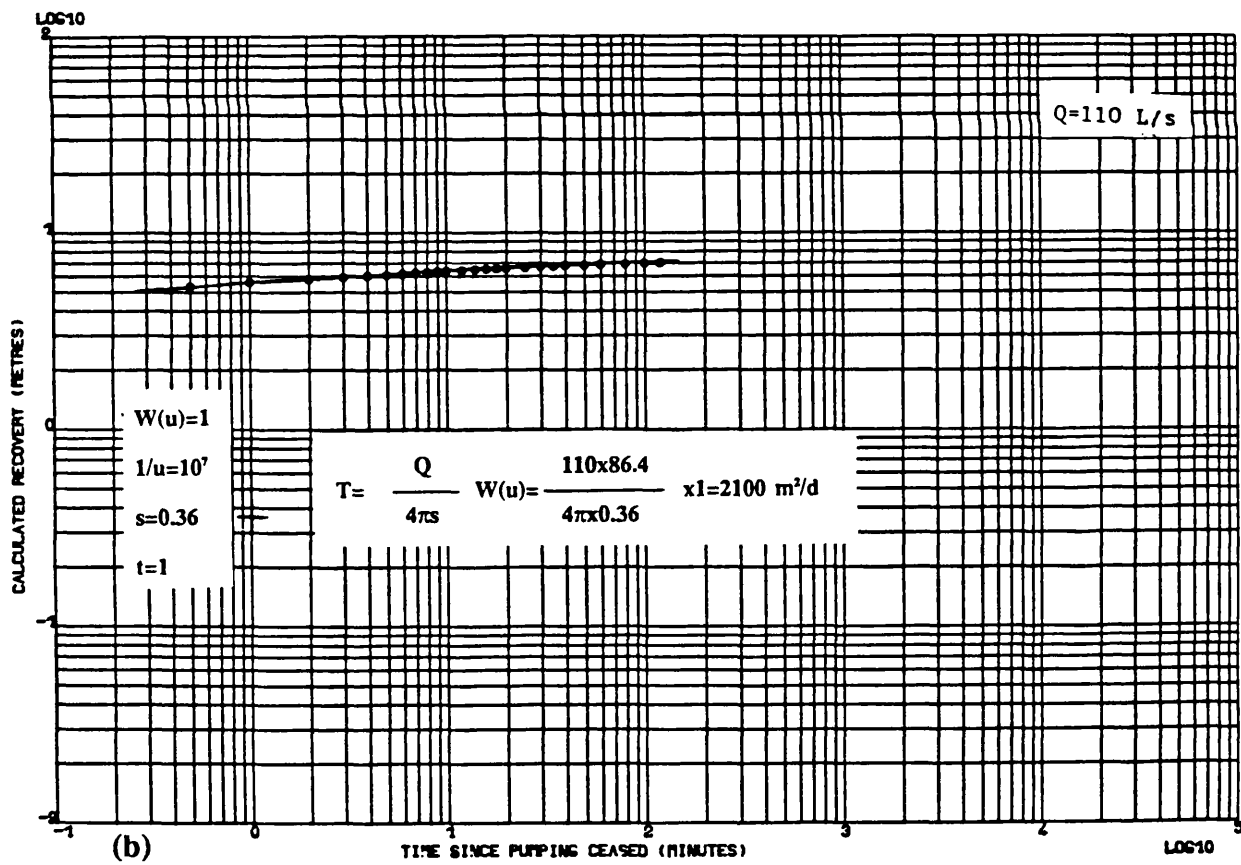
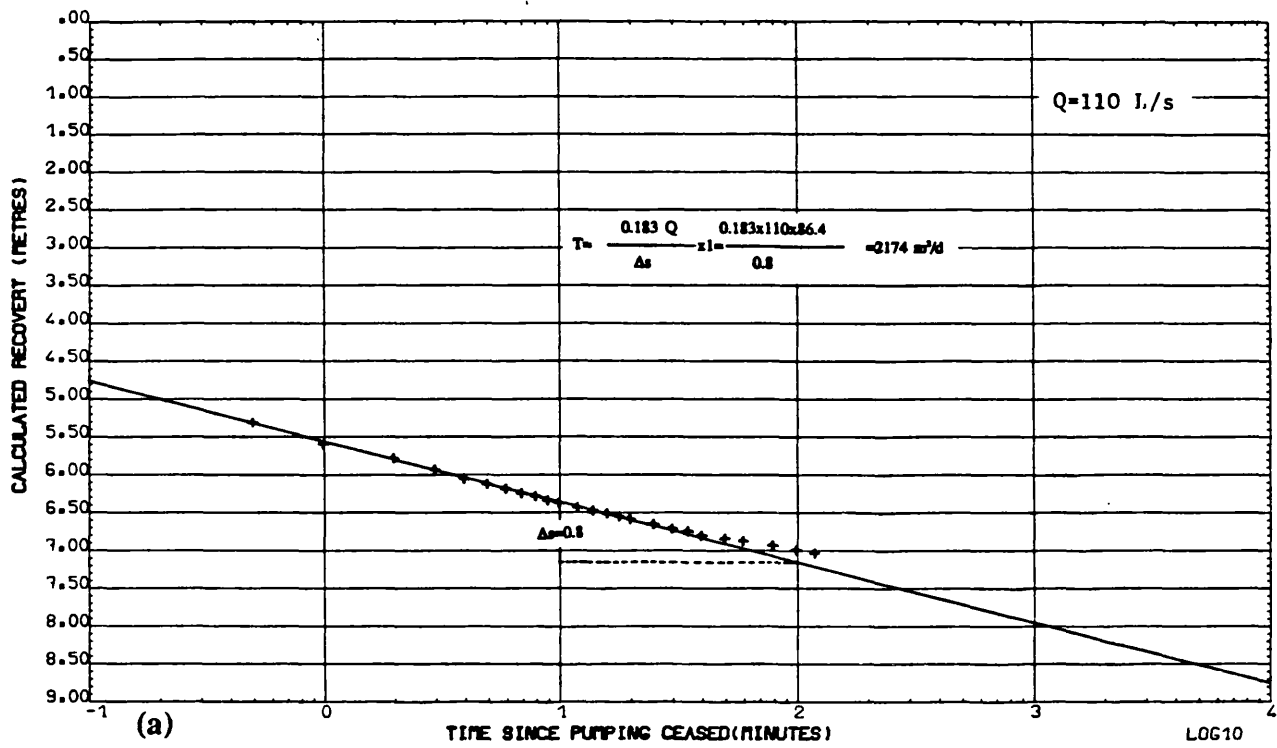


Fig. A5.10 PW TPSW8, Calculated Recovery plots: (a) Straight line method, (b) Type curve method.

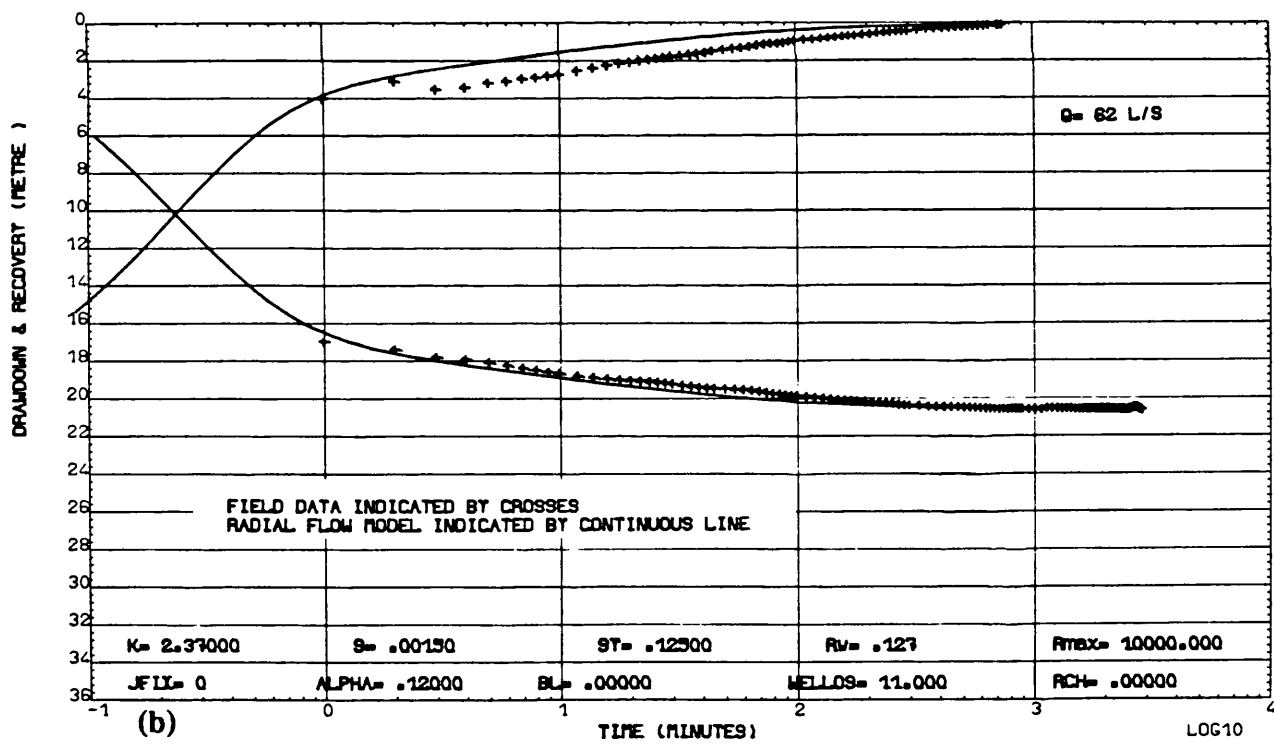
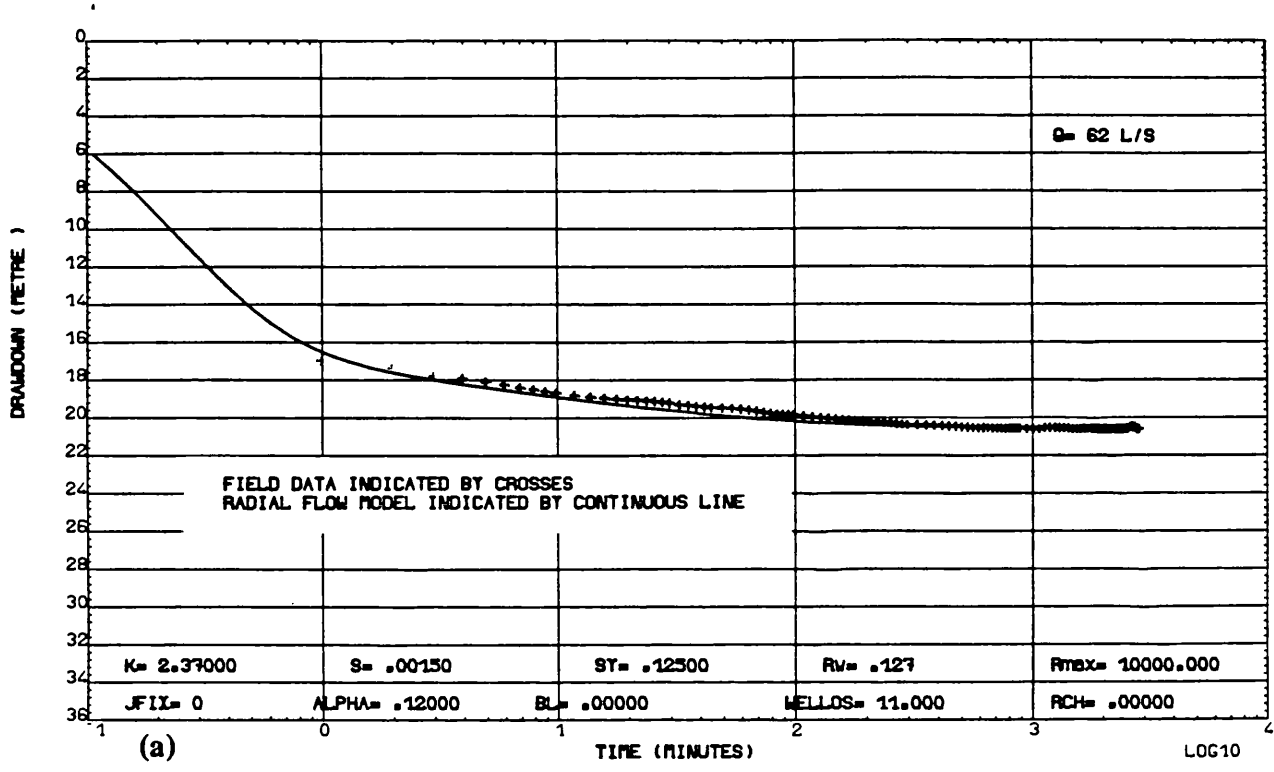


Fig. A5.11 PW SW5, Model analysis: (a) Without recovery, (b) With recovery.

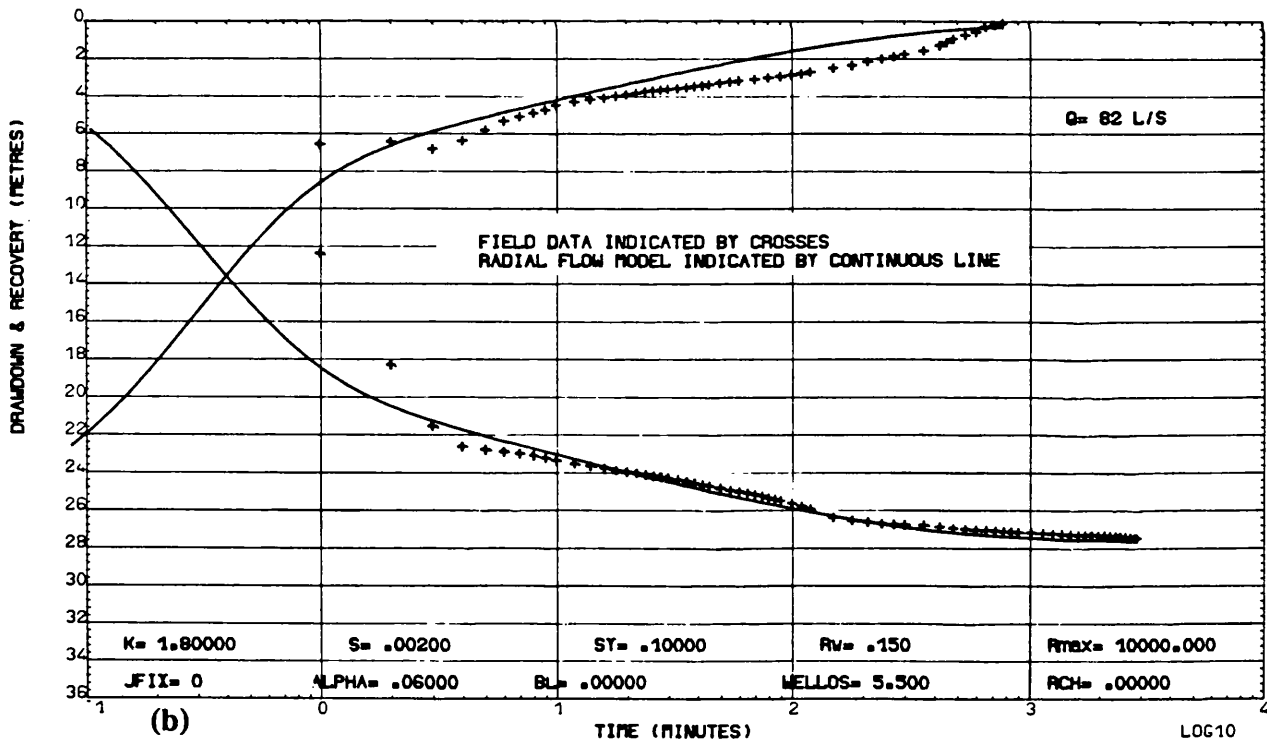
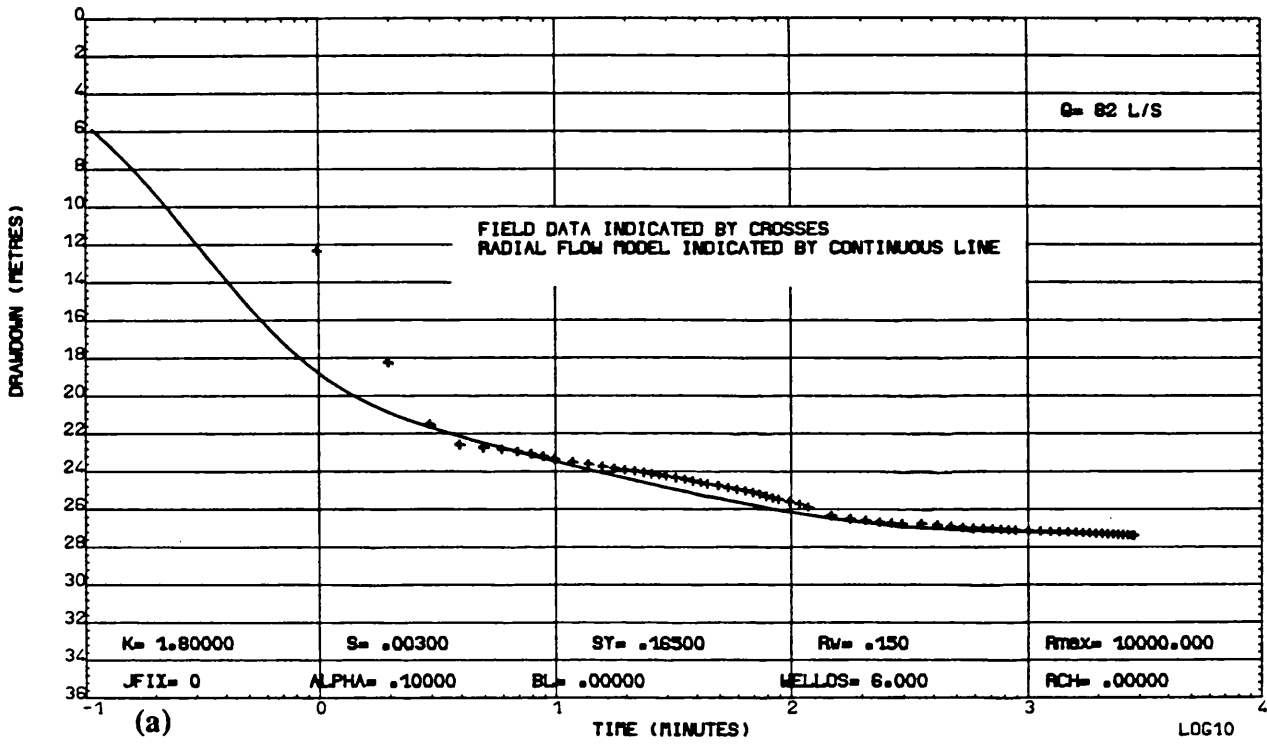


Fig. A5.12 PW SW8, Model analysis: (a) Without recovery, (b) With recovery.

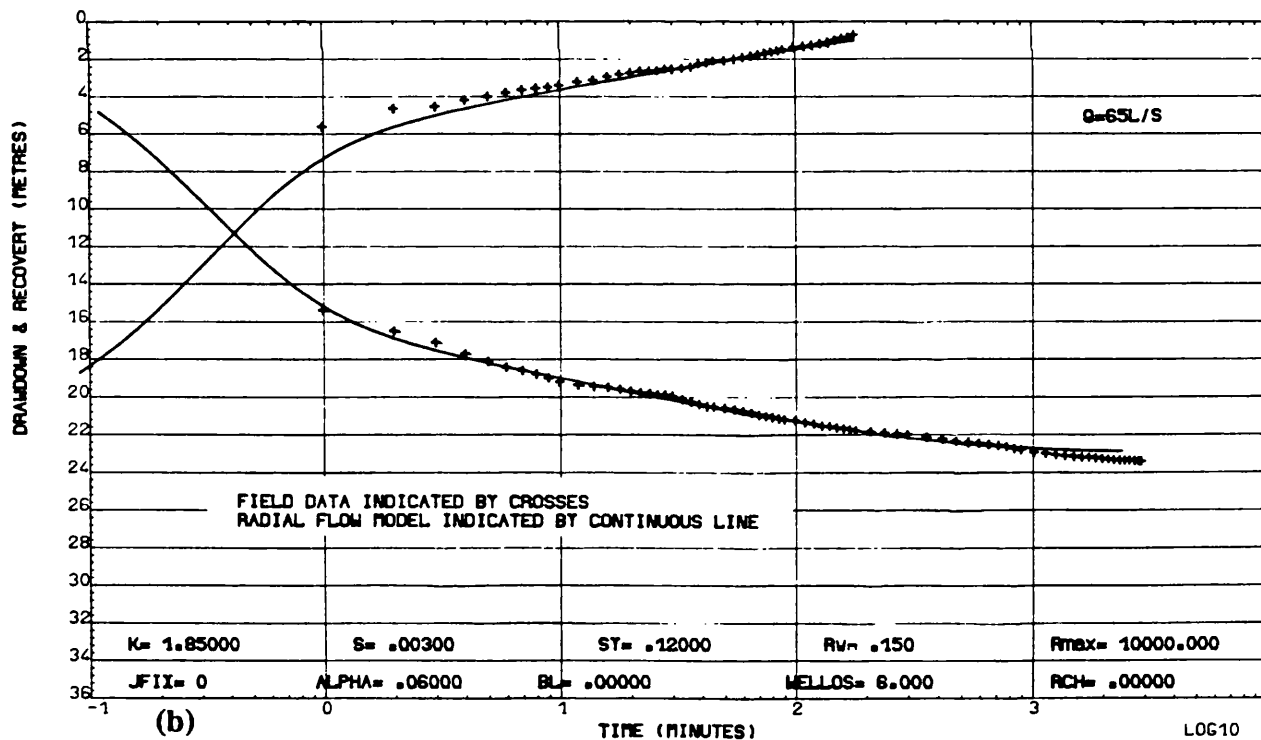
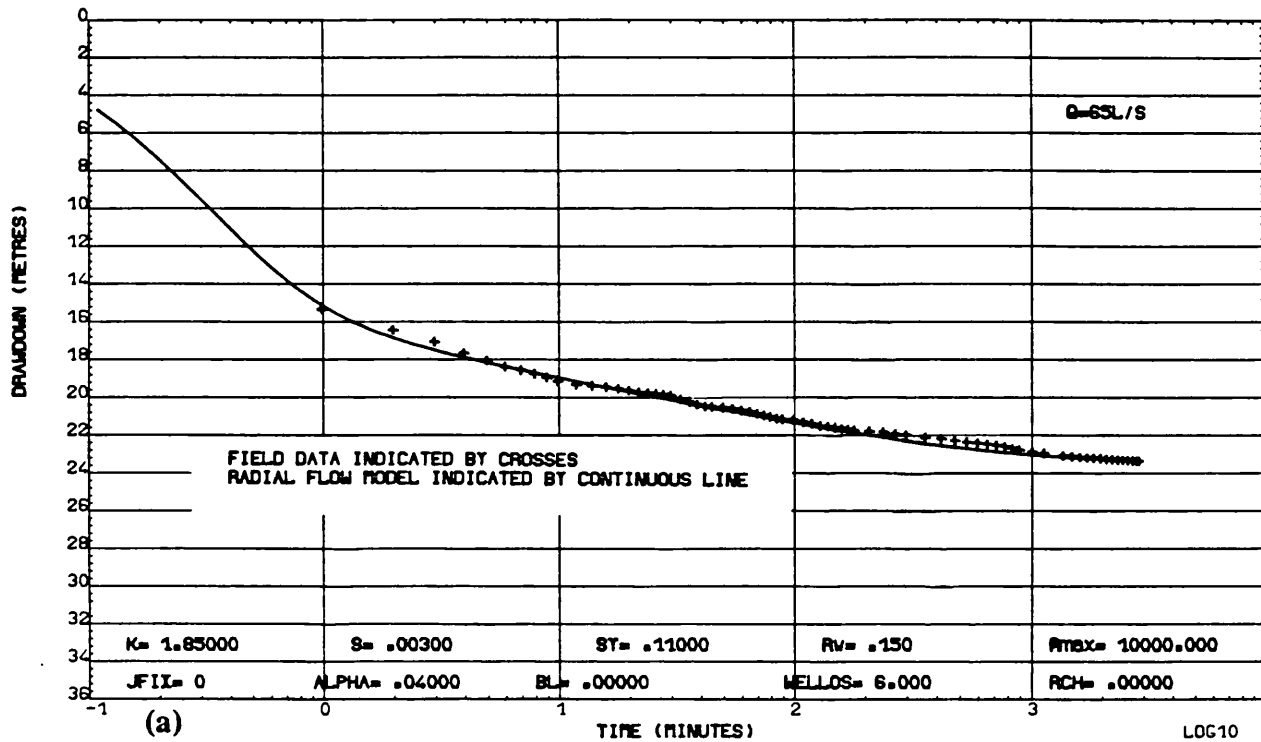


Fig. A5.13 PW SW10, Model analysis: (a) Without recovery, (b) With recovery.

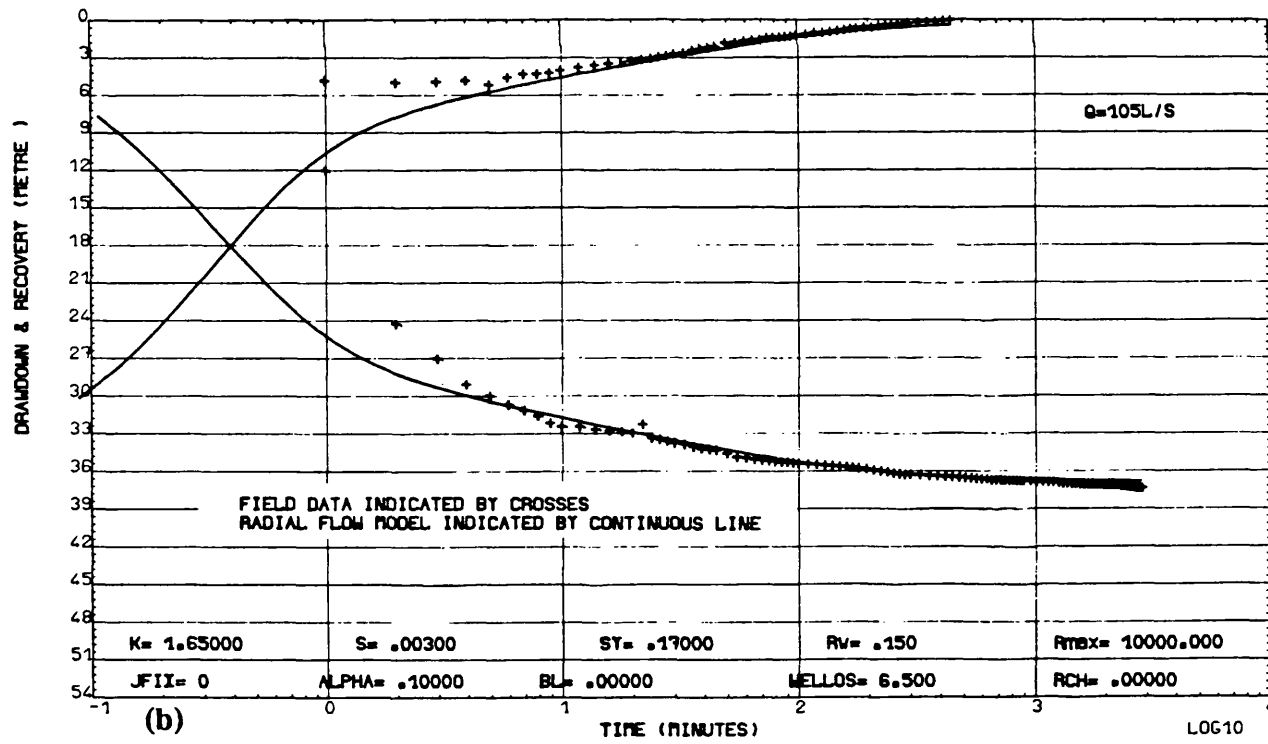
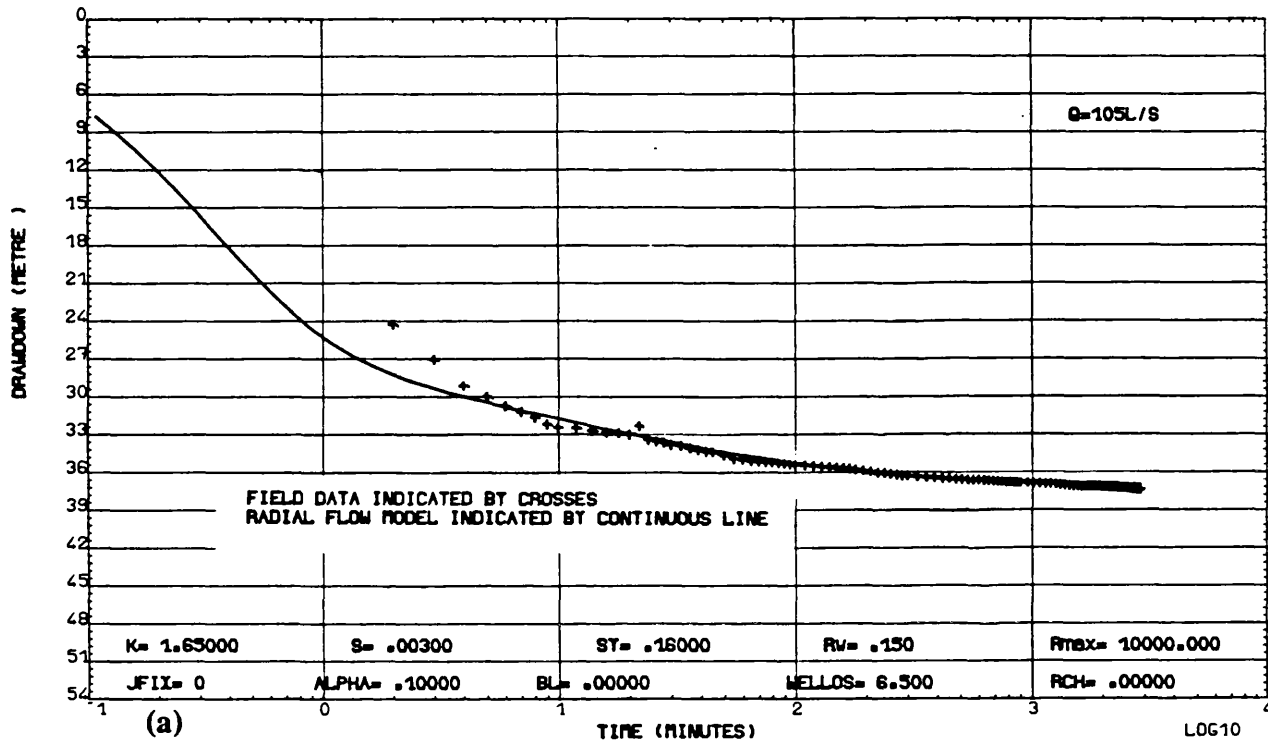


Fig. A5.14 PW SW11, Model analysis: (a) Without recovery, (b) With recovery.



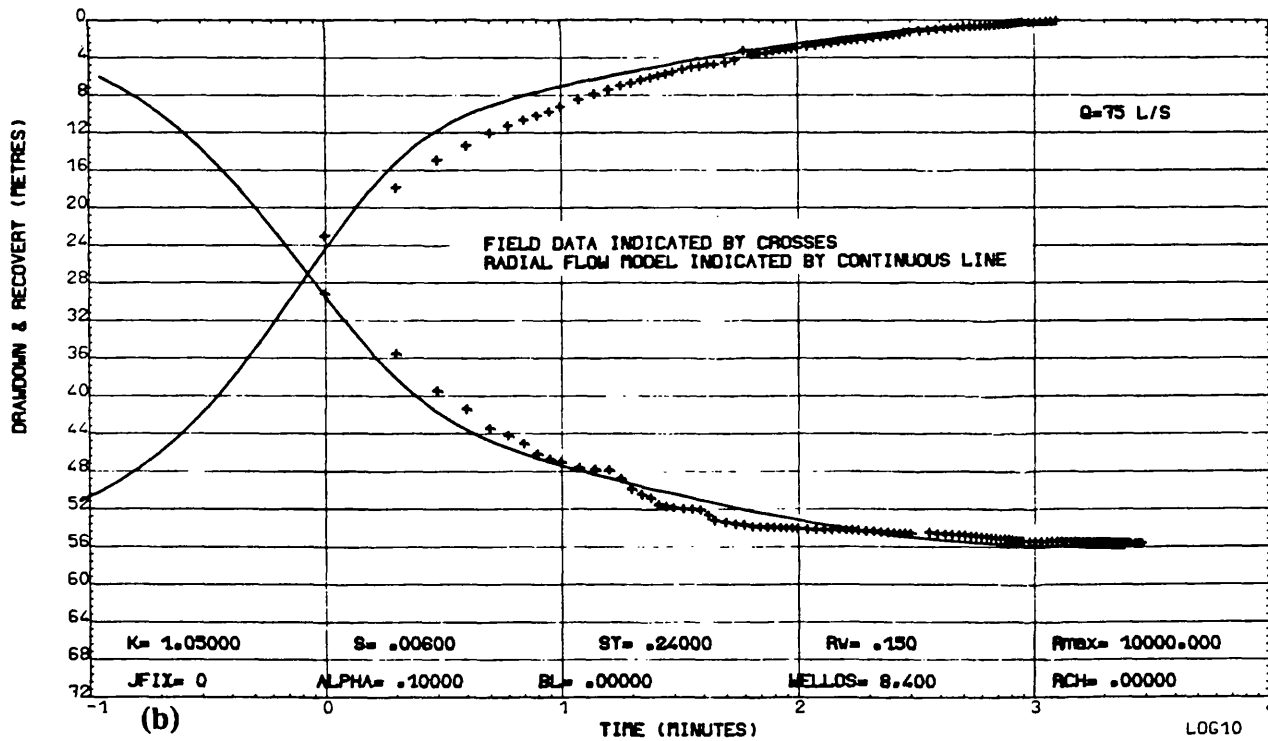
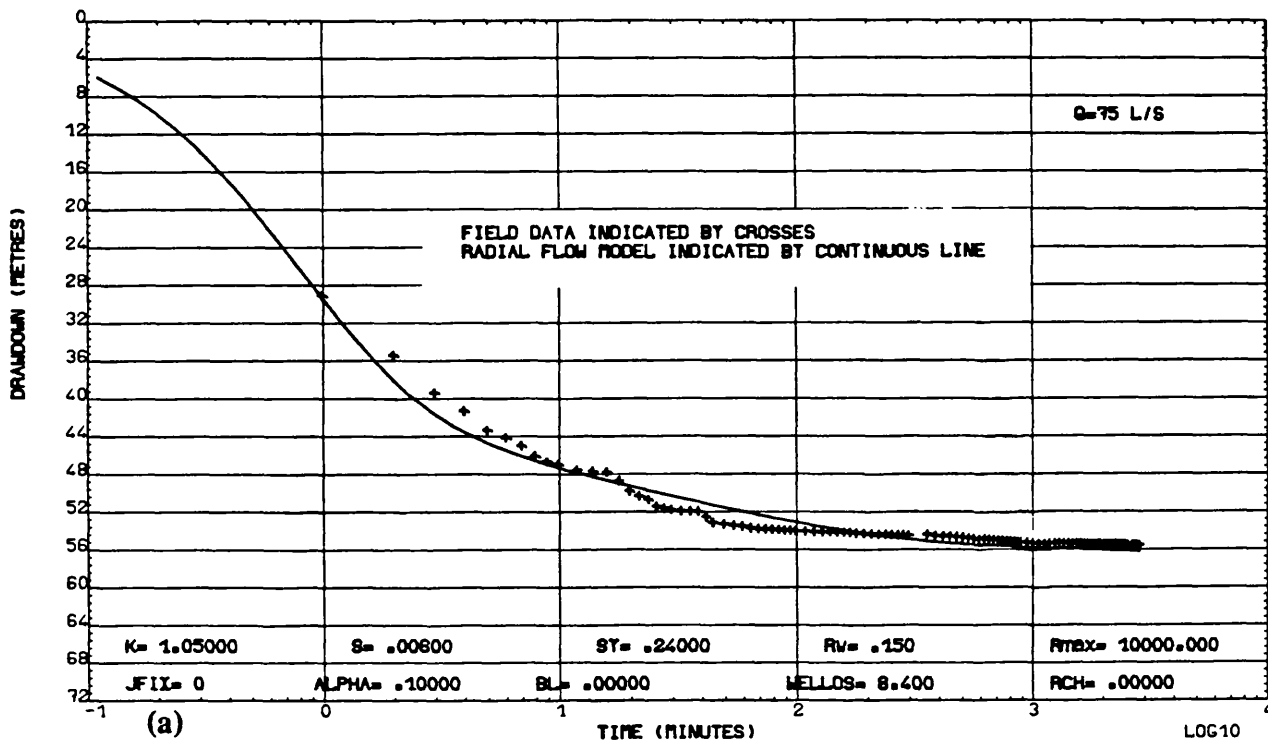


Fig. A5.15 PW SW13, Model analysis: (a) Without recovery, (b) With recovery.

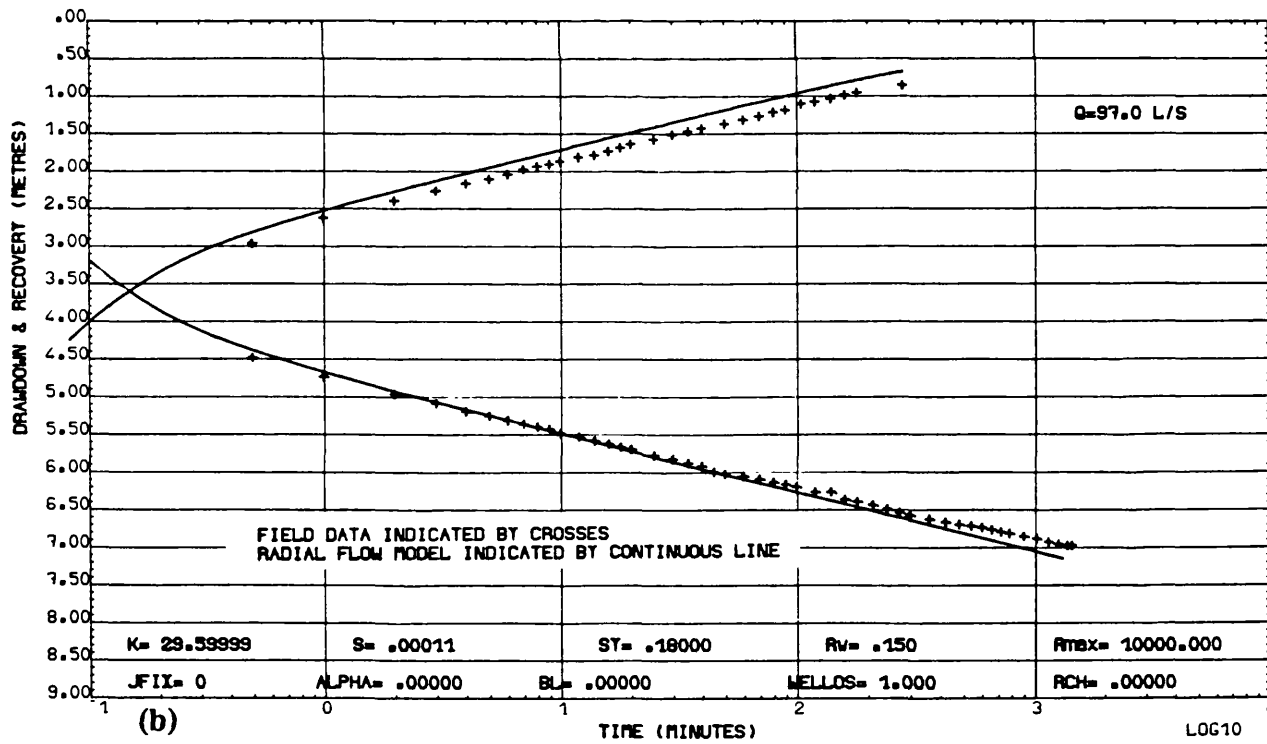
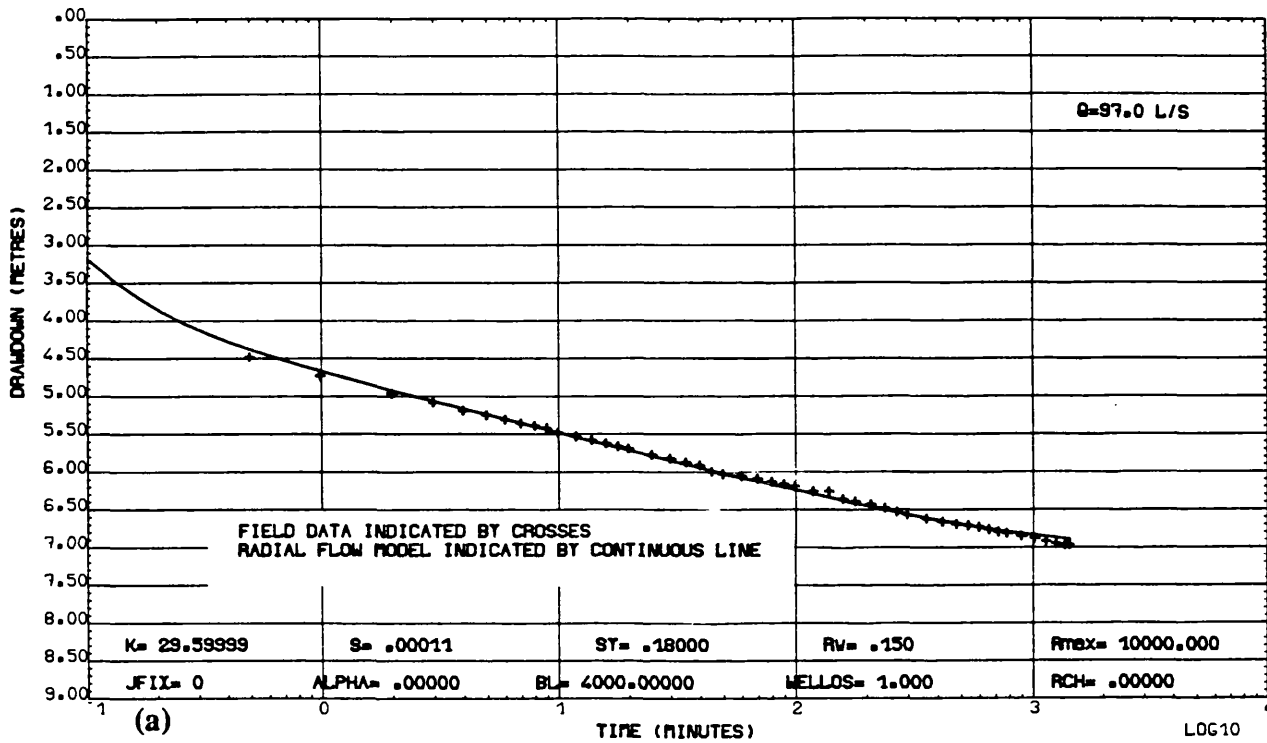


Fig. A5.16 PW TPSW4, Model analysis: (a) Without recovery, (b) With recovery.

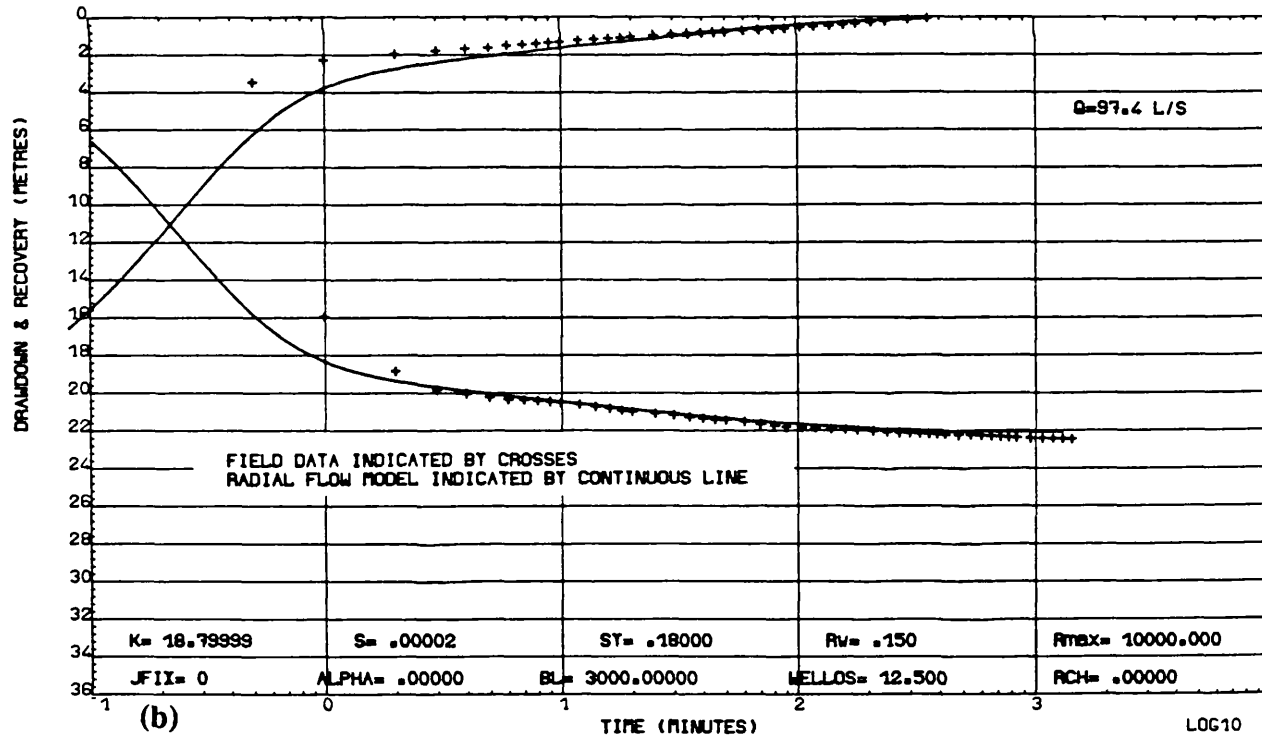
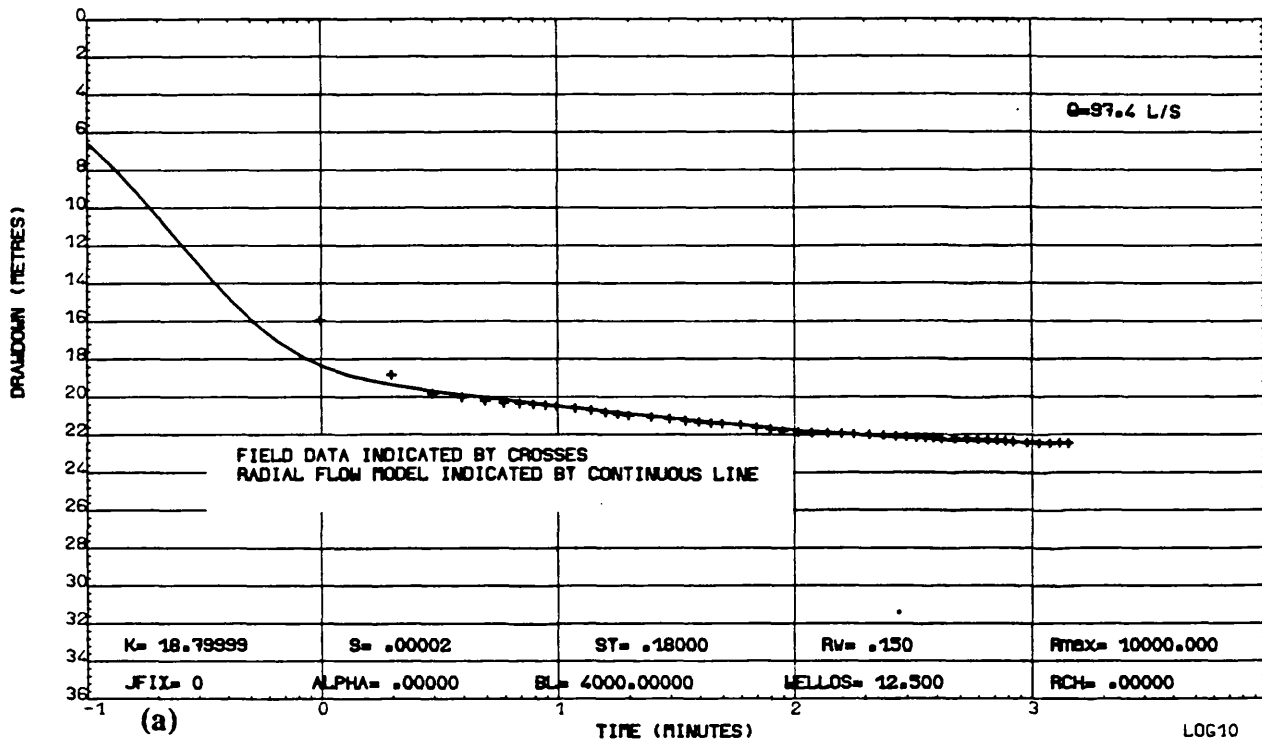


Fig. A5.17 PW TPSW6, Model analysis: (a) Without recovery, (b) With recovery.

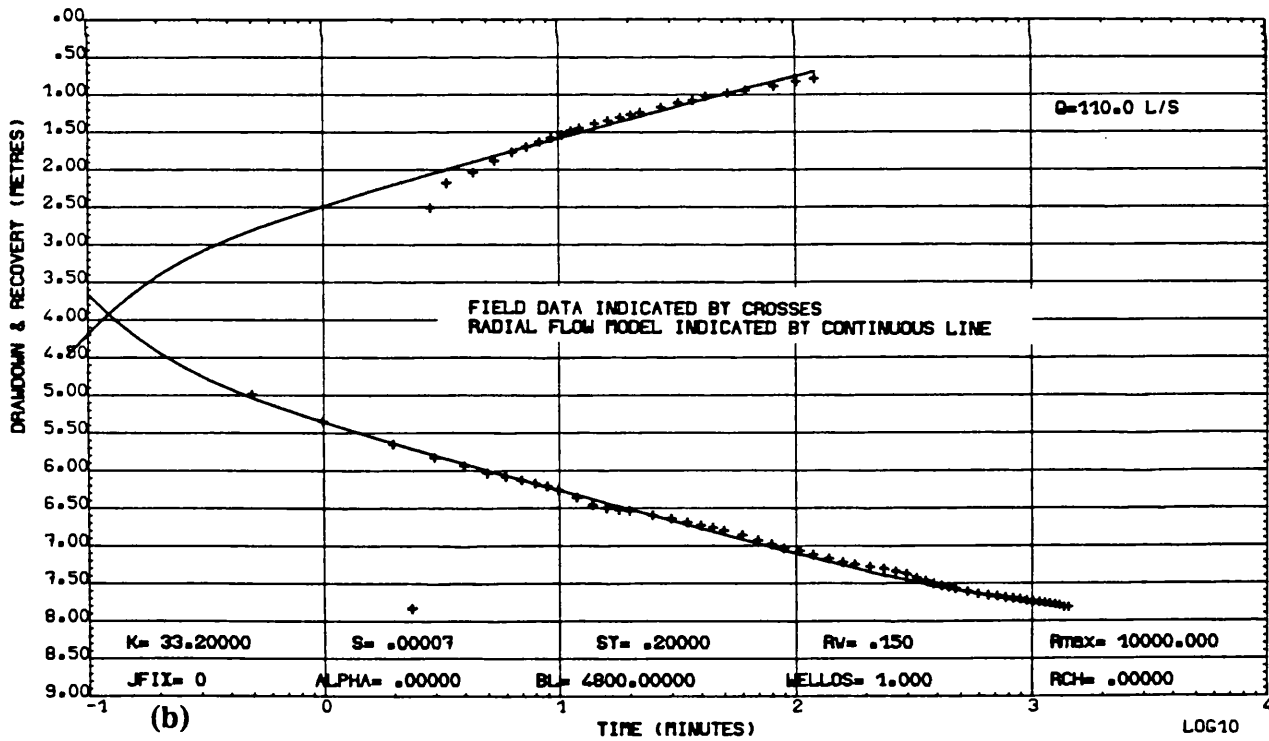
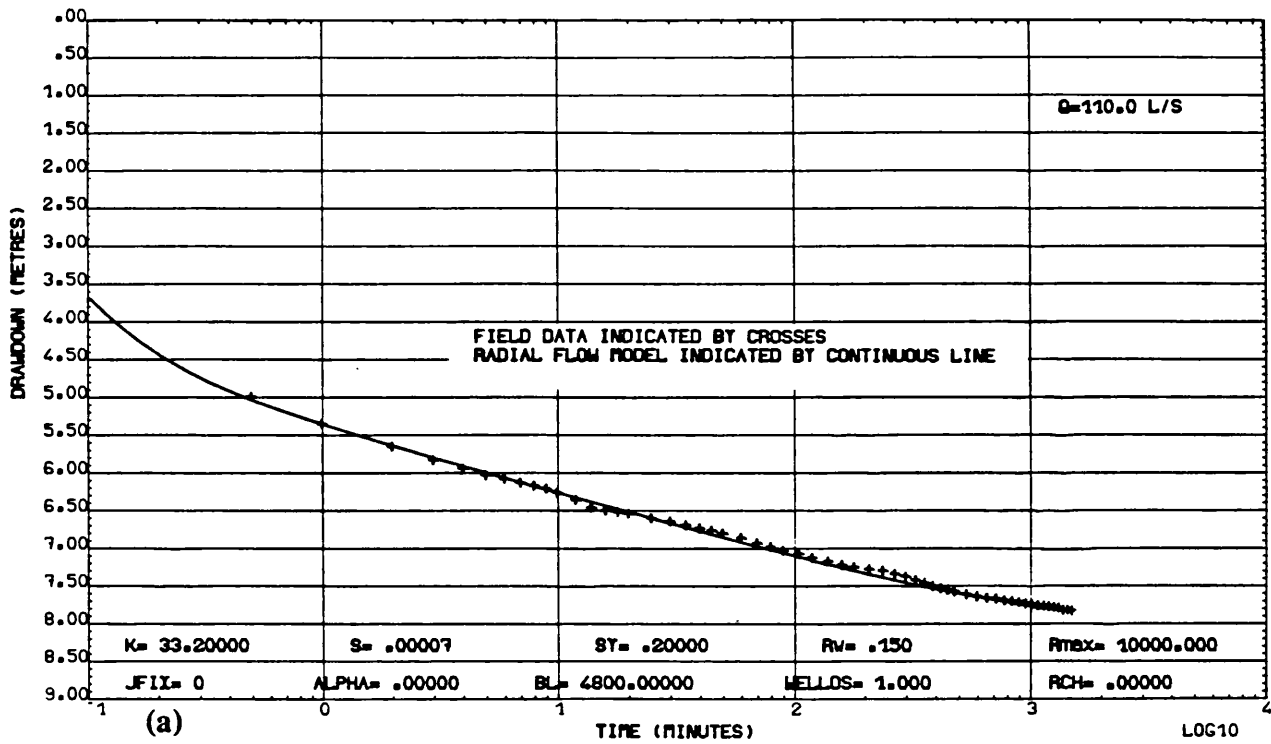


Fig. A5.18 PW TPSW8, Model analysis: (a) Without recovery, (b) With recovery.

**Appendix 6 Plots of Step-Drawdown Test analysis.**

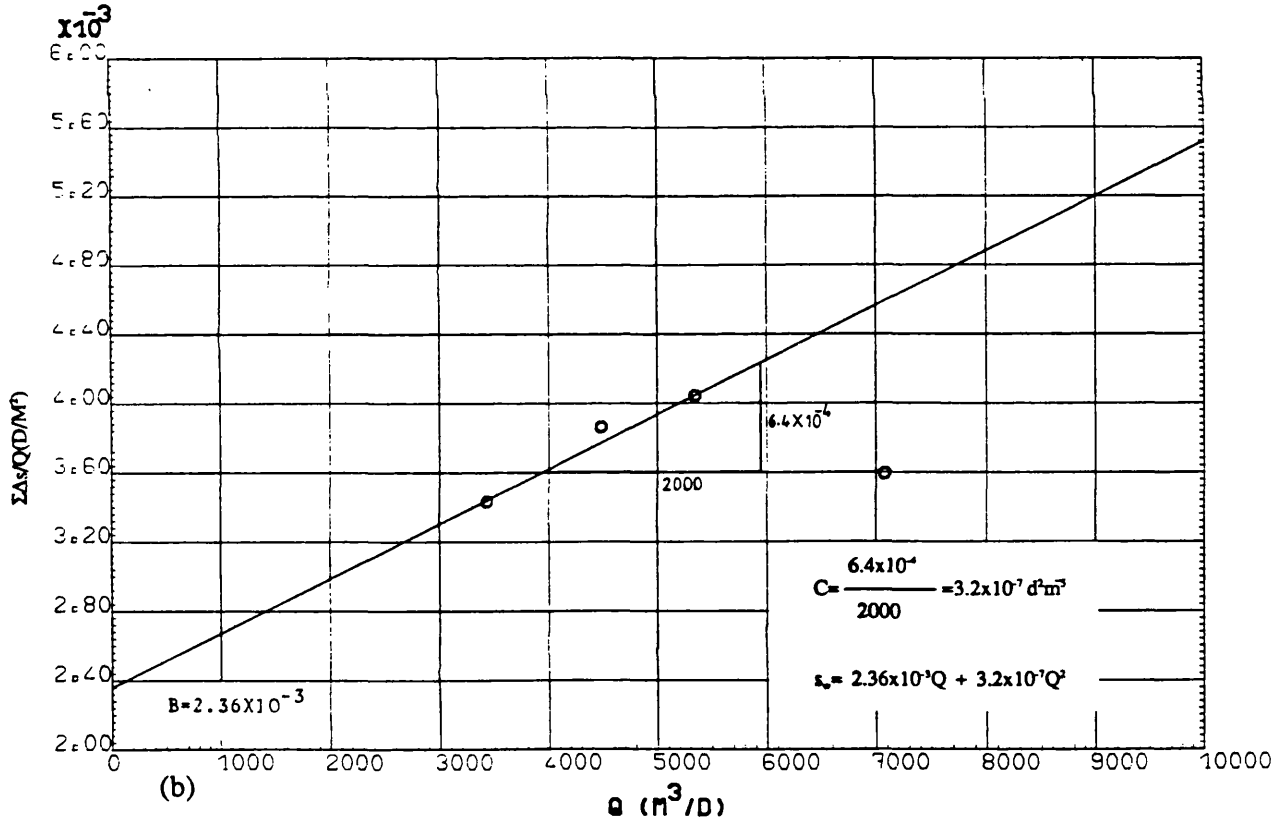
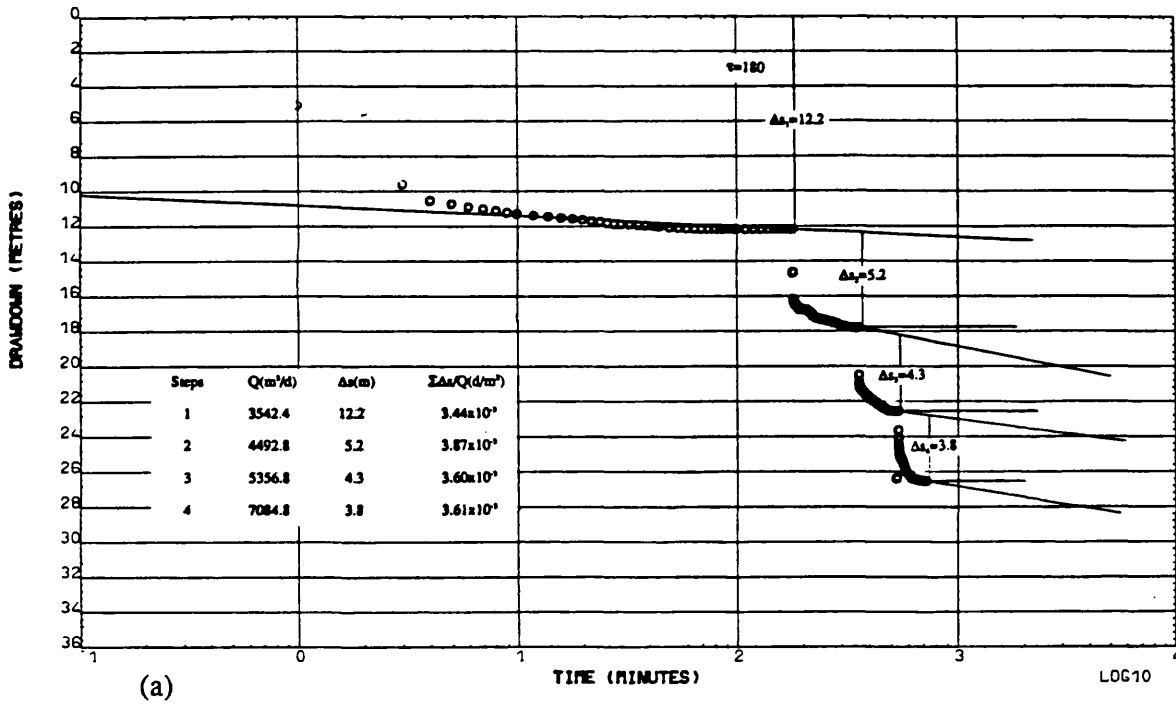


Fig. A6.1 PW SW8, Step-Drawdown test: Bruin & Hudson method, (a) data handling, (b) data plot.

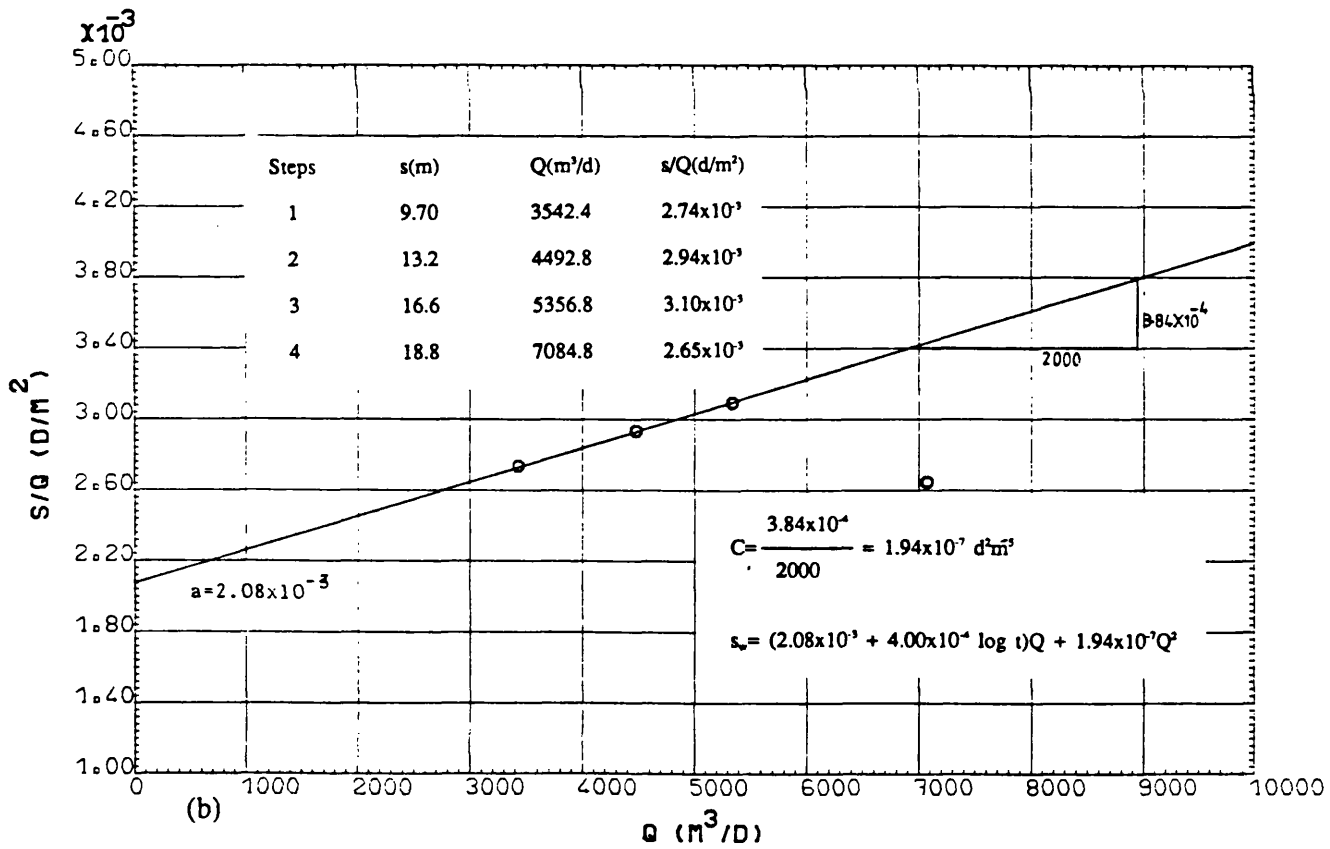
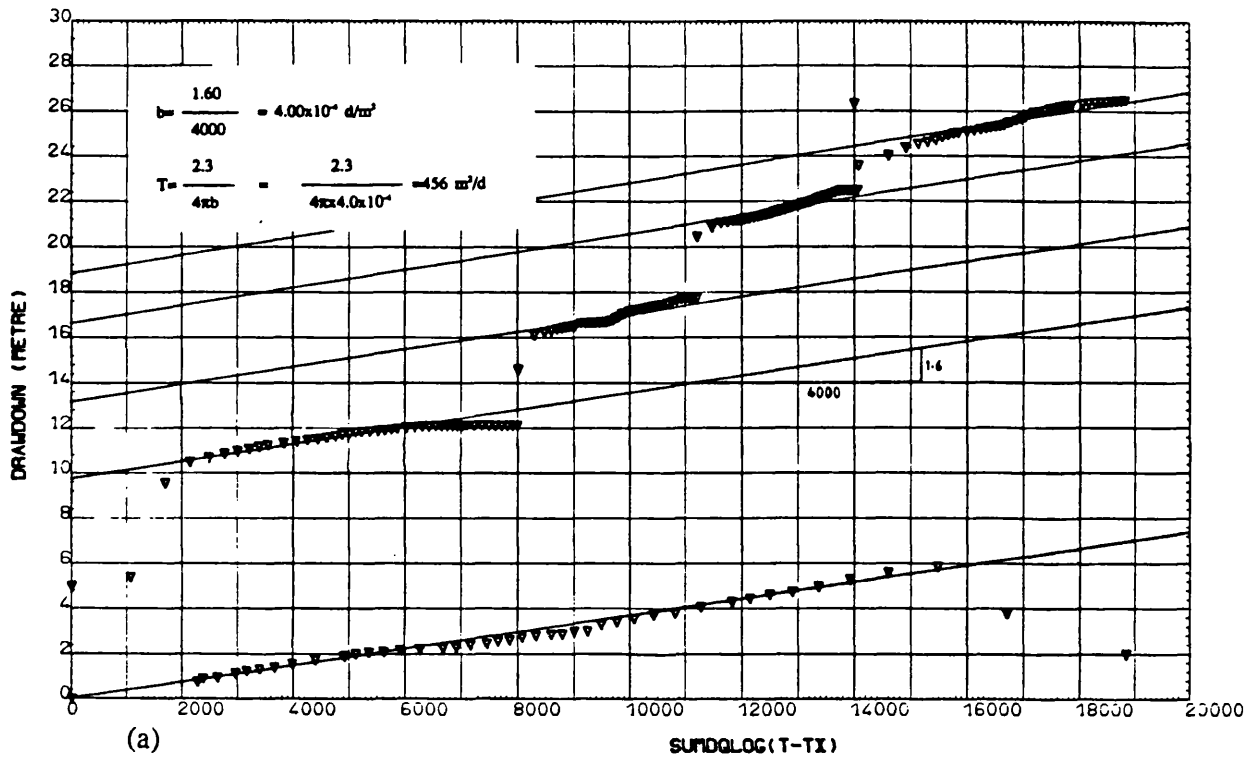
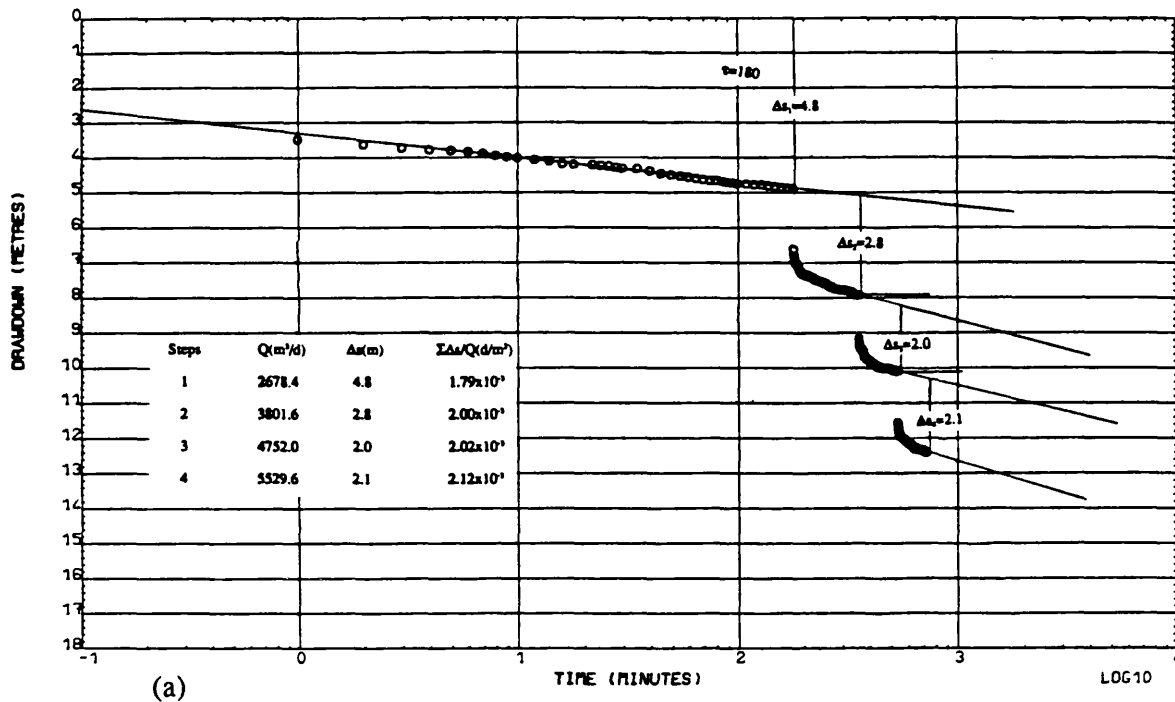
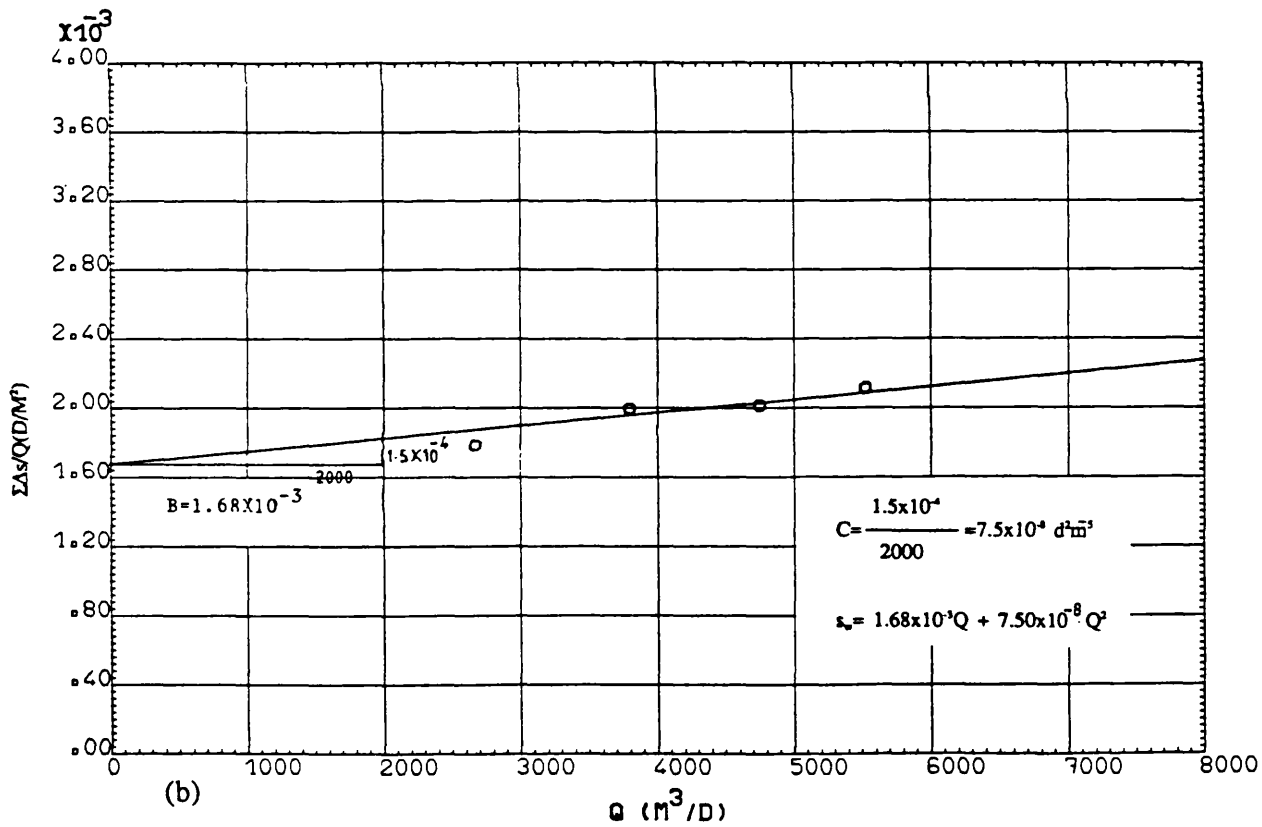


Fig. A6.2 PW SW8, Step-Drawdown test: Eden & Hazel method, (a) data handling, (b) data plot.



(a)



(b)

Fig. A6.3 PW JW1, Step-Drawdown test: Bruin & Hudson method, (a) data handling, (b) data plot.



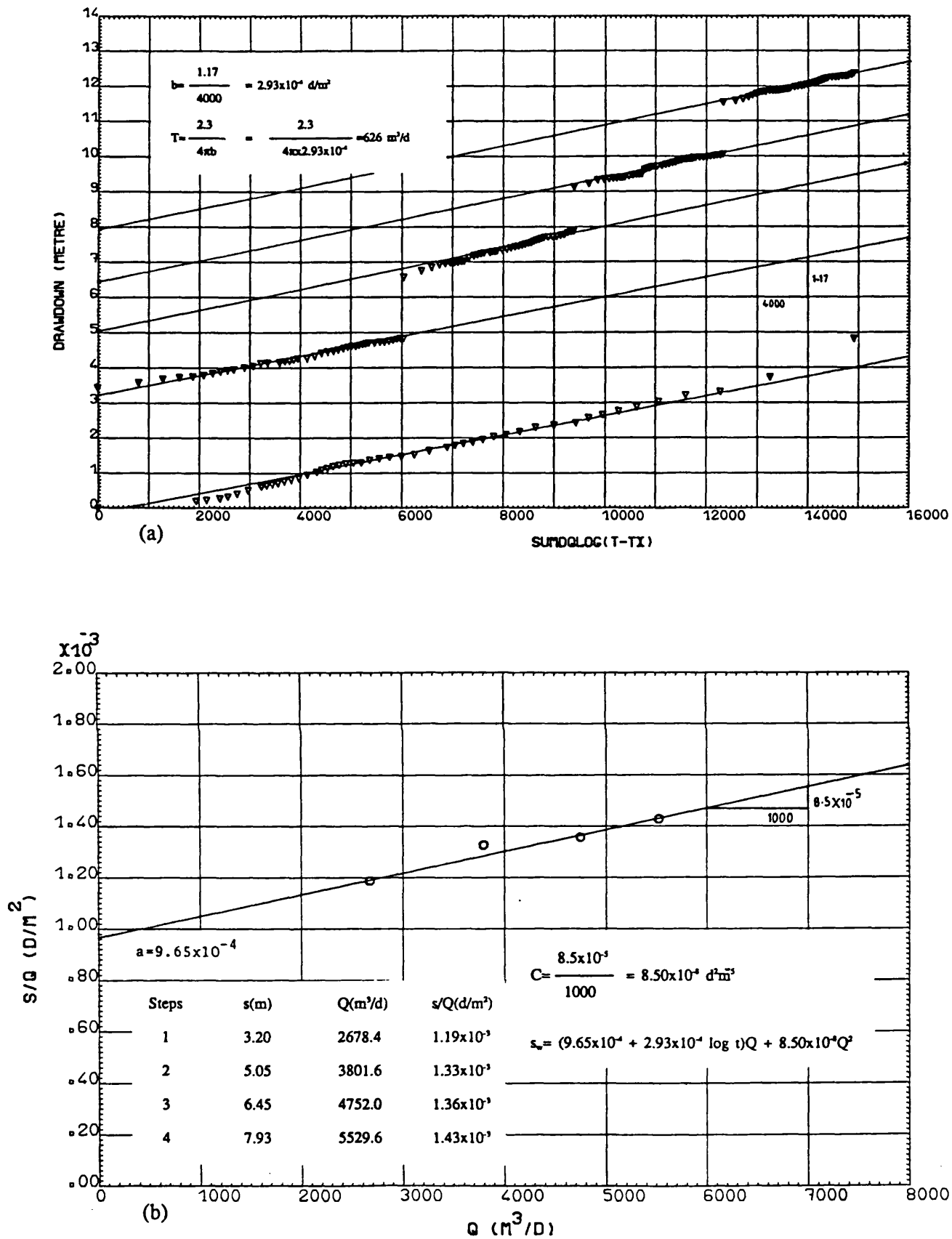


Fig. A6.4 PW JW1, Step-Drawdown test: Eden & Hazel method, (a) data handling,

(b) data plot.

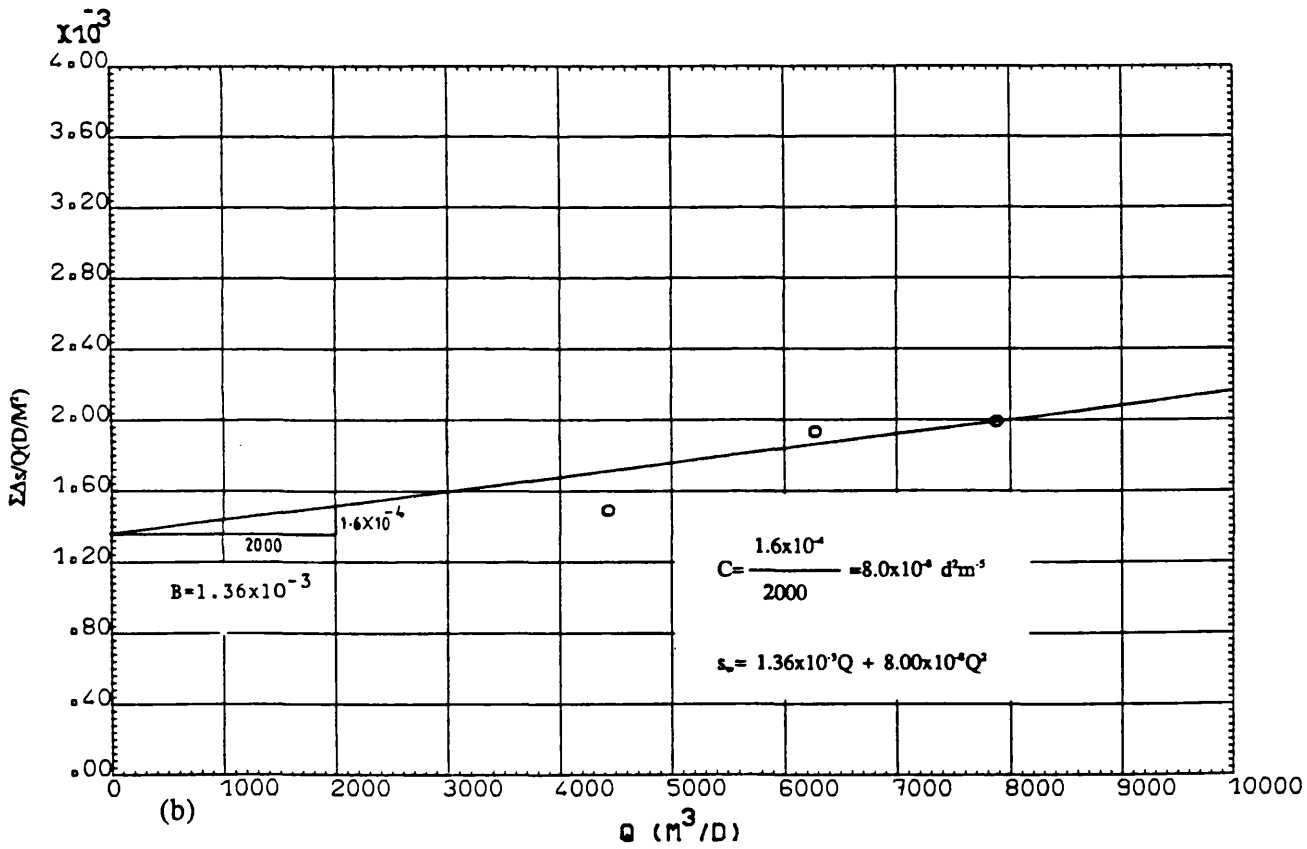
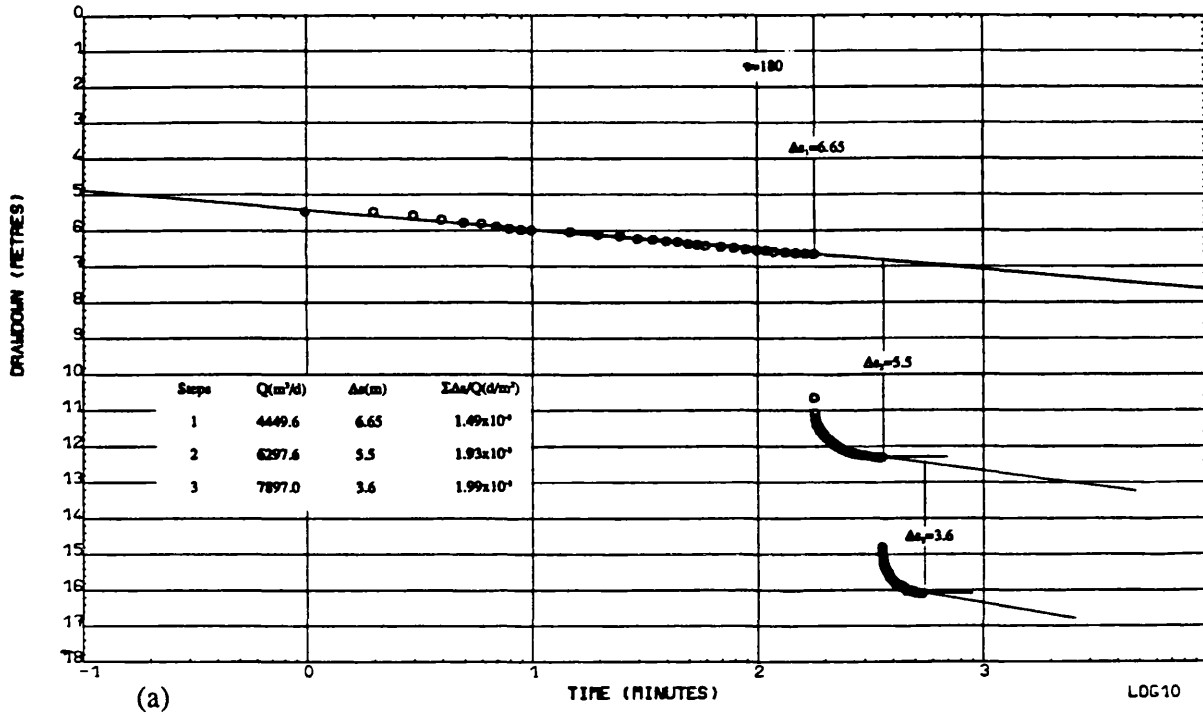


Fig. A6.5 PW TPSW1, Step-Drawdown test: Bruin & Hudson method, (a) data handling, (b) data plot.

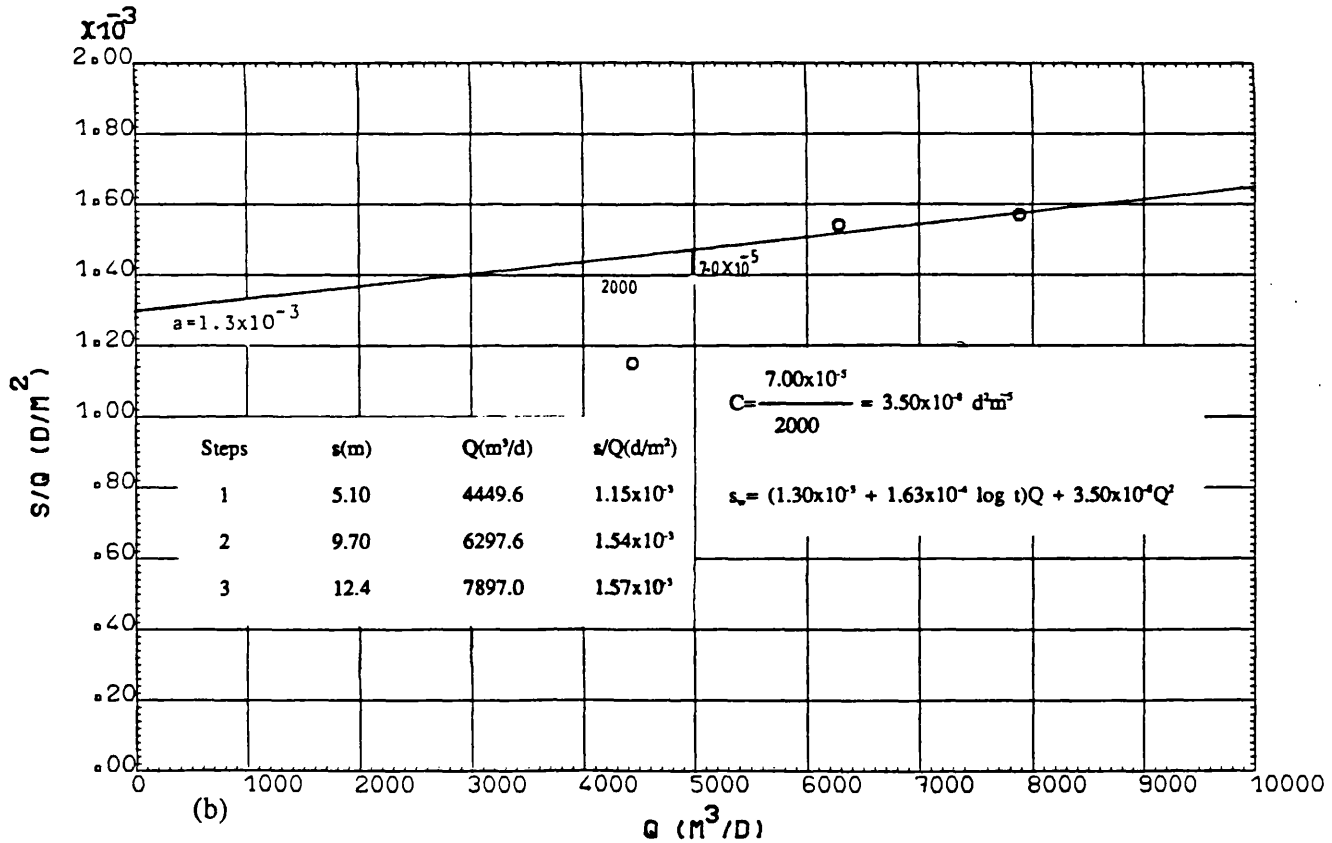
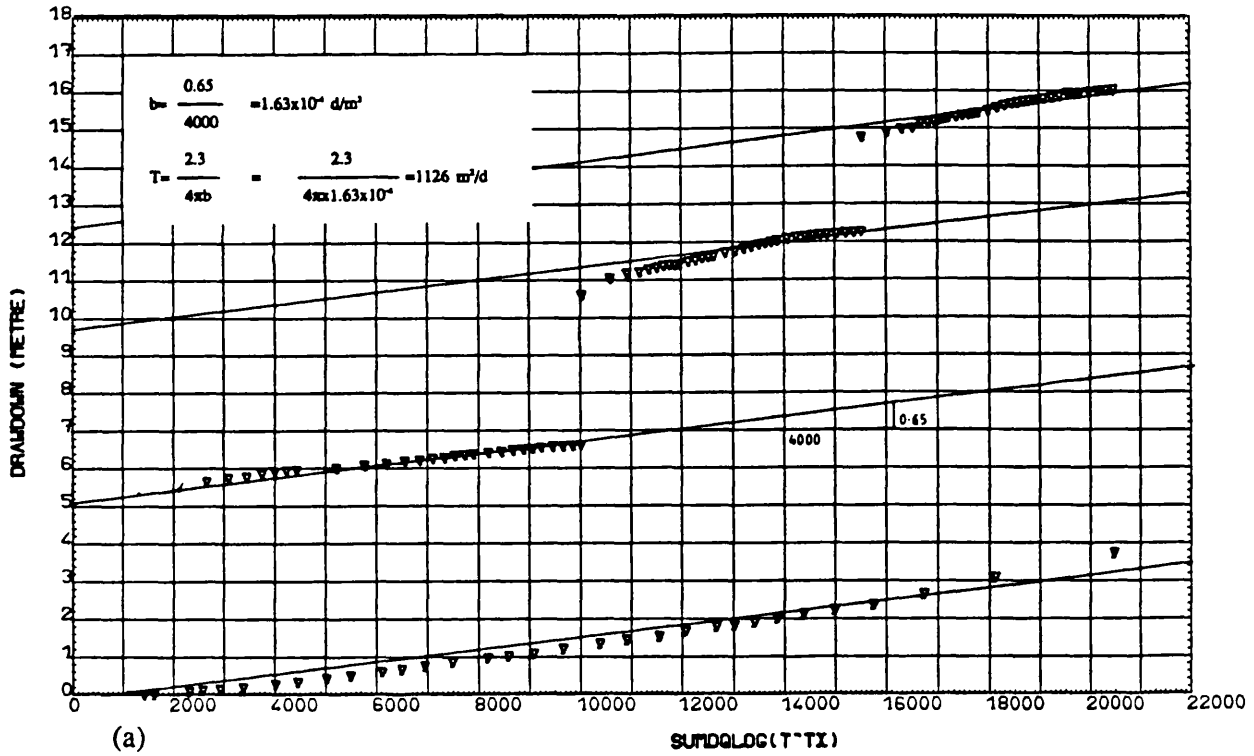


Fig. A6.6 PW TPSW1, Step-Drawdown test: Eden & Hazel method, (a) data handling, (b) data plot.

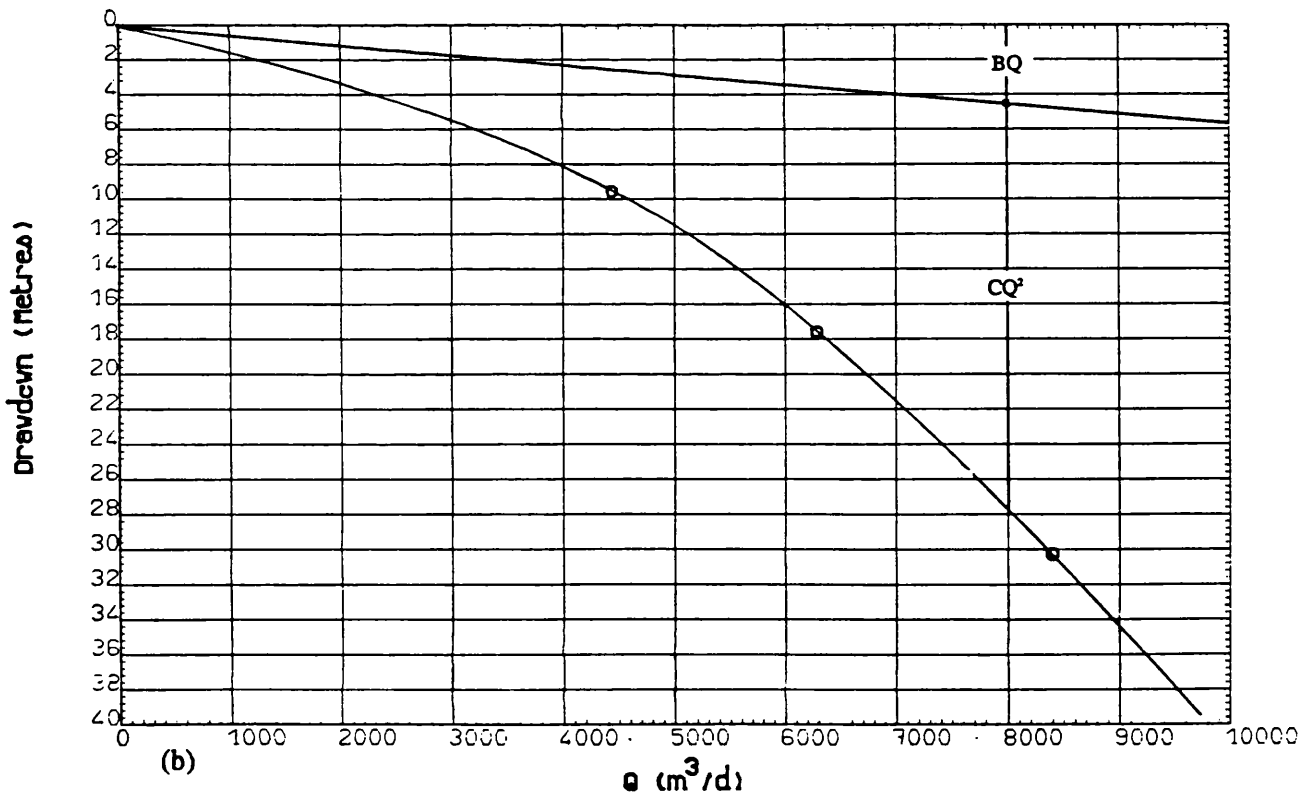
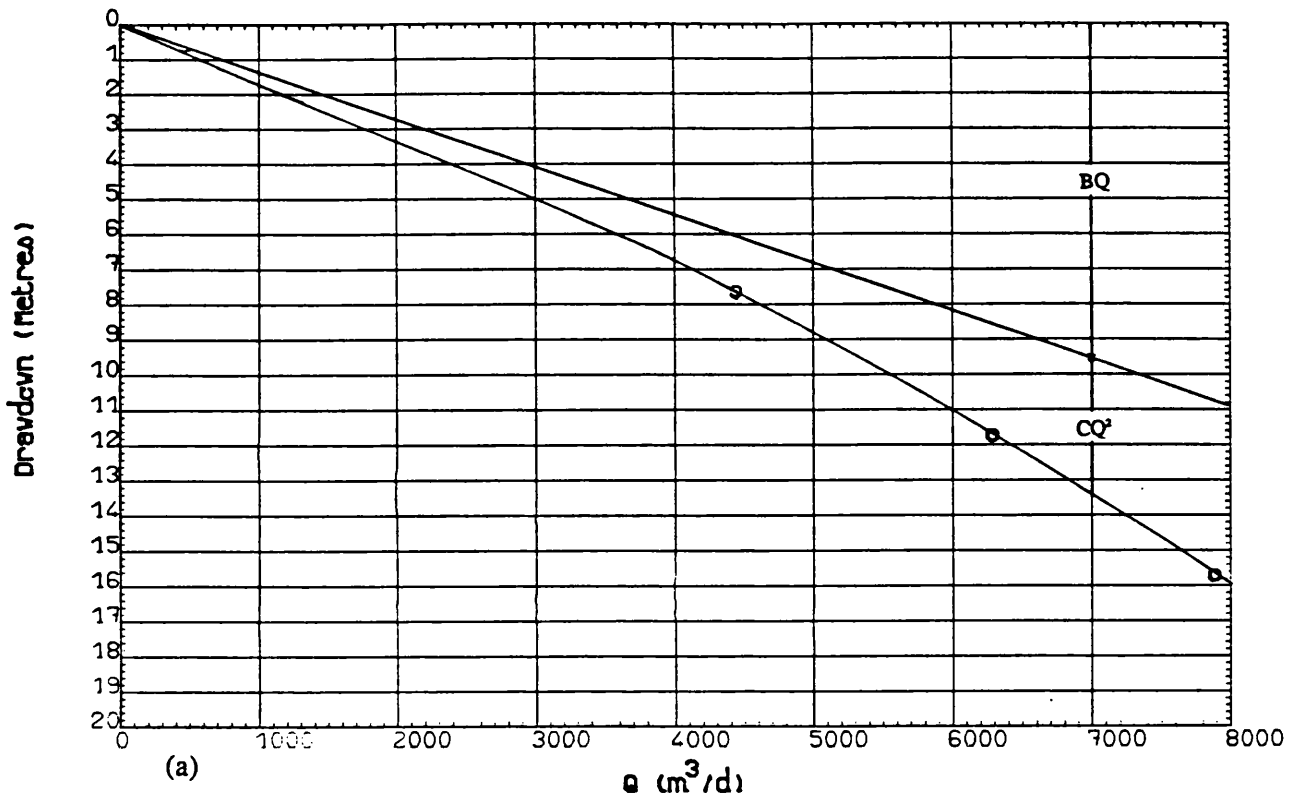


Fig. A6.7 Step-Drawdown test: Theoretical drawdown - yield curve, (a) PW TPSW1, (b) PW TPSW3.

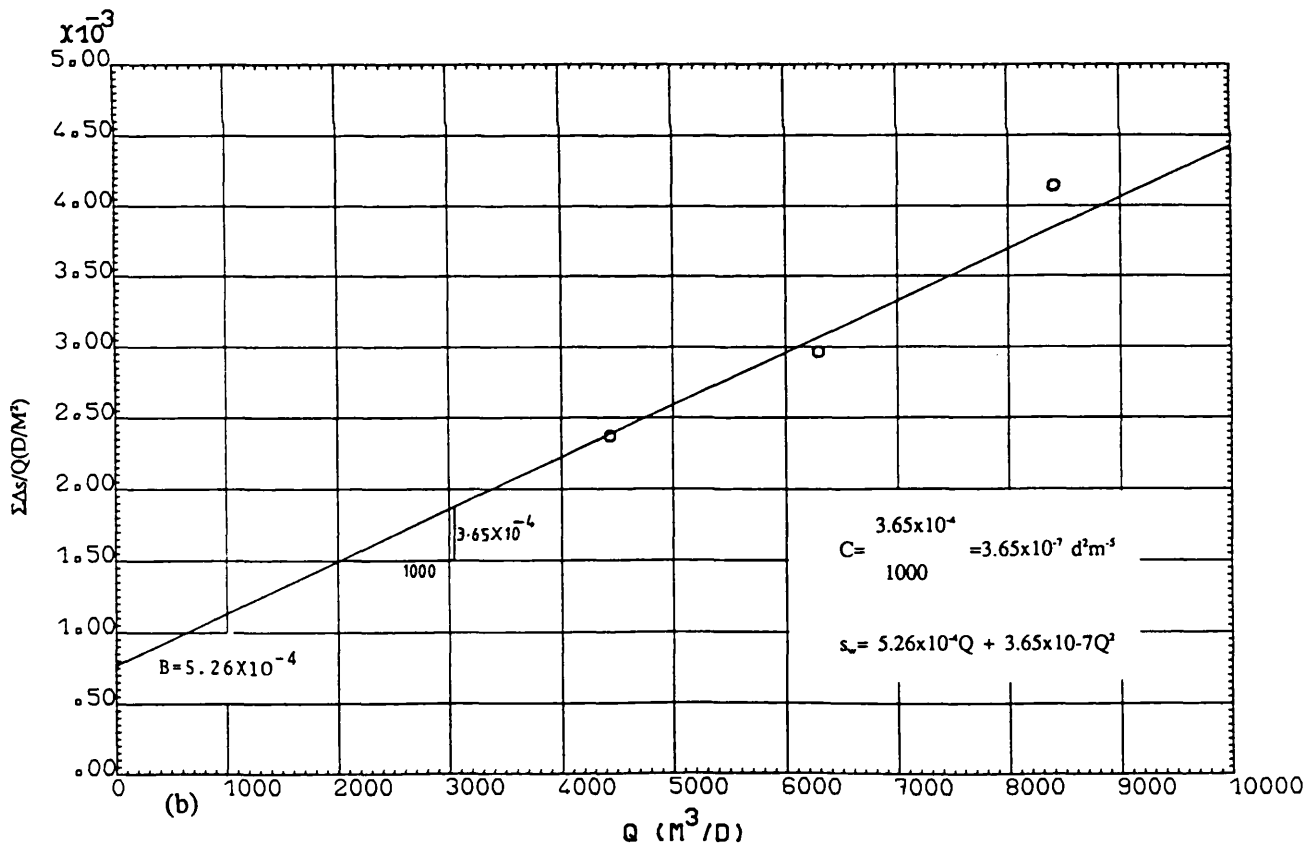
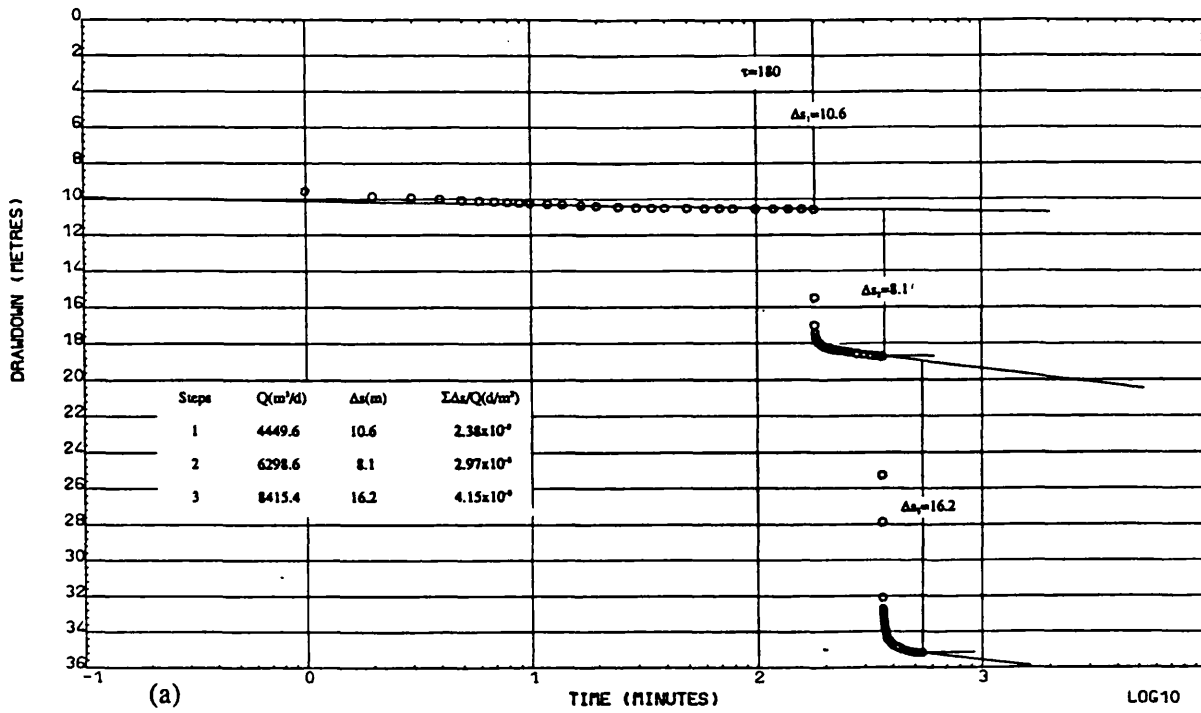


Fig. A6.8 PW TPSW3, Step-Drawdown test: Bruin & Hudson method, (a) data handling, (b) data plot.

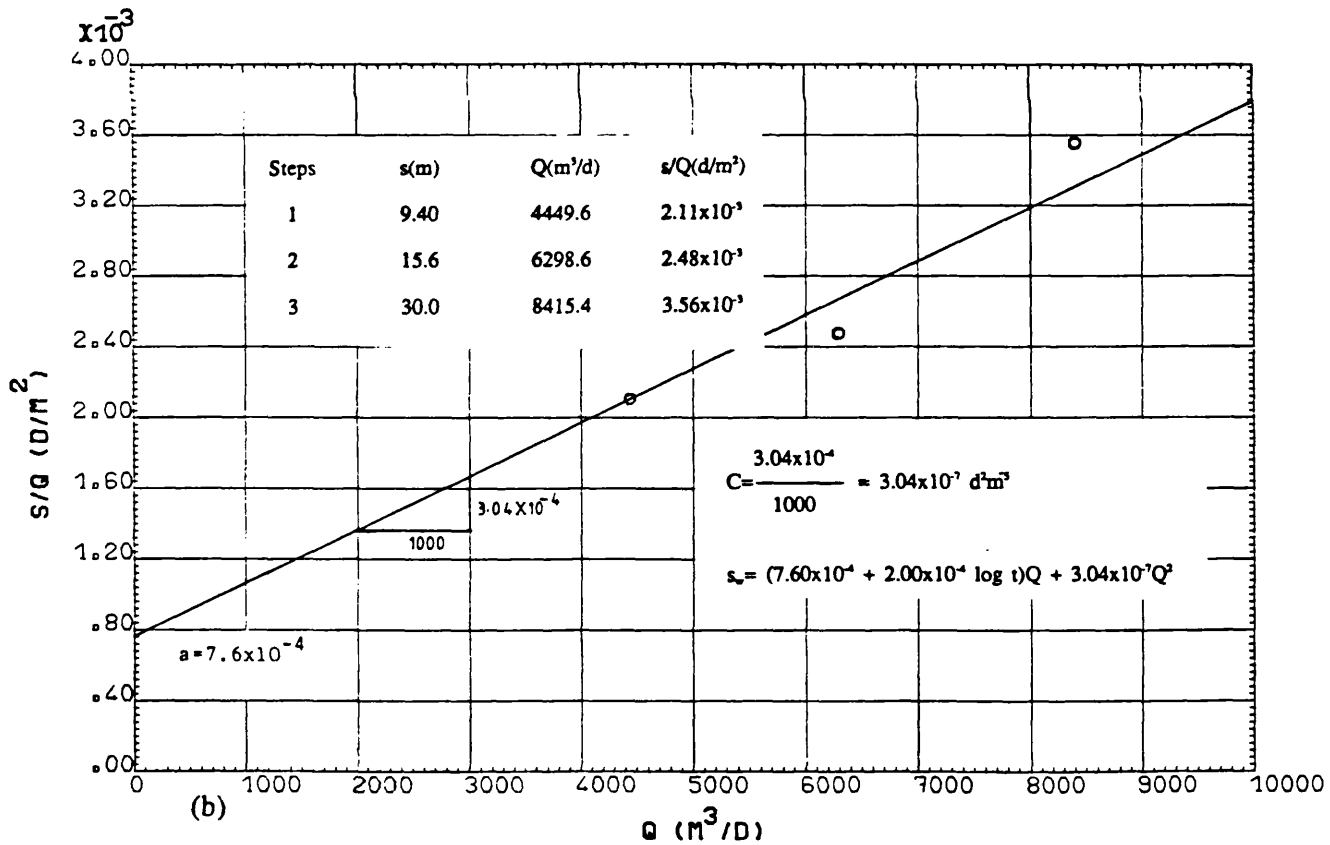
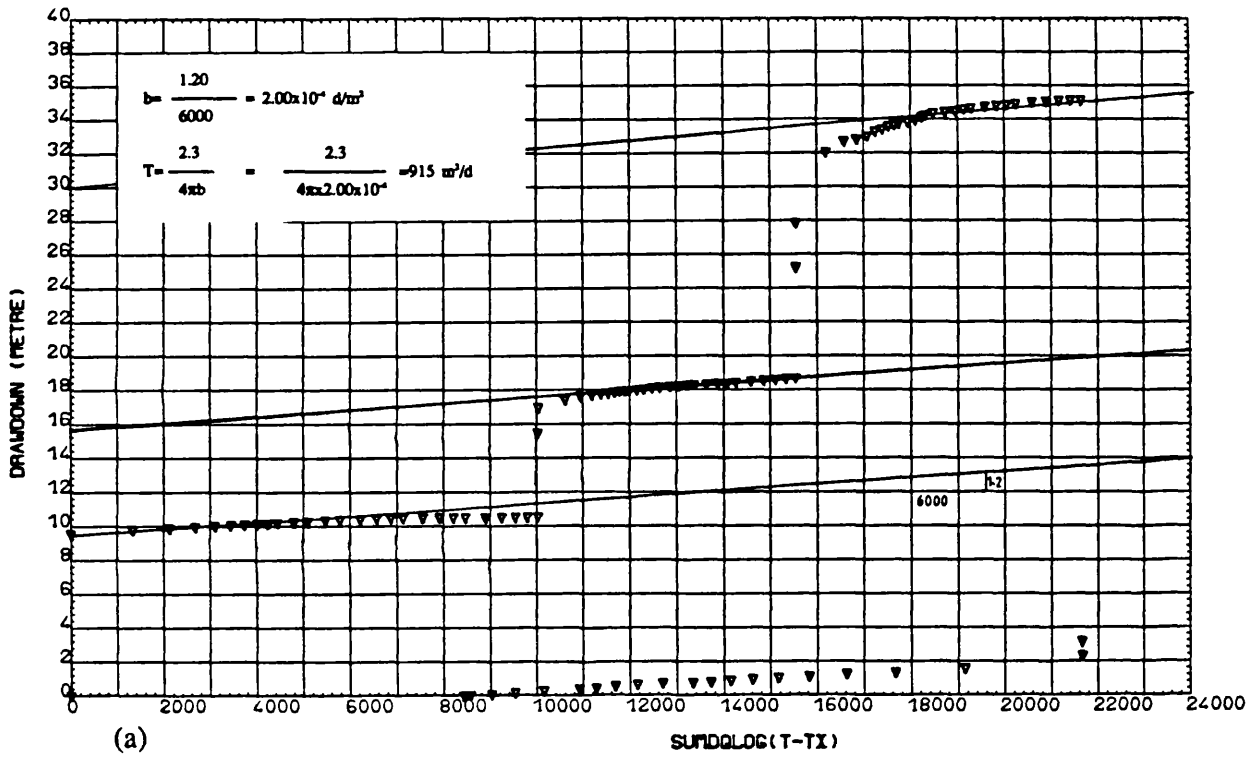


Fig. A6.9 PW TPSW3, Step-Drawdown test: Eden & Hazel method, (a) data handling, (b) data plot.

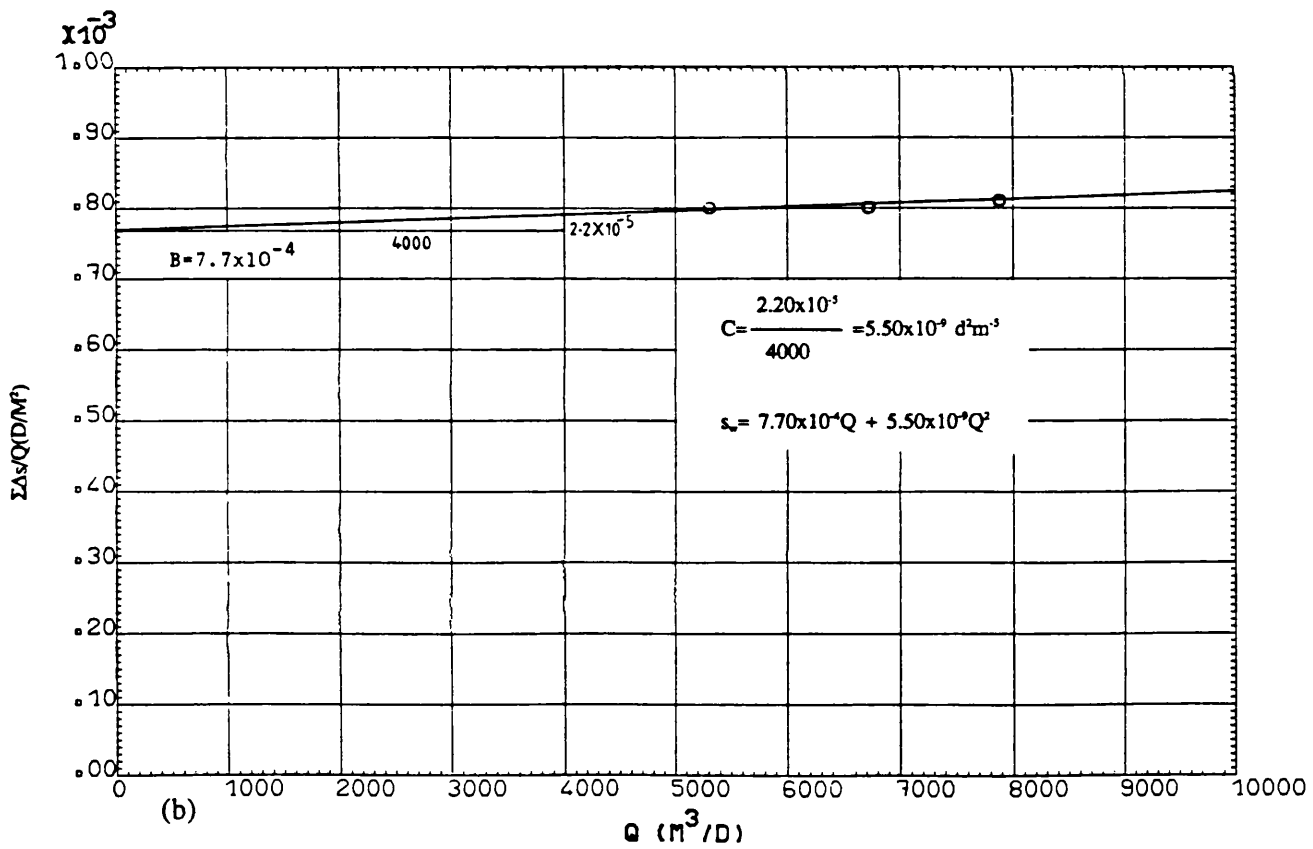
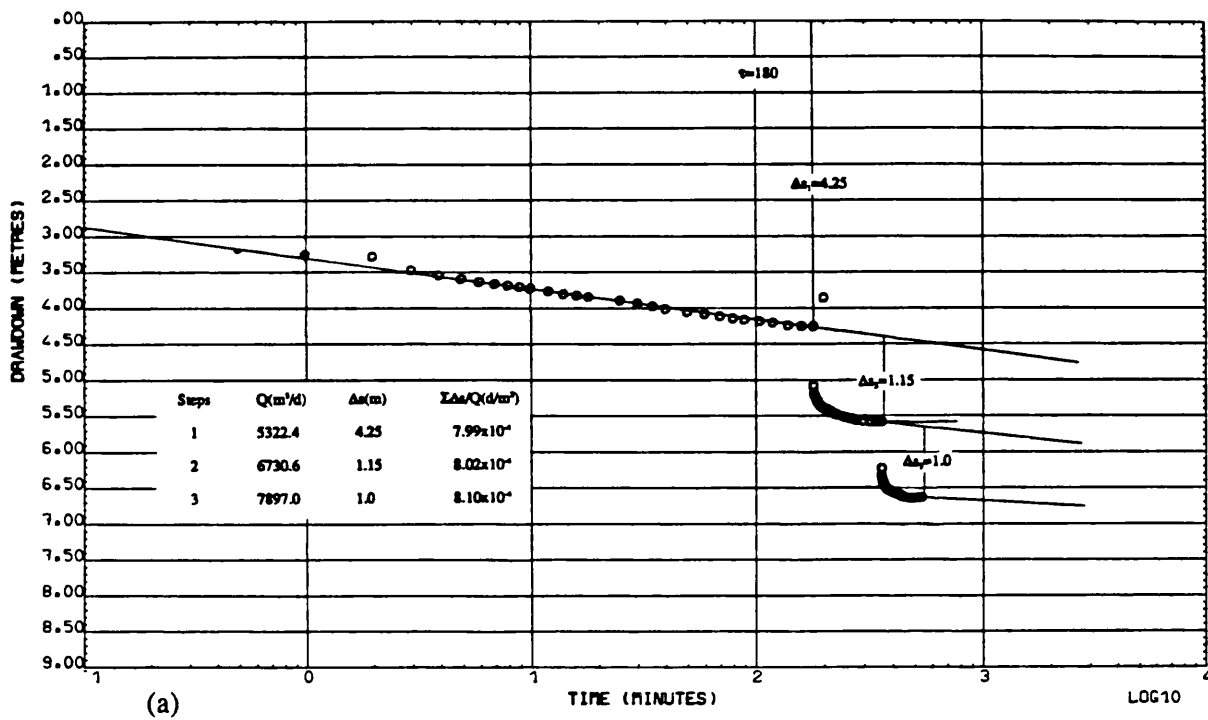


Fig. A6.10 PW TPSW4, Step-Drawdown test: Bruin & Hudson method, (a) data handling,

(b) data plot.

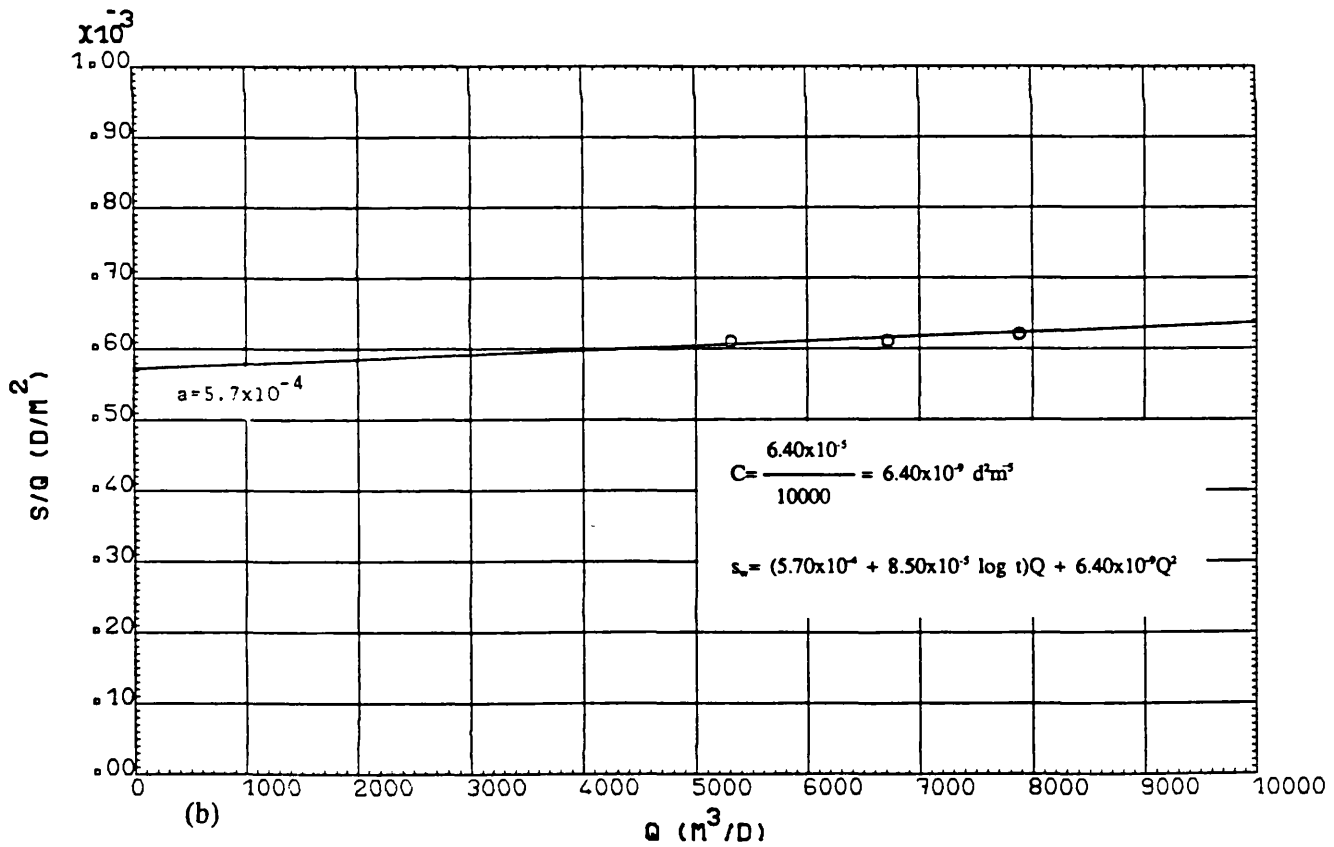
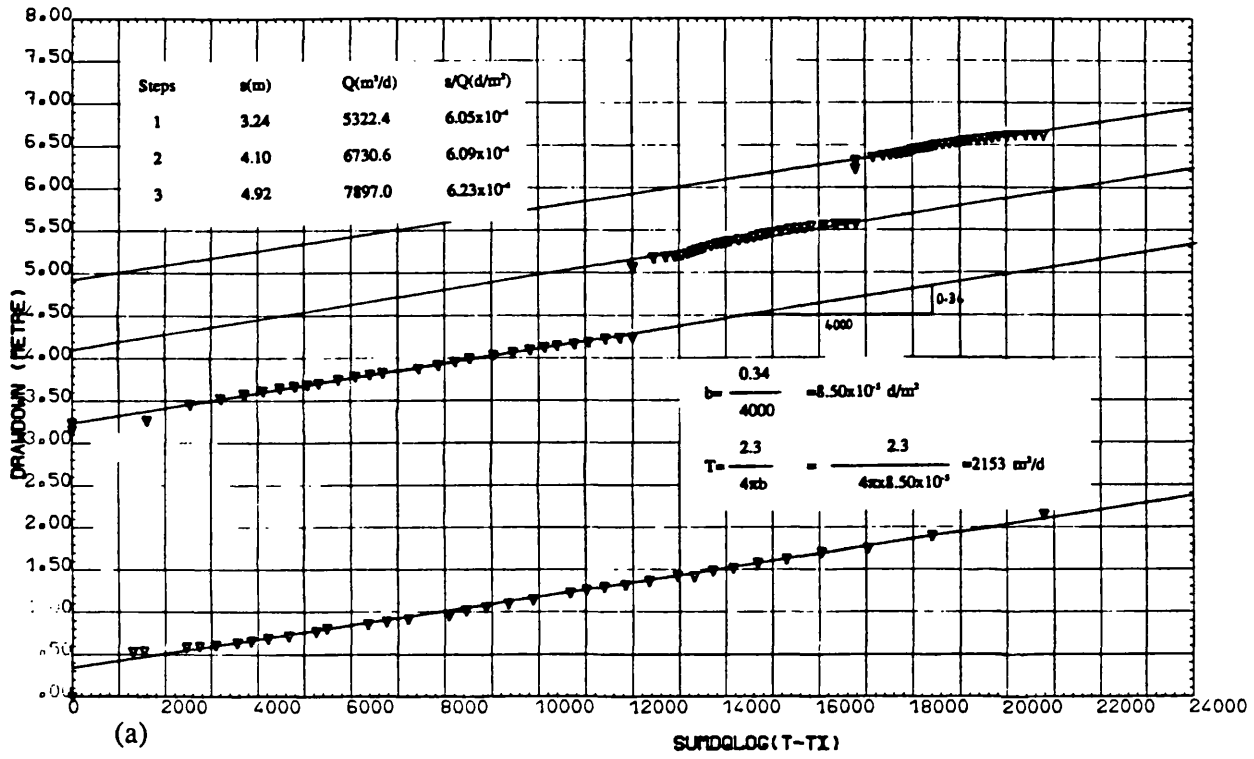


Fig. A6.11 PW TPSW4, Step-Drawdown test: Eden & Hazel method, (a) data handling, (b) data plot.



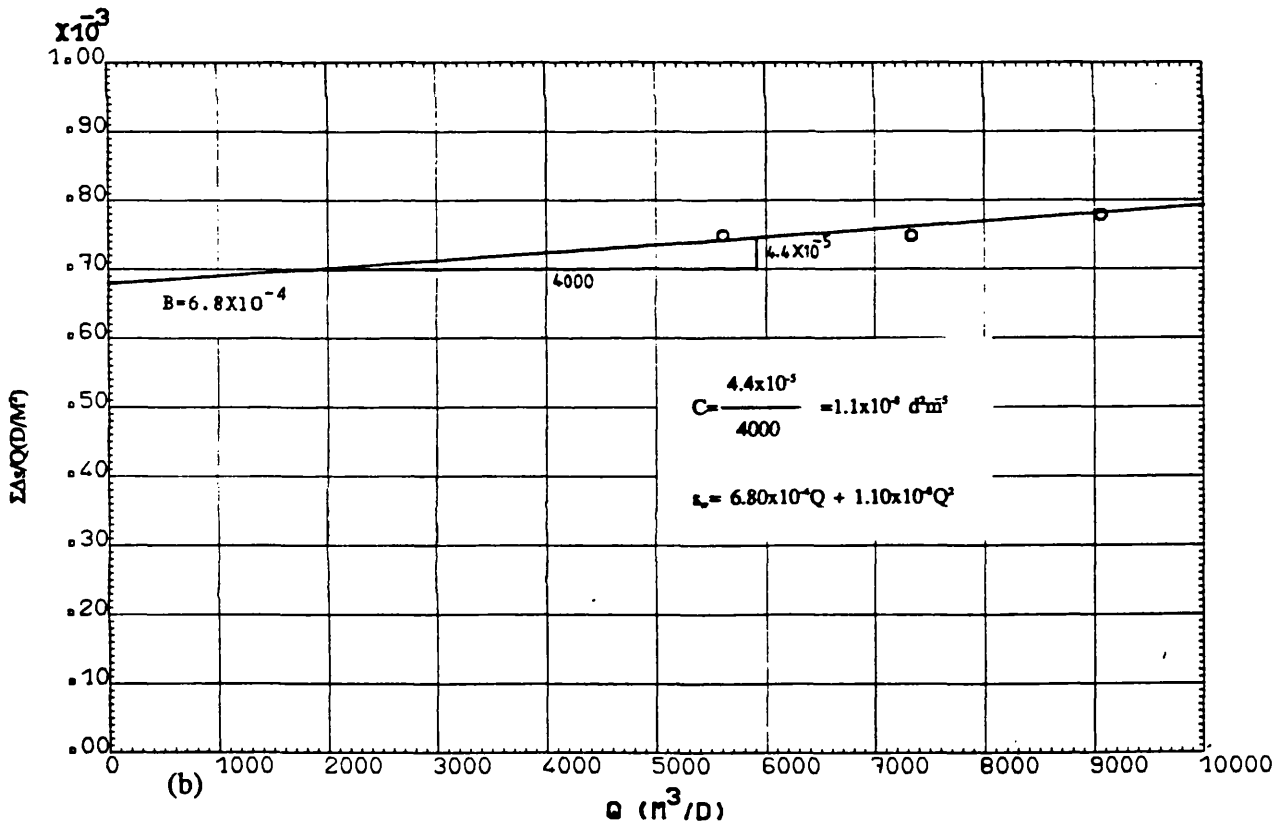
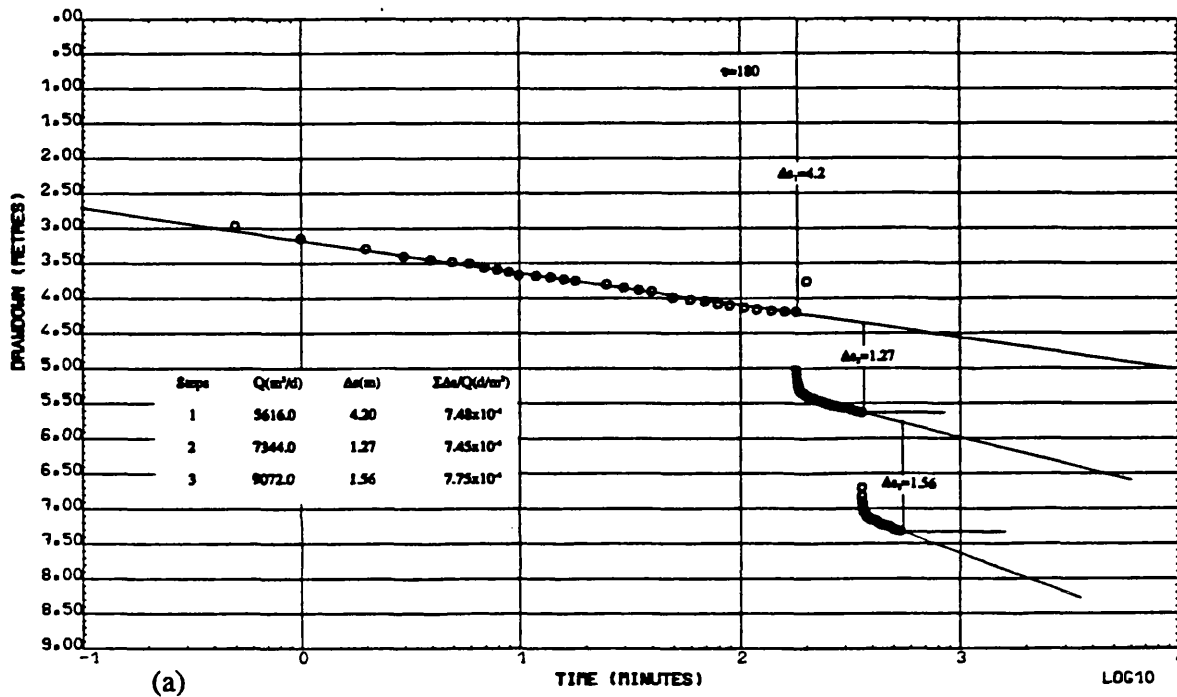


Fig. A6.12 PW TPSW8, Step-Drawdown test: Bruin & Hudson method, (a) data handling, (b) data plot.

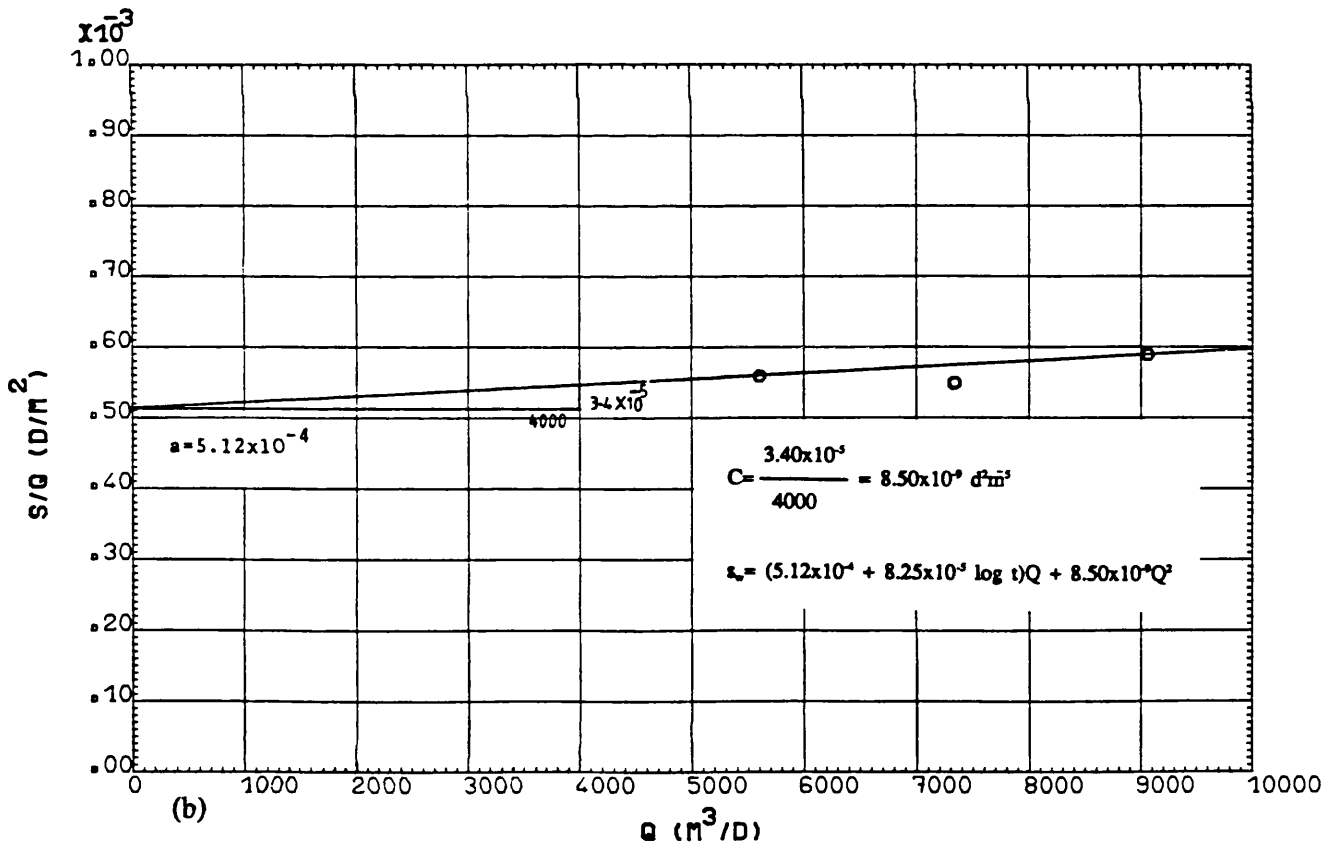
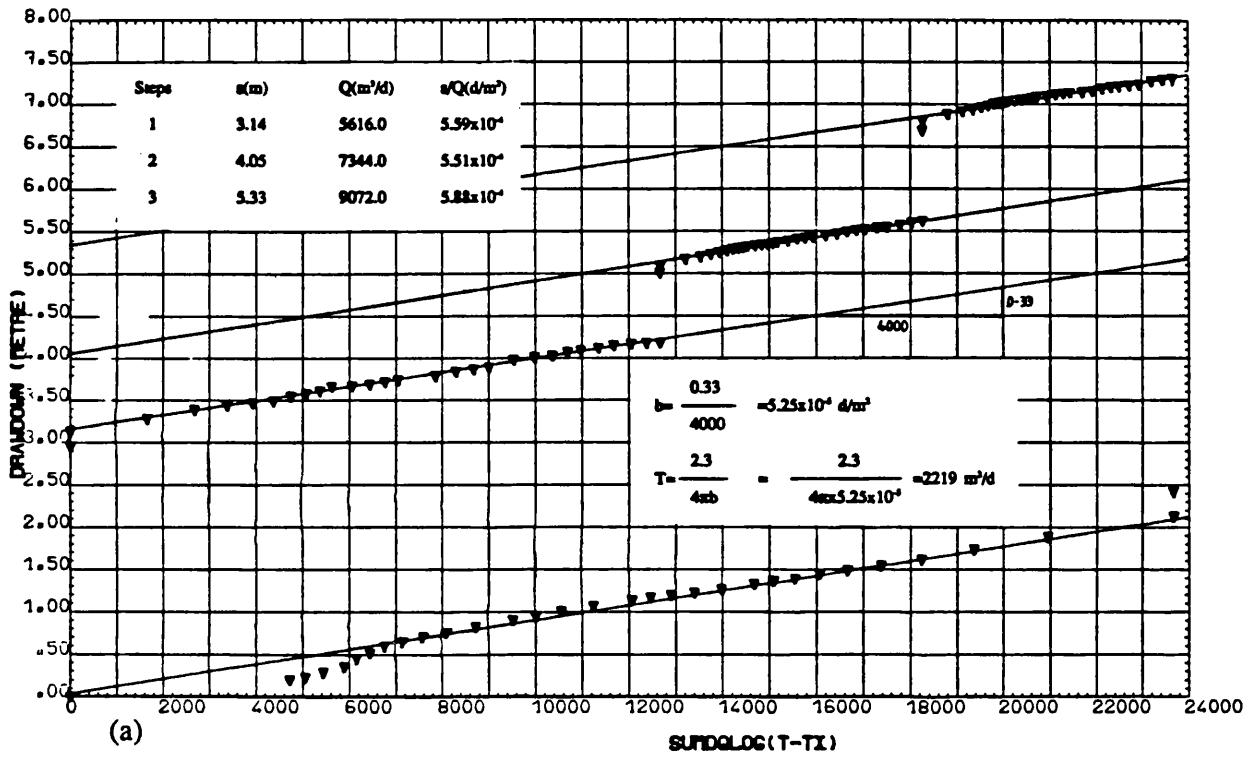


Fig. A6.13 PW TPSW8, Step-Drawdown test: Eden & Hazel method, (a) data handling, (b) data plot.

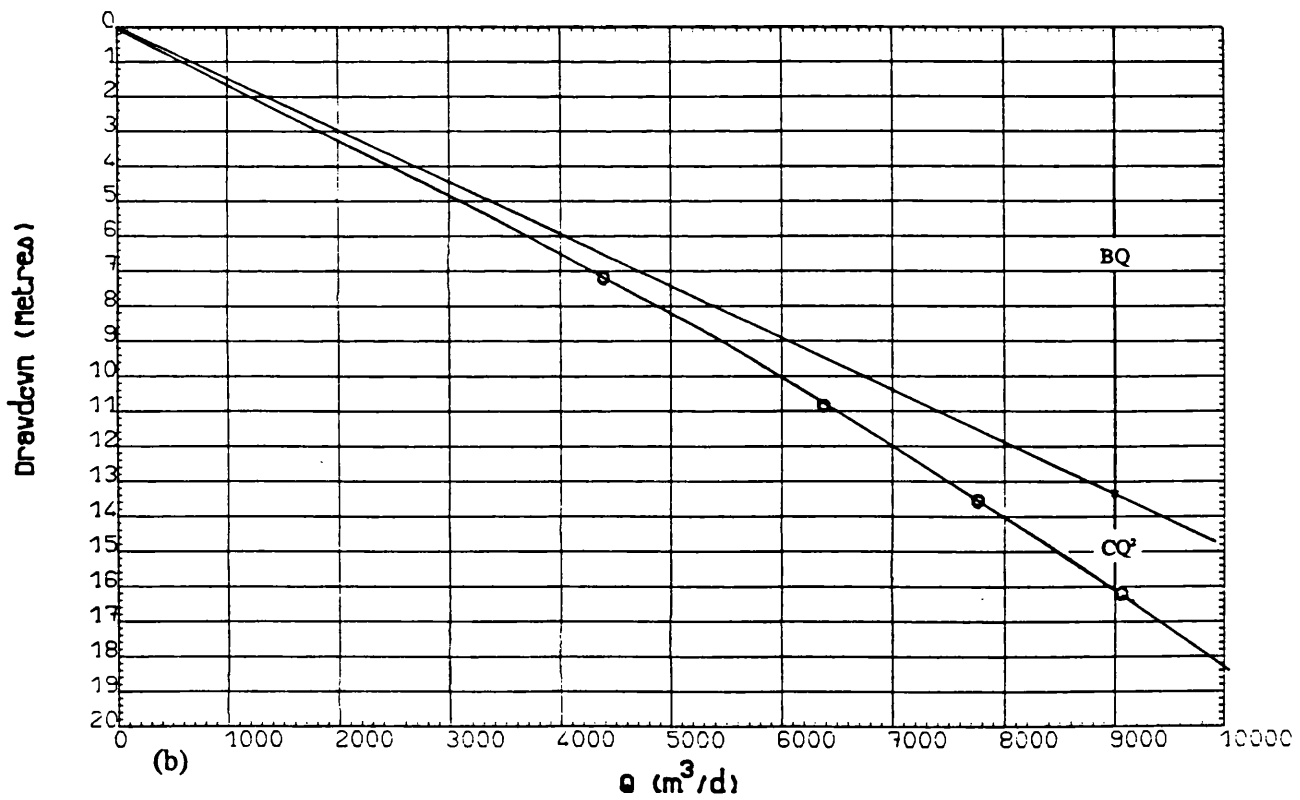
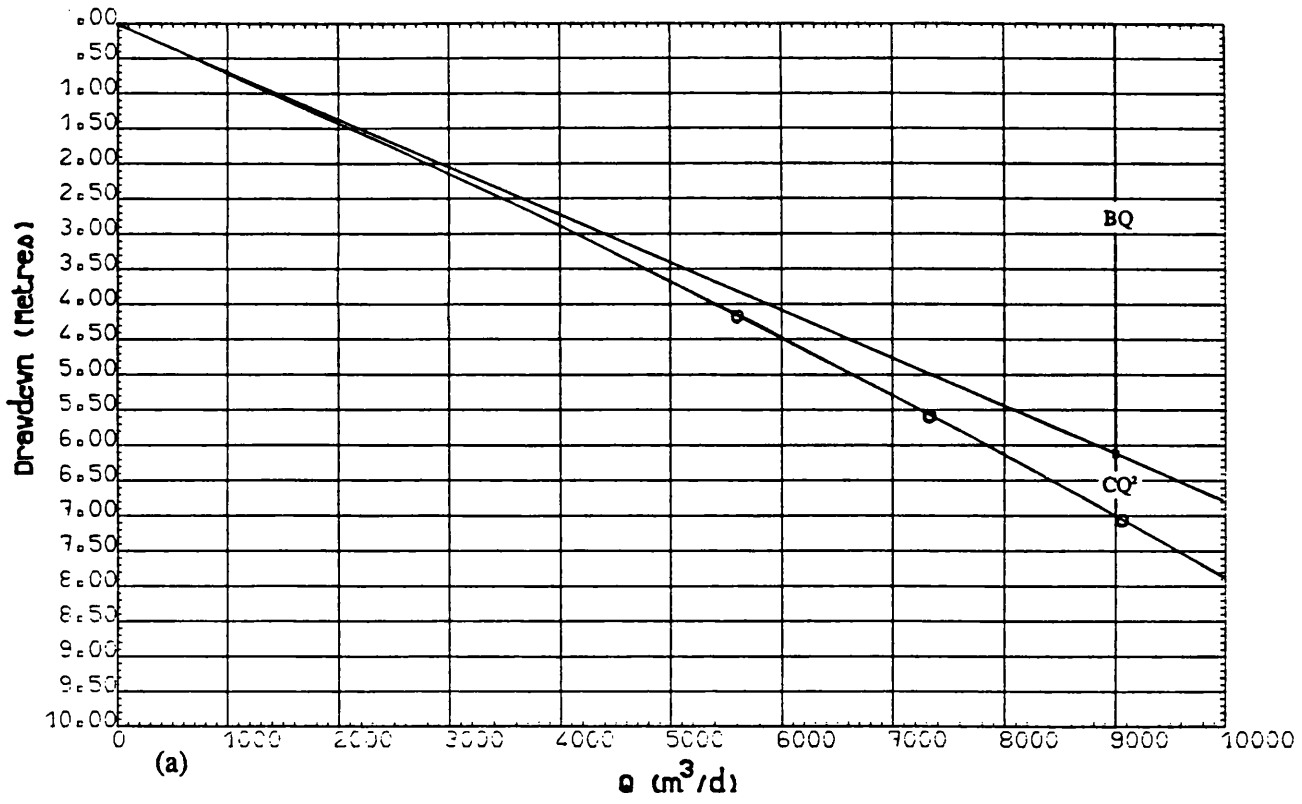


Fig. A6.14 Step-Drawdown test: Theoretical drawdown - yield curve, (a) PW TPSW8,  
(b) PW PTW1.

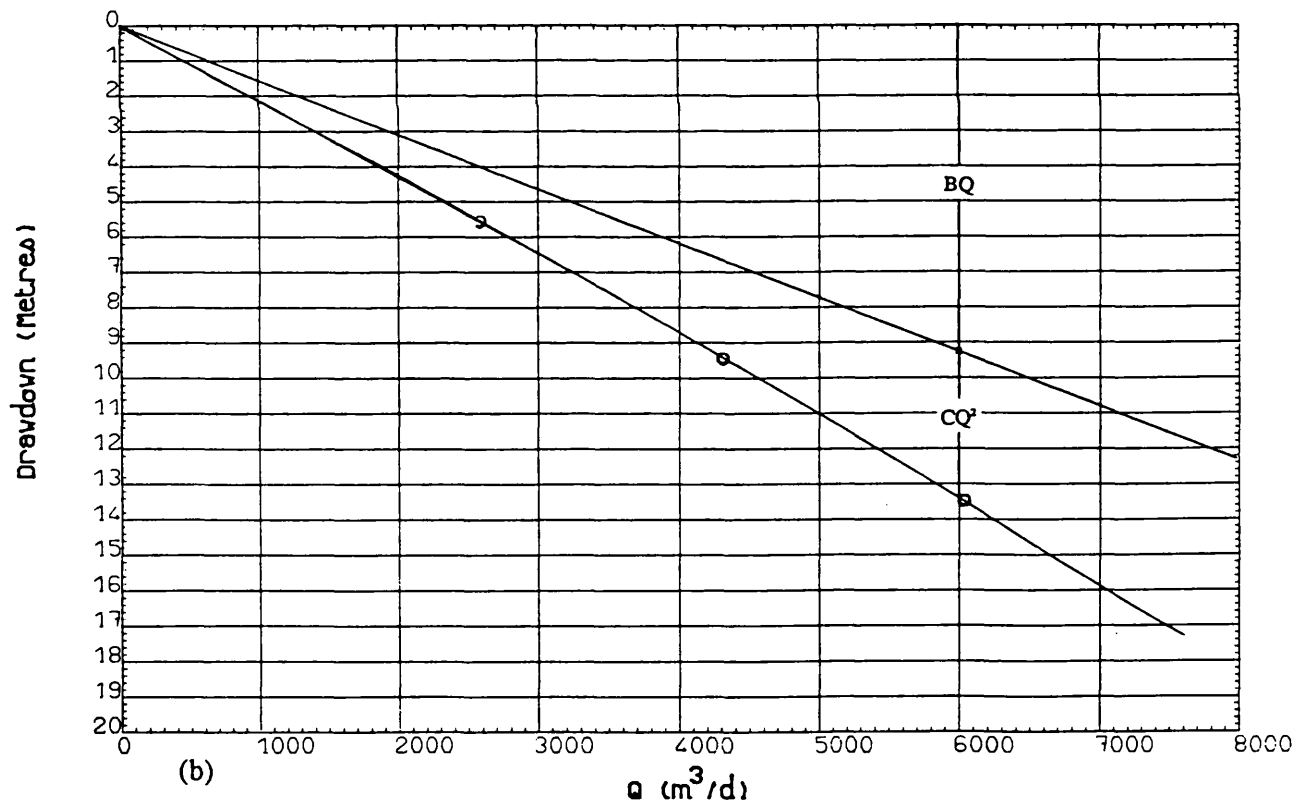
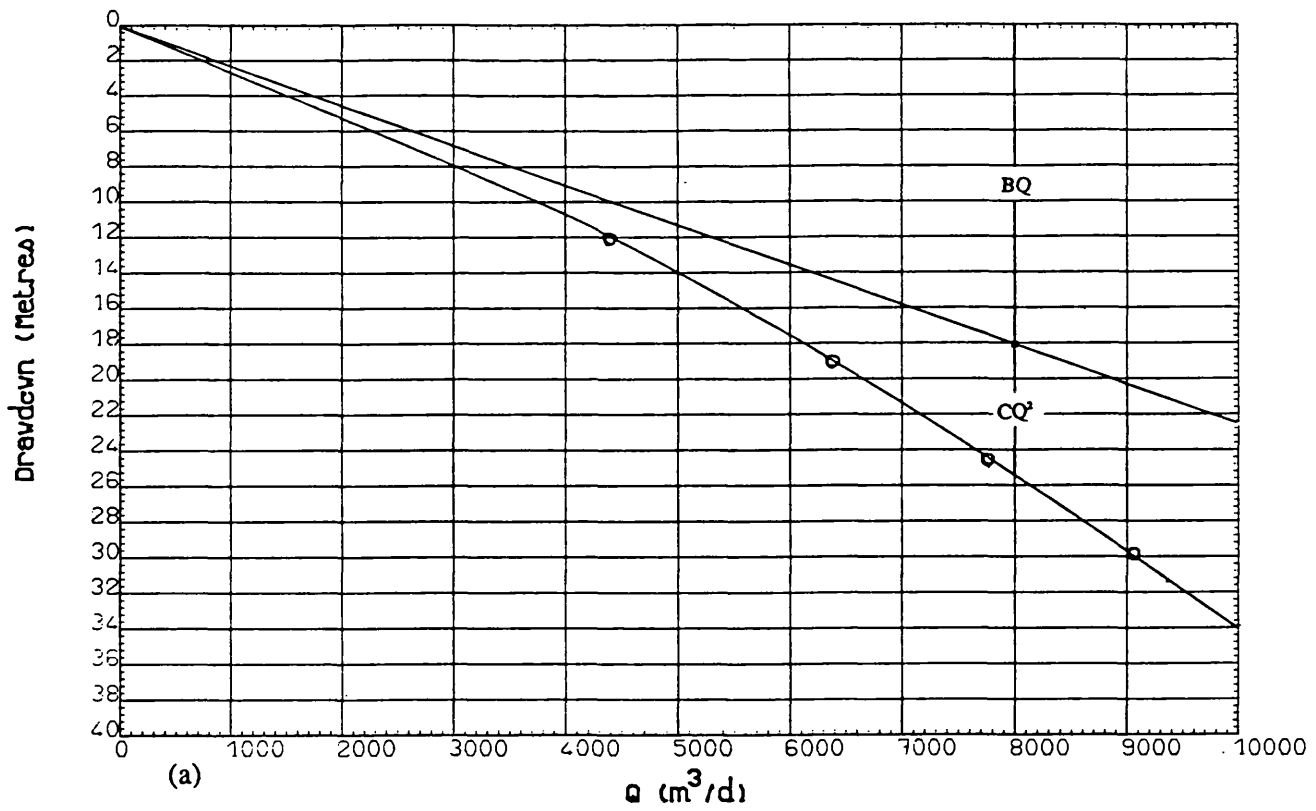


Fig. A6.15 Step-Drawdown test: Theoretical drawdown - yield curve, (a) PW PTW2,  
(b) PW PTW3.

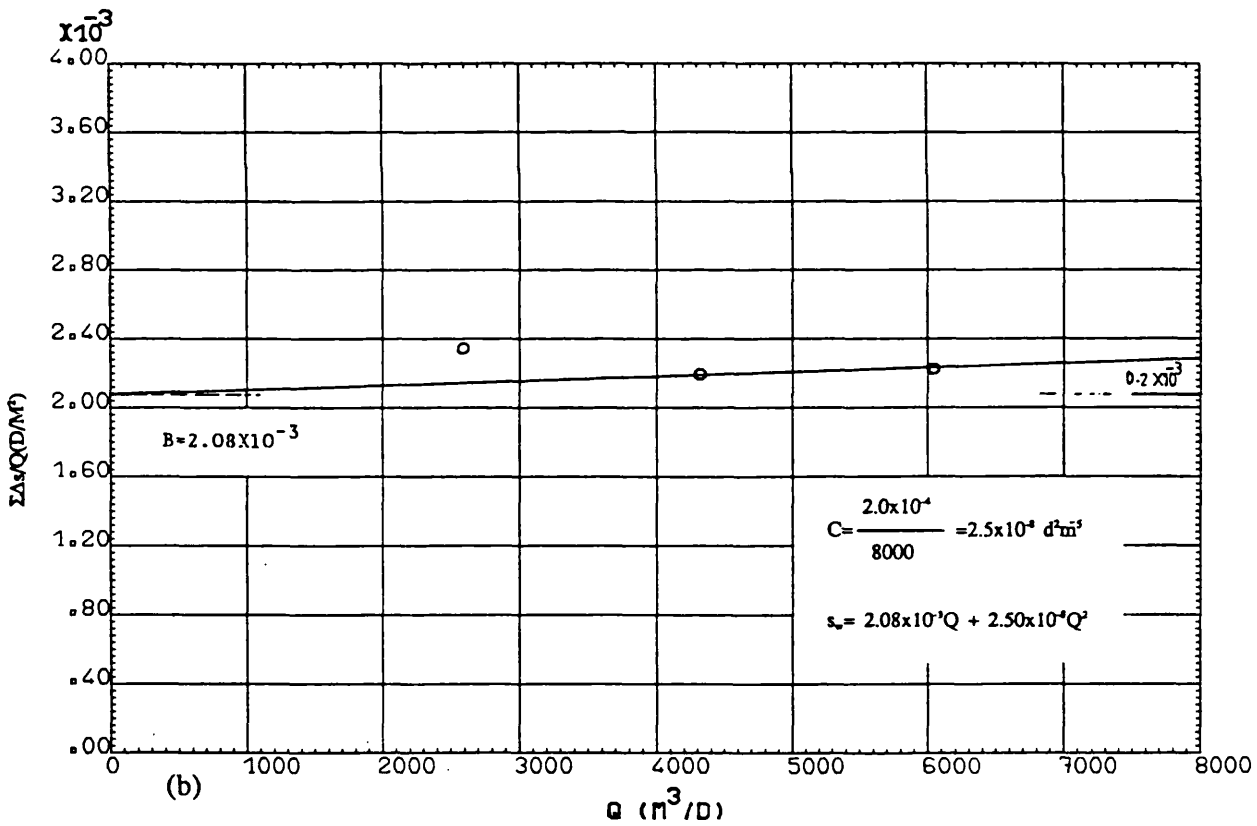
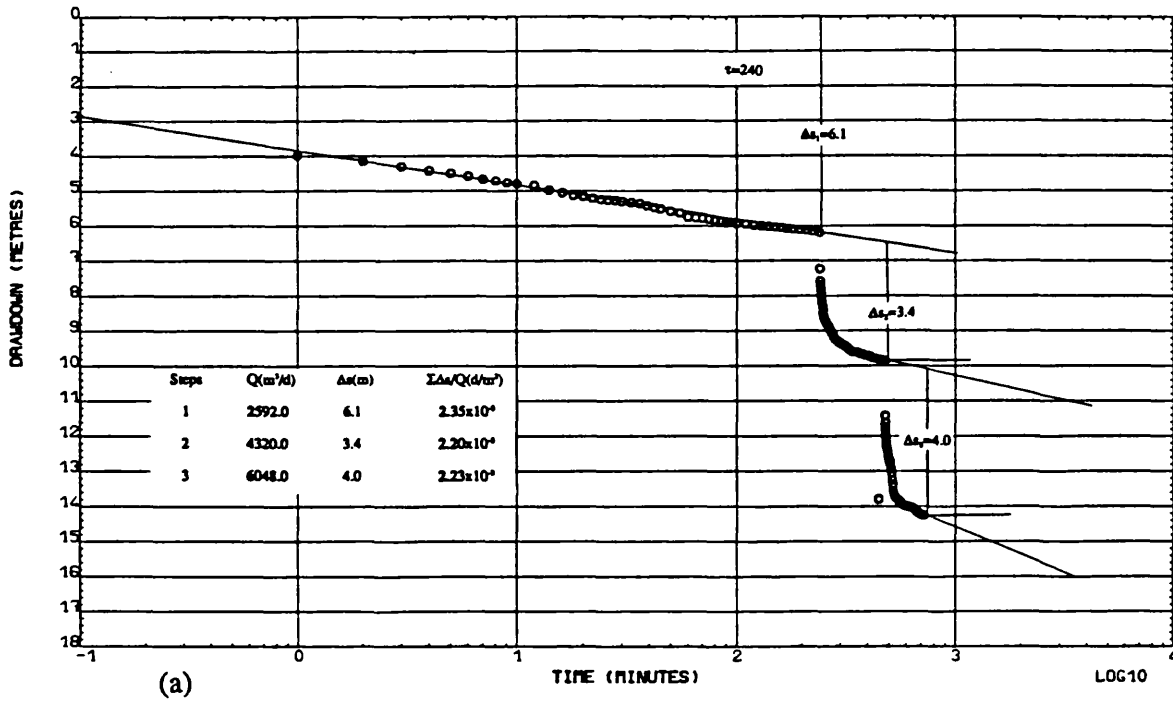


Fig. A6.16 PW PTW3, Step-Drawdown test: Bruin & Hudson method, (a) data handling, (b) data plot.

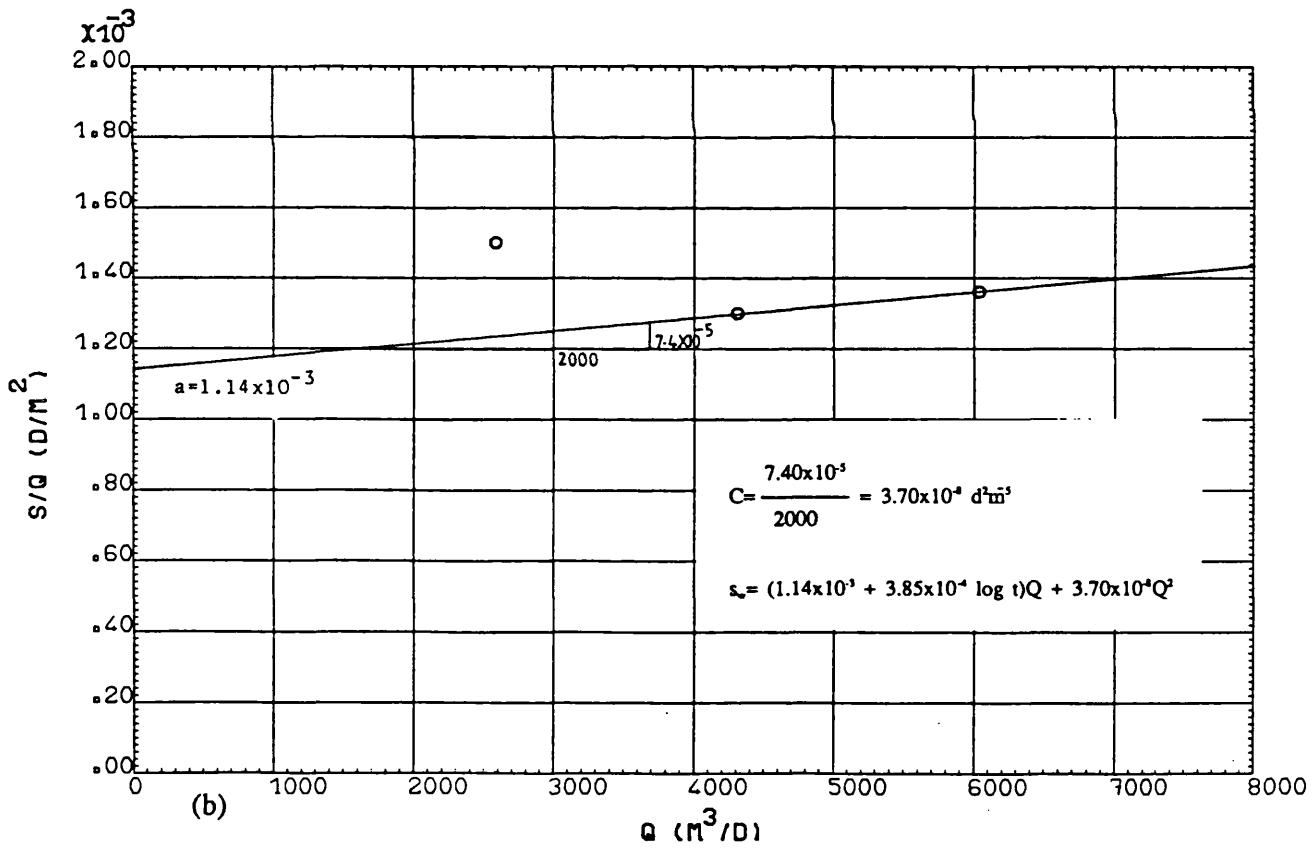
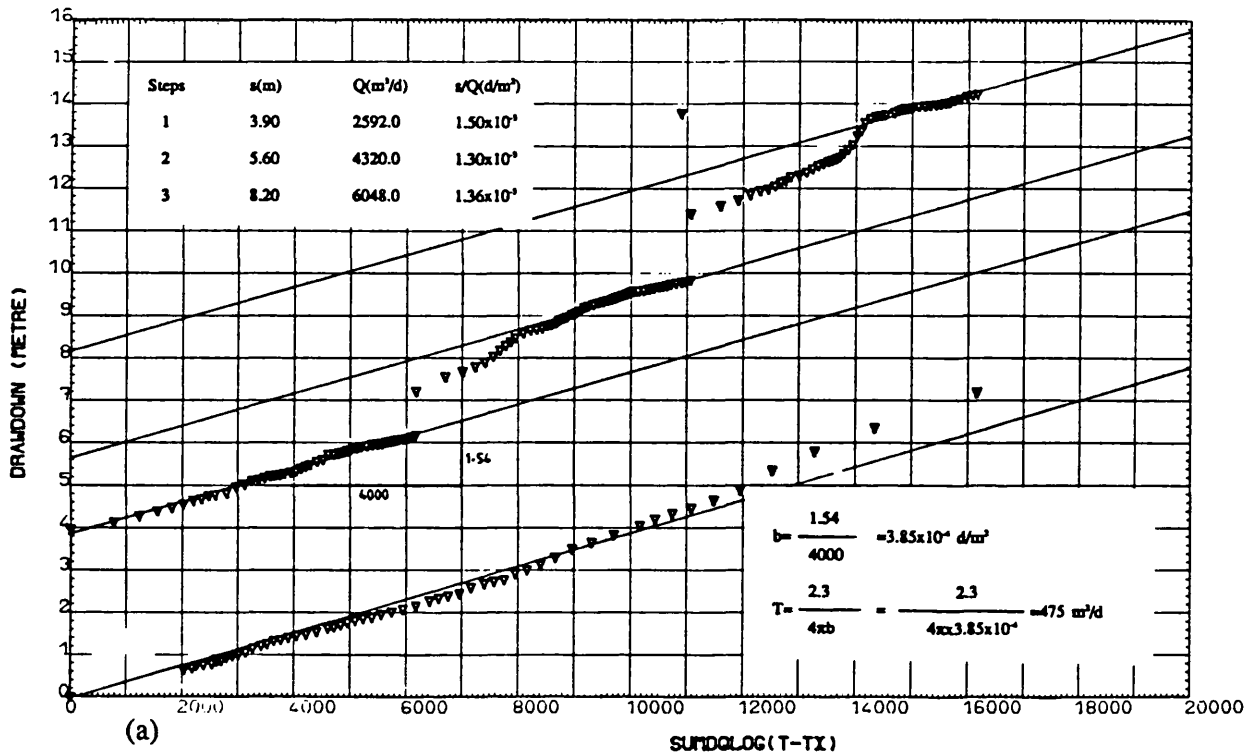


Fig. A6.17 PW PTW3, Step-Drawdown test: Eden & Hazel method, (a) data handling, (b) data plot.

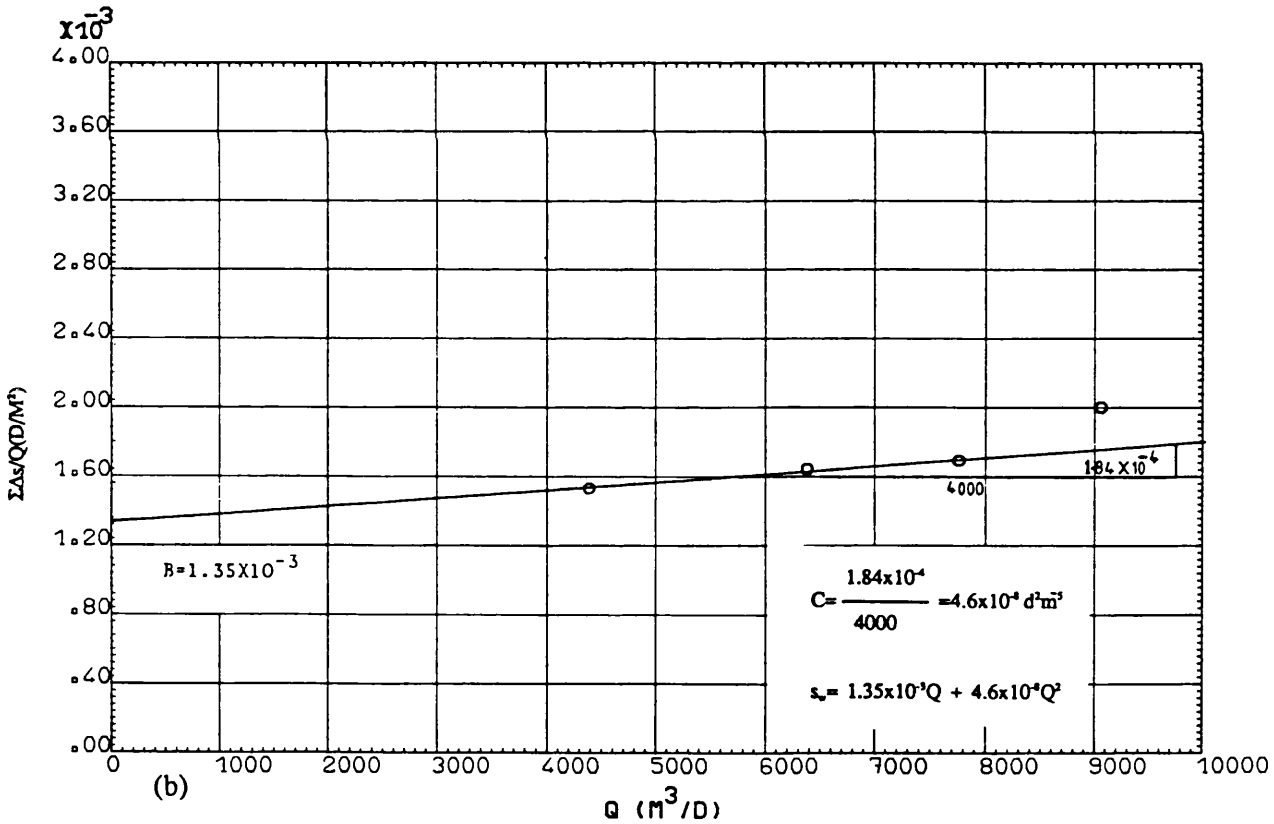
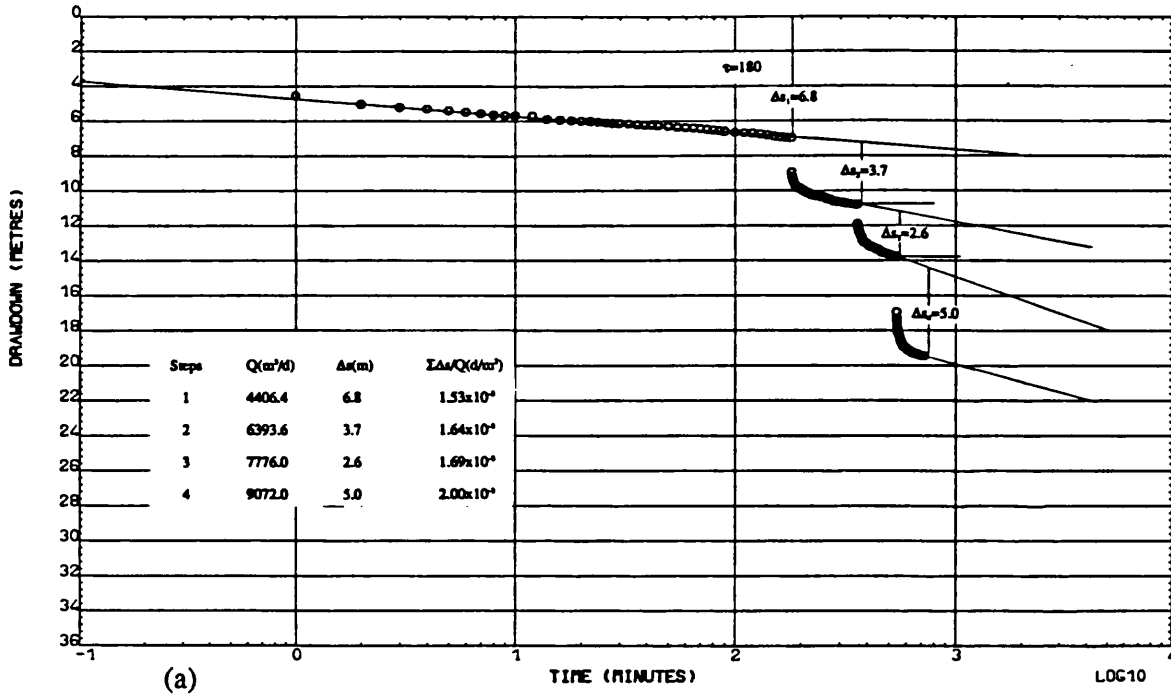


Fig. A6.18 PW PTW4, Step-Drawdown test: Bruin & Hudson method, (a) data handling, (b) data plot.

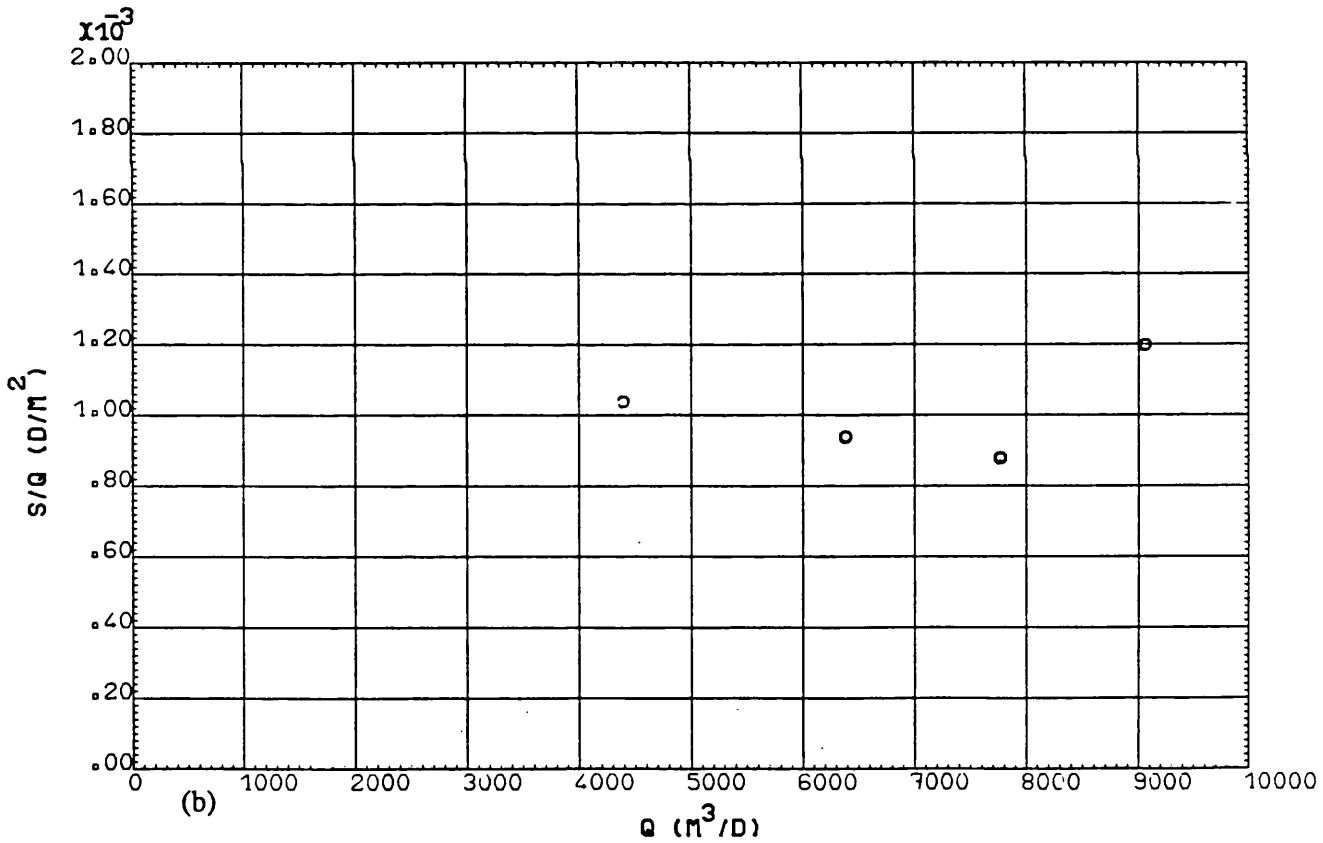
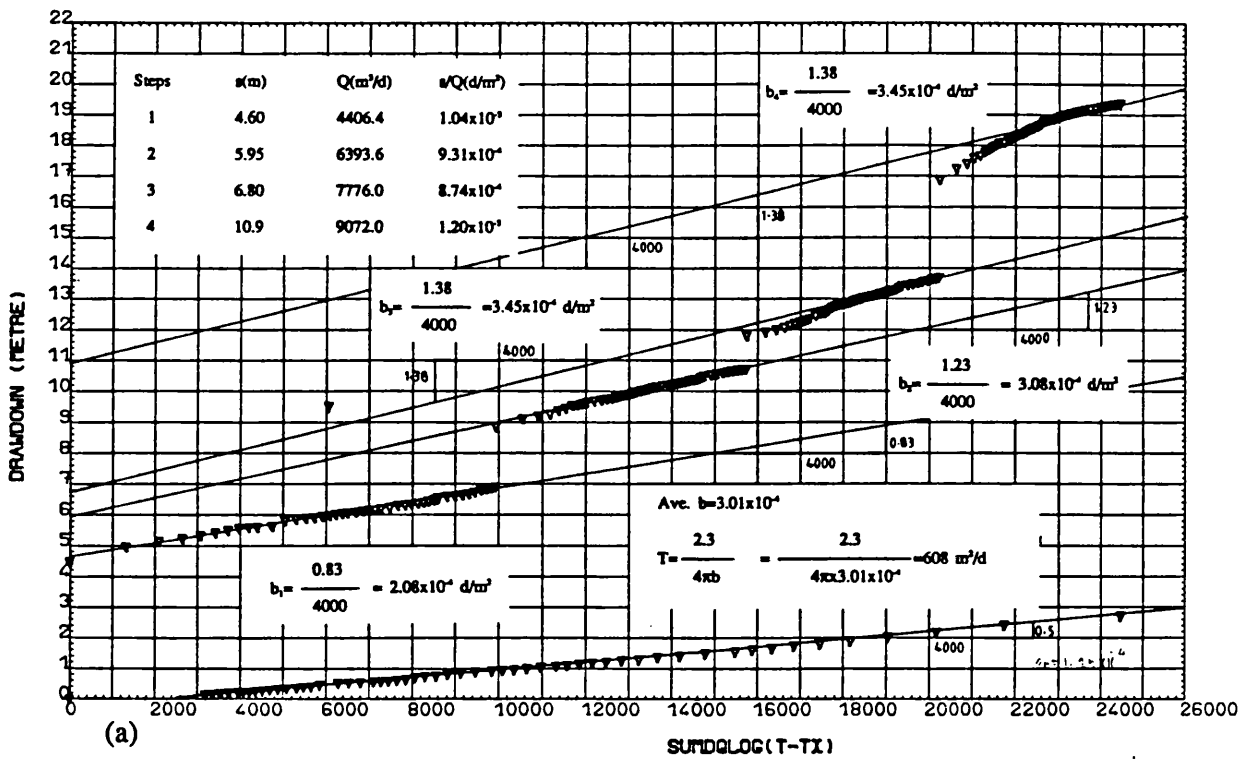


Fig. A6.19 PW PTW4, Step-Drawdown test: Eden & Hazel method, (a) data handling, (b) data plot.



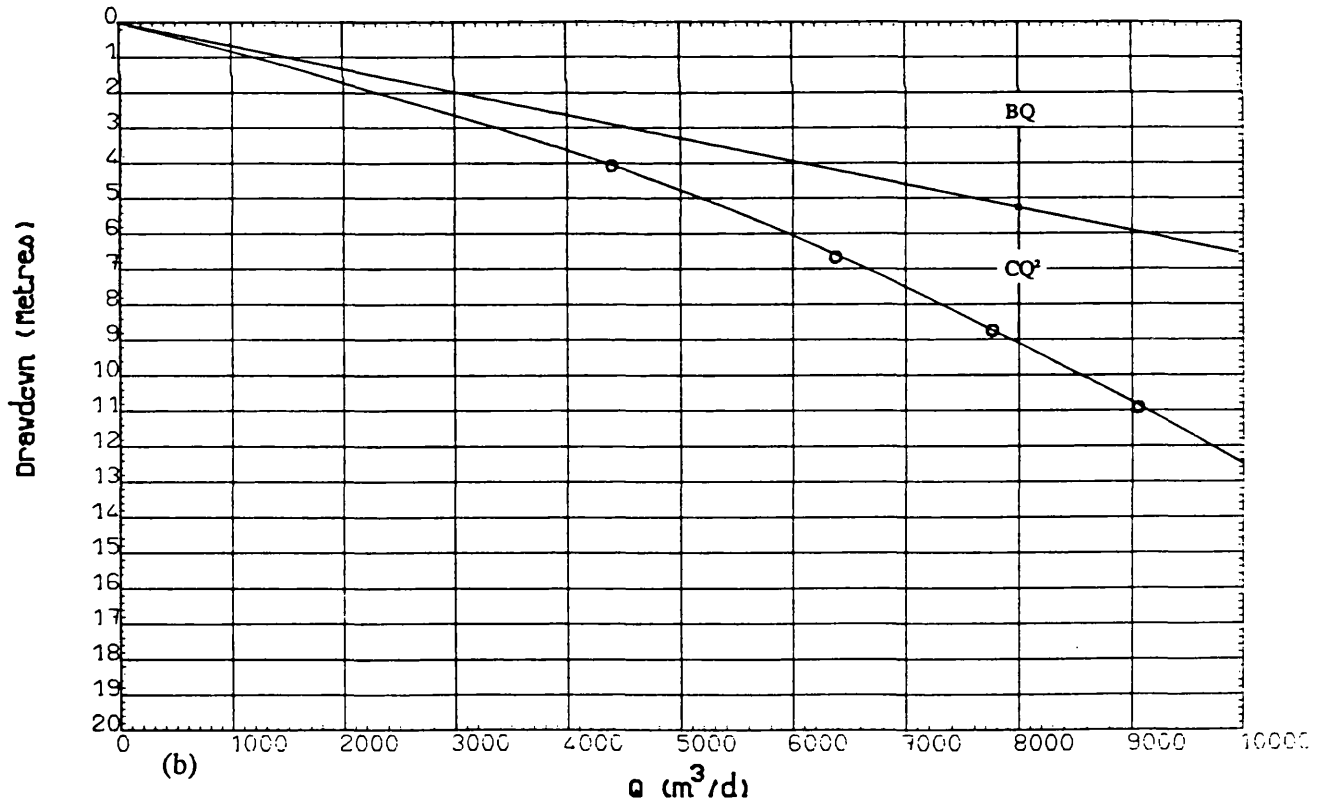
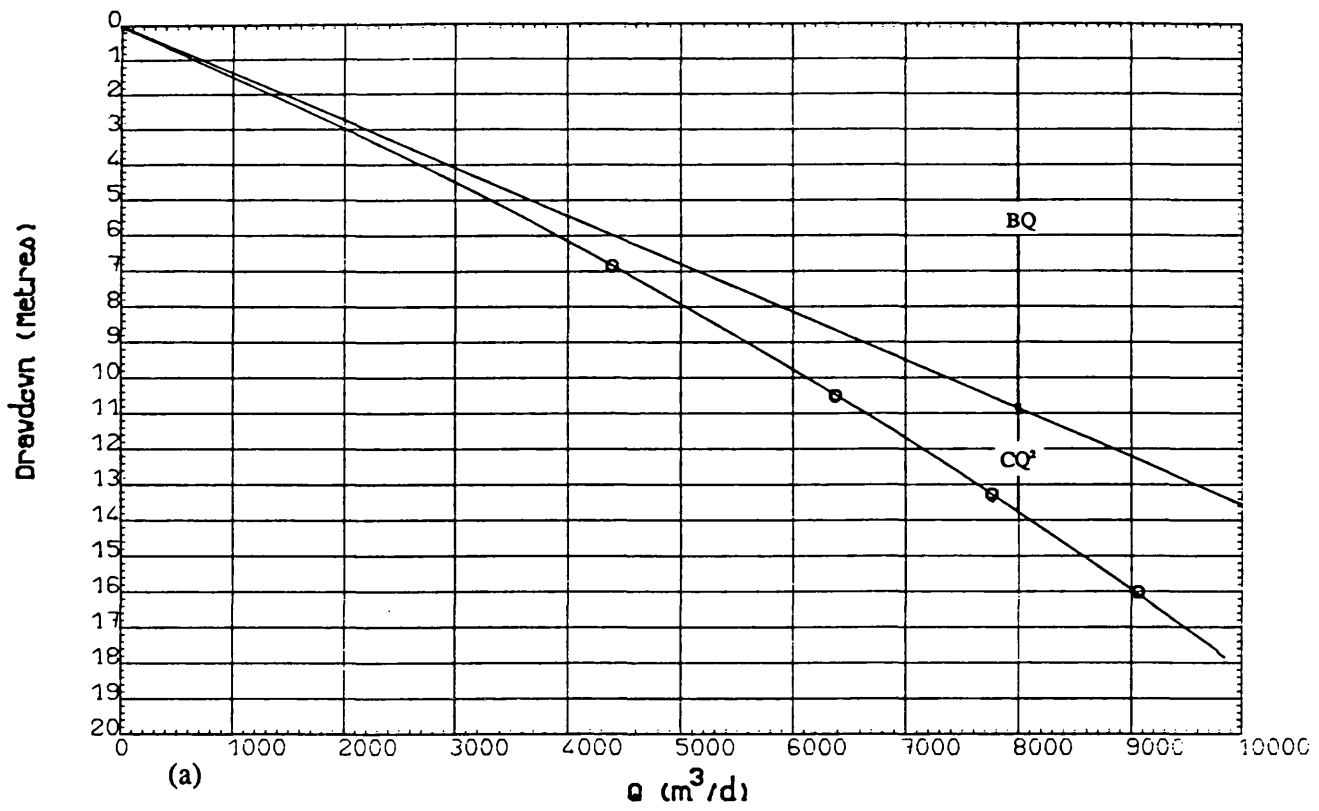
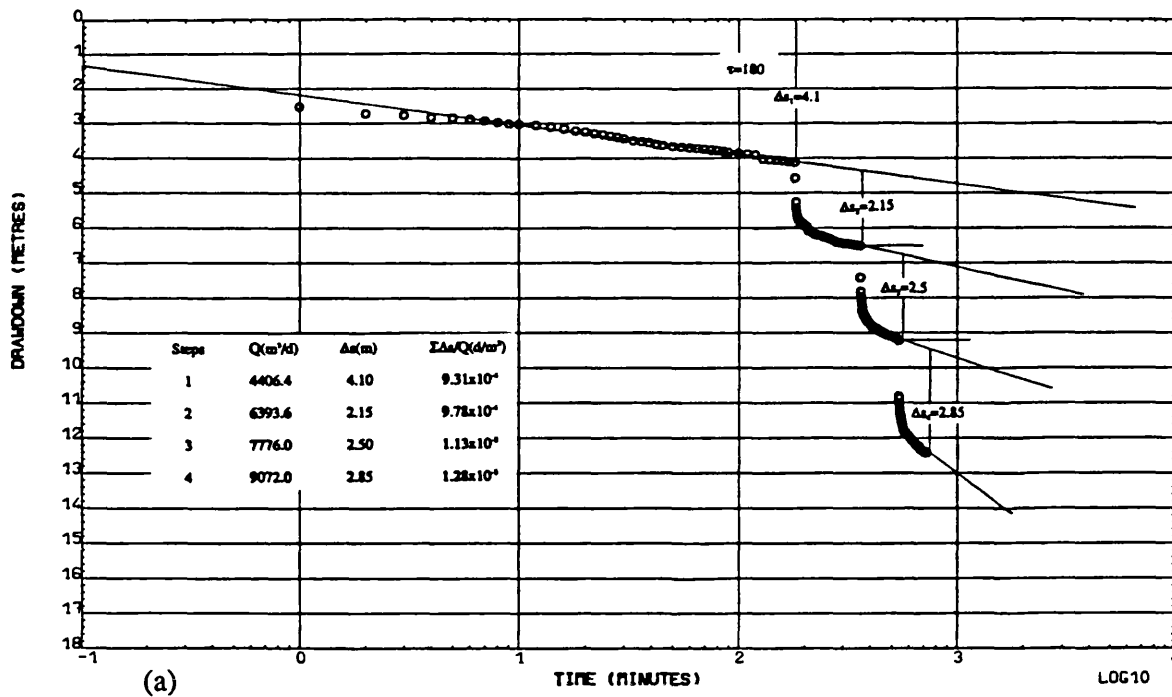
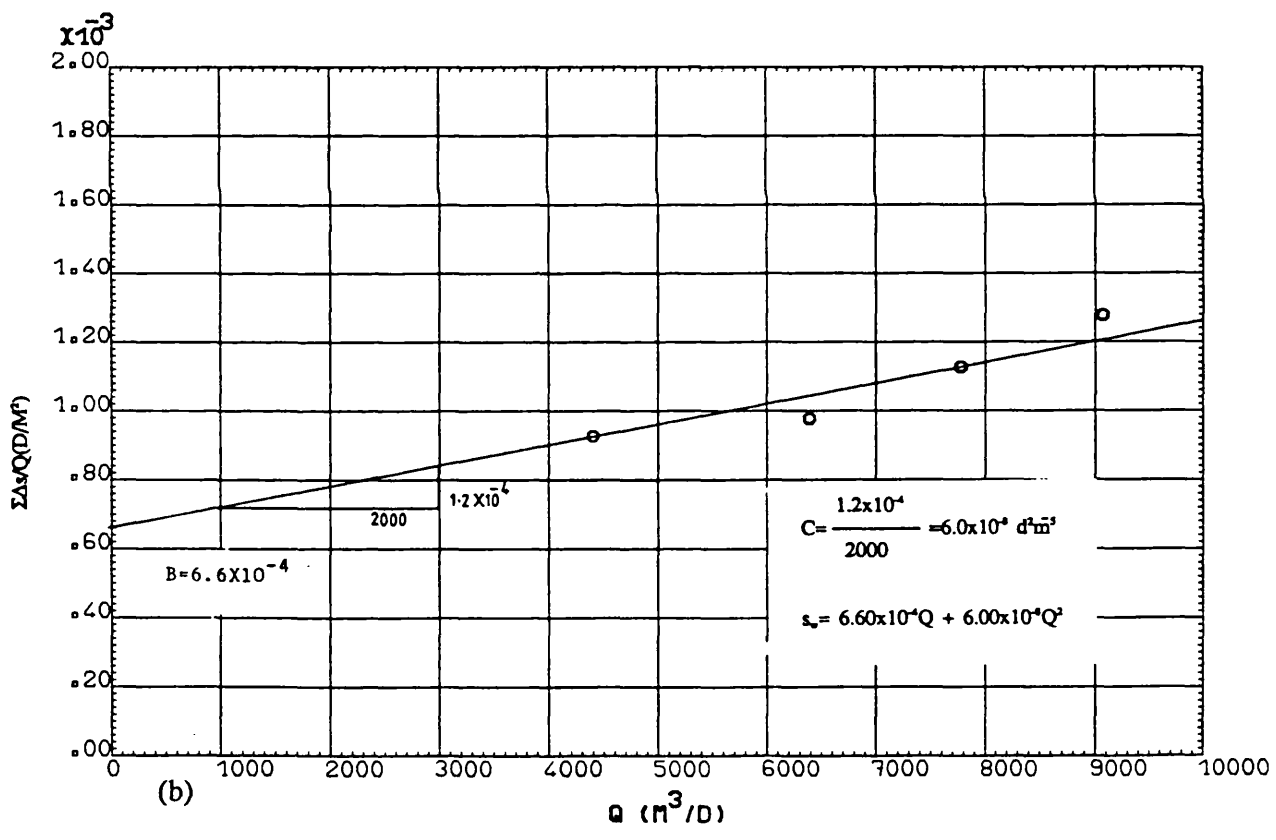


Fig. A6.20 Step-Drawdown test: Theoretical drawdown - yield curve, (a) PW PTW4, (b) PW PTW5.



(a)



(b)

Fig. A6.21 PW PTW5, Step-Drawdown test: Bruin & Hudson method, (a) data handling, (b) data plot.

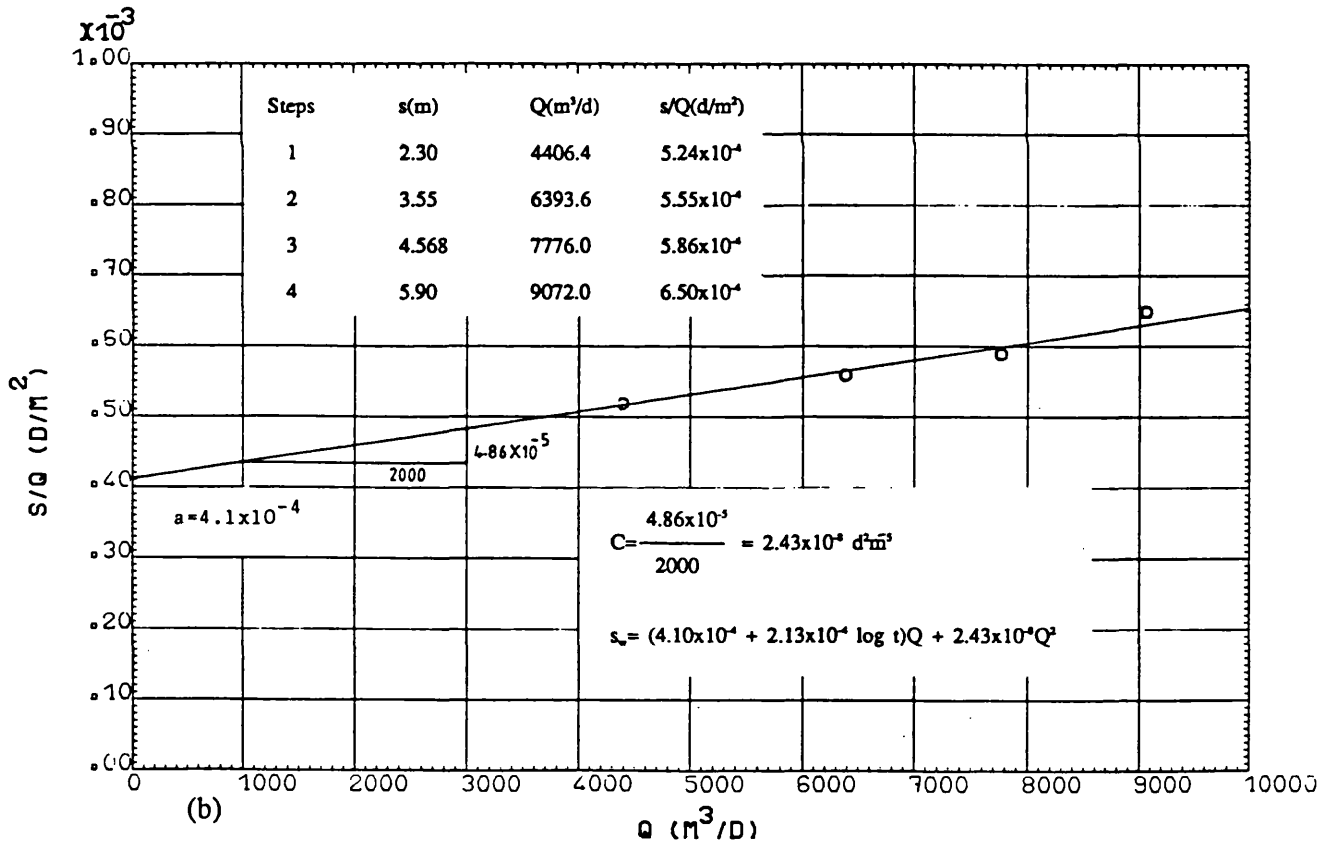
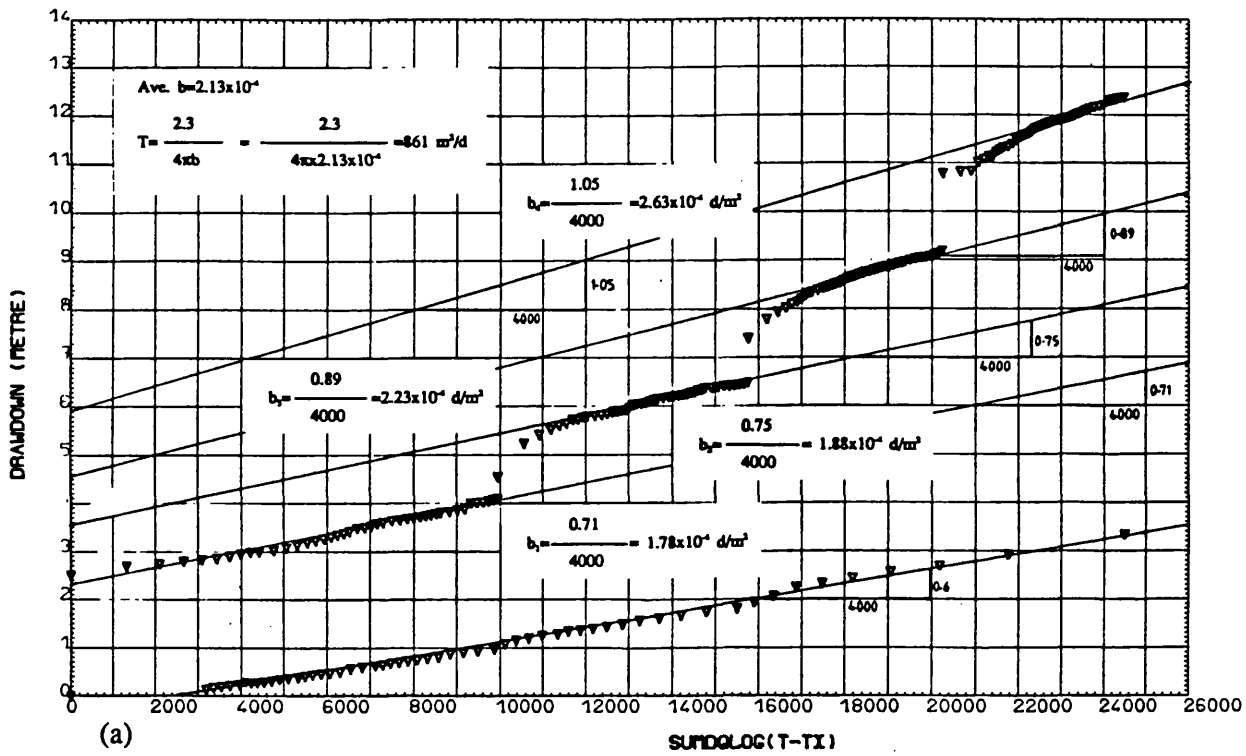


Fig. A6.22 PW PTW5, Step-Drawdown test: Eden & Hazel method, (a) data handling, (b) data plot.

**Appendix 7 Results of Chemical Analyses for Ground Water in  
the Area (Oct. 1987).**

**Appendix 7: Results of chemical analyses for ground water in the area (Oct. 1987).**

Hydrochemical data of the Tabriz Plain (October 1987)

Samp. No.	Samp. Grid Ref.	Ca	Mg	Na	HCO <sub>3</sub>	SO <sub>4</sub>	Cl	pH	EC µS/cm	TDS mg/l	% Error	RSC meq/l	SAR meq/l	Hard. CaCO <sub>3</sub>	Chemical Formula (Kurtlov formula)
6	40L-40D	46.1 2.30 31.7	41.33 3.40 46.8	35.9 1.56 21.5	268.5 4.403 60.3	105.7 2.20 30.1	24.8 0.70 9.60	6.8	730	490	0.29	-	0.92	285	HCO <sub>3</sub> , SO <sub>4</sub> , Cl Mg Ca Na 490-----6.8
10	39K-9D	90.2 4.50 43.3	42.54 3.50 33.6	55.2 2.40 23.1	213.6 3.53 34.0	225.7 4.70 45.6	74.5 2.10 20.4	7.6	1025	680	0.49	-	1.20	400	SO <sub>4</sub> , HCO <sub>3</sub> , Cl Ca Mg Na 680-----7.6
11	39K-6S	100.2 5.00 40.0	54.69 4.50 36.0	69.0 3.00 24.0	274.6 4.50 36.3	259.4 5.40 43.5	88.6 2.50 20.2	7.8	1240	820	0.40	-	1.37	475	SO <sub>4</sub> , HCO <sub>3</sub> , Cl Ca Mg Na 820-----7.8
12	38K-7D	160.3 8.00 25.0	194.5 16.0 50.0	183.9 8.000 25.0	451.6 7.41 23.4	879.0 18.28 57.7	212.7 6.00 18.9	7.2	3000	2040	0.47	-	2.31	1200	SO <sub>4</sub> , HCO <sub>3</sub> , Cl Mg Ca/Na 3000-----7.2
13	36K-26S	144.3 7.20 30.9	62.00 5.10 21.9	253.0 11.01 47.2	213.6 3.50 15.1	754.1 15.69 67.6	141.8 4.00 17.2	7.8	2290	1550	0.25	-	4.44	650	SO <sub>4</sub> , Cl HCO <sub>3</sub> Na Ca Mg 1550-----7.8
14	39J-1S	82.2 4.10 12.4	229.7 18.89 56.9	234.5 10.20 30.7	1281.4 21.01 63.1	350.6 7.29 21.9	177.3 5.00 15.0	7.3	3300	2210	0.18	-	3.01	1150	HCO <sub>3</sub> , SO <sub>4</sub> , Cl Mg Na Ca 2210-----7.3
15	37J-27D	200.4 10.0 45.1	87.52 7.20 32.4	115.0 5.00 22.5	427.1 7.004 31.8	480.3 10.00 45.4	177.3 5.00 22.7	6.8	2190	1470	0.46	-	1.70	860	SO <sub>4</sub> , HCO <sub>3</sub> , Cl Ca Mg Na 1470-----6.8
32	32Q-9Q	84.2 4.20 35.9	24.31 2.00 17.1	126.5 5.50 47.0	183.1 3.00 25.5	269.0 5.60 47.4	113.4 3.20 27.1	6.9	1160	780	0.40	-	3.12	310	SO <sub>4</sub> , Cl HCO <sub>3</sub> Na Ca Mg 780-----6.9

Ion concentration: line 1 in mg/l; line 2 in ppm; line 3 in % epm

In the sample grid references, the final letters S, D and Q refer to shallow, deep wells and qanat respectively

Hydrochemical data of the Tabriz Plain (continued)

33	32Q-15Q	128.3 6.40 38.1	41.33 3.40 20.2	160.9 7.00 41.7	262.4 4.30 25.6	313.6 6.52 38.8	212.7 6.00 35.7	7.3	1670	1100	0.07	-	3.16	490	1100	SO <sub>4</sub> , Cl, HCO <sub>3</sub> Na Ca Mg	7.3
35	32R-19Q	64.1 3.200 47.8	18.23 1.50 22.4	46.0 2.00 29.9	262.4 4.30 71.4	44.2 1.00 15.3	28.4 0.80 13.3	8.0	680	450	5.30	-	1.30	235	450	HCO <sub>3</sub> , SO <sub>4</sub> , Cl Ca Na Mg	8.0
36	32S-1Q	220.4 11.00 33.7	48.62 4.00 12.3	404.6 17.60 54.0	549.2 9.01 27.7	528.3 11.00 33.8	443.1 12.50 38.5	7.0	3200	2110	0.16	-	6.43	750	2110	Cl, SO <sub>4</sub> , HCO <sub>3</sub> Na Ca Mg	7.0
37	34N-4D	44.1 2.20 46.8	12.16 1.00 21.3	34.5 1.50 31.9	170.9 2.80 59.4	63.4 1.32 27.9	21.3 0.60 12.7	7.7	470	310	0.03	-	1.19	160	310	HCO <sub>3</sub> , SO <sub>4</sub> , Cl Ca Na Mg	7.7
38	33N-8D	56.1 2.80 40.0	14.57 1.20 17.1	69.0 3.00 42.9	213.6 3.50 49.7	127.3 2.65 37.6	31.9 0.90 12.8	7.9	710	470	0.36	-	1.60	353	470	HCO <sub>3</sub> , SO <sub>4</sub> , Cl Na Ca Mg	7.9
40	30N-6D	66.1 3.30 6.8	97.24 8.00 16.6	850.6 37.00 76.6	207.5 3.40 7.1	465.9 9.69 20.2	1240.8 35.00 72.8	8.0	4800	3160	0.22	-	15.57	565	3160	Cl, SO <sub>4</sub> , HCO <sub>3</sub> Na Mg Ca	8.0
41	33M-17D	164.3 8.20 46.0	34.03 2.80 15.7	157.3 6.84 38.4	390.5 6.40 35.8	302.6 6.29 35.2	184.3 5.200 29.0	7.0	1800	1200	0.16	-	2.92	550	1200	HCO <sub>3</sub> , SO <sub>4</sub> , Cl Ca Na Mg	7.0
42	32M-139D	460.9 23.00 46.9	109.4 9.00 18.4	390.8 17.00 34.7	189.2 3.10 6.3	398.7 8.30 17.0	1240.0 37.49 76.7	7.0	4880	3200	0.11	-	4.25	1600	3200	Cl, SO <sub>4</sub> , HCO <sub>3</sub> Ca Na Mg	7.0
43	30M-2D	60.1 3.00 9.4	34.03 2.80 8.8	597.7 26.00 81.8	225.8 3.70 11.6	393.9 8.19 25.7	709.0 20.00 62.7	8.2	3200	2090	0.15	-	15.27	290	2090	Cl, SO <sub>4</sub> , HCO <sub>3</sub> Na Ca Mg	8.2
44	34L-47D	166.3 8.30 34.3	8.51 0.70 2.9	349.5 15.20 62.8	500.4 8.21 34.1	401.5 8.35 34.7	265.9 7.50 31.2	7.3	2400	1580	0.30	-	7.17	450	1580	SO <sub>4</sub> , HCO <sub>3</sub> , Cl Na Ca Mg	7.0

Hydrochemical data of the Tabriz Plain (continued)

45	34L-21D	186.4 9.30 38.8	57.13 4.70 19.6	229.9 10.00 41.7	500.3 8.205 34.1	160.9 3.347 13.9	443.1 12.50 52.0	7.5	2400	1580	0.11	-	3.78	700	1580	Cl HCO <sub>3</sub> , SO <sub>4</sub> Na Ca Mg	7.5
46	33L-69D	551.1 27.50 53.3	103.3 8.500 16.5	358.6 15.60 30.2	280.7 4.60 8.9	595.6 12.39 23.8	1240.4 35.00 67.3	6.5	5300	3500	0.38	-	3.68	1800	3500	Cl SO <sub>4</sub> , HCO <sub>3</sub> Ca Na Mg	6.5
47	33L-46D	40.1 2.00 14.1	48.62 4.00 28.2	188.5 8.200 57.8	360.0 5.90 41.9	273.8 5.70 40.4	88.6 2.50 17.7	8.3	1400	930	0.35	-	4.73	300	930	HCO <sub>3</sub> , SO <sub>4</sub> , Cl Na Mg Ca	8.3
48	33L-38D	250.5 12.50 24.0	164.1 13.50 25.9	597.7 26.00 50.0	274.6 4.503 8.6	533.1 11.09 21.1	1311.7 37.00 70.3	7.5	5000	3300	0.57	-	7.08	1350	3300	Cl SO <sub>4</sub> , HCO <sub>3</sub> Na Mg Ca	7.8
49	32L-10D	46.1 2.30 6.5	81.44 6.69 18.9	609.2 26.50 74.7	213.6 3.50 9.9	422.7 8.79 24.9	815.4 23.00 65.2	8.0	3500	2280	0.29	-	12.49	450	2280	Cl SO <sub>4</sub> , HCO <sub>3</sub> Na Mg Ca	8.0
50	31L-13D	64.1 3.20 8.4	85.09 7.00 18.3	643.7 28.00 73.3	317.3 5.20 13.7	374.6 7.80 20.5	886.3 25.00 65.8	7.8	3780	2400	2.69	-	12.40	510	2400	Cl SO <sub>4</sub> , HCO <sub>3</sub> Na Mg Ca	7.8
51	36K-25D	110.2 5.50 35.8	80.16 6.59 42.9	75.4 3.28 21.3	231.9 3.80 24.9	456.3 9.49 62.1	70.9 2.00 13.1	6.8	1530	1030	0.24	-	2.92	450	1030	SO <sub>4</sub> , HCO <sub>3</sub> , Cl Mg Ca Na	6.8
52	35K-30D	216.4 10.95 36.2	48.64 4.00 13.4	345.0 15.01 50.4	286.8 4.70 15.7	542.7 11.29 37.6	496.3 14.00 46.7	7.5	3000	1980	0.31	-	5.51	740	3000	Cl SO <sub>4</sub> , HCO <sub>3</sub> Na Ca Mg	7.5
53	34K-31D	501.0 25.00 41.3	91.50 7.52 12.4	644.0 28.01 46.3	274.6 4.50 7.5	360.2 7.49 12.5	1702.1 48.00 80.0	7.5	6100	3950	0.45	-	6.95	1625	3950	Cl SO <sub>4</sub> , HCO <sub>3</sub> Na Ca Mg	7.5
54	33K-10D	200.4 10.00 18.8	113.1 9.30 17.4	781.7 34.00 63.8	305.1 5.00 9.4	288.2 6.00 11.3	1488.9 42.00 79.2	7.4	5400	3500	0.30	-	10.94	965	3500	Cl SO <sub>4</sub> , HCO <sub>3</sub> Na Ca Mg	7.4

Hydrochemical data of the Tabriz Plain (continued)

55	36J-33S	340.7 17.00 27.4	121.55 10.00 16.1	804.7 35.00 56.5	610.2 10.00 16.4	720.5 14.98 24.6	1276.2 36.00 59.0	7.2	6000	3900	0.83	-	12.00	1350	3900	Cl SO <sub>4</sub> , HCO <sub>3</sub> , Na Ca Mg	7.2
56	36J-4S	90.2 4.50 16.4	36.47 3.00 10.9	459.8 20.00 72.7	537.0 8.81 31.8	235.4 4.90 17.7	496.3 14.00 50.5	7.3	2780	1800	0.36	1.3	10.33	375	1800	Cl HCO <sub>3</sub> , SO <sub>4</sub> , Na Ca Mg	7.3
57	35J-8D	86.2 4.30 10.1	41.33 3.40 8.0	804.7 35.00 82.0	213.6 3.50 8.2	297.8 6.19 14.5	1169.9 33.00 77.3	8.1	4300	2800	0.02	-	17.84	385	2800	Cl SO <sub>4</sub> , HCO <sub>3</sub> , Na Ca Mg	8.1
58	34J-11D	160.3 8.00 26.8	94.81 7.79 26.2	321.9 14.00 47.0	274.6 4.50 15.1	307.4 6.39 21.4	673.6 19.00 63.5	7.5	3000	1980	0.16	-	4.98	790	1980	Cl SO <sub>4</sub> , HCO <sub>3</sub> , Na Ca Mg	7.5
59	31R-23S	240.5 12.00 32.2	27.96 2.30 6.2	528.8 23.00 61.7	976.3 16.00 43.2	653.2 13.59 36.6	265.9 7.50 20.2	7.0	3720	2460	0.28	1.7	8.60	715	2460	HCO <sub>3</sub> , SO <sub>4</sub> , Cl Na Ca Mg	7.0
60	31R-8S	74.2 3.70 45.1	27.96 2.30 28.0	50.6 2.20 26.8	335.6 5.50 66.9	82.6 1.72 20.9	35.5 1.00 12.2	7.3	820	540	0.13	-	1.27	300	540	HCO <sub>3</sub> , SO <sub>4</sub> , Cl Ca Mg Na	7.3
61	30R-5S	140.3 7.00 32.3	66.85 5.500 25.3	211.5 9.200 42.4	793.3 13.00 59.8	132.1 2.75 12.6	212.7 6.00 27.6	7.3	2180	1460	0.14	0.5	3.68	625	1460	HCO <sub>3</sub> , SO <sub>4</sub> , Cl Na Ca Mg	7.3
64	31O-5D	204.4 10.20 51.0	27.96 2.30 11.5	172.4 7.500 37.5	274.6 4.50 22.6	451.5 9.39 47.2	212.7 6.00 30.2	7.1	1680	1310	0.26	-	3.00	625	1310	SO <sub>4</sub> , Cl HCO <sub>3</sub> , Ca Na Mg	7.1
67	27J-10D	106.2 5.30 30.3	93.59 7.69 44.0	103.5 4.50 25.7	262.4 4.30 24.7	148.9 3.10 17.8	354.5 10.00 57.5	7.9	1730	1120	0.28	-	1.77	650	1120	Cl HCO <sub>3</sub> , SO <sub>4</sub> , Mg Ca Na	7.9
68	30I-54D	36.1 1.80 43.9	18.23 1.500 36.5	18.4 0.80 19.5	195.3 3.20 77.7	25.0 0.52 12.6	14.2 0.40 9.7	7.7	410	270	0.28	-	0.62	165	270	HCO <sub>3</sub> , SO <sub>4</sub> , Cl Ca Mg Na	7.7



Hydrochemical data of the Tabriz Plain (continued)

69	30I-15D	36.1 1.80 37.5	17.02 1.40 29.1	36.8 3.30 33.3	201.4 3.30 68.1	36.0 0.75 15.4	28.40 0.801 16.5	7.7	480	320	0.54	0.1	1.26	160	320	$\frac{\text{HCO}_3, \text{Cl SO}_4}{\text{Ca Na Mg}} = 7.7$
70	29I-27D	58.1 2.90 43.3	27.96 2.30 34.3	34.5 1.50 22.4	299.0 4.90 72.9	25.0 0.52 7.7	46.10 1.30 19.3	7.4	680	450	0.19	-	0.93	260	450	$\frac{\text{HCO}_3, \text{Cl SO}_4}{\text{Ca Na Mg}} = 7.4$
71	28I-2D	46.1 2.30 32.0	37.68 3.10 43.0	41.4 1.80 25.0	170.9 2.80 38.5	71.1 1.48 20.3	106.4 3.00 41.2	7.5	725	480	0.57	-	1.10	270	480	$\frac{\text{Cl HCO}_3, \text{SO}_4}{\text{Mg Ca Na}} = 7.5$
72	26I-3D	90.2 4.50 40.6	54.7 4.50 40.5	48.3 2.10 18.9	213.6 3.50 31.8	48.0 1.00 9.1	230.4 6.500 59.1	7.3	1100	720	0.45	-	1.00	450	720	$\frac{\text{Cl HCO}_3, \text{SO}_4}{\text{Ca Mg Na}} = 7.3$
73	25I-59D	40.1 2.00 51.6	12.16 1.000 25.8	20.1 0.87 22.6	140.4 2.303 59.8	55.2 1.15 29.8	14.2 0.40 10.4	7.5	385	260	0.31	-	0.73	150	260	$\frac{\text{HCO}_3, \text{SO}_4, \text{Cl}}{\text{Ca Mg Na}} = 7.5$
74	24I-4D	40.1 2.00 45.5	12.16 1.000 22.7	32.2 1.40 31.8	164.8 2.70 61.7	51.9 1.08 24.6	21.3 0.60 13.7	7.7	435	290	0.20	-	1.14	150	290	$\frac{\text{HCO}_3, \text{SO}_4, \text{Cl}}{\text{Ca Na Mg}} = 7.7$
75	34H-4S	112.2 5.600 7.1	156.8 12.89 16.4	1379.4 60.00 76.4	518.7 8.51 10.8	504.3 10.49 13.3	2127.0 59.98 75.9	7.9	8000	5300	0.31	-	19.73	3000	5300	$\frac{\text{Cl SO}_4, \text{HCO}_3}{\text{Na Mg Ca}} = 7.9$
76	34H-2S	150.3 7.50 12.1	203.0 16.70 26.8	873.6 38.00 61.1	500.4 8.207 13.0	758.9 12.78 25.1	1382.6 39.00 61.9	6.8	6400	4200	0.63	-	10.92	1210	4200	$\frac{\text{Cl SO}_4, \text{HCO}_3}{\text{Na Mg Ca}} = 6.8$
77	31H-28D	74.2 3.70 19.3	76.58 6.300 32.8	211.5 9.20 47.9	189.2 3.10 16.2	192.1 4.00 20.9	425.4 12.00 62.8	7.8	1900	1240	0.27	-	4.11	500	1240	$\frac{\text{Cl SO}_4, \text{HCO}_3}{\text{Na Mg Ca}} = 7.8$
78	31H-19D	56.1 2.80 38.9	29.17 2.40 33.3	46.0 2.00 27.8	274.6 4.50 62.4	34.6 0.72 10.0	70.9 2.00 27.7	7.7	730	490	0.17	-	1.24	260	490	$\frac{\text{HCO}_3, \text{Cl SO}_4}{\text{Ca Mg Na}} = 7.7$

Hydrochemical data of the Tabriz Plain (continued)

79	30H-22D	56.1 2.80 59.6	14.59 1.20 25.5	16.1 0.70 14.9	189.2 3.10 66.7	26.4 0.55 11.8	35.5 1.00 21.5	7.7	460	310	0.49	-	0.49	200	310	$\frac{\text{HCO}_3, \text{Cl SO}_4}{\text{Ca Mg Na}}$ 7.7
80	29H-19D	40.1 2.00 32.3	36.47 3.00 48.4	27.6 1.20 19.4	268.5 4.40 73.3	28.8 0.60 10.0	35.5 1.00 16.7	7.4	600	400	1.60	-	0.65	250	400	$\frac{\text{HCO}_3, \text{Cl SO}_4}{\text{Mg Ca Na}}$ 7.4
81	25H-9D	34.1 1.70 35.9	27.96 2.30 48.5	17.0 0.74 15.6	177.0 2.90 61.8	52.8 1.10 23.4	24.8 0.70 14.9	8.0	470	310	0.14	-	0.52	200	310	$\frac{\text{HCO}_3, \text{SO}_4, \text{Cl}}{\text{Mg Ca Na}}$ 8.0
82	24H-1D	86.2 4.30 30.1	36.47 3.00 21.0	160.9 7.00 49.0	256.3 4.20 29.8	230.5 4.79 34.0	180.8 5.100 36.2	7.7	1400	920	0.71	-	3.69	360	920	$\frac{\text{Cl SO}_4, \text{HCO}_3}{\text{Na Ca Mg}}$ 7.7
83	23H-17D	64.2 3.20 31.4	36.47 3.00 29.4	92.0 4.00 39.2	256.3 4.20 41.6	67.2 1.40 13.8	159.5 4.500 44.5	7.6	1000	670	0.51	-	2.27	310	670	$\frac{\text{Cl HCO}_3, \text{SO}_4}{\text{Na Ca Mg}}$ 7.6
84	23H-5D	76.2 3.80 18.3	48.62 4.00 19.2	298.9 13.00 62.5	323.4 5.30 24.4	163.3 3.40 15.7	460.9 13.00 59.9	7.5	2150	1400	2.11	-	6.58	390	1400	$\frac{\text{Cl HCO}_3, \text{SO}_4}{\text{Na Mg Ca}}$ 7.5
85	35G-16S	300.6 15.00 27.8	109.4 9.00 16.7	689.7 30.00 55.6	518.7 8.51 15.6	43.2 0.90 1.7	1595.3 45.00 82.7	7.0	5500	3600	0.37	-	8.66	1200	3600	$\frac{\text{Cl HCO}_3, \text{SO}_4}{\text{Na Ca Mg}}$ 7.0
86	34G-1Q	74.2 3.70 20.7	51.05 4.200 23.4	229.9 10.00 55.9	280.7 4.60 25.6	441.9 9.19 51.1	148.9 4.200 23.3	7.0	1810	1220	0.26	-	5.03	395	1220	$\frac{\text{SO}_4, \text{HCO}_3, \text{Cl}}{\text{Na Mg Ca}}$ 7.0
87	33G-2Q	64.1 3.20 34.8	34.03 2.800 30.4	73.6 3.20 34.8	244.1 4.00 43.9	169.1 3.52 38.6	56.7 1.60 17.5	8.2	920	610	0.43	-	1.85	300	610	$\frac{\text{HCO}_3, \text{SO}_4, \text{Cl}}{\text{Ca/Na Mg}}$ 8.2
88	32G-2S	220.4 11.00 17.2	97.24 8.00 12.5	1034.6 45.00 70.3	262.4 4.303 6.5	562.0 11.68 17.7	1772.5 50.00 75.8	7.7	6500	4300	1.52	-	14.60	950	4300	$\frac{\text{Cl SO}_4, \text{HCO}_3}{\text{Na Ca Mg}}$ 7.3

Hydrochemical data of the Tabriz Plain (continued)

89	22G-9D	56.1 2.80 25.5	38.90 3.200 29.1	115.0 5.00 45.5	305.1 5.00 45.1	139.4 2.900 26.1	113.4 3.200 28.8	8.0	1100	730	0.46	-	2.89	300	730	$\frac{\text{HCO}_3, \text{Cl}, \text{SO}_4}{\text{Na Mg Ca}}$ 8.0
90	32F-4D	220.4 11.00 25.6	109.4 9.00 20.9	528.8 23.00 53.5	378.3 6.204 14.1	542.7 11.30 25.7	939.4 26.49 60.2	7.3	4100	2680	1.14	-	7.27	1000	2680	$\frac{\text{Cl SO}_4, \text{HCO}_3}{\text{Na Ca Mg}}$ 7.3
91	21F-5D	70.1 3.500 29.2	64.42 5.300 44.1	73.6 3.20 26.7	335.6 5.504 45.5	245.0 5.096 42.1	53.20 1.500 12.4	7.8	1220	810	0.44	-	1.53	440	810	$\frac{\text{HCO}_3, \text{SO}_4, \text{Cl}}{\text{Mg Ca Na}}$ 7.8
92	27H-17Q	72.1 3.600 44.3	29.17 2.400 29.6	48.7 2.12 26.1	353.9 5.804 71.1	60.5 1.26 15.4	39.0 1.100 13.5	7.5	820	530	0.29	-	1.22	300	530	$\frac{\text{HCO}_3, \text{SO}_4, \text{Cl}}{\text{Ca Mg Na}}$ 7.5
93	27H-12Q	52.1 2.60 43.3	29.17 2.40 40.0	23.0 1.00 16.7	280.7 4.603 76.1	50.4 1.048 17.3	14.20 0.400 6.6	7.2	600	400	0.45	-	0.63	250	400	$\frac{\text{HCO}_3, \text{SO}_4, \text{Cl}}{\text{Ca Mg Na}}$ 7.2
94	26H-3Q	56.1 2.80 45.2	26.74 2.200 35.5	27.6 1.20 19.4	262.4 4.303 69.2	77.8 1.62 26.0	10.60 0.300 4.8	7.0	620	420	0.19	-	0.76	250	620	$\frac{\text{HCO}_3, \text{SO}_4, \text{Cl}}{\text{Ca Mg Na}}$ 7.0
95	25H-7Q	60.1 3.00 67.4	7.29 0.60 13.5	19.5 0.85 19.1	152.6 2.50 56.8	72.1 1.50 34.1	14.20 0.400 9.1	7.2	440	290	0.49	-	0.63	180	290	$\frac{\text{HCO}_3, \text{SO}_4, \text{Cl}}{\text{Ca Mg Na}}$ 7.2
96	22G-11Q	44.1 2.20 59.1	9.72 0.80 21.5	16.6 0.72 19.4	122.0 2.00 52.9	66.3 1.38 36.5	14.20 0.400 10.6	7.2	380	250	0.77	-	0.59	150	250	$\frac{\text{HCO}_3, \text{SO}_4, \text{Cl}}{\text{Ca Mg Na}}$ 7.2
97	27G-12Q	60.1 3.00 66.7	14.59 1.20 26.7	6.9 0.30 6.7	164.8 2.70 60.3	71.1 1.48 33.0	10.60 0.300 6.7	8.0	442	290	0.19	-	0.21	210	290	$\frac{\text{HCO}_3, \text{SO}_4, \text{Cl}}{\text{Ca Mg Na}}$ 8.0
98	30F-11Q	64.1 3.20 61.5	19.45 1.60 30.8	9.20 0.40 7.7	195.3 3.20 62.8	67.2 1.40 27.4	17.70 0.50 9.8	7.8	510	340	0.95	-	0.26	240	340	$\frac{\text{HCO}_3, \text{SO}_4, \text{Cl}}{\text{Ca Mg Na}}$ 7.8

Hydrochemical data of the Tabriz Plain (continued)

99	21E-4Q	70.1 3.50 46.2	42.54 3.50 46.2	13.3 0.60 7.6	335.6 5.50 72.4	62.4 1.30 17.1	28.40 0.80 10.5	7.5	750	510	0.20	-	1.07	350	510	$\frac{\text{HCO}_3, \text{SO}_4, \text{Cl}}{\text{Ca/Mg Na}}$ 7.5
102	31H-26D	74.2 3.70 19.3	76.61 6.30 32.8	211.6 9.21 47.9	189.1 3.10 16.2	192.1 4.00 20.9	425.5 12.00 62.8	7.5	4000	2700	0.28	-	7.3	900	2700	$\frac{\text{Cl SO}_4, \text{HCO}_3, \text{Na Mg Ca}}{\text{Na Mg Ca}}$ 7.5
103	31H-12D	32.1 1.60 22.7	32.83 2.70 38.2	63.5 2.76 39.1	207.4 3.40 48.0	66.3 1.40 19.5	81.60 2.30 32.5	8.1	710	470	0.13	-	1.88	215	470	$\frac{\text{HCO}_3, \text{Cl SO}_4, \text{Na Mg Ca}}{\text{Na Mg Ca}}$ 8.1
104	21I-20D	48.1 2.40 35.3	34.05 2.80 41.2	36.8 1.60 23.5	207.4 3.40 49.9	140.3 2.92 42.8	17.70 0.50 7.3	7.4	680	450	0.14	-	0.99	260	450	$\frac{\text{HCO}_3, \text{SO}_4, \text{Cl Mg Ca Na}}{\text{Mg Ca Na}}$ 7.4
105	26I-21D	130.3 6.50 48.2	66.88 5.50 40.7	34.5 1.50 11.1	274.6 4.50 33.1	182.5 3.80 27.9	187.9 5.30 39.0	7.1	1360	890	0.36	-	0.61	600	890	$\frac{\text{Cl HCO}_3, \text{SO}_4, \text{Ca Mg Na}}{\text{Ca Mg Na}}$ 7.1
106	30I-43D	40.1 2.00 52.6	9.73 0.80 21.0	23.0 1.00 26.3	164.7 2.70 73.0	24.0 0.50 13.5	17.7 0.50 13.5	7.5	375	250	1.36	-	0.85	140	250	$\frac{\text{HCO}_3/\text{SO}_4, \text{Cl Ca Na Mg}}{\text{Ca Na Mg}}$ 7.5
107	31I-9D	40.1 2.00 25.3	36.48 3.00 37.8	67.2 2.92 36.9	225.7 3.70 46.6	108.1 2.25 28.3	70.9 2.00 25.2	7.0	800	530	0.16	-	1.85	250	530	$\frac{\text{HCO}_3, \text{SO}_4, \text{Cl Mg Na Ca}}{\text{Mg Na Ca}}$ 7.0
108	35I-D	72.1 3.600 7.7	38.91 3.20 6.8	920.0 40.02 85.5	231.8 3.80 8.3	537.9 11.19 24.3	1099.3 31.00 67.4	7.8	4400	2900	0.89	-	21.69	340	2900	$\frac{\text{Cl SO}_4, \text{HCO}_3, \text{Na Ca Mg}}{\text{Na Ca Mg}}$ 7.8
109	36I-D	56.1 2.80 8.2	42.56 3.50 10.2	644.0 28.01 81.6	201.3 3.30 9.4	321.8 6.69 19.1	886.5 25.00 71.4	7.9	3600	2350	0.98	-	15.78	315	2350	$\frac{\text{Cl SO}_4, \text{HCO}_3, \text{Na Mg Ca}}{\text{Na Mg Ca}}$ 7.9
110	34J-10D	76.2 3.80 25.7	60.80 5.00 33.8	138.0 6.00 40.6	323.4 5.30 35.6	172.9 3.60 24.1	212.7 6.00 40.3	7.8	1500	990	0.32	-	2.86	440	990	$\frac{\text{Cl HCO}_3, \text{SO}_4, \text{Na Mg Ca}}{\text{Na Mg Ca}}$ 7.8

Hydrochemical data of the Tabriz Plain (continued)

111	21E-16D	130.3 6.50 36.7	60.80 5.00 28.2	142.6 6.20 35.0	732.1 12.00 67.2	216.1 4.50 25.2	48.20 1.36 7.6	6.9	1800	1200	0.44	0.5	2.59	575	$\frac{\text{HCO}_3, \text{SO}_4, \text{Cl}}{\text{Ca Na Mg}} \frac{1200}{6.9}$
112	21E-19Q	90.2 4.50 19.3	158.08 13.00 55.8	133.4 5.80 24.9	640.6 10.50 45.0	384.2 7.99 34.2	172.3 4.86 20.8	7.4	2360	1580	0.12	-	1.96	875	$\frac{\text{HCO}_3, \text{SO}_4, \text{Cl}}{\text{Mg Na Ca}} \frac{1580}{7.4}$
113	21F-16Q	80.2 4.00 25.7	97.28 8.00 51.3	82.8 3.60 23.1	549.1 9.01 57.4	225.7 4.70 29.9	70.9 2.00 12.7	7.4	1580	1040	0.32	-	1.47	600	$\frac{\text{HCO}_3, \text{SO}_4, \text{Cl}}{\text{Mg Ca Na}} \frac{1040}{7.4}$
114	22F-5Q	80.2 4.00 39.2	38.91 3.200 31.4	69.0 3.00 29.4	488.1 8.01 78.8	65.3 1.36 13.4	28.4 0.80 7.9	7.5	1020	670	0.19	0.8	1.58	360	$\frac{\text{HCO}_3, \text{SO}_4, \text{Cl}}{\text{Ca Mg Na}} \frac{670}{7.5}$
115	22G-3D	72.1 3.60 29.5	43.78 3.60 29.5	115.0 5.00 41.0	292.9 4.80 38.4	187.3 3.90 31.2	134.8 3.80 30.4	7.8	1200	790	1.22	-	2.64	360	$\frac{\text{HCO}_3, \text{SO}_4, \text{Cl}}{\text{Na Ca/Mg}} \frac{790}{7.8}$
116	22G-11D	72.1 3.600 31.3	42.56 3.50 30.4	101.2 4.40 38.3	353.9 5.80 50.6	128.7 2.68 23.3	106.4 3.00 26.1	7.8	1140	760	0.07	-	1.84	574	$\frac{\text{HCO}_3, \text{Cl SO}_4}{\text{Na Ca Mg}} \frac{760}{7.8}$
117	30G-10D	80.2 4.00 42.1	36.48 3.00 31.6	57.5 2.50 26.3	353.9 5.80 60.9	20.2 0.42 4.4	117.0 3.30 34.6	7.4	950	630	0.12	-	1.34	476	$\frac{\text{HCO}_3, \text{Cl SO}_4}{\text{Ca Mg Na}} \frac{630}{7.4}$
118	31G-D	72.1 3.60 41.8	29.18 2.40 27.9	59.8 2.60 30.3	274.6 4.50 53.3	117.7 2.45 29.0	53.2 1.50 17.8	8.2	850	570	0.86	-	1.5	300	$\frac{\text{HCO}_3, \text{SO}_4, \text{Cl}}{\text{Ca Na Mg}} \frac{570}{8.2}$
119	33G-3S	48.1 2.40 29.3	41.34 3.40 41.4	55.2 2.40 29.3	231.8 3.80 46.6	136.9 2.85 34.9	53.2 1.50 18.4	8.0	810	540	0.31	-	1.41	290	$\frac{\text{HCO}_3, \text{SO}_4, \text{Cl}}{\text{Mg/Ca Na}} \frac{540}{8.0}$
120	25H-7D	52.1 2.60 35.0	38.91 3.20 43.1	37.3 1.62 21.9	231.8 3.80 51.0	103.3 2.15 28.8	53.2 1.50 20.1	7.8	750	500	0.20	-	0.95	290	$\frac{\text{HCO}_3, \text{SO}_4, \text{Cl}}{\text{Mg Ca Na}} \frac{500}{7.8}$

Hydrochemical data of the Tabriz Plain (continued)

121	31O-21D	28.1	7.30	41.4	195.2	2.4	17.7	7.8	380	250	0.73	1.2	1.8	100	250	$\frac{\text{HCO}_3, \text{Cl SO}_4}{\text{Na Ca Mg}}$ 7.8
		1.40	0.60	1.80	3.20	0.050	0.50									
		36.9	15.8	47.4	85.4	1.3	13.3									
122	31O-24D	911.8	273.6	529.0	274.6	264.2	2836.8	7.1	8800	5750	0.55	-	3.94	3400	5750	$\frac{\text{Cl SO}_4, \text{HCO}_3}{\text{Ca Na Mg}}$ 7.1
		45.50	22.50	23.01	4.50	5.50	80.00									
		50.0	24.7	25.3	5.0	6.1	88.9									
123	30P-31S	821.6	231.2	202.4	353.9	778.1	1649.4	6.3	6800	4400	0.22	-	1.61	3000	6400	$\frac{\text{Cl SO}_4, \text{HCO}_3}{\text{Ca Mg Na}}$ 6.3
		41.00	19.00	8.80	5.80	16.20	46.50									
		59.6	27.6	12.8	8.5	23.6	67.9									
124	31P-23D	200.4	103.4	197.8	244.0	518.7	432.6	6.8	2680	1770	0.20	-	2.83	925	1770	$\frac{\text{Cl SO}_4, \text{HCO}_3}{\text{Ca Na Mg}}$ 6.8
		10.00	8.50	8.60	4.00	10.79	12.20									
		36.9	31.4	31.7	14.8	40.0	45.2									
125	31P-52S	270.5	72.96	177.1	701.6	220.9	390.1	7.3	2700	1780	0.18	-	2.47	975	1780	$\frac{\text{HCO}_3, \text{Cl SO}_4}{\text{Ca Na Mg}}$ 7.3
		13.50	6.00	7.70	11.51	4.60	11.00									
		49.6	22.0	28.3	42.5	17.0	40.6									
126	30G-77D	190.4	44.99	110.4	634.5	173.9	141.8	7.0	1800	1200	0.06	-	1.87	660	1200	$\frac{\text{HCO}_3, \text{Cl SO}_4}{\text{Ca Na Mg}}$ 7.0
		9.50	3.70	4.80	10.40	3.62	4.00									
		52.8	20.5	26.7	57.7	20.1	22.2									
127	30Q-82S	1142.3	279.70	828.0	640.6	264.2	3616.9	6.8	11500	7500	0.85	-	5.69	4000	7500	$\frac{\text{Cl HCO}_3, \text{SO}_4}{\text{Ca Na Mg}}$ 6.8
		57.00	23.00	36.02	10.50	5.495	102.00									
		49.1	19.8	31.0	8.9	4.7	86.4									
128	30Q-100D	180.4	54.72	124.2	640.6	144.1	195.0	7.5	1900	1270	0.26	-	2.08	675	1270	$\frac{\text{HCO}_3, \text{Cl SO}_4}{\text{Ca Na Mg}}$ 7.5
		9.00	4.500	5.40	10.50	3.00	5.50									
		47.6	23.8	28.6	55.3	15.8	28.9									
129	30Q-106D	90.2	30.40	156.4	488.1	124.9	117.0	7.7	1400	930	0.36	1.0	3.63	350	930	$\frac{\text{HCO}_3, \text{Cl SO}_4}{\text{Na Ca Mg}}$ 7.7
		4.50	2.50	6.80	8.01	2.60	3.30									
		32.6	18.1	49.3	57.6	18.7	23.7									
130	31Q-48D	130.3	103.4	197.8	244.0	571.6	266.0	7.8	2350	1550	0.45	-	3.14	750	1550	$\frac{\text{SO}_4, \text{HCO}_3, \text{Cl}}{\text{Na Mg Ca}}$ 7.8
		6.50	8.50	8.60	4.00	11.89	7.50									
		27.5	36.0	36.5	17.1	50.8	32.1									

Hydrochemical data of the Tabriz Plain (continued)

131	30R-8D	196.4 9.80 30.0	105.8 8.70 26.6	326.6 14.21 43.4	793.1 13.00 40.2	461.1 9.59 29.7	345.6 9.75 30.1	7.2	3250	2140	0.55	-	4.67	925	$\frac{2140}{\text{Na Ca Mg}}$ 7.2
132	32R-13S	96.2 4.80 56.5	18.24 1.50 17.6	50.6 2.20 25.9	396.6 6.50 76.3	82.6 1.72 20.2	10.60 0.30 3.5	7.5	850	550	0.12	0.2	1.24	315	$\frac{550}{\text{Ca Na Mg}}$ 7.5
133	32R-2S	66.1 3.30 40.7	26.75 2.20 27.2	59.8 2.60 32.1	366.1 6.00 73.6	74.5 1.55 19.0	21.30 0.60 7.4	7.7	820	540	0.34	0.5	1.57	275	$\frac{540}{\text{Ca Na Mg}}$ 7.7
134	32Q-3Q	44.1 2.20 21.0	52.29 4.300 40.9	92.0 4.00 38.1	213.5 3.50 33.2	213.7 4.45 42.1	92.2 2.60 24.7	7.4	1060	710	0.21	-	5.82	325	$\frac{710}{\text{SO}_4, \text{HCO}_3, \text{Cl}}$ 7.4
135	33Q-6Q	60.1 3.00 40.0	24.30 2.00 26.6	57.5 2.50 33.4	207.4 3.40 44.8	96.1 2.00 26.3	78.0 2.20 28.9	7.9	790	505	0.68	-	1.58	250	$\frac{505}{\text{HCO}_3, \text{Cl SO}_4}$ 7.9
136	31R-4Q	80.2 4.00 55.6	12.16 1.00 13.9	50.6 2.20 30.6	311.8 5.11 71.1	51.9 1.08 15.0	35.50 1.00 13.9	7.3	715	480	0.90	0.1	1.39	250	$\frac{480}{\text{HCO}_3, \text{SO}_4, \text{Cl}}$ 7.3
137	32R-16Q	64.1 3.20 44.4	21.89 1.80 25.0	50.6 2.20 30.6	305.1 5.00 69.0	69.6 1.45 20.0	28.4 0.80 11.0	8.0	730	490	0.37	-	1.39	250	$\frac{490}{\text{HCO}_3, \text{SO}_4, \text{Cl}}$ 8.0
138	32R-27Q	90.2 4.50 67.2	2.40 0.200 2.9	46.0 2.00 29.9	317.3 5.20 75.4	52.8 1.10 15.9	21.3 0.60 8.7	7.6	690	460	1.50	0.4	1.29	240	$\frac{460}{\text{HCO}_3, \text{SO}_4, \text{Cl}}$ 7.6
139	32R-30Q	72.1 3.60 54.5	2.43 0.20 3.0	64.4 2.80 42.5	305.1 5.00 75.2	55.2 1.15 17.3	17.7 0.50 7.5	7.7	660	430	0.39	1.2	2.03	190	$\frac{430}{\text{HCO}_3, \text{SO}_4, \text{Cl}}$ 7.7
140	21E-1Q	44.1 2.20 39.3	34.05 2.80 50.0	13.8 0.60 10.7	244.0 4.00 72.1	40.8 0.85 15.3	24.8 0.70 12.6	7.6	550	360	0.45	-	0.38	250	$\frac{360}{\text{HCO}_3, \text{SO}_4, \text{Cl}}$ 7.6

Hydrochemical data of the Tabriz Plain (continued)

141	31E-2Q	110.2 5.50 24.3	66.88 5.50 24.3	266.8 11.61 51.3	305.1 5.00 22.4	773.3 16.08 72.2	42.60 1.20 5.4	7.7	2200	1450	0.70	-	4.95	550	1450	SO, HCO, Cl Na Ca/Mg	7.7
143	32F-2Q	731.5 36.50 18.0	316.16 26.00 12.8	3220.0 140.00 69.1	244.0 4.00 2.0	528.3 11.00 5.4	6737.4 190.40 92.7	7.3	20000	13000	0.71	-	25.04	3125	13000	Cl SO, HCO, Na Ca Mg	7.3
144	22G-1Q	80.2 4.00 27.0	58.37 4.80 32.4	138.0 6.00 40.6	305.1 5.00 33.4	182.5 3.80 25.3	219.9 6.20 41.3	7.8	1500	990	0.66	-	2.86	440	990	Cl HCO, SO, Na Mg Ca	7.8
145	22G-5Q	60.1 3.00 41.7	24.32 2.00 27.8	50.6 2.20 30.6	213.5 3.50 48.3	122.5 2.55 35.1	42.6 1.20 16.6	6.8	730	480	0.36	-	1.39	250	480	HCO, SO, Cl Ca Na Mg	6.8
146	27H-26Q	104.2 5.200 28.4	82.69 6.80 37.1	144.9 6.30 34.4	475.9 7.81 42.9	283.4 5.90 32.4	159.6 4.50 24.7	7.0	1800	1200	0.27	-	2.57	600	1200	HCO, SO, Cl Mg Na Ca	7.0
147	34L-5Q	154.3 7.70 37.6	48.64 4.00 19.5	202.4 8.80 42.9	366.1 6.00 29.0	413.1 8.59 41.5	216.3 6.10 29.5	6.9	2100	1420	0.47	-	3.64	584	1420	SO, Cl HCO, Na Ca Mg	6.9
148	37I-29D	180.4 9.00 42.9	12.16 1.00 4.8	253.0 11.01 52.4	457.6 7.51 35.6	411.1 8.55 40.6	177.3 5.00 23.7	7.3	2120	1400	0.11	-	4.92	500	1400	SO, HCO, Cl Na Ca Mg	7.3
149	35K-27D	220.4 11.00 24.7	91.24 7.50 16.8	598.0 26.01 58.4	275.6 4.52 10.0	360.2 7.492 16.6	1170.2 33.00 73.3	7.5	4600	2990	0.56	-	8.55	925	2990	Cl SO, HCO, Na Ca Mg	7.5
150	37K-8D	70.1 3.50 9.9	46.21 3.80 10.8	644.0 28.01 79.3	292.9 4.80 13.7	374.6 7.79 22.2	797.9 22.50 64.1	8.0	3500	2300	0.30	-	14.66	365	2300	Cl SO, HCO, Na Mg Ca	8.0



Hydrochemical data of the Tuff aquifer, Tabriz area (October 1987)

Samp. No.	Samp. Ref.	Grid	Ca	Mg	Na	HCO <sub>3</sub>	SO <sub>4</sub>	Cl	pH	EC μS/cm	TDS mg/l	% Error	RSC meq/l	SAR meq/l	Hard. CaCO <sub>3</sub>	Chemical Formula (Kurlov formula)
1	41M-17D		24.1 1.20 37.5	9.73 0.80 25.0	27.6 1.20 37.5	122.0 2.00 62.9	32.7 0.68 21.4	17.7 0.50 15.7	7.7	315	210	0.36	-	1.2	100	$\frac{\text{HCO}_3, \text{SO}_4, \text{Cl}}{\text{Ca/Na Mg}} \frac{7.7}{7.7}$
2	41M-19D		20.0 1.00 43.4	3.65 0.30 13.1	23.0 1.00 43.5	97.6 1.60 70.8	12.5 0.26 11.5	14.2 0.40 17.7	7.8	228	150	0.83	-	1.24	65	$\frac{\text{HCO}_3, \text{Cl SO}_4}{\text{Na Ca Mg}} \frac{7.8}{7.8}$
3	41M-22D		20.0 1.00 45.4	2.43 0.20 9.1	23.0 1.00 45.5	97.6 1.60 74.4	7.2 0.15 7.0	14.2 0.40 18.6	7.7	215	140	1.08	0.4	1.29	60	$\frac{\text{HCO}_3, \text{Cl SO}_4}{\text{Na Ca Mg}} \frac{7.7}{7.7}$
4	41M-27D		28.1 1.40 38.9	7.29 0.60 16.6	36.8 1.60 44.4	134.2 2.201 62.9	28.8 0.60 17.1	24.8 0.70 20.0	7.6	355	230	1.45	0.2	1.60	100	$\frac{\text{HCO}_3, \text{Cl SO}_4}{\text{Na Ca Mg}} \frac{7.6}{7.6}$
5	41M-31D		50.1 2.50 53.2	12.16 1.00 21.3	27.6 1.20 25.5	231.8 3.80 81.2	18.3 0.38 8.1	17.7 0.50 10.7	7.5	465	305	0.20	0.3	0.91	175	$\frac{\text{HCO}_3, \text{Cl SO}_4}{\text{Ca Na Mg}} \frac{7.5}{7.5}$
6	42M-1D		64.1 3.20 59.2	12.16 1.00 18.5	27.6 1.20 22.2	256.2 4.20 77.1	16.8 0.35 6.4	31.9 0.90 16.5	6.9	545	360	0.48	-	0.83	210	$\frac{\text{HCO}_3, \text{Cl SO}_4}{\text{Ca Na Mg}} \frac{6.9}{6.9}$
7	42M-2D		140.3 7.00 56.0	24.31 2.00 16.0	80.5 3.50 28.0	671.2 11.0 87.3	9.6 0.20 1.6	49.6 1.40 11.1	6.0	1260	835	0.42	-	1.65	450	$\frac{\text{HCO}_3, \text{Cl SO}_4}{\text{Ca Na Mg}} \frac{6.0}{6.0}$
8	42M-8D		44.1 2.20 45.8	9.72 0.80 16.6	41.4 1.80 37.5	164.7 2.70 56.0	63.4 1.32 27.4	28.4 0.80 16.6	7.3	480	320	0.22	-	1.47	150	$\frac{\text{HCO}_3, \text{SO}_4, \text{Cl}}{\text{Ca Na Mg}} \frac{7.3}{7.3}$
9	42M-10D		20.0 1.0 45.0	9.72 0.8 36.0	9.7 0.42 19.0	109.8 1.80 80.0	2.4 0.05 2.2	14.2 0.40 17.8	7.3	220	150	0.72	-	0.45	90	$\frac{\text{HCO}_3, \text{Cl SO}_4}{\text{Ca Mg Na}} \frac{7.3}{7.3}$

Hydrochemical data of the Tuff aquifer, Tabriz area (continued)

10	42M-11D	54.1 2.70 57.4	12.16 1.00 21.3	23.0 1.00 21.3	207.4 3.40 71.6	26.4 0.55 11.6	28.4 0.80 16.9	7.6	475	320	0.54	-	0.74	185	$\frac{\text{HCO}_3, \text{Cl SO}_4}{\text{Ca Na/Mg}}$ 320
11	42M-17D	54.1 2.70 62.8	7.30 0.60 14.0	23.0 1.00 23.3	231.8 3.80 89.4	2.4 0.05 1.2	14.2 0.40 9.4	7.4	425	280	0.56	0.5	0.78	165	$\frac{\text{HCO}_3, \text{Cl SO}_4}{\text{Ca Na Mg}}$ 280
12	42M-28D	20.0 1.00 52.6	1.20 0.10 5.2	18.4 0.80 42.2	91.5 1.50 79.9	3.8 0.08 4.2	10.6 0.30 15.9	7.0	186	120	0.48	0.4	1.08	55	$\frac{\text{HCO}_3, \text{Cl SO}_4}{\text{Ca Na Mg}}$ 120
13	42M-34D	28.1 1.40 42.5	13.38 1.10 33.3	18.4 0.80 24.2	152.5 2.50 76.5	13.0 0.27 8.3	17.7 0.50 15.3	7.0	325	210	0.47	-	0.96	125	$\frac{\text{HCO}_3, \text{Cl SO}_4}{\text{Ca Mg Na}}$ 210
14	41N-1D	44.1 2.20 48.9	15.81 1.30 28.9	23.0 1.00 22.2	207.4 3.40 73.9	24.0 0.50 10.9	24.8 0.70 15.2	7.4	450	300	1.09	-	0.76	175	$\frac{\text{HCO}_3, \text{Cl SO}_4}{\text{Ca Mg Na}}$ 300
15	41N-4D	50.1 2.50 56.8	8.51 0.70 15.9	27.6 1.20 27.3	213.5 3.50 81.4	9.6 0.20 4.6	21.3 0.60 14.0	7.7	432	290	1.13	0.3	0.91	160	$\frac{\text{HCO}_3, \text{Cl SO}_4}{\text{Ca Na Mg}}$ 290
18	42N-3D	30.1 1.50 50.0	3.65 0.30 10.0	27.6 1.20 40.0	134.2 2.20 73.8	23.1 0.48 16.1	10.6 0.30 10.0	7.5	298	200	0.38	0.4	1.26	90	$\frac{\text{HCO}_3, \text{SO}_4, \text{Cl}}{\text{Ca Na Mg}}$ 200
19	32N-11Q	76.2 3.80 43.2	14.59 1.20 13.6	87.4 3.80 43.2	152.6 2.50 28.8	172.9 3.560 41.3	92.2 2.60 29.9	7.5	870	590	0.60	-	2.4	250	$\frac{\text{SO}_4, \text{Cl HCO}_3}{\text{Ca/Na Mg}}$ 590
20	32N-32Q	80.2 4.00 44.5	12.16 1.00 11.1	91.7 3.99 44.4	146.4 2.40 26.6	150.3 3.13 34.6	124.1 3.50 38.8	7.6	900	600	0.21	-	2.53	250	$\frac{\text{Cl SO}_4, \text{HCO}_3}{\text{Ca Na Mg}}$ 600
21	34N-53Q	46.1 2.300 34.9	18.23 1.50 22.7	64.4 2.80 42.4	140.4 2.30 35.4	105.7 2.20 33.8	70.9 2.00 30.8	7.7	650	430	0.76	-	2.03	190	$\frac{\text{HCO}_3, \text{SO}_4, \text{Cl}}{\text{Ca Na Mg}}$ 430

Hydrochemical data of the Tuff aquifer, Tabriz area (continued)

22	35N-3Q	72.1 3.600 46.7	7.30 0.60 7.8	80.5 3.50 45.5	268.4 4.40 57.3	90.3 1.88 24.5	49.6 1.40 18.2	7.5	760	500	0.14	-	2.03	190	500	$\frac{\text{HCO}_3, \text{SO}_4, \text{Cl}}{\text{Ca Na Mg}}$ 7.5
23	35N-14Q	80.2 4.00 63.5	9.73 0.80 12.7	34.5 1.50 23.8	256.2 4.20 67.8	57.6 1.20 19.3	28.4 0.80 12.9	7.2	620	410	0.82	-	0.97	240	410	$\frac{\text{HCO}_3, \text{SO}_4, \text{Cl}}{\text{Ca Na Mg}}$ 7.2
24	31O-2Q	90.2 4.50 45.9	27.96 2.30 23.5	69.0 3.00 30.6	170.9 2.80 28.9	163.3 3.40 35.0	124.1 3.50 36.1	7.3	965	635	0.52	-	1.63	340	635	$\frac{\text{Cl SO}_4, \text{HCO}_3}{\text{Ca Na Mg}}$ 7.3
25	32O-7Q	132.3 6.60 43.2	26.74 2.20 14.4	149.4 6.50 42.5	140.4 2.30 15.0	377.0 7.84 51.1	184.3 5.20 33.9	6.9	1520	1000	0.14	-	3.10	440	1000	$\frac{\text{SO}_4, \text{Cl HCO}_3}{\text{Ca Na Mg}}$ 6.9
26	33O-1Q	80.2 4.00 46.0	23.09 1.90 21.8	64.4 2.80 32.2	158.7 2.60 29.9	140.3 2.92 33.5	113.4 3.20 36.7	7.5	870	580	0.10	-	1.63	295	580	$\frac{\text{Cl SO}_4, \text{HCO}_3}{\text{Ca Na Mg}}$ 7.5
27	34O-2Q	42.1 2.10 44.7	13.37 1.10 23.4	34.5 1.50 31.9	164.8 2.70 57.1	44.7 0.93 19.6	39.0 1.10 23.2	7.8	470	310	0.33	-	1.19	160	310	$\frac{\text{HCO}_3, \text{Cl SO}_4}{\text{Ca Na Mg}}$ 7.8
28	34O-3Q	40.1 2.00 45.5	14.59 1.20 27.3	27.6 1.20 27.3	170.9 2.80 62.9	31.2 0.65 14.6	35.5 1.00 22.5	7.3	445	290	0.59	-	0.95	160	290	$\frac{\text{HCO}_3, \text{Cl SO}_4}{\text{Ca Mg/Na}}$ 7.3
29	32P-4Q	94.2 4.70 44.8	34.03 2.80 26.6	69.0 3.00 28.6	195.3 3.20 30.8	201.7 4.20 40.3	106.4 3.00 28.9	7.3	1040	690	0.48	-	1.55	375	690	$\frac{\text{SO}_4, \text{HCO}_3, \text{Cl}}{\text{Ca Na Mg}}$ 7.3
30	32P-18Q	60.1 3.00 42.2	17.02 1.40 19.7	62.1 2.70 38.1	146.5 2.40 33.4	120.1 2.500 34.7	81.5 2.30 31.9	7.5	720	470	0.70	-	1.82	220	470	$\frac{\text{SO}_4, \text{HCO}_3, \text{Cl}}{\text{Ca Na Mg}}$ 7.5
31	32P-25Q	44.1 2.20 42.3	12.16 1.00 19.2	46.0 2.00 38.5	164.7 2.70 51.7	49.0 1.02 19.5	53.2 1.50 28.7	7.8	520	340	0.20	-	1.58	160	340	$\frac{\text{HCO}_3, \text{Cl SO}_4}{\text{Ca Na Mg}}$ 7.8

Hydrochemical data of the Tuff aquifer, Tabriz area (continued)

32	32P-33Q	46.1 2.30 45.1	12.16 1.00 19.6	41.4 1.80 35.3	152.5 2.50 50.0	38.4 0.80 16.0	60.3 1.70 34.0	7.7	500	330	1.0	-	1.40	165	330	$\frac{\text{HCO}_3, \text{Cl}, \text{SO}_4}{\text{Ca Na Mg}}$ 7.7
33	32P-48Q	78.2 3.90 39.8	25.54 2.10 21.4	87.4 3.80 38.8	176.9 2.90 29.9	153.7 3.20 33.0	127.6 3.60 37.1	7.7	970	640	0.55	-	2.19	300	640	$\frac{\text{Cl}, \text{SO}_4, \text{HCO}_3}{\text{Ca Na Mg}}$ 7.7
34	32P-50Q	46.1 2.30 46.0	8.51 0.70 14.0	46.0 2.00 40.0	207.4 3.40 66.7	33.6 0.70 13.7	35.5 1.00 19.6	7.8	510	335	1.0	0.4	1.63	150	335	$\frac{\text{HCO}_3, \text{Cl}, \text{SO}_4}{\text{Ca Na Mg}}$ 7.8
35	33Q-1Q	68.1 3.400 36.5	27.96 2.300 24.7	82.8 3.60 38.7	201.4 3.30 34.2	160.9 3.35 34.7	106.4 3.00 31.1	7.8	960	630	1.86	-	2.08	300	630	$\frac{\text{SO}_4, \text{HCO}_3, \text{Cl}}{\text{Na Ca Mg}}$ 7.8
36	35N-4D	60.1 3.00 68.2	4.86 0.40 9.1	23.0 1.00 22.7	219.7 3.60 82.2	18.3 0.38 8.7	14.2 0.40 9.1	7.5	435	290	0.17	0.2	0.77	170	290	$\frac{\text{HCO}_3, \text{Cl}, \text{SO}_4}{\text{Ca Na Mg}}$ 7.5
37	36L-11Q	76.2 3.80 44.2	14.59 1.20 13.9	82.8 3.60 41.9	231.8 3.802 44.5	117.7 2.45 28.6	81.5 2.30 26.9	7.3	850	560	0.32	-	2.28	250	560	$\frac{\text{HCO}_3, \text{SO}_4, \text{Cl}}{\text{Ca Na Mg}}$ 7.3
38	36L-9Q	79.2 3.95 40.5	26.74 2.20 22.5	82.7 3.60 36.9	183.1 3.00 31.4	162.3 3.38 35.3	113.4 3.20 33.4	7.0	950	630	0.13	-	5.54	300	630	$\frac{\text{SO}_4, \text{Cl}, \text{HCO}_3}{\text{Ca Na Mg}}$ 7.0
39	39L-4Q	50.1 2.500 37.3	20.66 1.70 25.3	57.5 2.50 37.3	195.3 3.20 48.5	100.9 2.10 31.8	46.1 1.30 19.7	7.3	660	440	0.73	-	1.73	210	440	$\frac{\text{HCO}_3, \text{SO}_4, \text{Cl}}{\text{Ca/Na Mg}}$ 7.3
40	39L-11Q	32.1 1.60 42.1	7.30 0.60 15.8	36.8 1.60 42.1	146.4 2.40 64.0	31.2 0.65 17.3	24.8 0.70 18.7	7.4	375	250	0.72	0.2	1.53	110	250	$\frac{\text{HCO}_3, \text{Cl}, \text{SO}_4}{\text{Ca/Na Mg}}$ 7.4
41	40L-13Q	30.1 1.502 36.6	12.16 1.000 24.4	36.8 1.60 39.0	140.4 2.300 56.9	60.0 1.25 30.8	17.7 0.499 12.3	6.9	405	260	0.64	-	1.43	125	260	$\frac{\text{HCO}_3, \text{SO}_4, \text{Cl}}{\text{Na Ca Mg}}$ 6.9

Hydrochemical data of the Tuff aquifer, Tabriz area (continued)

42	41L-5Q	70.1 3.500 42.7	30.40 2.50 30.5	50.6 2.20 26.8	305.1 5.00 61.9	128.7 2.68 33.1	14.2 0.40 5.0	6.3	810	540	0.72	-	1.27	300	540	$\frac{\text{HCO}_3, \text{SO}_4, \text{Cl}}{\text{Ca Mg Na}}$ 6.3
43	35M-5Q	40.1 2.00 37.8	18.23 1.50 28.3	41.4 1.80 34.0	170.9 2.800 53.4	93.7 1.95 37.1	17.7 0.50 9.50	7.3	525	350	0.46	-	1.36	175	350	$\frac{\text{HCO}_3, \text{SO}_4, \text{Cl}}{\text{Ca Na Mg}}$ 7.3
44	36M-1Q	48.1 2.400 37.5	19.45 1.60 25.0	55.2 2.40 37.5	183.1 3.00 47.6	86.5 1.80 28.5	53.2 1.50 23.8	7.2	630	420	0.79	-	1.70	200	420	$\frac{\text{HCO}_3, \text{SO}_4, \text{Cl}}{\text{Ca/Na Mg}}$ 7.2
45	41M-8Q	40.1 2.00 47.6	12.16 1.00 23.8	27.6 1.20 28.6	152.5 2.50 59.3	63.4 1.32 31.2	14.2 0.40 9.5	7.4	420	280	0.23	-	0.98	150	280	$\frac{\text{HCO}_3, \text{SO}_4, \text{Cl}}{\text{Ca Na Mg}}$ 7.4
46	32N-3Q	140.3 7.00 50.4	12.16 1.00 7.10	137.9 6.00 42.9	207.5 3.40 24.1	336.2 7.00 49.6	131.2 3.70 26.2	7.1	1390	940	0.35	-	3.0	400	940	$\frac{\text{SO}_4, \text{Cl HCO}_3}{\text{Ca Na Mg}}$ 7.1
47	35L-18Q	126.3 6.30 50.4	14.59 1.20 9.6	115.0 5.00 40.0	292.9 4.80 38.7	196.9 4.10 33.0	124.1 3.50 28.2	8.0	1230	810	0.42	-	2.58	375	810	$\frac{\text{HCO}_3, \text{SO}_4, \text{Cl}}{\text{Ca Na Mg}}$ 8.0
48	36L-1D	56.1 2.80 39.4	32.8 2.70 38.0	36.8 1.60 22.6	256.3 4.20 53.1	111.4 2.32 29.3	49.6 1.40 17.7	7.9	715	470	5.47	-	0.96	278	470	$\frac{\text{HCO}_3, \text{SO}_4, \text{Cl}}{\text{Ca Mg Na}}$ 7.9
49	36L-5D	60.1 3.00 41.7	34.05 2.80 38.9	32.2 1.40 19.5	183.0 3.00 42.3	110.5 2.30 32.4	63.8 1.80 25.3	7.2	710	470	0.70	-	0.82	290	470	$\frac{\text{HCO}_3, \text{SO}_4, \text{Cl}}{\text{Ca Mg Na}}$ 7.2
50	36L-8D	68.1 3.40 45.3	7.30 0.60 8.0	80.5 3.50 46.7	170.8 2.80 36.9	148.9 3.10 40.8	60.3 1.70 22.4	7.1	760	510	0.66	-	2.47	200	510	$\frac{\text{SO}_4, \text{HCO}_3, \text{Cl}}{\text{Na Ca Mg}}$ 7.1
51	37L-2D	60.1 3.0 41.7	17.0 1.4 19.4	64.4 2.8 38.9	213.6 3.50 48.3	122.5 2.55 35.1	42.5 1.2 16.5	7.0	730	490	0.35	-	1.89	220	490	$\frac{\text{HCO}_3, \text{SO}_4, \text{Cl}}{\text{Ca Na Mg}}$ 7.0

Hydrochemical data of the tuff aquifer, Tabriz area (continued)

52	38L-3D	36.1	17.07	27.6	152.5	73.0	14.2	7.6	445	300	0.22	-	1.11	160	300	$\frac{\text{HCO}_3, \text{SO}_4, \text{Cl}}{\text{Ca Mg Na}}$	7.6
		1.80	1.40	1.20	2.50	1.52	0.400										
		40.9	31.9	27.3	56.6	34.4	9.1										
53	38L-5D	74.2	26.74	66.7	305.1	139.3	35.5	7.1	890	600	0.56	-	1.69	295	600	$\frac{\text{HCO}_3, \text{SO}_4, \text{Cl}}{\text{Ca Na Mg}}$	7.1
		3.73	2.20	2.90	5.00	2.90	1.00										
		42.0	25.0	33.0	56.2	32.5	11.2										
54	39L-3S	60.1	17.02	75.9	244.0	124.9	35.5	7.8	765	510	0.65	-	2.22	220	510	$\frac{\text{HCO}_3, \text{SO}_4, \text{Cl}}{\text{Na Ca Mg}}$	7.8
		3.00	1.40	3.30	4.00	2.60	1.00										
		38.9	18.2	42.9	52.6	34.2	13.2										
55	39L-4S	46.1	29.18	87.4	213.5	193.1	35.5	7.7	850	570	0.11	-	2.48	235	570	$\frac{\text{SO}_4, \text{HCO}_3, \text{Cl}}{\text{Na Mg Ca}}$	7.7
		2.30	2.40	3.80	3.50	4.02	1.00										
		27.1	28.2	44.7	41.1	47.1	11.8										
56	40L-34D	54.1	15.81	57.5	207.4	108.1	28.4	7.5	640	420	0.38	-	1.77	200	420	$\frac{\text{HCO}_3, \text{SO}_4, \text{Cl}}{\text{Ca Na Mg}}$	7.5
		2.70	1.30	2.50	3.40	2.25	0.80										
		41.5	20.0	38.5	52.7	34.9	12.4										
57	41L-1D	26.1	14.59	27.6	134.2	49.5	17.7	7.0	370	240	0.38	-	1.07	125	240	$\frac{\text{HCO}_3, \text{SO}_4, \text{Cl}}{\text{Ca Na/Mg}}$	7.0
		1.30	1.20	1.20	2.20	1.03	0.50										
		35.2	32.4	32.4	59.0	27.6	13.4										
58	41L-7S	84.2	14.59	101.2	170.8	242.6	70.9	7.7	980	665	0.22	-	2.68	270	665	$\frac{\text{SO}_4, \text{HCO}_3, \text{Cl}}{\text{Na Ca Mg}}$	7.7
		4.20	1.20	4.40	2.80	5.05	2.00										
		42.9	12.2	44.9	28.4	51.2	20.3										
59	40M-1D	136.3	48.62	64.4	286.8	264.2	117.0	6.7	1340	880	0.37	-	1.20	540	880	$\frac{\text{SO}_4, \text{HCO}_3, \text{Cl}}{\text{Ca Mg Na}}$	6.7
		6.80	4.00	2.80	4.70	5.50	3.300										
		50.0	29.4	20.6	34.8	40.7	24.4										
60	40M-3Q	30.1	12.16	46.0	122.0	84.1	28.4	7.2	460	300	0.53	-	1.79	125	300	$\frac{\text{HCO}_3, \text{SO}_4, \text{Cl}}{\text{Na Ca Mg}}$	7.2
		1.50	1.00	2.00	2.00	1.75	0.80										
		33.4	22.2	44.4	44.0	38.4	17.6										
61	41M-1D	20.0	7.30	18.4	109.8	5.8	17.7	7.8	242	160	0.46	0.2	0.89	80	160	$\frac{\text{HCO}_3, \text{Cl SO}_4}{\text{Ca Na Mg}}$	7.8
		1.00	0.60	0.80	1.80	0.12	0.50										
		41.6	25.0	33.4	74.4	5.0	20.6										

Hydrochemical data of the tuff aquifer, Tabriz area (continued)

62	41M-7D	36.1 1.80 45.0	14.59 1.20 30.0	23.0 1.00 25.0	152.5 2.50 61.8	45.6 0.95 23.4	21.3 0.60 14.8	7.4	405	270	0.61	-	0.82	150	270	$\frac{\text{HCO}_3, \text{SO}_4, \text{Cl}}{\text{Ca Mg Na}} = 7.4$
63	41M-11D	76.2 3.80 54.3	14.59 1.20 17.1	46.0 2.00 28.6	305.1 5.00 72.5	52.8 1.10 15.9	28.4 0.80 11.6	6.8	690	460	0.72	-	1.26	300	460	$\frac{\text{HCO}_3, \text{SO}_4, \text{Cl}}{\text{Ca Na Mg}} = 6.8$
64	42N-13D	24.1 1.20 54.6	3.65 0.30 13.6	16.1 0.70 31.8	109.8 1.80 81.1	10.6 0.22 9.9	7.10 0.20 9.0	7.6	222	150	0.41	-	0.81	75	150	$\frac{\text{HCO}_3, \text{SO}_4, \text{Cl}}{\text{Ca Na Mg}} = 7.6$
65	41N-6D	36.1 1.80 49.7	8.51 0.70 19.3	25.8 1.12 31.0	183.1 3.00 83.4	19.2 0.40 11.1	7.10 0.20 5.6	7.4	360	240	0.29	-	1.0	125	240	$\frac{\text{HCO}_3, \text{SO}_4, \text{Cl}}{\text{Ca Na Mg}} = 7.4$